Outer Continental Shelf Environmental Assessment Program

Final Reports of Principal Investigators

Volume 64   November 1989

It is suggested that reports in this volume be cited as follows:

Payne, J. R., J. R. Clayton, Jr., G. D. McNabb, Jr., B. E. Kirstein, C. L. Clary, R. T. Redding, J. S. Evans, E. Reimnitz, and E. W. Kempema. 1989. Oil–ice–sediment interactions during freezeup and breakup. U.S. Dep. Commer., NOAA, OCSEAP Final Rep. 64: 1–382.

Kirstein, B. E., and C. L. Clary. 1989. User's manual for the computer codes: OILSPMXS, SPMONLY, OILSPM3. U.S. Dep. Commer., NOAA, OCSEAP Final Rep. 64: 383–448.

OUTER CONTINENTAL SHELF

ENVIRONMENTAL ASSESSMENT PROGRAM

Final Reports of Principal Investigators

Volume 64

November 1989

Outer Continental Shelf Environmental Assessment Program

Final Reports of Principal Investigators

C O N T E N T S

OIL–ICE–SEDIMENT INTERACTIONS DURING FREEZEUP AND BREAKUP

by

James R. Payne, John R. Clayton, Jr., G. Daniel McNabb, Jr.,
Bruce E. Kirstein, Cheryl L. Clary, Robert T. Redding, John S. Evans,
Erk Reimnitz (U.S.G.S.), and Ed W. Kempema (U.S.G.S.)

Applied Environmental Sciences Department
Science Applications International Corporation
4224 Campus Point Court
San Diego, California 92121

Final Report
Outer Continental Shelf Environmental Assessment Program
Research Unit 680

June 30, 1989

ACKNOWLEDGMENTS

FOREWORD

The original three-year program, entitled "Oil-Ice Sediment Interactions during Freezeup and Breakup," was envisioned and designed to examine the interactions of oil, ice and suspended particulate material, with a major emphasis on how the dynamics of different types of growing (and existing) sea ice in arctic and subarctic waters may influence sediment transport as suspended particulate material (SPM) and, therefore, oil/SPM interactions. This information was then to be utilized in developing a generic, nonsite-specific computer model that could be used to predict oil/SPM interactions in cold marine waters. As a result, most of the effort during the first one and one-half years of the program was directed at studying frazil and slush ice interactions with SPM. In the middle of the second year of this contract, however, the program scope was changed by NOAA and MMS to eliminate or postpone the ice formation dynamics components of the study and focus entirely on experimentation to measure the kinetics of oil/SPM interactions and the rates of SPM (both oiled and unoiled) sedimentation in support of the computer modeling efforts to predict these phenomena.

The interaction kinetics measurements and sedimentation studies were completed to provide data to validate and support computer model development and allow user-selected choices of SPM type, oil type (fuel oil versus fresh or weathered crude oil), and salinity conditions when running the computer code to predict environmental impacts from oil/SPM interactions and sedimentation. The computer codes developed during this project are one-dimensional, and they predict reaction rates of oil droplets and SPM, as controlled by the aforementioned variables. They are primarily useful as scoping tools for estimating what changes can be expected when the independent variables are changed.

Earlier MMS- and Department of Transportation (DOT)- sponsored studies on oil droplet dispersion and oil droplet/SPM interactions (Delvigne et al., 1987; Bowmeester and Wallace, 1986; Payne et al., 1987b) had not proceeded as far and sucessfully as desired by early 1987, and the Oil/Ice/SPM Program was viewed as the most logical way to address aspects of the phenomena for which

5

data were still incomplete or only partly understood. Hence, the program scope of work was changed, and the research focus was redirected as described in the following report.

Because of the mid-course change in program scope, this report is segregated such that the results from the two studies are presented as distinct and independent components. The first, which includes Sections 1 through 7 and constitutes the majority of the report, presents the results of computer model development and the oil/SPM interaction kinetics and sedimentation measurements completed since October 1987. These sections are accompanied by a separate, stand-alone document, which contains the Computer Users Manual and computer code (Kirstein and Clary, 1989). By virtue of the change in program scope, these sections (1 through 7) and the stand-alone Users Manual are considered by NOAA and MMS to be the most important. The second component of the report, which is contained entirely in Section 8, considers the original, but only partially completed, ice/SPM dynamics studies undertaken during the first one and one-half years of the program.

During the interim between the preparation of the original Draft Final Report for this program and the incorporation of NOAA/MMS review comments, the EXXON VALDEZ oil spill occurred in Prince William Sound, Alaska. The contract was then further modified to allow field validation of oil weathering and oil/SPM interactions, and the results of those studies are contained in Appendix B of this report.

TABLE OF CONTENTS

7

TABLE OF CONTENTS (Continued)

10

TABLE OF CONTENTS (Continued)

13

LIST OF FIGURES (Continued)

15

16

LIST OF TABLES

17

1.0   EXECUTIVE SUMMARY

1.1   PROGRAM OBJECTIVES AND RELEVANCE TO OCSEAP'S ANALYSIS OF OUTER CONTINENTAL SHELF OIL AND GAS DEVELOPMENT ACTIVITIES

One of the goals of the NOAA Outer Continental Shelf Environmental Assessment Program (OCSEAP) was to develop predictive capabilities for defining the magnitude of potential environmental impacts from Outer Continental Shelf (OCS) oil and gas development activities. In support of that goal, the objective of this program and previous NOAA- and MMS-sponsored studies (e.g., Payne et al., 1984a and 1984b; 1987a and 1987b) was therefore to develop predictive models that could describe the qualitative and quantitative chemical weathering and fate of crude oil and refined petroleum products released to the marine environment. Outdoor wave tank studies on subarctic oil spills in ice-free waters and the development of the NOAA model for open-ocean oil weathering are described in Payne et al., 1984a. Modifications to the experimental program and computer code to allow development of a predictive model for the weathering of oil in the presence of sea ice are considered in Payne et al., 1987a.

In the development of these models, a True Boiling Point (TBP) distillation cut approach was used to characterize the oils, and as such, the models are applicable to a wide variety of crude oil types and distillate products. Furthermore, with this distillate cut (or pseudocomponent) approach, it is possible to get a more accurate estimate of the overall mass balance of the slick (including the nondistillable residuum). At the time of their development, however, neither of the NOAA models considered oil droplet interactions with suspended particulate material (SPM) and sedimentation. Therefore, requirements for measuring and modeling those phenomena were first considered in Payne et al., 1987b. That program provided for the successful development of an analytical technique suitable for measuring oil droplet/SPM interaction rate constants. Unfortunately, limited time and resources prevented application of the technique to a wide variety of oil and SPM types. As a result, the current program was ultimately modified (as discussed in the Foreword) to obtain the necessary oil/SPM interaction rate constant data and allow for the completion of the mathematical derivations and model-development activities necessary to

21

provide computer-based mass transport calculations for interacting oil droplets and SPM.

Section 2 of this report provides a brief overview of previous field and laboratory studies of oil/SPM interactions, and it serves as a general introduction to the studies of oil/SPM interactions and model development contained in Sections 3-7. Section 3.0 considers the computer code development, and it provides the assumptions, derivations, and equations that have been incorporated into the computer model. As discussed in Section 3, the model is based on experimental studies of oil/SPM interactions, and various user-defined parameters can be adjusted using experimental data to simulate oil/SPM interactions with a variety of SPM and oil types. Thus, the model development was completed in concert with field sampling and laboratory studies, wherein data from these experiments were ultimately incorporated into the model code, used to verify modeling assumptions, or tabulated for user-specified input for particular scenarios. The methods and materials used for SPM sampling and characterization are provided in Section 4.1; whole-oil droplet/SPM interactions are described in Section 4.2; settling velocity determinations are in Section 4.3, and molecular-scale interactions are considered in 4.4. The results and discussion section for the laboratory experiments is organized in the same fashion and follows as Section 5.0. Section 6.0 stands as a separate discussion of the implementation of the computer model utilizing the information and results contained in Sections 3 through 5. In addition, it provides examples of the computer model output, or results, to assist the user in data interpretation and utilization. Section 7.0 presents the conclusions drawn from this study and is divided into the three major areas of focus; SPM/droplet interactions (7.1), settling (7.2), and molecular adsorption (7.3). As noted in the Foreword, Section 8 is reserved entirely for oil/ice/SPM studies completed during the first one and one-half years of the program before the experimental focus was re-directed to eliminate the ice studies. Quality assurance and quality control (QA/QC) concerns and references for both the oil/SPM and oil/ice/SPM studies are presented in Sections 9.0 and 10.0, respectively. Appendix A presents the results of subcontracted mineralogical determinations on the different SPM/sediment types examined in this program, and Appendix B contains the results of oil weathering

22

and oil/SPM field validation studies using the EXXON VALDEZ incident in Prince William Sound as a spill of opportunity. As required by the contract, the Oil/SPM User's Manual and Computer Code are published as a separate, stand-alone document (Kirstein and Clary, 1989).

1.2   MODEL DERIVATION AND CODE DEVELOPMENT/UTILIZATION (SECTIONS 3 AND 6)

The purpose of the modeling work discussed in this report was to develop a scoping technique to evaluate the effect of oil/suspended particulate material interactions as a removal process for oil dispersed in the water column. The assumptions, derivations, and equations required for development of the computer code are presented in Section 3, and Section 6 stands as a separate discussion of the implementation of the computer model utilizing the information and results from laboratory experiments described in Sections 4 and 5. In addition, Section 6 provides examples of the computer model output to assist the user in data interpretation and utilization. Specifically, mass transport calculations for interacting oil droplets and SPM in a one-dimensional water column are presented to illustrate the procedures necessary to implement the various models in realistic environmental situations. Additional instructions on the implementation and use of the computer models, including assumptions and limitations, are presented in the stand-alone User's Manual (Kirstein and Clary, 1989).

The basis for the mathematical model used in this report is the rate of reaction of oil droplets and SPM, and it is proportional to the concentration of each. The proportionality constants are the turbulent energy dissipation rate, the particle-particle sticking coefficient and geometric factors. Particle- particle kinetics was originally described by M. Smoluchowski (1916), and more recently, Birkner and Morgan (1968) presented an experimental study similar to the oil/SPM prgram. Thus, the model used, not developed, for oil/SPM kinetics is essentially a well-known general particle-particle kinetics expression. The use of the particle-particle kinetics expression in a volume that is not uniform (i.e., the ocean instead of a well-mixed vessel) in no way affects the kinetics expression used. However, the one-dimensional models that incorporate the oil/SPM expression are quite

limited in that they are one-dimensional. The one-dimensional models are useful only for the purposes of estimating what changes can be expected when the independent variables are changed. In the development of the model code(s), it was necessary to develop three separate cases: Oil fluxed from the surface into the water column alone, SPM fluxed from the bottom into the water column alone, and oil and SPM each fluxed into the water column and allowed to interact to form agglomerates which can then settle to the bottom at user specified sedimentation rates.

In order to use the model which describes interacting oil droplets and SPM in a one-dimensional water column that is initially oil free, a source term for both oil and SPM is required. The source term for the oil droplets can be obtained from NOAA's Open Ocean Oil-Weathering Code (Payne, et al., 1984a) which predicts the rate at which oil droplets are dispersed into the water column. This oil dispersion rate is used as a boundary condition in the form of an oil flux as a function of time. Since the oil-weathering code only predicts the flux and does not provide an equation form, the oil flux is actually used in mathematical form as a series of decaying exponentials. The one-dimensional models presented in Section 3 are based on a single exponential type boundary condition, and thus, to use a series of exponentials, the calculated results for each exponential are then added together.

In the development of the oil droplet dispersion model, the coordinate system used is one dimensional in the vertical. The model describes the concentration profile for the oil droplets and provides boundary conditions for flux of oil from the water surface and loss at the bottom. The model considers: 1) the mass of oil dispersed into the water column (per unit area), 2) the mass of free oil droplets in the profile (per unit area), 3) the mass of oil lost through oil/SPM interactions (per unit area), and 4) the oil mass lost at the bottom (sedimented and diffused out of the water column, per unit area).

The model which describes the SPM in the water column is based on an SPM source term at the lower boundary. This SPM source term is self-limiting with respect to the maximum SPM concentration that can be attained in the water column. Necessarily, this source term must be obtained from experience or

24

observations of sediment transport. Thus, the particles are fluxed from the bottom and may either attach to oil droplets or return to the bottom. Again, the coordinate system is one dimensional in the vertical, and the model defines concentration profiles throughout the water column with boundary conditions for flux of sediment from the bottom and no particle loss through the surface. Parameters considered in the model include particle settling velocity, turbulent diffusivity, a sediment flux source term from the bottom, and a first-order sediment deposition return rate to the bottom. The SPM model calculates: 1) the mass of SPM fluxed in from the bottom (per unit area), 2) the total mass of SPM in the water column (per unit area), and 3) the mass of SPM lost due to reaction with oil droplets (per unit area).

The model which describes the interaction of oil droplets and SPM is first order with respect to each species. The rate constant is a function of the turbulent energy dissipation rate and other multiplicative lumped parameters. These lumped parameters are particle shape, particle sizes and particle sticking coefficients. The reason lumped parameters are used is that the "exact" nature of the variables are not known, while the nature of an idealized spherical particle is known which is what the theory is based on. This interaction model can be applied to a well-mixed volume of water, such as a homogeneous reaction vessel, or applied to a nonhomogeneous volume where concentrations change as a function of position. Both of these applications are extremes of more classical mathematical descriptions of similar material balances in other fields of science and engineering.

Thus, the oil droplet and SPM model considers oil droplets being dispersed into the water column from the surface and sediment being fluxed into the water column from the bottom. The oil droplets and SPM collide and stick to form SPM agglomerates at specific rate constants that are entered by the user. As shown by the matrix in Table 1-1, experimentally determined rate constants for nine sediment or SPM types with a variety of fresh and weathered crude oils and distillate products, as well as salinities, are available (in Section 5) to the user for utilization in the model. Where the results of experimentation with these variables indicated a change in interaction rate constants, additional investigations were undertaken as described in Section 5.

Table 1-1

Experimental Variables Investigated for Oil Droplet/SPM Interactions and Sedimentation

| | OIL TYPE/SALINITY LEVEL: | | | | | | | | |
| | unweathered PB crude: | | | weathered PB crude: | | | unweathered fuel oil: | | |
PARTICLE TYPE:	SW	SW/FW (1:1)	FW	SW	SW/FW (1:1)	FW	SW	SW/FW (1:1)	FW
NATURAL PARTICULATES:									
Grewingk glacial till (<53 um)	●	●	O	●		O	●	O	O
Yukon Delta sediment (<53 um)	●	●	●	●	●	●	O	O	O
Turnagain Arm SPM	O		'	O			O		
Beaufort Sea sediment (<53 um)	O			O			O		
Beaufort Sea peat (<53 um)	O			O					
Peard Bay sediment (<53 um)	O			O					
Prudhoe Bay sediment (<53 um)	O			O					
Kotzebue sediment (<53 um)	O			O					
Jakolof Bay sediment (<53 um)	O						O		
CONTROL PARTICULATES:									
Aluminum oxide grit (10 um)	O								
DVB polyspheres (1-20 um)	O								

NOTES:

O = oil droplet/SPM interaction experiment

● = oil droplet/SPM interaction and sedimentation experiments

PB crude = Prudhoe Bay crude oil

SW = seawater

FW = freshwater

SW/FW (1:1) = 1:1 mix of seawater and freshwater

26

When the experimental results from the extremes of one variable type (e.g., fresh vs weathered oil or high Total Organic Carbon (TOC) vs low TOC loading on the SPM types) failed to show a change in rate constants (see below), additional experimental activities were discontinued. In addition, it was found using the extremes of SPM/sediment types with all three oils that there were no oil/SPM interactions in fresh water. Therefore, as shown by Table 1-1, it was not necessary to complete all possible experimental combinations for all oil and SPM types at all salinities in order to complete the matrix and provide the necessary data for model utilization.

The coordinate system in the model is again one dimensional in the vertical, and the model defines concentration profiles for free oil droplets, unoiled suspended particulate material, and oil/SPM agglomerates. For the oil droplets, parameters considered include the rise or fall velocity, turbulent diffusivity, flux of oil droplets from the surface, a decay constant for the flux of oil, and a rate constant for oil droplet removal due to interaction with suspended particulate material. The boundary conditions for the SPM in the water column include the flux of sediment from the bottom, and the parameters considered include particle settling velocity, turbulent diffusivity, the flux-source term from the bottom, a first-order sediment deposition rate, and finally, a user-specified rate constant for SPM removal due to interaction with free oil droplets.

In completing the mathematical solutions for the oil/SPM interaction model, it was not possible to obtain an analytical solution because of the SPM and oil droplet concentration cross terms. Therefore, solutions were obtained using a Crank-Nicolson finite-difference numerical-integration algorithm and an iteration at each time step on trial vectors.

In considering the oil/SPM agglomerate profile, the final boundary conditions state that when the oil/SPM agglomerate reaches the bottom, it is removed. The removal of oil/SPM agglomerates at the bottom is a mathematical specification of this boundary condition. Clearly, other specifications such as Lavaestu's (discussed below) could be used, but, in order to calculate how many oil-SPM agglomerates then return to the water column, a time-dependent

model coupled to a water-column model (with two coupled partial differential equations) would be required. This was ultimately determined to be too complicated, and it was decided to use the technical approach presented for reasons of simplicity and illustration.

Laevastu and Fukahara (1985) present mathematical models to calculate oil sedimentation (or deposition of oil) as a function of an instantaneous or continuous source with or without a thermocline present, and also a model to calculate the decay of oil on the bottom. The sedimentation models are essentially compartmental models in that these models are not based on transport through the water column due to dispersion (or turbulent diffusion). Compartment models are well mixed throughout. Therefore, this type of model is not the same technical approach used in the oil-SPM models where transport by dispersion is used. As a result, it is not possible to use the sedimentation information presented by Laevastu and Fukahara to derive a dispersion-based model.

Laevastu and Fukahara specifically postulate an accumulation of sedimented oil in the bottom nepheloid layer with subsequent decay. Decay signifies the oxidative degradation of aromatic compounds, as well as oil being buried into the sediment, and the "decay" formula is an exponential with various (negative) factors. Thus, more than one process is considered in this model, and all processes are essentially lumped into one.

The various oil-SPM models can be (re)derived with a bottom nepheloid layer, i.e., a compartment between the water column and the bottom. However, it is likely that analytical solutions could not be obtained with a reasonable expenditure of effort, and numerical methods would be required to solve them. Since the information concerning the nepheloid layer with respect to oil accumulation is somewhat sketchy, it did not (and does not) appear to be worthwhile carrying out the transport derivations and obtaining the subsequent solutions. While mathematically the effort will yield "correct" equations, the predictions with respect to physical reality (verification) would not be advanced.

Among other parameters considered in the oil/SPM model develolped in the current program, the agglomerate settling velocity can be entered by the user, and here again, a number of settling velocity experiments were completed with a variety of oil/SPM types (see Table 1-1). Therefore, experimental data presented in Section 5 may again be utilized as input to the oil/SPM interaction model. In addition, as discussed above, model parameters include turbulent diffusivity and a user-specified constant for the rate of oil/SPM agglomerate product formation.

For the oil/SPM agglomerates, material balance equations are presented for: 1) the mass of agglomerate in the water column (per unit area), 2) the mass of agglomerate produced by the oil droplets and sediment (per unit area), and 3) the mass of agglomerate lost at the bottom (per unit area per unit time).

In considering the collision frequency for dilute suspensions of particles in a well-mixed volume, model parameters include the energy dissipation per unit mass of fluid per unit time, the kinematic viscosity of the fluid, particle radii, and particle number densities. Simplifying assumptions and conversions of number densities to more commonly used concentrations (mg/L) allow the development of a working equation for predicting the loss of oil droplets due to collisions and adherence to SPM particles. This equation is derived in Section 3.0 and uses experimental measurements of interaction rate constants which can be entered by the user for predicting oil/SPM interactions with a variety of oil and SPM types.

The ultimate movement of oil droplets in the water column is either to the surface as buoyant droplets or to the bottom as oil-SPM agglomerates. Thus, the illustrative models presented in Sections 3 and 6 are designed to predict an oil-free water column at large times and provide a total material balance for the oil to predict the the mass of oil that is deposited in the bottom sediments.

In evaluating these models, it is important to recognize that they are one dimensional. Thus, in the example cases considered in Section 6, there are

no advective or diffusive oil-loss mechanisms, and calculated oil concentrations are much higher than those ever observed in the ocean. Nevertheless, the modeling approach is extremely useful in providing a "worst-case" upper-bound estimate of sediment-bound oil concentrations, and the calculations provide an estimate of the time required for things to happen in the water column. Also, the sensitivity of the input parameters can be investigated to learn what is or is not important with respect to a specific objective. For example, the oil deposition mechanisms are the boundary conditions at the bottom for the oil and the oil-SPM agglomerate, and the relative importance of these two processes can be investigated with respect to the parameters which will affect them (i.e., oil rise velocity, oil-SPM reaction rate and oil-SPM settling velocity).

It should also be noted that these calculations (codes) are not usable by interfacing them with other codes (i.e., with an ocean circulation code). The only part of the calculation which is usable is the oil-SPM reaction rate which is of the form: $\alpha_c CS$. This reaction rate is written on a per-unit-volume basis, and an (existing) ocean-circulation model in three dimensions then must integrate this expression for the loss of oil, loss of SPM, and production of oil-SPM agglomerates. Thus, the relatively simple reaction rate expression is quite difficult to use in an environmental situation, if for no other reason than the environmental situations of interest are three dimensional.

1.3   RESULTS OF OIL DROPLET/SPM INTERACTION RATE CONSTANT DETERMINATIONS, SEDIMENTATION STUDIES AND MOLECULAR SCALE ADSORPTION MEASUREMENTS (SECTIONS 4 AND 5)

1.3.1   Experimental Approach

The apparatus and experimental protocol used to obtain kinetic rate constants for interactions between dispersed oil droplets and SPM in the water column are similar to those described in Payne et al., 1987b. Details of the experimental protocols are described in Sections 4.2.1 through 4.2.7. To estimate rate constants for interactions between dispersed oil droplets and SPM

in an experiment, number densities of "free" oil droplets were determined over time during the experiment. Differences in the natural buoyancy of free oil droplets compared to oiled SPM agglomerates were used to separate the unreacted oil from oil-SPM agglomerates and unreacted SPM. Number densities of free oil droplets were then determined by photomicroscopy using specially prepared microscope slides for enumeration of free oil droplets. In addition to the photomicroscopy techniques, determinations of total SPM loads (in mg/L) and total dispersed oil quantities (in mg/L) in reaction solutions were also completed by more conventional gravimetric techniques and flame-ionization-detector gas chromatography, respectively.

Experiments were performed with a number of variables to evaluate possible effects of those variables on whole oil droplet SPM interaction rate constants. The major variables evaluated in the experiments were suspended particulate material type, oil type, salinity, and turbulence.

1.3.2   Sediment/SPM Characterization

In order to examine the effects on interaction rate constants arising from variations in SPM types, a total of eight sediment and one SPM types were collected and tested according to procedures discussed in Section 4. The eight sediment types and one SPM type analyzed were considered to be representative of a variety of coastal Alaskan waters. These sediments included materials collected from Turnagain Arm (SPM), Kachemak Bay (Grewingk glacial till), Jakolof Bay, Prudhoe Bay, Kotzebue Sound, Peard Bay, Beaufort Sea sediments, Beaufort Sea peat, and Yukon River Delta sediments. Both surface scrapings of the uppermost 1-4 mm of subtidal fine-grained materials and SPM collected directly by filtration from the water column were considered. The purpose of collecting true suspended particulate material from the water column by filtration was to allow comparison with other sedimentary samples collected from subtidal sources in the other regions considered. The detailed characterization of all sediment and SPM types, as well as measured oil/SPM interaction rate constants with the different SPM types, illustrated that the collection method did not significantly affect results in the oil/SPM

31

interaction studies. Each of the sediment/SPM types listed above were characterized for the following chemical and physical properties: total organic carbon, grain size, hydrocarbon content, mineralogy, solids density, and particle number density. These parameters were then used to evaluate similarities and differences among the SPM types and to help explain experimental differences in oil/SPM interaction rate constants.

In addition to the natural sediment and SPM samples described above, two commercially available particulate phases were used in oil/SPM interaction rate constant studies for control purposes. The commercially available particulate phases consisted of aluminum oxide grit (approximately 10-μm diameter) and polystyrene divinylbenzene spheres (1 to 20-μm diameter). These materials were utilized as "standard materials" which could be available for use as controls in future studies should other investigators wish to replicate the studies presented in this report.

1.3.3   Oil/SPM Rate Determinations

While all sediment particles were < 53 μm in diameter, great ranges in particle sizes were observed both among and within particular sediment types. The greatest number densities for particles < 10 μm in diameter occurred in Grewingk glacial till, although high number densities in this size class were also present in the Beaufort Sea and Peard Bay sediment samples. While particles < 10 μm were present in all of the sediment types, larger particles approaching 50 μm in diameter were common in Yukon Delta sediment, Jakolof Bay sediment, Kotzebue sediment, Prudhoe Bay sediment, and Turnagain Arm SPM.

Utilization of data for number densities and gravimetric loads (mg/L) allowed for number densities of particles per unit mass to be determined for each sediment type. These data are presented in Section 5.1 and allow relationships between particle number density and sediment mass for each sediment and SPM type to be obtained. Not surprisingly, Grewingk glacial till showed the highest number density of particles per unit dry weight, while Yukon Delta sediment exhibited the lowest.

Results of TOC analyses show relatively little variation in the one SPM and eight sediment types. The values range from a low of 2 mg/g dry weight for Grewingk glacial till to a high of 14.2 mg/g dry weight for Prudhoe Bay sediment. These levels are in agreement with a recently published statistical review of surface sediment contaminant levels (Bronson, 1988) for 48 sediment samples collected from the Northern Bering Sea.

Much greater variations between sediment and SPM types were observed for background hydrocarbon contents. Levels of background hydrocarbons ranged from extremely low concentrations for Yukon Delta sediment (> 0.05 μg/g) to high concentrations for Jakolof Bay sediment (862 μg/g). Most of the chromatographic profiles show a predominance of odd carbon n-alkanes that are either skewed towards heavier molecular-weight compounds (i.e., Prudhoe Bay, Beaufort Sea, and Kotzebue sediment samples) or are more evenly distributed throughout the intermediate molecular-weight range (Beaufort Sea peat, Jakolof Bay, and Peard Bay sediments and Turnagain Arm SPM).

The results of mineralogical analysis demonstrated that alpha-quartz was the major constituent in all of the sediment and SPM types. Feldspar accounted for intermediate amounts in five of the eight samples and minor amounts in the remaining three. The following minerals were also found: kaolinite in Beaufort Sea sediment, calcite in Prudhoe Bay sediment, chlorite in Kotzebue sediment, and sanadine/microcline in Yukon Delta sediment.

From the sediment characterization data, it appeared that the eight sediment and one SPM type selected for oil/SPM interaction studies were sufficiently varied while still being representative of coastal Alaskan sedimentary or SPM types. Because of the time-consuming nature and logistical problems associated with collection of large volumes of natural SPM, most of the oil droplet SPM interaction experiments were conducted with sieved, natural sediment types. However, in order to evaluate the possibility of an introduced bias resulting from the use of sieved sediments as opposed to the true natural SPM, the true SPM collected from Turnagain Arm was used in certain experiments. As noted above, the results of the physical and chemical property determinations indicated that no inherent disparities in properties occurred between Turnagain

Arm SPM and the other sediment types. Consequently, comparisons of experimental results for oil/SPM interactions using the sieved natural sediments versus those for the one true SPM appear to be appropriate and valid.

The major objective of the laboratory experimental efforts was to evaluate interaction kinetics between whole oil droplets and suspended sedimentary materials, such that the lumped reaction coefficient α_c (the rate constant for removal of "free" oil droplets due to reaction with SPM particles) could be determined. Effects of differences among a number of pertinent environmental variables (sediment or SPM type, quantity and type of oil, salinity and turbulence level) upon values of α_c were investigated.

The rate constant for oil/SPM interactions k can be described by the equation:

$$k = \alpha \ (\epsilon/\nu)^{1/2} S$$

where S is the excess SPM concentration in the experimental reaction solution. ϵ is the energy dissipated per unit mass of water per unit time. ν is the kinematic viscosity of the aqueous medium and α is the "lumped" reaction coefficient taking into account not only geometric factors such as heterogeneous size distributions of the oil droplets and SPM but also the "sticking" factor between oil droplets and SPM. Excess SPM refers to the situation where oil droplets and SPM are reacting and the depletion of SPM is so small that its loss can be neglected. This can be illustrated where the SPM "count" is 100 (or 10) times that of the oil droplets. When the reaction proceeds to completion the SPM count will still be essentially 100 (really 99). Since the reaction rate is proportional to concentrations, the SPM is in excess and the SPM concentration appears constant.

Determinations of values for the "lumped" reaction coefficient α were the primary purpose of the laboratory experiments summarized in this report. Section 5.2.2 presents experimental data derived for both the reaction constant k and the "lumped" reaction coefficient (α) for all experiments conducted in the program. The data indicate that large differences in values for k do not

appear to be in evidence either among or within the various SPM types. In light of the fact that total oil loadings in experiments varied by more than a factor of 10, the relatively small variations in values for k indicate that the total number of oil droplets reacting with SPM in a particular experiment was proportional to the amount of oil present. While these data might lead one to conclude that no substantial differences exist among the oil droplet SPM interactions for the various sediment and SPM types, it is important to note that the interaction term in the algorithms for the model codes is the "lumped" reaction coefficient α. When values for α are considered, distinction between the various SPM types become apparent with overall values differing by a factor of almost 40 (i.e., -0.0075 cm^3/g to -0.29 cm^3/g).

In an attempt to explain these differences, mean values for the reaction coefficients α for various SPM types were compared with other physical and chemical properties of the SPM including: density per unit mass, the fraction of the total sediment occurring in the 0-2 μm particle size range, total organic carbon, specific density, and total resolved hydrocarbon content. Results of the statistical analyses indicated that of the five independent variables, particle number density per unit mass showed the highest correlation (r = 0.902) with the values for the reaction coefficient α. A slightly lower degree of correlation (r = 0.798) existed with the values for sediment fractions comprising the 0-2 μm particle-size range. The remaining three variables (TOC, specific density, and total resolved hydrocarbon content) showed no significant correlations with the reaction coefficient α (r = 0.355, 0.032, and 0.321, respectively).

Because the SPM types considered come from a variety of locations in Alaska, it seems plausible to suggest that the reaction coefficients (α) for SPM from other locations might be extrapolated if appropriate information pertaining to particle number densities for specific SPM types can be obtained as described in Section 5.2.2.1 of this report. This latter information can be derived by either detailed light microscopy or possibly by comparing limited light microscopic observations with detailed particle-size analyses by the pipette method.

Four types of oil were used in the experiments: 1) unweathered Prudhoe Bay crude oil; 2) 12-day weathered Prudhoe Bay crude oil from wave tank studies (see Payne et al., 1984a); 3) unweathered No. 1 fuel oil; and 4) naturally weathered North Slope crude oil spilled from the R/T GLACIER BAY grounding in Cook Inlet in 1987. In addition to the different types of oil, varying quantities of a given oil type were also used in experiments (i.e., to change the oil/SPM ratio). Oil concentrations in experimental solutions ranged from low to medium to high levels. For fresh Prudhoe Bay crude oil, these low, medium, and high levels yielded concentrations of 4-8, 8-44, and 80-105 mg/L, respectively. For 12-day weathered Prudhoe Bay crude oil, the low, medium, and high levels yielded concentrations of 14-26, 43-112, and 240-310 mg/L, respectively. Interactions between dispersed oil droplets and SPM were investigated for four oil types, and within the scatter inherent to the data there did not appear to be substantial differences between the values for k of the four oil types considered, implying that oil droplet SPM interactions were essentially independent of the type of oil present.

Experiments were performed at three general salinity levels: 1) full-strength seawater; 2) 1:1 mixtures of seawater and freshwater; and 3) freshwater. Results indicated that salinity had a strong controlling influence on reaction rates for dispersed oil droplets and the sediment types considered. Specifically, very low rates of reaction (i.e., k values approaching 0) were observed for SPM types in freshwater, while substantially higher rates were observed in both half-strength and full-strength seawater. Comparable effects of salinity on associations of dispersed oils and fatty acids with SPM or mineral phases have been shown by other investigators (e.g., Bassin and Ichiye, 1977; Meyers and Quinn, 1973); however, these earlier investigations were done by equilibrium studies and did not investigate the rate of oil/SPM interactions.

A limited number of experiments were performed at varying energy dissipation rates or turbulence levels. The energy dissipation rate ϵ for all of the experiments was estimated from the volume of the reaction vessel, the value for the kinematic viscosity of the aqueous medium, and measurements of the torque and propeller shaft rpms used in the experimental medium during

experiments. For the oil droplet/SPM interaction model and experimental approach to be valid, the natural logarithm of the oil droplet number data must decline as a straight line over time and the rate constant k describing the interaction must vary as the square root of the energy dissipation rate ϵ. Experiments were performed to evaluate this relationship, and the data in Section 5.2.2.4 indicate that the expected relationship between the experimentally derived values for k and ϵ was satisfied for the different turbulence levels examined. Consequently, the experimental values confirmed the expected theoretical relationships between turbulence and oil/SPM interaction rate constants, although the data available for this comparison were limited.

In addition to the oil/SPM interaction rate determinations, solutions of source materials from each oil/SPM interaction experiment were used for SPM settling velocity (or sedimentation) experiments. By utilizing oiled SPM from the oil/SPM interaction rate studies, relatively well-defined prehistories were available for the oiled SPM particles (for example, types of SPM, types and quantities of oil, salinity, and turbulence levels). In addition, time-course changes in the number densities and sizes of the SPM and oil/SPM agglomerates were available for the SPM phases used in the sedimentation experiments. Variables evaluated for potential effects on SPM settling velocities included suspended particulate material type, oil type and amount, and salinity. Experiments were performed with two types of SPM -- Grewingk glacial till and Yukon River Delta sediment. These two sediment types encompass the extreme ranges for not only particle sizes but also oil droplet/SPM reaction coefficients observed for all particulate types used in the experimental programs. Oiled SPM for settling chamber experiments were derived from parent stirred reaction vessel studies that used either unweathered Prudhoe Bay crude oil, 12-day weathered Prudhoe Bay crude oil, or unweathered No. 1 fuel oil. In addition, varying amounts of blended oil were used in parent stirred reaction vessel experiments, such that SPM for the settling chamber studies used SPM with varying degrees of prior oiling. Settling chamber experiments were also performed at three salinities: full-strength seawater, half-strength seawater, and freshwater.

Section 5.3 presents the values for SPM settling velocities. Significant differences in mean settling velocities between the two experimental SPM types were observed. Grewingk glacial till was comprised almost exclusively of particles < 10 μm in diameter, and < 25 % of the total SPM load by weight had settled below the specified sampling depth in the settling chamber after 1 hr. In contrast, > 90 % of the Yukon Delta sediment had settled below the sampling depth after 1 hr due to sedimentation of larger particles (i.e., approaching 50 μm in diameter).

Because the quantity of oil that became associated with SPM in the stirred reaction vesel experiments was directly related to the amount of oil in the reaction vessel, SPM with differing amounts of agglomerated oil were produced and subsequently used in various settling chamber experiments. Data presented in Section 5.3.2.2 clearly illustrate that increasing quantities of oil in parent stirred reaction vessel experiments ultimately produced higher settling velocities for SPM particles in follow-on settling chamber studies.

Full-strength and half-strength seawater produced certain degrees of flocculation in the smaller size classes of SPM, leading to greater sedimentation of "flocculated" SPM in solutions with these elevated salinities.

In addition to investigating whole-oil droplet/SPM interactions, SPM/molecular scale interactions also were investigated through the development of Freundlich isotherms for individual dissolved aromatic hydrocarbon components and mixtures of the more water-soluble hydrocarbon components contained in distillation cuts of Prudhoe Bay crude oil. The distillation cut approach was utilized to provide data which would be useful for dissolution and adsorption considerations for individual components contained in individual distillation cuts of Prudhoe Bay crude oil and refined petroleum products. As discussed in Section 1.1, the distillation cut approach is used for characterization of all oil types used in the NOAA oil weathering computer model codes, and NOAA and MMS personnel have expressed an interest in characterizing the dissolution/adsorption behavior of "distillate cuts" (or more accurately components within each cut) to couple dissolution behavior/evaporation losses calculated by the model for each disillate cut fraction.

38

Because of the sheer number of compounds comprising crude oil and refined distillate products, the models developed by SAIC to date have taken a "pseudocompound" approach. This approach adopts distillate cuts as manageable subsets of whole crude oil. The finite number of water-soluble compounds contained in a given cut can easily be handled in an isotherm experiment and yet still provide data that reflects the crude oil source. Therefore, iso-therms were developed for the soluble compounds contained in four distillate cuts of Prudhoe Bay crude oil using Grewingk glacial till and one cut using Turnagain Arm SPM and Yukon Delta sediment.

The Freundlich isotherm determinations were used to determine upward boundary conditions of molecular sorption values for each of the compounds and mixtures considered. In addition, the experimental procedure provided for de-termination of partition coefficients, K_p (concentration on SPM/concentration in solution, at equilibrium). In examining the results of molecular scale interactions with SPM, Section 5.4 presents the maximum adsorption capacity for a variety of individual molecular species and SPM types. These adsorption capacities are determined for toluene, ethylbenzene, m,p-xylene, o-xylene, ethylmethylbenzene, C_3-benzene, and several distillate cuts of Prudhoe Bay crude oil. A range of adsorption capacities were observed for Turnagain Arm SPM, Grewingk glacial till, and Yukon Delta sediment, with markedly different isotherm plots being obtained for the different SPM types. Differences were attributed to particle-size differences and the SPM organic carbon content. The values reported represent the maximum capacities that the SPM could adsorb under experimentally ideal (environmentally worst-case) conditions. Capacities in the marine environment are bound to be substantially lower than those reported because of the exceedingly high dissolved phase concentrations required for the experiments. Furthermore, from an overall mass balance perspective, it should be noted that molecular adsorption of dissolved components from seawater is not a significant mechanism for the removal and deposition of lower molecular weight aromatic components to benthic sediments. From these results, it is clear that SPM/dissolved or molecular-scale inter-actions account for only a minuscule fraction of the mass of oil potentially

39

removed from a surface slick when compared to dispersed whole-oil droplet/SPM interactions.

Calculated partition coefficient values (K_p) are presented along with coefficients of variation arising from replicate measurements for a wide variety of lower molecular weight aromatic components and three SPM types. A general trend of increasing K_p values with increasing molecular weight was observed. By combining these measured K_p values with estimated water column concentrations and measured concentrations for dissolved phase oil components in real spill events, predicted concentrations of adsorbed components on SPM (assuming a very high 200 mg/L SPM load) were presented. Using this approach, more realistic dissolved molecular-scale adsorption levels are presented in Section 5.4. Predicted levels of molecular-scale/SPM adsorption range from 70 ppb to 3900 ppb for the variety of individual compounds and SPM components examined. As would be expected, these predicted molecular adsorption levels are well below the maximum adsorption capacities determined through isotherm development. Further, it should be noted that desorption will occur as an SPM particle is exposed to clean water, unless the adsorption mechanisms involve an unlikely chemical reaction. Additional data are presented to correlate molecular scale adsorption levels with SPM-dependent parameters including TOC, mineralogy, hydrocarbon content, number density, solids density, and grain-size distributions. The octanol water-partition coefficient (K_{ow}) and partition coefficient (K_p) are also examined, and it was observed that all K_p values increased with increasing K_{ow} and molecular weight and with decreasing solubility. SPM adsoption capacity appeared to be strongly affected by initial dissolved component concentrations, and suspended particle number densities and available surface area appear to effect adsorption of individual components onto SPM.

1.4   RESULTS OF SEA/ICE DYNAMICS EXPERIMENTS TO EXAMINE OIL/ICE INTERACTIONS (SECTION 8)

Sections 8.1 through 8.6 present the results from a number of studies undertaken to provide additional information and data on the processes responsible for incorporation of seabed sediments and suspended particulate material

into nearshore sea ice layers. The primary thrust of these studies was on understanding the sediment/SPM entrainment processes responsible for generating a seasonal ice canopy with widely varying, but significant (up to 1600 mg/L) sediment burdens. These studies were undertaken to ultimately allow predictive modeling of oil weathering and sedimentation for oil interacting with sea ice containing heavy sediment loads.

Initially, wave tank experiments were conducted to investigate sediment/SPM scouring and resuspension by actively growing frazil and slush ice interacting directly with the bottom (Section 8.3). Results of the wave tank studies illustrated that it was possible to generate slush ice samples containing elevated levels of suspended particulate material with fine-grained sediments; however, it was also apparent that, in general, the concentration of SPM in the slush ice field was less than the background suspended particulate material load in the water column (e.g., see Table 8-3). Furthermore, the data demonstrated that there was a significant reduction in the sediment load in the slush ice with time, due to the turbulence regime introduced by passing wave trains.

Because of the somewhat ambiguous results obtained with the wave tank experiments, racetrack flume experiments were undertaken to observe interactions of frazil and anchor ice with fine-grained sediment, both in suspension and as bed material in fresh and saltwater systems. The results from these studies clearly demonstrated that SPM concentrations in surface frazil and slush ice were significantly higher (up to 3300 mg/L) than water column SPM loads (700 mg/L) immediately after the supercooling event leading to frazil ice formation. As in the wave tank experiments, however, frazil ice concentrations subsequently decreased until, after several hours, they were lower than the corresponding water column samples (e.g., see Table 8-4). Nevertheless, careful control of the sampling times such that water and frazil ice samples were obtained during the critical phase when seawater frazil may be sticky (i.e., during the transition from the temperature minimum T_m to the equilibrium temperature T_e) allowed for the generation of data which strongly suggested that frazil crystals adhere to suspended particulate materials when there is significant supercooling and active ice growth. These crystals may then lose

their adhesive properties when the temperature rises to the equilibrium temperature following the supercooled state. Interestingly, in these studies, the presence of petroleum contaminants did not appear to affect the incorporation of sediment into a saltwater frazil ice cover. Thus, racetrack flume experiments demonstrated that oil contaminated sediment may be incorporated into the ice cover during storms occurring in the fall, and this may be a potential source for pollutant transport and dispersal.

The results of the wave tank and racetrack flume experiments described in Section 8.3 showed that sediment-laden ice could be generated under experimental conditions but that subsequent cleansing of the ice would occur due to natural turbulence under certain conditions. Therefore, a large number of self-cleaning mechanisms for surface ice canopies were examined, as described in Section 8.4. Studies to look at selective size fractionation of SPM retained in slush ice experiencing wave turbulence clearly showed preferential retention of finer-grained materials in the ice canopy. Specifically, after 10 minutes of wave turbulence, the SPM retained in the ice consisted of 11% mud (9% silt and 2% clay) and 88% sand; whereas, material collected raining out of the ice surface was 98.6% sand with only 1.4% mud (1.1% silt and 0.3% clay).

As noted above, self-cleaning of slush ice and frazil ice in the racetrack flume was also noted with time. Based on simultaneous measurements of SPM loads in the water column and surface ice layer, it was determined that the drop in SPM load in the slush ice was due to a change in its adhesive properties with time, in addition to the simple act of physically knocking SPM out of the ice layer due to current- and wave-induced turbulence.

An additional mechanism of self-cleaning of sediments in sea ice canopies was discovered, which dealt with the movement of fine-grained sediment particles in seawater and freshwater slush ice slurries during freeze-front advances. Photographic and gravimetric analyses of the final distributions of sediments in several experiments clearly demonstrated that movement of sediment particles within an ice canopy can occur during the freezing process. Laboratory and larger-scale studies demonstrated that sediment particles could be moved horizontally as well as vertically under the influence of advancing

freeze fronts in aqueous slush ice slurries and that this movement could be due to forces other than gravity alone. Not surprisingly, smaller particles had a greater tendency to "migrate."

From the results presented in Sections 8.3 and 8.4, it became clear that the formation of dirty, sediment-laden ice was dependent on the unique, stochastic sequential development of a storm event and subsequent freezeup. Therefore, several new hypotheses were developed to explain observed sediment loads in natural ice canopies. These are described in detail in Section 8.5, which presents the results of experiments designed to validate the hypothesis that SPM-laden slush ice will retain its sediment load only if the weather lies down quickly after a storm event and that the natural wave-dampening effect of the slush ice prevents further rainout of the sediment from the ice canopy as it freezes. Specifically, it was proposed that if a storm occurs during fall freezeup and the water is supercooled to the point that frazil ice maintains itself in an "active" state for a sustained period, then significant adhesion of SPM might occur. However, even if the frazil is not maintained in a sticky state, the platelets could also be capable of passively scavenging (filtering) high loads of suspended particulate material from the water column as they work their way to the surface after the storm subsides. As this SPM-laden frazil ice reaches the surface, it can then either undergo self-cleaning, as observed in the wave tank and racetrack flume experiments described in Sections 8.3 and 8.4 or freeze in place, entrapping its sediment load if the weather lies down quickly, in such a way that residual wave turbulence subsides to the point that additional self-cleaning of the ice by turbulent mechanisms is not a factor. In this manner, high concentrations of suspended particulate material in a seasonal canopy would result as observed in the field.

To test this hypothesis, experiments were undertaken in the wave tank to demonstrate first that a heavy SPM load could be established by physical entrapment from underlying SPM-laden waters and be maintained in the ice canopy under experimental conditions when turbulence was eliminated. Specifically, relatively clean (140 mg/L) slush ice was physically mixed into SPM-laden seawater (276 mg/L) within a 20-cm diameter cylinder vertically inserted through the surface slush ice all the way to the bottom of the tank. This

43

slush ice was then allowed to resurface in the absence of any additional turbulence, and the SPM loads in the ice canopy within the cylinder were measured at nearly 1080 mg/L compared to the control area, which was not subjected to physical entrainment, at 140 mg/L. With subsequent freezing, the ice loading within the slush ice control area outside of the cylinder and within the stirred cylinder itself decreased; however, an elevated level of 591 mg/L of SPM was maintained within the ice canopy that had been rapidly mixed into underlying SPM-rich water and then allowed to freeze in the absence of further turbulence. Thus, the results of the cylinder experiment demonstrated that high levels of SPM could be generated in the wave tank system; however, even in this instance there was some evidence of self-cleaning, which may have been due to the advancing freeze front mechanism described in Section 8.4.5.

Experiments undertaken to evaluate the potential for horizontal and vertical filtration of SPM by frazil and slush ice from the water column were also conducted in the Kasitsna Bay wave tank, and results from those studies are presented in Section 8.5.3. Significant concentration and entrapment of suspended particulate material were routinely observed as SPM-laden water was allowed to filter through the slush ice, and in each case, significantly elevated SPM loads were obtained in the slush ice compared to the feed water and drain water (i.e., the filtered seawater after passing through the slush ice layer). As described in Section 8.5.3, there appeared to be little variation in filtration efficiency when either unoiled or previously oiled SPM materials were used.

Section 8.5.4 discusses the results of a number of experiments designed to examine the scavenging of suspended particulate material by rising frazil ice platelets contained in a 91-cm x 7.6-cm column of seawater containing a known and measured concentration of SPM. In these experiments, a limited amount of clean frazil ice was introduced into the experimental column, and the column was then subjected to a series of end-for-end inversions. After each inversion, the column was held in a stationary vertical position in such a way that the frazil ice platelets, which rose due to their natural buoyancy, were exposed to suspended particulate material during their ascent. By repeating the end-for-end inversion a number of times, it was possible to

44

simulate frazil ice rising through a 20-m water column. At the conclusion of the experiment, the system was allowed to stand in place in the cold room at Kasitsna Bay until all the frazil/slush ice congealed at the surface. The water then was drained, and both the slush ice and drain water were analyzed for SPM loads. The data from these experiments (Table 8-9) clearly suggested that the simple rising of loose frazil platelets through the water column was sufficient to scavenge SPM, overcome the negative buoyancy of the SPM particles, and result in an elevated SPM load in the upper ice canopy. Concentration factors of up to twofold were observed for slush ice compared to drain water; however, it was believed that the lack of more enhanced removal of SPM from the water column during the inversion experiments was due to the fact that the frazil platelets were not in an active or sticky stage of growth because it was impossible to maintain the water in the inversion column experiments at a supercooled state.

Because of the problem with supercooling in the inversion experiments, additional experiments were undertaken within the cold room where frazil ice crystals were allowed to form in situ at the base of a vertical experimental column and then rise through SPM-laden water by their own buoyancy as they grew in the supercooled fluid. The results of those experiments are presented in Section 8.5.5, and in this instance, a total of 20 different experiments were undertaken with low (Table 8-10), medium (Table 8-11), and high (Table 8-12) SPM loads, both with and without previous oiling. All of the experiments were completed in replicate in order to provide a statistically valid data base on frazil ice scavenging phenomena. The data from this series of experiments clearly showed that rising and growing active frazil ice platelets can significantly remove suspended particulate material from the water column, and it appeared that this process was slightly more efficient with unoiled than with previously oiled SPM.

In the execution of this series of experiments, the collection of subsamples of slush ice, interstitial water, and pre- and postfreeze water column samples allowed overall mass balance estimates to be completed. Through these studies, it was clear from the mass balance data that both active scavenging of SPM onto rising and possibly sticky frazil ice and passive entrain-

45

ment of SPM-laden water into interstitial spaces are important mechanisms for entraining high loads of SPM in surface ice canopies.

With the successful completion of the vertical column study using a dry ice/methanol foot bath to initiate and catalyze frazil ice formation at the base of the column, additional experiments were undertaken using a thermally jacketed column. The purpose of these latter studies was to control and obtain data on the heat-transfer process during the frazil ice formation and SPM scavenging event. Such data are essential for any attempt at eventually modeling the interactions of oil, ice, and suspended particulate material.

The results from the jacketed column experiments are presented in Section 8.6. From the initial studies, it was clear that most of the independent variables (SPM size distribution and concentration, total oil concentration, oil type and degree of weathering, level of turbulence, degree of supercooling, and heat-transfer rate to the environment) could be controlled, or at least measured and compared to ice formation rates and crystal size. Thus, at the conclusion of the initial scoping experiments in February 1987, it was apparent that although some aspects of the system operation still needed refinement, the jacketed column system was itself essentially ready for additional studies.

As described in the Foreword, the scope of work for the program was changed before additional modeling activities and experiments with this system could be completed. Nevertheless, the system is still in existence at the NOAA Laboratory at Kasitsna Bay, and with minor additional effort, it could be utilized, should additional frazil ice/SPM interaction studies be desired in the future as part of some other study. It clearly showed great promise and coupled with the results from the other vertical column experiments presented in Section 8.5 is believed to be the obvious direction for continued studies required for any approach at modeling oil/ice/SPM interactions.

2.0   OIL/SPM INTERACTIONS INTRODUCTION

Since 1979 Science Applications International Corporation (SAIC) has been involved in the development of computer models designed to simulate the behavior of crude oil and refined petroleum products as they weather in the marine environment. The original model addressed the open-ocean oil-weathering processes of evaporation, dissolution, emulsification, and spreading as functions of wind speed, air temperature, sea state, and starting oil composition (Payne et al., 1984a). As the logical progression in subroutine development, SAIC derived the algorithms and code needed to evaluate (and predict) the physical and chemical changes occurring as oil weathers in the presence of first and multiyear sea ice (Payne et al., 1987a). Further investigations into the modeling of oil-weathering behavior have addressed the nature of oil interactions with suspended particulate material (SPM) and are the topic of this and previous (Payne et al., 1987b.) reports. As with the sea ice study, the oil/SPM interaction investigation has resulted in the development of a subroutine compatible with the original open ocean weathering computer model.

Interactions between spilled oil and SPM are important because they represent a major potential pathway for the deposition of hydrocarbons in coastal environments. These interactions can occur through two primary and generally simultaneous mechanisms: 1) discreet oil droplets "sticking" to suspended particulate material, and 2) adsorption by SPM of individual dissolved molecules.

Molecular scale interactions are negligible considering the overall mass balance of an oil slick; however, under certain conditions they may create adverse environmental conditions for biota (Payne et al., 1987b). On the other hand, oil droplet (or macroscale) interactions with SPM are known to have affected vast percentages of the mass of oil present in certain spills. The 1969 Santa Barbara Channel blowout (Kolpack, 1971 and Wolfe, 1987) and the IXTOC-1 well blowout (Boehm and Fiest, 1980 and Payne et al. 1980) are both instances where dispersed oil droplet interactions with SPM have resulted in the transport of significant quantities of surface oil to benthic sediments. Following the TSESIS oil spill in the Baltic Sea, approximately 10-15% of the

300 tons of spilled oil were transported by sedimentation of SPM-adsorbed oil. The high oil flux in this instance was due to the large SPM concentrations resulting from turbulent resuspension of bottom sediments (Johansson et.al., 1980). Furthermore, spills in areas of elevated SPM concentrations, particularly in nearshore waters, can exhibit rapid dispersal and oil removal due to interactions with frontal zone SPM (Forrester, 1971; Kolpack, 1971).

The rates of both types of interactions (molecular and marcoscale) may be dependent on a number of factors including oil composition (and degree of weathering), physical and chemical properties of the SPM, salinity, temperature, and turbulence. The variable of SPM concentration also appears to contribute significantly to the vertical transport of oil. At low (< 10 ppm) SPM levels, little transport of oiled particles is expected. Under moderate (10 to 100 ppm) levels, significant sorption can occur provided that there is adequate mixing of oil and particulates. Finally, massive sinking of oil may be possible under conditions of higher (> 100 ppm) SPM concentrations (Boehm, 1987).

Many investigators (Gearing et.al., 1979 and 1980; Zurcher and Thuer, 1978; Winters, 1978; de Lappe et.al., 1979; Boehm and Fiest, 1980; Meyers and Quinn, 1973; and Payne et al., 1984a) have reported on the selective partitioning between lower and higher molecular-weight aromatic compounds during the dissolution and molecular-scale adsorption process. Many of the results have pointed to the role of the SPM clay fraction and organic carbon loadings on SPM, as well as the chemical properties, especially solubility and the octanol-water partition coefficient, of the dissolved species in trying to explain the adsorption mechanism. Often contradictory results confound the ability to predict reliably the potential for or effects of molecular-scale sorption onto particulates. Meanwhile a complete understanding of the nature of macroscale droplet interactions has remained somewhat elusive because of the relatively random character of the dispersion process coupled with methods incapable of determining the sought-after rate constants (see for example, Payne et al., 1987b).

Therefore, during the first phase of this oil/SPM interaction study, a great deal of effort was devoted to the development of an analytical technique suitable for the measurement of oil droplet/SPM interaction rate constants (see for example, Payne et al., 1987b). Once this technique had been evaluated in terms of reliability, reproducibility, and practicality and compared against other candidate methods, it was utilized to obtain oil/SPM interaction rate constants on a wide variety of oil and SPM types. In particular, the last phase of this study (which is the subject of Sections 3 through 7 of this report) has focused on examining the effect on rate constants resulting from variations in SPM type, oil type and degree of weathering, salinity, oil level, and turbulence. Furthermore, rate constant variations attributable to SPM type were subdivided and evaluated according to total organic carbon concentration, hydrocarbon content, mineralogy, grain size, solids density, and number density.

Based on these experiments, the most profound effect on rate constants results from variations in salinity and to a lesser degree on SPM number density. Algorithms that incorporate the rate constant and effects of the most pronounced variables have been coded as "add on" subroutines to the existing open-ocean oil-weathering model. This also has the advantage of allowing the user to select the degree of weathering, as well as the type of oil (or distillate product) before the initiation of modeled SPM interactions. In addition, the effect of oil on sedimentation rates has been investigated concurrently with the rate constant determinations, and aspects of dissolved-compound adsorption were experimentally determined through the development of a number of adsorption isotherms and partition coefficients. Details of these and other experiments are presented in the following sections of this report.

3.0 MODEL DERIVATION

The purpose of the experimental and modeling work discussed here is to develop a scoping technique to evaluate the effect of oil-suspended-particulate-material (SPM) interactions as a removal process for oil dispersed in the water column. Particulate scavenging of oil droplets will impact the fate of an oil slick from both a disappearance-over-time aspect and from the standpoint of the ultimate fate of the oil (bottom deposition, bioimpacts, etc.). The following sections present a discussion of the scoping models that have been developed. Section 3.1 presents an overview of the mathematical derivations of the computer models and the parameters used in these models. Section 3.2 presents discussions of considerations pertinent to the mathematical derivation and experimental validation of the whole oil droplet/SPM interaction rate constants.

3.1 MATHEMATICAL MODELS

3.1.1 Oil Droplet Model (with Excess SPM)

Consider oil droplets being dispersed into a water column uniformly loaded with suspended particulate material (in excess). These drops collide with and stick to the SPM at a rate of α_c. The coordinate system used is one dimension (in x) with x = 0 at the surface and increasing x values in the downward direction (down is in the plus direction) with a total depth of l. The concentration profile, C (in the vertical dimension only) for the oil droplets is described by

$$\frac{\partial C}{\partial t} + v_x \frac{\partial C}{\partial x} = \frac{\partial}{\partial x}(k \frac{\partial C}{\partial x}) - \alpha_c C \qquad (1)$$

with boundary conditions

$$v_x C - k \frac{dC}{dx} = N_0 e^{-\gamma t} \text{ at } x = 0 \qquad (2)$$

and

$$C = 0 \quad \text{at} \quad x = l \, . \tag{3}$$

The parameters are given by

v_x = (rise or fall) velocity in the + x direction (down)

k = turbulent diffusivity (assumed dispersion constant)

N_o = flux of oil at the surface at t = 0

g = decay constant for the flux of oil.

The second boundary condition, describing the loss mechanism at the bottom, states that when oil reaches the bottom it is removed (from the water column). The equation (1) above describes only the free oil droplets.

Using Laplace Transformations, the subsidiary equations are (Carslaw & Jaeger, 1959)

$$\frac{d^2\bar{C}}{dx^2} - \frac{v_x}{k} \frac{d\bar{C}}{dx} - \frac{p + \alpha_c}{k} \bar{C} = 0 \tag{4}$$

$$v_x\bar{C} - k \frac{d\bar{C}}{dx} = \frac{N_0}{p + \gamma} \quad \text{at} \quad x = 0 \tag{5}$$

$$\bar{C}(l) = 0. \tag{6}$$

Solving this equation with the boundary conditions yields

$$\bar{C} = \frac{N_0 e^{ax} \sinh \xi (l - x)}{(p + \gamma)\left[(-\frac{v_x}{2}) \sinh \xi l + k\xi \cosh \xi l\right]} \tag{7}$$

where

$$\xi = \left[\left(\frac{v_x}{2k}\right)^2 + \frac{p + \alpha_c}{k}\right]^{1/2} \tag{8}$$

51

In the following equations define

$$a = \frac{v_x}{2k} \tag{9}$$

Next, inverting the Laplace transform yields the vertical concentration profile

$$C(x,t) = \left[\frac{N_0 e^{ax} e^{-\gamma t} \sinh \bar{\xi} (l - x)}{\frac{v_x}{2} \sinh \bar{\xi} l + k \bar{\xi} \cosh \bar{\xi} l} \right]$$

$$- \frac{4N_0 k e^{ax}}{l} \sum_i \frac{\beta_i \sin \beta_i (1 - x/l) e^{-[\alpha + k(a^2 + \beta_i^2/l^2)]t}}{[\gamma - \alpha_c - k(a^2 + \beta_i^2/l^2)][(2k + l v_x) \cos \beta_i - 2k \beta_i \sin \beta_i]} \tag{10}$$

where the β_i's are the roots of

$$\beta_i \cot \beta_i + \frac{l v_x}{2k} = 0 \quad \text{and} \quad \bar{\xi} = [a^2 + \frac{\alpha_c - \gamma}{k}]^{1/2} \tag{11}$$

From equation 10, the following calculations can then be made.

1. The mass of free oil drops in the profile (total oil in the water column) per unit area is given by

$$\int_0^l C(x,t) \, dx \tag{12}$$

2. The mass of oil lost through reaction (oil/SPM interactions) per unit area is given by

$$\alpha_c \int_0^T \int_0^l C(x,t) \, dx \, dt \tag{13}$$

52

3. The oil mass lost at the bottom (sedimented and removed from the water column) per unit area is given by

$$\int_0^T \left\{ \upsilon_x C - k \frac{dC}{dx} \right\}_l dt \tag{14}$$

4. The oil dispersed into the water column per unit area is

$$\frac{N_o}{\gamma} (1 - e^{-\gamma t}) \tag{15}$$

In order to verify the calculated results, the sum of items 1, 2 and 3 (above) must equal item 4.

3.1.2   Suspended Particulate Matter (SPM) Model

Consider SPM being dispersed into a water column. The particles are fluxed from the bottom and may either attach to oil droplets or return to the bottom. The model(s) only handle SPM that is fluxed from (or to) the bottom because the models are one-dimensional. The analytical model for SPM has a zero initial condition for the SPM concentration profile and it cannot be changed since this condition uniquely defines the solution. The numerical model for reacting oil droplets and SPM (steady state) can have an arbitrary initial condition for the SPM (to simulate SPM levels derived from another source such as a river) or oil-droplet concentration profiles; however, only "zero" and a steady-state profile for SPM are available in the coding. The coordinate system used is again one dimension in x with x = 0 at the surface and a total depth of l .   The concentration profile, S (in the vertical dimension) for the SPM is described by:

$$\frac{\partial S}{\partial t} + v_x \frac{\partial S}{\partial x} = \frac{\partial}{\partial x} (k \frac{\partial S}{\partial x}) - \alpha_s S \tag{1}$$

with boundary conditions

$$v_x S - k \frac{dS}{dx} = -F_0 + k_s S \text{ at } x = l \tag{2}$$

and

$$v_x S - k \frac{dS}{dx} = 0 \quad \text{at } x = 0 \tag{3}$$

The first boundary condition describes the flux of sediment from the bottom. The parameters are given by

v_x = particle settling velocity

k = turbulent diffusivity

F_o = constant flux source term from the bottom

k_s = first-order sediment deposition rate at the bottom

Using Laplace Transformations, the subsidiary equations are (Carslaw & Jaeger, 1959)

$$\frac{d^2 \bar{S}}{dx^2} - \frac{v_x}{k} \frac{d\bar{S}}{dx} - \frac{(p + \alpha_s)}{k} \bar{S} = 0 \tag{4}$$

with

$$v_x \bar{S} - k \frac{d\bar{S}}{dx} = - \frac{F_o}{p} + k_s \bar{S} \quad \text{at } x = l \tag{5}$$

$$v_x \bar{S} - k \frac{d\bar{S}}{dx} = 0 \quad \text{at } x = 0 \tag{6}$$

Solving this equation with the boundary conditions yields

$$\bar{S} = \frac{F_o e^{a(x-l)}}{p} \left\{ \frac{v_x \sinh \xi x + 2k\xi \cosh \xi x}{[k_s v_x + 2k(\alpha + p)] \sinh \xi l + 2k_s k\xi \cosh \xi l} \right\} \tag{7}$$

$$\text{where } \xi = \left[a^2 + \frac{\alpha_s + p}{k} \right]^{1/2} \tag{8}$$

and $a = \dfrac{v_x}{2k}$ (9)

Next, inverting the transform yields the vertical concentration profile

$$S(x,t) = F_0 e^{a(x-l)} \left\{ \frac{v_x \sinh \xi_0 x + 2k\xi_0 \cosh \xi_0 x}{(k_s v_x + 2k \alpha_s) \sinh \xi_0 l + 2k_s k \xi_0 \cosh \xi_0 l} \right.$$

(10)

$$\left. - \sum_{i=1}^{\infty} \frac{\beta_i [v_x \sin \Phi x + 2k \Phi \cos \Phi x] e^{-[\alpha + k(a^2 + \Phi^2)]t}}{[a + k(a^2 + \Phi^2)] [\beta_i (2k + k_s l) \sin \beta_i - l(ak_s l + k_s - kl(a^2 + \Phi^2) \cos \beta_i)]} \right\}$$

where $\Phi = \dfrac{\beta_i}{l}$ and $\xi_0 = \left[a^2 + \dfrac{\alpha_s}{k}\right]^{1/2}$ (11)

and the β_i's are the roots of

$$\beta_i \cot \beta_i = \frac{kl}{k_s} \left[a^2 + \Phi^2\right] - al$$ (12)

From equation 10, the following calculations can then be made:

1. The total mass of SPM in the water column per unit area is given by

$$\int_0^l S(x,t) \, dx$$ (13)

2. The mass of SPM lost due to reactions with oil droplets per unit area is given by

as $\alpha_s \displaystyle\int_0^T \int_0^l S(x,t) \, dx \, dt$ (13)

3. The mass of SPM fluxed in from the bottom per unit area is given by

$$\int_0^T \left\{ v_x S - k \frac{dS}{dx} \right\}_l dt$$ (13)

In order to verify the calculated results, the sum of items 2 and 3 must equal that of 1.

3.1.3   Oil Droplet and SPM Model

Consider oil droplets being dispersed into a water column from the surface and sediment being fluxed into the water column from the bottom. The oil droplets and SPM collide and stick to form an oil-SPM agglomerate at a specific rate. The coordinate system used is one dimension (in x) with x = 0 at the surface and increasing x values in the downward direction (down is the plus direction) with a total depth of l . The concentration profile, C (in the vertical dimension only), for the oil droplets is described by

$$\frac{\partial C}{\partial t} + v_c \frac{\partial C}{\partial x} = \frac{\partial}{\partial x}(k \frac{\partial C}{\partial x}) - \alpha_c CS \tag{1}$$

with boundary conditions

$$v_c - k\frac{dc}{dx} = N_0 e^{-\gamma t} \quad \text{at } x = 0 \tag{2}$$

and

$$C = 0 \text{ at } x = l \tag{3}$$

The parameters are given by:

v_c = (rise or fall) velocity in the x direction

k = turbulent diffusivity

N_0 = flux of oil droplets at the surface at t = 0

g = decay constant for the flux of oil

a_c = rate constant for oil droplet removal

The second boundary condition (Eq. 3), describing the oil-droplet loss of mechanism at the bottom, states that when oil reaches the bottom it is removed.

The concentration profile, S (in the vertical dimension only), for SPM is described by

$$\frac{\partial S}{\partial t} + v_s \frac{\partial S}{\partial x} = \frac{\partial}{\partial x}(k \frac{\partial S}{\partial x}) - \alpha_s CS \qquad (4)$$

with boundary conditions

$$v_s S - k \frac{dS}{dx} = - F_0 + k_s S \text{ at } x = l \qquad (5)$$

and

$$v_s S - k \frac{dS}{dx} = 0 \text{ at } x = 0 \qquad (6)$$

The first boundary condition describes the flux of sediment from the bottom. The parameters are given by

v_s = particle settling velocity

k = turbulent diffusivity

F_0 = constant flux source term from the bottom

k_s = first-order sediment deposition rate

a_s = rate constant for SPM removal

The solutions to the above equation set (Eqs. 1 and 4) cannot be obtained analytically because of the cross term CS. Solutions can be obtained using a Crank-Nicolson finite-difference numerical integration algorithm and an iteration at each time step on trial vectors for C and S. In order to check the mass balance for both oil droplets and SPM, the same mass quantities as described by equations (12) through (15) for oil, and equations (13) through (15) for SPM can be calculated (numerically).

Finally, the oil/SPM agglomerate profile, W, is described by

$$\frac{\partial W}{\partial t} + v_w \frac{\partial W}{\partial x} = \frac{\partial}{\partial x}(k \frac{\partial W}{\partial x}) + \alpha_w CS \qquad (7)$$

with boundary conditions

$$v_w W - k \frac{dW}{dx} = 0 \text{ at } x = 0 \tag{8}$$

and

$$W = 0 \text{ at } x = l \tag{9}$$

The last boundary condition states that when the agglomerate reaches the bottom it is removed. The parameters are given by

v_w = agglomerate settling velocity

k = turbulent diffusivity

a_w = rate constant for agglomerate production

The material balance equations for the oil/SPM agglomerate are

1. The mass of agglomerate in the water column per unit area is given by

$$\int_0^l W(x,t) \, dx \tag{10}$$

2. The mass of agglomerate produced by the oil droplets and sediment per unit area is given by

$$\alpha_w \int_0^T \int_0^l CS \, dx \, dt$$

3. The mass of agglomerate lost at the bottom per unit area is given by

$$\int_0^T \left\{ v_w W - k \frac{dW}{dx} \right\}_l dt$$

The verification of the calculation of the agglomerate profile is obtained from the sum of items 1 and 2, which must equal item 3.

3.1.4   Boundary Conditions and Parameter Estimations

Parameters that must be specified in order to perform a calculation are N_o and γ for oil droplets, and F_o and k_s for the SPM. The parameter N_o is the initial oil-dispersion (droplet) flux with (typical) units of $grams/(cm^2 sec)$, and γ is the decay constant with typical units of 1/sec. The primary motivation for using a decaying exponential to describe the oil droplet dispersion source term is the observation that these calculated results from the open-ocean oil-weathering code (Letter to Mauri Pelto from B.E. Kirstein, May 25, 1983; and letter to Dave Liu from B.E. Kirstein, July 1, 1983) plot as a straight line on a semilog graph (or a sum of straight lines). The only way to obtain these parameters from the open-ocean oil-weathering code is to run the code for a specified case, plot the results for oil-droplet dispersion, and fit the calculated results to a straight line. While this can be time consuming and somewhat tedious, another quicker (but less accurate) way is to assume (from experience) that a certain thickness of oil will decay by 1/2 in a given time. For example, suppose a 1/2-cm thick spill will disperse at a rate such that the thickness will be 1/4 cm in 6 hr. The defining equation for this "half-life" is

$$\frac{T}{T_o} = \exp(-\lambda t)$$

and

$$t_{1/2} = 0.693/\lambda$$

So if $t_{1/2} = 6$ hr $= 2.16 \times 10^4$ sec, $\lambda = 4.6 \times 10^{-5}$ sec^{-1}. Now, the total oil dispersed in any time frame through one cm^2 is

$$\text{oil dispersed} = (T_o - T) * 1\ cm^2 * \rho_o$$

or

$$W = \text{oil dispersed} = T_o(1 - \exp[-\lambda t]) * 1 \text{ cm}^2 * \rho_o$$

and the flux is the derivative of the total oil dispersed, and is

$$\text{flux} = T_o\lambda \exp[-\lambda t] * 1 \text{ cm}^2 * \rho_o$$

For this case with $\rho_o = 0.8 \text{ gm/cm}^3$, the lead coefficient N_o is

$$N_o = T_o\lambda\rho_o = 1.8 \times 10^{-5} \text{ gm/(cm}^2 \text{ sec)}$$

Thus, knowing in a general sense how an oil spill behaves with respect to dispersion, an estimate (only) of the boundary condition parameters for oil can be quickly obtained.

The parameters F_o and k_s for the SPM (bottom) boundary condition were chosen partly for a mathematical reason. Any SPM model must have a self-limiting source term or the water column could load to unrealistic sediment quantities. Therefore, a "back flux" of sediment to the bottom must occur which is proportional to how much sediment exits in the water. Mathematically this "back flux" is written as k_sS where k_s is a first order rate constant that multiplies the sediment concentration at the lower boundary. Since flux has units of $\text{gm/(cm}^2 \text{ sec)}$ and the sediment concentration, S, has units of gm/cm^3, k_s has units of cm/sec. The constant flux term F_o is what initially loads sediment into a clean water column, and when k_sS equals F_o, the net flux of sediment into the water column becomes zero. In order to estimate what typical parameters can be, consider that the water-column concentration of SPM can be 2 gm/l (as it has been observed at Beluga Point in Turnagain Arm of Cook Inlet), and this loading can be achieved in 6 hr; further assume the water is approximately 10 m deep. Thus, for each cm^2 of bottom area and water column, there is 1000 cm^3 of water containing a total of 1 gm of sediment. The differential equation for a well-mixed water column (even though it is not) is

$$l \frac{dS}{dt} = F_0 - k_sS$$

where l is the depth. A solution for S is

$$S = \frac{F_o}{k_s} (1 - \exp\left[-\frac{k_s}{l}t\right])$$

Thus, for large times, $S \longrightarrow F_o/k_s$. Hence, if 6 hr is about the time required to load the water column with sediment, let

$$F_o = 1 \text{ gm}/(1 \text{ cm}^2 * 6 \text{ hr}) = 4.6 \times 10^{-5} \text{ gm/cm}^2 \text{ sec}$$

and since $S = 0.001 \text{ gm/cm}^3$

$$k_s = F_o/S = 0.046 \text{ cm/sec}$$

It should be emphasized that the preceding calculations are only examples of how values for pertinent variables would be used in the model algorithms.

3.2   RATE CONSTANT CONSIDERATIONS

Theoretical and practical aspects of particle-particle interactions as they pertain to whole-oil droplet/SPM interactions have been addressed in previous NOAA/MMS programs (e.g., Section 2.1 in Payne et al., 1987b). Information presented in Sections 3.2.1 through 3.2.3 below provides further definition and clarification of these concepts.

3.2.1   Derivation of Working Equations Applicable for Oil/SPM Kinetics

The collision frequency for dilute suspensions of particles in a well-mixed volume can be expressed as

$$R = 1.3 \left[\epsilon/\nu\right]^{1/2} (r_i + r_j)^3 n_i n_j \tag{1}$$

where

R is the collision frequency

ϵ is the energy dissipation per unit mass of fluid per unit time

ν is the kinematic viscosity

r_i, r_j are the particle radii for species i and j

n_i, n_j are the particle number densities for species i and j

The rate of loss of particles due to collision and sticking to form an agglomerate is the above equation multiplied by a "sticking" coefficient denoted as α; i.e.,

$$R = -1.3 \, \alpha \, [\epsilon/\nu]^{1/2} \, (r_i + r_j)^3 \, n_i n_j$$

When the simplifying assumptions are made that oil droplets and SPM in a narrow-size range behave as a monosized population, and when units are converted to concentration (mg/L) instead of number densities, an equation may be obtained which describes representative interaction rates. The working equation for the rate of loss of oil droplets due to collision and adherence to SPM particles is:

$$dC/dt = -1.3 \, \alpha \, [\epsilon/\nu]^{1/2} \, CS \qquad (2)$$

where C and S are the concentrations for oil droplets and SPM particles, respectively.

If the concentration of SPM is kept constant (i.e., the SPM concentration is in great excess), then the equation may be further simplified to

$$dC/dt = -kC \qquad (3)$$

where $k = 1.3 \, \alpha \, [\epsilon/\nu]^{1/2} \, S$. Integration of this equation yields:

$$\ln C/C_o = -kt \qquad (4)$$

where C_o is the initial oil concentration. This equation is the basis for determining k from the slope of the measured oil-droplet concentration versus time data. The oil-droplet concentration measurements must plot as a straight line in order to verify the assumption of excess SPM.

3.2.2   Rate Constants for SPM Loses and Oil/SPM Production

Experimental measurements as presented in Section 5.2 yield only rate constants for oil droplet losses, not SPM losses or oil/SPM agglomerate production. However, since the kinetics describe a material balance for these three species, the latter two constants can be derived if the oil droplet and SPM particle (average) masses are known. The oil droplet and SPM kinetic expression is based on particle-particle collision and is rewritten in terms of species concentration of mass per volume. Thus, if one oil droplet of mass M_c "reacts" with one SPM particle of mass M_s, the rate of mass loss of SPM relative to oil will be M_s/M_c. To illustrate this concept in a mathematical sense, consider the rate of collision and sticking between particles i and j:

$$R = kn_i n_j$$

where all the parameters are "lumped" into k, and n_i and n_j are number densities (i.e., number of particles per unit volume). Now, the rate of loss of particle i is

$$dn_i/dt = - kn_i n_j$$

and for j is

$$dn_j/dt = - kn_i n_j .$$

Multiply both sides of the equation for the rate of loss of i by the mass per particle i to obtain

$$dC_i/dt = - k C_i n_j$$

63

and multiply both sides of the equation for the rate of loss of j by the mass per particle j to obtain

$$dC_j/dt = - kn_i C_j .$$

Continuing, multiply and divide the right-hand side of dC_i/dt by the mass of particle j to obtain

$$dC_i/dt = - kC_i C_j/M_j .$$

Likewise, multiply and divide the right-hand side of dC_j/dt by the mass of particle i to obtain

$$dC_j/dt = - kC_i C_j/M_i .$$

Now suppose the rate constant for the loss of oil droplets is "known" from measurements to be α_c in the following expression:

$$dC/dt = - \alpha_c CS$$

and it is required to determine α_s in

$$dS/dt = - \alpha_s CS .$$

From the preceding equations, it can be seen that

$$\alpha_c = k/M_s$$

and

$$\alpha_s = k/M_c$$ stand alone as $\alpha_s = (M_s/M_c) \alpha_c$ as asserted. Likewise, the rate constant for oil/SPM agglomerate production is

$$\alpha_w = \alpha_c + \alpha_s .$$

3.2.3   Rate Constant Scaling With Respect to Particle Size

In order to illustrate how the rate equation, and hence the rate constant, changes with respect to particle size, consider the defining equation as given in the previous sections

$$R = 1.3 \ [\epsilon/\nu]^{1/2} \ (r_i + r_j)^3 \ N_i N_j$$

where ϵ is the energy dissipation rate per unit mass of fluid, ν is the kinematic viscosity, r_i and r_j are the radii of particles i and j present at number densities N_i and N_j. Multiplying and dividing by the mass of particles i and j yields

$$R = 1.3 \ [\epsilon/\nu]^{1/2} \ (r_i + r_j)^3 \ N_i N_j \ (M_i/M_i)(M_j/M_j)$$

or

$$R = 1.3 \ [\epsilon/\nu]^{1/2} \ (r_i + r_j)^3 \ C_i C_j /(M_i M_j)$$

where now C_i and C_j are mass concentrations.

The mass of a particle is the equivalent volume (spherical) multiplied by the particle material intrinsic density, or for particle i

$$M_i = \rho_i \ (4/3) \ \pi r_i^3$$

Eliminating particle masses yields

$$R = \frac{1.3 \left[\dfrac{\epsilon}{\upsilon}\right]^{1/2} (r_i + r_j)^3 \ C_i C_j}{\dfrac{16}{9}\pi^2 \ \rho_i \rho_j \ r_i^3 r_j^3}$$

In order to account for "sticking" to form an i-j agglomerate, a multiplication factor β is introduced to yield

$$R_{i-j} = \frac{1.3 \, \beta \left[\frac{\epsilon}{\upsilon}\right]^{1/2}}{\frac{16}{9} \pi^2 \rho_i \rho_j} \left(\frac{r_i + r_j}{r_i r_j}\right)^3 C_i C_j$$

Comparing the above to the working equation used to analyze the laboratory data, i.e.,

$$R_{c-s} = \alpha [\epsilon/\nu]^{1/2} \, SC$$

In Section 5.2 yields the identification of α as

$$\alpha = \frac{1.3 \, \beta}{\frac{16}{9} \pi^2 \rho_i \rho_j} \left(\frac{r_i + r_j}{r_i r_j}\right)^3$$

Thus, the rate constant α varies as the above cubic function of the particle radii. Since the environmental sediment is not spherical, these radii must be interpreted as some equivalent radii (such as that similar to an aerodynamic radius).

Therefore, suppose that a rate constant is measured in the laboratory using a sediment of equivalent radius r_{j1} (conditions #1) and that it is necessary to predict the rate constant for the same type of sediment with radius r_{j2} (conditions #2). Dividing the defining equation for condition #2 by that for #1 yields

$$\alpha_2 = \alpha_1 \left[\frac{(r_i + r_{j2})r_{j1}}{(r_i + r_{j1})r_{j2}}\right]^3$$

For the purpose of illustration suppose that r_i denotes an oil droplet radius of 1 μm, r_{j1} denotes the first experimental sediment radius of 5 μm, and r_{j2} is the second sediment radius of 10 μm. Then by direct calculation $\alpha_2 = 0.77\alpha_1$. This example illustrates that the sediment concentrations of conditions #1 and #2 can remain the same, but yet the rate constant will change as the sediment particle size changes.

These illustrations are intended to provide a basis for scaling specific laboratory results to other conditions which may be encountered in the environment. Note that the laboratory experiments were conducted using oil droplets with radii on the order of 1-10 μm and sediment radii on the order 5-20 μm. If it is found that oil droplets and sediment in environmental situations are significantly different, then the above equation can be used to predict the net change of the rate constant from known conditions.

4.0   METHODS AND MATERIALS

4.1   SPM SAMPLING AND CHARACTERIZATION

In order to examine the effects on interaction rate constants arising from variations in SPM types, a total of eight sediment types were collected and tested according to procedures provided in Sections 4.2, 4.3, and 4.4. This section presents the collection methods used to acquire the sediment/SPM types deemed representative of coastal Alaskan waters. Also provided are the method procedures or references, where appropriate, for the physical/chemical characterization parameters.

Collection Methods

The eight types of sediment/SPM and the method of collection are listed below:

1) Turnagain Arm - seawater filtration

2) Grewingk Glacier - sediment surface scraping

3) Jakolof Bay - sediment surface scraping

4) Prudhoe Bay - ocean sediment grab sample

5) Kotzebue - ocean sediment grab sample

6) Peard Bay - ocean sediment grab sample

7) Beaufort Sea - ocean sediment grab sample

8) Yukon Delta - sediment surface scraping

SPM was collected nearshore from the water column in Turnagain Arm (Cook Inlet, near Anchorage, AK) on November 7, 1987. Relatively high turbulence levels were encountered during the SPM sampling as indicated by visibly high current velocities at the SPM sampling locations. The purpose of collecting true SPM was for comparison with samples collected from sedimented sources (all the other types). The Turnagain Arm SPM was obtained by pumping seawater through a 1-μm grade, porous, stainless-steel filter that has a surface

68

area of approximately 0.5^2. A double-acting diaphragm pump, that delivered roughly 50 psi at the filter housing, was employed to collect sufficient quantities of SPM for experimental and characterization purposes.

Sediments from Grewingk Glacier and Jakolof Bay were collected in August and November 1987, respectively, by carefully scraping the uppermost 2-5 mm of the surface of depositional areas. The sediment from Grewingk Glacier, located on the southern portion of the Kenai Peninsula, was obtained from eddy areas along Grewingk Creek, which flows from the glacial melt water lake into Kachemak Bay. Jakolof Bay is an estuarine area, also located off of Kachemak Bay, that receives freshwater input from Jakolof Creek. At this site, the sediment was acquired from depositional areas uncovered at low tides towards the center of the bay. The harvested sediments were placed into Teflon screw-capped jars and frozen until preparation prior to testing (see Section 4.2.3).

The remaining sediments--Beaufort Sea, Kotzebue, Yukon Delta, Peard Bay, and Prudhoe Bay--were collected as part of other NOAA or MMS sponsored projects. With the exception of the Yukon Delta sediment, all were collected using a grab sampler by Erk Reimnitz during August and September 1985. The Beaufort Sea sediment was obtained midway between Harrison Bay and Barrow, in 36 m of water, with the following identifiers: 85-AER-5, Line 15, JD 243. Peard Bay sediment (85-AER-2) was collected in 52 ft of water, NNW of Cape Franklin. Prudhoe Bay sediment (85-AER-8) was collected < 200 m west of W. Dock in 1.5 m of water. The sampling site for Kotzebue sediment was located west of Kotzebue in 63 ft of water. The sediment obtained from the Yukon Delta was collected by Lt. Cmdr. Mike Myers using surface-scrape techniques. All of these sediment samples were frozen after collection until their use during interaction testing.

In addition, peat--an organic, nonsedimentary material--was subjected to interaction rate determinations. The peat was collected by Bill Benji of MMS in August 1986 along the coast of the Beaufort Sea and frozen until tests were conducted in July 1988.

Each of the eight sediments/SPM types listed above were characterized for the following chemical or physical properties: total organic carbon (TOC), grain size, hydrocarbon content, mineralogy, solids density, and number density. A method reference or procedural account is provided below for each of these parameters, and results of the measurements can be found in Section 5.1.

- TOC levels were determined according to modified (for solids) EPA method 415. A Zirtex Dorman Model #PIR-2000 TOC analyzer accomplishes carbon compound oxidation by pyrolosis with the generated CO_2 concentration measured with an infrared (IR) detector.

- Grain-size distributions were measured by the Pipette Method of Particle-Size Analysis, as described in Methods of Soil Analysis, Part 1 Physical and Mineralogical Properties (C.A. Black, et al., 1965).

- Solids-density measurements were made using a pyncnometer according to Method BS 1377:1975, Test 6 (B), which can be found in the Manual of Soil Laboratory Testing, Vol.1, Soil Classification and Compaction Tests.

- Mineralogy was determined with a Philips Electronics X-ray diffractometer equipped with a crystal monochrometer. Detailed method descriptions along with instrument operating parameters can be found in Appendix C.

- Number densities were obtained by photomicroscopy techniques as detailed in Section 4.2.6.

- Hydrocarbon-content determinations were accomplished by solvent extraction with volume reduction and subsequent analysis by flame ionization detector gas chromatography (FID-GC). Briefly, approximately 20 g (wet weight) of sediment were extracted with 50 ml of methanol, followed by 50 ml of 1:1 methanol: DCM, and, finally, two 50-ml portions of DCM. All extracts were combined and back-extracted with 50 ml of 3% saltwater, which was subsequently extracted with 25 ml DCM, which is added to the combined extracts. Solvent-reduction techniques employed the standard Kuderna-Danish concentrators; instrumental analysis by FID-GC is described in detail in Payne et al. (1984a).

4.2   WHOLE-OIL DROPLET/SUSPENDED PARTICULATE MATERIAL (SPM) INTERACTIONS

The apparatus and experimental protocol used to obtain kinetic rate constants for interactions between dispersed whole-oil droplets and SPM in a water

70

column are similar to those described in Payne et al. (1987b). For the current NOAA-sponsored program, the protocols for the whole-oil droplet/SPM interaction experiments are described in Sections 4.2.1 through 4.2.7. Variables incorporated into experiments for the rate constant measurements are described in Section 4.2.8. All experiments were performed at the NOAA field laboratory at Kasitsna Bay, AK.

4.2.1   Reaction Vessel

All whole oil droplet-SPM interaction experiments were performed with the configuration shown schematically in Figure 4-1. Photographs of the complete apparatus (including a stirred reaction vessel) and a close-up of the torque meter are shown in Figures 4-2 and 4-3, respectively. The reaction vessel was normally a 4-L glass beaker, although a 10-L beaker was used on occasion. Volumes for reaction solutions were either 3.5 or 9.5 L in the 4- or 10-L vessels, respectively. The shaft and propeller connected to the variable-speed motor were used to generate specified turbulence levels in the experimental reaction solution. Torque and revolutions-per-minute (rpm) generated by the propeller were recorded with a torque meter and an rpm-counting device connected in-line between the motor and the propeller shaft. The torque meter was purchased from General Thermodynamics (Model M-1 with torsion bar #M1-005). The digital rpm-counting device was constructed for this project. The torque and rpm measurements were used to estimate values for energy dissipation per unit time in the reaction solution.

4.2.2   Preparation of Water for Reaction Solutions

Seawater for experiments was obtained from the resident seawater pumping system at the laboratory. Freshwater was obtained through a separate pumping system from a natural creek adjacent to the lab. Larger particles were initially removed from both the seawater and freshwater by vacuum-filtration through glass-fiber filters (1 μm nominal pore size). All of this prefiltered water then received a final vacuum filtration through polycarbonate membrane filters (0.4 μm pore size) immediately before use in experiments.

71
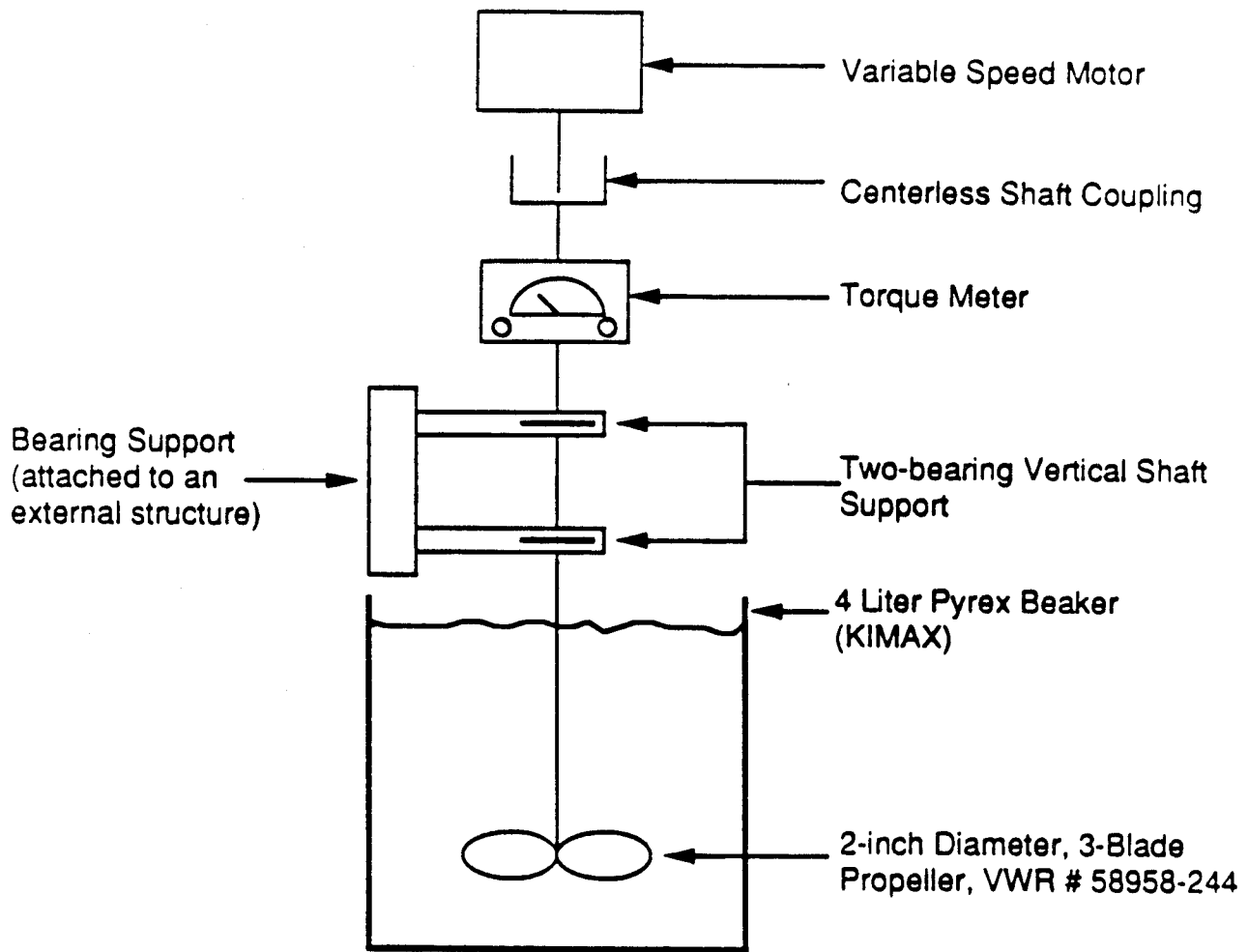
Figure 4-1.   Experimental Hardware Used to Determine Oil-SPM Interaction Kinetics
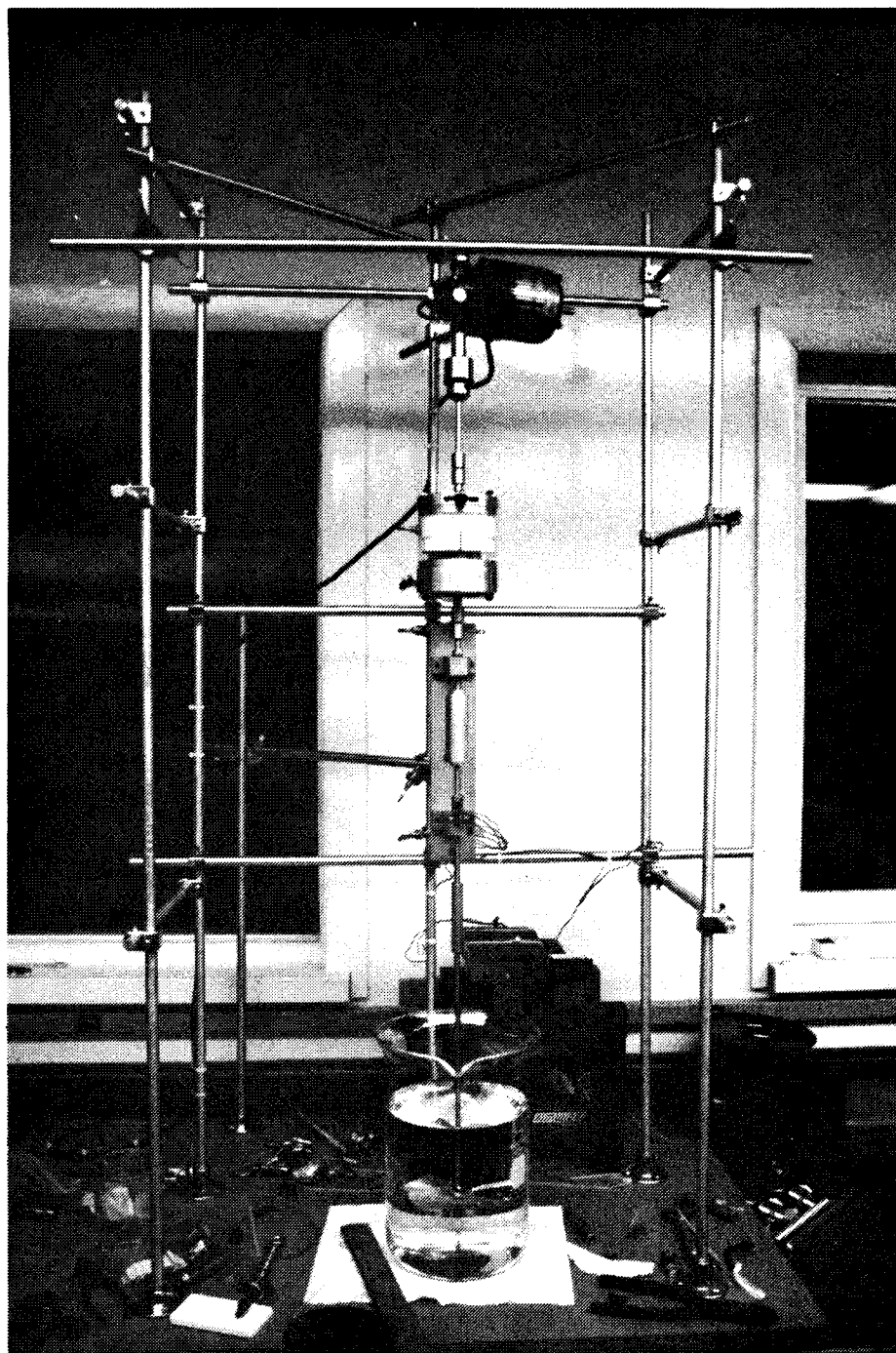
Figure 4-2.   Photograph of the Complete Stirred Reaction Apparatus
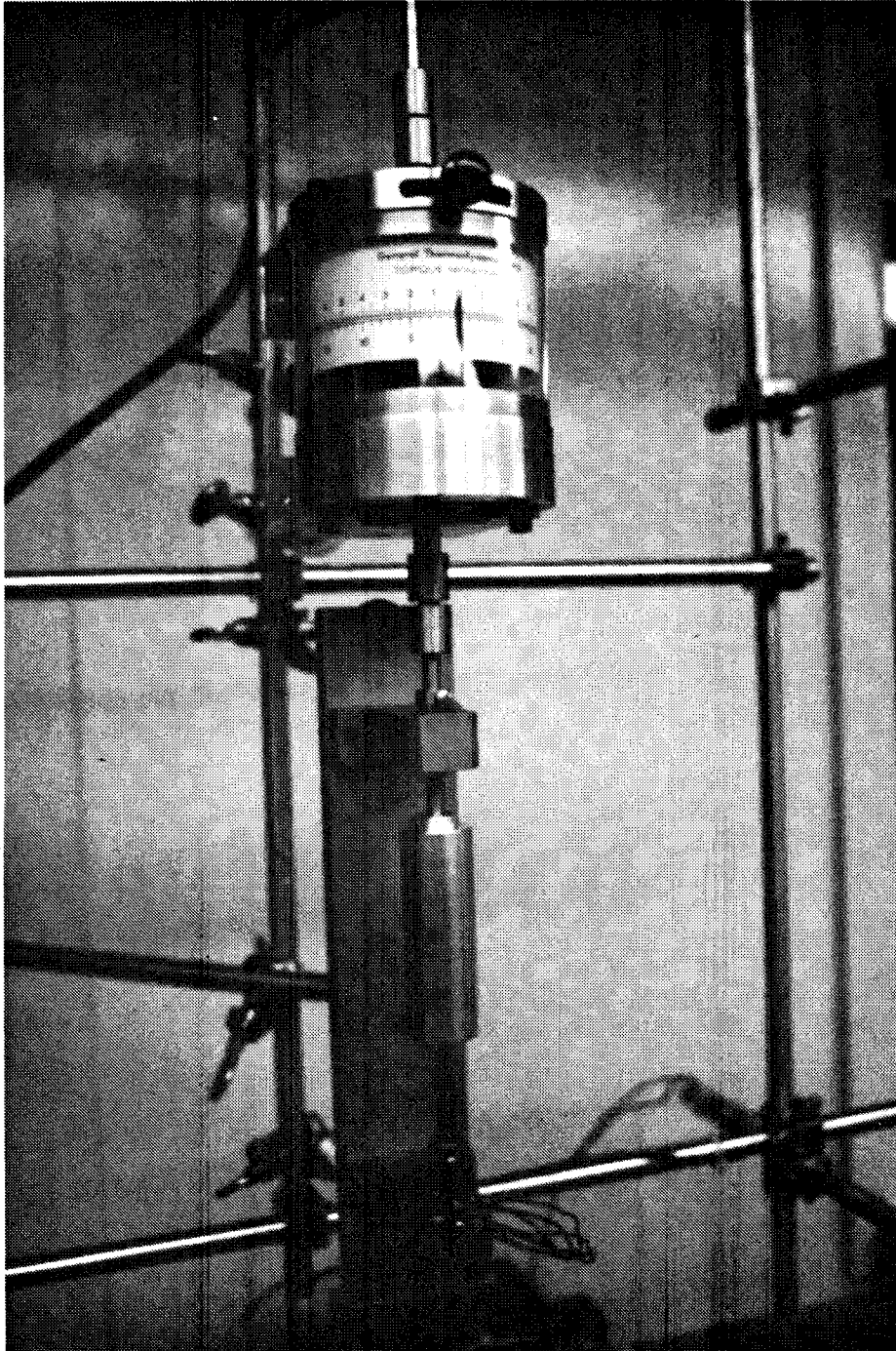
Figure 4-3.   Photograph of Torque Meter

74

4.2.3   Preparation of SPM for Reaction Solutions

As elaborated in Section 4.2.8.1, a variety of particulate types were utilized in oil droplet/SPM interaction experiments. These SPM types included eight natural sediments, one natural marine SPM and two commercially available particle phases. If not used immediately, the natural sediment and SPM phases were stored frozen. Immediately prior to experiments, all of the natural sediments were presized with a 53 μm geological sieve and only particles passing through the sieve (i.e., particles < 53 μm in diameter) were used. Neither the natural marine SPM nor the commercially available particulate phases were sieved prior to their use in experiments.

4.2.4   Preparation of Dispersed Oil Droplets for Reaction Solutions

Dispersed oil droplets in aqueous phases for experiments were prepared with a defined protocol. The protocol involved mechanical blending of a specified amount of oil in 750 ml of 0.4 μm filtered water (Section 4.2.2) in a commercial multiple-speed blender (i.e., Hamilton Beach Scovill 7-Speed Blender). Quantities of oil used in the "blending" process included 4, 16, or 64 drops for unweathered oils (i.e., Prudhoe Bay crude and No. 1 fuel oil); 6, 24, or 96 drops for 12 day weathered Prudhoe Bay crude oil; or recorded weights for naturally weathered North Slope crude oil recovered from the R/T Glacier Bay spill event in July 1987 in Cook Inlet, AK. To produce dispersed oil droplets in the desired size range of 1-10 μm in the 750 mL "blending" solution, the preparative procedure routinely involved the following steps: the blender was 1) turned "on" at a specified setting ("6") for 5 sec, 2) "off" for 60 sec and 3) "on" for an additional 5 sec. After remaining stationary for 5 min, the larger oil droplets forming a slick on the surface of the "blended" solution were removed with sorbent tissues. Observations with a light microscope (see Section 4.2.6) indicated that oil droplets remaining in suspension of the final "blended" solutions (i.e., after removal of the surface oil slick) were almost always < 10 μm in diameter. Figures 4-4, 4-5 and 4-6 present FID-GC chromatograms depicting the initial 3.5-min and 26-min reaction time sample for fresh Prudhoe Bay crude, 12-day weathered Prudhoe Bay crude, and No. 1 fuel oil, respectively. As seen, minor amounts of the lighter weight compounds are lost

Figure 4-4. GC/FID Chromatograms Depicting: A) fresh Prudhoe Bay crude time O, B) time 3.5 min., and C) time 26 min.
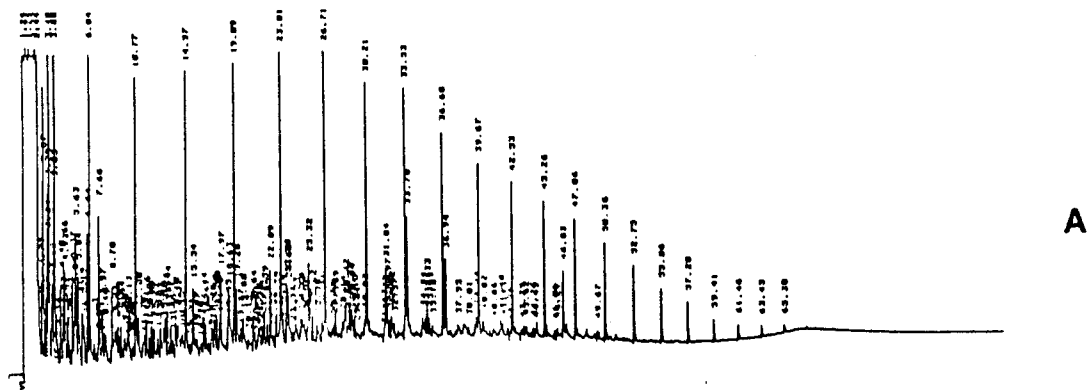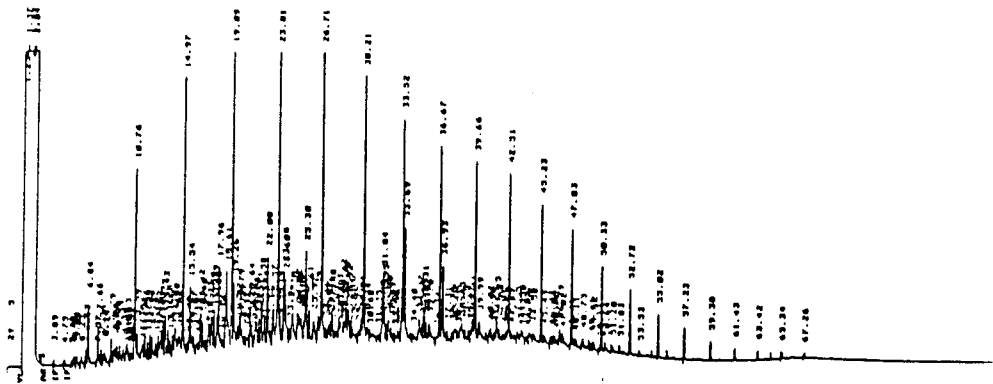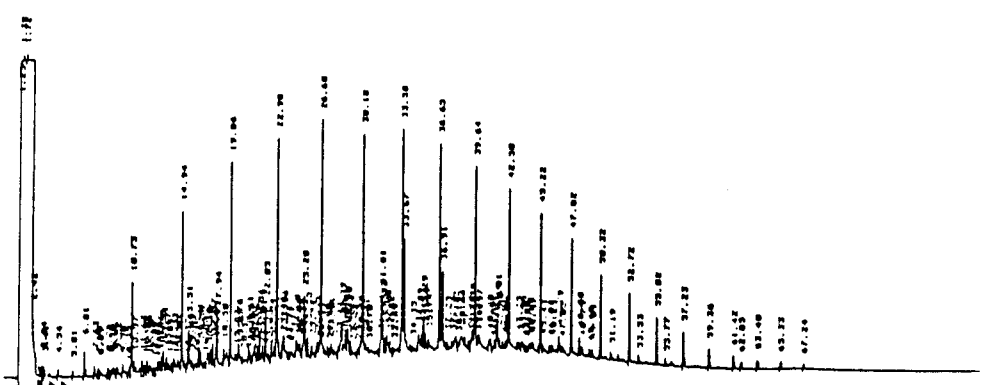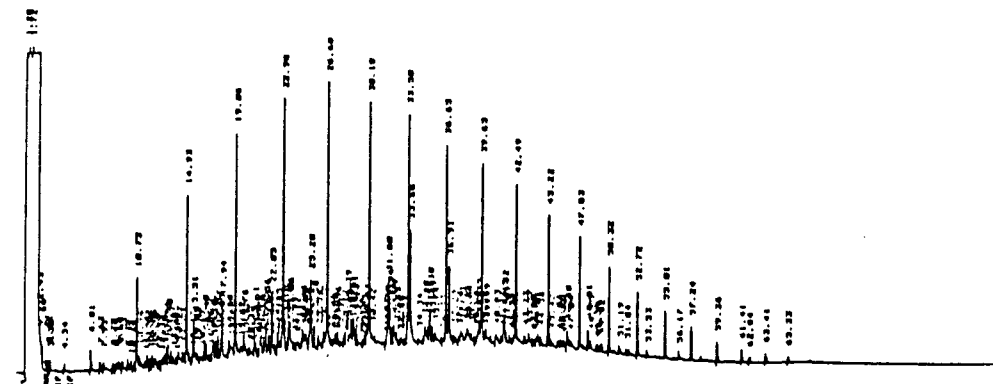
Figure 4-5. GC/FID Chromatograms Depicting: A) 12-day weathered Prudhoe Bay crude time , B) time 3.5 min., and C) time 26 min.

77
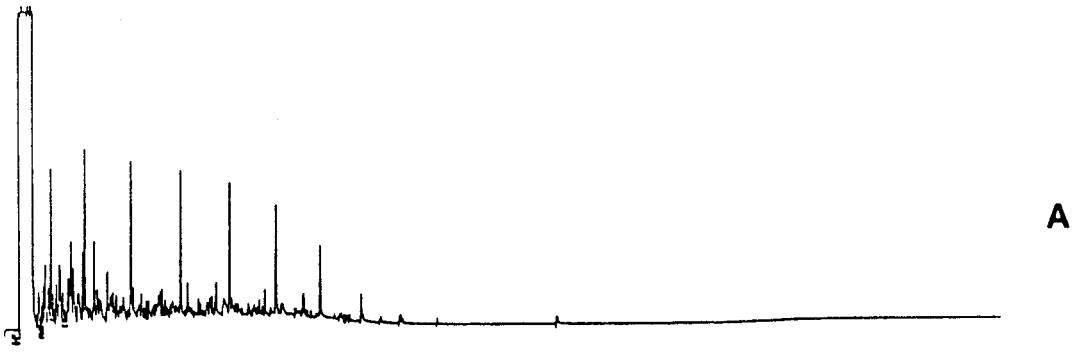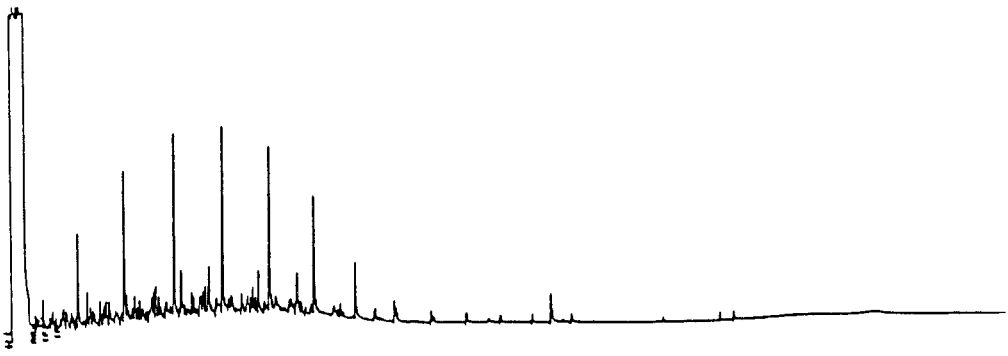
Figure 4-6.   GC/FID Chromatograms Depicting: A) Kasitsna Bay fuel oil time O, B) time 3.5 min.,
and C) time 26 min.

during the blending process for the fuel oil and the fresh Prudhoe Bay crude; however, the composition of the oil remains unchanged during the reaction experiment.

4.2.5 Stirred Reaction Vessel Experiment for Whole-Oil Droplet/SPM Interactions

For experiments containing both dispersed oil droplets and SPM, a volume of a parent SPM solution (Section 4.2.3) was added to the stirred reaction vessel containing an appropriate volume of 0.4 μm filtered water (i.e., either seawater, freshwater, or a 1:1 v:v mixture of seawater and freshwater; Section 4.2.2). The volume of parent SPM solution added to the reaction vessel was adjusted to ensure that number densities of SPM particles would be substantially in excess of those for dispersed oil drops. Number density ratios for SPM particles to oil droplets at the start of experiments were always > 3. The experiment was initiated upon addition of the "blended" oil solution to the reaction vessel containing the filtered water and SPM. Total solution volumes for experiments (i.e., filtered water + "blended" oil solution + SPM) were 3.5 L and 9.5 L for the 4- and 10-L reaction vessels, respectively. All experiments were conducted at room temperature, with solution temperatures ranging between 17°C and 23°C over all experiments.

For the purpose of determining the oil droplet/SPM interaction rate constant in a given experiment, 50 μL aliquots of the stirred oil droplet-SPM-water solution were removed from the reaction vessel at specified times and transferred to specially designed microscope slides that served as counting chambers. Times for collection of 50 μL aliquots were 1, 2, 3, 5, 7, 9, 11, 13, 15, 20 and 25 min after the addition of the "blended" oil solution to the reaction vessel. Discussions of the design of the microscope slide-counting chambers and their utilization for oil droplet and SPM number-density determinations are presented in Section 4.2.6. In addition to the 50 μL aliquots transferred to the microscope slides, two 50-mL samples were also collected from the homogeneously stirred solution in the reaction vessel near the beginning and end of each experiment (e.g., at 3.5 and 26 min). The latter samples were used to determine total SPM loads and suspended oil quantities in the

reaction solution (Section 4.2.7) and to assess that these quantities did not change substantially over the course of the experiment.

In addition to the above-described experiments that included additions of both oil droplets and SPM to reaction vessel solutions, control experiments were conducted on a routine basis. These experiments were performed in a manner identical to that described above, except that either oil droplets or SPM particles were not added to the reaction solutions.

4.2.6   Determination of Whole-Oil Droplet and SPM Number Densities in Reaction Solutions

To estimate rate constants for interactions between dispersed oil droplets and SPM in an experiment, number densities of "free" oil droplets (i.e., droplets without associated SPM) had to be determined over time during experiments. Because of density differences between the oil droplets and the aqueous media in experiments, the "free" oil had a natural tendency to rise toward the surface of solutions. Rise velocities of approximately 0.4 μm/sec (or 15 mm/hr) for "free" oil droplets with a 5 μm diameter and a density of 0.8-0.9 g/cm^3 were estimated using Stokes Law. In contrast, oiled SPM agglomerates (i.e., oil droplets that had "reacted" with SPM) as well as "unreacted" SPM had densities greater than that of the aqueous medium, causing these particulate phases to sink in the aqueous medium. These density differences between the "free" oil drops and that of the oil/SPM agglomerates and "free" SPM were subsequently used to distinguish number densities of "free" oil droplets over time in experiments for the purpose of estimating oil droplet/SPM interaction rate constants.

During a stirred vessel experiment (Section 4.2.5), each 50 μL aliquot collected over time was transferred onto the middle of a microscope slide as shown in Figure 4-7. The microscope slide contained two stacked cover slips at each end. The height of the stacked cover slips was approximately 0.5 mm. A final cover slip was then placed on top of the end stacks, effectively "capping" the sample and providing flat upper and lower surfaces to the water/oil/SPM droplet. A sample volume of 50 μL was sufficient to ensure that

Sample of oil-SPM, 50 µl,
placed between ends, "cap"
added to form flat upper surface
and prevent evaporation

Rectangular cover slip
to form "cap"

Standard slide

Two # 2 cover slips
stacked at each end
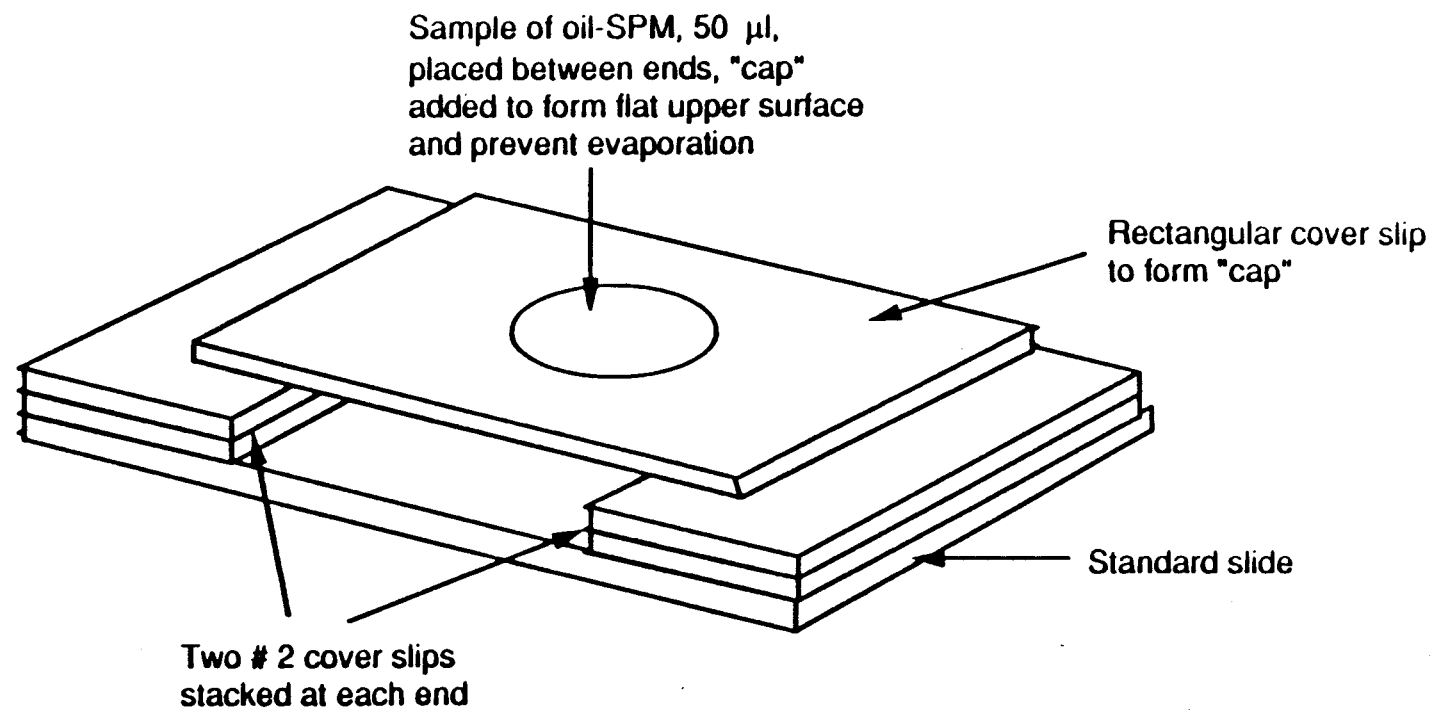
Note: This drawing is not to scale

Figure 4-7. Microscope Slide Arrangement for Viewing Oil Droplets and SPM

the aqueous solution on the slide contacted the undersurface of the top cover slip, yielding a total sample depth of approximately 0.5 mm on the slide. At the Stokes rise velocity specified above for 5-μm diameter oil droplets (i.e., 15 mm/hr), all "free" oil droplets in the sample on the slide would reach the upper cover slip in approximately 100 sec. In contrast, oil/SPM agglomerates and "free" SPM on the slide would sink to the bottom of the "capped" sample.

A Nikon Labophot light microscope (#HFX-11) equipped with phase contrast and 35mm and Polaroid film camera attachments was used to photographically document number densities and visible characteristics of "free" oil droplets, oil/SPM agglomerates, and "free" SPM in samples on the microscope slides. All photomicrographs were taken at a magnification of 100X. Because of depth-of-field focus considerations, only "free" oil droplets were observed when the focal plane of the microscope was adjusted to the top of the "capped" sample (i.e., the undersurface of the top cover slip). "Free" SPM and oil/SPM agglomerates that sank to the bottom of the water/oil/SPM sample on the slide were not visible in the focal plane of the "free" oil droplets. By adjusting the focal plane down, however, SPM and oil/SPM agglomerates could be observed in the absence of any visible "free" oil droplets. To ensure sufficient time for the necessary vertical separations between "free" oil droplets and the SPM and oil- SPM agglomerates on a slide, samples were routinely not counted until 15-30 min after they were collected from the stirred reaction vessel.

Photomicrographs were also obtained of a stage micrometer. Comparison between photomicrographs of the micrometer and sample slides made it possible to determine the sizes of oil droplets, SPM, and oil/SPM agglomerates as well as the horizontal dimensions for the entire field of a photomicrograph. The combination of the horizontal dimensions of the photomicrograph field and the total sample depth on the microscope slide (i.e., 0.5 mm) made it possible to estimate the total sample volume contained in the overall field of view of a photomicrograph. Consequently, number densities per photomicrograph for "free" oil droplets (upper focal plane of the slide) as well as SPM and oil/SPM agglomerates (lower focal plane) could be transformed into values per unit volume for a sample.

82

Although photomicrographs of sample slides were obtained with both 35 mm black-and-white (Kodak TMAX-100) and Polaroid film, the 35 mm medium was preferred due to its slightly better resolution properties. For each sample, five fields-of-view were randomly chosen for photographic documentation of number densities of either "free" oil droplets (upper focal plane) and/or SPM and oil/SPM agglomerates (lower focal plane). Mean values for numbers of "free" oil droplets in the five fields on a given sample slide were used in calculations for oil droplet/SPM interaction rate constants (see Section 5.2).

4.2.7 Determination of Total SPM and Oil Quantities in Reaction Solutions

The 50-mL sample volumes collected near the beginning and end of stirred reaction vessel experiments were used to obtain estimates for both total oil loads and total SPM in a given experiment. The procedure is identical to that described in Payne et al. (1987b). Briefly, the 50-mL volume for a given sample was vacuum-filtered (< 10 cm Hg) through a preweighed, 47-mm diameter polyester membrane filter (0.4-μm pore size; Nuclepore). If the experimental aqueous medium was comprised of full or partial seawater, the filter received a final vacuum rinse with freshwater to remove residual sea salts. All seawater and freshwater filtrates were discarded. Sequential vacuum filtrations through the filter were then performed with 1) 10 mL methanol and 2) 30 mL methylene chloride. The latter solvent filtrates were retained for the oil load measurements.

For a total SPM load determination, the solvent-rinsed polyester membrane filter was placed in a desiccator until constant filter weight measurements were obtained. The difference between the initial tare weight for the filter and its final weight containing solvent-rinsed SPM was used to determine the total SPM load in the sample. Because the polyester filters were highly efficient in retaining "free" oil droplets as well as SPM, the final sample filtration rinses with methanol and methylene chloride were necessary to obtain SPM weight estimates independent of accompanying oil quantities present as either "free" oil droplets or oil/SPM agglomerates in the 50-mL sample volume.

83

For total oil load determinations, the methanol and methylene chloride fractions from the membrane filtration step were combined, reduced to appropriate volume with a water bath and N_2 blowdown, and analyzed for oil content and composition by flame ionization detector-gas chromatography (FID-GC). Quantities of oil in resulting chromatograms of sample extracts were determined by comparison with accompanying chromatograms of standard solutions containing known concentrations of the parent oil used in a given experiment. For experiments using unweathered and 12-day weathered Prudhoe Bay crude oil and naturally weathered North Slope crude oil, quantities of oil in experimental samples were estimated by comparing peak areas in sample extracts with standard solutions of unweathered Prudhoe Bay crude oil for the following eight n-alkane and isoprenoid compounds: $n-C_{16}$, $n-C_{17}$, pristane, $n-C_{18}$, phytane, $n-C_{19}$, $n-C_{20}$ and $n-C_{21}$. For experiments using unweathered No. 1 fuel oil, quantities of oil were estimated by comparing peak areas in sample extracts with parent oil standards (No. 1 fuel oil) for the following five n-alkane compounds: $n-C_{12}$, $n-C_{13}$, $n-C_{14}$, $n-C_{15}$ and $n-C_{16}$. A Hewlett-Packard 5840A gas chromatograph located at the NOAA field laboratory at Kasitsna Bay was used for all FID-GC analyses.

4.2.8   Experimental Variables

Experiments were performed with a number of variables to evaluate possible effects of those variables on whole-oil droplet/SPM interaction rate constants. A listing of all experiments is presented in Table 4-1. Included in the table are values for the salinity, SPM load, and oil load used in each experiment. Methods to measure the latter variables are presented in Sections 4.2.7 and 4.2.8.3. Discussions of the major variables evaluated in experiments are presented in Sections 4.2.8.1 through 4.2.8.4.

4.2.8.1 Suspended Particulate Material (SPM) Types

Types of SPM used in experiments included eight natural sediments collected from a variety of coastal environments in Alaska, one natural SPM collected from marine waters in Turnagain Arm near Anchorage, AK, and two commercially available particulate phases. Collection procedures and sample

84

Table 4-1

Summary of Whole-Oil Droplet/SPM Interaction and SPM Settling Velocity Experiments

Salinity (ppt)	Sediment Type	Sed Amount (mg/L)	Oil Type	Oil Amount (mg/L)	RX Exp[a]	Pic Typ[b]	Drop Count[c]	Setl Exp[d]	Date
30.0	Grewingk till (< 53 μm)	62.7	None	0.0		—		Y	11-15-87
30.0		63.8		0.0		—		Y	07-11-88
0.0		61.5	Unweathered Prudhoe Bay crude	35.7	X	T	X		07-09-88
14.0		56.7		18.4	X	T	X	Y	07-10-88
30.0		51.4		4.1	X	P	X	Y	11-17-87
30.0		52.1		19.9	X	T	X		07-28-87
30.0		53.9		12.9	X	T	X		07-28-87
30.0		47.9		19.3	X	P	X		07-30-87
30.0		—		NA	X	P	X		07-30-87
30.0		—		NA	X	P	X		08-03-87
30.0		44.6		10.9	X	T	X		08-26-87
30.0		47.1		15.3	X	T	X		08-26-87
30.0		47.8		17.4	X	P	X		08-29-87
30.0		—		NA	X	P	X		08-30-87
30.0		40.5		24.2	X	P	X		09-02-87
30.0		67.7		7.9	X	T	X		10-07-87
30.0		42.5		24.7	X	P	X		11-14-87
30.0		54.7		14.4	X	P	X	Y	11-16-87
30.0		55.7		79.2	X	P		Y	11-18-87
0.0		63.4	12-day weathered Prudhoe Bay crude	99.0	X	T	X		07-09-88
29.0		62.2		26.1	X	T	X	Y	07-17-88
29.0		59.5		83.9	X	T	X	Y	07-15-88
29.0		60.9		54.9	X	T	X		07-15-88
29.0		63.5		43.2	X	T	X		07-15-88
30.0		58.2		307.6	X	T		Y	07-13-88
0.0		56.6	Unweathered No. 1 fuel oil	7.1	X	T	X		07-18-88
15.0		69.0		32.4	X	T	X		07-18-88
30.0		68.4		32.8	X	T	X	Y	07-19-88
30.0		55.4	R/T Glacier Bay weathered North Slope crude	1.2	X	P	X		08-03-87
30.0	Turnagain Arm SPM	180.0	Unweathered Prudhoe Bay crude	18.6	X	T	X		11-12-87
29.0		356.8		25.8	X	P	X		07-17-88
29.0		416.4	12-day weathered Prudhoe Bay crude	58.4	X	P	X		07-17-88
30.0		319.8	Unweathered No. 1 fuel oil	24.9	X	P	X		07-18-88
0.0	Yukon Delta sed (< 53 μm)	390.1	None	0.0		—		Y	02-15-88
0.0		756.2		0.0		—		Y	04-20-88
13.5		516.2		0.0		—		Y	02-18-88
29.0		447.0		0.0		—		Y	02-17-88
29.0		830.0		0.0		—		Y	04-21-88
0.0		453.3	Unweathered Prudhoe Bay crude	44.2	X	T	X	Y	02-20-88
14.0		526.7		31.5	X	T	X	Y	02-24-88
28.0		508.7		40.6	X	T	X	Y	02-21-88
29.0		614.1		105.4	X	T	X	Y	02-23-88

Table 4-1 (Continued)

Salinity (ppt)	Sediment Type	Sed Amount (mg/L)	Oil Type	Oil Amount (mg/L)	RX Exp[a]	Pic Typ[b]	Drop Count[c]	Setl Exp[d]	Date
0.0	Yukon Delta sed (< 53 µm)	690.1	12-day weathered Prudhoe Bay crude	68.6	X	T	X	Y	04-18-88
14.0	(Cont.)	776.5		71.2	X	T	X	Y	04-19-88
29.0		707.5		19.0	X	T	X	Y	04-16-88
29.0		782.2		49.2	X	T	X	Y	04-15-88
29.0		789.2		286.6	X	T	X	Y	04-17-88
0.0		408.6	Unweathered No. 1 fuel oil	32.9	X	T	X		07-20-88
14.0		485.4		28.8	X	T	X		07-20-88
30.0		554.0		25.6	X	P	X		07-19-88
30.0	Beaufort Sea sed (< 53 µm)	136.5	Unweathered Prudhoe Bay crude	23.6	X	T	X		07-10-88
30.0		139.4	12-day weathered Prudhoe Bay crude	112.2	X	P	X		07-12-88
30.0		128.4	Unweathered No. 1 fuel oil	21.6	X	T	X		07-15-88
30.0		138.2		48.0	X	P	X		07-18-88
30.0	Beaufort Sea peat (< 53 µm)	130.6	Unweathered Prudhoe Bay crude	21.6	X	T	X		07-10-88
30.0		115.3	12-day weathered Prudhoe Bay crude	98.6	X	P	X		07-12-88
30.0	Peard Bay sed (< 53 µm)	152.1	Unweathered Prudhoe Bay crude	30.3	X	T	X		07-11-88
30.0		132.9	12-day weathered Prudhoe Bay	69.5	X	P	X		07-13-88
30.0	Prudhoe Bay sed (< 53 µm)	203.4	Unweathered Prudhoe Bay crude	32.1	X	T	X		07-11-88
30.0		209.8	12-day weathered Prudhoe Bay crude	88.0	X	P	X		07-13-88
30.0	Kotzebue sed (< 53 µm)	231.2	Unweathered Prudhoe Bay	31.1	X	T	X		07-11-88
30.0		232.8	12-day weathered Prudhoe Bay crude	77.3	X	T	X		07-14-88
30.0	Jakolof Bay sed (< 53 µm)	32.5	Unweathered Prudhoe Bay crude	29.2	X	P	X		07-25-87
30.0		49.9		16.3	X	P	X		07-27-87
30.0		60.0		17.0	X	T	X		11-06-87
30.0		53.0		25.0	X	T	X		11-06-87
30.0		57.0		NA	X	T	X		11-07-87
30.0		60.0		23.0	X	T	X		11-08-87
30.0		363.0	Unweathered No. 1 fuel oil	37.9	X	T	X		07-19-87
30.0	Aluminum oxide grit	62.4	Unweathered Prudhoe Bay crude	25.9	X	T	X		10-04-87
30.0	(10 µm)	205.7		22.4	X	T	X		10-05-87
30.0		221.3		26.4	X	T	X		10-06-87
30.0		266.1		10.2	X	T	X		11-10-87
30.0		263.5		4.8	X	T	X		11-11-87
30.0	DVB polyspheres (1-20 µm)	NA	Unweathered Prudhoe Bay crude	NA	X	T	X		10-08-87

Table 4-1 (Continued)

Salinity (ppt)	Sediment Type	Sed Amount (mg/L)	Oil Type	Oil Amount (mg/L)	RX Exp[a]	Pic Typ[b]	Drop Count[c]	Setl Exp[d]	Date
0.0	None	—	Unweathered Prudhoe Bay crude	38.8	X	T	X		02-1988
13.0		—		30.7	X	T	X		02-19-88
30.0		—		14.8	X	P	X		07-29-87
30.0		—		23.0	X	P	X		08-31-87
30.0		—		7.8	X	P	X		11-13-87
30.0		—		22.6	X	P	X		11-12-87
30.0		—		31.5	X	T	X		02-19-88
0.0		—	12-day weathered Prudhoe Bay crude	62.0	X	T	X		04-13-88
29.0		—		13.8	X	T	X		04-14-88
29.0		—		44.1	X	T	X		04-13-88
30.0		—	R/T Glacier Bay weathered North Slope crude	5.3	X	P	X		08-02-87
30.0		—	Unweathered No. 1 fuel oil	8.3	X	P	X		07-14-88

[a] RX Exp: X = oil droplet/SPM interaction experiment performed
[b] Pic Type: photomicrographs taken with TMAX-100 film (T) or Polaroid film (P)
[c] Drop Count: photomicrographs counted for oil drop numbers
[d] Setl Exp: Y = settling chamber experiment performed with solution generated in parent oil droplet/SPM interaction study

locations for the natural sediments and the Turnagain Arm SPM are presented in greater detail in Section 4.1. Briefly, the eight natural sediments are the following: 1) Beaufort Sea sediment, 2) Beaufort Sea peat, 3) glacial till collected from melt waters of the Grewingk Glacier near Kachemak Bay, AK, 4) Jakolof Bay (a small embayment adjacent to Kachemak Bay), 5) Kotzebue sediment, 6) Peard Bay sediment, 7) Prudhoe Bay sediment and 8) Yukon River Delta sediment. All eight sediment types (but not the Turnagain Arm SPM) were passed through a 53-μm geological sieve, and only those particles passing through the sieve were used in experiments. The commercially available particulate phases used in certain experiments consisted of commercial aluminum oxide grit (approximately 10-μm diameter particles), or polystyrene divinylbenzene (DVB) spheres (1-20-μm diameter particles). Neither the grit nor the polystyrene spheres were sieved before their use in experiments.

4.2.8.2 Oil Types

Four types of oil were used in experiments: 1) unweathered Prudhoe Bay crude oil, 2) 12-day weathered Prudhoe Bay crude oil, 3) unweathered No. 1 fuel oil and 4) naturally weathered North Slope crude oil. The 12-day weathered Prudhoe Bay crude was generated in an outdoor, flow-through seawater tank at the NOAA field laboratory at Kasitsna Bay. Discussions of the preparation, composition and rheological properties of this oil are presented in Payne et al. (1987b). The naturally weathered North Slope crude oil was supplied by Dr. Carol Ann Manen and was derived from oil released into Cook Inlet, AK following the grounding of the vessel R/T Glacier Bay near Kenai, AK in July 1987.

In addition to the different types of oil, varying quantities of a given oil type were also used in experiments. For example, quantities of un- weathered Prudhoe Bay crude oil used in the initial "blending" procedure (Section 4.2.4) included 4, 16, or 64 drops. As measured by FID-GC analyses of sample extracts (Section 4.2.7), the latter quantities of unweathered Prudhoe Bay crude oil (i.e., 4, 16, and 64 drops) resulted in oil concentration ranges in experimental solutions of 4-8, 8-44, and 80-105 mg/L, respectively. The quantities of 12-day weathered Prudhoe Bay crude oil used for the "blending" procedure included 6, 24, and 96 drops, which resulted in experimental oil concentrations of 14-26, 43-112, and 240-310 mg/L, respectively. All experi- ments performed with No. 1 fuel oil used 16 drops of oil in the blending proce- dure, which resulted in experimental oil concentrations of 7-48 mg/L.

4.2.8.3 Salinity

Experiments were performed at three general salinity levels: 1) full strength seawater (28-30 ppt), 2) 1:1 mixtures of seawater and freshwater (13-14 ppt) and 3) freshwater (0 ppt). All salinity determinations were made with a Reichert temperature-compensated refractometer.

4.2.8.4 Turbulence

A limited number of experiments were performed at varying energy dis-
sipation or turbulence levels in the stirred reaction vessel. As discussed in
Section 5.2.1, the energy dissipation rate for an experiment was estimated from
the volume of the reaction solution, the value for the kinematic viscosity of
the aqueous medium, and measurements for the torque and propeller shaft rpms
during the experiment.

4.3   SPM SETTLING VELOCITY EXPERIMENTS

Solutions of source material for all SPM settling velocity experiments
(i.e., both "oiled" and "unoiled" SPM) were obtained from stirred reaction ves-
sels at the conclusion of experiments used to generate whole-oil droplet/SPM
interaction rate constants (i.e., Section 4.2). Several advantages were de-
rived from this coupling of settling velocity experiments to oil/SPM interac-
tion rate studies. First, relatively well-defined prehistories were available
for "oiled" SPM particles used in the settling velocity experiments. For exam-
ple, information on variables contributing to the generation of "oiled" SPM
particles (e.g., types of SPM, types and quantities of oil, salinity and turbu-
lence levels in the stirred reaction vessels) as well as time-course changes in
number densities and sizes of SPM, "free" oil droplets, and oil/SPM
agglomerates during the stirred reaction experiment were available. And, sec-
ond, use of "oiled" SPM generated from a parent oil/SPM interaction rate study
provided for an efficient utilization of available experimental time (i.e.,
both oil droplet/SPM interaction rate constants and settling velocity
. information were generated from a common experiment).

4.3.1   Experimental Protocol for Settling Chamber Experiments

The protocol for the SPM settling velocity experiments involved minor
modifications of traditional pipette methods used for sediment particle-size
analyses (e.g., Siebert, 1979; Head, 1980; Allen, 1981). At the conclusion of a
stirred reaction vessel experiment (Section 4.2.5), the remaining oil droplet/
SPM/water solution in the stirred reaction vessel was homogeneously mixed.

89

One-liter volumes were transferred to each of three settling chambers (i.e., 1-L glass graduated cylinders). The cylinders were then maintained in undisturbed states. Sample volumes of 50 mL were withdrawn from a set depth in each settling chamber (18.5 cm below the initial air-water interface) at specified time intervals. Sampling times of 0 min, 20 min, 2 hr, 4 hr, 6 hr, 8 hr and 20 hr following the start of a settling experiment were chosen to provide sufficient resolution for SPM settling velocities. Following the final sample withdrawal at 20 hr, the air-water interface was only 4.1 cm above the depth from which the final sample was collected. All experiments were performed at room temperature, and care was taken to ensure that solution temperatures did not change during the time course of sample withdrawals from the settling chambers. For all of the experiments, water temperatures in settling chambers ranged from 17°-23°C.

Using previously described procedures for gravimetric measurements of SPM loads (Section 4.2.7), the 50-mL sample volumes withdrawn at specific sampling times from a settling chamber were vacuum-filtered onto tared polyester membrane filters and processed for their salt-free, oil-free SPM weight determinations. Mean values for SPM concentrations (i.e., mg dry weight/liter) from the three settling chambers in a given experiment were calculated for each sampling time. Values for mean settling velocities (i.e., distance settled/unit time) and the percent weight fractions of the total SPM load characterized by a particular mean settling velocity also were calculated using data collected for 1) mean distances between the air-water interface and the chamber sampling depth at a given sampling time, 2) time differences between sequential sampling events and 3) declines in gravimetric concentrations for SPM between sequential sampling events. Using procedures described in Section 4.2.6, photomicrographs were routinely taken for samples withdrawn from the settling chambers. With the protocol discussed in Section 4.2.7, oil loads were also determined from samples withdrawn from the settling chamber in one experiment to allow for temporal comparisons between measurements for SPM and oil loads.

In addition to experiments using "oiled" SPM, appropriate control experiments using "unoiled" SPM were performed. Parent solutions for the latter

control experiments were derived from "control" stirred reaction vessel experiments that had not received any additional oil.

4.3.2   Experimental Variables

To evaluate effects of certain variables on settling velocities of SPM, settling chamber experiments were performed with parent solutions obtained from selected stirred reaction vessel experiments. The settling experiments and their corresponding parent stirred reaction vessel solutions have been summarized in Table 4-1. Variables evaluated for potential effects on SPM settling velocities are discussed below in Sections 4.3.2.1 through 4.3.2.3.

4.3.2.1   Suspended Particulate Material (SPM) Types

Settling chamber experiments were performed with two types of SPM: Grewingk glacial till (<53 μm) and Yukon River Delta sediment (<53 μm). As discussed in Sections 5.1 and 5.3.2, these two SPM types encompassed the extremes in particle-size ranges for all sediment types investigated in this NOAA-sponsored program.

4.3.2.2   Oil Types

"Oiled" SPM used in settling chamber experiments were derived from parent stirred reaction vessel studies that utilized either unweathered Prudhoe Bay crude oil, 12-day weathered Prudhoe Bay crude oil, or unweathered No. 1 fuel oil. The SPM solutions for settling chamber experiments involving unweathered and 12-day weathered Prudhoe Bay crude oil were also derived from stirred reaction vessel experiments that utilized different amounts of the given oil type in the initial "blending" procedure (see Section 4.2.4). By using approximately the same amount of a given sediment type and varying the amount of "blended" oil in the stirred reaction vessel experiments, SPM with differing degrees of "oiling" was produced for the subsequent use in the settling chamber studies.

91

4.3.2.3 Salinity

Settling chamber experiments were performed with parent stirred reaction vessel solutions generated at three salinities: 1) full seawater (28-30 ppt), 2) 1:1 mixtures of seawater and freshwater (13-14 ppt), and 3) freshwater (0 ppt).

4.4   SPM/MOLECULAR SCALE INTERACTIONS

The interaction (sorption behavior) of SPM with petroleum hydrocarbons on the <u>molecular</u> scale was investigated through the development of Freundlich isotherms (H.J. Forwalt, et al., 1986; Calgon Corporation; Rohm and Haas Co.). This approach is useful because it provides the maximum adsorption capacity of the SPM tested for individual dissolved molecular compounds at a specified concentration in seawater. Thus, by conducting the tests with near-saturation levels of dissolved hydrocarbons, the upward boundary of molecular sorption values has been determined. In addition, the experimental procedure provided for a means to determine the partition coefficient, K_p (by difference only). A brief discussion of the Freundlich isotherm and experimental methods is followed in Section 5.4 by the results of experimentation using this technique.

For this particular application, the Freundlich isotherm is a plot of adsorbate (dissolved hydrocarbon) concentration in seawater versus the adsorbate concentration on the adsorbent (the SPM) at equilibrium. The general formula for the isotherm is:

$$X/M = K(C_f)^{1/n}$$

where $X = C_o - C_f$, which is the amount of dissolved hydrocarbon adsorbed from a given volume of seawater. M is the SPM dry weight; C_f is the amount of dissolved hydrocarbon remaining in the seawater after equilibration with the SPM; and K and 1/n are constants. A log-log plot of this equation (X/M vs C_f) yields a straight line that, when extrapolated to C_o, provides the equilibrium (maximum) adsorption capacity.

92

Because of the sheer number of compounds comprising crude oil, the models developed by SAIC to date have taken a "pseudocompound" approach. This approach adopts distillate cuts as manageable subsets of whole crude oil. For this same reason--to limit the vast number of compounds contained in whole crude to something manageable--determinations of molecular-scale interactions have relied on the distillate cut for convenient experimental material. The finite number of water-soluble compounds contained in a given cut can be easily handled in an isotherm experiment, yet still provide data that reflect the crude oil source.

Therefore, isotherms were developed for the soluble compounds contained in four distillate cuts of Prudhoe Bay crude oil using Grewingk glacial till and one cut using Turnagain Arm SPM and Yukon Delta sediment according to the following procedures. First, the distillate cut of interest was equilibrated over a 24- to 48-hr period with filtered (0.45 μm) seawater by carefully layering approximately 4 ml of the cut on approximately 2 L of seawater in a separatory funnel. The seawater, now containing the soluble cut components, is the initial (C_o) test liquor. Figure 4-8 depicts FID-GC chromatograms of the equilibrated seawater for the different cuts investigated. Cut selection was based on the desire to incorporate a wide molecular-weight range of soluble hydrocarbons. And, as seen, Cut #4 (210°-232°F) contains mainly volatile aromatics, while Cuts #7 (282°-304°F) and #10 (349°-368°F) impart intermediate and higher molecular weight aromatics respectively. There were only three soluble components imparted from the still pot bottoms (> 415°F).

For each batch test, a series of six 125 ml, amber glass, septa screw-capped bottles were dosed with varying amounts of SPM ranging from 0 to 10 g (on a dry weight basis). The C_o seawater was then dispensed through a pressurized in-line filter (to avoid including any oil micelles present) into each bottle and capped with no head space. The bottles were then agitated on a wrist-action shaker for 24-hr. All equilibrations were conducted at 26°C. Each sample was vacuum-filtered and the aqueous phase extracted 3 times with 25 mL of solvent. The solvent extracts were volume-reduced using standard Kuderna-Danish evaporation techniques and then analyzed by capillary FID-GC.
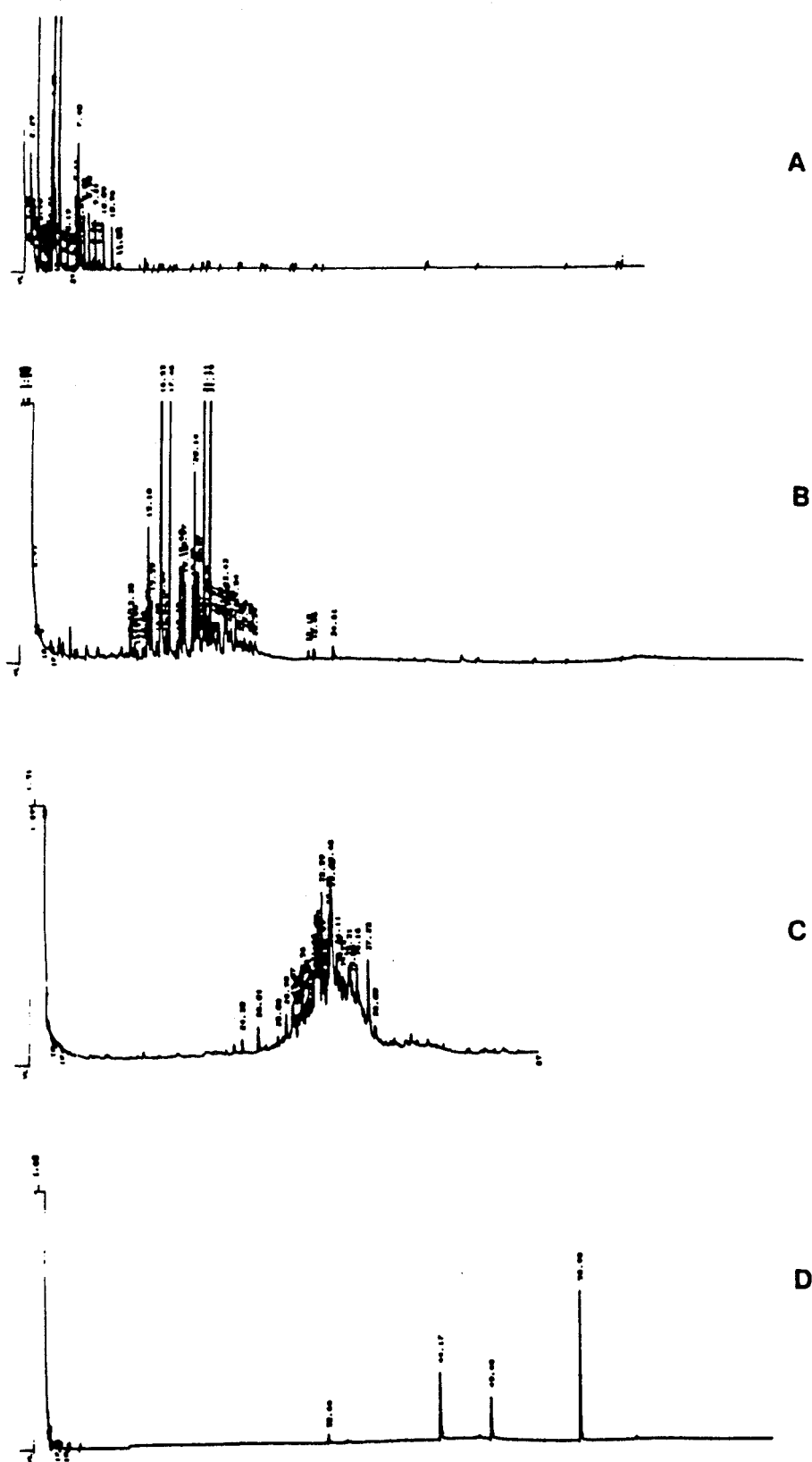
Figure 4-8. Chromatograms Depicting Initial (C₀) Seawater Equilibrations of A) Cut #4 (BP range 210°-232°F), B) Cut #7 (BP range 282°-304)°F, C) Cut #10 (BP range 349°-368°F), and D) bottoms (BP range 415°F and above)

94

K_p values were calculated from the individual component isotherm data by difference. In other words, the concentration of the compound adsorbed onto the SPM was determined by subtracting the mass measured in the aqueous phase from the mass contained in the initial (C_o) feed then dividing by the grams of dry SPM contained in the equilibration vessel. The K_p then is simply the concentration on the SPM divided by the concentration in solution (measured) at equilibrium. The results of both the isotherm development and the K_p determinations are provided in Section 5.4.

5.0   RESULTS AND DISCUSSION

5.1   SPM CHARACTERISTICS

In order to investigate oil/SPM interactions using representative, yet varied, SPM types, nine sediment/SPM sources from coastal regions in Alaska were sampled as described in Section 4.1. Each sediment or SPM type was characterized for a variety of physical and chemical parameters to evaluate the effect on oil/SPM interaction rates arising from differences in sediment or SPM properties. The physical characterization of the sediment or SPM types included grain-size distributions, particle-size characteristics and solids densities, while chemical characterizations included TOC analyses, hydrocarbon contents and mineralogical information.

Physical Properties

Photomicrographs of the eight natural sediment types and the Turnagain Arm SPM used for experiments are shown in Figure 5-1. The accompanying photograph of the micrometer allows for size estimates to be extrapolated for particles in each of the sediment and SPM prints. While all sediment particles were appropriately smaller than 53 μm (i.e., the sediments had been passed through a 53-μm geological sieve), great ranges in particle sizes can be observed not only among but also within particular sediment types. The greatest number densities for particles < 10 μm in diameter appear to occur in Grewingk glacial till, although high numbers are also present in the Beaufort Sea and Peard Bay sediment samples. While particles < 10 μm are present in all of the sediment types, larger particles approaching 50 μm in diameter are common in Yukon Delta sediment, Jakolof Bay sediment, Kotzebue sediment, Prudhoe Bay sediment, Beaufort Sea peat and the Turnagain Arm SPM. Biological contributions to the Jakolof Bay sediment and, particularly, the Beaufort Sea peat are in distinct evidence with the visible presence of diatoms.

The results of grain-size determinations on the sediment and SPM types by the pipette method are summarized in Table 5-1 and are illustrated in Figure 5-2. As indicated in the figure, a spectrum of particle sizes is present in

96
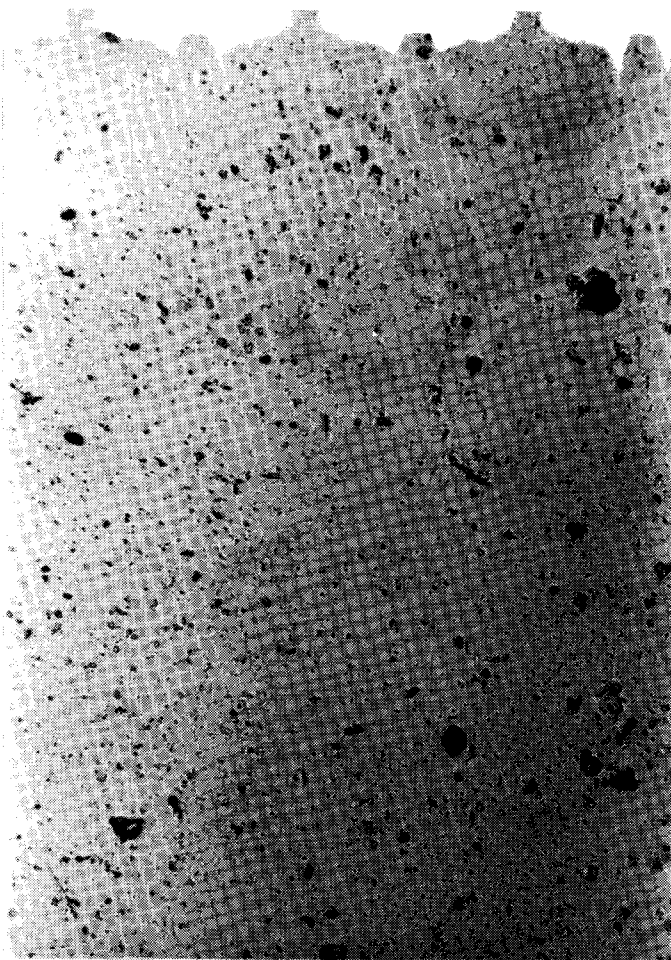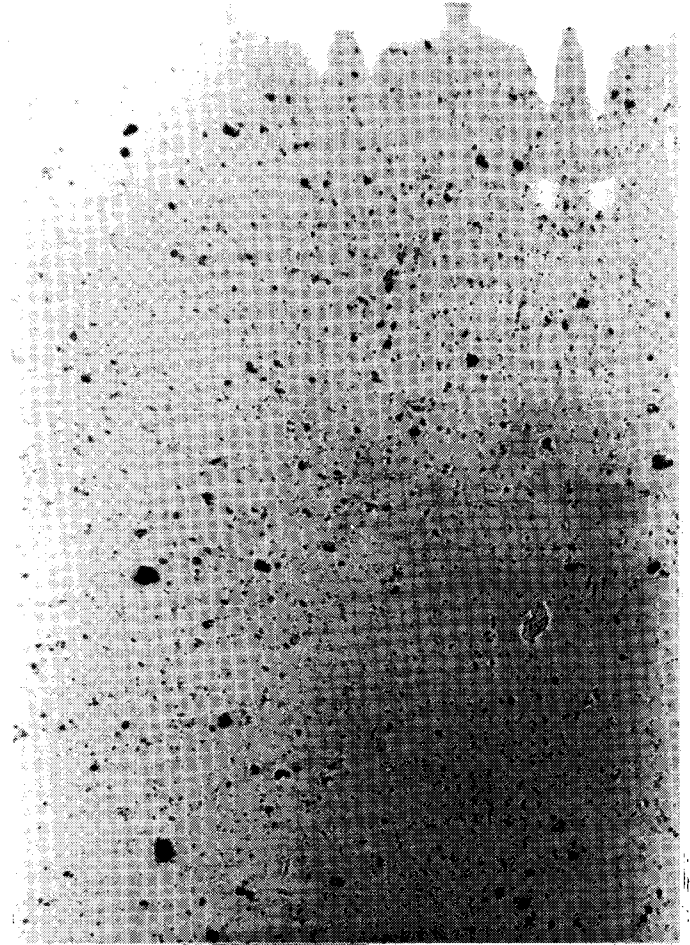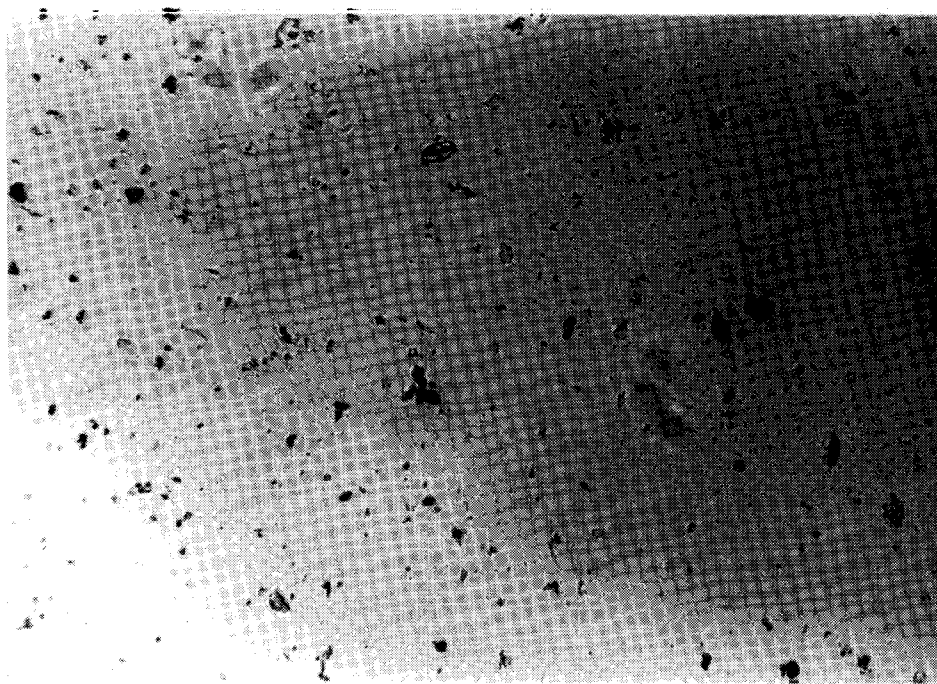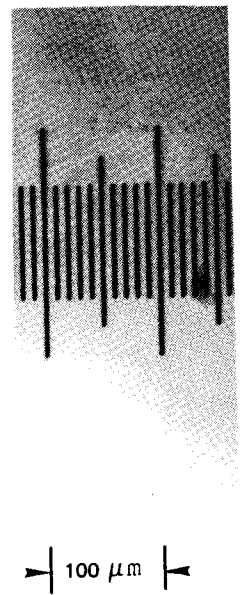
Figure 5-1. Photomicrographs of the Sediment/SPM Types used for Experimentation From A) Turnagain Arm, B) Beaufort Sea, C) Kotzebue, D) Grewingk Glacier, E) Peard Bay, F) Prudhoe Bay, G) Jakolof Bay, H), Yukon Delta, and I) Beaufort Sea (peat)

Figure 5-1. (Continued) Photomicrographs of the Sediment/SPM Types used for Experimentation From A) Turnagain Arm, B) Beaufort Sea, C) Kotzebue, D) Grewingk Glacier, E) Peard Bay, F) Prudhoe Bay, G) Jakolof Bay, H), Yukon Delta, and I) Beaufort Sea (peat)

98

G

H

I
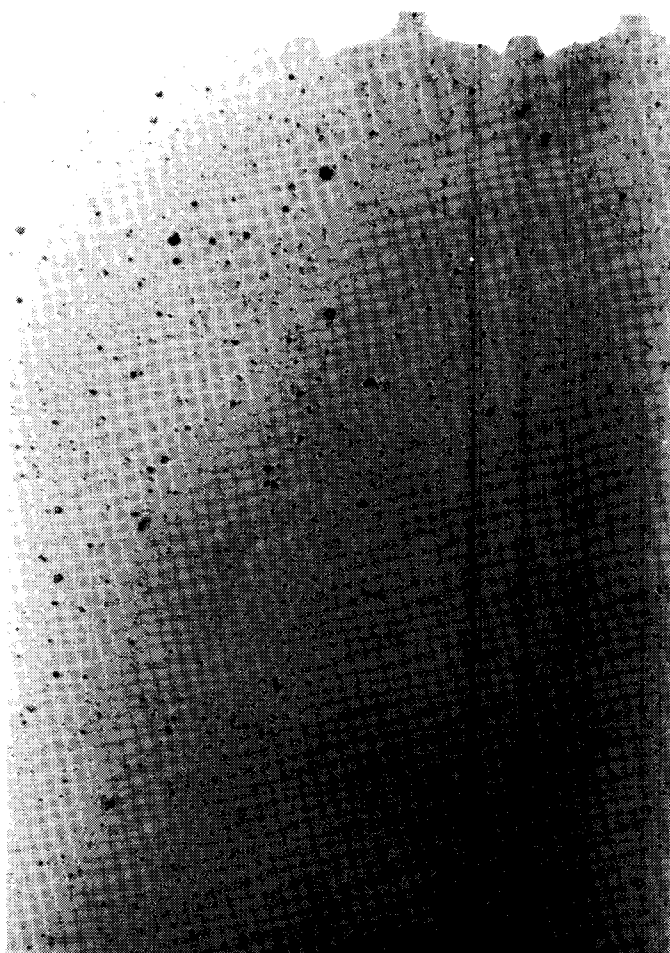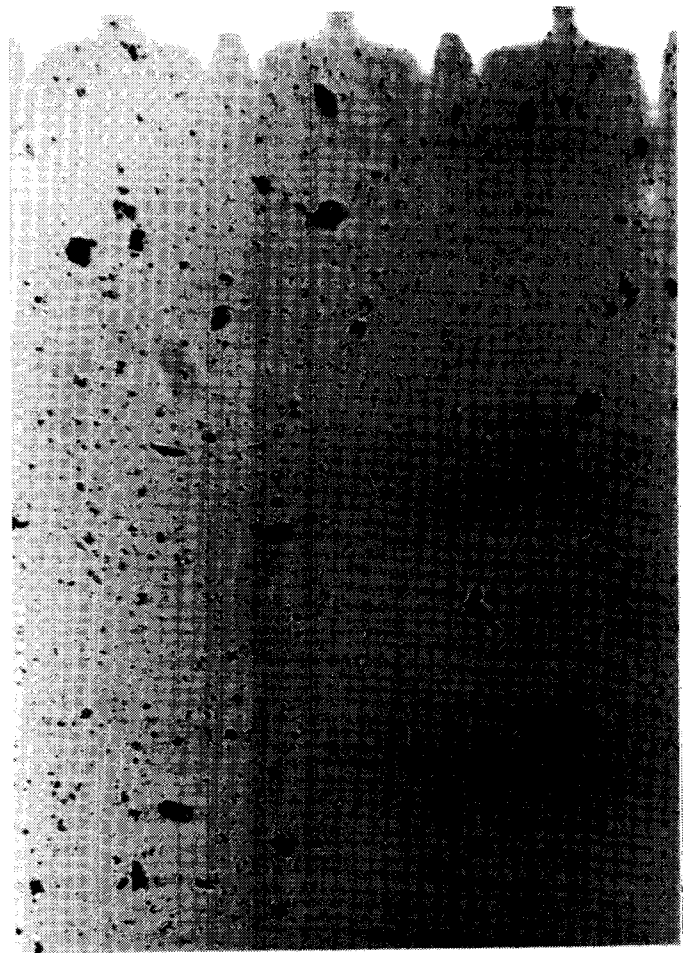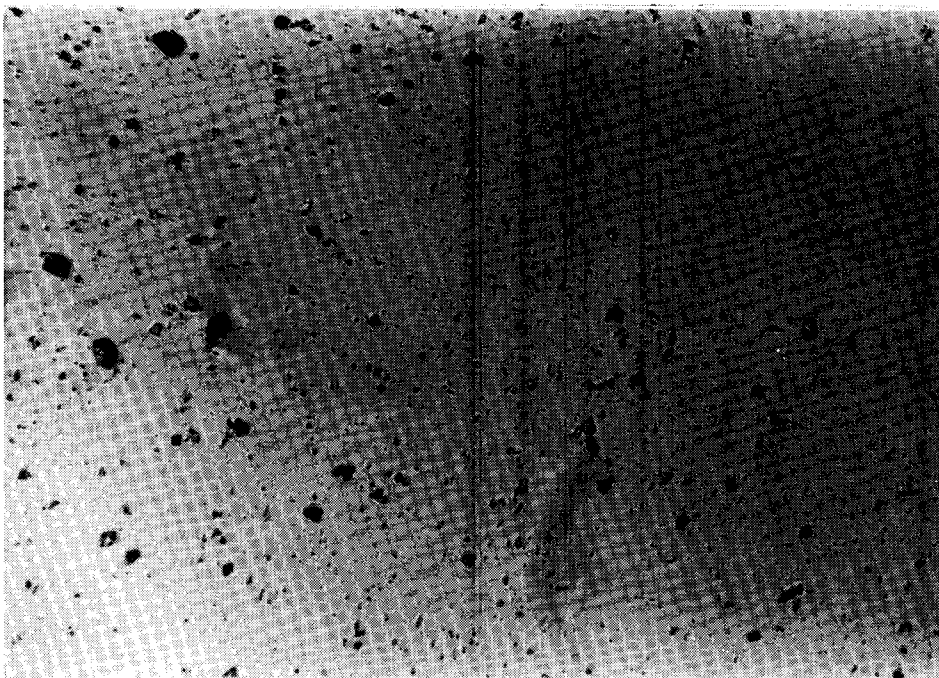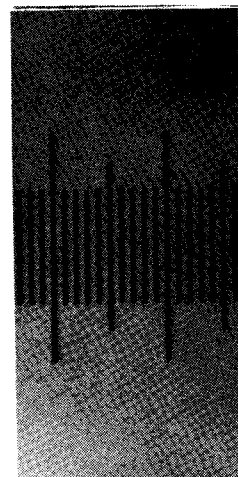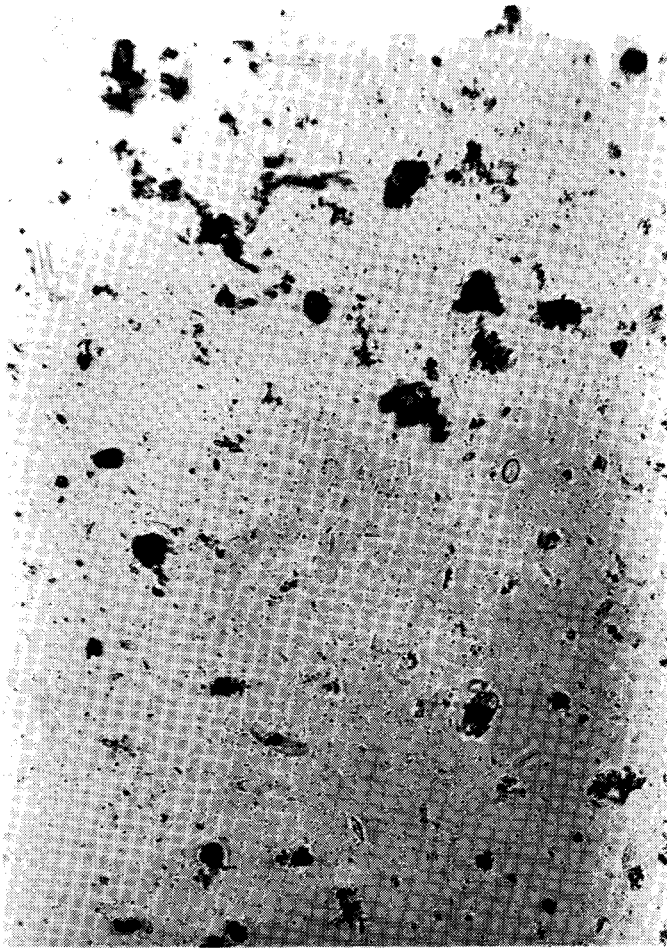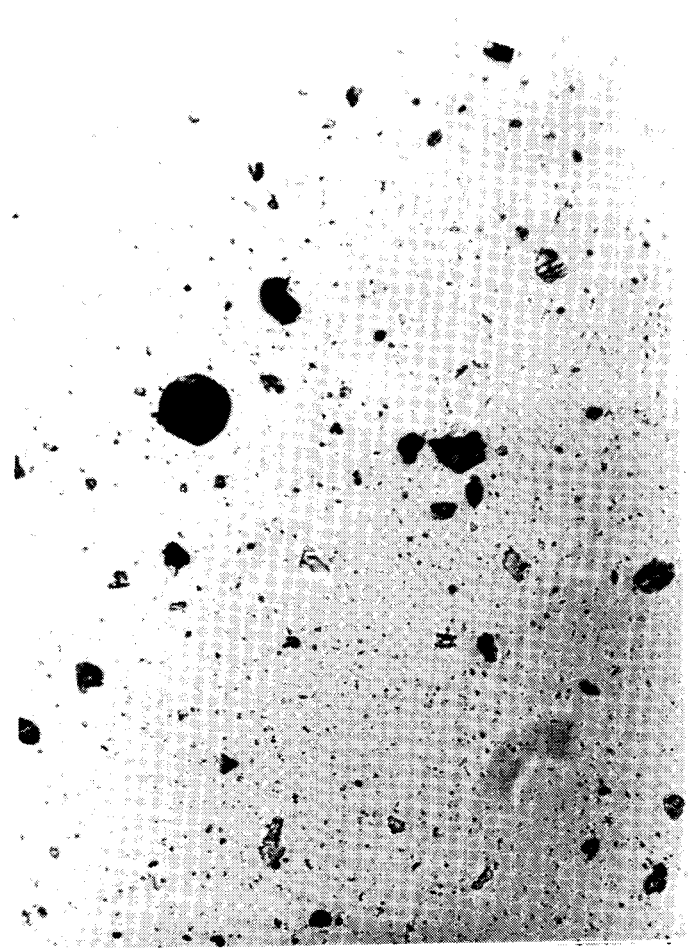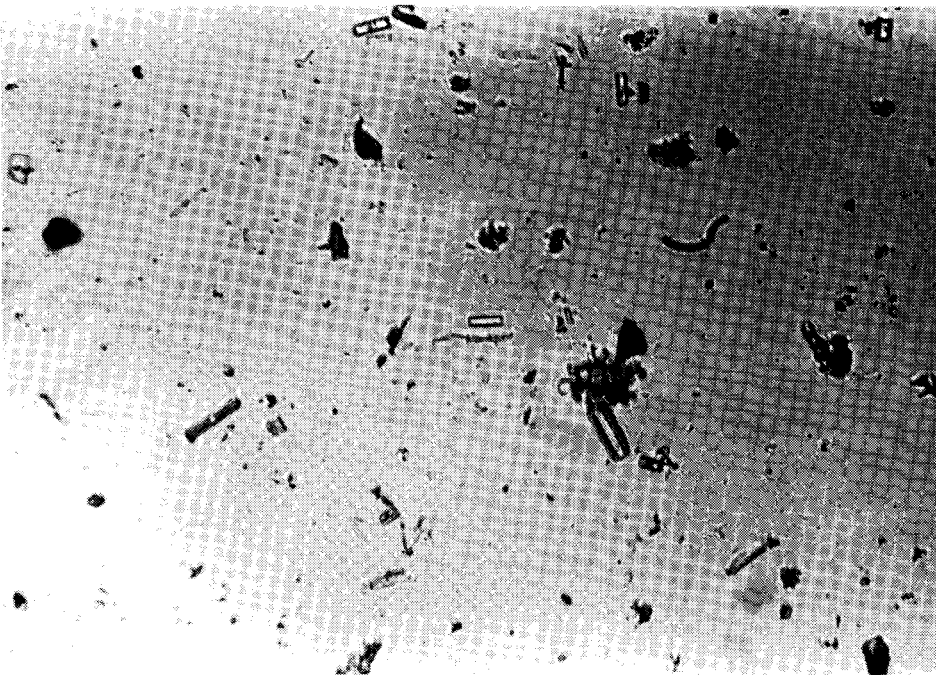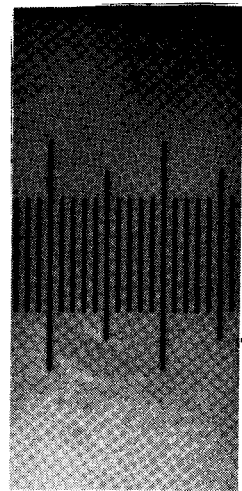
$\rightarrow$ | 100 μm | $\leftarrow$

Figure 5-1.   (Continued) Photomicrographs of the Sediment/SPM Types used for Experimentation From A) Turnagain Arm, B) Beaufort Sea, C) Kotzebue, D) Grewingk Glacier, E) Peard Bay, F) Prudhoe Bay, G) Jakolof Bay, H), Yukon Delta, and I) Beaufort Sea (peat)

Table 5-1

Grain-Size Distribution for Various Alaskan Marine Sediments

SPM Site[a]	SIZE INTERVAL WEIGHT PERCENTAGE (%)			
	0–2 μm	2–5 μm	5–20 μm	20–53 μm
Jakolof Bay	35.1	13.6	19.5	31.8
Peard Bay	43.8	16.8	29.8	9.6
Prudhoe Bay	22.7	11.1	35.6	30.6
Kotzebue	24.1	11.3	38.7	25.9
Turnagain Arm	10.5	3.8	11.1	74.6
Grewingk Glacier	51.6	26.6	18.6	3.2
Yukon Delta	6.9	1.6	14.4	77.1
Beaufort Sea	44.6	16.3	27.8	11.3

[a] all sediments were sieved to < 53 μm except for Turnagain Arm (see Section 4.1)

each of the sediment and SPM types. All of the size classifications display certain degrees of variation, but the 0-2 μm and 20-53 μm size classes show the greatest differences from sediment to sediment. The range in the fine fraction (0-2 μm) is from a low of 6.9% of the total sediment for Yukon Delta to a high of 51.6% for Grewingk glacial till. Other high percentages of fine fractions include Beaufort Sea sediment (44.6%), Peard Bay sediment (43.8%) and Jakolof Bay sediment (35.1%). As discussed in Section 4.1, all sediment phases (i.e., excluding the Turnagain Arm SPM) were sieved to < 53 μm prior to their use in experiments. Particle-size distributions in the Turnagain Arm SPM relative to the other sediment types yielded the second lowest percentage of fines and the second highest percentage in the 20-53 μm size class. The abundance of larger particles in the Turnagain Arm SPM reflects the high turbulence regime under which this SPM was collected in the field (see description of SPM sampling in Section 4.1).

Further information pertaining to sizes of particles contributing to the natural sediment and SPM phases was obtained from the photomicrographs and
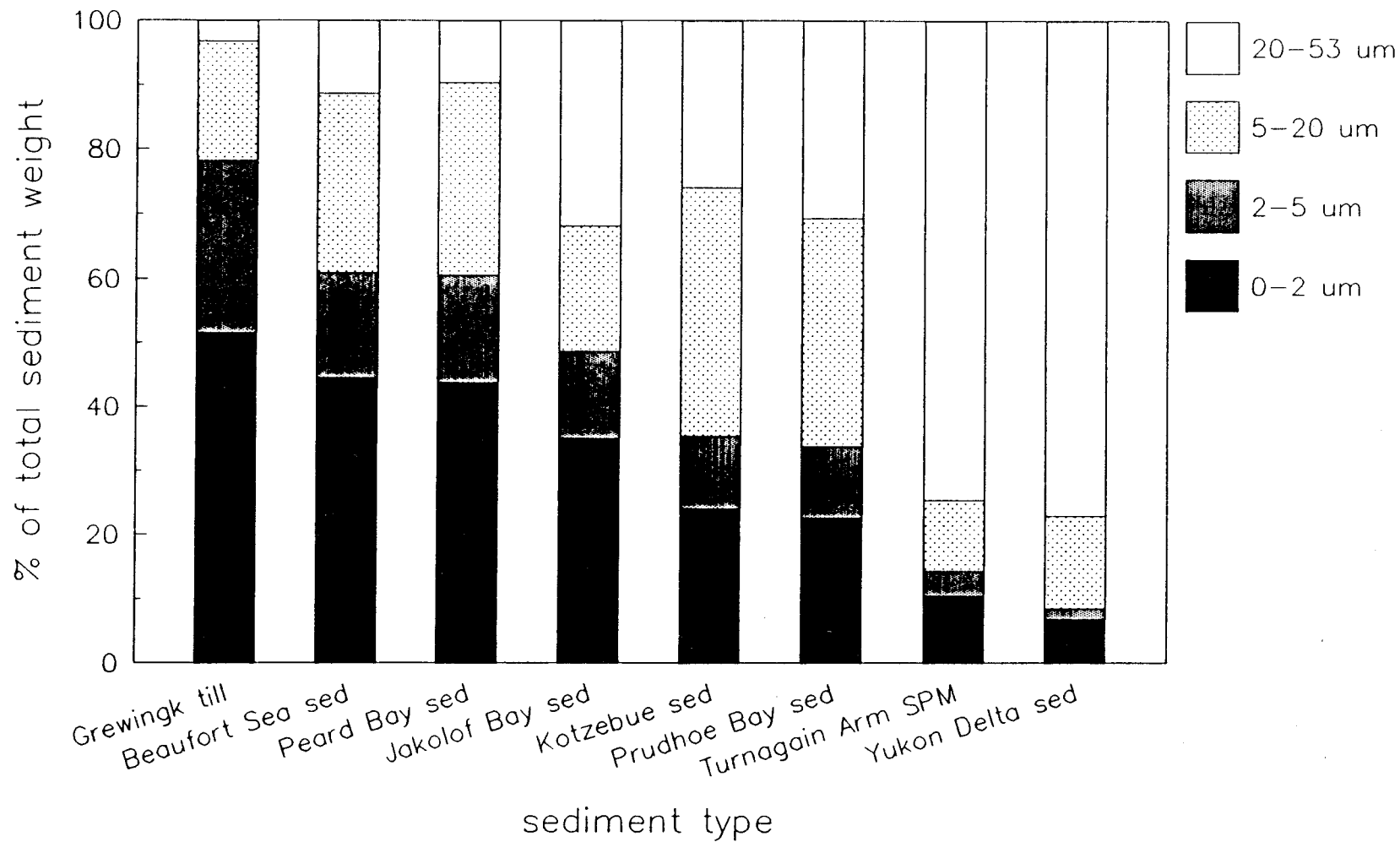
Figure 5-2. **Distributions of Total Sediment Weights in Different Particle-Size Classes for Sediment and SPM Types used in Whole-Oil Droplet/SPM Interaction and Settling Velocity Experiments**

gravimetric weight measurements of the various particle types in experimental suspensions. Number densities of particles per unit volume in solutions were determined from photomicrographs with the procedure described in Section 4.2.6. Gravimetric measurements of SPM loads per unit volume in the same solutions were made with the procedure described in Section 4.2.7. Utilization of data from these two measurements allowed for number densities of particles per unit mass to be determined for each sediment or SPM type. The results are summarized in Figure 5-3 for the eight natural sediments and one natural SPM type used in experiments. The relationships between particle number density and sediment mass for each of the sediment and SPM types is also illustrated in Figure 5-4. As evidenced in Figure 5-3, Grewingk glacial till showed the highest number density of particles per unit dry weight, while the Yukon Delta sediment exhibited the lowest. Because number densities per unit mass will be inversely related to the average size of particles, this information provides additional insight into the size spectra of particles comprising the various sediment and SPM types. From the information in Figures 5-2 and 5-4, Grewingk till was characterized by the greatest number of small particles, while Yukon Delta sediment was characterized by much higher abundances of larger particles. These trends are confirmed by the observations from the photomicrographs of the various sediment and SPM types (Figure 5-1).

The results of specific density determinations in the various sediment and SPM types are summarized in Table 5-2 and, for the most part, show expected trends. The lowest values (i.e., 2.51) were measured in Prudhoe Bay and Peard Bay sediments. The highest values were measured in Yukon Delta sediment and Grewingk glacial till (2.77 and 2.76, respectively). An insufficient amount of Jakolof Bay sediment was present to allow for a specific density measurement.

Chemical Properties

Tables 5-3 through 5-5 present the results of the chemical characterizations. Figure 5-5 presents FID chromatograms of background hydrocarbon compositions in each of the various types of sediment and SPM.

SEDIMENT TYPE:

Grewingk till (<53 um)

Beaufort Sea sed (<53 um)

Peard Bay sed (<53 um)

Turnagain Arm SPM

Prudhoe Bay sed (<53 um)

Jakolof Bay sed (<53 um)

Beaufort Sea peat (<53 um)

Kotzebue sed (<53 um)

Yukon Delta sed (<53 um)

0   20   40   60   80   100   120   140   160   180   200

NUMBER DENSITY (10^9 particles/g dry weight)
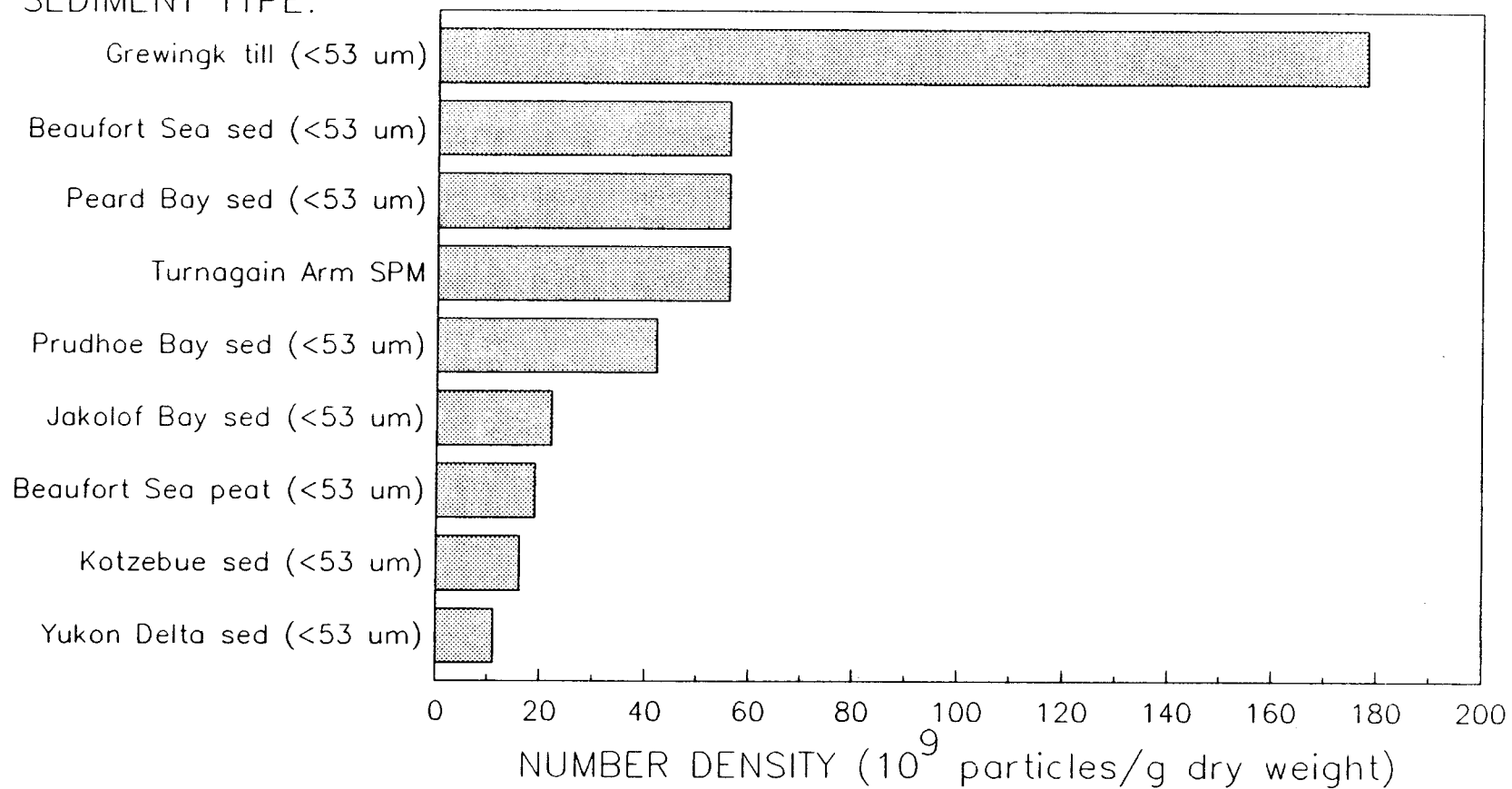
Figure 5-3.   **Particle Number Densities Per Unit Dry Weight for Sediment and SPM Types used in Whole-Oil Droplet/SPM Interaction and Settling Velocity Experiments**

103
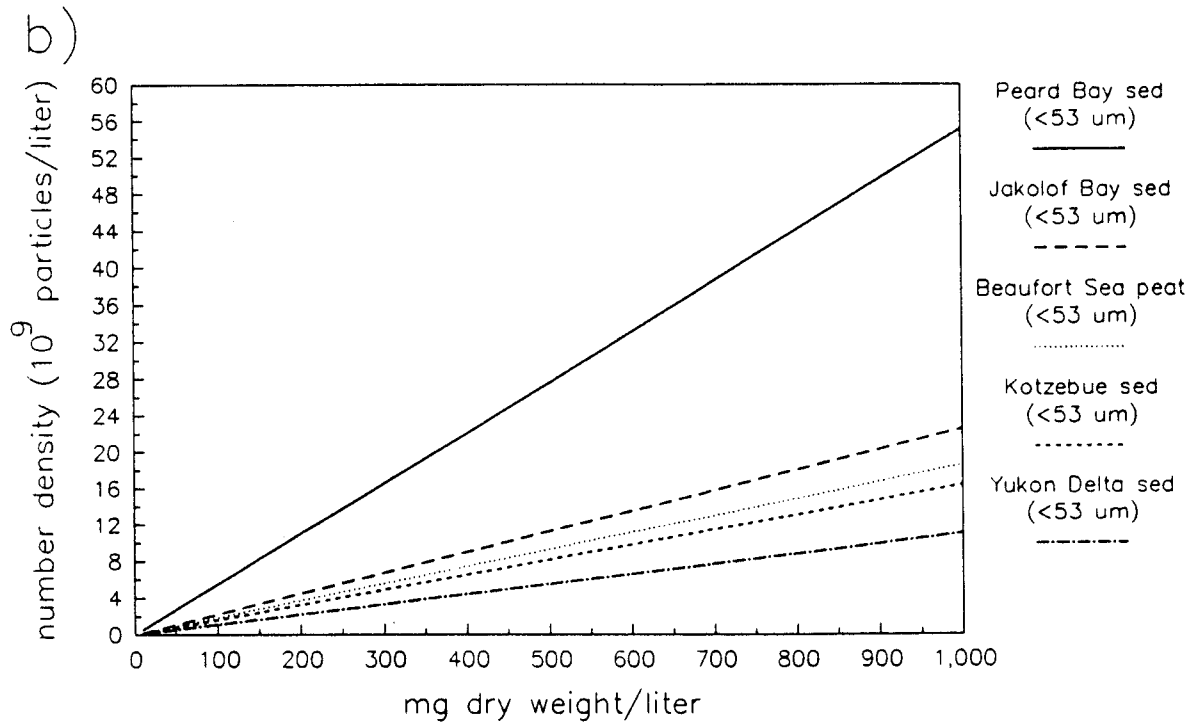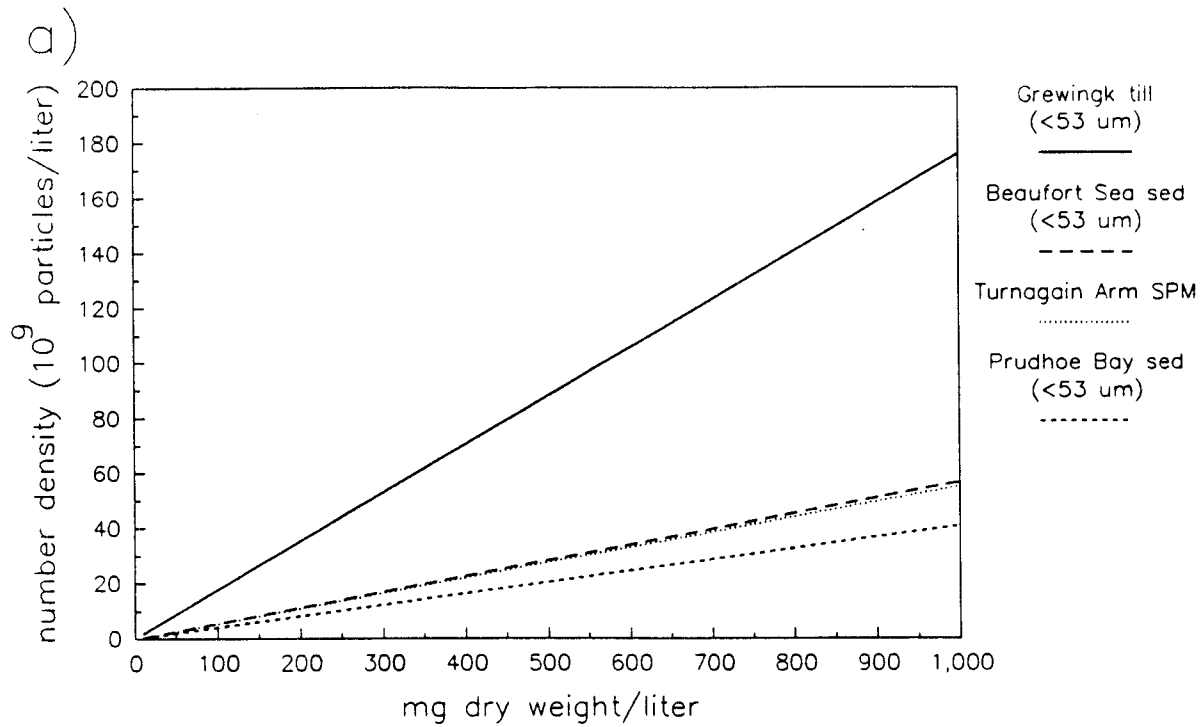
Figure 5-4. **Particle Number Densities Per Unit Volume Versus Dry Weight Per Unit Volume for Sediment and SPM Types Used in Whole-Oil Droplet/SPM Interaction and Settling Velocity Experiments**

104

Table 5-2

Solids Density of Various Alaskan Marine Sediments

SPM Site	Density (g/cm^3)
Yukon Delta	2.77
Peard Bay	2.51
Turnagain Arm	2.64
Beaufort Sea	2.55
Prudhoe Bay	2.51
Kotzebue	2.70
Grewingk Glacier	2.76
Jakolof Bay	NA[a]

[a] not analyzed due to insufficient sample

Table 5-3

Total Organic Carbon (TOC) Concentrations for Various Alaskan Marine Sediments

SPM Site	TOC Concentration (µg/g)[a]
Turnagain Arm (Rep 1)	3,960
Turnagain Arm (Rep 2)	5,340
Grewingk Glacier	2,050
Beaufort Sea	6,150
Prudhoe Bay (Rep 1)	14,700
Prudhoe Bay (Rep 2)	13,700
Kotzebue (Rep 1)	7,510
Kotzebue (Rep 2)	7,630
Peard Bay	11,500
Yukon Delta (Rep 1)	5,470
Yukon Delta (Rep 2)	5,220
Jakolof Bay	6,490

[a] based on sample dry weights

Table 5-4

Background Hydrocarbon Content of Various Alaskan Marine Sediments

SPM Site	Total Resolved Hydrocarbon Concentration (mg/g)[a]
Turnagain Arm	3.4
Grewingk Glacier (Rep 1)	2.2
Grewingk Glacier (Rep 2)	1.2
Beaufort Sea	8.3
Prudhoe Bay	26
Kotzebue	43
Peard Bay	18
Yukon Delta (Rep 1)	0.05
Yukon Delta (Rep 2)	0.05
Peat	78
Jakolof Bay	862

[a] based on sample dry weights

Table 5-5

Summary of the X-Ray Diffraction Mineralogy

Sample	Alpha-Quartz	Feldspar	Chlorite	Illite	Kaolite	Other
Beaufort Sea	Major	Minor+	Minor+	Minor+	Intermediate	—
Jakolof	Major	Intermediate	Minor	Trace	Minor	—
Peard Bay	Major	Minor	Minor+	Minor-	Minor	Olivine?
Prudhoe Bay	Major	Minor+	Minor	Minor+	Minor+	Calcite (Intermediate) Dolomite (Minor+)
Kotzebue	Major	Intermediate	Intermediate	Minor+	Minor	Olivine?

Sample	Alpha-Quartz	Feldspar	Chlorite	Mica	Other
Turnagain	Major	Intermediate+	Minor	Minor	Hornblende (Minor)
Yukon	Major	Intermediate+	Trace?	Trace	Sanadine/Microcline (Intermediate)
Grewingk	Major	Intermediate+	Minor+	Trace	Hornblende (Trace)
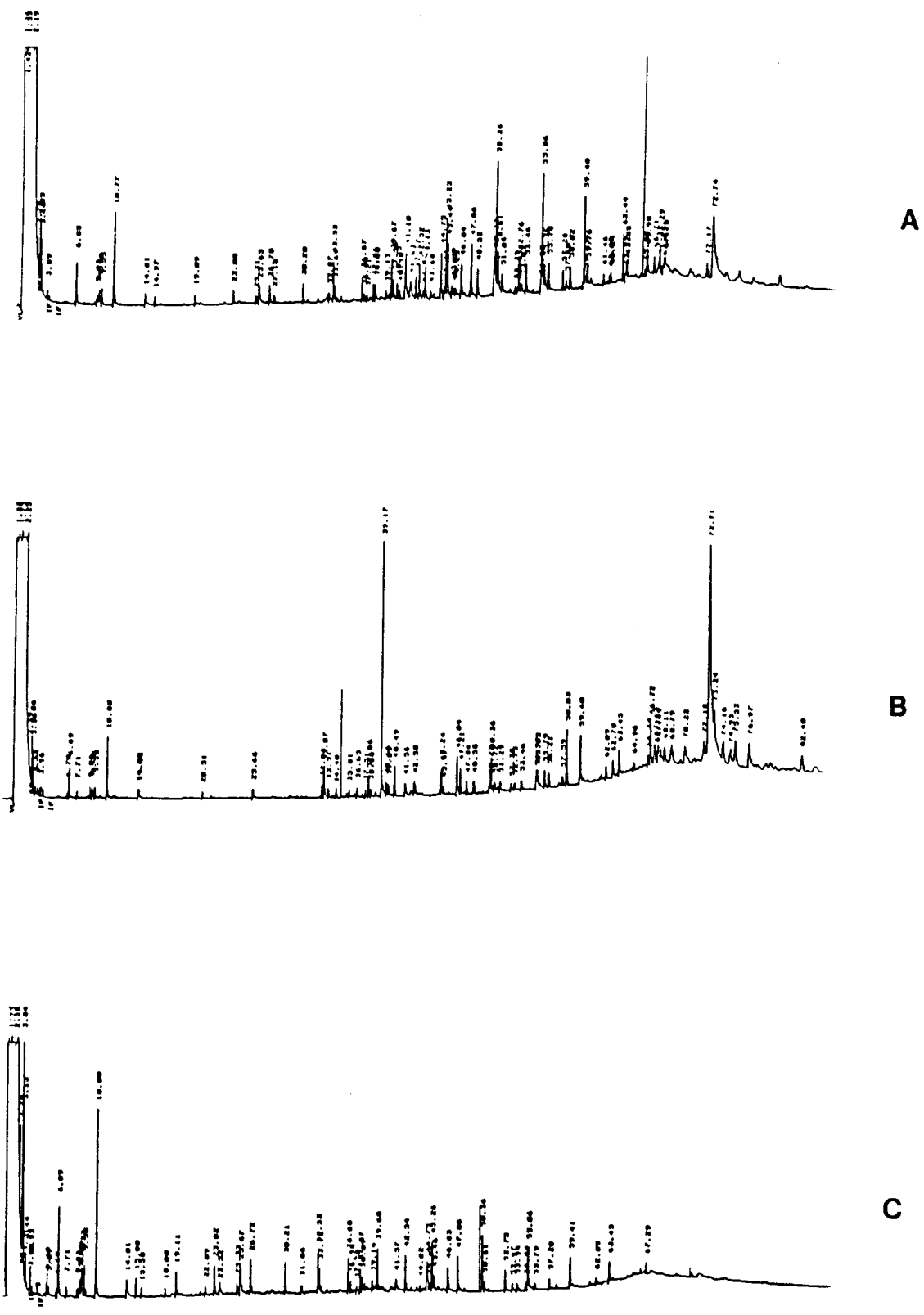
Figure 5-5.   GC/FID Chromatograms Depicting: A) Prudhoe Bay sediment, B) Beaufort Sea
sediment, and C) Beaufort Sea peat

107

Figure 5-5. (Continued) GC/FID Chromatograms Depicting: A) Prudhoe Bay sediment, B) Beaufort Sea sediment, and C) Beaufort Sea peat

108

G

H

Figure 5-5. (Continued) GC/FID Chromatograms Depicting: A) Prudhoe Bay sediment, B) Beaufort Sea sediment, and C) Beaufort Sea peat

109
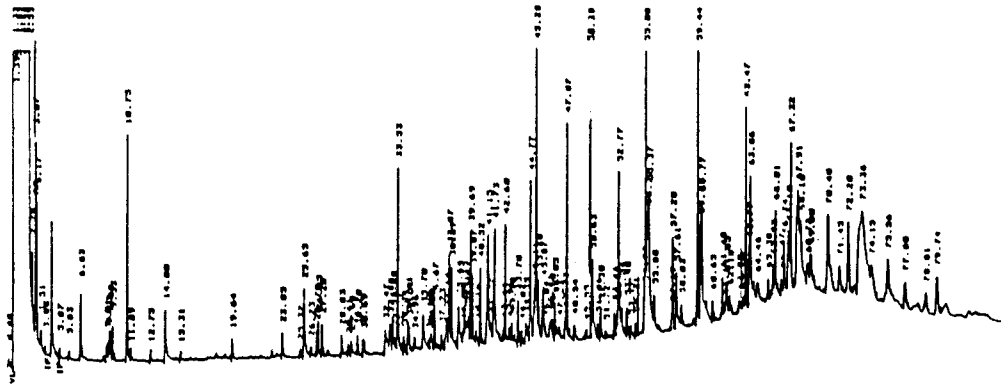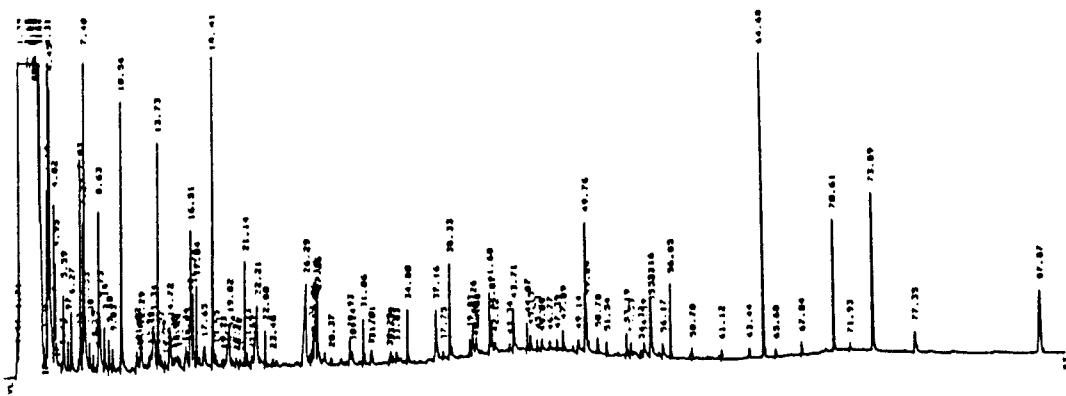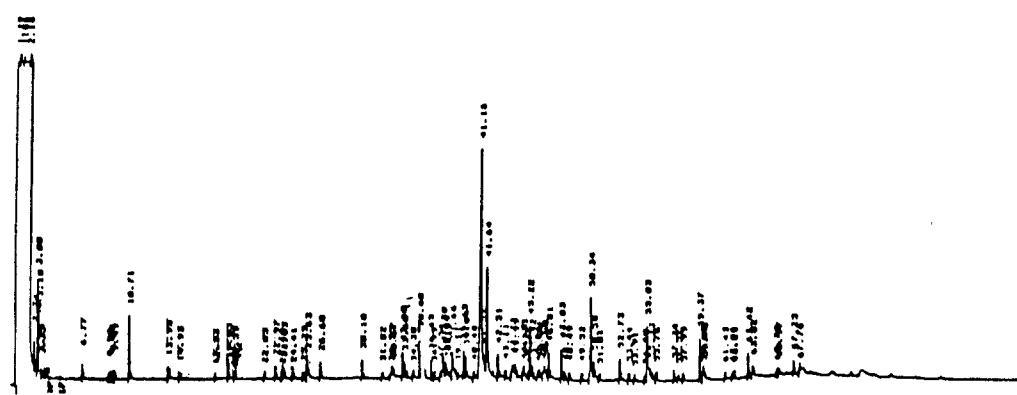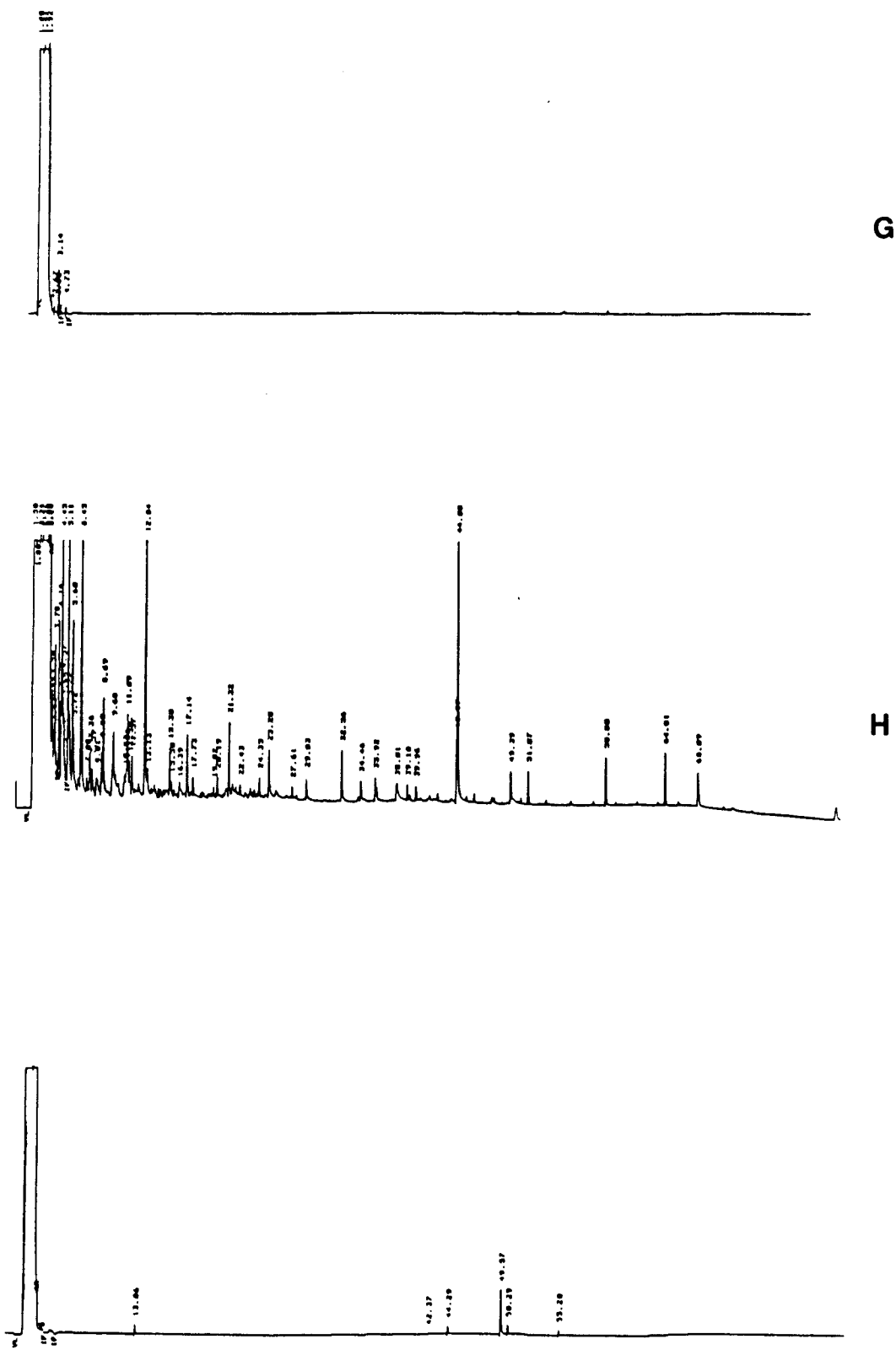
The results of TOC analyses (Table 5-3) show relatively little variation among the eight sediment and SPM types in the table. The values range from a low of 2050 μg/g dry weight for Grewingk glacial till to a high of 14,200 μg/g dry weight for Prudhoe Bay sediment. With the exception of Peard Bay sediment at 11,500 μg/g, the remaining five sample TOC levels fall roughly between 4500 and 7500 μg/g. These levels are in agreement with recently published statistical review of surface sediment contaminant levels (Bronson, 1988) that calculates a geometric mean of 5635 μg TOC/g dry weight for 48 sediment samples collected from the northern Bering Sea.

Much greater variation between the sediment and SPM types is seen in Table 5-4 and Figure 5-5 for hydrocarbon contents. In this case, the levels of background hydrocarbons range from extremely low concentrations for Yukon Delta sediment (< 0.05 μg/g) to high concentrations for Jakolof Bay sediment (862 μg/g). The FID chromatograms in Figure 5-5 show a noteworthy absence of hydrocarbon peaks in both the Yukon Delta sediment and the Grewingk glacial till. Most of the other profiles show a predominance of odd carbon n-alkanes that are either skewed toward the heavier molecular-weight end (i.e., Prudhoe Bay, Beaufort Sea and Kotzebue sediment samples) or are more evenly distributed in the Beaufort Sea peat, the Jakolof Bay and Peard Bay sediments, and the Turnagain Arm SPM. In the previously mentioned statistical review (Kaplan, et al., 1979 and 1980), the raw data show tabularized results of detailed hydrocarbon analyses of Norton Sound sediments. The latter data also reflect a higher degree of variability in hydrocarbon levels from different sediment sources as opposed to the corresponding variability in TOC concentrations.

Complete results of the sediment and SPM mineral content as determined by X-ray diffraction (including strip-chart recordings and a discussion of the results) are provided in Appendix C. The results are summarized in Table 5-5. As indicated in the table, alpha-quartz is the major constituent in all of the sediment and SPM types. Feldspar accounts for intermediate amounts in five of the eight samples and minor amounts in the remaining three samples. Intermediate amounts of the following minerals were found: kaolinite in Beaufort Sea sediment, calcite in Prudhoe Bay sediment, chlorite in Kotzebue sediment, and

110

sanadine/microcline in Yukon Delta sediment. Minor and/or trace amounts of mica, hornblend, illite, and dolomite were detected in certain samples.

From the information pertaining to the above physical and chemical properties, it appears that the eight sediments and one SPM type selected for oil/SPM interaction studies are sufficiently varied, while still being representative of coastal Alaskan sedimentary or SPM types. Because of the time-consuming nature and logistical problems associated with the collection of large volumes of natural SPM, most of the oil droplet/SPM interaction experiments were conducted with the sieved, natural sediment types. However, in order to evaluate the possibility of an introduced bias resulting from the use of sieved sediments as opposed to true natural SPM, one in situ SPM type was collected from Turnagain Arm and used in certain experiments. The results of the above physical and chemical property determinations indicate that no inherent disparities in properties occurred between the Turnagain Arm SPM and the various sediment types. Consequently, comparisons of experimental results using the sieved natural sediments with those of the one true SPM (i.e., Turnagain Arm) appear to be appropriate and valid.

5.2   WHOLE-OIL DROPLET/SPM INTERACTION KINETICS

The derivation and pertinent characteristics of algorithms central to the mathematical models developed for this program (i.e., the oil droplet model with excess SPM, the SPM model, and the oil droplet and SPM model) are discussed in Section 3.2. The major objective of laboratory experimental efforts to evaluate interaction kinetics between whole-oil droplets and suspended sedimentary materials for the models was to derive values for the "lumped" reaction coefficient α_c (i.e., the rate constant for removal of "free" oil droplets due to reaction with SPM particles). Effects of variations in a number of pertinent environmental variables (i.e., sediment or SPM type, quantity and type of oil, salinity, and turbulence level) upon values of α_c were investigated. In the end, values for α_c in the context of realistic variations in the environmental variables of interest can be used in the corresponding mass balance equations in the models in Section 3.2.

111

5.2.1   Conceptual Approach

The experimental approach used to investigate interactions between whole oil droplets and SPM is described in detail in Section 4.2. The major effort of the approach involved documentation and quantitation of declines in number densities of "free" oil droplets (i.e., oil droplets that had not reacted with SPM) over time in turbulent reaction solutions containing oil droplets and SPM. A prerequisite for the implementation of the experimental approach that was used required that number densities of SPM particles be substantially in excess of those for "free" oil droplets. As noted in Section 4.2.5, ratios of number densities of SPM to oil droplets at the start of all experiments were always > 3. The initial equation for analyzing data from the oil droplet/SPM interaction experiments is

$$C = C_0 e^{(-k)t} \quad \text{or} \quad \ln(C/C_0) = -kt$$

where C is the number density of "free" oil droplets at time t, C_0 is the number density at time t_0, and k is the reaction rate constant describing the decline in "free" oil droplets over time. Values for k were calculated from least-squares fits of the "free" oil droplet data to the above equation(s). Although the stirred reaction vessel experiments were routinely conducted for 25 min the interaction rate constants (k) were only determined for data from the first 15 min of reactions. In the context of the experimental approach in Section 4.2.5, the units for k were reciprocal minutes.

The rate constant k can also be described by the equation

$$k = \alpha(\epsilon/\upsilon)^{1/2}S$$

where S is the (excess) SPM concentration in the experimental reaction solution, ϵ is the energy dissipated per unit mass of water per unit time, υ is the kinematic viscosity of the aqueous medium and α is the "lumped" reaction coefficient taking into account not only geometric factors such as heterogeneous size distributions of the oil droplets and SPM but also the "sticking" factor between oil droplets and SPM. Determinations of values for the "lumped"

112

reaction coefficient α were the primary purpose of the laboratory experiments summarized in this section of this report.

In addition to the oil droplet number density data that allowed for calculations of values for k, necessary information for the following parameters was also recorded for specific experiments:

1) torque (τ) in ounce(force)-inches,

2) propeller speed (w) in revolutions per minute (rpm),

3) the total SPM concentration (S) in mg dry wt/L, and

4) the total solution volume (V) in the stirred reaction vessel.

The values for these five essential items (i.e., k, τ, w, S and V) were then used to calculate the following parameters:

1) energy dissipation (E) in ergs/sec,

2) $(\epsilon/\upsilon)^{1/2}$, and

3) α in units of cm^3/g.

The value for energy dissipated per unit time by the rotating propeller was calculated as follows:

$$E \text{ in ergs/sec} = (w \text{ rpm})(\tau \text{ ounce-inches})(7400)$$

where the number 7400 takes into account unit conversion factors. The energy dissipated per unit time per unit mass by the rotating propeller is then calculated as:

$$\epsilon \text{ in ergs/g-sec} = (E \text{ in ergs/sec})(V \text{ in liters})(1000)$$

where 1000 is again a necessary unit conversion factor. When the values for k are converted to units of sec^{-1} and SPM concentrations (S) are converted to units of g/cm^3, the "lumped" reaction coefficient of interest (α) can be calculated for a particular reaction vessel solution using an appropriate value for

113

the kinematic viscosity (v) of the reaction medium (i.e., 0.01 cm^2/sec for experiments performed in this report). The value for α is calculated as:

$$\alpha = k/[(\epsilon/\upsilon)^{1/2}S].$$

For the purpose of demonstrating the end result of deriving pertinent values for α, consider the following values:

1) torque (τ) = 0.5 ounce-inch

2) propeller speed (w) = 400 rpm

3) slope of "free" oil droplet number density data (k) = -0.10 min^{-1}

4) SPM concentration (S) = 100 mg dry wt/L, and

5) reaction solution volume (V) = 3.5 L.

Carrying through the calculations with these "experimental" values as an example, one derives a value of 0.081 cm^3/g for the "lumped" reaction coefficient α.

It should be noted that the coefficient α is not used directly in the material balance equations described in Section 3. The appropriate reaction term actually appears in the mathematical derivations as either $\alpha_c C$ when SPM is in excess or $\alpha_c CS$ when SPM is not in excess. In either instance, values for α_c are typically in units of g/cm^3-sec. Thus, in the case where SPM is in excess,

$$\alpha_c = \alpha(\epsilon/\upsilon)^{1/2}S,$$

which is the same form used for the experimental measurements made in this program (i.e., see protocol described in Section 4.2.5 and results summarized in Section 5.2.2). When SPM is not in excess, the reaction coefficient is described by the equation:

$$\alpha_c = \alpha(\epsilon/\upsilon)^{1/2}.$$

If values for the SPM concentration (S) of 1 g/L (i.e., 0.001 g/cm^3) and $(\epsilon/\upsilon)^{1/2}$=10 sec^{-1} are used in a situation where the SPM is in excess, then the value for the reaction coefficient becomes:

$$\alpha_c - (0.081 \text{ cm}^3/\text{g})(10 \text{ sec}^{-1})(0.001 \text{ g/cm}^3) - 0.00081 \text{ sec}^{-1}.$$

Thus, the value for the term $\alpha_c C$ in material balance calculations has units of g/cm^3-sec, which are the same as those for dC/dt. At the same time, the value for α_c becomes the following if SPM is not in excess:

$$\alpha_c - 0.81 \text{ cm}^3/\text{g-sec}.$$

The preceding calculations are presented as examples of "experimentally" derived rate constants or coefficients that could be used in the appropriate algorithms for the computer code models described in Sections 3.2 and 6 (i.e., OILSPMXS if the SPM is in excess and OILSPM3 if SPM is not in excess in Section 6).

5.2.2   Experimentally Derived Whole-Oil Droplet-SPM Interaction Rate Constants

As indicated previously in Table 4-1, a large number of laboratory experiments were performed to obtain values for whole-oil droplet-SPM interaction rate constants. To provide environmental relevance to results that could then be used in the model codes discussed in Sections 3.2 and 6, the laboratory experiments intentionally incorporated variations in a number of pertinent environmental parameters, including SPM types, quantities and types of oil, salinity and turbulence levels.

As noted in Section 4.2, photomicrography played an integral part in the studies of oil droplet/SPM interactions. Examples of photomicrographs obtained from experiments are illustrated in Figure 5-6. The figure contains prints for 1) dispersed oil droplets, 2) unreacted or "unoiled" Grewingk glacial till and 3) oil/SPM agglomerates following interaction between the till and oil droplets. The latter photograph illustrates that the oil droplets could become "coated" with SPM following interactions between the two phases.
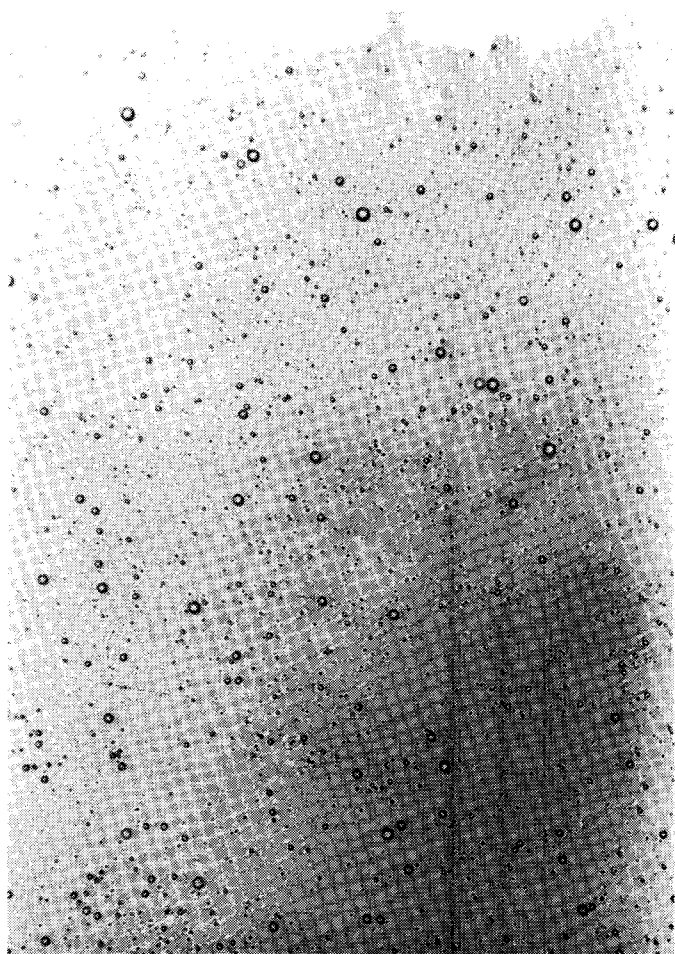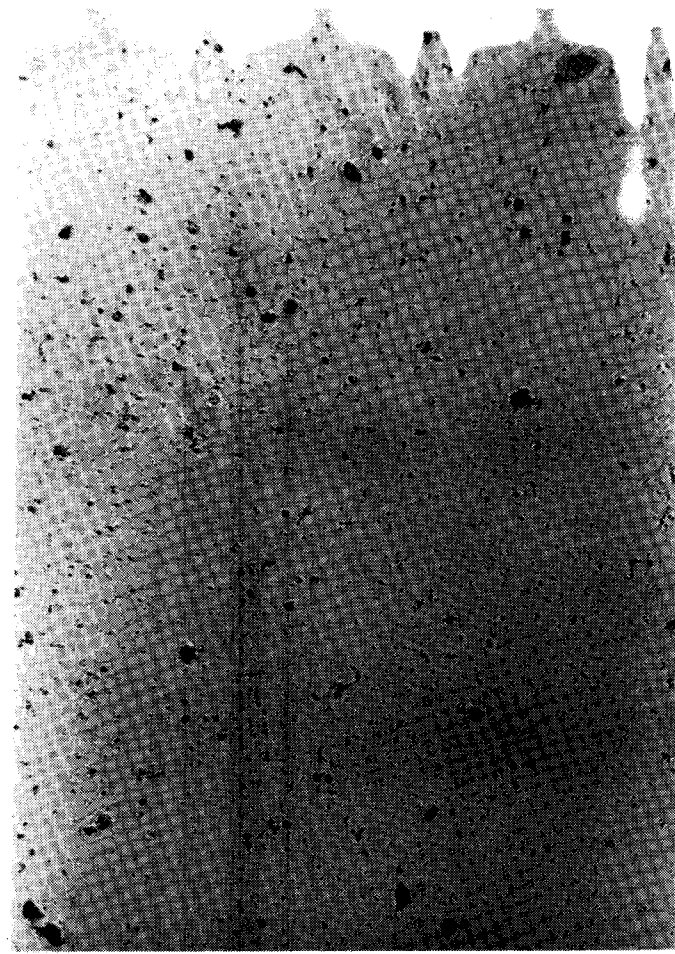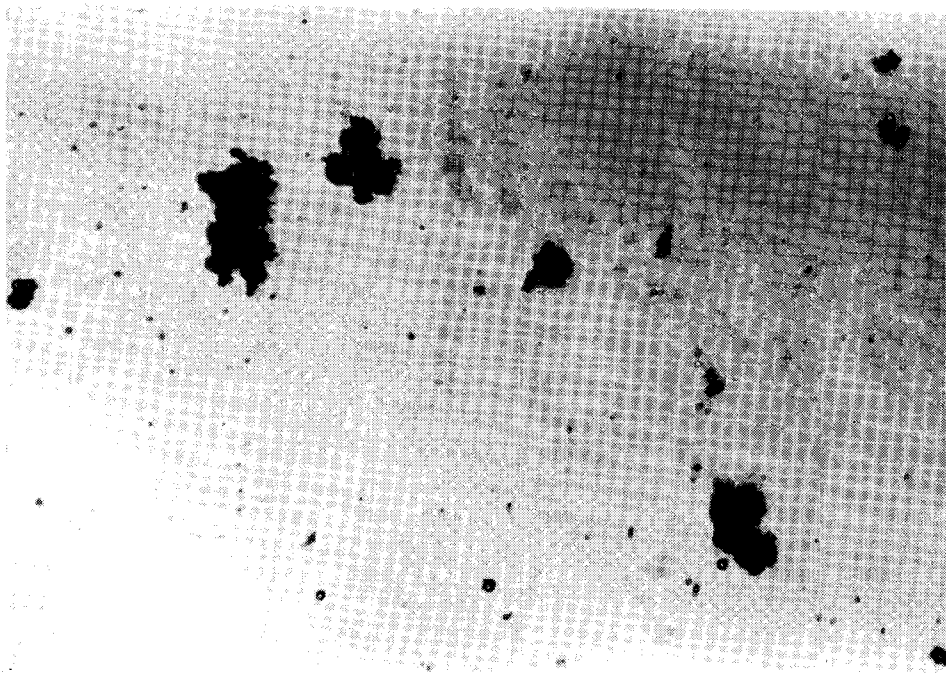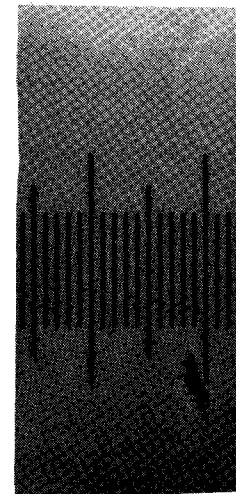
Figure 5-6. Examples of Photomicrographs from Reaction Rate Determination Experiments Showing the A) oil droplet component, B) the SPM component, and C) the oil-SPM agglomerates

Furthermore, the focal plane of the microscope for the photograph of the oil/SPM agglomerates (i.e., Figure 5-6c) was the same as that for the unreacted till (Figure 5-6b). Consequently, the oil/SPM agglomerates tended to sink in the water column (i.e., they behaved like unreacted SPM in this sense). Should comparable oil/SPM agglomerates be formed in real-world situations, their behavior would tend to favor transfer of oil to benthic environments.

Quantitation of interactions between whole oil droplets and SPM was done by determining changes in number densities of "free" oil droplets over time in photomicrographs from a given stirred reaction vessel experiment. The number density data for the oil droplet counts were subsequently transformed to their natural logarithm equivalents and a linear-regression line fitted to the data. Equations describing changes in number densities of "free" oil droplets are the following:

$$C = C_0 e^{k(t)} \quad \text{or} \quad \ln(C) = \ln(C_0) + (k)t$$

where C and C_0 are numbers of "free" oil droplets per photomicrograph at times t and t_0, respectively, and k is the rate constant describing the change in the number density of the droplets over time. A typical illustration of data generated by this approach is presented in Figure 5-7. Number density data in the figure are shown for two experiments: 1) a reaction vessel containing unweathered Prudhoe Bay crude oil and Yukon Delta sediment that had been sieved to < 53 μm and 2) the corresponding control experiment that contained unweathered Prudhoe Bay crude, but no SPM. In the absence of any reaction between "free" oil droplets and SPM, there should be no change in the number density of oil droplets over time. This is shown in the figure for the control experiment that had no SPM. In contrast, a logarithmic decline in the number densities for "free" oil droplets (i.e., translated to a linear decline following transformation of data to natural logarithm equivalents) would be expected when interactions occur between oil droplets and SPM. This is shown in the figure for the experiment containing oil and Yukon Delta SPM. The slopes of the linear regression lines fitted to the data correspond to the rate constants (k) for interactions between "free" oil droplets and available SPM. In conjunction with accompanying experimental measurements for the volume of a reaction
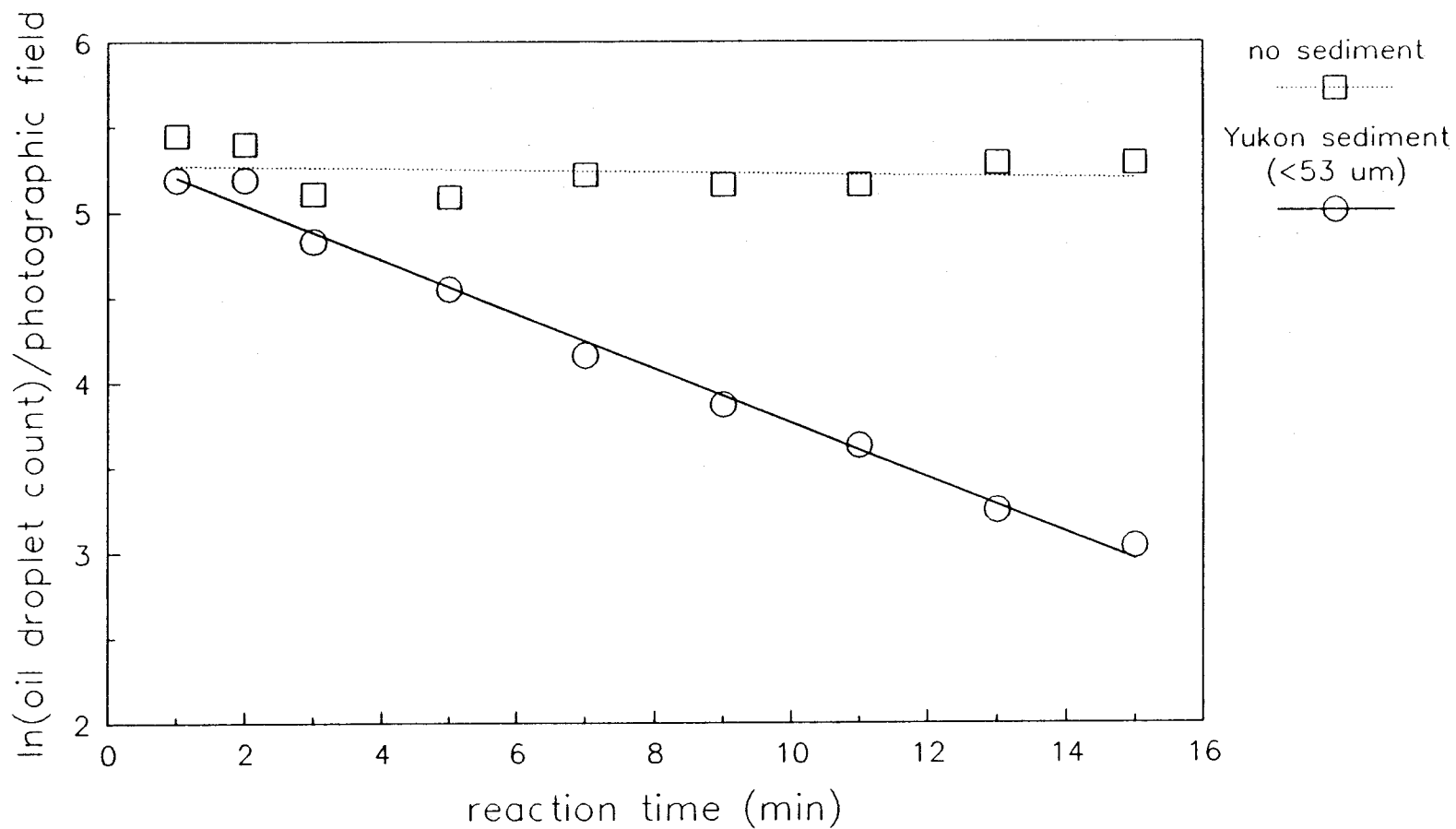
Figure 5-7. **Representative Data Plots Used to Generate Rate Constants "k" for Interactions Between Whole-Oil Droplets and SPM**

Values for "k" are equivalent to the slopes of the linear regression lines fitted to the data in the figure. Unweathered Prudhoe Bay crude oil at 30-40 mg/L was used for both experiments.

solution, the total SPM load, and the torque and rotation speed of the stirring paddle, a value for k can be used to calculate a number for the "lumped" reaction coefficient (α) for interactions between oil droplets and SPM using equations presented in Section 5.2.1.

In order to attribute declines in "free" oil droplet number densities to oil/SPM interactions, control experiments in stirred reaction vessels were conducted with oil but no SPM. Theoretically, these experiments should yield values of 0 for the reaction rate constant k. Table 5-6 summarizes information from a number of these control experiments, and includes not only regression values for k but also indications of whether the values were significantly different from 0 (alpha - 0.05 level). In only one instance was a value for k determined to be different from 0, and the value for rejection of the null hypothesis of k - 0 in this one exception was only slightly greater than that required for accepting the null hypothesis.

Table 5-6

Summary of Interaction Rate Constants "k" for Control Experiments Containing Oil But No SPM

Oil Type	Oil Amount (mg/L)	Salinity (ppt)	Rate Constant k (min^{-1})
Unweathered Prudhoe Bay crude oil	38.8	0.0	0.02
	30.7	13.0	-0.02
	14.8	30.0	0.01
	23.0	30.0	-0.00
	7.8	30.0	0.01
	22.6	30.0	0.02*
	31.5	30.0	-0.01
12-day weathered Prudhoe Bay crude	62.0	0.0	0.01
	13.8	29.0	0.01
	44.1	29.0	-0.01
R/T Glacier Bay weathered North Slope crude	5.3	30.0-	-0.01
Unweathered No.1 fuel oil	8.3	30.0	-0.00

*values for k that are significantly different from 0 at the $\alpha = 0.05$ level are indicated by *

119

The approach utilizing declines in "free" oil droplet number densities was applied to all experimental data designed to investigate interactions between oil droplets and SPM. All data for values of both the reaction constant (k) and the "lumped" reaction coefficient (α) from experiments having both oil and SPM are summarized in Table 5-7. Also included in the table are items of information from each experiment for SPM types and quantities, oil types and quantities, salinities, reaction solution volumes, and torques and propeller rotation speeds. Values for k are calculated for every experiment, and those values that are significantly different from 0 at the alpha - .05 level (i.e., denoting some statistically significant change in oil droplet number densities over time) are indicated by a "Y" in the appropriate column. Because essential items of information (e.g., torque and rpm values) were missing for certain experiments, values for the "lumped" reaction coefficient α could not be determined for every experiment. Discussions of the relevance of the values for k and α in the context of the experimental variables of interest are presented in Sections 5.2.2.1 through 5.2.2.4.

5.2.2.1 Effect of SPM Type

Oil droplet/SPM interaction rate constants were evaluated in experiments for eight natural sediments and one natural SPM collected in or near various coastal environments in Alaska. These sediment and SPM types included the following: Beaufort Sea sediment (< 53 μm), Beaufort Sea peat (< 53 μm), Grewingk glacial till (< 53 μm), Jakolof Bay sediment (< 53 μm), Kotzebue sediment (< 53 μm), Peard Bay sediment (< 53 μm), Prudhoe Bay sediment (< 53 μm), Yukon River Delta sediment (< 53 μm) and Turnagain Arm SPM. As indicated, all of the sediment phases were presieved through a 53 μm geological sieve prior to their use in experiments, while the Turnagain Arm SPM not sieved.

Although data pertaining to individual experiments can be extracted from Table 5-7, values for reaction rate constants k for the various SPM types are summarized in Figure 5-8. In the figure, data are illustrated as means and ranges for the sum of numbers for a given SPM type. For presentation purposes, values for k are only taken from experiments having oil loads of 8-110 mg/L and

120

Table 5-7

Summary of Experimental "k" and "alpha" Oil Droplet/SPM Interaction Constants

Salinity (ppt)	Sediment Type	Sed Amt (mg/L)	Oil Type	Oil Amt (mg/L)	Rx k Slope[a]	Sig?[b]	Rx Sol Vol (L)[c]	Rx rpm[d]	Rx torque (oz-in)	Energy diss rate (ergs/cc-sec)	Rx alpha (cm^3/g)	Date
0.0	Grewingk till (< 53 μm)	61.5	Unweathered Prudhoe Bay crude	35.7	0.02	Y	3.5	400	0.50	423	0.0270	07-09-88
14.0		56.7		18.4	-0.05	Y	3.5	400	0.50	423	-0.0676	07-10-88
30.0		51.4		4.1	-0.08	Y	3.5	400	0.50	423	-0.1255	11-17-87
30.0		52.1		19.9	-0.18	Y	3.5					07-28-87
30.0		53.9		12.9	-0.19	Y	3.5					07-28-87
30.0		47.9		19.3	-0.08	Y	3.5	400	0.50	423	-0.1423	07-30-87
30.0		—		NA	-0.08	Y	3.5					07-30-87
30.0		—		NA	-0.09	Y	3.5					08-03-87
30.0		44.6		10.9	-0.16	Y	3.5					08-26-87
30.0		47.1		15.3	-0.11	Y	3.5	400	0.33	282	-0.2319	08-26-87
30.0		47.8		17.4	-0.06	Y	3.5	400	0.50	423	-0.0943	08-29-87
30.0		—		NA	-0.08	Y	3.5	400	0.50	423		08-30-87
30.0		40.5		24.2	-0.06	Y	3.5	400	0.50	423	-0.1187	09-02-87
30.0		67.7		7.9	-0.15	Y	9.5	300	0.75	175	-0.2789	10-07-87
30.0		42.5		24.7	-0.08	Y	3.5	400	0.50	423	-0.1554	11-14-87
30.0		54.7		14.4	-0.08	Y	3.5	400	0.50	423	-0.1242	11-16-87
0.0		63.4	12-day weathered Prudhoe Bay crude	99.0	-0.01	N	3.5	400	0.50	423	-0.0089	07-09-88
29.0		62.2		26.1	-0.08	Y	3.5	400	0.50	423	-0.1049	07-17-88
29.0		59.5		83.9	-0.07	Y	3.5	400	0.50	423	-0.1020	07-15-88
29.0		60.9		54.9	-0.08	Y	3.5	400	0.50	423	-0.1081	07-15-88
29.0		63.5		43.2	-0.10	Y	3.5	400	0.50	423	-0.1259	07-15-88
0.0		56.6	Unweathered No. 1 fuel oil	7.1	-0.02	Y	3.5	400	0.50	423	-0.0268	07-18-88
15.0		69.0		32.4	-0.10	Y	3.5	400	0.50	423	-0.1208	07-18-88
30.0		68.4		32.8	-0.08	Y	3.5	400	0.50	423	-0.0930	07-19-88
30.0		55.4	R/T Glacier Bay weathered North Slope crude	1.2	-0.09	Y	3.5	400	0.50	423	-0.1317	08-03-87
30.0	Turnagain Arm SPM	180.0	Unweathered Prudhoe Bay crude	18.6	-0.16	Y						11-12-87
29.0		356.8		25.8	-0.11	Y	3.5	400	0.50	423	-0.0257	07-17-88

Table 5-7 (Continued)

Salinity (ppt)	Sediment Type	Sed Amt (mg/L)	Oil Type	Oil Amt (mg/L)	Rx k Slope[a]	Sig?[b]	Rx Sol Vol (L)[c]	Rx rmp[d]	Rx torque (oz-in)	Energy diss rate (ergs/ cc-sec)	Rx alpha (cm^3/g)	Date
29.0	Turnagain Arm SPM (Cont.)	416.4	12-day weathered Prudhoe Bay crude	58.4	-0.12	Y	3.5	400	0.50	423	-0.0239	07-17-88
30.0		319.8	Unweathered No. 1 fuel oil	24.9	-0.17	Y	3.5	400	0.50	423	-0.0425	07-18-88
0.0	Yukon Delta sediment (< 53 μm)	453.3	Unweathered Prudhoe Bay crude	44.2	0.01	Y	3.5	400	0.50	423	0.0024	02-20-88
14.0		526.7		31.5	-0.09	Y	3.5	400	0.50	423	-0.0142	02-24-88
28.0		508.7		40.6	-0.15	Y	3.5	400	0.50	423	-0.0232	02-21-88
29.0		614.1		105.4	-0.06	Y	3.5	400	0.50	423	-0.0075	02-23-88
0.0		690.1	12-day weathered Prudhoe Bay crude	68.6	-0.01	Y	3.5	400	0.50	423	-0.0015	04-18-88
14.0		776.5		71.2	-0.21	Y	3.5	400	0.50	423	-0.0221	04-19-88
29.0		707.5		19.0	-0.14	Y	3.5	400	0.50	423	-0.0166	04-16-88
29.0		782.2		49.2	-0.17	Y	3.5	400	0.50	423	-0.0177	04-15-88
29.0		789.2		286.6	-0.14	Y	3.5	400	0.50	423	-0.0144	04-17-88
0.0		408.6	Unweathered No. 1 fuel oil	32.9	-0.03	Y	3.5	400	0.50	423	-0.0066	07-20-88
14.0		485.4		28.8	-0.10	Y	3.5	400	0.50	423	-0.0165	07-20-88
30.0		554.0		25.6	-0.07	Y	3.5	400	0.50	423	-0.0108	07-19-88
30.0	Beaufort Sea sediment (< 53 μm)	136.5	Unweathered Prudhoe Bay crude	23.6	-0.12	Y	3.5	400	0.50	423	-0.0706	07-10-88
30.0		139.4	12-day weathered Prudhoe Bay crude	112.2	-0.12	Y	3.5	400	0.50	423	-0.0691	07-12-88
30.0		128.4	Unweathered No. 1 fuel oil	21.6	-0.15	Y	3.5	400	0.50	423	-0.0946	07-15-88
30.0		138.2		48.0	-0.09	Y	3.5	400	0.50	423	-0.0527	07-18-88
30.0	Beaufort Sea peat (< 53 μm)	130.6	Unweathered Prudhoe Bay crude	21.6	-0.05	Y	3.5	400	0.50	423	-0.0339	07-10-88
30.0		115.3	12-day weathered Prudhoe Bay crude	98.6	-0.05	Y	3.5	400	0.50	423	-0.0363	07-12-88
30.0	Peard Bay sediment (< 53 μm)	152.1	Unweathered Prudhoe Bay crude	30.3	-0.14	Y	3.5	400	0.50	423	-0.0723	07-11-88
30.0		132.9	12-day weathered Prudhoe Bay crude	69.5	-0.10	Y	3.5	400	0.50	423	-0.0632	07-13-88

Table 5-7 (Continued)

Salinity (ppt)	Sediment Type	Sed Amt (mg/L)	Oil Type	Oil Amt (mg/L)	Rx k Slope[a]	Sig?[b]	Rx Sol Vol (L)[c]	Rx rpm[d]	Rx torque (oz-in)	Energy diss rate (ergs/ cc-sec)	Rx alpha (cm³/g)	Date
30.0	Prudhoe Bay sediment (< 53 µm)	203.4	Unweathered Prudhoe Bay crude	32.1	-0.07	Y	3.5	400	0.50	423	-0.0275	07-11-88
30.0		209.8	12-day weathered Prudhoe Bay crude	88.0	-0.10	Y	3.5	400	0.50	423	-0.0399	07-13-88
30.0	Kotzebue sediment (< 53 µm)	231.2	Unweathered Prudhoe Bay crude	31.1	-0.06	Y	3.5	400	0.50	423	-0.0209	07-11-88
30.0		232.8	12-day weathered Prudhoe Bay crude	77.3	-0.07	Y	3.5	400	0.50	423	-0.0234	07-14-88
30.0	Jakolof Bay sediment (< 53 µm)	32.5	Unweathered Prudhoe Bay crude	29.2	-0.12	Y						07-25-87
30.0		49.9		16.3	-0.06	Y						07-27-87
30.0		60.0		17.0	-0.13	Y	3.5					11-06-87
30.0		53.0		25.0	-0.12	Y	3.5					11-06-87
30.0		57.0		NA	-0.09	Y	3.5					11-07-87
30.0		60.0		23.0	-0.10	Y	3.5					11-08-87
30.0		363.0	Unweathered No. 1 fuel oil	37.9	-0.08	Y	3.5	400	0.50	423	-0.0180	07-19-88
30.0	Aluminum oxide grit (10 µm)	62.4	Unweathered Prudhoe Bay crude	25.9	-0.04	Y	3.5	360	0.33	253	-0.0671	10-04-87
30.0		205.7		22.4	-0.08	Y	3.5	350	0.33	246	-0.0413	10-05-87
30.0		221.3		26.4	-0.08	Y	3.5	350	0.33	246	-0.0384	10-06-87
30.0		266.1		10.2	-0.06	Y	9.5	226	0.50	88	-0.0401	11-10-87
30.0		263.5		4.8	-0.12	Y	9.5	392	1.50	458	-0.0355	11-11-87
30.0	DVB polyspheres (1–20 µm)	NA	Unweathered Prudhoe Bay crude	NA	-0.15	Y	3.5	360	0.50	370		10-08-87

[a] Rx k Slope: reaction rate constant (k) determined from linear regression fit to data for ln (oil droplet number) versus time
[b] Sig?: Y = k significantly different from 0 at $\alpha = 0.05$; N = k not significantly different from 0 at $\alpha = 0.05$
[c] Rx Sol Vol: volume of solution for stirred reaction vessel experiment
[d] Rx rpm: rate of turning of propeller shaft for stirred reaction vessel experiment
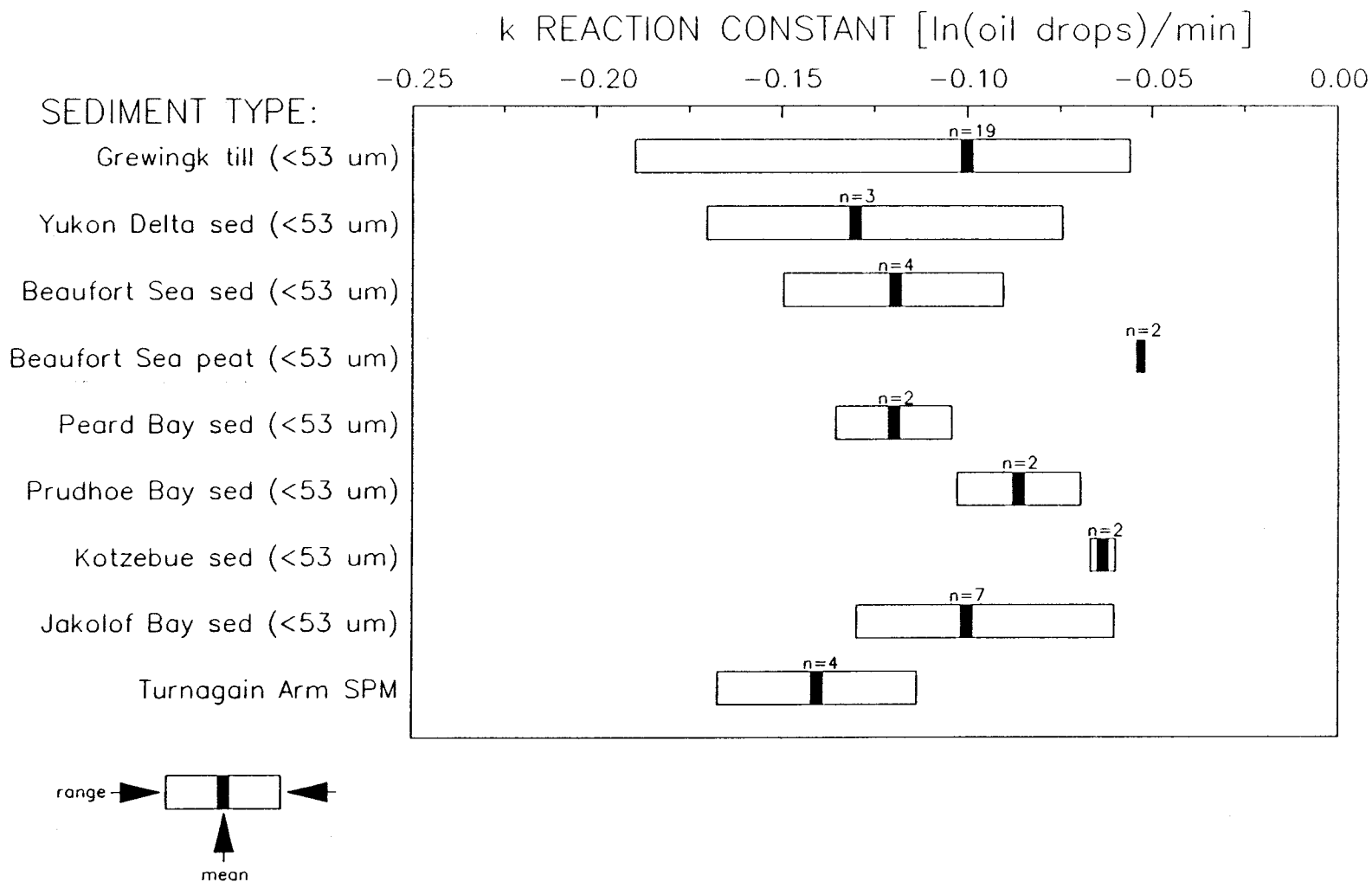
Figure 5-8. Summary of Whole-Oil Droplet/SPM Interaction Rate Constants ("k") for Different Sediment and SPM Types

All data are from experiments with full-strength seawater (28–30 ppt) and oil loads of 7–112 mg/L). Data are presented as means with indicated minimum/maximum ranges (n = number of data points to determine a given mean value).

124

using full seawater as the reaction medium (see Section 5.2.2.3 for effects of salinity). As indicated in the figure, all values for k are within a factor of 4 of each other, and this range can be encountered within a single sediment type (e.g., Grewingk till). Consequently, large differences in values for k do not appear to be in evidence either among or within the various SPM types. In light of the fact that total oil loadings in experiments varied by more than a factor of 10 (see Table 5-7), the relatively small variation in values for k indicate that the total number of oil droplets reacting with SPM in a particular experiment was proportional to the amount of oil present (e.g., see equations describing the relationship between the reaction constant k and oil droplet number density in Section 5.2.2).

The information in Figure 5-8 might lead one to conclude that no substantial differences exist among the oil droplet/SPM interactions for the various sediment and SPM types. However, the important interaction term in the algorithms of the model codes in Section 3 is the "lumped" reaction coefficient α. Values for the coefficient α then need to be considered for those experiments having data for all of the necessary algorithm components. Results summarizing the calculated values for α are illustrated in Figure 5-9. Distinctions between the various SPM types become more apparent in the latter figure, with overall values differing by a factor of almost 40 (i.e., -0.0075 cm^3/g to -0.29 cm^3/g). In an attempt to explain these differences, mean values for the reaction coefficients α for various SPM types were compared with other physical and chemical properties of the SPM, including particle number densities per unit mass (i.e., Section 5.1 and Figure 5-3), the fraction of the total sediment occurring in the 0-2 μm particle size range (Figure 5-2), total organic carbon, specific density, and total resolved hydrocarbon content. The data for all of these variables (including mean values for α) are summarized in Table 5-8. Using data in this table, regression analyses were performed with values for the reaction coefficient α being the dependent variable and the other parameters being considered as independent variables. Results of these statistical analyses are summarized in Table 5-9. Of the five independent variables, particle number density per unit mass showed the highest correlation with the values for the reaction coefficient α. A slightly lower degree of correlation (i.e., significant at alpha - 0.05 but not at alpha - 0.01)

125
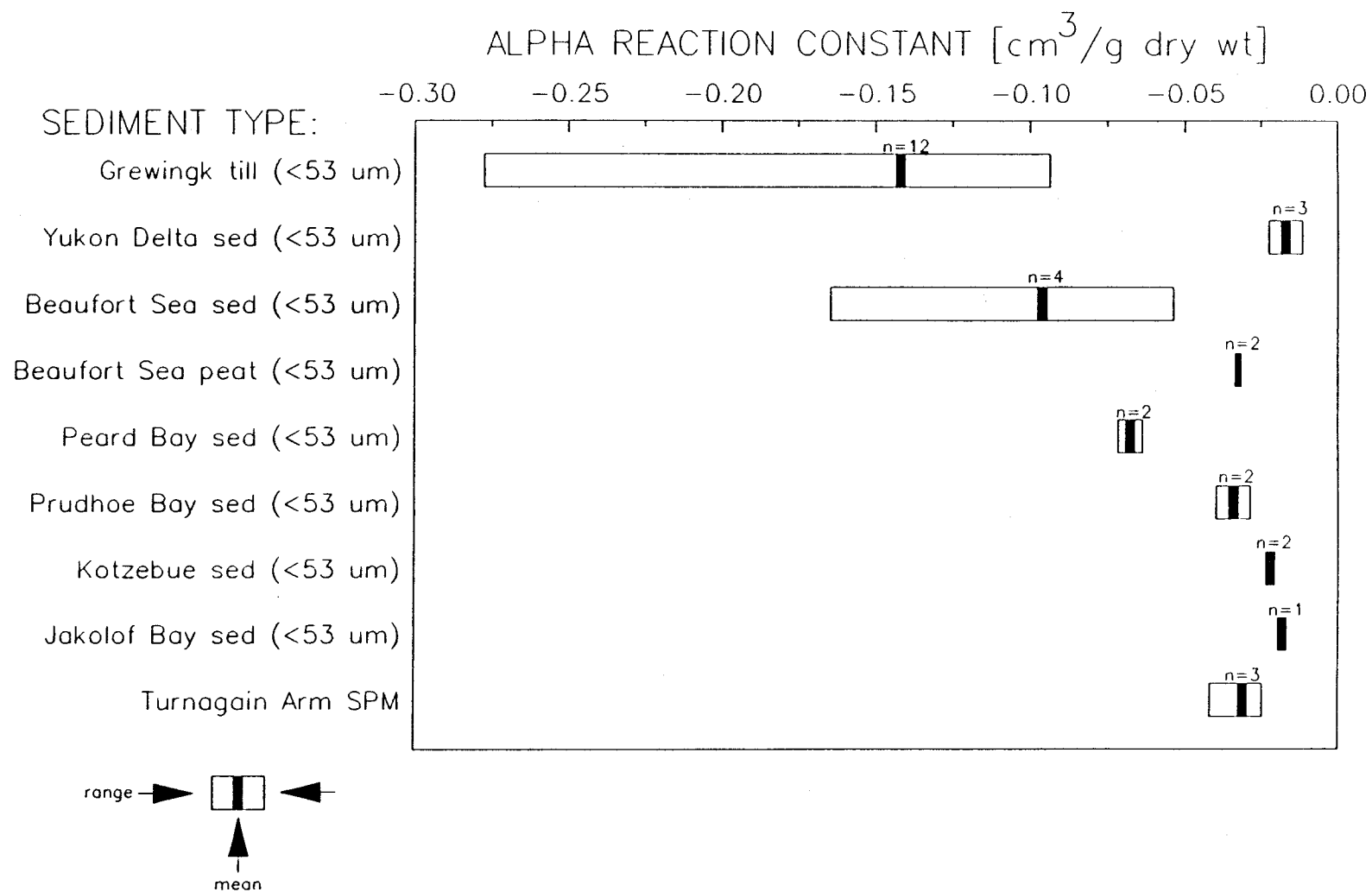
Figure 5-9. Summary of "alpha" Reaction Coefficients for Interactions Between Whole-Oil Droplets and SPM for Different Sediment and SPM Types

The data are from the same experiments summarized in Figure 5-8.

Table 5-8

Summary of Mean "alpha" Reaction Coefficients and Physical and Chemical Properties for SPM Types Used in Whole-Oil Droplet/SPM Interaction Experiments

SPM Type	Mean Rx "alpha" (cm^3/g)	Part. No. Density $(10^9/g)$	Sed. Fract. in 0-2 μm Size Range (%)	TOC (mg/g)	Density (g/cm^3)	Tot. Res. Hydrocarb. $(\mu g/g)$
Beaufort Sea sediment (< 53 μm)	-0.096	56	44.6	6.15	2.55	8.3
Beaufort Sea peat (< 53 μm)	-0.032	19	NA	NA	NA	78.0
Grewingk till (< 53 μm)	-0.142	178	51.6	2.05	2.76	1.7
Jakolof Bay sediment (< 53 μm)	-0.018	22	35.1	6.49	NA	862.0
Kotzebue sediment (< 53 μm)	-0.022	16	24.1	7.57	2.70	43.0
Peard Bay sediment (< 53 μm)	-0.068	56	43.8	11.50	2.51	18.0
Prudhoe Bay sediment (< 53 μm)	-0.034	42	22.7	14.20	2.51	26.0
Turnagain Arm SPM	-0.031	56	10.5	4.65	2.64	3.4
Yukon Delta sediment (< 53 μm)	-0.017	11	6.9	5.35	2.77	> 0.05

NA = not available

Table 5-9

Regression Analyses of "alpha" Reaction Coefficients Versus Selected Physical and Chemical Properties of Various SPM Types Tested
(dependent variable: alpha reaction constant $(cm^3/g$ dry weight)

Independent Variable	n	t_s	Probability
Particle No. Density (10^9 particles/g dry wt)	9	-5.54**	0.999
Sed. Fract. in 0-2 μm size range (%)	8	-3.25*	0.982
Total Organic Carbon (mg/g dry wt)	8	0.93	0.611
Background Density	7	-0.07	0.055
Total Resolved Hydrocarbons (μg/g dry wt)	9	0.90	0.600

Significant values for t_s at $\alpha = 0.01$ and 0.05 levels are indicated by ** and *, respectively.

existed with the values for the sediment fractions comprising the 0-2 μm particle-size ranges. The remaining three variables (TOC, specific density, and total resolved hydrocarbon content) showed no significant correlations with the reaction coefficient α. The relationship between the reaction coefficients α and particle number densities per unit mass for the nine sediment and SPM types is shown graphically in Figure 5-10 along with a linear regression fit to the data. The value of 0.81 for the square of the correlation coefficient (r^2) indicates that approximately 80% of the variability in the values for α among the sediment and SPM types can be correlated with the number density values. Because the SPM types considered in Figure 5-10 come from a variety of locations in Alaska, it seems plausible to suggest that reaction coefficients (α) for SPM from other locations might be extrapolated from the regression line in Figure 5-10, if appropriate information pertaining to particle number densities for specific SPM types can be obtained. The latter information can be derived by either detailed light microscopy (e.g., counting particles as in Figure 5-1) or possibly by comparing limited-light microscopy with particle-size analyses (i.e., coupling information and data from sources such as both Figures 5-1 and 5-2).

5.2.2.2 Effect of Oil Type

Interactions between dispersed oil droplets and SPM were investigated for four types of oil: 1) unweathered Prudhoe Bay crude, 2) 12-day weathered Prudhoe Bay crude, 3) naturally weathered North Slope crude collected from the R/T Glacier Bay grounding incident and 4) unweathered No. 1 fuel oil. Because both the type of SPM and the salinity of the reaction medium were found to affect rates of interaction (Sections 5.2.2.1 and 5.2.2.3, respectively), evaluations of effects of the different oil types on oil droplet/SPM interactions were only performed for individual SPM types at a common salinity. By utilizing a single SPM type, values for reaction rate constants (k) could be compared directly. However, the populations of experimental data available for single SPM types at a given salinity were limited. Such a comparison is presented in Figure 5-11 for Grewingk glacial till in seawater. Within the scatter inherent to the data, there do not appear to be substantial differences between the values for k for the four oil types, implying that the oil droplet/SPM interactions were essentially independent of the type of oil present.

128
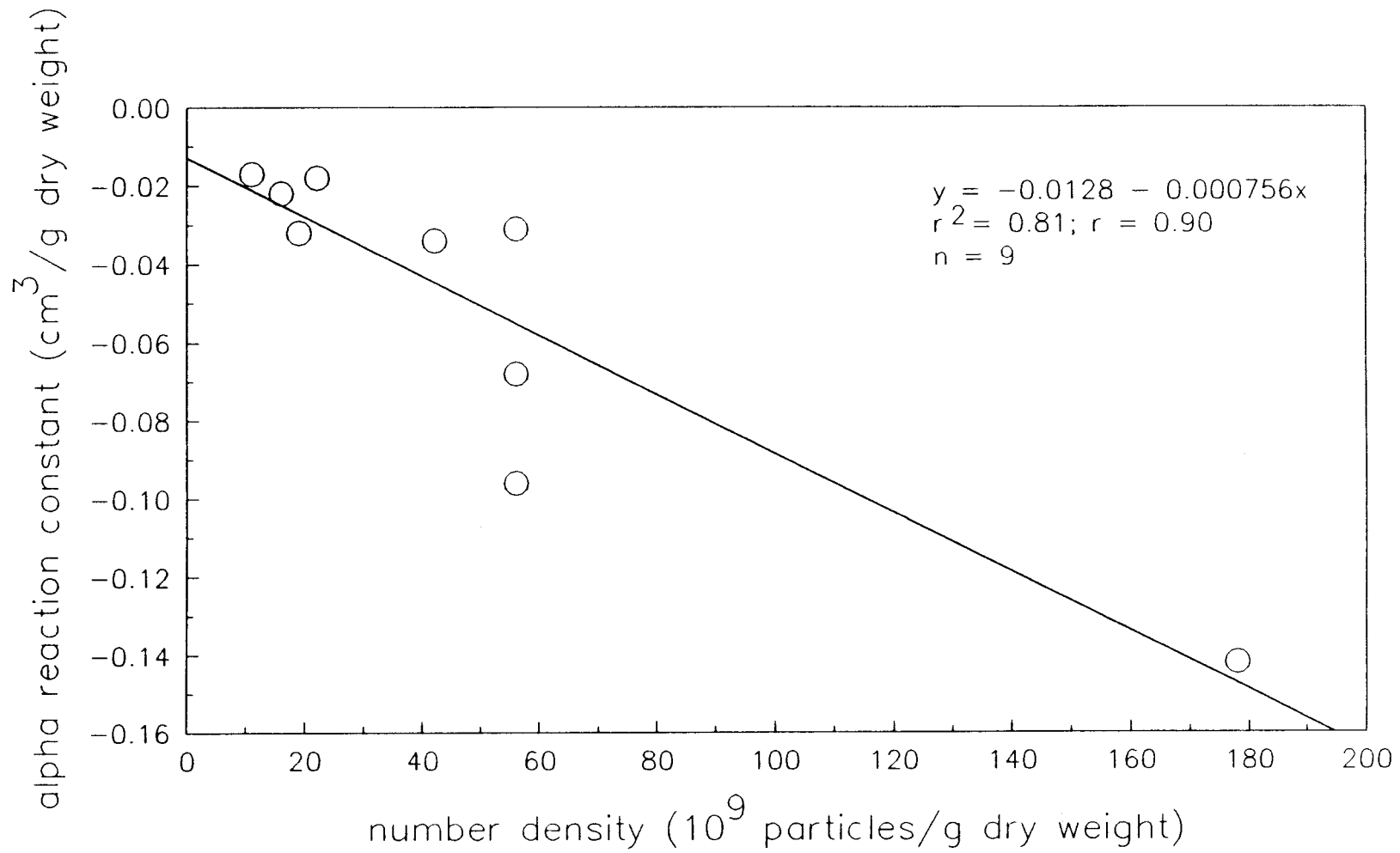
Figure 5-10.   Linear Regression Fit of Mean Values for "alpha" Reaction Coefficients to Corresponding Particle Number Densities for Different Sediment and SPM Types (see Table 5-8)
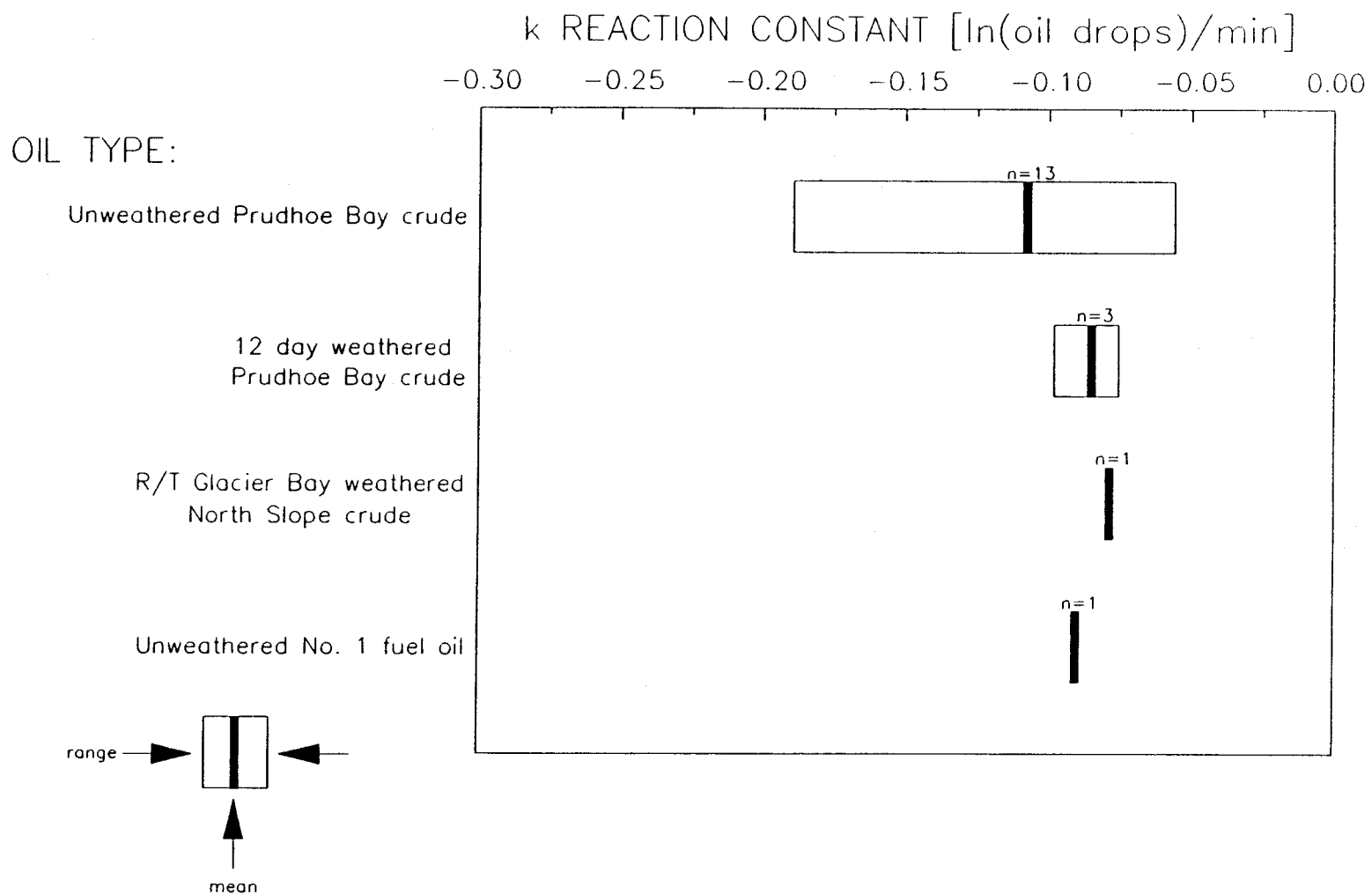
Figure 5-11. Summary of Whole-Oil Droplet/SPM Interaction Rate Constants ("k") for Different Oil Types

All experiments performed with Grewingk glacial till (< 53 μm) in full-strength seawater.

5.2.2.3 Effect of Salinity

Because rates of oil/SPM interactions are dependent on SPM types, comparisons of the effects of salinity on oil droplet/SPM interactions had to be considered for only single types of SPM. This again produced limitations in the total number of data that could be used. However, as illustrated in Figure 5-12, salinity appears to have a strong controlling effect on reaction rates for both Yukon Delta sediment and Grewingk till. For example, very low rates of reaction (i.e., k values approaching 0) were observed with both SPM types in freshwater, while substantially higher rates were observed in both half-strength and full-strength seawater. Comparable effects of salinity on associations of dispersed oils and fatty acids with SPM or mineral phases have been shown by other investigators (e.g., Bassin and Ichiye, 1977; Meyers and Quinn, 1973)

5.2.2.4 Effect of Turbulence

As developed in Section 5.2, the rate constant k for interactions between whole oil droplets and SPM can be described by the equation

$$k = \alpha(\epsilon/\upsilon)^{1/2}S$$

where S is the SPM concentration, ϵ is the energy dissipated per unit mass of water per unit time, υ is the kinematic viscosity of the aqueous medium and α is the "lumped" reaction coefficient. For experimental data to be valid for this equation, the natural logarithm of oil droplet number data must decline as a straight line over time and the rate constant k must vary as the square root of the energy dissipation rate.

To evaluate whether values for k would follow the expected relationship with the energy dissipation rate (ϵ), two experiments were performed with the following conditions: both experiments were conducted in 10-L beakers (9.5 L of reaction solution) and utilized aluminum oxide grit (10-μm diameter particles; 330-mg dry wt/L as the SPM phase and unweathered Prudhoe Bay crude as the oil phase. In one experiment the propeller shaft rotation rate (w) and

131

a) Yukon Delta sed (<53 um)

k REACTION CONSTANT [ln(oil drops)/min]

SALINITY:

b) Grewingk till (<53 um)

k REACTION CONSTANT [ln(oil drops)/min]
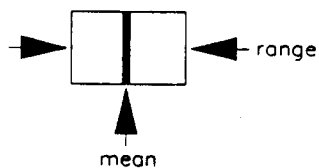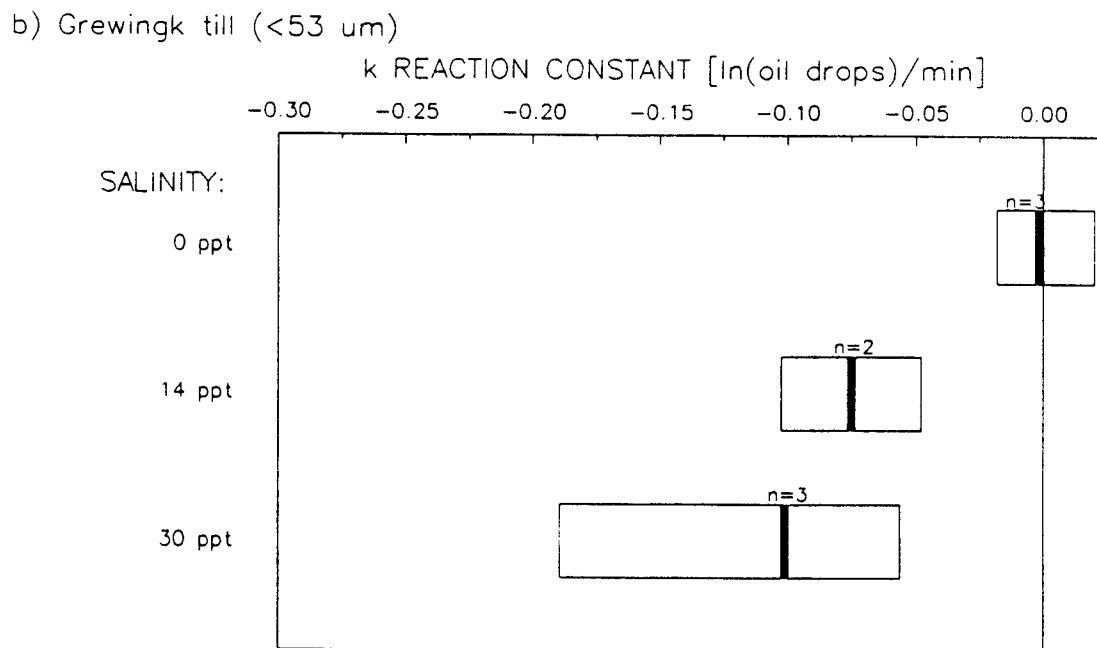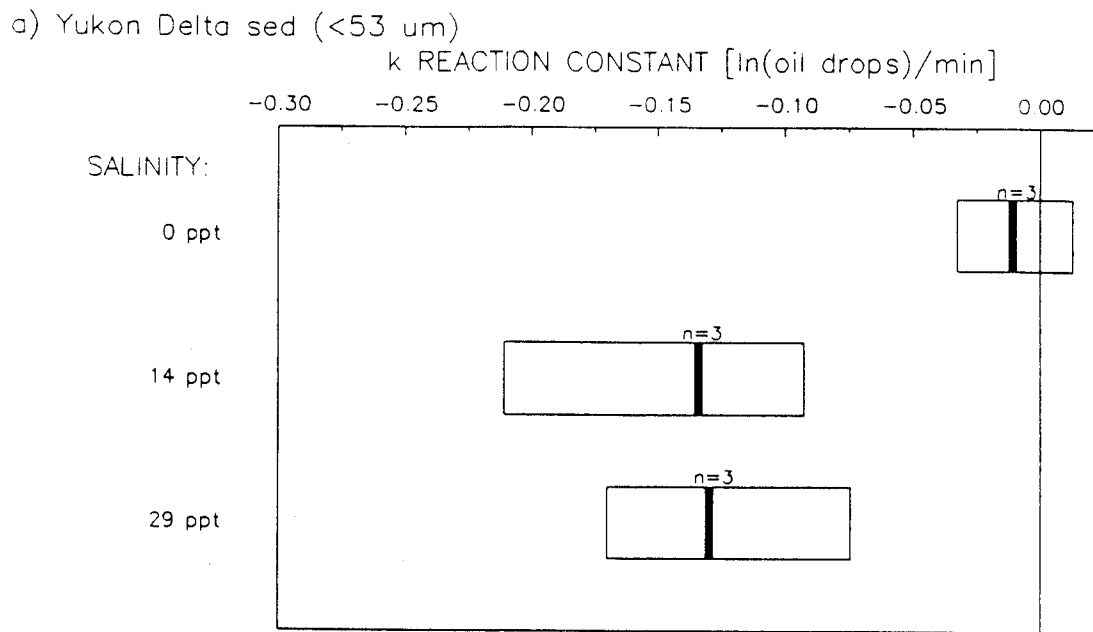
SALINITY:

Figure 5-12. Summary of Whole-Oil Droplet/SPM Interaction Rate Constants ("k") at Different Salinities

(a) Yukon River Delta sediment (< 53 μm). (b) Grewingk glacial till (< 53 μm).

132

torque (τ) were 226 rpm and 0.5 ounce-inches, respectively. The values resulted in a number for the energy dissipation per unit time of:

$$E_1 = (w)(\tau)(7400) = 8.4 \times 10^5 \text{ ergs/sec.}$$

In the second experiment, the propeller rotation rate and torque were 393 rpms and 1.5 ounce-inches, respectively, yielding the following value for E:

$$E_2 = 4.4 \times 10^6 \text{ ergs/sec.}$$

Because all experimental variables in the two experiments were identical except for the values of E, the ratio of the numbers for k in the two experiments should be $k_2/k_1 = [(4.4 \times 10^6)]^{1/2}/[(8.4 \times 10^5)]^{1/2}$ or 2.3. At the same time, the torque meter had a certain amount of "bounce" in its values that was estimated to produce an error of $\pm$ 20% in readings. Taking this into account, the ratio of the square root of the energy dissipation rates for the two experiments is 2.3 with a limit of error of 0.3 based on the error estimates for the torque readings. Regression analyses of the "free" oil droplet data in photomicrographs from the two experiments yielded values for k_2 and k_1 of -0.112 $\pm$ 0.025 and -0.062 $\pm$ 0.023, respectively. The latter values produce a value of 1.8 for the ratio of k_2/k_1. The confidence interval for the latter values of k is based on a specified confidence limit of 0.8 for a two-tailed test (Miller and Freund, 1965). Assuming no bias (i.e., errors will tend to cancel), the limit of error for the latter ratio of k_2/k_1 is 0.78 (Shoemaker and Garland, 1962). Thus, analysis of errors yields a ratio of the slopes for the two sets of data of 1.8 with a limit of error of 0.8. Finally, comparison between the values for the ratios of k_2/k_1 calculated with the two techniques (i.e., 2.3 with a limit of error of 0.3, and 1.8 with a limit of error of 0.8) indicate that the expected relationship between experimentally derived values for k and E was satisfied for the different turbulence levels. Consequently, the experimental values confirmed the expected theoretical relationships between turbulence and oil/SPM interaction rate constants, although the data available for this comparison were limited.

5.3   SPM SETTLING VELOCITIES

In Section 5.2.2 and Figure 5-6, photomicrographs from the stirred reaction vessel experiments documented the formation of oil/SPM agglomerates following interactions between SPM and whole-oil droplets. Furthermore, the oil/SPM agglomerates in Figure 5-6 occurred in the focal plane of the SPM rather than that of the oil droplets, indicating that the agglomerates were denser than the aqueous medium and tended to sink in the water column. Because of the changes in the morphological appearance of oil/SPM agglomerates relative to parent SPM (see Figure 5-6), it is reasonable to expect that "oiling" of particles could affect the settling velocities of the particles. If the latter supposition is true, the potential exists for transport of oil to benthic environments through the sinking of "oiled" particles. A number of studies under both natural and semicontrolled conditions have documented that oil can be transferred to bottom sediments (Bassin and Ichiye, 1977; Gearing et al., 1980; Hartung and Klingler, 1968; Johansson et al., 1980; Lee et al., 1978; Wade and Quinn, 1980).

To evaluate effects of oil on settling velocities of selected SPM types, a number of settling chamber studies were conducted in conjunction with the stirred reaction vessel experiments. For this purpose, the solutions generated in the stirred vessels were transferred to settling chambers, and the SPM loads remaining in suspension over time were monitored. General information specific to the individual settling chamber experiments and their parent stirred reaction vessel solutions have been summarized in Table 4-1.

5.3.1   Conceptual Approach

As described in Section 4.3.1, the approach for the settling velocity studies involved collection and measurement of SPM loads in samples from settling chambers over time. Figure 5-13 illustrates the rationale behind this approach. At the start of an experiment, a solution is homogeneously mixed to ensure that all particles are evenly distributed in the suspending medium. The solution is then maintained in an undisturbed state and samples are withdrawn

134
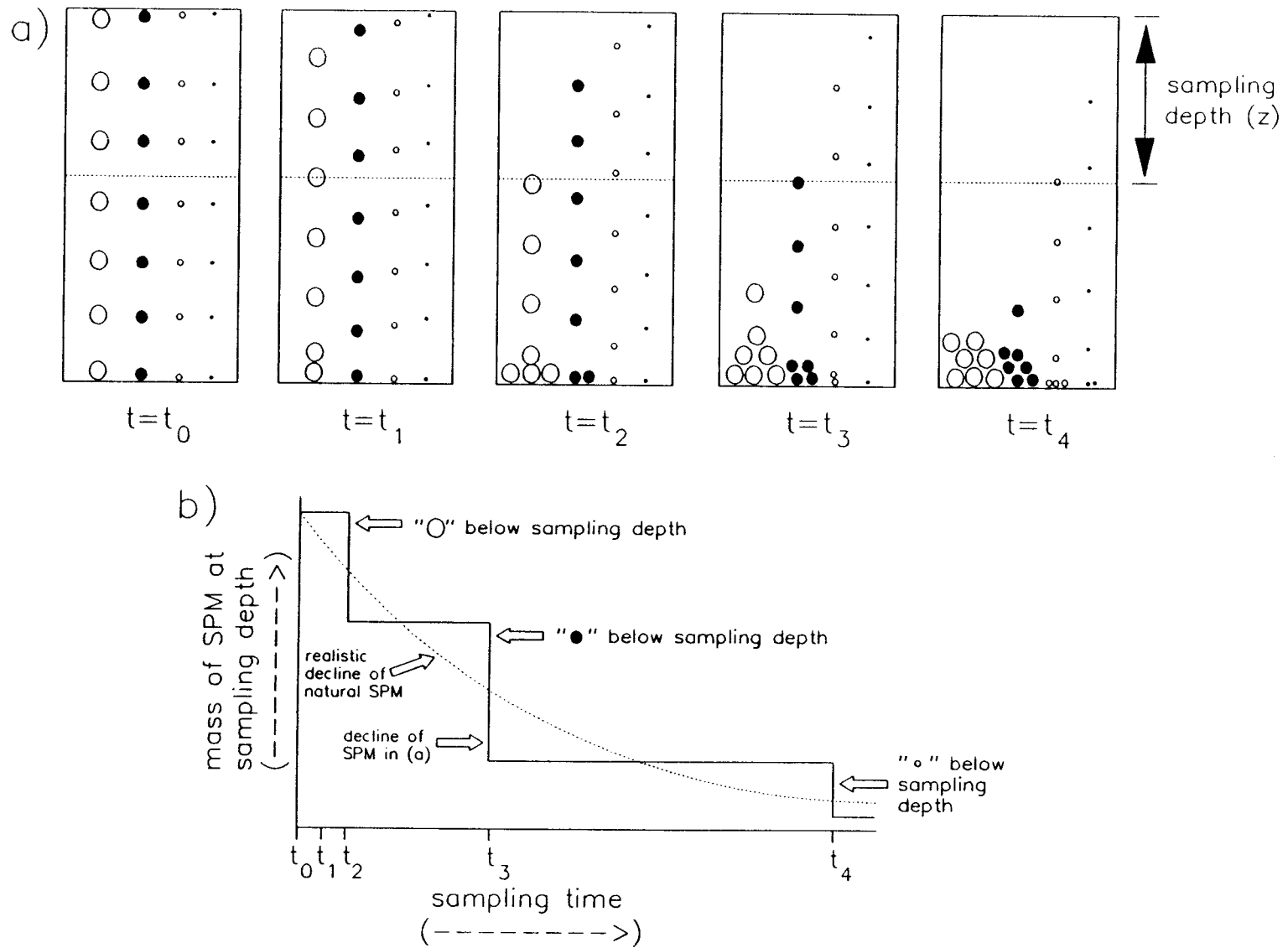
Figure 5-13. Schematic Illustration of Approach Used in Particle-Settling Velocity Experiments

(a) Vertical distributions of particles with different settling velocities over time (i.e., time = t_0 to t_4) relative to the sample collection depth (z).
(b) Representative time-course plots for measurements of gravimetric SPM loads at depth "z", with solid line denoting decline for particles in (a) and dashed line representing decline in an SPM sample comprised of a broader range of particle sizes.

over time from a specified depth. For the sake of analogy, particles charac-
terized by only a limited number of sizes and settling velocities are illus-
trated in Figure 5-13. When particles of a specific type sink below the
collection depth in the chamber, subsequent samples will reflect a correspond-
ing decrease in the total SPM load. In conjunction with the situation illus-
trated in part (a) of Figure 5-13, the decline in the SPM load would follow the
step-wise pattern shown in part (b) of the figure. Settling velocities for
particles of type x would be calculated with the formula:

$$v_x = z/(t_x - t_0)$$

where v_x is the settling velocity, z is the sampling depth in the chamber, t_0
is the starting time for the experiment, and t_x is the time at which particle x
sinks below the sampling depth. While part (b) of Figure 5-13 illustrates a
stepwise decline for SPM concentrations, natural sedimentary or SPM material
will normally be comprised of broad ranges of particle shapes and sizes (e.g.,
see Figures 5-1 and 5-2). Consequently, suspended sediments or SPM in real-
world situations will be more likely to mimic the more gradual decline for SPM
loads indicated by the "dotted" line in Figure 5-13b.

5.3.2   Experimental Settling Velocity Results

Settling velocity experiments were performed with two sediment types
that had been presized to < 53 μm before use in parent stirred reaction vessel
experiments: 1) Grewingk glacial till and 2) Yukon River Delta sediment. Be-
cause both sediment types were homogeneously suspended in solutions at the
start of experiments, these sedimentary phases will subsequently be referred to
as SPM. Based on information presented in Sections 5.1 and 5.2.2.1, the Grew-
ingk till and the Yukon Delta sediment encompassed the extreme ranges for not
only particle sizes (e.g., Figures 5-1 through 5-4) but also reactivity coeffi-
cients with whole-oil droplets (e.g., Table 5-8 and corresponding data in
Figure 5-10). Experiments were conducted with the two types of SPM to evaluate
effects of the following variables on settling velocities: 1) SPM type, 2) oil
type and quantity and 3) salinity.

5.3.2.1 Effect of SPM Type

Because the size distributions of particles in the Grewingk till and Yukon Delta sediments were very different from each other (e.g., Figure 5-2), it would seem reasonable to expect that settling velocity properties for the two SPM types would also be very different. This is confirmed in Figure 5-14 that illustrates plots of the portions of the total SPM loads remaining in suspension over time for experiments conducted in seawater with no oil additions. For Grewingk till that was comprised almost exclusively of particles <10 μm in diameter, less than 25% of the total SPM load by weight had settled below the sampling depth in the settling chamber after 1 hr. In contrast, >90% of the Yukon Delta sediment was no longer sampled at this time due to the sedimentation of larger particles (i.e., approaching 50 μm in diameter). Because depths of sampling in the chamber and specific sampling times were recorded, the information illustrated in Figure 5-14 could be incorporated into the equation presented in Section 5.3.1 to calculate mean settling velocities for various weight % fractions of the two SPM types. These results are shown in Figure 5-15. Again, the differences in the settling velocity properties for the two SPM types are clearly apparent.

5.3.2.2 Effect of Oil Amount and Type

As described in Section 4.2.4, stirred reaction vessel experiments were often performed with different quantities of oil added in the initial "blending" procedure. This resulted in different total amounts of oil being available for reaction with the SPM (e.g., see Table 4-1 for summaries of oil loads in experiments that were ultimately used for settling velocity studies). Because the quantity of oil that became associated with SPM was directly related to the amount of oil in a stirred reaction vessel (see Section 5.2.2.1), SPM with differing amounts of agglomerated oil were produced and then used for settling chamber experiments. In light of this fact, the effect of "oil loading" (i.e., varying amounts of oil associated with SPM) on settling velocities of SPM could be evaluated. For example, Figure 5-16 presents data for declines in SPM loads of Grewingk till over time from experiments that had different loads

137

138
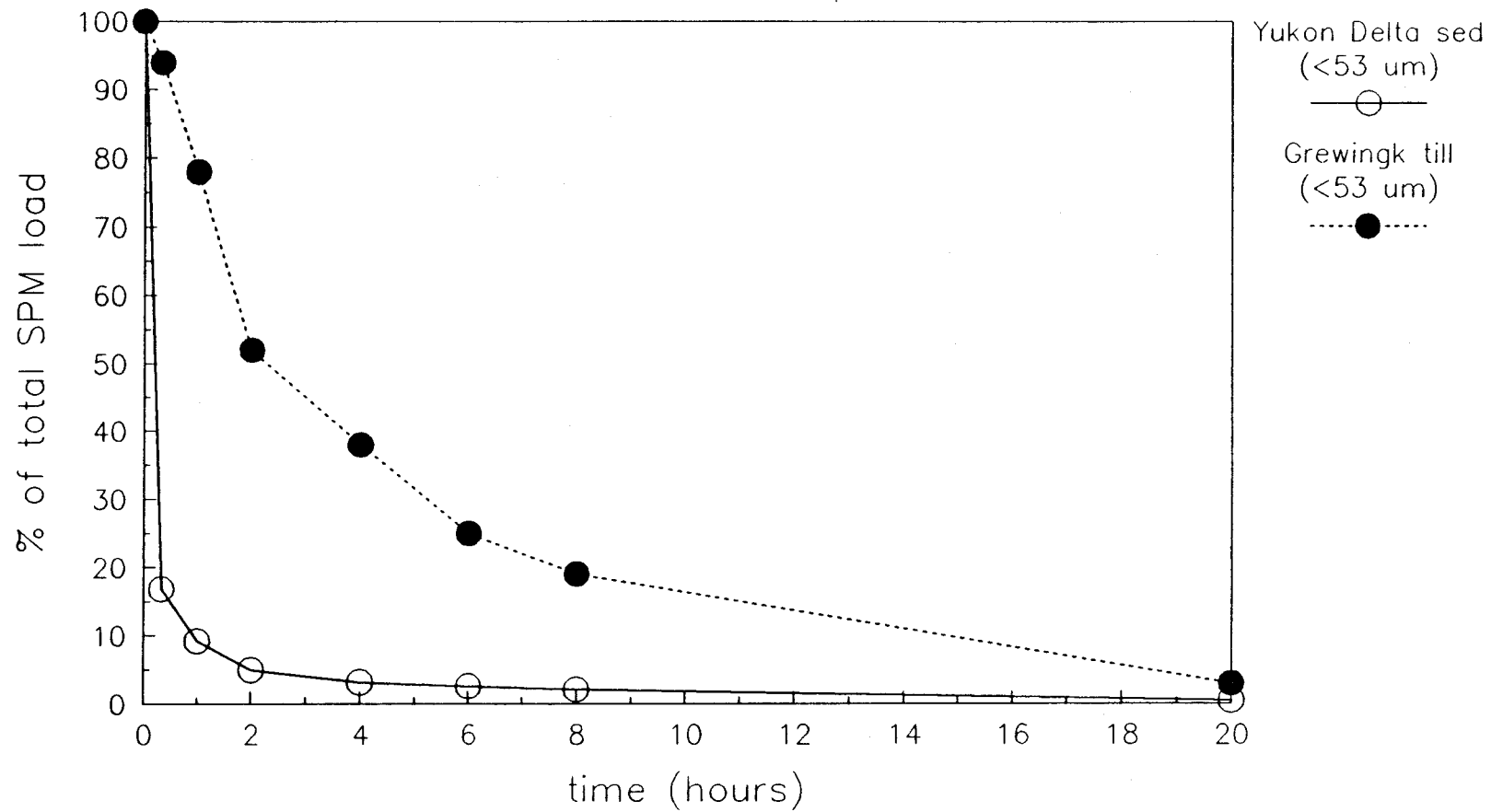
Figure 5-14. **Weight % of Total SPM Load Remaining in Suspension at Sampling Depth Over Time for Yukon River Delta Sediment (< 53 µm) and Grewingk Glacial Till (< 53 µm)**

Both experiments performed in full-strength seawater with no prior "oiling" of sediment.
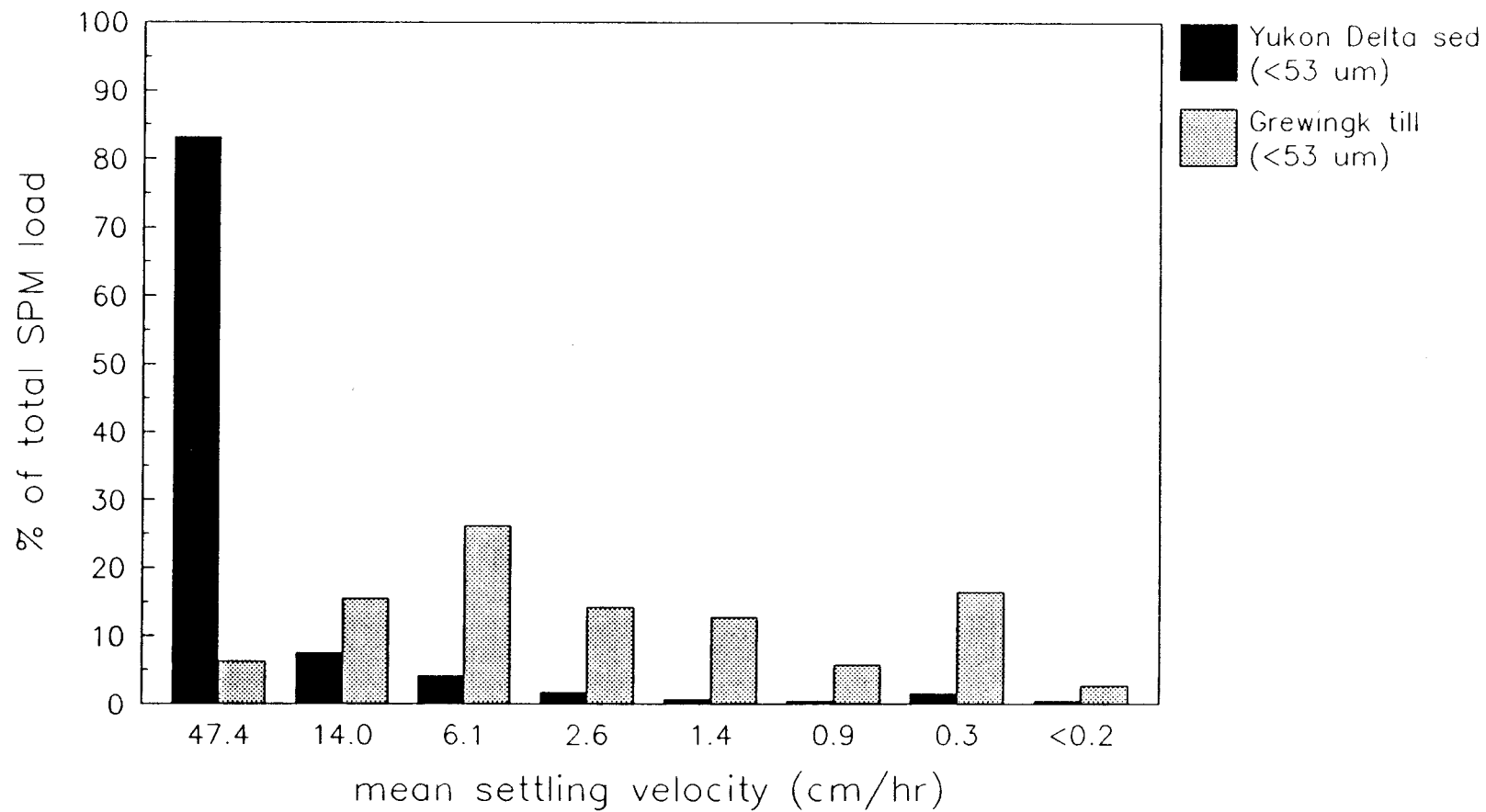
Figure 5-15.   Weight % of Total SPM Loads Corresponding to Given Mean Particle Settling Velocities for the Data Illustrated in Figure 5-14
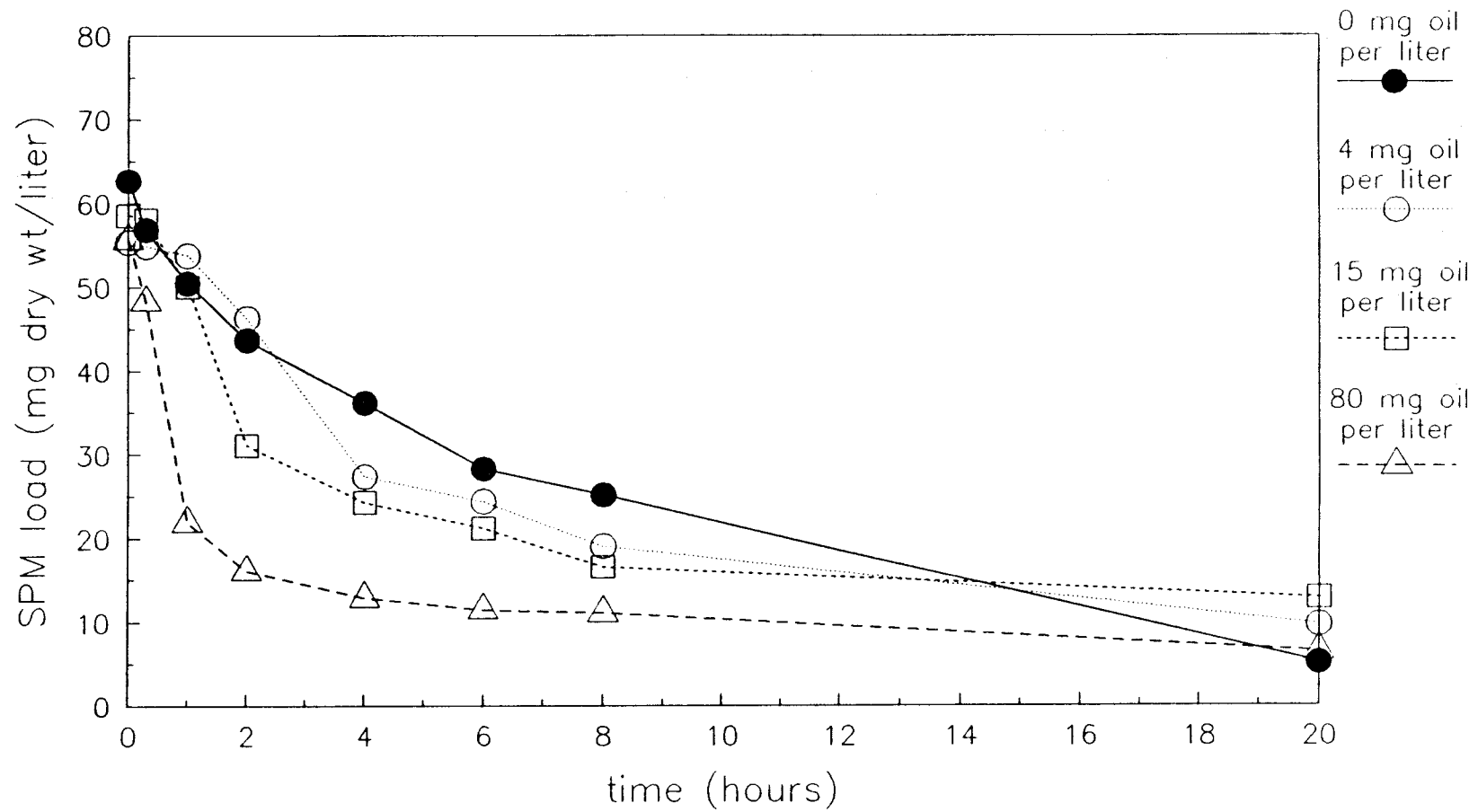
Figure 5-16. **SPM Loads Remaining in Suspension at Sampling Depth Over Time for SPM Previously Exposed to Different Oil Levels**

All data are for Grewingk glacial till (< 53 μm) in full-strength seawater with unweathered Prudhoe Bay crude oil.

of unweathered Prudhoe Bay crude oil. The numbers for oil in the figure represent values for total oil per liter of seawater in the parent stirred reaction vessel experiments. The data illustrate that the increasing quantities of oil in a parent reaction vessel experiment ultimately produced higher settling rates for SPM particles. Manipulating the data in Figure 5-16 to yield mean settling velocities (i.e., distance settled per unit time) and comparing the resulting values for the different levels of oil to that of the control (i.e., no oil) produced the plots in Figure 5-17. The latter figure illustrates the shift toward higher settling velocities with higher oil loadings. While Figures 5-16 and 5-17 provide information for Grewingk till and unweathered Prudhoe Bay crude oil, Figures 5-18 and 5-19 provide identical information for the same till with 12-day weathered Prudhoe Bay crude oil. The same general trends are observed, with higher oil loadings producing shifts toward higher settling velocities for the SPM. Comparable plots are presented for Yukon Delta SPM with unweathered Prudhoe Bay crude oil (Figures 5-20 and 5-21) and 12-day weathered Prudhoe Bay crude oil (Figures 5-22 and 5-23). While the effects upon Yukon Delta SPM are less dramatic than with Grewingk till, it still appears that there are shifts toward higher settling velocities for the Yukon SPM with higher oil loadings. It seems probable that the smaller effect on settling velocities for Yukon SPM may derive from the fact that the reactivity of the Yukon sediment with oil was substantially lower than that of Grewingk till (see Section 5.2.2.1 and in particular values for the reaction coefficient a in Table 5-8). It is interesting to note that Bassin and Ichiye (1977) concluded that inherent coagulation properties of oils and suspended clays did not appear to affect sedimentation rates of oil. However, from results presented in this report, it appears that increasing quantities of oil associated with SPM produced progressively greater rates of sedimentation for SPM and, hence, any associated oil.

In addition to investigating the overall sedimentation of oiled SPM, an attempt was made to determine whether agglomerated oil was uniformly distributed over the entire size spectrum of SPM in a given experiment. To accomplish this purpose, one filter sample from each sampling time was analyzed for oil content as well as SPM load in one settling chamber experiment. The specific experiment involved Yukon Delta SPM and 12-day weathered Prudhoe Bay

141
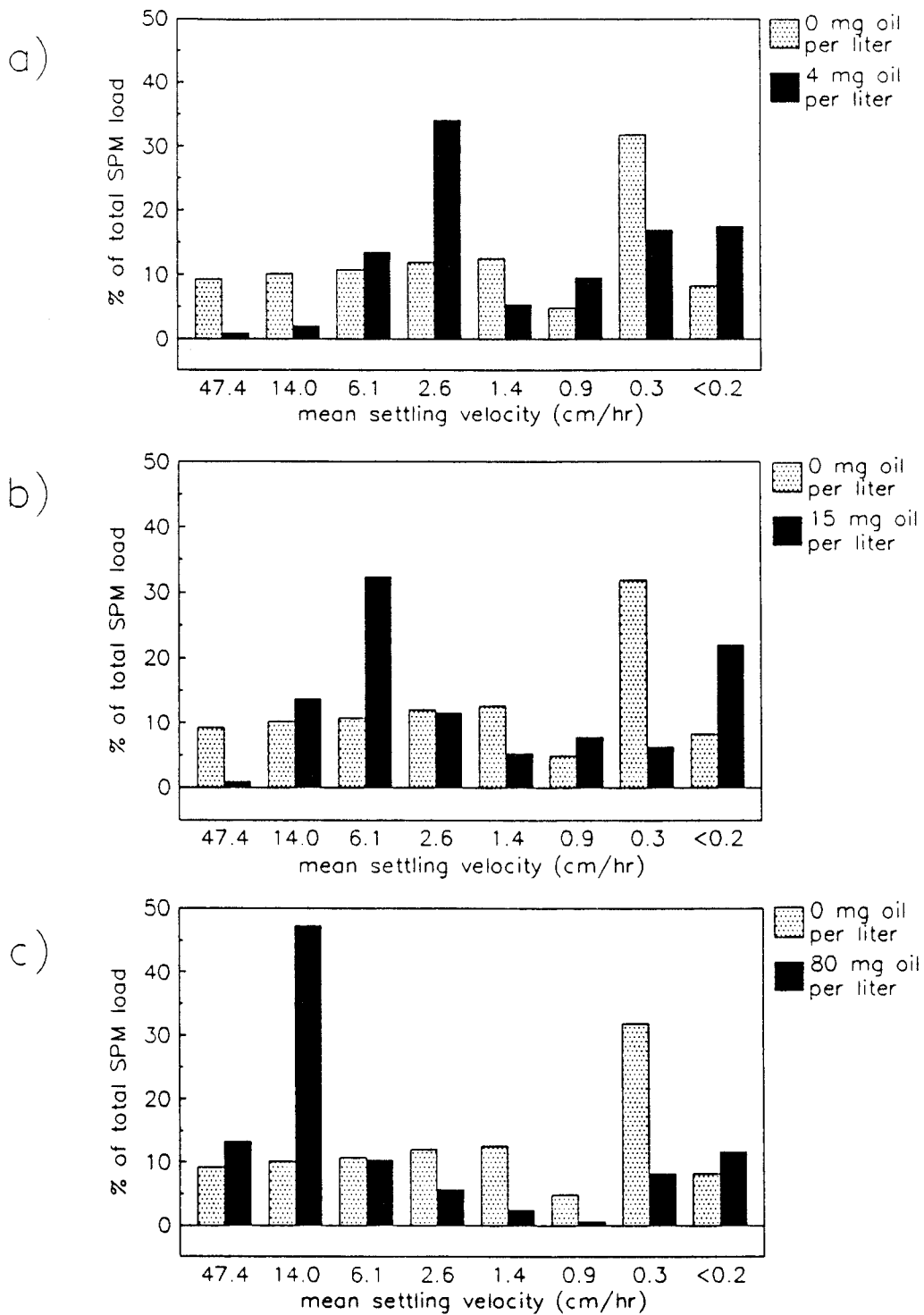
Figure 5-17. **Weight % of Total SPM Loads Corresponding to Given Mean Particle Settling Velocities for the Data Illustrated in Figure 5-16**

Experiments with the following oil load exposures are compared with an unoiled control: (a) 4 mg oil/L, (b) 15 mg oil/L, and (c) 80 mg oil/L.

142
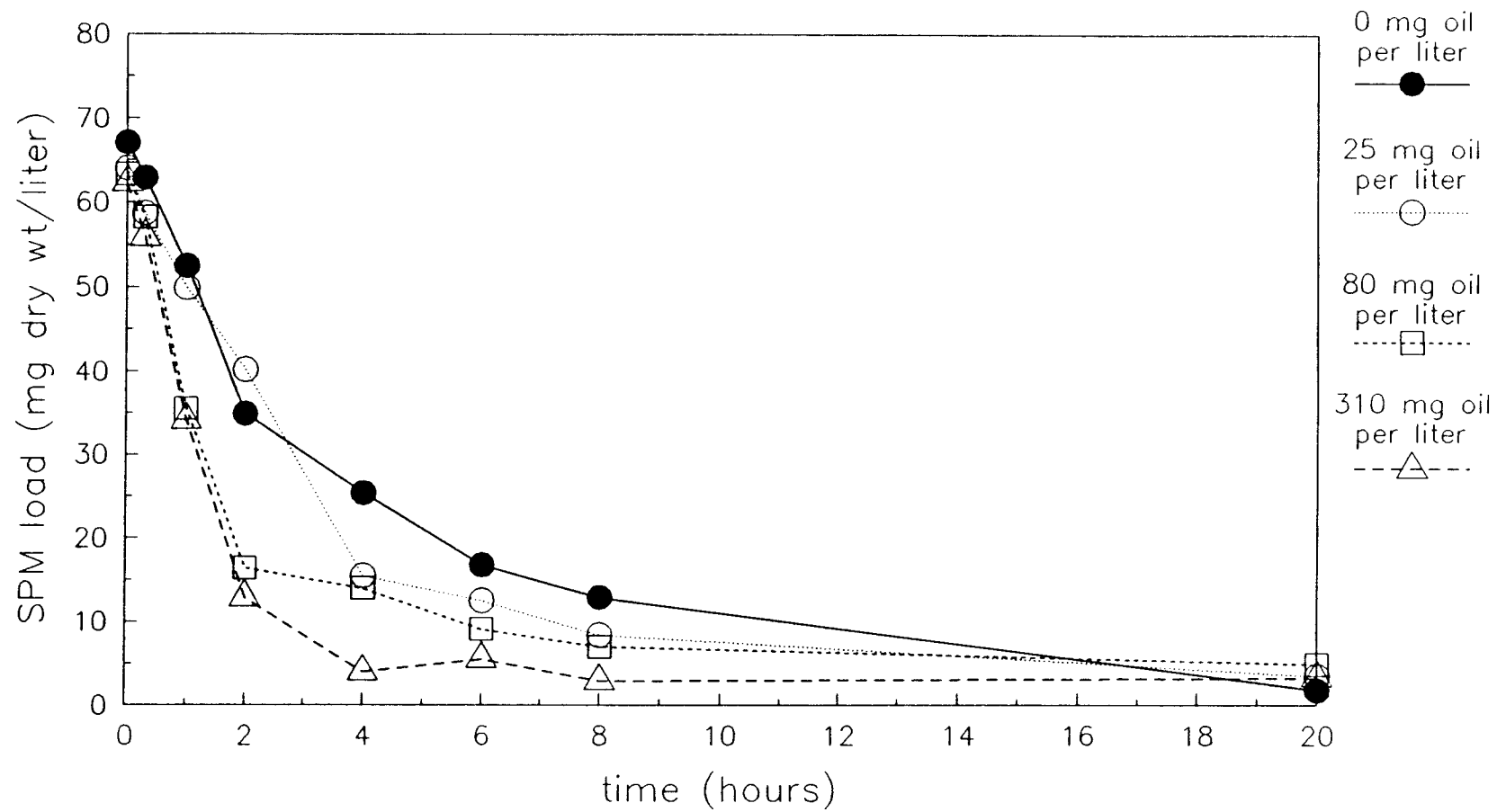
Figure 5-18. Identical to Figure 5-16, Except 12-Day Weathered Prudhoe Bay Crude Oil Used with Grewingk Glacial Till in Seawater
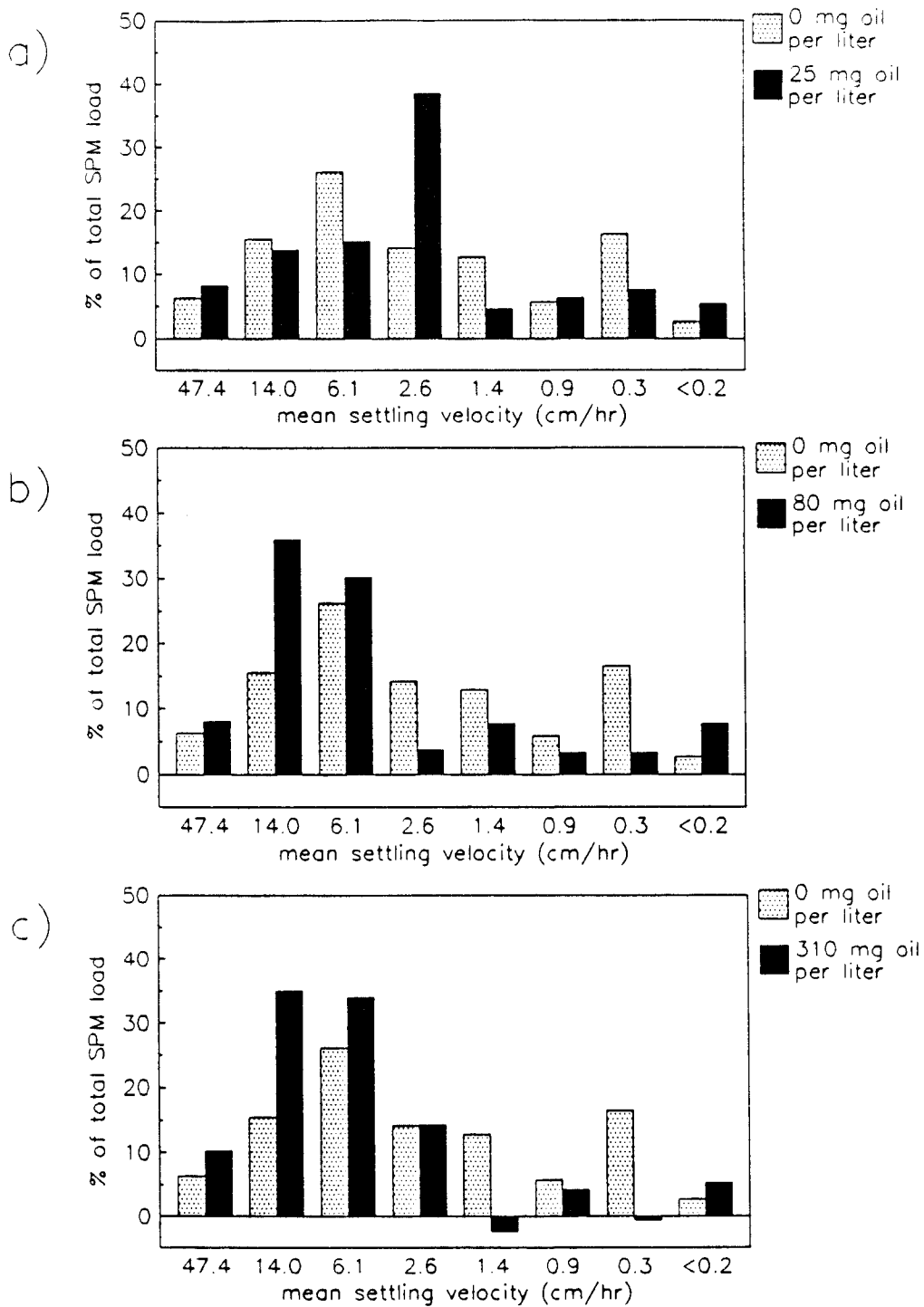
Figure 5-19. Weight % of Total SPM Loads Corresponding to Given Mean Particle Settling Velocities for the Data Illustrated in Figure 5-18

Experiments with the following oil load exposures are compared with an unoiled control: (a) 25 mg oil/L, (b) 80 mg oil/L, and (c) 310 mg oil/L.
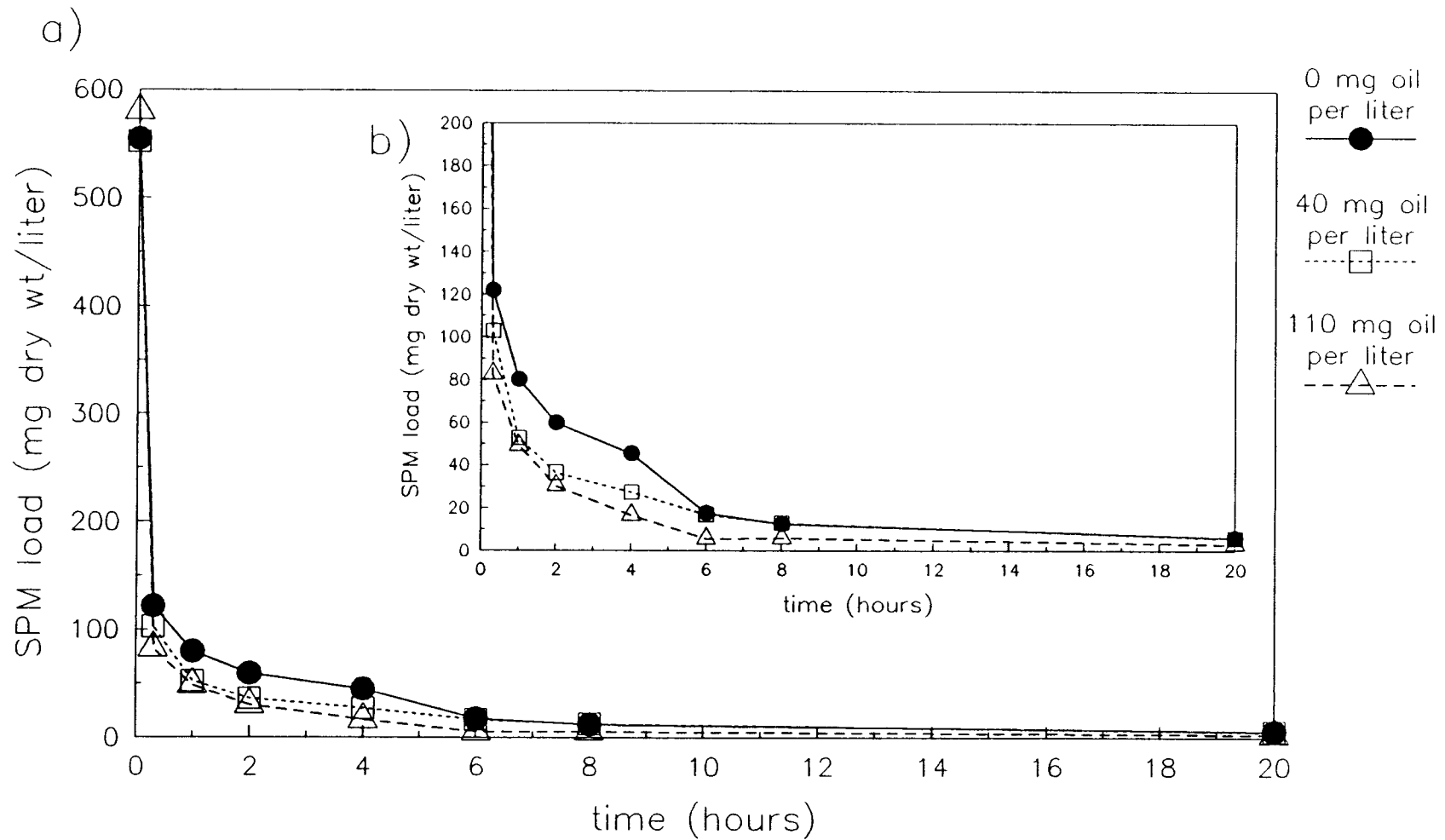
Figure 5-20. **SPM Loads Remaining in Suspension at Sampling Depth Over Time for SPM Previously Exposed to Different Oil Levels**

All data are for Yukon River Delta sediment (< 53 μm) in full-strength seawater with unweathered Prudhoe Bay crude oil. (a) All data. (b) Data for SPM load scale of 0–200 mg/L to allow better visualization of trends.
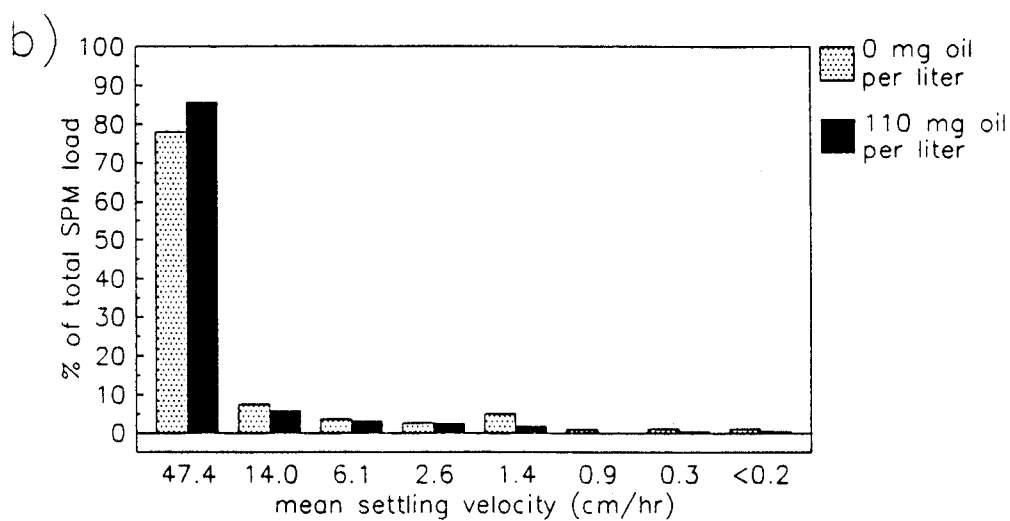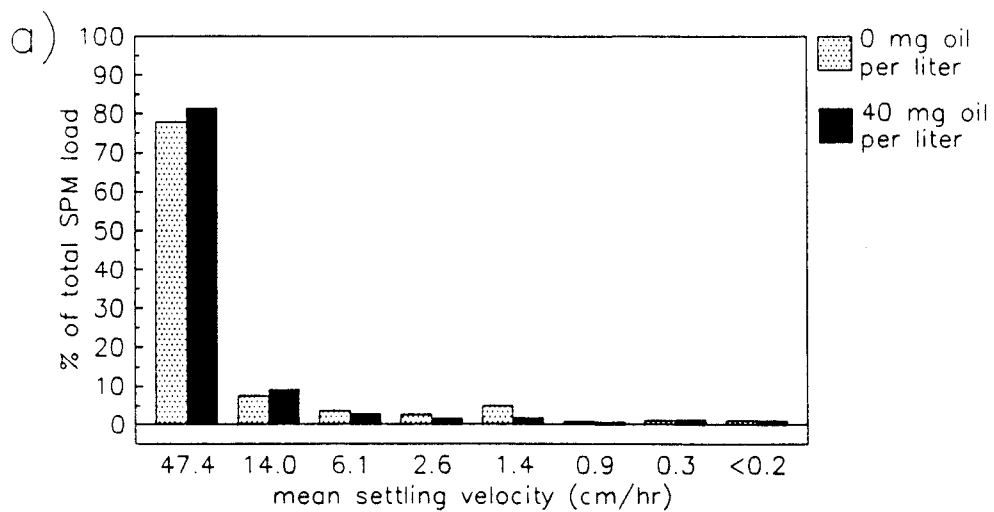
Figure 5-21. Weight % of Total SPM Loads Corresponding to Given Mean Particle Settling Velocities for the Data Illustrated in Figure 5-20

Experiments with the following oil load exposures are compared with an unoiled control: (a) 40 mg oil/L and (b) 110 mg oil/L.
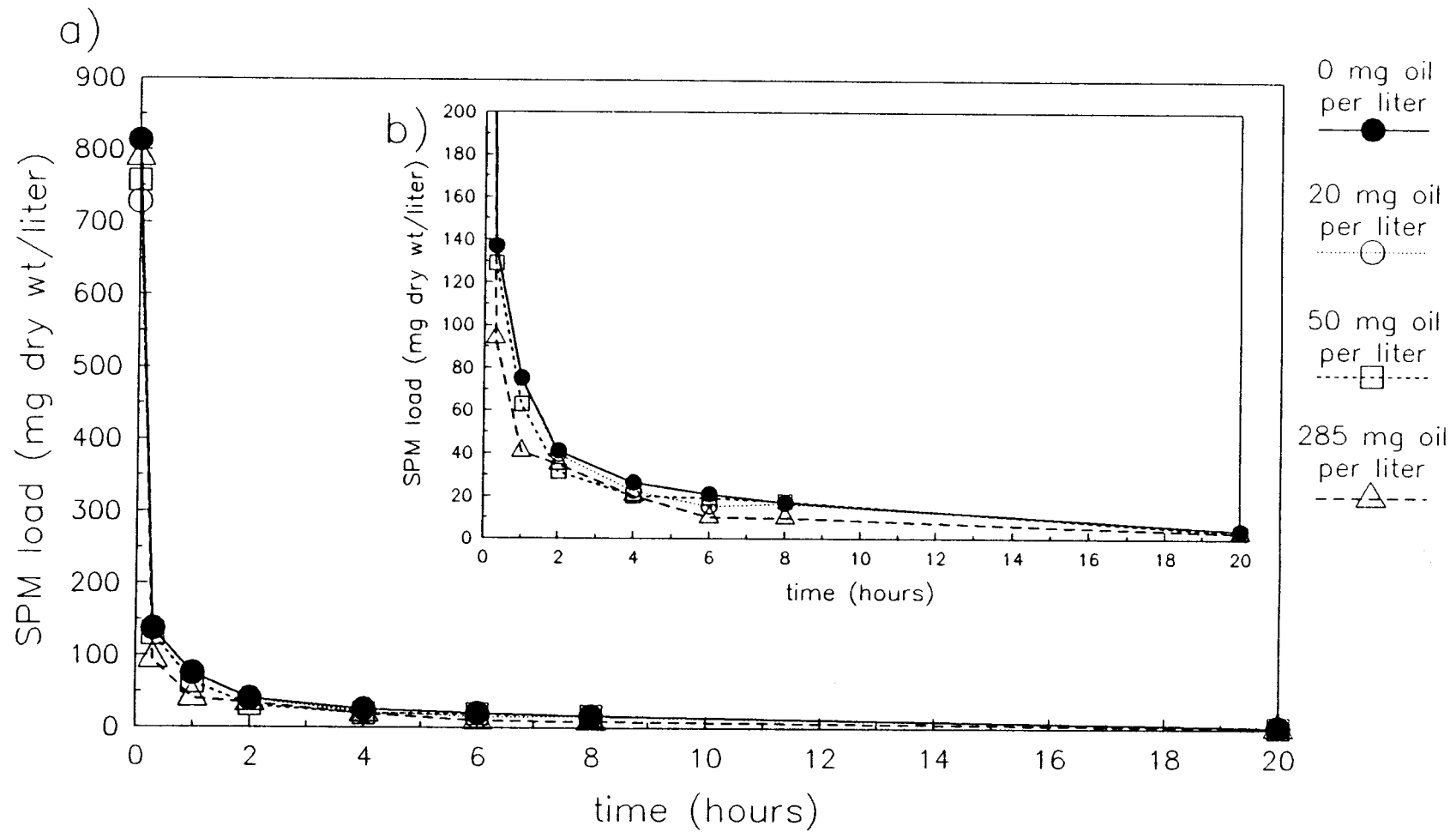
Figure 5-22. **Identical to Figure 5-20, Except 12-Day Weathered Prudhoe Bay Crude Oil Used with Yukon Delta River Sediment in Seawater**
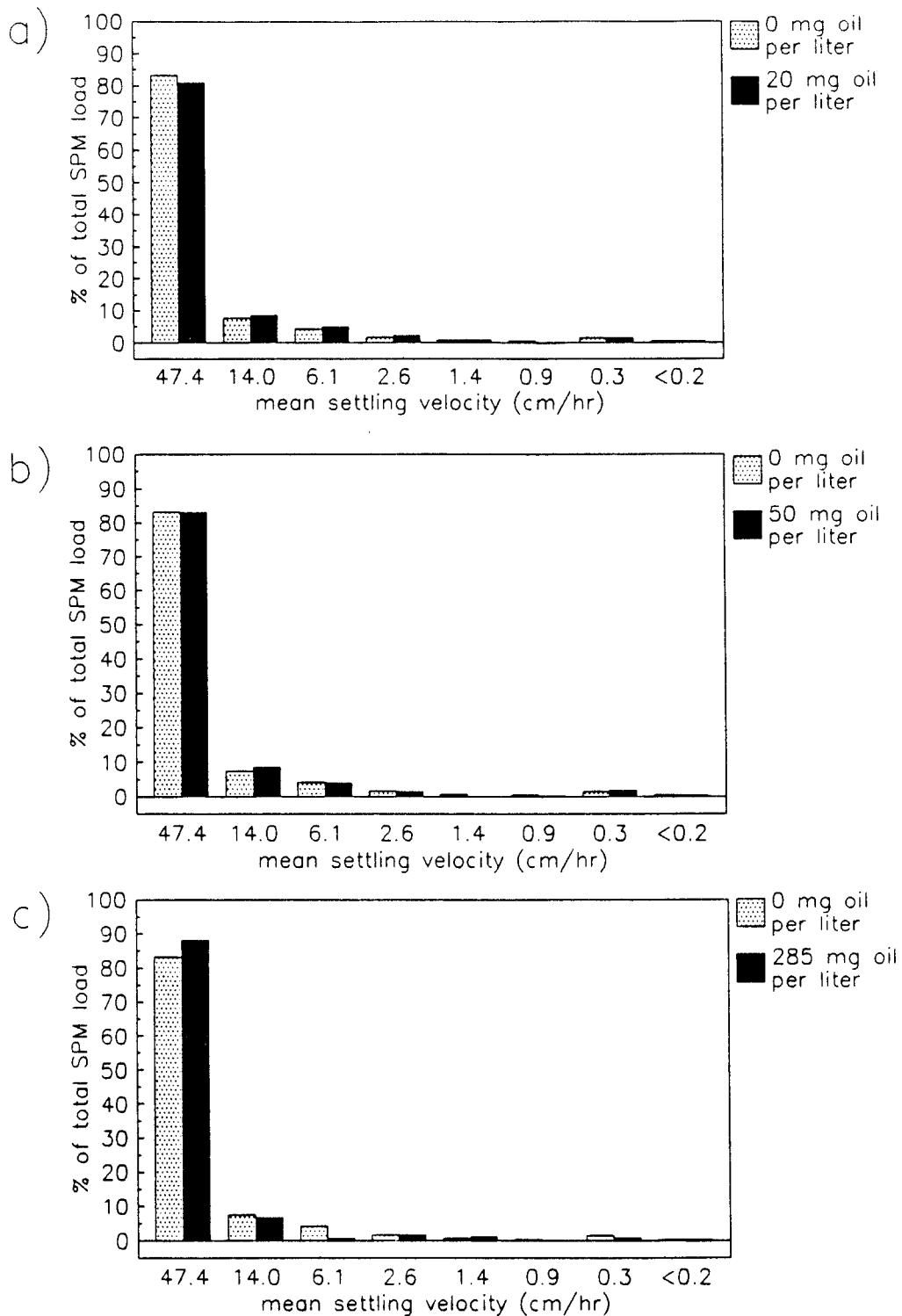
Figure 5-23. Weight % of Total SPM Loads Corresponding to Given Mean Particle Settling Velocities for the Data Illustrated in Figure 5-22

Experiments with the following oil load exposures are compared with an unoiled control: (a) 20 mg oil/L, (b) 50 mg oil/L, and (c) 285 mg oil/L.

crude oil in seawater. Results of the analyses of the SPM loads and the oil contents over time are illustrated in Figure 5-24. While values for both variables follow the anticipated rapid decline expected for Yukon Delta SPM, the decline does not appear to be as abrupt for the oil. Figure 5-25 again presents both sets of data following their transcription to appropriate settling velocity values. If oil were evenly distributed over the entire size spectrum of SPM particles, one would expect close agreement between trends in the data for the SPM loads and the oil concentrations. Because the latter situation was not exactly indicated (see Figure 5-25), it appears that oil was preferentially associating with particles that settled at velocities slightly lower than those of the "heaviest" SPM. Similar preferential associations of oil with "smaller" sediment particles in a controlled marine ecosystem are noted in Wade and Quinn (1980).

5.3.2.3 Effect of Salinity

Effects of salinity on settling velocities of particles were also investigated for Yukon Delta SPM. Figures 5-26 and 5-27 illustrate declines in SPM loads over time on two occasions with "unoiled" SPM. In both figures, the SPM loads in freshwater remain slightly elevated at the later sampling times. It would appear that this reflects a certain degree of flocculation in the smaller size ranges of SPM in seawater as well as the 1:1 mixture of seawater and freshwater, leading to greater sedimentation of "flocculated" SPM in the two solution mediums with higher salinities. Comparable data are shown for "oiled" SPM for unweathered Prudhoe Bay crude oil (Figure 5-28) as well as 12-day weathered Prudhoe Bay crude oil (Figure 5-29). Both of the latter figures illustrate trends similar not only to each other but also to the data in Figures 5-26 and 5-27 where no oil was present. In the context of these experiments, it does not appear that the sedimentation behaviors of "oiled" versus "unoiled" SPM are substantially affected by salinity. This is in contrast to results presented in Hartung and Klingler (1968) that show increased rates of sedimentation of oil at lower salinities. In light of results presented in Section 5.2.2.3 and Figure 5-12 that indicate only extremely limited tendencies for oil to interact with sediments in freshwater, it is unclear how Hartung and Klingler could obtain increased sedimentation of oil at

149
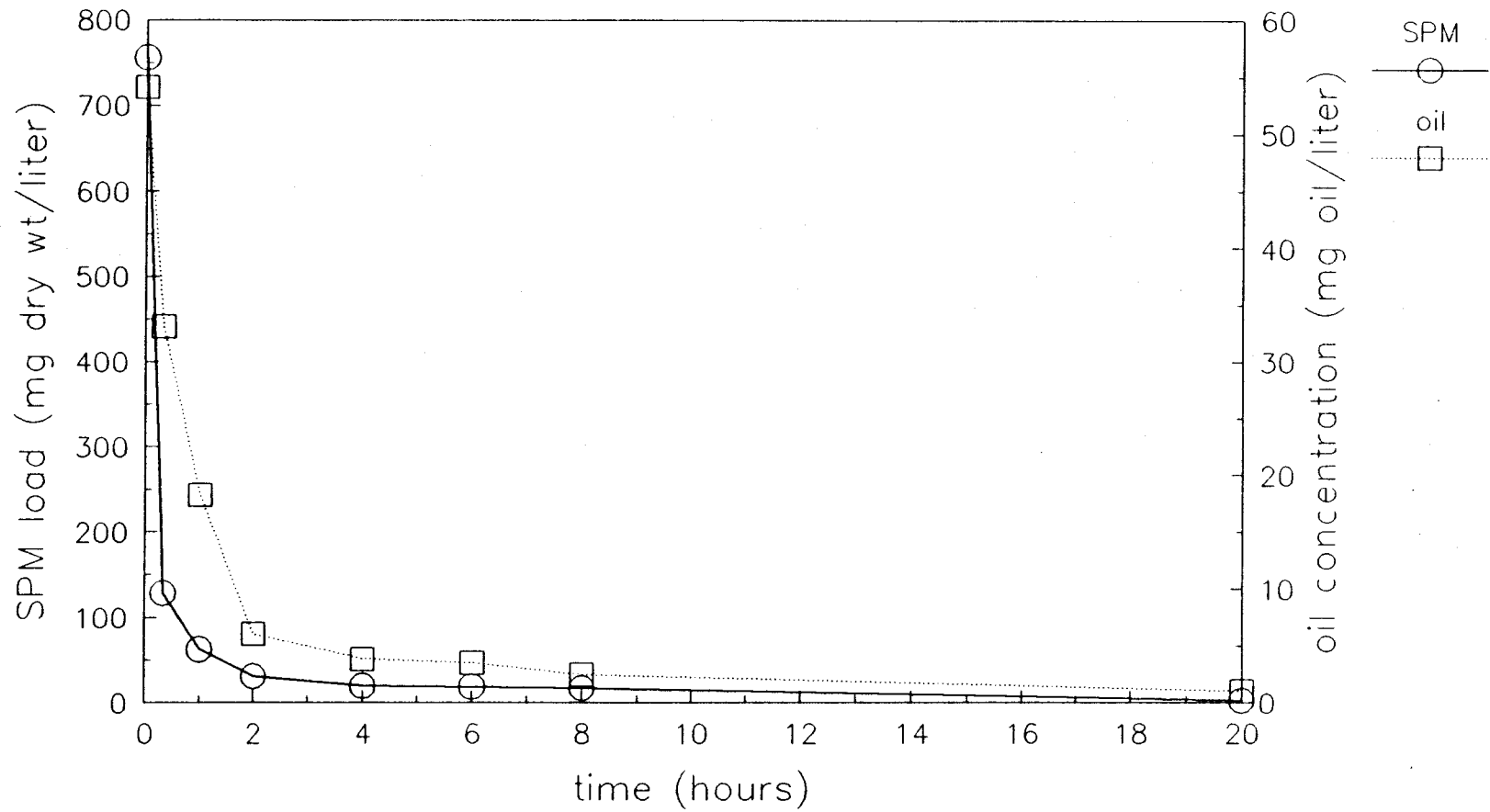
Figure 5-24. **Comparison Between Time-Course Declines in SPM Loads and Oil Concentrations Retained on Filters in a Settling Chamber Experiment**

The experiment involved Yukon Delta River sediment (< 53 µm) in seawater with 12-day weathered Prudhoe Bay crude oil.
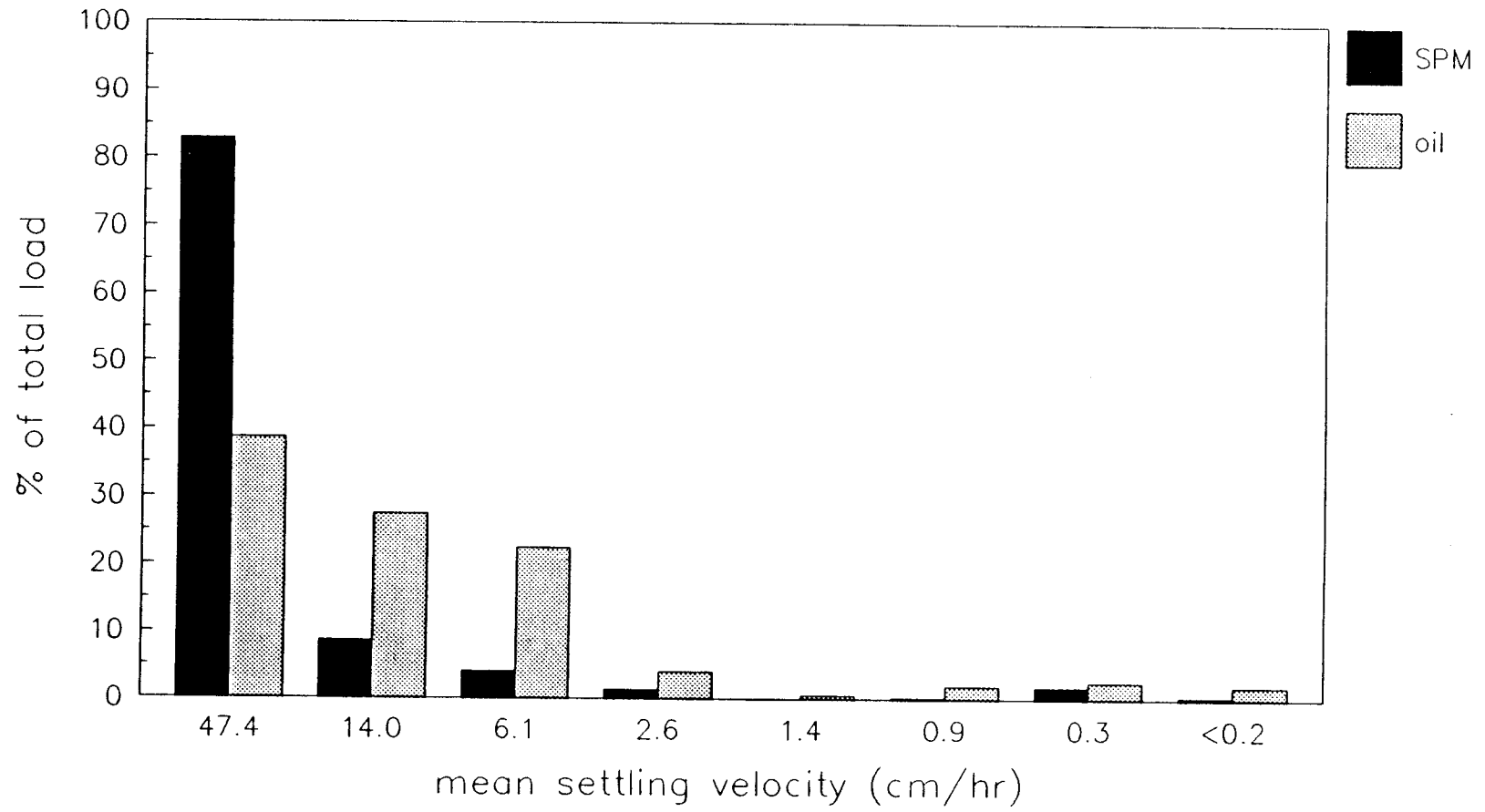
Figure 5-25. Percent of Total Loads for SPM and Oil Corresponding to Given Mean Settling Velocities for the Data Illustrated in Figure 5-24
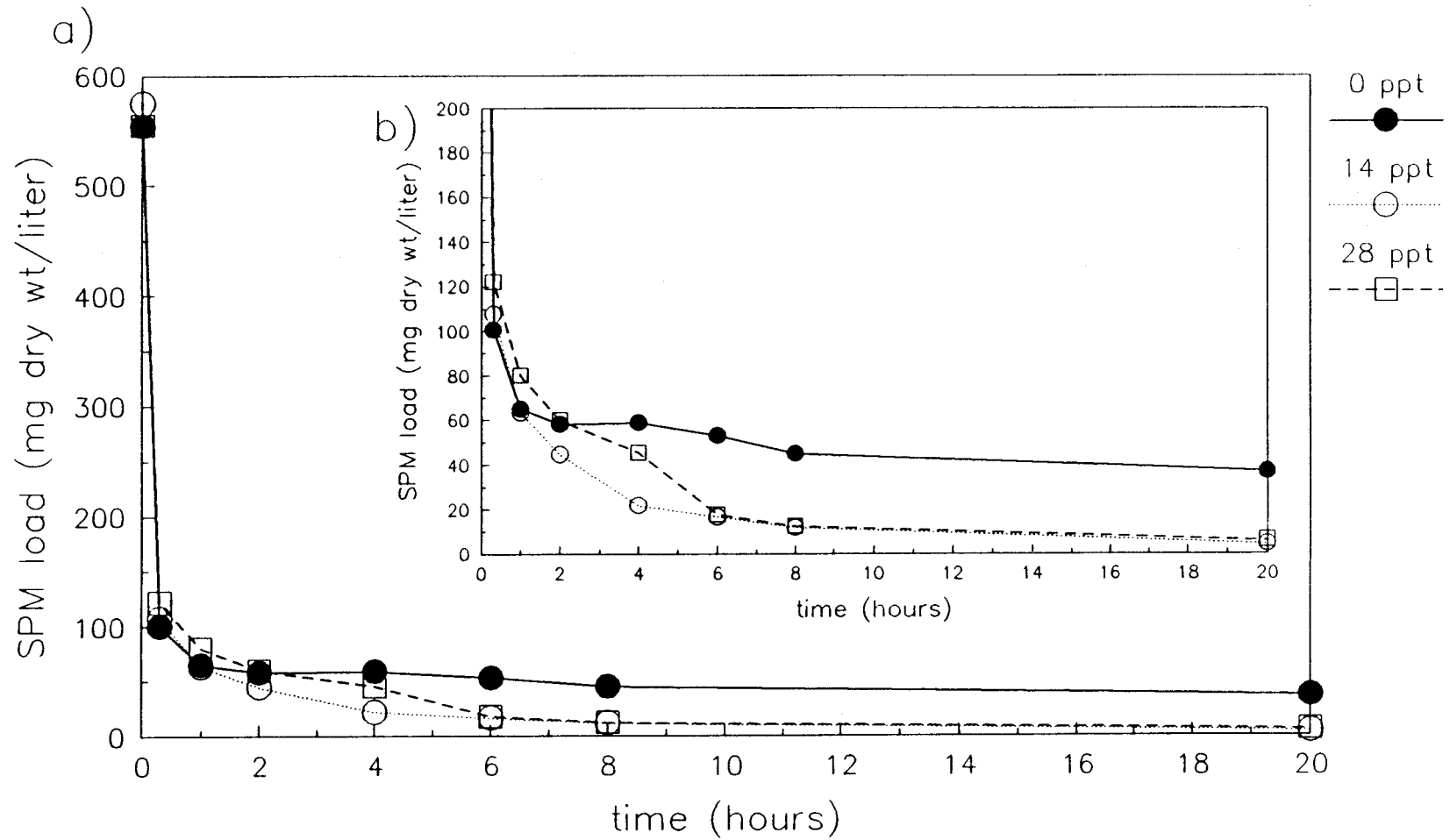
Figure 5-26. **SPM Loads for "Unoiled" Yukon River Delta Sediment (< 53 μm) Remaining in Suspension at Sampling Depth Over Time at Different Salinity Levels**

Sediment had not been previously exposed to oil. (a) All data. (b) Data for SPM load scale of 0–200 mg/L to allow better visualization of trends.
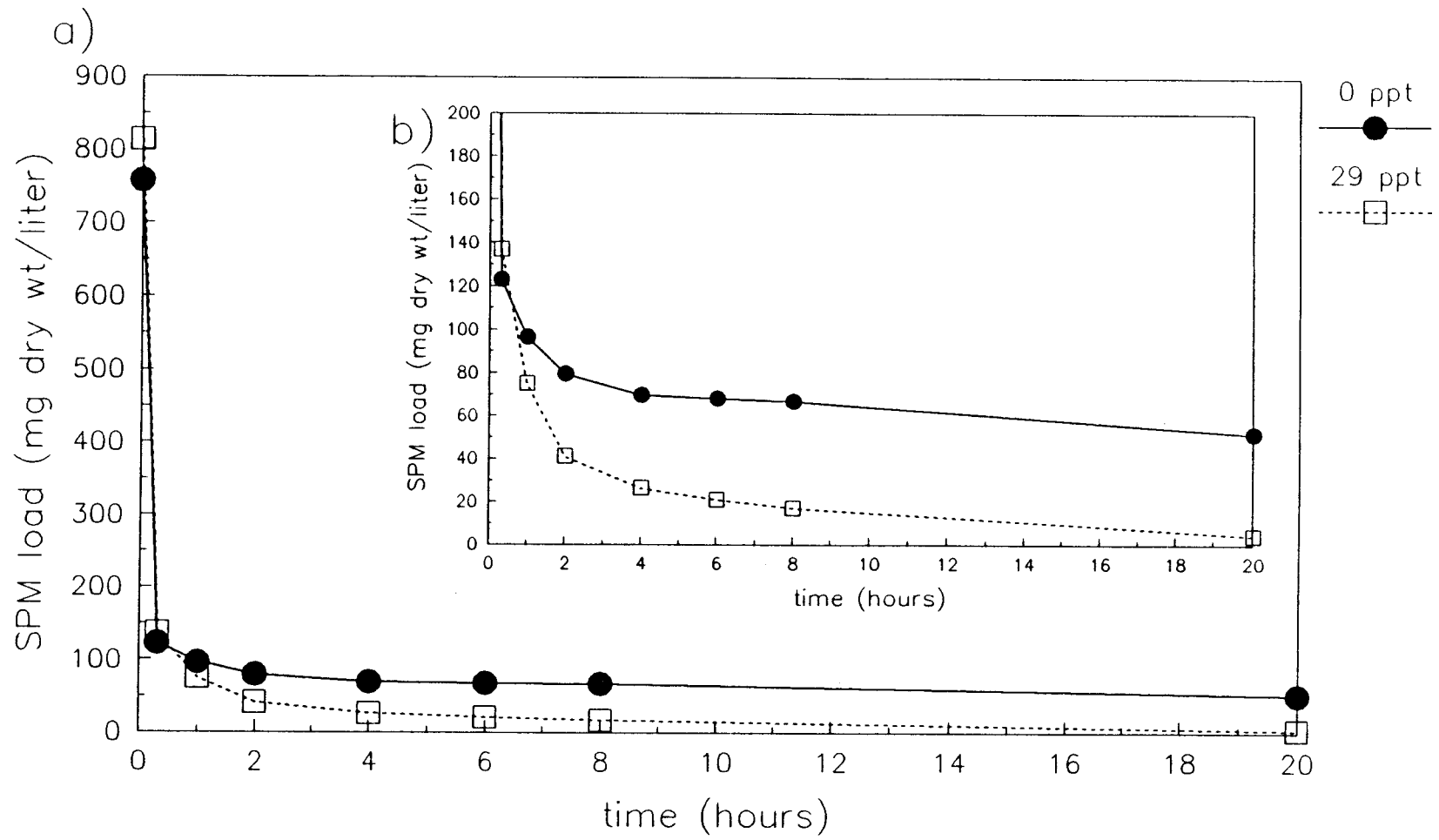
Figure 5-27.   Data for Experiments Identical to Those Summarized in Figure 5-26

153
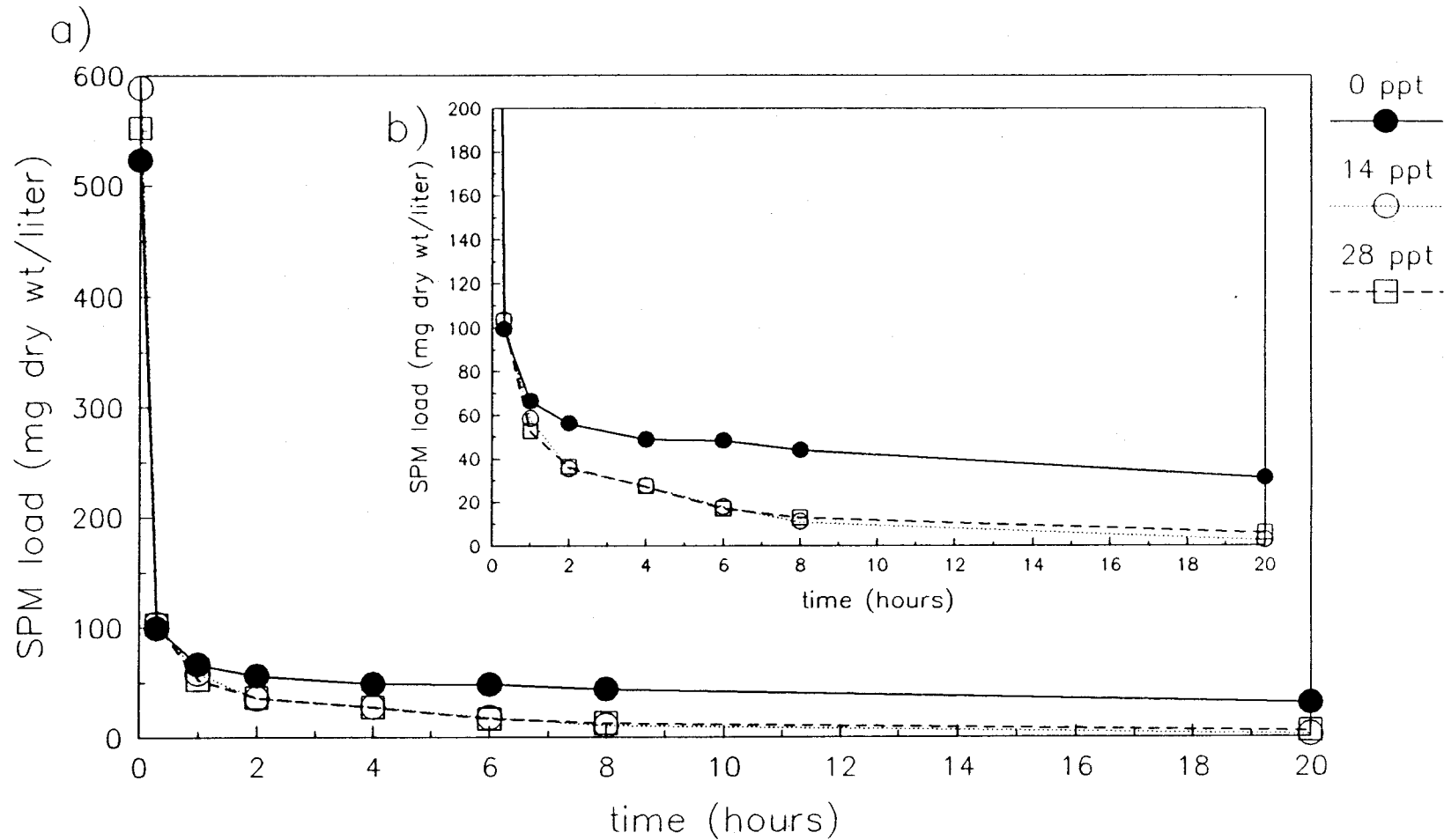
Figure 5-28. **SPM Loads for "Oiled" Yukon River Delta Sediment (< 53 μm) Remaining in Suspension at Sampling Depth Over Time at Different Salinity Levels**

Sediment had not been previously exposed to Prudhoe Bay crude oil. (a) All data. (b) Data for SPM load scale of 0–200 mg/L to allow better visualization of trends.

154
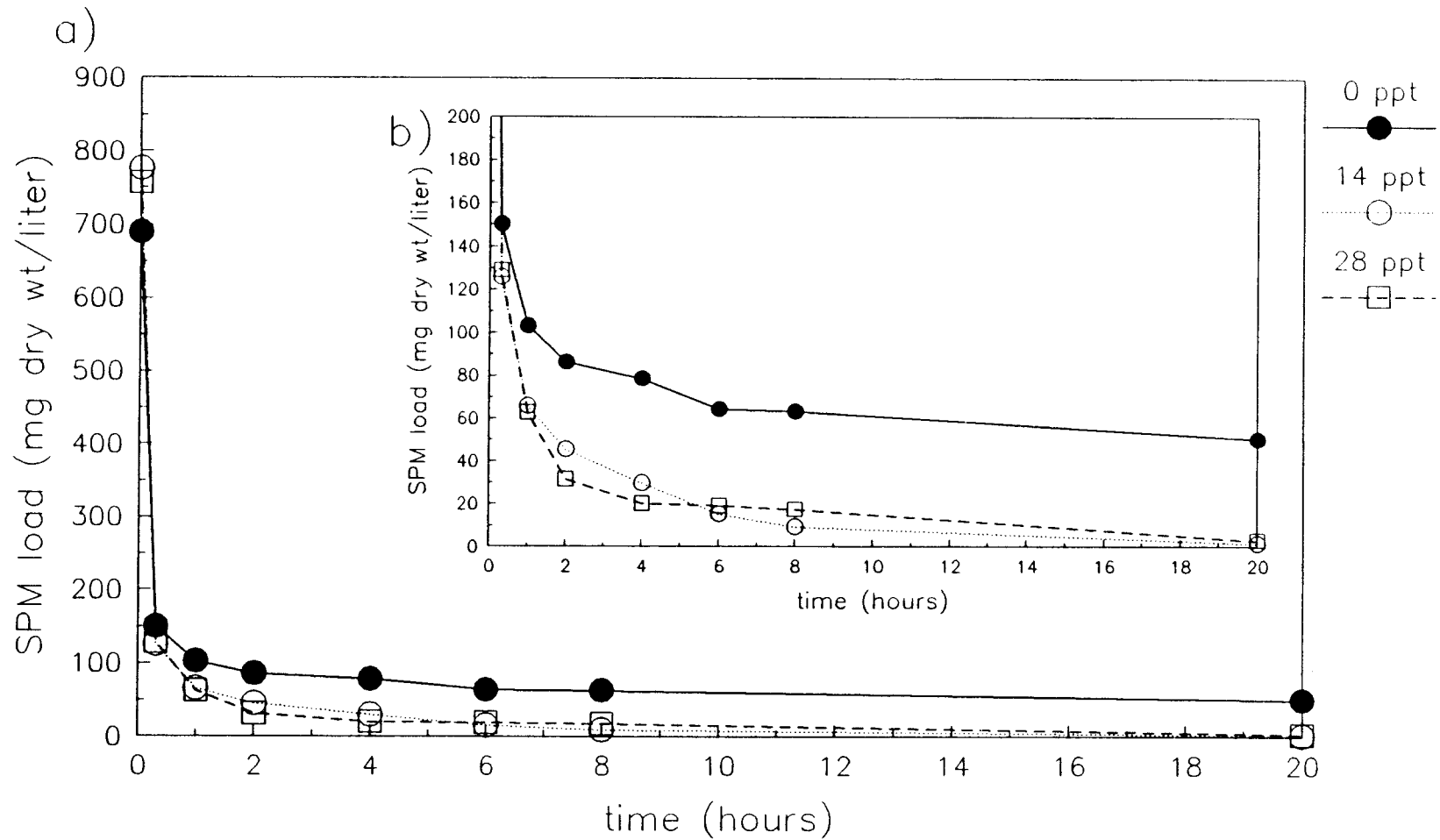
Figure 5-29. **SPM Loads for "Oiled" Yukon River Delta Sediment (< 53 μ) Remaining in Suspension at Sampling Depth Over Time at Different Salinity Levels**

Sediment had been previously exposed to 12-day weathered Prudhoe Bay crude oil. (a) All data. (b) Data for SPM load scale of 0–200 mg/L to allow better visualization of trends.

lower salinities. The results in this report documenting higher rates of interaction between oil droplets and SPM at higher salinities and the implication that this has for subsequent sedimentation of "oiled" SPM appear to be in agreement with conclusions arrived at by Bassin and Ichiye (1977).

5.4 MOLECULAR ADSORPTION LEVELS

A discussion of the utility and development of the isotherm, and how it can be applied to the determination of molecular-scale interactions with SPM has been presented earlier as Section 4.4. The development of isotherms has resulted in the determination of the maximum adsorption capacity for a variety of individual molecular species. In addition, the method for arriving at the isotherm lends itself to the calculation of the equilibrium partition coefficient. The following discussion presents the results of these measurements along with predictions of realistic sorption levels based on actual spill-event dissolved-component concentrations. The use of distillate cuts as convenient experimental material arises, in part, from the need to limit the number of compounds tested as well as to conform to the approach already adopted by the previous modeling efforts.

Isotherm plots of X/M vs C_f are presented as Figures 5-30 and 5-31 for Cuts #4 and #7 for Grewingk glacial till, respectively. Figure 5-32 depicts isotherms of Cut #7 compounds for Yukon Delta sediment. The X/M intercept at C_o provides the maximum individual molecular adsorption capacity at the initial dissolved concentration. These values are presented (along with the initial concentration in seawater and the isotherm linear correlation coefficient) in Tables 5-10 and 5-11 . As seen in Table 5-10 and Figure 5-30, for compounds contained in Cut #4, the nearly identical isotherm slopes and the almost direct correlation between capacity and initial (C_o) concentration suggest that a single adsorption mechanism is operational.

On the other hand, Table 5-11 and Figure 5-31 show varying isotherm slopes and little direct dependence of capacity on initial concentration for compounds in Cut #7. This suggests more complex adsorption mechanism(s) for these intermediate molecular-weight aromatics. It should be noted, however,
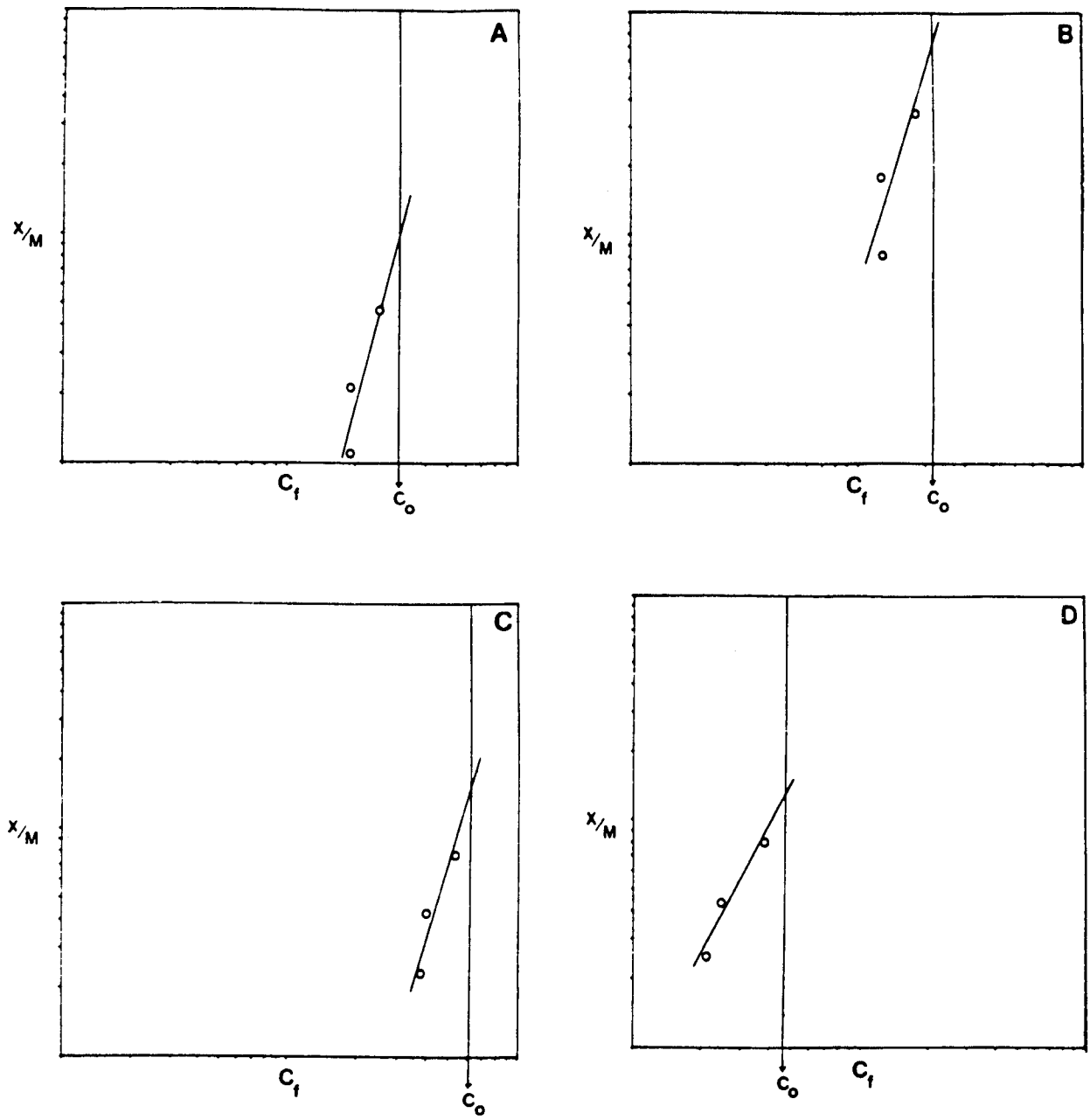
Figure 5-30.   Selected Isotherms for Grewingk Glacial Till and Cut #4 Components: A) Toluene,
B) Ethylbenzene, C) O-xylene, and D) Ethylmethylbenzene
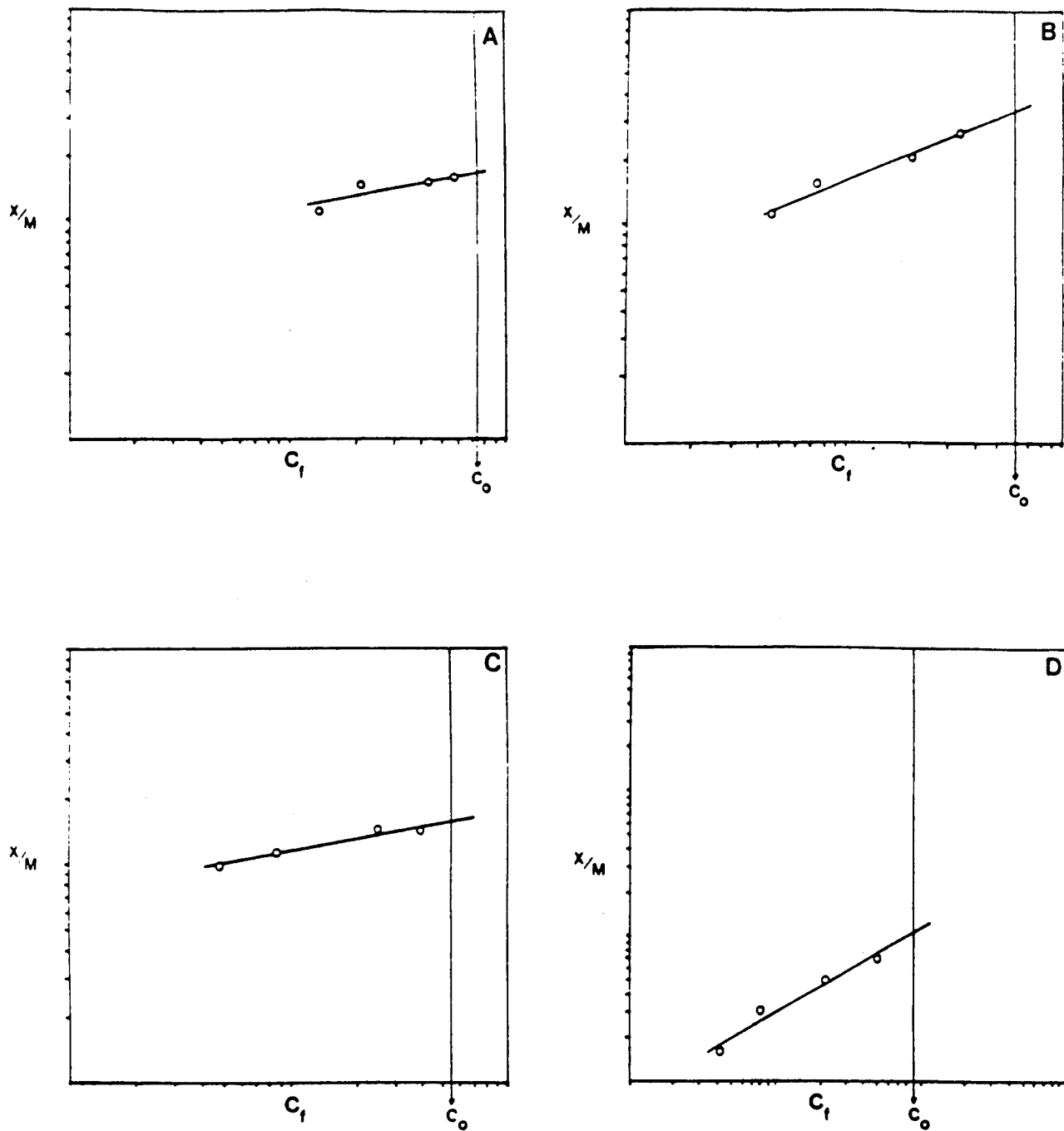
Figure 5-31. Selected Isotherms for Grewingk Glacial Till and Cut #7 Components: A) naphthalene, B) 2-methylnaphthalene, C) 1-methylnaphthalene, and D) 1,1'-biphenyl

158
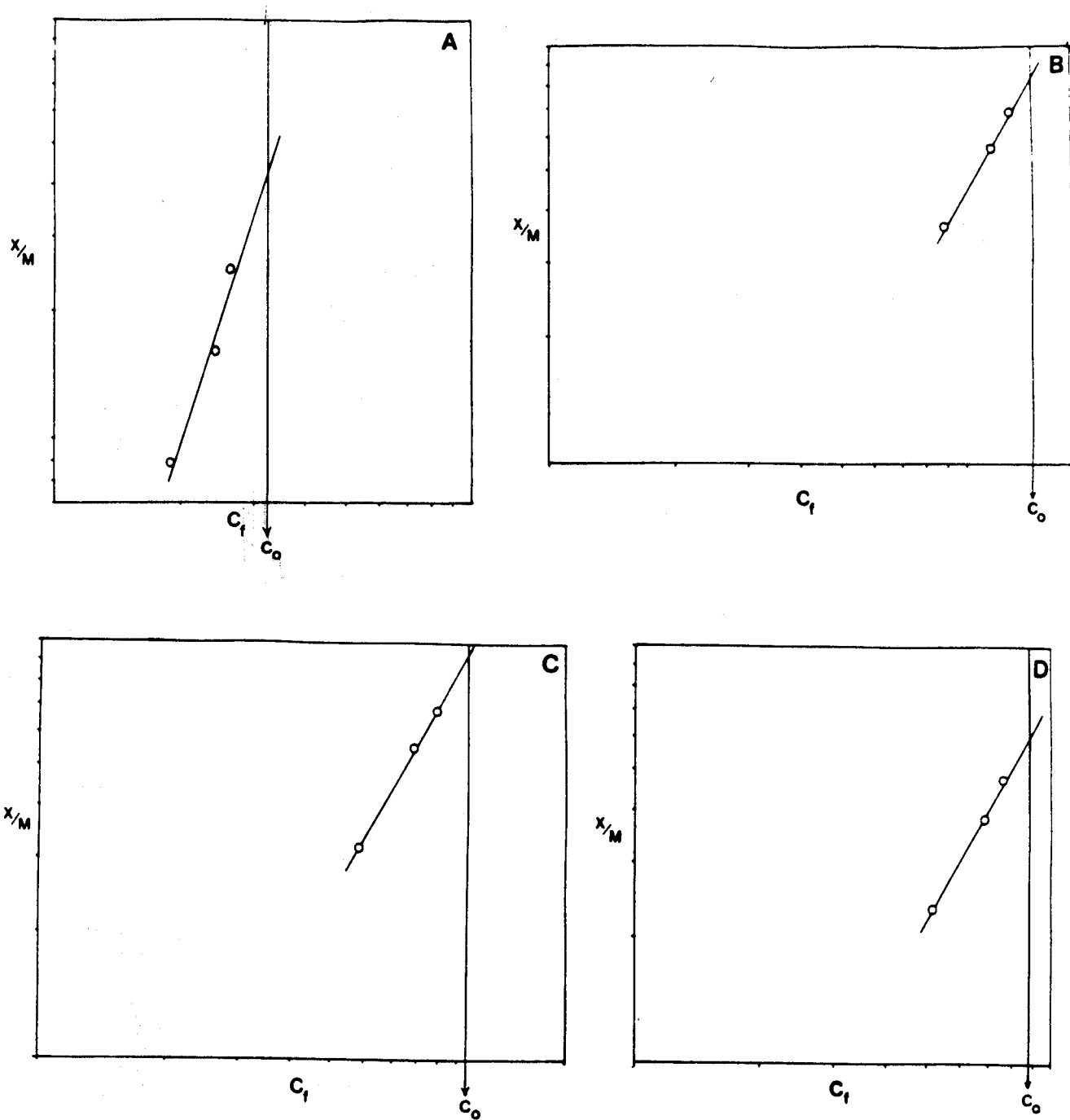
Figure 5-32. Selected Isotherms for Yukon Delta Sediment and Cut #7 Components: A) Naphthalene, B) 2-methylnaphthalene, C) 1-methylnaphthalene, and D) 1,1'-biphenyl

Table 5-10

Adsorptive Capacities of Grewingk Glacial Till[a] for Cut #4 Dissolved Hydrocarbons

Compounds	Concentration in Seawater (μg/l)	Maximum Adsorptive Capacity (μg/g)	Linear Correlation Coefficient
Toluene	7,230	250	.844
Ethylbenzene	5,400	170	.778
m&p-xylene	27,300	660	.867
o-xylene	15,400	360	.907
Ethylmethylbenzene	1,160	36	.972
C_3-benzene	450	11	.920
C_3-benzene	484	14	.974

[a] Attempts to determine adsorptive capacities for Yukon Delta sediment were unsuccessful due to inadequate dosage/concentration bracketing.

Table 5-11

Comparison of Adsorptive Capacities of Two Sediment Types for Cut #7 Dissolved Hydrocarbons

Compound	Concentration in Seawater (μg/l)	MAXIMUM ADSORPTIVE CAPACITY (μg/g)/LCC[a]	
		Grewingk Glacier	Yukon Delta
Tetramethylbenzene	25.2	2.5/.983	3.8/.977
C_4-benzene	75.5	2.5/.929	4.0/.885
Naphthalene	1,110	35/.889	75/.997
2-methylnaphthalene	842	61/.986	84/.999
1-methylnaphthalene	723	30/.906	54/.997
1,1'-biphenyl	31.2	1.6/.828	1.9/.957

[a] LCC indicates linear correlation coefficient

160

that these adsorbtive capacities are partially dependent on the initial concentrations by virtue of the saturation levels of starting material. That is, although a one-to-one concentration-to-capacity relationship does not exist for Cut #7, the capacities will depend on the relative initial concentrations.

Nevertheless, the maximum adsorption capacities of Grewingk glacial till ranged from a low of 1.6 μg/g for 1,1'-biphenyl to a high of 660 μg/g for m&p-xylenes. Maximum adsorptive capacities were obtained for Yukon Delta sediment with Cut #7 only because of experimental "bracketing" problems encountered during Cut #4 isotherm development. Yukon Delta sediment adsorption capacities for Cut #7 are uniformly higher than those of Glacial till (Table 5-11) and range from 1.9 μg/g for 1,1'-biphenyl to 84 μg/g for 2-methylnaphthene. This uniformly higher capacity for Yukon Delta sediment may be a result of the higher TOC levels displayed by Yukon Delta sediment compared to Grewingk till (see Section 5.1).

In addition to the values shown in Tables 5-10 and 5-11, one isotherm was developed for Glacial till for an unidentified C_{14}-carboxylic acid contained in the oil distillate bottoms; at a seawater concentration of 27.0 μg/l the capacity of Glacial till for this compound was 6.7 μg/g.

Because the oil weathering model utilizes a pseudocomponent (i.e., distillate cut) approach to account for the oil's mass balance, a slightly modified version of the above tests was conducted using Cut #10. In this experiment, a single capacity was developed for the cut as a whole in order to establish the SPM's capacity for an entire distillate cut. In addition, the variation arising from differences in SPM composition was investigated by examining three SPM types.

Figure 5-33 presents the isotherms developed for the sum of all Cut #10 resolved peaks and, as seen, markedly different plots were obtained for the three SPM types. Table 5-12 shows a range of capacities from 1.0 μg/g for Turnagain Arm SPM to 22 μg/g for Grewingk glacial till with Yukon Delta sediment falling in between at 7.1 μg/g. Theses differences are often attributed to the effects on sorption of 1) the particle-size distribution, which also

161
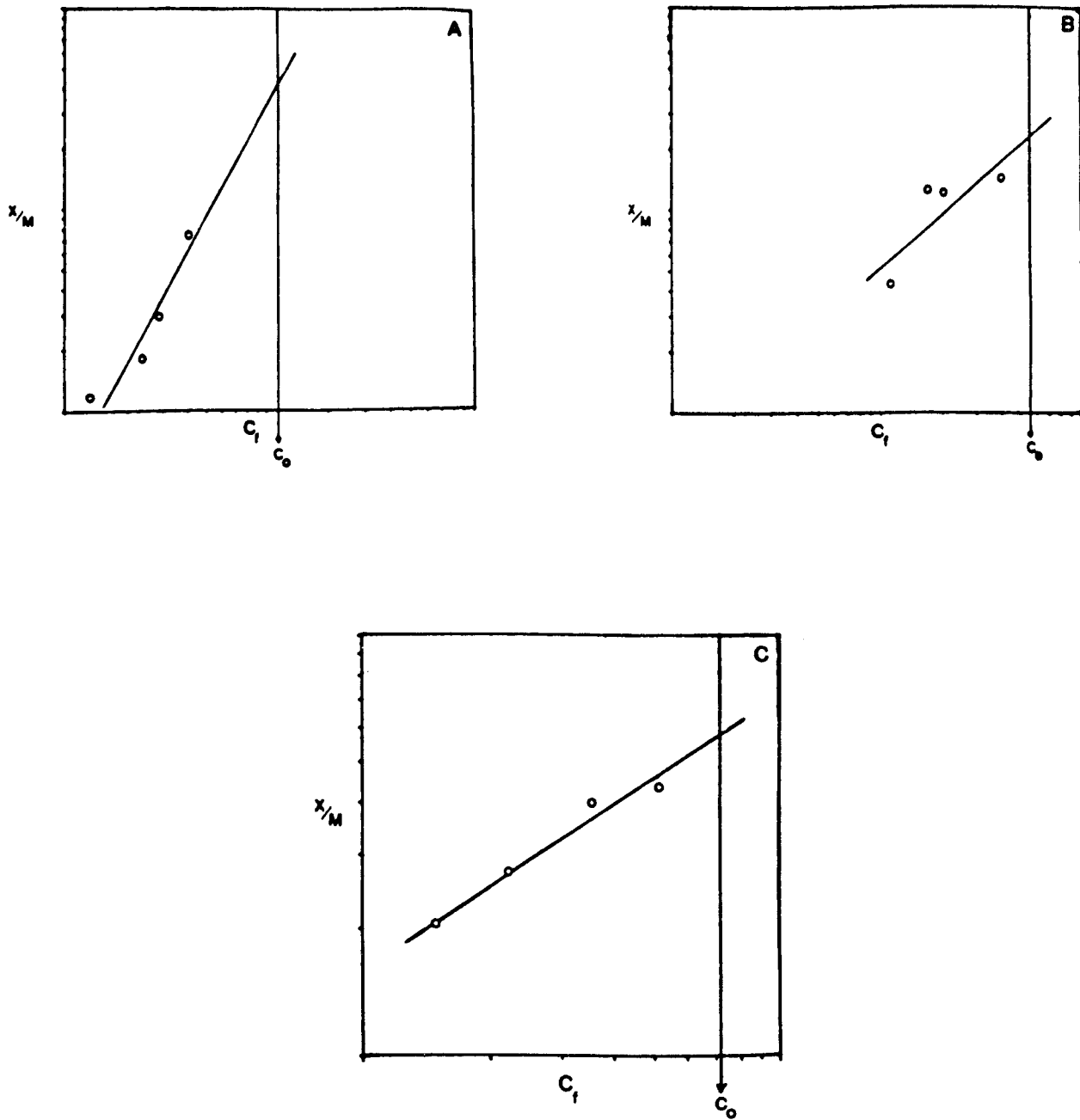
Figure 5-33.   Isotherms of Total Cut #10 Soluble Components with A) Grewingk glacial till, B) Turnagain Arm SPM, and C) Yukon Delta sediment

162

Table 5-12

Comparison of Adsorptive Capacities of Three Sediment Types for Total[a] Cut #10 Dissolved Hydrocarbons

SPM Type	Maximum Adsorptive Capacity[b] ($\mu g/g$)	Linear Correlation Coefficient
Turnagain Arm	1.0	.892
Grewingk Glacier	22	.954
Yukon Delta	7.1	.981

[a] sum of all Cut #10 resolved compounds
[b] initial Cut #10 concentration in seawater was 54.4 $\mu g/L$ with a coefficient of variation of 40% based on experimental triplicates

affects number density and available surface area, and 2) SPM organic carbon loading (Karickhoff et al., 1978). (See Section 5.1 for sediment/SPM characterization data.)

It should be emphasized here that the values reported throughout this discussion so far represent the maximum capacity that SPM could adsorb under ideal (designed) conditions. Ideal conditions for maximum adsorption would dictate a packed column of SPM and a suitably long contact time with cut equilibrated seawater as the influent. Of course ocean conditions are hardly ideal (from this respect), and capacities in the marine environment are bound to be substantially lower than those reported here.

To put these adsorption capacities into perspective, isotherms were developed for toluene and ethylbenzene using a granular-activated carbon from Hydro-Darco. At similar initial concentrations the activated-carbon capacity was 53 mg/g for toluene and 15 mg/g for ethylbenzene. These capacities are

163

orders of magnitude greater than the levels determined for glacial till (see Table 5-10).

Given the results presented above, and keeping in mind that they represent the upward boundary (ie. under designed conditions), it becomes apparent that SPM/dissolved or molecular-scale interactions account for only a minuscule fraction of the mass of oil potentially removed when compared to dispersed, whole-oil droplet/SPM interactions (see Section 5.2). However, in order to obtain realistic sorption values, as opposed to the maximum levels provided above, the isotherm experimental data were used to obtain partition coefficient (K_p) values for the individual dissolved molecular compounds. Cuts #4 and #7 for Grewingk glacial till and Yukon Delta sediment and total Cut #10 compounds for all three types of SPM were investigated. The results of this effort are presented below.

Calculated K_p values can be found in Table 5-13 along with the coefficient of variation (CV) arising from replicate measurements. As seen, the K_p values range from 12.9 to 204 for Grewingk glacial till, and from 26.3 to 86.0 for Yukon Delta sediment for Cuts #4 and #7 compounds. Most apparent from these

Table 5-13

Predicted Levels of Molecular-Scale/SPM Adsorption

Compound	Grewingk	K_p (CV)[a] Yukon	Turnagain	Estimated Maximum Water Column Concentration (ppb)	PREDICTED CONCENTRATION[b] ON SPM (ppb) Grewingk	Yukon	Turnagain
Toluene	18.5 (31)	28.0 (30)	NA[c]	140	2,500	3,900	NA
Ethylbenzene	21.1 (21)	29.2 (9)	NA	20	420	580	NA
m & p-xylene	17.4 (31)	26.3 (19)	NA	60	1,000	1,600	NA
o-xylene	12.9 (39)	28.2 (25)	NA	30	390	840	NA
Ethylmethylbenzene	20.6 (27)	34.5 (15)	NA	4	80	130	NA
C$_3$-benzene	16.8 (31)	35.8 (14)	NA	4	70	140	NA
C$_3$-benzene	22.6 (19)	29.7 (13)	NA	8	180	240	NA
Tetramethylbenzene	55.1 (18)	86.0 (36)	NA	3	160	250	NA
C$_4$-benzene	39.6 (22)	57.3 (16)	NA	10	400	570	NA
Naphthalene	70.9 (54)	60.5 (14)	NA	20	1,400	1,200	NA
2-methylnaphthalene	196 (52)	84.1 (16)	NA	15	2,800	1,200	NA
1-methylnaphthalene	138 (70)	68.0 (15)	NA	10	1,300	670	NA
1,1'-biphenyl	204 (100)	80.8 (29)	NA	2	390	160	NA
Cut #10	134 (47)	17.9 (20)	50.7 (46)	~10	1,300	170	500

[a] Kp indicates the average partition coefficient – concentration on SPM/concentration in solution at equilibrium. CV is the coefficient of variation based on triplicate measurements.
[b] predictions based on measured Kps, real spill event dissolved aromatic water column concentrations, and an SPM level of 200 mg/l
[c] not analyzed

data is the general trend of increasing K_p with increasing molecular weight. The resolved compound K_p for total Cut #10 was 134 for Glacial till, 17.9 for Yukon Delta, and 50.7 for Turnagain Arm. These values appear to correlate well with number density.

Also included in Table 5-13 are estimated maximum water column concentrations for each of the investigated compounds. These values were obtained from measurements coinciding with, for the most part, real spill events (Brooks et al., 1980; McAuliffe, 1977a and b; Payne et al., 1984). By combining the measured K_p values with these estimated water column concentrations and assuming an ocean SPM loading of 200 mg/l, the predicted concentration on the SPM has been calculated. The following equation was used to predict these more realistic dissolved molecular-scale sorption levels.

$$C_s = \frac{C_i V_1}{V_1/K_p + S}$$

Where C_s = the concentration on the SPM (μg/g), C_i = the initial concentration in seawater (μg/l), V_1 = the volume of seawater (l), K_p = the partition coefficient (unitless), and S = the SPM loading (g). The above formula arises from rearrangement and substitution of the simple mass balance equation:

$$C_i V_1 = C_1 V_1 + C_s S$$

with $K_p = C_s/C_1$. The above equation states simply that the total mass of compound x contained in a given volume is equal to the sum of the mass on the SPM and mass remaining in the aqueous phase.

Solving for C_s yields the predicted concentrations on SPM presented in the last few columns of Table 5-13. For the target compounds listed, the predicted SPM concentrations ranged from 70 ppb (for a C_3-benzene) to 2800 ppb (for 2-methylnaphthalene) for Grewingk glacial till, and from 130 ppb (for ethylmethylbenzene) to 3900 ppb (for toluene) for Yukon Delta sediment. The predicted levels for total Cut #10 compounds were 1300, 170, and 500 ppb for Glacial till, Yukon Delta sediment, and Turnagain Arm SPM, respectively.

165

As expected, the predicted molecular sorption levels--based on measured K_p and realistic water column aromatic compound and SPM concentrations--are well below the maximum adsorption capacities determined through isotherm development. The realistic predicted concentrations are in the ppb range, while the maximum adsorption capacities are in the ppm range. Furthermore, unless the adsorption mechanism involves an unlikely chemical reaction, then desorption will occur as the SPM particle is exposed to clean water. The reversible nature of the sorption process will over time (and/or distance), decrease the levels of aromatic compound loading even further.

In an effort to correlate molecular-scale adsorption levels with SPM-dependent parameters, the three types of SPM examined were analyzed for total organic carbon (TOC), mineralogy by X-ray diffraction, hydrocarbon content, solids density, number density, and grain-size distribution. Tables 5-1 through 5-5 and Appendix C provide the results of these determinations in detail. In addition, it has been suggested (Sabljic', 1987), that reliable predictions can often be made based on certain molecular properties such as structure, the octanol-water partition coefficient (K_{ow}) or solubility. Therefore, Table 5-14 provides the log K_{ow} and solubility in seawater for the compounds of interest.

A review of SPM characteristics and molecular properties versus adsorption behavior reveals principally only a few expected trends:

- K_p is found to increase with an increase in K_{ow}, decreasing solubility, and increasing molecular weight

- SPM adsorption capacity appears to be strongly affected by initial dissolved component concentrations

- SPM capacity for Cut #10 components correlates (loosely) with both number density and the > 2 μm grain-size fraction.

Figure 5-34 shows in histogram fashion the overall absence of recognizable trends. As seen, number density correlates with the fine (< 2 μm) grain-size fraction, and both appear to relate inversely with TOC. Beyond that the abili-

Table 5-14

Octanol/Water Partition Coefficients (log K_{ow}) and Seawater Solubilities for Selected Aromatic Compounds

Compound	Log K_{ow}[a]		Solubility[b] (ppm)
Toluene	2.65	2.69[c]	379
Ethylbenzene	3.13	2.84[d]	111
m-xylene	3.20		106
p-xylene	3.18		111
o-xylene	3.13		130
Ethylmethylbenzene	3.53		—
Trimethylbenzene	3.55		31–48 (isomer range)
Naphthalene	3.35	3.37[e]	22
		3.31[e]	
2-methylnaphthalene	3.86		25[f]
1-methylnaphthalene	3.87		26[f]
1,1'-biphenyl	3.95		4.8

[a] All log K_{ow} values were obtained from Environmental Science and Technology, Vol. 19, No. 6, June 1985, pp. 522–529, except where noted.
[b] All solubility values are from Fate and Weathering of Petroleum Spills in the Marine Environment, R.E. Jordan and J.R. Payne, Ann Arbor Science Publications, 1980, pp 31–41.
[c] Environmental Science and Technology, Vol. 11, No. 5, May 1977, pp 475–478
[d] Environmental Science and Technology, Vol. 17, No. 4, April 1983, pp 227–231
[e] Environmental Science and Technology, Vol. 18, No. 1, January 1984, pp 31–34
[f] measured in distilled water

ty to unveil trends is hampered severely. Given this lack of coherent trends, any attempt to promote a correlation factor based on SPM variables would amount only to pure conjecture. On the other hand, differences in SPM types aside, there are several estimation methods available (Lyman et al., 1982) that can be used with reasonable success to predict partitioning behavior based on chemical properties. These estimation methods make use of chemical properties that are, for the most part, easily found in the literature such as solubility, octanol-water partition coefficient, or molecular structure. (The interested reader is directed to Chapter 4 of the Lyman reference.)

In the case of examining the molecular adsorption behavior of various SPM types, the most reliable approach remains to perform the necessary measurements. Short of conducting the determinations, approximations can be
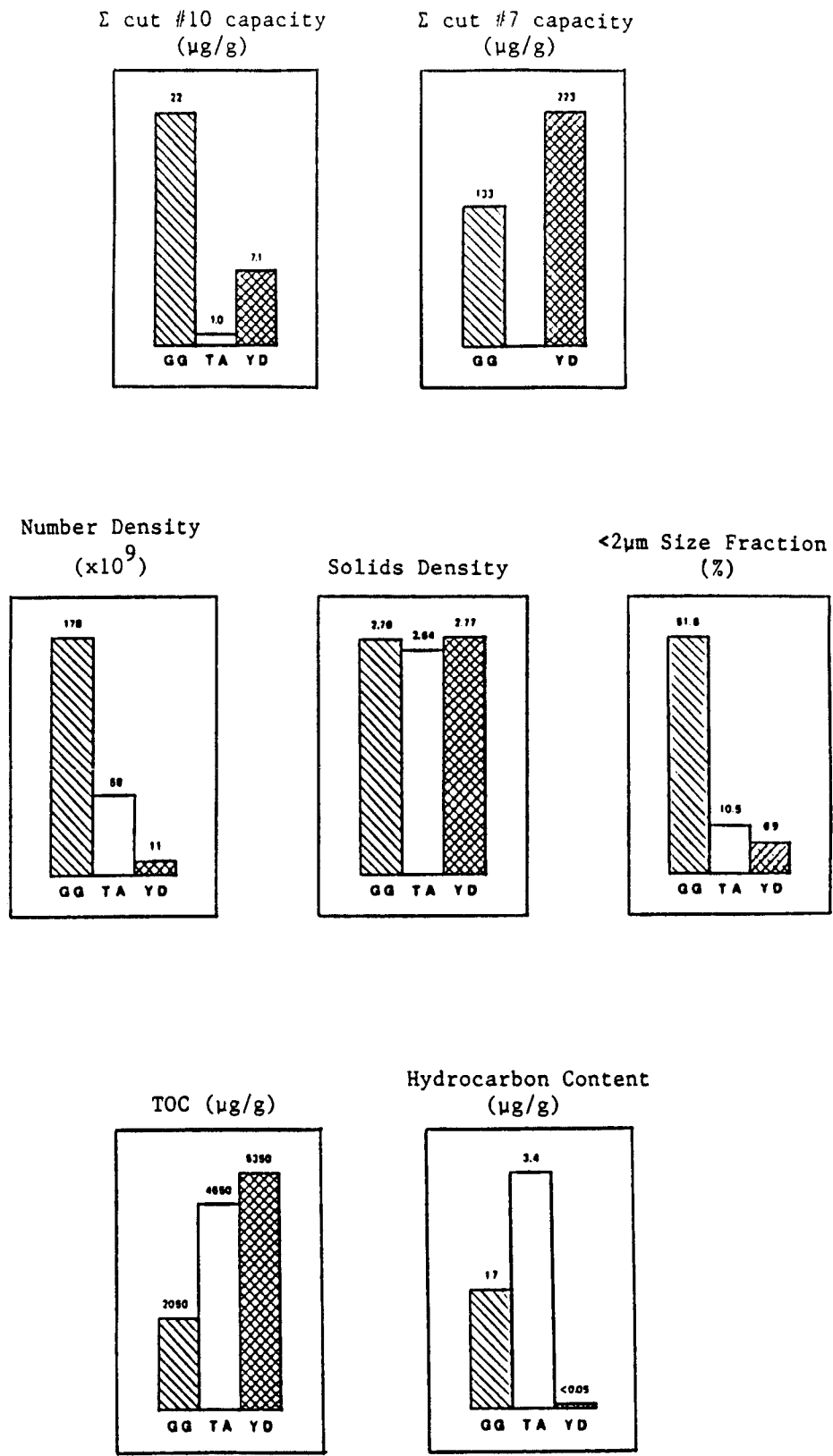
Figure 5-34. Histograms of SPM Variables and Cut Capacities Where: GG = Grewingk Glacial Till, TA = Turnagain Arm Sediment, and YD = Yukon Delta Sediment

168

predicted though the prudent selection of an appropriate estimation method. The data provided in this section are actual measurements and, as such, should be regarded as more reliable than estimated methods. The ability to predict interaction results through parameter correlations currently remains limited to chemical properties inherent in the molecule of interest.

In summary, although the correlation factor for SPM/molecular adsorption is elusive, measurement is the option that can provide the needed information. And, based on the measured values determined during this project and keeping in mind the reversible nature of the process, it is apparent that compared to droplet/SPM interactions, molecular adsorption levels are of little environmental concern.

6.0   CODE DESCRIPTIONS

6.1   CODE-USE DESCRIPTION: OILSPMXS

The mathematical model that describes the interaction of oil droplets with excess SPM is coded in BASIC and named OILSPMXS.BAS. The mathematics are described in Section 3.1. This code should be run from a compiled and linked executable file. The executable file should be a "stand-alone" and not require a run-time library.

Upon running OILSPMXS by typing the .EXE file name, the screen will display a prompt asking the user if the parameters are to be "edited" or "entered," as illustrated in Table 6-1. The user can then enter "edit" as illustrated and previously stored values of the parameters will be displayed as shown in Table 6-2. It is recommended that the user "edit" parameters rather than "enter" because the stored parameters are in the range of interest of the environmental applications. Any of the displayed parameters can be changed, i.e., edited by typing "yes," to the prompt, as illustrated in Table 6-2. Upon entering "yes" the parameter line number that is to be changed is entered, in this case the depth is changed to 20 m. After each edit the entire parameter list is displayed. The code will continue execution only after "no" is entered at the parameter-change prompt as illustrated in Table 6-3.

The code executes in the compiled and linked mode in a few seconds, and the initial output is a summary of the input parameters and the roots of the transcendental function (also referred to as eigenvalues) for the problem. Each page of the output begins with a header identifying the code name and version. This information is coded into the source through character strings and any user that changes the code is urged also to make these changes (in the first few lines of the source). By doing this, a record is maintained that can be of great value in documenting results. An example of the first page of output is illustrated in Table 6-4.

The calculated oil droplet concentration profile for a user-entered time of 1 hr is illustrated in the output in Table 6-5. The dimensionless

170

Table 6-1.   Initial Screen Prompt From OILSPMXS.BAS.

```
OIL DROPLETS INTERACTING WITH EXCESS SPM.
CODE NAME IS OILSPMXS.BAS, VERSION OF 8-3-88 @ 0718

WANT TO EDIT OR ENTER INPUT PARAMETERS ? edit
```

Table 6-2.   Screen Display of Parameter Editing From OILSPMXS.BAS.

```
OIL DROPLETS INTERACTING WITH EXCESS SPM.
CODE NAME IS OILSPMXS.BAS, VERSION OF 8-3-88 @ 0718

1.  RISE VELOCITY, CM/SEC = .001
2.  TURBULENT DIFFUSIVITY, CM*CM/SEC = 100
3.  DEPTH, METERS = 10
4.  NUMBER OF ROOTS = 25
5.  ROOT ERROR LIMIT = 1.000D-06
6.  EXPONENTIAL FLUX TERM, 1/SEC = 4.600D-05
7.  INITIAL OIL FLUX, GRAM/(CM*CM*SEC) = 1.800D-05
8.  DISAPPEARANCE RATE CONSTANT, 1/SEC = 9.400D-04
9.  NUMBER OF DEPTH VALUES = 27
10. PRINT THE ROOTS? YES

WANT TO CHANGE ANY? yes

ENTER THE LINE NUMBER TO BE CHANGED? 3

ENTER THE DEPTH, METERS ? 20
```

Table 6-3.   Screen Display of Parameters to be Used in Calculation, with a Final User Response of "no", From OILSPMXS.BAS.

```
OIL DROPLETS INTERACTING WITH EXCESS SPM.
CODE NAME IS OILSPMXS.BAS, VERSION OF 8-3-88 @ 0718

1.  RISE VELOCITY, CM/SEC = .001
2.  TURBULENT DIFFUSIVITY, CM*CM/SEC = 100
3.  DEPTH, METERS = 10
4.  NUMBER OF ROOTS = 25
5.  ROOT ERROR LIMIT = 1.000D-06
6.  EXPONENTIAL FLUX TERM, 1/SEC = 4.600D-05
7.  INITIAL OIL FLUX, GRAM/(CM*CM*SEC) = 1.800D-05
8.  DISAPPEARANCE RATE CONSTANT, 1/SEC = 9.400D-04
9.  NUMBER OF DEPTH VALUES = 27
10. PRINT THE ROOTS? YES

WANT TO CHANGE ANY? no
```

171

Table 6-4.   Printed Output of Problem Parameters From OILSPMXS.BAS.

```
CODE NAME IS OILSPMXS.BAS, VERSION OF 8-3-88 @ 0718
RUN TIME = 07:15:01, RUN DATE = 08-03-1988

THIS CODE SOLVES THE TRANSIENT ADVECTION-DISPERSION EQUATION FOR
OIL DROPLETS WITH FIRST-ORDER REACTION LOSS.

PROBLEM IDENTIFICATION: PRE-LOADED PARAMETER TEST CASE

OIL DROPLET RISE VELOCITY =   .001  CM/SEC, DEPTH =   10   METERS

TURBULENT DIFFUSIVITY =  100   CM*CM/SEC

ERROR LIMIT FOR THE ROOTS =   1.000D-06

VX*L/(2*K) =  -5.000D-03 UNITLESS

THE 25 ROOTS OF F(BETA) = BETA*COTANGENT(BETA) + VX*L/(2*K)

          ROOT          F(BETA)        ERROR CODE
        1.568D+00     -4.111D-07          1
        4.711D+00      3.831D-07          1
        7.853D+00     -7.362D-08          1
        1.100D+01     -2.266D-08          1
        1.414D+01      4.998D-07          1
        1.728D+01      3.937D-07          1
        2.042D+01     -4.653D-07          1
        2.356D+01     -8.318D-08          1
        2.670D+01      2.939D-07          1
        2.984D+01      3.739D-07          1
        3.299D+01      1.577D-07          1
        3.613D+01     -5.745D-07          1
        3.927D+01      3.101D-07          1
        4.241D+01     -7.179D-07          1
        4.555D+01      6.801D-07          1
        4.869D+01     -9.371D-07          1
        5.184D+01      5.586D-08          1
        5.498D+01      6.808D-07          1
        5.812D+01      7.541D-07          1
        6.126D+01      5.503D-08          1
        6.440D+01      2.015D-07          1
        6.754D+01     -9.391D-07          1
        7.069D+01     -5.765D-08          1
        7.383D+01      9.708D-07          1
        7.697D+01     -6.114D-07          1

EXPONENTIAL FLUX TERM =   4.600D-05 1/SEC

INITIAL OIL FLUX =  1.800D-05 GRAMS/(CM*CM*SEC)

FIRST ORDER DISAPPEARANCE RATE CONSTANT, 1/SEC =   9.400D-04 1/SEC

ZETA-BAR IS REAL ( <> VX/(2*K) ) AND EQUAL TO  2.990D-03 1/CM (IZBAR = 1)
```

Table 6-5.   Calculated Oil-Droplet Concentration Profile at 1 Hour From OILSPMXS.BAS.

```
CODE NAME IS OILSPMXS.BAS, VERSION OF 8-3-88 @ 0718
RUN TIME = 07:15:01, RUN DATE = 08-03-1988

CALCULATED RESULTS ********************************

CONCENTRATION PROFILE (GM/CC) FOR TIME =  1.000D+00 HOURS
DIMENSIONLESS TIME, K*T/L**2 =  3.600D-01

         DEPTH          OIL CONC
         (CM)           (GM/CC)
       0.000D+00       5.040D-05       (SURFACE)
       3.846D+01       4.484D-05
       7.692D+01       3.988D-05
       1.154D+02       3.546D-05
       1.538D+02       3.152D-05
       1.923D+02       2.800D-05
       2.308D+02       2.487D-05
       2.692D+02       2.207D-05
       3.077D+02       1.957D-05
       3.462D+02       1.733D-05
       3.846D+02       1.534D-05
       4.231D+02       1.355D-05
       4.615D+02       1.195D-05       -
       5.000D+02       1.052D-05
       5.385D+02       9.225D-06
       5.769D+02       8.062D-06
       6.154D+02       7.011D-06
       6.538D+02       6.057D-06
       6.923D+02       5.187D-06
       7.308D+02       4.390D-06
       7.692D+02       3.654D-06
       8.077D+02       2.969D-06
       8.462D+02       2.327D-06
       8.846D+02       1.717D-06
       9.231D+02       1.131D-06
       9.615D+02       5.614D-07
       1.000D+03       0.000D+00       (BOTTOM)

TOTAL GRAMS OF OIL DISPERSED INTO THE WATER COLUMN =  5.972D-02

GRAMS OF FREE OIL DROPS IN THE WATER COLUMN =  1.507D-02
GRAMS OF OIL DROPS ATTACHED TO SPM =  4.147D-02
GRAMS OF FREE OIL DROPS ATTACHED TO THE BOTTOM =  3.179D-03

TOTAL GRAMS OF OIL ACCOUNTED FOR IN THE CALCULATION =  5.972D-02
```

time printed just under the time of 1 hr is printed to provide the user with a number which can be used to gauge how close the results are to a steady-state value. Typically, dimensionless times greater than 1.0 are indicative of a result that is very close to steady state, and entering a greater time will not markedly change the results. However, this dimensionless time is printed only as a gauge, and in some cases the steady state may be a zero-concentration profile. Note in the calculated results in Table 6-5 that the oil droplet concentration varies from 5.04×10^{-5} g/cm^3 (50.4 ppm) at the surface to 1.05×10^{-5} g/cm^3 (10.5 ppm) at a depth of 5 m, and to 0 g/cm^3 at the bottom. The zero concentration at the bottom is the result of the (imposed) boundary condition described in the derivation.

A total material balance summary for oil droplets is printed after the concentration profile. This summary provides information with respect to the quantity of oil droplets dispersed into the water at the surface, in this example 0.0597 g at 1 hr; the mass of unattached oil droplets in the water, 0.0151 grams; oil attached to SPM, 0.0415 g; and oil attached to the bottom, 0.0032 g. The latter three masses must sum to the mass of oil dispersed in order to "close" the material balance. Thus, the last line of output accounts for 0.0597 g of oil. The material balance must close for each calculation; lack of successful closure indicates an error in the calculation.

The oil droplet concentration profile at 10 hr is presented in Table 6-6 and is to be compared with the profile at 1 hr in Table 6-5. Note that the 10-hr concentrations are considerably decreased relative to the 1-hr concentrations. This is due to the loss of oil through reaction and loss of oil to the bottom. Note that the dispersion is modeled as a decaying exponential, (line #6 in Table 6-2) and as a result the oil droplet flux from the surface goes to zero at large time(s).

The sample problem illustrated in Tables 6-1 through 6-6 is based on an $(\epsilon/\nu)^{1/2}$ value of 10 sec^{-1}. However, a review of the literature (Table 6-7) for energy dissipation rates in the ocean shows that a value of 0.01 $erg/cm^3/sec$ can be expected (and down to 0.0003 $erg/cm^3/sec$ also). On a per-unit mass-of-fluid basis this value becomes 0.01 cm^2/sec^3, and dividing by

Table 6-6.   Calculated Oil-Droplet Concentration Profile at 10 Hours From OILSPMXS.BAS.

```
CODE NAME IS OILSPMXS.BAS, VERSION OF 8-3-88 @ 0718
RUN TIME = 07:15:01, RUN DATE = 08-03-1988

CALCULATED RESULTS ********************************

CONCENTRATION PROFILE (GM/CC) FOR TIME =  1.000D+01 HOURS
DIMENSIONLESS TIME, K*T/L**2 =  3.600D+00

          DEPTH           OIL CONC
          (CM)            (GM/CC)
        0.000D+00       1.145D-05        (SURFACE)
        3.846D+01       1.020D-05
        7.692D+01       9.083D-06
        1.154D+02       8.087D-06
        1.538D+02       7.197D-06
        1.923D+02       6.404D-06
        2.308D+02       5.695D-06
        2.692D+02       5.062D-06
        3.077D+02       4.496D-06
        3.462D+02       3.990D-06
        3.846D+02       3.537D-06
        4.231D+02       3.131D-06
        4.615D+02       2.767D-06
        5.000D+02       2.439D-06
        5.385D+02       2.144D-06
        5.769D+02       1.877D-06
        6.154D+02       1.636D-06
        6.538D+02       1.416D-06
        6.923D+02       1.215D-06
        7.308D+02       1.030D-06
        7.692D+02       8.583D-07
        8.077D+02       6.984D-07
        8.462D+02       5.478D-07
        8.846D+02       4.046D-07
        9.231D+02       2.667D-07
        9.615D+02       1.325D-07
        1.000D+03       0.000D+00        (BOTTOM)

TOTAL GRAMS OF OIL DISPERSED INTO THE WATER COLUMN =  3.166D-01

GRAMS OF FREE OIL DROPS IN THE WATER COLUMN =  3.459D-03
GRAMS OF OIL DROPS ATTACHED TO SPM =  2.843D-01
GRAMS OF FREE OIL DROPS ATTACHED TO THE BOTTOM =  2.881D-02

TOTAL GRAMS OF OIL ACCOUNTED FOR IN THE CALCULATION =  3.166D-01
```

Table 6-7

Observed Energy Dissipation Rates

Depth (m)	$\epsilon(\text{ergs/cm}^3/\text{sec})$	Reference
1	6.4 E-2	Liu (1985)
1–2	3.0 E-2	Stewart & Grant (1962)
15	3.0 E-2	Stewart & Grant (1962)
15	2.5 E-2	Grant et al. (1968)
15	1.0 E-2	Liu (1985)
27	5.2 E-3	Grant et al. (1968)
36	1.5 E-1	Belyaev (1975)*
40	2.65 E-3	Liu (1985)
43	3.0 E-3	Grant et al. (1968)
58	4.8 E-3	Grant et al. (1968)
73	1.9 E-3	Grant et al. (1968)
89	3.4 E-4	Grant et al. (1968)
90	3.1 E-4	Grant et al. (1968)
100	6.25 E-4	Liu (1985)
140	3.7 E-2	Belyaev (1975)*

*in Raj (1977)

<u>Unit Conversions</u>
$1 \text{ erg/cm}^3/\text{sec} = 1 \text{ cm}^2/\text{sec}^3 \text{ water}$
$= 10^{-4} \text{ W/kg water}$
$= 10^{-7} \text{ W/cm}^3$

Reference:
Kirstein et al., "Observed Energy Dissipation Rates," Interim Report, Integration of Suspended Particulate Matter and Oil Transportation Study, submitted to MMS, November 1, 1985.

a kinematic viscosity of $0.01 \text{ cm}^2/\text{sec}$ yields $(\epsilon/\nu)^{1/2} = 1 \text{ sec}^{-1}$. The rate constant for oil droplet loss with excess SPM at 100 mg/L then will be $0.000094 \text{ sec}^{-1}$ (decreased by a factor of 10 from the previous case). Calculated results for this rate constant at 1 and 10 hr are presented in Tables 6-8 through 6-10. Note that the free oil droplet concentration profile with the decreased α_c in Table 6-8 is greater than that in Table 6-5. The reason for this difference is that in the case with a smaller oil-loss-rate constant, more oil remains in the water column. This is also illustrated by the mass of oil attached to SPM at 1 hour; for $\alpha_c = 0.00094$ the oil mass attached is 0.0415 g (Table 6-5) while for $\alpha_c = 0.000094$ the oil mass attached is 0.00834 g (Table 6-9). The corresponding calculation at 10 hr is presented in Table 6-10 and is to be compared with Table 6-6.

176

6.2   CODE-USE DESCRIPTION: SPMONLY

The mathematical model which describes the transport of SPM with a first-order reaction loss is coded in BASIC and named SPMONLY.BAS. The mathematics is described in Section 3.1.2. This code should be run from a compiled and linked executable file. The executable file should be a "stand-alone" and not require a run-time library.

Upon running SPMONLY by typing in the .EXE file name, the screen will display a prompt asking the user if the parameters are to be "edited" or "entered." It is recommended that the user enter "edit" because the parameters stored in the code are in the range of interest of environmental applications. Any of the displayed parameters can be changed, i.e., edited, by typing "yes" in response to the prompt. Upon entering "yes" the parameter line number that is to be changed is entered. After each edit the entire parameter list is displayed. The code will continue to execute only after "no" is entered at the parameter-change prompt as illustrated in Table 6-11.

Upon entering "no" the prompt will ask the user if cotangent values from Abramowitz and Stegun are to be used. The Abramowitz and Stegun cotangent values are double-precision cotangent values as described in the Handbook of Mathematical Functions (M. Abramowitz and I.A. Stegun, page 76). The reason this cotangent calculation was used is the recognition that (some) BASIC software does not have double-precision trigonometric functions, and in the early stages of coding, an error limit of less than 1.D0-05 could not be attained in solving for the roots of the transcendental function (eigenfunction). Most of the time it will make no difference if the Abramowitz and Stegun cotangent values are used or if the single-precision machine function is used. For the example illustrated in Table 6-11, "no" is entered. The prompt will then ask for a time to calculate the SPM concentration profile.

The results of a calculation are illustrated in Tables 6-12 through 6-14. Table 6-12 provides documentation of the code name and version, an echo of the input parameters, and the roots of the transcendental function (eigen-

Table 6-8. Printed Output of Problem Parameters From OILSPMXS.BAS (with $a_c = 0.000094$ sec^{-1}).

```
CODE NAME IS OILSPMXS.BAS, VERSION OF 8-3-88 @ 0718
RUN TIME = 10:42:31, RUN DATE = 08-03-1988

THIS CODE SOLVES THE TRANSIENT ADVECTION-DISPERSION EQUATION FOR
OIL DROPLETS WITH FIRST-ORDER REACTION LOSS.

PROBLEM IDENTIFICATION: PRE-LOADED PARAMETER TEST CASE

OIL DROPLET RISE VELOCITY =  .001  CM/SEC, DEPTH =  10  METERS

TURBULENT DIFFUSIVITY =  100  CM*CM/SEC

ERROR LIMIT FOR THE ROOTS =  1.000D-06

VX*L/(2*K) = -5.000D-03 UNITLESS

THE 25 ROOTS OF F(BETA) = BETA*COTANGENT(BETA) + VX*L/(2*K)

          ROOT          F(BETA)         ERROR CODE
        1.568D+00      -4.111D-07           1
        4.711D+00       3.831D-07           1
        7.853D+00      -7.362D-08           1
        1.100D+01      -2.266D-08           1
        1.414D+01       4.998D-07           1
        1.728D+01       3.937D-07           1
        2.042D+01      -4.653D-07           1
        2.356D+01      -8.318D-08           1
        2.670D+01       2.939D-07           1
        2.984D+01       3.739D-07           1
        3.299D+01       1.577D-07           1
        3.613D+01      -5.745D-07           1
        3.927D+01       3.101D-07           1
        4.241D+01      -7.179D-07           1
        4.555D+01       6.801D-07           1
        4.869D+01      -9.371D-07           1
        5.184D+01       5.586D-08           1
        5.498D+01       6.808D-07           1
        5.812D+01       7.541D-07           1
        6.126D+01       5.503D-08           1
        6.440D+01       2.015D-07           1
        6.754D+01      -9.391D-07           1
        7.069D+01      -5.765D-08           1
        7.383D+01       9.708D-07           1
        7.697D+01      -6.114D-07           1

EXPONENTIAL FLUX TERM =  4.600D-05 1/SEC

INITIAL OIL FLUX =  1.800D-05 GRAMS/(CM*CM*SEC)

FIRST ORDER DISAPPEARANCE RATE CONSTANT, 1/SEC =  9.400D-05 1/SEC

ZETA-BAR IS REAL ( <> VX/(2*K) ) AND EQUAL TO  6.928D-04 1/CM (IZBAR = 1)
```

Table 6-9. Calculated Oil-Droplet Concentration Profile at 1 Hour From OILSPMXS.BAS (with a_c=0.000094 sec^{-1}).

```
CODE NAME IS OILSPMXS.BAS, VERSION OF 8-3-88 @ 0718
RUN TIME = 10:42:31, RUN DATE = 08-03-1988

CALCULATED RESULTS ********************************

CONCENTRATION PROFILE (GM/CC) FOR TIME =  1.000D+00 HOURS
DIMENSIONLESS TIME, K*T/L**2 =  3.600D-01

        DEPTH           OIL CONC
        (CM)            (GM/CC)
       0.000D+00       9.647D-05       (SURFACE)
       3.846D+01       9.068D-05
       7.692D+01       8.512D-05
       1.154D+02       7.977D-05
       1.538D+02       7.463D-05
       1.923D+02       6.970D-05
       2.308D+02       6.498D-05
       2.692D+02       6.044D-05
       3.077D+02       5.610D-05
       3.462D+02       5.193D-05
       3.846D+02       4.794D-05
       4.231D+02       4.411D-05
       4.615D+02       4.044D-05
       5.000D+02       3.691D-05
       5.385D+02       3.353D-05
       5.769D+02       3.027D-05
       6.154D+02       2.713D-05
       6.538D+02       2.410D-05
       6.923D+02       2.117D-05
       7.308D+02       1.832D-05
       7.692D+02       1.556D-05
       8.077D+02       1.286D-05
       8.462D+02       1.022D-05
       8.846D+02       7.625D-06
       9.231D+02       5.063D-06
       9.615D+02       2.526D-06
       1.000D+03       0.000D+00       (BOTTOM)

TOTAL GRAMS OF OIL DISPERSED INTO THE WATER COLUMN =  5.972D-02

GRAMS OF FREE OIL DROPS IN THE WATER COLUMN =  4.073D-02
GRAMS OF OIL DROPS ATTACHED TO SPM =  8.342D-03
GRAMS OF FREE OIL DROPS ATTACHED TO THE BOTTOM =  1.064D-02

TOTAL GRAMS OF OIL ACCOUNTED FOR IN THE CALCULATION =  5.972D-02
```

Table 6-10. Calculated Oil-Droplet Concentration Profile at 10 Hours From OILSPMXS.BAS (with $a_c = 0.000094$ sec^{-1}).

```
CODE NAME IS OILSPMXS.BAS, VERSION OF 8-3-88 @ 0718
RUN TIME = 10:42:31, RUN DATE = 08-03-1988

CALCULATED RESULTS *********************************

CONCENTRATION PROFILE (GM/CC) FOR TIME =   1.000D+01 HOURS
DIMENSIONLESS TIME, K*T/L**2 =   3.600D+00
```

DEPTH (CM)	OIL CONC (GM/CC)	
0.000D+00	2.988D-05	(SURFACE)
3.846D+01	2.855D-05	
7.692D+01	2.725D-05	
1.154D+02	2.597D-05	
1.538D+02	2.471D-05	
1.923D+02	2.346D-05	
2.308D+02	2.224D-05	
2.692D+02	2.102D-05	
3.077D+02	1.983D-05	
3.462D+02	1.865D-05	
3.846D+02	1.748D-05	
4.231D+02	1.632D-05	
4.615D+02	1.518D-05	
5.000D+02	1.405D-05	
5.385D+02	1.293D-05	
5.769D+02	1.182D-05	
6.154D+02	1.071D-05	
6.538D+02	9.619D-06	
6.923D+02	8.531D-06	
7.308D+02	7.450D-06	
7.692D+02	6.375D-06	
8.077D+02	5.305D-06	
8.462D+02	4.238D-06	
8.846D+02	3.175D-06	
9.231D+02	2.115D-06	
9.615D+02	1.057D-06	
1.000D+03	0.000D+00	(BOTTOM)

```
TOTAL GRAMS OF OIL DISPERSED INTO THE WATER COLUMN =   3.166D-01

GRAMS OF FREE OIL DROPS IN THE WATER COLUMN =   1.434D-02
GRAMS OF OIL DROPS ATTACHED TO SPM =   1.028D-01
GRAMS OF FREE OIL DROPS ATTACHED TO THE BOTTOM =   1.995D-01

TOTAL GRAMS OF OIL ACCOUNTED FOR IN THE CALCULATION =   3.166D-01
```

Table 6-11. Screen Display of Parameter List for SPMONLY.BAS.

```
SUSPENDED-PARTICULATE-MATTER (SPM) CALCULATION
CODE NAME IS SPMONLY.BAS, VERSION OF 8-4-88 @ 0746

1.  TERMINAL VELOCITY, CM/SEC =  .001
2.  TURBULENT DIFFUSIVITY, CM*CM/SEC =  100
3.  DEPTH, METERS =  10
4.  NUMBER OF ROOTS =  25
5.  ROOT ERROR LIMIT =  1.000D-06
6.  SPM-LOSS RATE CONSTANT, 1/SEC =  9.400D-07
7.  FLUX RATE, GM/SEC*CM*CM =  4.600D-05
8.  DEPOSITION RATE, CM/SEC =  4.600D-02
9.  NUMBER OF DEPTH VALUES =  49
10. PRINT THE ROOTS? YES

WANT TO CHANGE ANY? N

DO YOU WANT ABRAMOWITZ & STEGUN COTANGENT VALUES? NO

ENTER THE TIME IN HOURS ? 1.

TIME ENTERED IS  1.000D+00

IS THIS CORRECT ? yes
```

function).   The code name and version are printed as a header on each page of output to provide a means of documenting results. These two identification items are coded into the source through character strings, and any user that changes the code is urged to make these changes also (in the first few lines of the source).

Tables 6-13 and 6-14 illustrate the calculated SPM profiles at 1 and 6 hr, respectively. At 1 hr the SPM concentration varies from 7.7×10^{-5} g/cm^3 (77 ppm) at the surface to 2.5×10^{-4} g/cm^3 (250 ppm) at the bottom, while at 6 hr the SPM at the surface is 5.4×10^{-4} g/cm^3 (540 ppm) and at the bottom 6.3×10^{-4} g/cm^3 (630 ppm). Note that the SPM profile is "flattening out" at 6 hr, i.e., the water column SPM concentration is approaching a steady state and is expected to be "flat".

```
CODE NAME IS SPMONLY.BAS, VERSION OF 8-4-88 @ 0746
RUN TIME = 08:12:02, RUN DATE = 08-04-1988

THIS CODE SOLVES THE 1-D TRANSIENT ADVECTION-DISPERSION EQUATION FOR SPM
(ANALYTICAL SOLUTION) WITH FIRST-ORDER REACTION LOSS.

TERMINAL VELOCITY =  1.000D-03 CM/SEC, DEPTH =  10.0 METERS

TURBULENT DIFFUSIVITY =  100.0 CM*CM/SEC

FLUX RATE FROM THE BOTTOM =  4.600D-05 GM/SEC*CM*CM

DEPOSITION RATE =  4.600D-02 CM/SEC

ERROR LIMIT FOR THE ROOTS =  1.000D-06

A = VX/(2*K) =  5.000D-06 1/CM

ROOTS CALCULATED USING MACHINE FUNCTIONS.

THE 25 ROOTS OF F(BETA)=BETA*COTANGENT(BETA)-K*((A*L)^2-A*KS*L+BETA^2)/(KS*L)

          ROOT          F(BETA)        ERROR CODE
        6.319D-01      1.685D-07           1
        3.281D+00      9.872D-07           1
        6.355D+00     -6.364D-07           1
        9.473D+00     -1.659D-07           1
        1.260D+01     -8.777D-07           1
        1.574D+01     -3.807D-07           1
        1.887D+01      4.496D-07           1
        2.201D+01      6.450D-07           1
        2.515D+01     -7.795D-07           1
        2.829D+01     -4.485D-08           1
        3.143D+01     -6.668D-07           1
        3.457D+01      9.841D-07           1
        3.771D+01      1.799D-07           1
        4.085D+01      5.034D-07           1
        4.399D+01      6.818D-07           1
        4.713D+01     -7.496D-07           1
        5.027D+01     -3.562D-07           1
        5.342D+01     -9.183D-07           1
        5.656D+01     -4.542D-07           1
        5.970D+01     -8.393D-07           1
        6.284D+01     -6.561D-07           1
        6.598D+01      7.975D-07           1
        6.912D+01     -9.499D-08           1
        7.226D+01      5.386D-07           1
        7.540D+01      3.503D-07           1

INITIAL SPM FLUX =  4.600D-05 GRAMS/(CM*CM*SEC)

FIRST-ORDER SPM DISAPPEARANCE RATE CONSTANT, 1/SEC =  9.400D-07 1/SEC
```

Table 6-13.   Printed Output From SPMONLY, SPM Profile at 1 Hour.

```
CODE NAME IS SPMONLY.BAS, VERSION OF 8-4-88 @ 0746
RUN TIME = 08:12:02, RUN DATE = 08-04-1988

CONCENTRATION PROFILES AT TIME =  1.000D+00 HOURS ************************
```

DEPTH	SPM CONC.
CM	GM/CM**3
0.000D+00	7.772D-05 (SURFACE)
2.083D+01	7.781D-05
4.167D+01	7.805D-05
6.250D+01	7.845D-05
8.333D+01	7.899D-05
1.042D+02	7.968D-05
1.250D+02	8.053D-05
1.458D+02	8.152D-05
1.667D+02	8.267D-05
1.875D+02	8.397D-05
2.083D+02	8.542D-05
2.292D+02	8.702D-05
2.500D+02	8.877D-05
2.708D+02	9.067D-05
2.917D+02	9.273D-05
3.125D+02	9.493D-05
3.333D+02	9.729D-05
3.542D+02	9.980D-05
3.750D+02	1.025D-04
3.958D+02	1.053D-04
4.167D+02	1.083D-04
4.375D+02	1.114D-04
4.583D+02	1.146D-04
4.792D+02	1.181D-04
5.000D+02	1.217D-04
5.208D+02	1.254D-04
5.417D+02	1.293D-04
5.625D+02	1.333D-04
5.833D+02	1.375D-04
6.042D+02	1.418D-04
6.250D+02	1.463D-04
6.458D+02	1.510D-04
6.667D+02	1.558D-04
6.875D+02	1.607D-04
7.083D+02	1.658D-04
7.292D+02	1.711D-04
7.500D+02	1.765D-04
7.708D+02	1.820D-04
7.917D+02	1.877D-04
8.125D+02	1.936D-04
8.333D+02	1.996D-04
8.542D+02	2.057D-04
8.750D+02	2.120D-04
8.958D+02	2.184D-04
9.167D+02	2.250D-04
9.375D+02	2.317D-04
9.583D+02	2.386D-04
9.792D+02	2.456D-04
1.000D+03	2.527D-04 (BOTTOM)

```
GRAMS OF SPM (UNATTACHED) IN THE WATER COLUMN = 1.362D-01
GRAMS OF SPM ATTACHED TO OIL =  2.395D-04

GRAMS OF SPM IN WATER + ATTACHED =  1.365D-01

GRAMS OF SPM FROM THE BOTTOM (FROM VX*C-K*DC/DX) = 1.365D-01
GRAMS OF SPM FROM THE BOTTOM (FROM -F0+KS*C) = 1.365D-01
```

Table 6-14.   Printed Output From SPMONLY, SPM Profile at 6 Hours.

```
CODE NAME IS SPMONLY.BAS, VERSION OF 8-4-88 @ 0746
RUN TIME = 08:12:02, RUN DATE = 08-04-1988

CONCENTRATION PROFILES AT TIME =  6.000D+00 HOURS **********************

        DEPTH              SPM CONC.
        CM                 GM/CM**3
     0.000D+00           5.395D-04  (SURFACE)
     2.083D+01           5.397D-04
     4.167D+01           5.399D-04
     6.250D+01           5.402D-04
     8.333D+01           5.406D-04
     1.042D+02           5.411D-04
     1.250D+02           5.416D-04
     1.458D+02           5.422D-04
     1.667D+02           5.429D-04
     1.875D+02           5.437D-04
     2.083D+02           5.445D-04
     2.292D+02           5.455D-04
     2.500D+02           5.465D-04
     2.708D+02           5.476D-04
     2.917D+02           5.487D-04
     3.125D+02           5.500D-04
     3.333D+02           5.513D-04
     3.542D+02           5.527D-04
     3.750D+02           5.541D-04
     3.958D+02           5.557D-04
     4.167D+02           5.573D-04
     4.375D+02           5.590D-04
     4.583D+02           5.608D-04
     4.792D+02           5.626D-04
     5.000D+02           5.645D-04
     5.208D+02           5.665D-04
     5.417D+02           5.686D-04
     5.625D+02           5.708D-04
     5.833D+02           5.730D-04
     6.042D+02           5.753D-04
     6.250D+02           5.776D-04
     6.458D+02           5.801D-04
     6.667D+02           5.826D-04
     6.875D+02           5.852D-04
     7.083D+02           5.879D-04
     7.292D+02           5.906D-04
     7.500D+02           5.934D-04
     7.708D+02           5.963D-04
     7.917D+02           5.992D-04
     8.125D+02           6.022D-04
     8.333D+02           6.053D-04
     8.542D+02           6.085D-04
     8.750D+02           6.117D-04
     8.958D+02           6.150D-04
     9.167D+02           6.183D-04
     9.375D+02           6.217D-04
     9.583D+02           6.252D-04
     9.792D+02           6.288D-04
     1.000D+03           6.324D-04  (BOTTOM)

GRAMS OF SPM (UNATTACHED) IN THE WATER COLUMN =  5.717D-01
GRAMS OF SPM ATTACHED TO OIL =  6.677D-03

GRAMS OF SPM IN WATER + ATTACHED =  5.784D-01

GRAMS OF SPM FROM THE BOTTOM (FROM VX*C-K*DC/DX) =  5.784D-01
GRAMS OF SPM FROM THE BOTTOM (FROM -F0+KS*C) =  5.784D-01
```

A total material balance for the SPM is printed below each concentration profile. SPM can reside in the water column or be removed from the water column through reaction with oil. These two masses <u>must</u> sum to the SPM mass put into the water column at the bottom. This is illustrated in Table 6-13 where 0.1362 g are in the water column and 0.000239 are attached to oil (by reaction). These two masses sum to 0.1365 g, which is equal to the SPM mass (fluxed) put into the water at the bottom by $-F_o + k_s C$ or the mass fluxed <u>away</u> <u>from</u> the bottom by $\nu_x C - k(dC/dx)$. Similar results are illustrated in Table 6-14.

6.3   CODE-USE DESCRIPTION: OILSPM3

The mathematical model which describes the interaction of oil droplets with SPM (not required to be in excess) is coded in BASIC and named OILSPM3.BAS. The "3" in the code name pertains to the fact that this model calculates <u>three</u> changing concentration profiles: oil droplets, SPM and oil-SPM agglomerate. The mathematics are described in Section 3.1.3. This code <u>must</u> be run from a compiled and linked executable file. The executable file should be a "stand-alone" and not require a run-time library.

Upon running OILSPM3 by typing the .EXE file name, the screen will display a prompt asking the user if the parameters are to be "edited" or "entered". It is recommended that the user enter "edit" because the parameters stored in the code are in the range of interest of environmental applications. Any of the displayed parameters can be changed, i.e., edited, by typing "yes" in response to the prompt. Upon entering "yes", the parameter line number that is to be changed is entered. After each edit the entire parameter list is displayed. The code will continue to execute only after "no" is entered at the parameter-change prompt as illustrated in Tables 6-15a and 6-15b. These two tables illustrate the parameter input list for OILSPM3. Table 6-15a illustrates mainly oil-related options and integration parameters such as the number of grid points. Since OILSPM3 is a numerical integration code, it is not possible just to enter a "time" and then calculate the concentration profiles. The code must integrate up to a specified time from an initial condition. The

185

Table 6-15a. First (of two) Screen Display of Parameters to be Used in Calculation, with a Final User Response of "no", From OILSPM3.

```
INTERACTING OIL DROPLETS AND SPM CALCULATION
CODE NAME IS OILSPM3.BAS, VERSION OF 8-9-88 @ 0643

1.   TURBULENT DIFFUSIVITY, CM*CM/SEC =  1.00D+02
2.   OIL RISING VELOCITY, CM/SEC =  1.00D-02
3.   OIL-SPM RATE CONSTANT FOR OIL LOSS, CC/(GM*SEC) =  9.40D-02
4.   OCEAN DEPTH, METERS =  1.00D+01
5.   NUMBER OF GRID POINTS =  49
6.   INITIAL OIL-DISPERSON FLUX SZERO, GRAMS/(CM*CM*SEC) =  1.80D-05
7.   OIL-DISPERSON GAMMA, 1/SEC =  4.60D-05
8.   MAXIMUM TIME, HOURS =  10.00
9.   PRINT INTERVAL, HOURS = 0.500
10.  USE STEADY-STATE OIL PROFILE TO START:  NO
11.  COUPLE THE CONCENTRATIONS:  YES
12.  COUPLING ITERATIONS =  3

WANT TO CHANGE ANY? no
```

Table 6-15b. Second Screen Display of Parameters to be Used in Calculation, with a Final User Response of "no", From OILSPM3.

```
INTERACTING OIL DROPLETS AND SPM CALCULATION
CODE NAME IS OILSPM3.BAS, VERSION OF 8-9-88 @ 0643

1.   SPM SETTLING VELOCITY, CM/SEC =  1.00D-03
2.   OIL-SPM AGGLOMERATE SETTLING VELOCITY, CM/SEC =  1.00D-03
3.   OIL-SPM RATE CONSTANT FOR SPM LOSS, CC/(GM*SEC) =  9.40D-02
4.   SPM SOURCE FLUX TERM, GM/(CM^2*SEC) =  4.60D-05
5.   SPM DEPOSITION RATE CONSTANT, CM/SEC =  4.60D-02
6.   USE STEADY-STATE SPM PROFILE TO START:  YES

WANT TO CHANGE ANY? no

TIME FOR UNITY DIMENSIONLESS TIME, HOURS =  2.814D-01

THE TIME STEP WILL BE THE ABOVE TIME DIVIDED BY   20.000

IS THIS ACCEPTABLE? yes
```

initial condition recommended for oil in the water column is zero, i.e., oil is spilled at time — 0, and this condition is implemented by line 10 in Table 6-15a, where a "no" is entered to the prompt: USE STEADY-STATE OIL PROFILE TO START.

This option exists for material-balance testing calculations only, and the user should always make sure that line 10 has a response of "no." Material-balance testing is used to make sure the code calculation accounts for all the masses in the water, which is difficult in numerical integrations because mass transfer changes rapidly in the initial stages of the calculation, i.e., the profiles are quite steep in the early stages of calculation. However, if a "smooth" profile, such as a steady-state profile, is used initially, the early integration errors do not exist; and for purposes of finding programming errors the calculated results are much easier to interpret.

Table 6-15b illustrates mainly SPM and oil/SPM agglomerate related parameters and the selection of the maximum allowable time step to be used in the Crank-Nicolson integration. Note that line 6 in this table specifies that a steady-state SPM profile is used to start the calculation. In other words, oil is spilled in water that has sediment. The dimensionless time referred to in this table is used as a gauge to select a maximum time step. Experience has resulted in selecting a time step on the order of 1/20 of this dimensionless time. It is recommended that at least 20 be entered, but if a larger number is entered, compute time will increase accordingly.

The code execute time is on the order of many minutes on a 80286-based personal computer. If an older 8088-based machine is used, expect one-half hour or longer. The initial output is illustrated in Table 6-16 where the code version is documented and the input parameters for the calculation are also documented.

Table 6-17a presents the calculated oil droplet, SPM, and oil/SPM concentration profiles at 0.5 hr, and Table 6-17b presents the total material balance for these species. The SPM concentration profile is close to 0.001 g/cm^3 because of the values selected for the SPM source flux [at 4.6×10^{-5}

Table 6-16.   Initial Output of Problem Parameters for OILSPM3.

```
FINITE-DIFFERENCE SOLUTION FOR INTERACTING OIL DROPLETS AND SPM.

CODE NAME IS OILSPM3.BAS, VERSION IS 8-9-88 @ 0643
RUN TIME WAS 06:42:48, AND RUN DATE WAS 08-09-1988

PROBLEM PARAMETERS ARE AS FOLLOWS:

VERTICAL TURBULENT DIFFUSIVITY, CM*CM/SEC =  100.00
WATER DEPTH, METERS =  10.0

OIL RISING VELOCITY, CM/SEC =  1.00D-02
OIL-SPM RATE CONSTANT FOR OIL LOSS, CC/(GM*SEC) =  9.400D-02
OIL DISPERSION RATE, GM/(CM*CM*SEC) = (0.18D-04)*EXP((-0.46D-04)*SECONDS)

SPM SETTLING VELOCITY, CM/SEC =  1.00D-03
OIL-SPM RATE CONSTANT FOR SPM LOSS, CC/(GM*SEC) =  9.40D-02
SPM BOTTOM SOURCE FLUX, GM/(CM^2*SEC) =  4.60D-05
SPM DEPOSITION RATE CONSTANT, CM/SEC =  4.60D-02

OIL-SPM AGGLOMERATE SETTLING VELOCITY, CM/SEC =  1.00D-03

TIME STEP, HOURS =  5.62D-03, INTEGRATION TIME, HOURS =  10.00
SPECIFIED PRINT INTERVAL, HOURS =  0.500

THE INITIAL OIL WATER-COLUMN LOADING, GRAMS =  0.000D+00
THE INITIAL SPM WATER-COLUMN LOADING, GRAMS =  9.950D-01
```

Table 6-17a. Calculated Oil-Droplet SPM and Oil-SPM Agglomerate Profiles at 0.5 Hour From OILSPM3.

```
FINITE-DIFFERENCE SOLUTION FOR INTERACTING OIL DROPLETS AND SPM.

CODE NAME IS OILSPM3.BAS, VERSION IS 8-9-88 @ 0643
RUN TIME WAS 06:42:48, AND RUN DATE WAS 08-09-1988


CONCENTRATION PROFILES AT TIME = 0.500 HOURS  ****************************
```

DEPTH (CM)	OIL CONC (GM/CC)	SPM CONC (GM/CC)	OIL-SPM CONC (GM/CC)	
0.000D+00	7.832D-05	9.856D-04	8.807D-06	(SURFACE)
2.083D+01	7.476D-05	9.858D-04	8.792D-06	
4.167D+01	7.131D-05	9.860D-04	8.747D-06	
6.250D+01	6.798D-05	9.863D-04	8.675D-06	
8.333D+01	6.476D-05	9.865D-04	8.578D-06	
1.042D+02	6.164D-05	9.868D-04	8.459D-06	
1.250D+02	5.864D-05	9.871D-04	8.320D-06	
1.458D+02	5.574D-05	9.874D-04	8.163D-06	
1.667D+02	5.294D-05	9.877D-04	7.990D-06	
1.875D+02	5.025D-05	9.880D-04	7.803D-06	
2.083D+02	4.765D-05	9.883D-04	7.605D-06	
2.292D+02	4.516D-05	9.886D-04	7.396D-06	
2.500D+02	4.276D-05	9.889D-04	7.179D-06	
2.708D+02	4.045D-05	9.892D-04	6.954D-06	
2.917D+02	3.824D-05	9.895D-04	6.724D-06	
3.125D+02	3.612D-05	9.899D-04	6.490D-06	
3.333D+02	3.408D-05	9.902D-04	6.252D-06	
3.542D+02	3.213D-05	9.905D-04	6.013D-06	
3.750D+02	3.027D-05	9.908D-04	5.772D-06	
3.958D+02	2.848D-05	9.911D-04	5.531D-06	
4.167D+02	2.677D-05	9.915D-04	5.291D-06	
4.375D+02	2.514D-05	9.918D-04	5.052D-06	
4.583D+02	2.358D-05	9.921D-04	4.816D-06	
4.792D+02	2.210D-05	9.924D-04	4.581D-06	
5.000D+02	2.068D-05	9.928D-04	4.350D-06	
5.208D+02	1.932D-05	9.931D-04	4.123D-06	
5.417D+02	1.803D-05	9.934D-04	3.899D-06	
5.625D+02	1.680D-05	9.937D-04	3.680D-06	
5.833D+02	1.562D-05	9.940D-04	3.465D-06	
6.042D+02	1.450D-05	9.943D-04	3.254D-06	
6.250D+02	1.343D-05	9.946D-04	3.048D-06	
6.458D+02	1.241D-05	9.949D-04	2.847D-06	
6.667D+02	1.144D-05	9.952D-04	2.651D-06	
6.875D+02	1.051D-05	9.955D-04	2.459D-06	
7.083D+02	9.622D-06	9.957D-04	2.271D-06	
7.292D+02	8.773D-06	9.960D-04	2.088D-06	
7.500D+02	7.959D-06	9.963D-04	1.910D-06	
7.708D+02	7.178D-06	9.966D-04	1.735D-06	
7.917D+02	6.428D-06	9.968D-04	1.564D-06	
8.125D+02	5.705D-06	9.971D-04	1.397D-06	
8.333D+02	5.007D-06	9.974D-04	1.233D-06	
8.542D+02	4.331D-06	9.976D-04	1.073D-06	
8.750D+02	3.674D-06	9.979D-04	9.143D-07	
8.958D+02	3.035D-06	9.981D-04	7.584D-07	
9.167D+02	2.410D-06	9.983D-04	6.044D-07	
9.375D+02	1.797D-06	9.986D-04	4.519D-07	
9.583D+02	1.192D-06	9.988D-04	3.006D-07	
9.792D+02	5.942D-07	9.990D-04	1.501D-07	
1.000D+03	0.000D+00	9.992D-04	0.000D+00	(BOTTOM)

189

Table 6-17b. Total Material Balance for Oil-Droplets, SPM and Oil-SPM Agglomerate at 0.5 Hour From OILSPM3.

```
MATERIAL BALANCE INFORMATION (FOR 1 CM*CM COLUMN OF WATER):

OIL IN THE WATER COLUMN, GRAMS = 2.688D-02
OIL LOST TO THE BOTTOM, GRAMS = 1.612D-03
OIL LOST THROUGH REACTION WITH SPM, GRAMS = 2.413D-03

OIL IN WATER + LOST AT BOTTOM + LOST THROUGH REACTION, GRAMS = 3.091D-02
OIL FLUXED INTO WATER + INITIAL LOADING, GRAMS = 3.109D-02


SPM (UNATTACHED) IN THE WATER COLUMN, GRAMS = 9.926D-01
SPM LOST THROUGH REACTION WITH OIL, GRAMS = 2.413D-03

SPM IN WATER + LOST THROUGH REACTION, GRAMS = 9.950D-01
SPM FLUXED INTO WATER AT BOTTOM + INITIAL LOADING, GRAMS = 9.950D-01


OIL-SPM AGGLOMERATE IN THE WATER COLUMN, GRAMS = 4.496D-03
OIL-SPM AGGLOMERATE FLUXED TO THE BOTTOM, GRAMS = 3.309D-04

OIL-SPM IN WATER + LOST TO BOTTOM, GRAMS = 4.827D-03
OIL-SPM AGGLOMERATE PRODUCED BY REACTION, GRAMS = 4.825D-03


VECTOR CONVERGENCE, OIL = 3.06D-14, SPM = 6.01D-15 ON  3 ITERATIONS.
```

$g/(cm^2 sec)$] and the SPM deposition rate constant (4.6×10^{-2} cm/sec). The oil droplet concentration profile ranges from 7.8×10^{-5} g/cm^3 (78 ppm) at the surface to 0 at the bottom. The zero concentration at the bottom is an imposed boundary condition and essentially results in an upper bound flux of oil to the bottom. Likewise, the oil/SPM agglomerate concentration is 0 at the bottom.

Table 6-17b illustrates the total material balance calculation for the three transporting species. Note that the oil fluxed into the water at the surface is 0.03109 g, while the calculation accounted for 0.03091 g as oil in the water, lost at bottom (transported to the bottom) and lost through reaction. This difference should be zero; but it is not because of numerical integration errors, and it can be made smaller by decreasing the grid spacing, the time step, or both. The SPM material balance closes by accounting for 0.9950 g, and the oil-SPM agglomerate almost closes by accounting for

0.004827 g in the water and lost to the bottom compared to 0.004825 g produced by reaction. Closing these material balances to four significant digits is considered reasonable given the assumptions and limitation of the data and calculation.

The oil droplet, SPM, and oil/SPM agglomerate concentration profiles and total material balance at 10 hr are presented in Tables 6-18a and 6-18b. Note that the time at the end of the calculation was 7:34 and the start time 6:42 for an integration to 10 hr with a time-step size of 0.00562 hr on a grid size of 20.83 cm (over 10 m, 51 grid points including 1 grid point outside each boundary for central differences). The SPM-concentration profile is still close to 0.001 g/cm^3 and the oil droplet concentration varies from 3.159 x 10^{-5} (32 ppm) at the surface to 0 at the bottom. This concentration is decreasing from the 0.5-hr value because the oil-dispersion source term is a decaying exponential. The oil/SPM agglomerate concentration varies from 2.168 x 10^{-5} g/cm^3 to 0; also, note this oil/SPM agglomerate concentration(s) is higher than the 0.5-hr value because the oil/SPM agglomerate has been produced over the 9.5-hr interval.

The total material balance at 10 hr presented in Table 6-18b illustrates that numerical integration errors improve (i.e., decrease) as the calculation "steps out" in time. Note that the oil put into the water from the surface is 0.3166 g while the calculation accounts for 0.3164 g. For the other two species, the material balances at close to four digits.

The vector convergence numbers that appear at the end of the each material balance calculation are the average final errors in trial vectors used in the calculation. In other words, to solve for an oil droplet concentration profile, the SPM concentration (vector) must be "guessed" and likewise to solve for the SPM-concentration profile the oil droplet concentration (vector) must be guessed. The average error in the concentrations is printed to indicate how well (or not) the calculation proceeded. For the case illustrated here the

Table 6-18a. Calculated Oil-Droplet, SPM and Oil-SPM Agglomerate Profiles at 10 Hours From OILSPM3.

```
FINITE-DIFFERENCE SOLUTION FOR INTERACTING OIL DROPLETS AND SPM.

CODE NAME IS OILSPM3.BAS, VERSION IS 8-9-88 @ 0643
RUN TIME WAS 06:42:48, AND RUN DATE WAS 08-09-1988


CONCENTRATION PROFILES AT TIME = 10.000 HOURS  ****************************

        DEPTH        OIL CONC       SPM CONC      OIL-SPM CONC
        (CM)         (GM/CC)        (GM/CC)        (GM/CC)
     0.000D+00      3.159D-05      9.366D-04      2.168D-05    (SURFACE)
     2.083D+01      3.081D-05      9.368D-04      2.167D-05
     4.167D+01      3.004D-05      9.371D-04      2.163D-05
     6.250D+01      2.927D-05      9.373D-04      2.157D-05
     8.333D+01      2.852D-05      9.375D-04      2.148D-05
     1.042D+02      2.777D-05      9.378D-04      2.136D-05
     1.250D+02      2.702D-05      9.381D-04      2.121D-05
     1.458D+02      2.629D-05      9.384D-04      2.105D-05
     1.667D+02      2.556D-05      9.387D-04      2.086D-05
     1.875D+02      2.483D-05      9.390D-04      2.064D-05
     2.083D+02      2.411D-05      9.393D-04      2.040D-05
     2.292D+02      2.340D-05      9.396D-04      2.014D-05
     2.500D+02      2.269D-05      9.400D-04      1.986D-05
     2.708D+02      2.199D-05      9.403D-04      1.955D-05
     2.917D+02      2.130D-05      9.407D-04      1.923D-05
     3.125D+02      2.061D-05      9.411D-04      1.888D-05
     3.333D+02      1.992D-05      9.415D-04      1.851D-05
     3.542D+02      1.924D-05      9.419D-04      1.813D-05
     3.750D+02      1.857D-05      9.423D-04      1.773D-05
     3.958D+02      1.790D-05      9.427D-04      1.731D-05
     4.167D+02      1.723D-05      9.432D-04      1.687D-05
     4.375D+02      1.657D-05      9.436D-04      1.641D-05
     4.583D+02      1.591D-05      9.441D-04      1.594D-05
     4.792D+02      1.526D-05      9.445D-04      1.546D-05
     5.000D+02      1.461D-05      9.450D-04      1.496D-05
     5.208D+02      1.397D-05      9.455D-04      1.444D-05
     5.417D+02      1.333D-05      9.460D-04      1.391D-05
     5.625D+02      1.269D-05      9.465D-04      1.337D-05
     5.833D+02      1.206D-05      9.470D-04      1.282D-05
     6.042D+02      1.143D-05      9.475D-04      1.225D-05
     6.250D+02      1.081D-05      9.480D-04      1.167D-05
     6.458D+02      1.019D-05      9.485D-04      1.108D-05
     6.667D+02      9.566D-06      9.490D-04      1.048D-05
     6.875D+02      8.950D-06      9.496D-04      9.876D-06
     7.083D+02      8.337D-06      9.501D-04      9.259D-06
     7.292D+02      7.727D-06      9.507D-04      8.633D-06
     7.500D+02      7.120D-06      9.512D-04      7.999D-06
     7.708D+02      6.515D-06      9.518D-04      7.358D-06
     7.917D+02      5.913D-06      9.523D-04      6.711D-06
     8.125D+02      5.313D-06      9.529D-04      6.057D-06
     8.333D+02      4.715D-06      9.535D-04      5.398D-06
     8.542D+02      4.119D-06      9.541D-04      4.734D-06
     8.750D+02      3.526D-06      9.546D-04      4.066D-06
     8.958D+02      2.934D-06      9.552D-04      3.394D-06
     9.167D+02      2.344D-06      9.558D-04      2.719D-06
     9.375D+02      1.756D-06      9.564D-04      2.042D-06
     9.583D+02      1.169D-06      9.570D-04      1.362D-06
     9.792D+02      5.839D-07      9.576D-04      6.814D-07
     1.000D+03      0.000D+00      9.582D-04      0.000D+00    (BOTTOM)
```

192

Table 6-18b. Total Material Balance for Oil-Droplets, SPM and Oil-SPM Agglomerate at 10 Hours From OILSPM3.

```
MATERIAL BALANCE INFORMATION (FOR 1 CM*CM COLUMN OF WATER):

OIL IN THE WATER COLUMN, GRAMS = 1.501D-02
OIL LOST TO THE BOTTOM, GRAMS = 2.001D-01
OIL LOST THROUGH REACTION WITH SPM, GRAMS = 1.013D-01

OIL IN WATER + LOST AT BOTTOM + LOST THROUGH REACTION, GRAMS = 3.164D-01
OIL FLUXED INTO WATER + INITIAL LOADING, GRAMS = 3.166D-01


SPM (UNATTACHED) IN THE WATER COLUMN, GRAMS = 9.458D-01
SPM LOST THROUGH REACTION WITH OIL, GRAMS = 1.013D-01

SPM IN WATER + LOST THROUGH REACTION, GRAMS = 1.047D+00
SPM FLUXED INTO WATER AT BOTTOM + INITIAL LOADING, GRAMS = 1.047D+00


OIL-SPM AGGLOMERATE IN THE WATER COLUMN, GRAMS = 1.358D-02
OIL-SPM AGGLOMERATE FLUXED TO THE BOTTOM, GRAMS = 1.890D-01

OIL-SPM IN WATER + LOST TO BOTTOM, GRAMS = 2.026D-01
OIL-SPM AGGLOMERATE PRODUCED BY REACTION, GRAMS = 2.025D-01


VECTOR CONVERGENCE, OIL = 9.98D-16, SPM = 6.55D-16 ON  3 ITERATIONS.

END OF RUN WAS 07:34:47
```

average error between "guessed" and "calculated" concentrations is 9.9 x 10-16 g/cm^3 for oil and 6.55 x 10^{-16} for SPM, which is considered small enough.

6.4   CODE LIMITATIONS AND PERSPECTIVE

An important aspect of the three calculations described here is that they are one dimensional. For the sample problems discussed, a water-column depth of 10 m is used and an area (top or bottom) of 1 cm^2.   Note that if 0.5 cm of oil is spilled and this oil transports into the water, the oil droplet concentration could be $0.4g/1000cm^3$ or 400 ppm if there are no oil-loss mechanisms.   For the case where oil is removed at the bottom the resulting concentrations will be lower.   Clearly this oil concentration is much higher than

193

that ever observed in the ocean. The main reason for not predicting a lower oil concentration is that the one-dimensional calculation does not consider horizontal dispersion or spreading of the oil. Thus, the one-dimension calculations are conservatively too high. Then the question arises: what good are the calculations?

Besides providing upper-bound estimates of concentrations, these calculations also provide an estimate of the time required for things to happen in the water column. Also, the sensitivity of the input parameters can be investigated to learn what is or is not important with respect to a specific objective. For example, the oil deposition mechanisms are the boundary conditions at the bottom for the oil and the oil/SPM agglomerate, and the relative importance of these two processes can be investigated with respect to the parameters which will affect them, i.e., oil-rise velocity, oil/SPM reaction rate and oil/SPM settling velocity.

These calculations (codes) are not usable by interfacing them with other codes, i.e., with an ocean-circulation code. The only part of the calculation which is usable is the oil/SPM reaction rate which is of the form: $\alpha_c CS$. This reaction rate is written on a per-unit-volume basis, and an (existing) ocean-circulation model in three dimensions then must integrate this expression for the loss of oil, loss of SPM, and production of oil/SPM agglomerate. Thus, the relatively simple reaction rate expression is quite difficult to use in an environmental situation, if for no other reason than the environmental situations of interest are three dimensional.

7.0   CONCLUSIONS

Derivations of algorithms for the oil/SPM interaction models are presented in Section 3 and descriptions of user interactions during the running of the model codes are presented in Section 6. Mass transport calculations for interacting oil droplets and SPM in a one-dimensional water column are presented in Section 3 to illustrate the procedures necessary for implementing the various models in realistic environmental situations. The models describing the interactions of oil droplets and SPM are first order with respect to each interacting species (i.e., oil drops and SPM), and the interaction rate constants are functions of turbulent energy dissipation rates and other multiplicative parameters. The interaction models can be applied to either a well-mixed volume of water (e.g., a homogeneously stirred reaction vessel) or a nonhomogeneous solution where concentrations change as a function of position. Both of these applications are extremes of more classical mathematical descriptions of similar material balances in other fields of science and engineering.

Experimental efforts to evaluate effects of relevant environmental variables on whole-oil droplet/SPM interactions and the resulting determinations of values for parameters to be incorporated into the model algorithms are summarized in Section 5.2. The results of the efforts from the laboratory experiments yielded the following observations:

- Values for interaction rate constants between whole-oil droplets and natural suspended particulate materials are dependent on the type of sediment or SPM available for an interaction. Natural particulate types used in laboratory experiments included the following: Grewingk glacial till (< 53 μm), Yukon River Delta sediment (< 53 μm), Beaufort sea sediment (< 53 μm), Beaufort Sea peat (< 53 μm), Jakolof Bay sediment (< 53 μm), Kotzebue sediment (< 53 μm), Peard Bay sediment (< 53 μm), Prudhoe Bay sediment (< 53 μm) and Turnagain Arm SPM.

  For the physical and chemical properties measured for the sediment/SPM types used in experiments, only values for particle

195

number densities and to a lesser extent the proportions of the SPM types occurring in the 0-2 μm size range showed significant correlations with interaction rate constants (α). Both of these parameters (i.e., number densities and the 0-2 μm weight fractions) reflect overall size distributions of particles in particular sediment/SPM types. Therefore, the interactions between the oil drops and particular SPM types were inversely related to the size and, as a corollary, the total surface area of the SPM particles.

Other sediment/SPM properties that had no significant correlation or effect on interaction rate constants between oil droplets and sediment/SPM types included chemical measurements related to the organic content of the sediment/SPM (i.e., total organic carbon and total resolved hydrocarbons) and the specific densities of the sediment/SPM.

- Values for interaction rate constants between whole-oil droplets and SPM were dependent on the salinity of the reaction medium. Definite interactions were observed at salinities of both 28-30 ppt (full-strength seawater) and 14-15 ppt (1:1 v:v mixtures of seawater and freshwater). The magnitudes of the interactions at these two salinity levels appeared to be essentially equal. In contrast, minimal or no interactions between oil droplets and SPM were observed at a salinity of 0 ppt (freshwater).

- Oil droplet/SPM interaction experiments were performed with four types of oil: unweathered Prudhoe Bay crude oil, 12-day weathered Prudhoe Bay crude, unweathered No. 1 fuel oil, and naturally weathered North Slope crude collected from the R/T Glacier Bay spill incident in Cook Inlet, AK. Within the scatter inherent to the data, no differences in absolute values for interaction rate constants were apparent for the different oil types.

- A limited number of oil droplet/SPM interaction experiments were performed at varying levels of turbulence in the reaction vessels. Rate constants calculated from these experiments conformed to

196

expected model predictions for effects of turbulence on rates of interaction between dispersed oil droplets and SPM.

From the standpoint of utilizing experimentally-generated data from Section 5.2 for the oil droplet/SPM interaction models described in Sections 3 and 6, the important values generated in the laboratory experiments are those for the oil droplet/SPM reaction coefficient (α). As described in Section 5.2.1, values for α are used in the following equations:

$$\alpha_c = \alpha(\epsilon/\nu)^{1/2}S$$

when SPM is in excess (i.e., model OILSPMXS.BAS in Section 6.1) and

$$\alpha_c = \alpha(\epsilon/\nu)^{1/2}$$

when SPM is not in excess (i.e., model OILSPM3.BAS in Section 6.3). In these equations, ϵ is the energy dissipation rate (see Table 6-7 for a summary of observed oceanic values for ϵ), ν is the kinematic viscosity (which can be approximated as 0.01 cm^2/sec for seawater and freshwater mediums), and S is the concentration of SPM in units of g dry wt/cm^3.

During an actual application of the OILSPMXS.BAS model, the user must supply the value for α_c in item 8 of Table 6-2. For the OILSPM3.BAS model, the user supplies the value for α_c in item 3 of Table 6-15a. In both instances, the user must first calculate values for α_c in the above equations from selected values of α, ϵ, ν and S. The values for α_c are then interactively "edited" into the appropriate model (e.g., at the specified locations in Tables 6-2 or 6-15a during the running of a model). Values of α for incorporation into the above equations can be derived from either individual experimental measurements presented in Table 5-7 or the summarized information in Table 5-8 and Figures 5-9 and 5-10. Table 5-8 and Figure 5-9 present summarized data for the experimental determinations of α for a variety of natural sediment and SPM types from Alaskan coastal and nearshore environments in seawater solutions. Because particle number densities for the various sediment and SPM types exhibited the highest correlation with experimentally derived values of α (Table 5-9), extrapolation of α values for other sediment or SPM types from

197

Figure 5-10 appears reasonable if number-density information for a particular sediment or SPM type is available or can be obtained.

In order to use the models describing interactions between oil droplets and SPM in a one-dimensional water column that is initially oil-free, a source term for both oil and SPM is required. The source term for the oil droplets can be obtained from NOAA's open ocean oil-weathering code, which predicts the rate at which oil droplets are dispersed into the water column. This oil dispersion rate is used as a boundary condition in the form of an oil flux as a function of time. Since the oil-weathering code only predicts the flux and does not provide information in the form of an equation, the oil flux is actually used in mathematical form as a series of decaying exponentials. The one-dimensional models developed for this program are based on a single exponential type boundary condition. To use a series of exponentials, the calculated results for each exponential are added together.

The model that describes the SPM in the water column is based on an SPM source term at the lower boundary. This source term is self-limiting with respect to the maximum SPM concentration that can be attained in the water column. The source term must be obtained from either experience or observations of sediment transport.

Eventual transport of oil droplets in the water column will be to either the air-water interface as buoyant droplets or to benthic regions as oil/SPM agglomerates. Thus, the models described in Sections 3 and 6 are ultimately designed to generate an oil-free water column at long times as well as provide estimates for total material balances of oil and predictions of quantities of oil deposited in bottom sediments.

As for transport of oil to benthic environments, results of experiments to evaluate sedimentation rates for natural sediment types in this program are summarized in Section 5.3. Experiments were performed with two sediment types (i.e., Grewingk glacial till and Yukon River Delta sediment) that encompassed the extremes in particle-size ranges for the nine sediment and SPM types utilized in various portions of the experimental programs. It would seem reasonable to expect that information generated for settling velocities

for these two SPM types should therefore encompass ranges of values expected for the other sediment and SPM tyes.

Settling velocities for the Grewingk glacial till and Yukon River sediment were investigated in the context of both prior interactions with varying amounts of unweathered or 12-day weathered Prudhoe Bay crude oil as well as varying salinity in the experimental medium. Information derived from the settling velocity studies can be summarized with the following points.

- While the average size distributions of particles in the Grewingk till and Yukon River sediment were substantially different from each other (i.e., the till was comprised of a much higher abundance of particles with diameters < 10 μm), both of these natural sediment types did contain particles encompassing a spectrum of size ranges. Correspondingly, the sedimentation experiments produced spectrums of particle settling velocities for each of the sediment types (e.g., see Figure 5-15).

- Both the Grewingk till and the Yukon River SPM were more efficiently removed from suspension (i.e., sedimented) at salinities of 28-29 ppt (full-strength seawater) and 14 ppt (a 1:1 v:v mixture of seawater and freshwater) as opposed to 0 ppt (freshwater). Effects of salinity on particle settling velocities were most pronounced for particles in the smaller size ranges, as indicated by the fact that differences in the sedimentation trends at the different salinities were most pronounced at later sampling times when only smaller particles remained in suspension (e.g., Figures 5-26 through 5-29). More effective sedimentation of particles in half-strength and full-strength seawater was due to flocculation of the smaller particles in the aqueous mediums characterized by higher ionic strengths.

- Prior oiling of SPM particles in stirred reaction vessel experiments resulted in higher sedimentation rates for particles. The magnitude of this effect was positively correlated with the degree of prior "oiling" of the SPM. The latter point was demonstrated by the fact

199

that progressively higher oil loads associated with SPM resulted in more rapid sedimentation of particles and skewing of sedimentation velocity envelopes for the spectrums of particles toward higher sedimentation velocities (Figures 5-16 through 5-19). Photomicrographs of samples of SPM used in sedimentation velocity experiments documented substantially larger sizes of oil/SPM agglomerates compared to unoiled parent SPM material (e.g., Figure 5-6). Consequently, "oiling" of SPM particles was accompanied by their agglomeration into larger "particle masses", which in turn produced enhanced rates of sedimentation for the particles and the associated oil.

- Limited evidence suggests that oil in sedimentation experiments was preferentially associated with smaller SPM particles. For example, analyses of both SPM loads and oil concentrations were measured in common samples collected over time in one of the sedimentation experiments involving Yukon River sediment and 12-day weathered Prudhoe Bay crude oil. The results demonstrated that measured quantities of oil declined more slowly than the SPM (Figures 5-24 and 5-25). Microscopic obserervations revealed that all of the oil in the samples appeared to be associated with SPM (i.e., no free oil drops were visible). Consequently, the more gradual declines in the oil loads would indicate that the oil was preferentially associating with smaller SPM particles that had greater tendencies to remain in suspension.

Information from the laboratory sedimentation experiments can be used in the models presented in Sections 3 and 6. Specifically, settling velocity values are entered in item 1 of Table 6-11 for the model describing transport of SPM (i.e., model SPMONLY.BAS in Section 6.2) and items 1 and 2 of Table 6-15b for the model describing interactions between oil droplets and SPM (i.e., model OILSPM3.BAS in Section 6.3). It must be noted, however, that results of the sedimentation studies performed during this program demonstrate that natural SPM types will normally consist of a variety of particle sizes and shapes that are characterized by different settling velocities. Consequently, selection of specific settling velocities for use in the models must be done

200

with care and an understanding of the limitations presented by spectrums of settling velocities normally encountered in natural SPM or sediment phases.

Within the context of the preceding recognized limitations, specific values of particle settling velocities for use in the models can be extracted from data contained in Figures 5-15, 5-17, 5-19, 5-21, 5-23 and 5-25. These figures contain settling velocity values for natural SPM types that not only encompass a broad range of particle sizes (i.e., primarily 20-50 μm for Yukon River sediment and < 5 μm for Grewingk till; Figure 5-2) but also incorporate effects of varying degrees of oil loading onto the SPM phases.

In addition to the whole-oil droplet/SPM interactions summarized above, experiments were also performed to evaluate and estimate the relative importance of molecular-scale interactions between dissolved oil components and SPM. These studies are summarized in Section 5.4. The experiments were conducted with the following boiling-point cuts from Prudhoe Bay crude oil: Cut #4, Cut #7 and Cut #10. Adsorptive capacities for Cut #10 as a whole as well as individual compounds from Cuts #4 and #7 were determined for Grewingk glacial till, Yukon River sediment, and Turnagain Arm SPM. Results from the experiments produced the following specific observations:

- Partition coefficients (K_p) for the compounds and/or cuts were observed to increase with higher values for octanol-water partition coefficients (K_{ow}), higher molecular weights and lower aqueous solubilities.

- SPM adsorption capacities appeared to be strongly influenced by the initial concentrations of the dissolved components.

- SPM adsorption capacities for Cut #10 components appeared to be correlated to a limited extent with both particle number densities and the weight fraction of the total SPM contained in the < 2-μm size range.

With the data generated in Section 5.4, calculations were made to estimate the environmental importance of the molecular-scale interactions

201

relative to those for whole-oil droplet/SPM interactions. The latter
computations indicated that molecular-scale interactions between dissolved oil
components and SPM would likely be of only minor importance for determining
ultimate distributions and fates of oil components.

8.0   SEA ICE DYNAMICS EXPERIMENTS TO EXAMINE OIL/ICE/SPM INTERACTIONS

8.1   INTRODUCTION

        The presence of sea ice has appreciable effects on the weathering
behavior and dispersion of spilled oil (e.g., Payne, et al., 1984b and 1987a).
Dynamic ice growth, decay, and transport processes will all affect spilled oil
(Thomas, 1984), and there are a number of important variables which must be
considered when attempting to predict the weathering behavior and fate of oil
spilled in the presence of ice. These variables include the age of the ice,
whether it is in a state of active growth or decay, the location of the spill
(underneath or on top of the ice), the type of oil spilled, and the physical
properties of the ice itself, including the ice crystal structure and the
presence of entrained sediments. While models developed by SAIC and others
(e.g. Payne et al., 1987a; Wotherspoon, et al., 1985; and Wilson and Mackay,
1986) allowed predictions of oil weathering behavior and interactions of oil
with first-year and multiyear ice, little information was available to allow
predictions concerning oil interactions with ice containing heavy sediment
loads. Therefore, the studies described in the following sections of this
report were undertaken to provide sufficient information and data to support a
computer model that could be used in concert with existing NOAA models
ultimately to predict oil weathering (and sedimentation) behavior under these
conditions. The primary thrust and initial focus of these studies was on
understanding the ice/sediment/SPM interaction and entrainment processes
responsible for generating a seasonal ice canopy with widely varying but
significant sediment burdens. Experiments were then planned in which free oil
droplets could be introduced to study their effect on sediment entrainment and
transport by seasonal ice canopies.

        As discussed by Osterkamp and Gosink (1984) and references therein,
incorporation of seabed sediments into nearshore sea ice layers is a common
phenomenon, particularly in areas of the Bering, Beaufort, and Chukchi Seas.
Sediment-laden ice is also often observed rising to the surface of northern
rivers on mornings following cold, clear nights (Barnes, 1982; Wigle, 1970; Ar-
den and Wigle, 1972; Michel, 1972; and Foulds and Wigle, 1974). Concentrations
of fine-grained sediments in sea ice have been reported as high as 1600 mg/L

203

(e.g., Campbell and Collin, 1958; Barnes and Fox, 1979; Barnes et al., 1982; Osterkamp and Gosink, 1984); concentration profiles of fine-grained sediments in sea ice are also frequently characterized by distinct vertical gradients comprising a surface layer with low sediment concentrations, an intermediate layer with high sediment concentrations, and a bottom layer of "clean" (i.e., essentially sediment-free) ice (Barnes et al., 1972; Barnes and Fox, 1979; Osterkamp and Gosink, 1984). Consequently, processes contributing to fine-grained sediment loads in sea ice can produce in situ concentrations substantially in excess of those in parent formation waters, as well as distinct vertical concentration gradients in the ice itself.

Sediment incorporation into ice may affect light transmittance properties, albedo, and the ice structure and mechanical strength. Additionally, ice movement followed by breakup represents a mechanism for transporting and redistributing significant quantities of entrapped sediments (Barnes et al., 1982; Naidu, 1979). This same mechanism may also be important for transporting and redistributing discharged materials from oil drilling operations, including muds and cuttings, as well as oil droplets or oiled sediments (Osterkamp and Gosink, 1984). The presence of weathered or fresh crude oil also may have important but unknown effects on ice/sediment interaction processes. Possible effects include alterations of sediment incorporation rates into ice, changes in the affinity of oiled particles (and flocs) for ice crystal surfaces, enhanced (or retarded) SPM filtration by slush ice, and perturbations to the susceptibility of oiled sediments to turbulent resuspension or reflotation.

Sediment is incorporated into fluvial and marine ice covers because of interactions of frazil ice, slush ice, and anchor ice with sediment in suspension and/or on the bottom. Frazil ice exists as fine spicules, plates, or discoids of ice crystals suspended in water (Kivisild, 1970). It forms in slightly supercooled water, usually occurring as discs ranging from 1 to 4 mm in diameter and 1 to 100 μm thick. Under certain conditions, frazil crystals become attached to bottom material or underwater objects, creating anchor ice. Although the formation, development, and properties of frazil have been the subject of many studies (summarized by Osterkamp, 1978; Martin, 1981, and

Tsang, 1982), the interactions of frazil and anchor ice with sediment are poorly understood.

Freshwater frazil and anchor ice in lakes and rivers cause many engineering problems, including flooding, interference with hydroelectric facilities, blockage of water supply intakes, interference with shipping, and damage to hydraulic structures (Carstens, 1966; Osterkamp, 1978). Therefore, it is not surprising that most studies have dealt with the engineering properties of frazil and anchor ice or have been aimed at understanding the meteorological and hydraulic conditions necessary for frazil and anchor-ice formation.

Fluvial and marine frazil and anchor ice commonly form in turbulent, supercooled water exposed to subfreezing air temperatures. Turbulence, caused by currents or wind-generated waves, inhibits formation of a surface ice cover and allows supercooling of the water column to some depth. In natural water bodies, this supercooling is less than 0.10°C (Schaefer, 1950; Wigle, 1970; Arden and Wigle, 1972). The time-temperature curve for water where frazil is produced has a characteristic shape (Figure 8-1) where the temperature decreases with time to some minimum temperature, T_m, and then rises to an equilibrium temperature (T_e) as frazil is formed (Tsang, 1982; Tsang and Hanley, 1985). T_e is slightly less than the freezing temperature, T_f, and the difference between these two, T_r or the residual temperature, is the driving force for continued frazil production in natural systems.

Frazil in supercooled <u>fresh</u> water is believed to be "active" or "sticky", exhibiting strong cohesive tendencies between individual ice crystals and between ice crystals and materials on the bottom (Carstens, 1966). Once frazil crystals form, they agglomerate to each other and form buoyant flocs 3 to 10 cm in diameter that rise to the water surface. Flocs evolve into surface slush ice or frazil pans when exposed to frigid air. Frazil pans can range from 2 to 10 m in diameter and exceed 1 m in thickness (Osterkamp and Gosink, 1983). The accumulation of frazil pans against an obstruction and subsequent freezing of the water between pans leads to the formation of a solid ice cover.
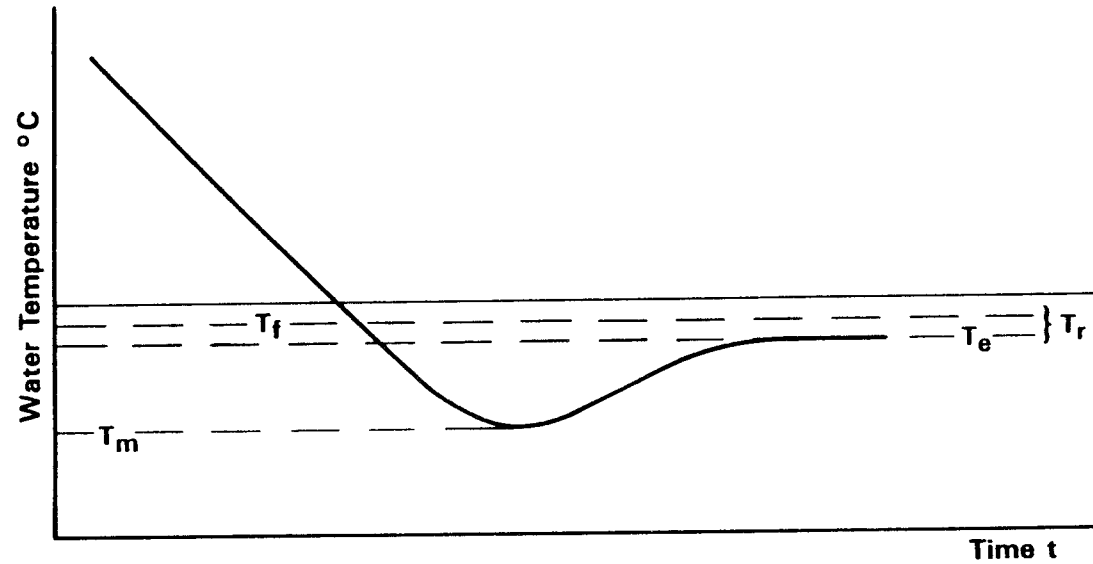
Figure 8-1   Idealized Time-Temperature Curve Showing Supercooling of a Water Body Leading to the Formation of Frazil Ice

T_m is the temperature minimum; T_e is the equilibrium temperature (i.e., that temperature at which heat lost to the atmosphere is equal to the heat released by the growing frazil ice crystals); T_f is the freezing point of the water, which may be below zero; and T_r is the residual temperature (i.e., the difference beteween T_e and T_f). This small residual temperature is the driving force for producing most frazil ice in natural systems (modified from Tsang and Hanley, 1985).

Previous research on <u>saltwater</u> frazil and anchor-ice formation suggests that, even in supercooled water, frazil platelets may not be sticky (Hanley and Tsang, 1984). This lack of stickiness is explained by salt rejection from the ice as a frazil crystal forms. This salt forms a thin layer of water with higher salinity and correspondingly lower freezing point around the frazil crystal, which in turn inhibits continued frazil growth and apparently also reduces the stickiness of the frazil crystal (Hanley and Tsang, 1984). In the Beaufort Sea, Kempema et al. (in prep.) found that accumulations of frazil slush on the sea surface are not sticky. However, Reimnitz et al. (1987) report observations of anchor ice that apparently formed from frazil adhering to the seafloor.

Potential mechanisms for sediment entrainment into surface ice canopies have been described by Campbell and Colin (1958); Benson and Osterkamp (1974); Larsen (1980b); Naidu (1980); Osterkamp and Gosink (1980); and Barnes et al. (1982) who suggested that the most likely mechanism for resuspending nearshore bottom sediments into ice is storms during the freezeup period. Initially, storm-induced turbulence can produce suspensions of fine-grained sedimentary materials in cold, shallow water columns in which frazil ice crystals are forming. If calm water conditions follow, the suspended sediment particles become entrained on or in the frazil crystals as the latter rise to form a seawater-slush ice layer near the water surface. In addition to entrapment by ascending frazil crystals, it has also been proposed that sediment particles may "stick" to newly formed frazil crystals in supercooled water (Osterkamp and Gosink, 1984). Another mechanism that has been documented to yield inclusions of larger sedimentary materials (as well as associated benthic fauna and flora) involves detachment of anchor ice from the seafloor in shallow-water areas (Dayton et al., 1969; Reimnitz et al., 1987). However, this mechanism does not appear to be adequate to explain either the high concentrations or the distinct vertical profiles of fine-grained sediments noted in ice cores.

Despite these proposed mechanisms, the exact processes responsible for incorporating sediments into the ice canopy are only poorly known, and existing information is largely empirical, based on observations from ice cores

207

collected at several locations in nearshore areas of Alaska. Schell (1980) reviewed a number of the possibilities, and proposed mechanisms (summarized in Table 8-1, can be divided into two categories: 1) direct contact between ice and bottom sediments and 2) interactions between suspended sediments and frazil ice during freezeup events. These two general types of interactions account for observations regarding the two classes of sediment types (coarse and fine-grained) found in ice cores (Benson and Osterkamp, 1974).

When this research program was initiated in the fall of 1985, there was little general consensus about which mechanisms were most important, or if all of the proposed mechanisms were tenable. Osterkamp and Gosink (1984) suggested that direct entrainment during freezeup and direct filtration by frazil ice crystals were the most likely mechanisms for sediment incorporation. However, direct entrapment during freezeup did not account for the extremely high sediment concentration factors observed in the ice canopies compared to observed SPM loads in the water column. Also, it was unclear that these processes could account for the observed localized spatial variability in sediment levels.

Table 8-1

**Possible Sediment/Ice Entrainment Processes
(from Osterkamp and Gosink, 1984)**

I) DIRECT ICE-BOTTOM SEDIMENT INTERACTIONS

- Entrainment in anchor ice, flotation, and incorporation into ice cover
- Entrainment of riverine anchor ice
- Entrainment by ice gouging
- Entrainment following sea bed freezing and reflotation

II) REMOVAL OF SUSPENDED SEDIMENTS FROM THE WATER COLUMN

- Direct entrainment of suspended sediments during freezeup
- Entrainment with frazil ice formed in leads and mixed underneath the ice cover
- Entrainment with sinking brine flow, interaction with suspended bottom sediments, and incorporation with ice growth
- Entrainment of bottom sediments with frazil ice crystals under conditions of strong turbulent mixing
- Direct filtration of suspended sediments from seawater

The processes responsible for incorporating sediments into frazil ice require a mechanism for efficiently filtering particles out of the water and for retaining sediment particles in growing ice crystals. Osterkamp and Gosink (1984) presented a theoretical discussion of ice crystal filtration of SPM to demonstrate that this process could account for the high sediment concentration factors observed in ice cores. However, the authors also suggested that the efficiency of ice crystal filtration and the permeability of frazil ice require experimental verification. Specific experiments designed to examine direct ice/sediment interactions and SPM entrainment and filtration processes, as well as other potential mechanisms for the formation of SPM-laden sea ice, are presented in the following sections.

Initially, experiments were conducted to investigate sediment resuspension and scouring of suspended particulate material (SPM) by actively growing frazil and slush ice interacting directly with the bottom (Section 8.3). As those experiments progressed, however, a number of self-cleaning mechanisms for slush ice in an active wave or current regime were discovered, and these are considered in Section 8.4. Based on the results of these initial studies, it was clear that the formation of dirty sediment-laden ice was dependent on the unique sequential development of a storm event and subsequent freezeup. Therefore, a number of new and/or modified hypotheses had to be developed to explain observed sediment loads in natural ice canopies. Section 8.5 presents the results from several direct filtration experiments and cold-room vertical column studies to examine the effects of SPM entrainment by actively growing _and rising_ frazil ice after a major storm event during fall freezeup. The results from these latter experiments were particularly promising and provided valuable insight on how a sediment-laden ice canopy might actually develop. Therefore, the vertical column experimental approach and equipment/instrumentation were modified, and Section 8.6 presents the results of initial studies to allow quantification of the heat-transfer processes during active frazil ice growth and sediment entrainment. Such data are critical for any modeling effort on predicting oil/ice/SPM interactions. Before additional experimentation or model development in this area could be completed, however, the program Scope of Work was changed to focus entirely on

209

the Oil/SPM interactions, which were described earlier in Sections 2.0 through 7.0.

8.2 EXPERIMENTAL SYSTEM AT KASITSNA BAY

8.2.1 Flow-Through Wave Tank System

From Section 8.1 it is apparent that numerous investigators have observed and collected slush ice containing entrapped sediments, and that a variety of hypotheses have been proposed to explain the incorporation of different sediment-size classes into the ice matrix. None of the hypotheses alone, however, is capable of fully explaining the field observations; and at the time this program was initiated, there were no systematic experimental data which had been collected under controlled laboratory conditions to investigate the phenomenon.

This experimental program was designed to examine several possible mechanisms that had been proposed to explain the formation of sediment-laden sea ice and the potential influence of these mechanisms on sediment and pollutant transport. Laboratory experiments were conducted using natural seawater in a flow-through wave-tank system and racetrack flume (Kempema, 1986) installed in a specially designed cold room at the NOAA Laboratory at Kasitsna Bay, Alaska. The wave tank and cold room chamber system have been described in detail elsewhere (Payne, et al., 1984b and 1987a).

Essentially, the experimental system consisted of a walk-in cold room equipped with a five-horsepower compressor and five-fan evaporator unit capable of maintaining the inside room at temperatures as low as -38°C. A 2,700-2,900 L flow-through seawater wave tank (3.5 m x 1.0 m x 0.9 m) was constructed inside the cold room for the frazil ice SPM interaction studies. Wave turbulence was provided by a submerged and hinged paddle attached to an adjustable eccentric drive-wheel powered by a one-horsepower motor (Figures 8-2 and 8-3). The sides, windows, and bottom of the tank were insulated with 2.3 cm of closed-cell foam to ensure that seawater cooling occurred primarily through the air/sea interface.
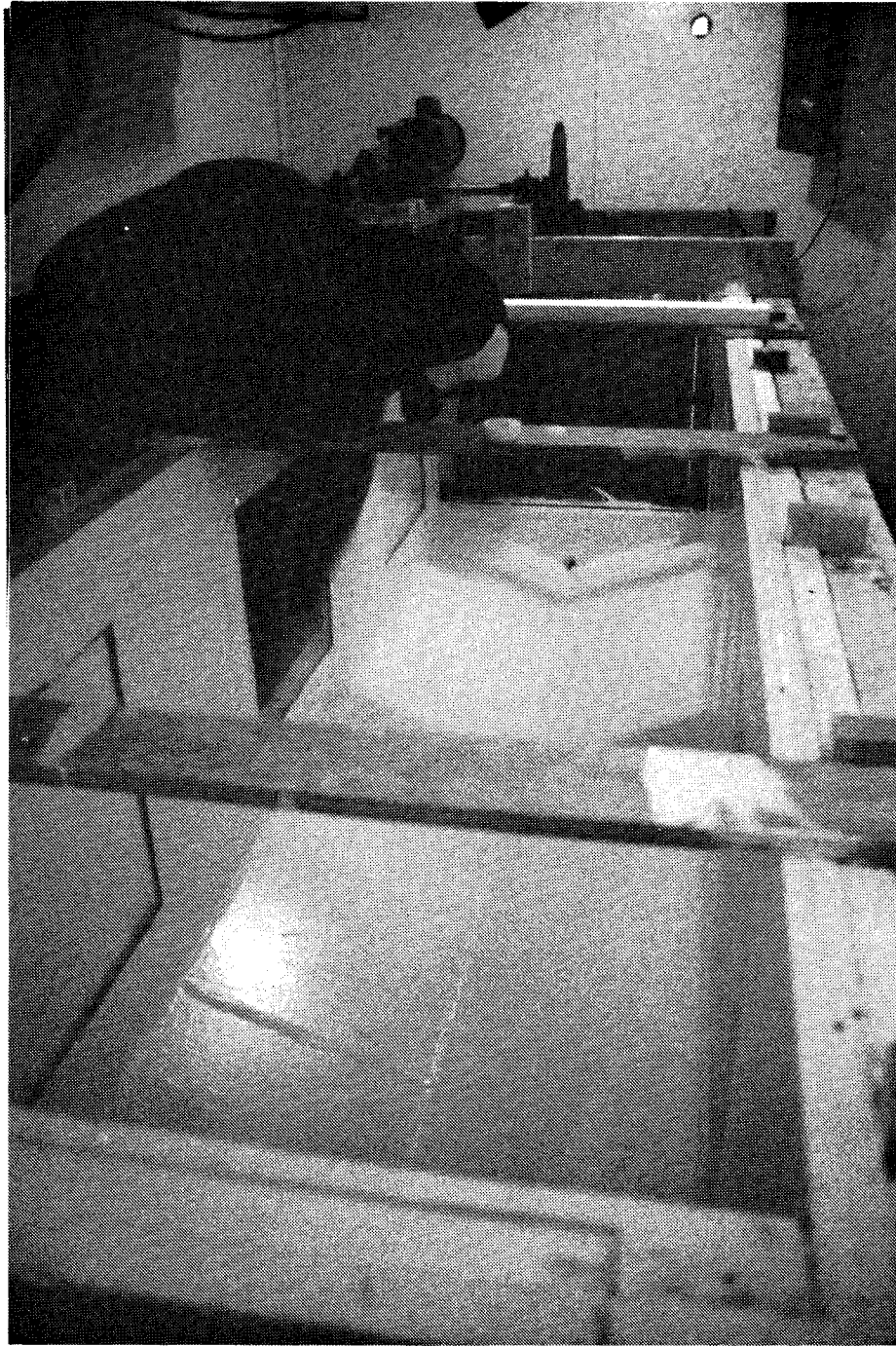
Figure 8-2. Overview of the 2700-Liter Wave Tank Installed in the Walk In Cold Room at Kasitsna Bay

Tank dimensions are 3.5 m x 1.0 m x 0.9 m. In the background of the figure, the paddle mechanism for generating wave turbulence can be observed. The seawater inlet for the flow-through system is at the base of the V immediately below the paddle.

Figure 8-3. Close-Up of the Wave Paddle System Driven by a 1-Hp Motor and Drive Shaft Connected to an Off-Center Eccentric Drive Wheel

Fresh seawater for the tank was pumped through PVC pipe from a depth of 3 m below the lowest low tide in Kasitsna Bay. This seawater was first passed through a countercurrent heat exchanger to recoup refrigeration capacity from the water exiting the wave tank when operated in the flow-through mode. The inlet for the fresh seawater entering the wave tank was located at the lowest point of the V-shaped tank bottom beneath the paddle. The position of the incoming seawater line was designed to allow sediment which settled out of the water column in the tank to be resuspended by the inlet flow. The external plumbing design (with its countercurrent heat exchanger) is shown schematically in Figure 8-4.

The wave tank was equipped with external PVC plumbing and impeller pumps connected to inlet and outlet flow headers shown in Figures 8-4 through 8-8. The inlet/outlet flow headers were designed to allow a diffuse flow of seawater to be introduced into one end of the tank and removed at the other. The outlet headers were located at approximately the same height as the inlet headers, but at the opposite end of the tank. This external plumbing loop was designed to provide a closed pump-around circuit to generate a water current through the tank which could be used to test Osterkamp and Gosink's "Filtration Hypothesis." By using this pump-around recirculating system with only ice-chamber water, the thermal requirements on the compressor and evaporator unit for the cold room were considerably less than if a higher simulated current flow were simply generated by increasing the flow-through rate of "fresh" but relatively warmer seawater from Kasitsna Bay. In-line digital flowmeters in an adjacent control room were installed to allow measurement of seawater flow rates through the wave tank. The system thus was designed and constructed to allow a simulated current flow to be established within a growing slush ice field. Temperature profiles within the growing slush ice fields and resulting sea ice canopies were measured with a vertical themistor array from Yellow Springs Instruments (Figure 8-9) located at the quiescent (or dead zone; e.g. see Bauer and Martin, 1983) end of the tank. Air temperatures were measured by two additional thermistor probes (which could be moved about the cold room) calibrated against a laboratory thermometer.
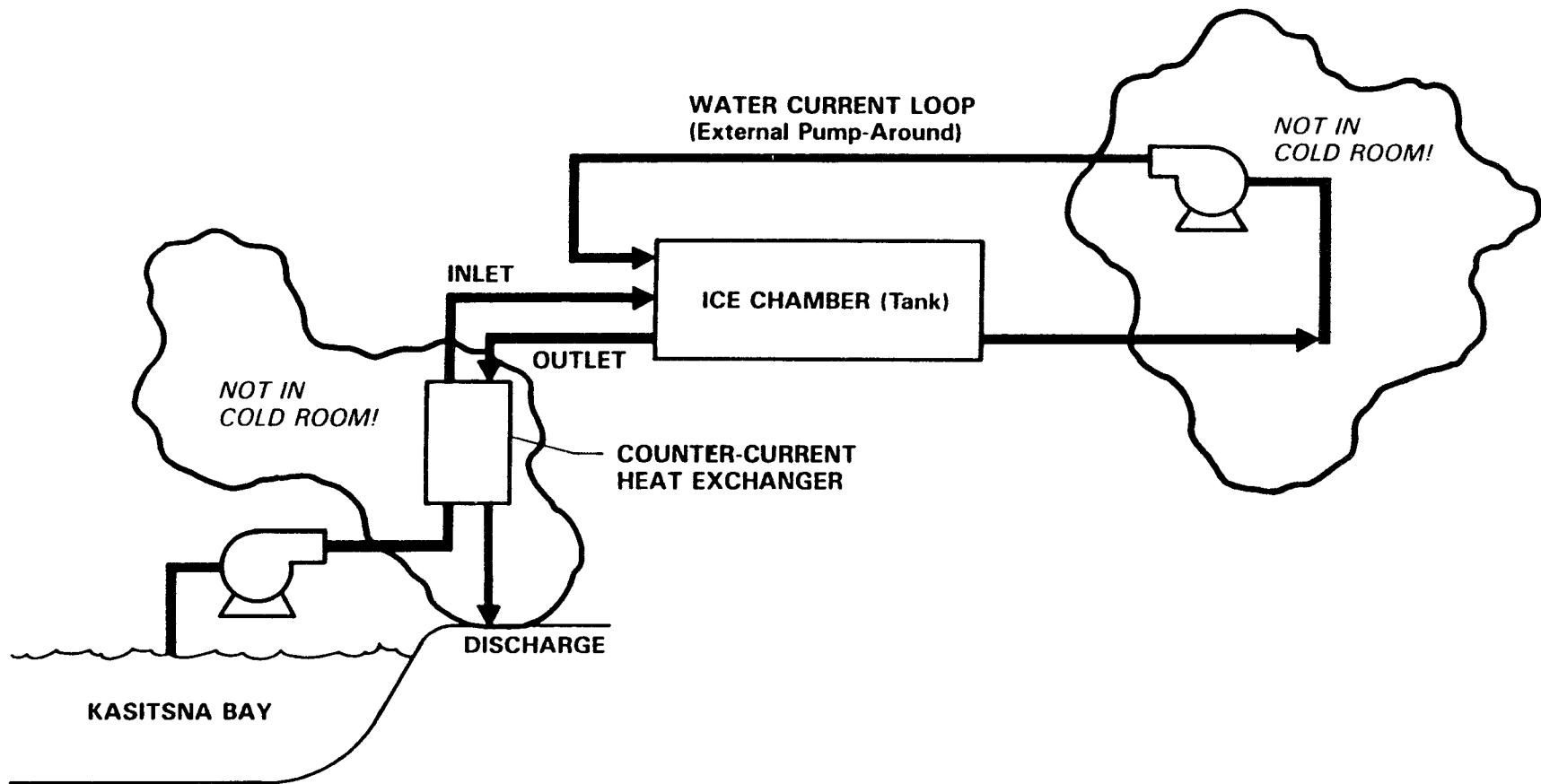
Figure 8-4. **Modified Ice Chamber Flow Loops for Experimental Program on Oil/Ice/Sediment Interactions**

Figure 8-5.   **Photograph of External Exhaust Headers at Dead-Zone End of Wave Tank**

These headers were later insulated with heat tape and foam insulation to prevent freezing during recirculation experiments.

Figure 8-6. **Photograph of the External Inlet Headers Into the Side of the Wave Tank Adjacent to the Paddle.**

These headers were later insulated with heat tape and foam insulation to prevent freezing during recirculation experiments.

216
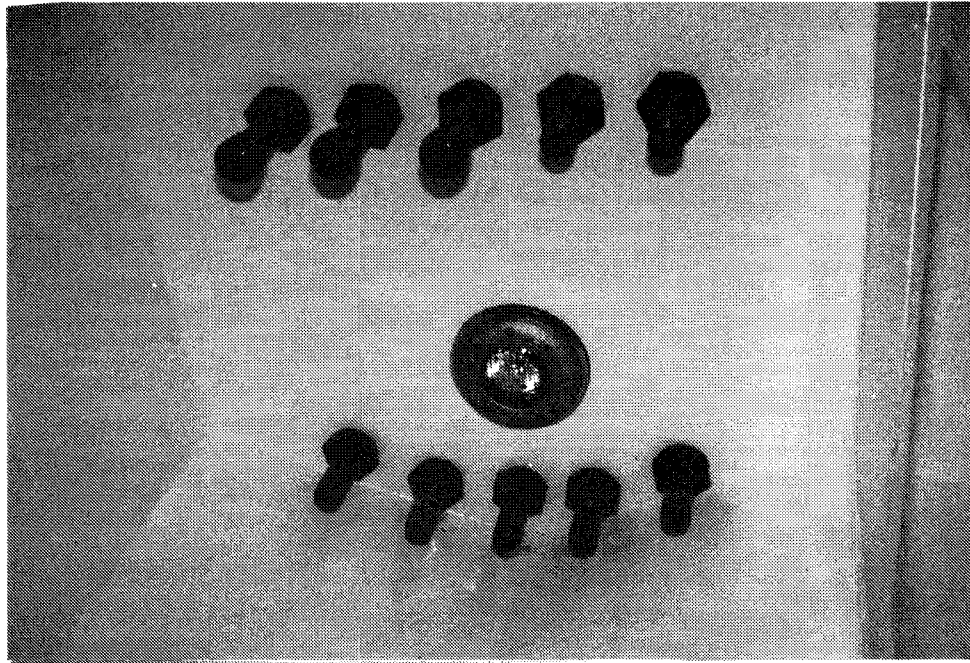
Figure 8-7. **Photograph of Internal Exhaust Headers and Underwater Light at the Dead-Zone End of the Wave Tank**

Note: 1-millimeter mesh plankton net was cemented to each exhaust header nipple to prevent entrainment of ice during flow-through seawater experiments. Also, the threaded end pieces could be capped to shut off flow as desired during experiments.
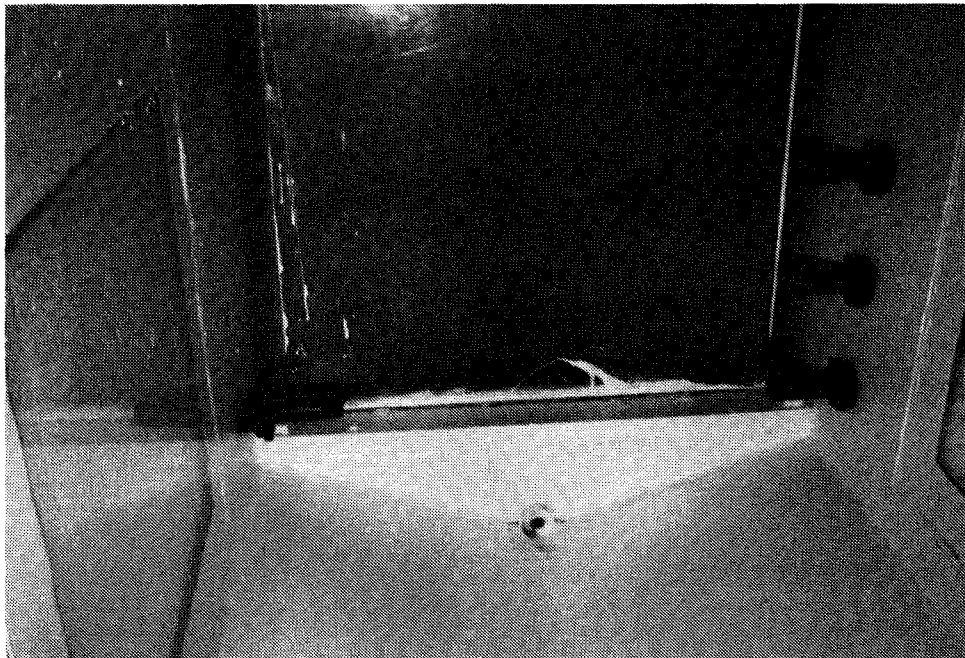
Figure 8-8. **Photograph of Internal Inlet Headers for Seawater Circulation System and Close-Up of Paddle in the Wave-Tank System**
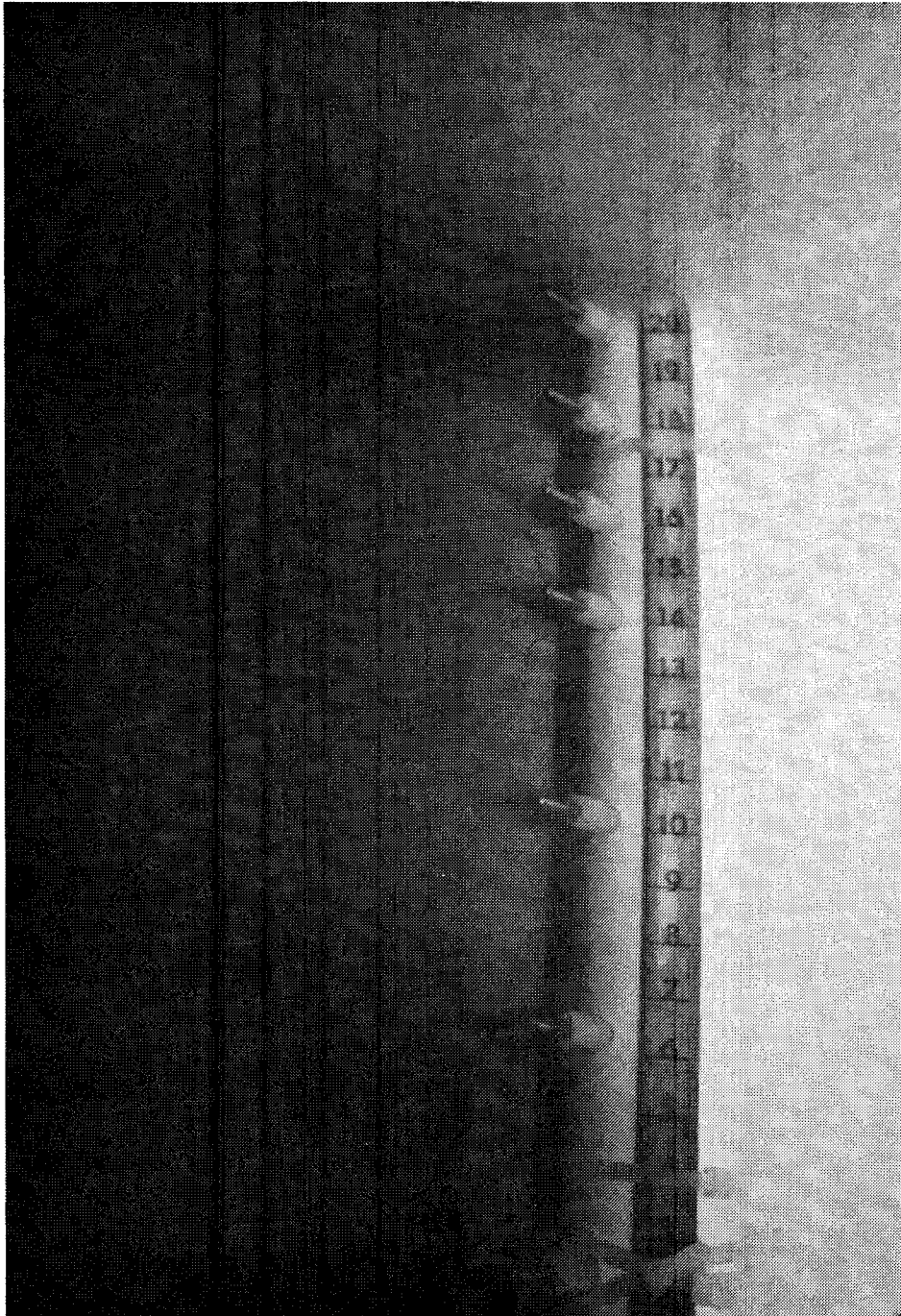
Figure 8-9. **Vertical Thermistor Array for Measurement of Seawater Temperatures and for Temperature Gradients in Surface Ice Canopies**

Two portable thermistors (not shown) were used for determination of air temperatures in the cold room during each experiment. The thermocouples were attached to a thermocouple readout unit located in the adjacent control room.

218

8.2.2   U.S. Geological Survey Racetrack Flume

The portable U.S.G.S. racetrack flume (Kempema, 1986) used in a number of the experiments was constructed of aluminum with plexiglas windows built into one straight segment (Figures 8-10 and 8-11). The flume was similar in shape to the one used by Carstens (1966) and was 1.2 m long, 75 cm wide, and 32 cm deep, with a channel width of 21 cm. The volume of water in the flume during an experiment was about 110 L. During use the flume was placed in the cold room and filled with a level layer of sand or finer-grained sediment 4 cm thick overlain by 17 cm of water. The aluminum sides of the flume were insulated with 1.5 cm of closed-cell foam, and the bottom with 5 cm of foam, so that the water cooled predominantly from the surface.

Currents in the flume were produced with a small plastic propeller, positioned in the back straight section of the flume and driven via a flexible shaft by a variable-speed electric motor. Current speeds in the flume could be varied from 30 to 70 cm/s. The shape of the flume and the rotary motion of the propeller resulted in nonuniform flow; thus, the reported current speeds are averages. Water temperatures during frazil ice experiments were measured with a portable thermistor probe attached to the digital thermistor array readout in the control room (accurate to +/- 0.025°C) or a U.S.G.S. thermistor system accurate to 0.004°C.

8.3   SEDIMENT RESUSPENSION BY DIRECT FRAZIL/SLUSH ICE INTERACTION

8.3.1   Introduction

It has been suggested that frazil ice may interact directly with bottom sediments under conditions of high turbulence in shallow, near-coastal waters. Larsen (1980) proposed that a transient form of anchor ice may form with frazil crystals adhering to seabed sediments. As the ice crystals continue to grow, their buoyancy increases; and it was hypothesized that they could lift the sediments to the surface where they may become part of the floating slush ice field which congeals and entraps them in place. This mechanism was also
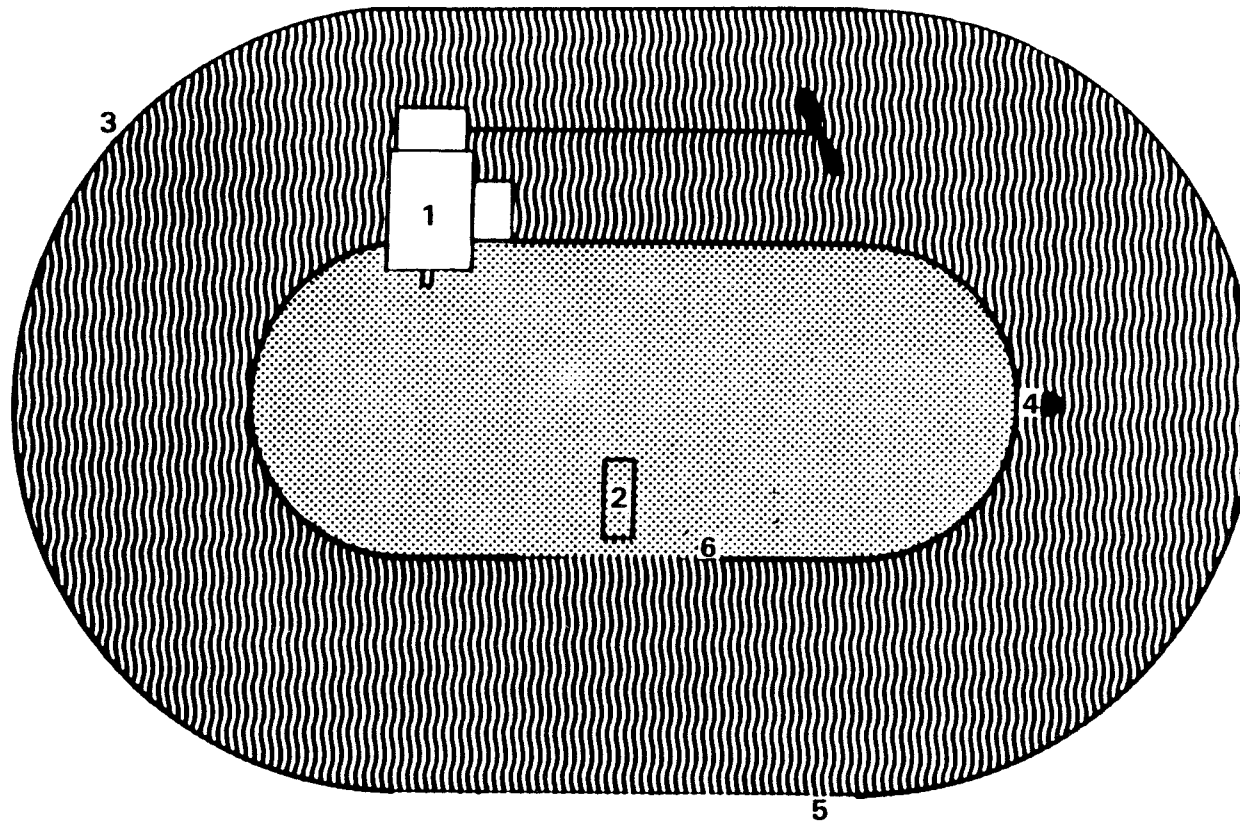
1. VARIABLE SPEED ELECTRONIC MOTOR
2. LIGHT
3. 1.5 cm INSULATION
4. THERMISTOR
5. PLEXIGLASS WINDOW

20 cm

Figure 8-10.   Plan View of USGS Racetrack Flume Illustrating: (1) variable-speed, electric motor attached to propeller, (2) light, (3) 1.5 cm thick insulation, (4) thermistor, and (5) plexiglas windows
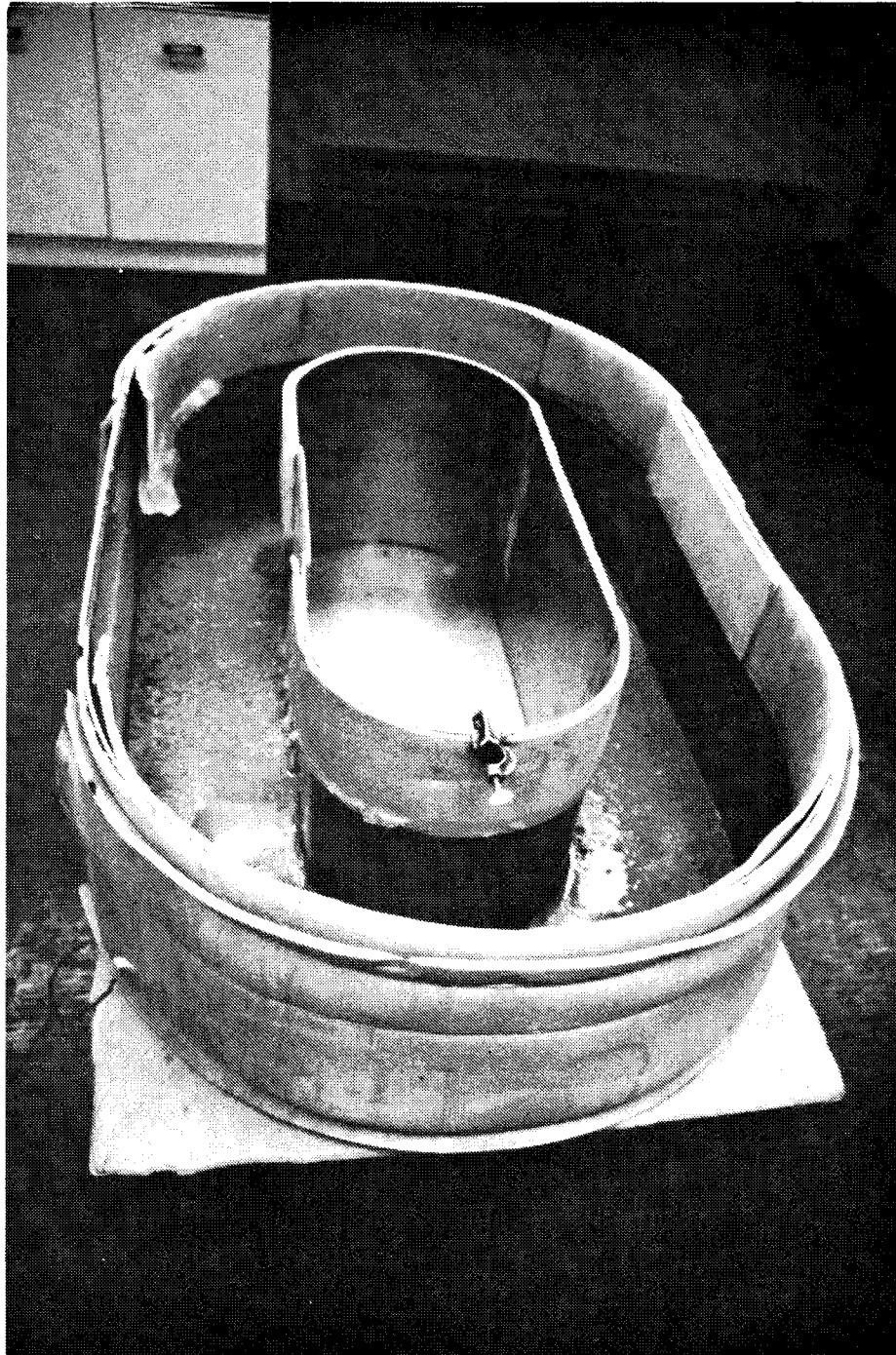
Figure 8-11. Photograph of the U.S. Geological Survey Racetrack Flume Before Installation into the Cold Room

believed to help explain the presence of larger sand grains and shell fragments observed in selected ice cores in the field.

8.3.2   Sloped-Table/Beach Face Experiments

8.3.2.1 Methods

Utilizing the cold room and wave-tank system described in Section 8.2, a series of sloped-table/beach-face experiments were undertaken to examine frazil ice/slush ice scouring of sediment due to direct ice platelet interactions with sediment in the presence of wave turbulence. A 1.8-m x 0.5-m artificial beach face was constructed of plywood and placed in the cold room wave tank, as shown schematically in Figure 8-12. The table surface was adjustable in such a way that the following parameters could be varied during an experiment:

- bottom slope

- bottom depth with respect to undulating slush ice and frazil ice matrix

- sediment type

- wave/slush ice turbulence

Figures 8-13 and 8-14 show photographs of the adjustable table system in the wave tank with a coarse (0.3 to 1.5 mm) sand-sediment matrix present for an initial series of scoping experiments. After installation of the artificial beach face and sedimentary material, the cold room and seawater in the wave-tank system were cooled to initiate the formation of frazil ice as described in Payne et al., 1987a.

Direct sediment resuspension/entrainment experiments were undertaken with two different sediment types. The first was a well-sorted sand sample from McDonald Spit and the second was a poorly sorted mixture of sand, silt,

WAVE PADDLE

SLUSH ICE/FRAZIL ICE
IN STANDING WAVE TRAIN

MOVABLE
SEDIMENT TRAY

OBSERVATION
PORT
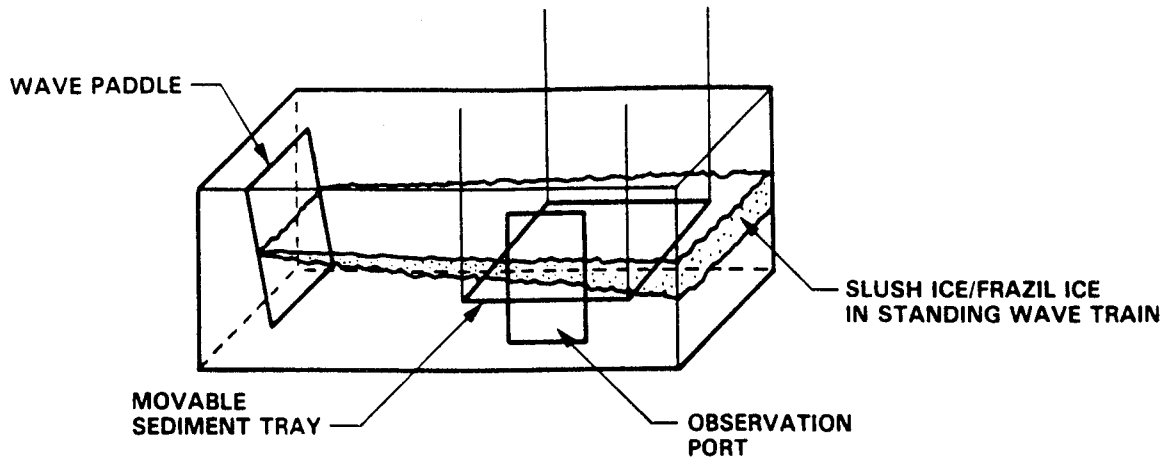
POSSIBLE EXPERIMENTAL PROGRAM VARIABLES (Side View)

SLUSH ICE/FRAZIL ICE

TANK
END

SIZED (SORTED) OR NATURAL
OILED VS. UN-OILED SEDIMENT
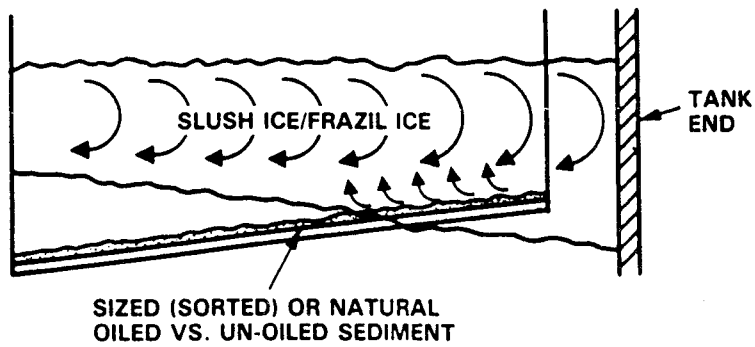
1. DIRECT SLUSH ICE/SEDIMENT
CONTACT IN STANDING WAVE
TRAIN TO EXAMINE HORIZONTAL
AND VERTICAL ENTRAINMENT
AND SPM MIGRATION.

2. INDIRECT ICE SCOURING BY
FRAZIL ICE CRYSTALS DRIVEN
TO BOTTOM.

SLUSH ICE

FRAZIL ICE
CRYSTALS ONLY

TANK
END
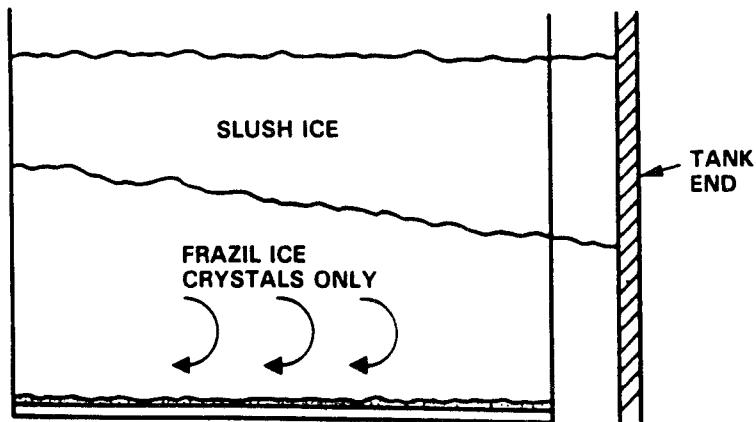
*VARIABLE EXPERIMENTAL
PARAMETERS:*

- BOTTOM SLOPE
- BOTTOM DEPTH WITH RESPECT
  TO UNDULATING SLUSH ICE
- SEDIMENT TYPE
- WAVE/SLUSH ICE TURBULENCE

Figure 8-12.   Overview of Sediment Tray Configuration in Frazil Ice Wave Chamber
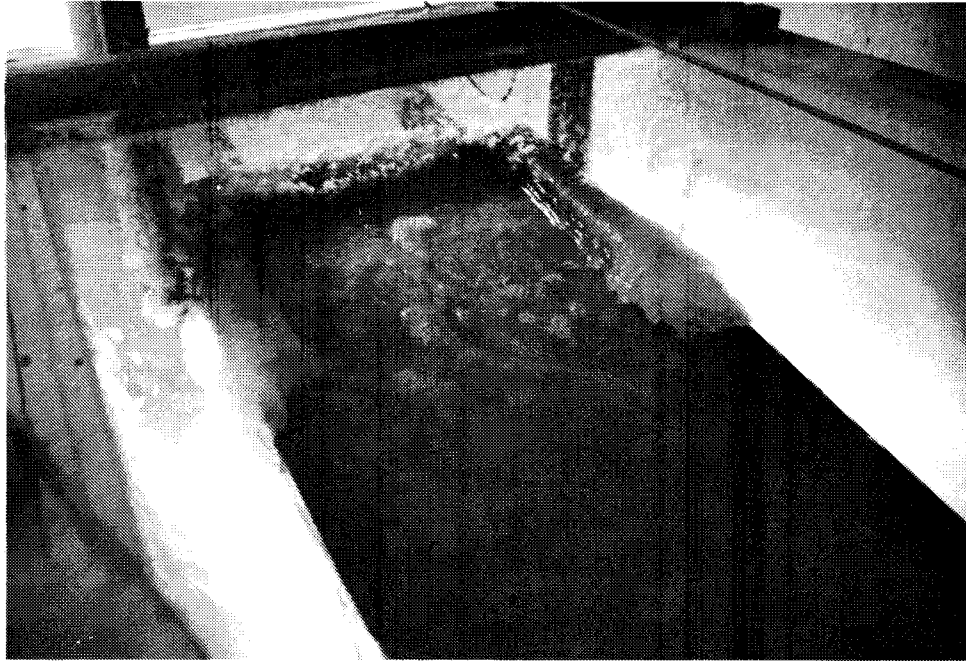
Figure 8-13. **Plywood Sloped Table/Beach Face Installed in Wave Tank**

The table was installed with a slope of 6:1. Note the upper 15 cm were in the splash zone above the air/sea interface.
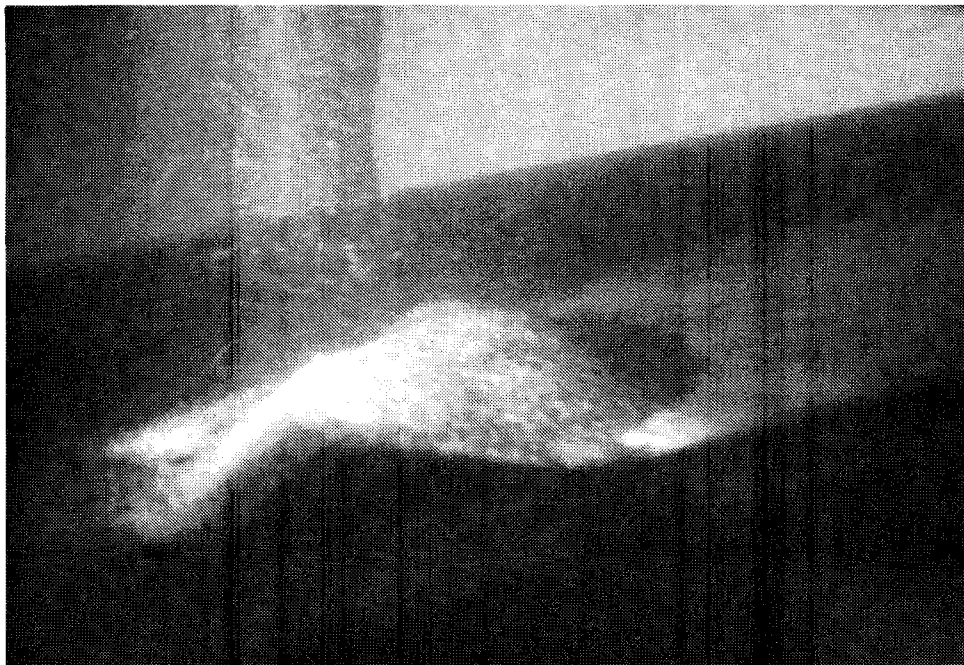
Figure 8-14. **Underwater View of Coarse-Grained Sediment (0.3 to 1.5 mm) on Beach Face With Traces of Frazil Ice in the Water Column Immediately Above the Sediment Matrix**

224

clay, and mud collected from Jakolof Bay. Table 8-2 and Figure 8-15 present the particle-size distribution data for these two sediment types.

In the initial experimental series, the tray was configured in such a way that the beach slope was 6:1. It was positioned at a depth which assured that breaking waves and newly formed slush ice would interact with the upper 10 cm of the exposed beach face while the remaining part of the adjustable table was beneath the water surface.

8.3.2.2 Results

At the initiation of the experiment approximately 400 gm of the well-sorted McDonald Spit sand were placed on the adjustable slope at the uppermost and middle sections of the beach face just under the air-sea interface. With wave turbulence, the sand was observed to be lifted off of the beach surface to a maximum depth of approximately 5 to 7 cm. Wave heights were measured at 12 to 18 cm. With time, some of this sand was moved up along the slope and deposited as a thin berm in the upper splash zone. Due to the turbulence on the beach face, additional sand grains were observed to be washed off the artificial slope, and these eventually settled to the bottom of the wave tank.

Just prior to frazil ice formation, a uniform water column temperature was measured at -1.77°C. When initial (time zero) frazil ice formation was noted, the turbulent regime established by the 12-18 cm amplitude wave train was sufficient to maintain frazil formation both above and below the beach plain, and little or no surface-ice accumulation was noted for at least 10-15 minutes. With the initial frazil ice formation, the orbital action of the waves moving up the beach surface could be easily observed; however, there was no evidence of any significant accumulation or scavenging of sedimentary material by the frazil ice during the first 20 minutes of the ice-formation event. Frazil crystals were observed suspended throughout the water column both above and below the beach face and, in general, these platelets had sizes ranging from 1 to 3 mm in diameter. On rare occasions, spicules of frazil ice containing sediment grains were observed suspended in the water column, and isolated grains of sand were observed in the growing ice canopy in clasts below

225

Table 8-2

Grain-Size Distributions for MacDonald Spit Sediment and Jakalof Bay 2 Sediment Used for Oil/Ice SPM Interaction Experiments

MACDONALD SPIT SEDIMENT

Phi Size	mm	PARTICLE SIZE DISTRIBUTION Adjusted Weight	Weight Percent	Cumulative Percent	OVERALL SIZE CLASS DISTRIBUTION Size Class	Weight Percent
-0.5	1.4142	0.6049	3.90	3.90	gravel	0.000
0.0	1.0000	1.8459	11.89	15.79	sand	99.957
0.5	0.7071	5.9874	38.56	54.35	silt	0.043
1.0	0.5000	5.7858	37.26	91.61	clay	0.000
1.5	0.3536	1.2875	8.29	99.90		
6.0	0.0156	0.0148	0.10	100.00		

JAKOLOF BAY 2 SEDIMENT

Phi Size	mm	PARTICLE SIZE DISTRIBUTION Adjusted Weight	Weight Percent	Cumulative Percent	OVERALL SIZE CLASS DISTRIBUTION Size Class	Weight Percent
0.5	0.7071	0.0219	0.30	0.30	gravel	0.000
1.0	0.5000	0.2029	2.80	3.10	sand	72.527
1.5	0.3536	0.5320	7.34	10.45	silt	22.954
2.0	0.2500	0.9544	13.17	23.62	clay	4.519
2.5	0.1768	1.2067	16.66	40.28		
3.0	0.1250	0.9653	13.32	53.60		
3.5	0.0884	0.7734	10.68	64.28		
4.0	0.0625	0.5978	8.25	72.53		
4.5	0.0442	0.2304	3.18	75.71		
6.0	0.0156	1.2144	16.76	92.47		
11.0	0.0005	0.5456	7.53	100.0		

226
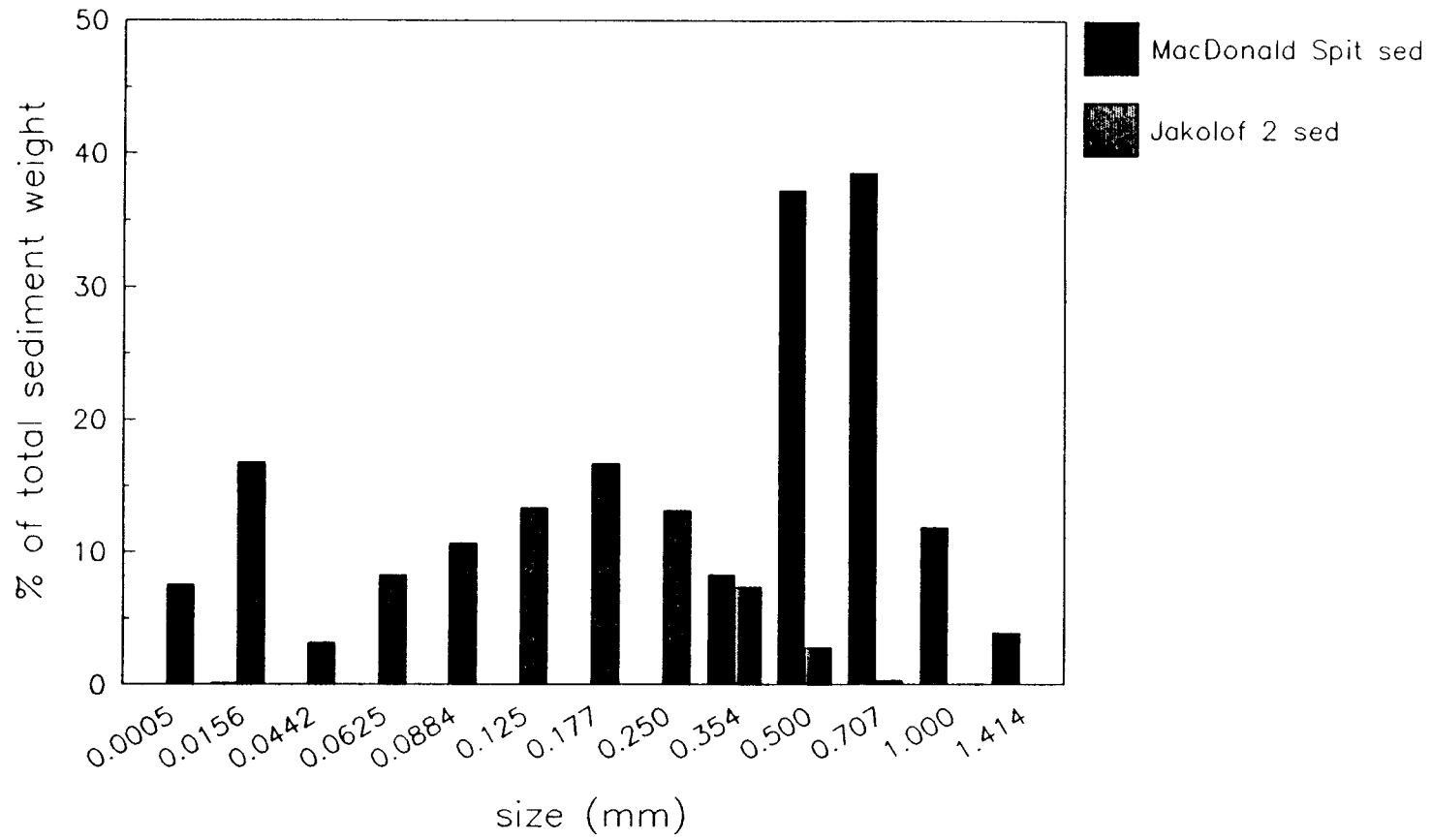
Figure 8-15.   Grain-Size Distributions for MacDonald Spit and Jakolof Bay 2 SPM

the frazil ice/air-sea interface after approximately 30-40 minutes. When such sediment-laden crystals were noted, however, the sand grains existed as entrapped species within the interstices of sintered frazil ice crystal flocs which were adhering to each other in the water column. That is, the sand grains did not appear to be _part_ of the ice crystal or a source of nucleation. From these observations it was not possible to determine if such icebound sediment grains were resuspended by "active" ice from the artificial beach face, or if the sand grains had first been washed off the beach face by wave turbulence and then possibly trapped by growing frazil during their fall to the bottom of the tank.

Approximately 1 hr after the initial formation of frazil ice, 1-2 cm of slush ice had accumulated underneath the beach slope surface and 2-3 cm had surfaced at the recirculating water supply headers at the aft (dead zone) end of the tank. Perhaps a dozen agglomerations of ice crystals containing sediment particles were observed in the water column, and several of these were noted to accumulate in the upper slush ice surface.

Because of the wave turbulence, there was not any accumulation of anchor or frazil ice on the submerged sediments contained on the artificial beach face, although there was a significant ice foot (Kaimoo) of sediment and ice which had accumulated at the upper end of the splash zone on the exposed beach face.

Approximately 3 hr after the initial frazil ice crystals were noted, a total of 3-6 cm of ice growth had occurred on the upper exposed surface of the beach face. Higher levels of slush ice had grown in the water column downslope from the beach face, resulting in observable wave and slush ice-mediated sediment migration on the artificial plain surface. As the slush ice accumulated on the water surface, wave turbulence throughout the tank was diminished, resulting in a significantly reduced concentration of suspended frazil ice in the water column. After 4 hours, the surface slush ice was 2 to 4 cm thick; however, as the slush ice field was worked by each passing wave, the grinding action of the individual 0.5 to 1 cm ice platelets on each other

228

was readily apparent, and the resulting action appeared to dislodge any sediment material which had previously been trapped.

Additional ice growth was allowed to occur under continued wave turbulence. After 24 hr the slush ice grew to a depth of 10 to 23 cm. Slush ice samples were then collected and melted for sediment determinations; however, they failed to show any accumulation of the sand-sized material.

8.3.3   Horizontal Table Experiments

8.3.3.1 Methods

The results from the sloping beach-face experiment suggested that very little, if any, sediment resuspension occurred and that the slush ice matrix itself may have been subject to self-cleaning. Therefore, the artificial beach-face surface was adjusted to position the horizontal plain to interact just with the bottom of the active slush ice field. This experiment was designed so that the slush ice matrix could interact with the sediment surface in the absence of the current set up by the waves passing up and down the beach slope in a transverse fashion. A total slush ice thickness of 18 cm was noted, and additional coarse-grained well-sorted sediment was added to the tray with a funnel, taking care not to incorporate any of the sediment into the overlying slush ice field. With continued wave agitation, the sediment in the horizontal tray was noted to form a series of berms on top of the tray itself, and some resuspension of very fine material could be seen moving back and forth between the berms with each passing wave. At the time of these adjustments, the underside of the ice surface was approximately 5 cm above the sediment, and no direct interaction occurred.

Additional ice growth was continued under wave turbulence, until the ice surface came into direct contact with the horizontal sediment surface; however, even then there was no significant accumulation of any sediment in the ice canopy. As a result, the experiment was terminated in the interest of attempting additional studies using much finer-grained sedimentary material. In addition, it was anticipated that the study should focus on the critical

moments of initial frazil ice formation, when the ice may be in a more active or "sticky" state and enhanced sediment accumulation might be expected. Therefore, in preparation for the next series of experiements, the cold room was allowed to warm, and all traces of older ice (less sticky) and coarse sedimentary material were cleaned from the tank.

The grain-size distribution data for the finer sedimentary material used in the subsequent experiments were presented in Table 8-2 (designated as "Jakolof 2"). As shown by the data in the table, a significant portion (72%) was still represented by sand; however, 27% was represented by mud (22.9% silt and 4.5% clay). A total of four wave-tank experiments were undertaken with this finer sedimentary material. In each experiment, the horizontal sediment layer was adjusted to just within the edge of the slush ice field being pumped by the wave train. The data from these finer-grained SPM experiments are presented in Table 8-3.

With the introduction of the finer sedimentary material, significant suspended particulate material loads could easily be maintained in the water column, as demonstrated by the SPM loads in the table; however, subsurface visibility was immediately reduced to zero. Therefore, all subsequent determinations of sediment entrainment by frazil and grease ice matrices and SPM loads in the water column had to be completed by gravimetric analyses.

Time-series samples of seawater and frazil ice were collected during the ice-formation events allowing simultaneous determinations of water and frazil ice SPM loads. To complete this activity, the paddle was temporarily turned off and 30 sec was allowed for frazil ice throughout the water column to reach the upper seawater surface before a water sample was siphoned from a depth of 45 cm. Sixty seconds after the paddle was turned off, the surface ice was collected with a 1-mm stainless-steel sieve, and after draining, the ice was transferred to a beaker where it was allowed to thaw.

SPM measurements were determined gravimetrically, as described in Section 4.2.7 and by Payne et al. (1987b). Briefly, a measured volume of a given sample was vacuum filtered (< 10 cm Hg) through a preweighed, 47-mm

Table 8-3

Results of Gravimetric Analyses of SPM Loads in Surface Slush Ice and the Water Column During Wave Tank Experiments

Date	Time (hr)	Elapsed Time (min)	SPM Type	SPM LOAD IN: Water (mg/L)	Ice (mg/L)	Comments
16-Feb-86	1520	0	Jakolof 2	636	(no ice)	
	1645	85		463	307	First slush ice at 1630 hrs
	1715	115		399	220	
	1800	160		368	238	
	2030	310		276	140	
18-Feb-86	1357	0	Jakolof 2	217	300	Sampled right at beginning of frazil ice formation
	1420	23		NA	157	
	1940	343		NA	59	Submerged ice from water column
	1940	343		NA	51	Surface slush ice from leading edge of ice wedge
19-Feb-86	1506	0	Jakolof 2	526	421	First slush ice scrapped off water surface
	1527	21		NA	370	Middle of slush ice field (W-6)
	1527	21		NA	240	At leading edge of slush ice field (W-5)
	1855	229		NA	166	Middle of slush ice field (W-6)
	1855	229		NA	40	At leading edge of slush ice field (W-2)
23-Feb-86	1230	0	Jakolof 2	464		
	1404	94		414	151	First accumulation of slush ice at water surface
	1640	250		278	104	Slush ice 8 cm thick at W-6
	1640	250		278	169	At leading edge of slush ice field at W-5
	2203	573		NA	47	
	2315	645		137	77	
	2315	645		137	104	Surface slush ice first mixed down into SPM-rich water column, then ice allowed to resurface

NA = not available

diameter polyester or polycarbonate membrane filter (0.4 μm pore size; Nuclepore). If subsequent methanol and methylene chloride extractions of the SPM on the filters were intended for FID-GC hydrocarbon analyses, the polyester membranes were used. Otherwise, the polycarbonate filters were used. The filter then received a final vacuum rinse with freshwater to remove residual sea salts, and all seawater and freshwater filtrates were discarded. For samples requiring hydrocarbon analyses, sequential vacuum filtrations through the filter were then performed with 1) 10 mL methanol and 2) 30 mL methylene chloride. The latter solvent filtrates were then concentrated by

Kuderna-Danish solvent reduction and analyzed by flame ionization detector-gas chromatography (FID-GC) as described in Section 4.2.7.

For a total SPM load determination, the freshwater and solvent-rinsed membrane filter was placed in a desiccator until constant filter-weight measurements were obtained. The difference between the initial tare weight for the filter and its final weight, containing solvent-rinsed SPM, was used to determine the total SPM load in the sample. Because the polyester filters were highly efficient in retaining "free" oil droplets as well as SPM, the final sample filtration rinses with methanol and methylene chloride were necessary to obtain SPM weight estimates independent of accompanying oil quantities present as either "free" oil droplets or oil/SPM agglomerates in the experiments in which oiled SPM was used.

8.3.3.2 Results

As shown by the data in Table 8-3, it was possible to generate slush ice samples containing elevated levels of suspended particulate material with this finer sediment source; however, it should also be noted that, in general, the concentrations of SPM in the ice were less than the background SPM loads in the water column. Furthermore, the data in the table demonstrate that there was a significant reduction of the sediment load in the slush ice with time due to the turbulence regime introduced by the passing wave trains. In addition to the gravimetric determination showing the self-cleaning nature of the surface ice, this could also be observed through the windows located in the sides of the tank. With increased elapsed time in each experiment, the upper surface of accumulating slush ice usually appeared to get whiter or cleaner.

There was one exception to the higher ratio of SPM in the water column compared to the SPM load in the slush ice. In this experiment (18 February 1986) the SPM load in the frazil ice was 300 mg/L compared to a background SPM load in the water column of 217 mg/L. That frazil ice sample was collected immediately at the initiation of the frazil ice-formation event when the frazil ice was believed to be in an active or sticky state. At the time these samples were collected, the water temperature was -1.9°C, and it may have just gone

through a minimal period of supercooling. However, even with continued time, a significant cleansing of the sediment load in the slush ice field was noted with subsequent values of 157 mg/L at 23 min, and 59 mg/L, and 51 mg/L at 343 min after the ice-formation event.

Thus, in as little as 23 minutes after the initial ice collection, the frazil ice showed a 50% reduction in SPM load. Of the two samples collected at 343 min, one was from the submerged frazil ice platelets immediately adjacent to the paddle (and believed to be freshly formed and possibly still "sticky"), and the other was from the surface slush ice at the leading edge of the ice wedge, which had been subjected to additional agitation in the wave field. The SPM concentrations in both samples were so close that it was not possible to distinguish any difference in sediment load. Nevertheless, this wave-tank experiment did show that high sediment loads (50% greater than the surrounding seawater) were observed in the slush ice immediately after the initial ice-formation event. Thus, there was some evidence for scavenging or stickiness in the frazil that was first formed in the wave-tank experiment; however, it was very short-lived and was not observed in the other experiments, when sampling was somewhat later and the surface slush ice was well worked by the wave train.

As evident from the data in Table 8-3, seawater samples were not always collected in parallel with frazil ice-sampling events, so there are only limited data to illustrate whether a decline in overall SPM load in the water column was also occurring over the time frame of these experiments. It is believed that this was the case, as shown by the data for the 16 and 23 February experiments in which both water column and ice canopy SPM determinations were completed. However, without data from all four experiments it is not possible to be certain of these results. The reduction in suspended particulate material loads in the water column is believed to have been caused by the decrease in turbulence due to the reduction in wave amplitude with time. The wave amplitude was significantly attenuated and eventually eliminated by the viscous nature of the growing slush ice field as the experiments progressed. Naturally, as the turbulence in the water column subsided, there

233

was no longer a driving force to maintain the higher SPM loads observed at the beginning of each experiment.

Because of the large volume of the wave tank, it took several days to clean it of all traces of ice and sediment between experiments. Therefore, it was impossible to complete and initiate experiments in a time-efficient manner. Furthermore, it was not possible to introduce sufficient turbulence to achieve adequate supercooling of the entire water volume without the "premature" formation of frazil ice. Therefore, additional experiments to examine the active form of frazil were conducted in the racetrack flume, rather than in the wave tank. With the flume, higher current speeds were possible, and the smaller water volume allowed more control of the supercooling phenomena. In addition, the smaller size of the system allowed a more rapid turnaround of experiments.

8.3.4 Racetrack Flume Experiments on Sediment Resuspension and Scavenging by Active Frazil Ice

8.3.4.1 Introduction

With the somewhat ambiguous results from of the wave tank experiments (designed to examine the scouring and entrainment of sediment by an undulating slush ice field interacting with a sediment bed), racetrack flume experiments were undertaken instead. These were designed to observe the interactions of frazil and anchor ice with fine-grained sediment, both in suspension and as bed material in fresh and saltwater systems. In addition to salinity, current speed and sediment type were varied to document their effects on sediment/ice interactions.

8.3.4.2 Methods

A total of six complete racetrack flume experiments were performed at Kasitsna Bay. For an experiment, the flume (see Section 8.2.2) was placed inside the walk-in cold room, and the inside air temperature was lowered to between -19 and -25°C. Air temperature was measured to +/-0.025°C with the digital thermistor array several times during each flume experiment. Water

temperature was measured with a thermistor accurate to 0.004°C. This thermistor was inserted to a water depth of 9 cm at a turn in the flume (Figure 8-10). Care was taken during the period of frazil formation to assure that no frazil stuck to the thermistor, which would have resulted in anomalously high temperature readings. To avoid this problem, the thermistor probe was mechanically cleaned during periods of frazil formation, or the probe was coated with silicone grease to retard the frazil adhesion. For these experiments, local seawater (salinity of 31-32 ppt) was used; and spot measurements of water temperature were recorded manually, so it was not possible to develop complete time-temperature curves. However, enough data points were collected to determine T_m and T_e and to determine the period of maximum frazil production and associated rise in temperature.

It is normally important to seed supercooled water to initiate the growth of frazil, and in carefully controlled laboratory experiments, it is relatively simple to get supercooling of at least 2°C (e.g., Hanley and Tsang, 1984). In these experiments, however, artificial seeding was not necessary. There were apparently enough ice crystals in the air that fell into the water to initiate frazil growth, and the degree of maximum supercooling was close to that seen in natural settings.

At all current speeds used in the flume, the sand moved as both bed load and suspended load. Well-developed ripples up to 7 cm high formed in the straight segments of the flume when current speeds were below 60 cm/s. At current speeds above 60 cm/s, these ripples were destroyed, and the sand assumed a flat-bed configuration. Because flow in the flume was not uniform, several dead spots or depositional areas formed, especially along the inside turns of the flume and the back straight segment just upstream of the propeller. In a similar fashion, along the outside of the turns and directly downstream from the propeller were areas of scouring. However, the area along the window generally maintained a cover of at least 2 cm of sediment throughout any given experiment, and it contained no regions of consistent scour or deposition. Flow conditions in the area of the window appeared uniform across the entire width of the channel; migrating bedforms usually reached from one wall of the channel to the other.

When possible, samples of frazil and anchor ice were collected to determine sediment concentrations. Ice samples were collected with a small strainer, and as much water as possible was shaken out of the ice before it was transferred to a beaker for melting. After the ice had melted, the sample was processed in the same way as the suspended-sediment samples (see Section 8.3.3.1).

In two experiments, sediment was contaminated with moderate levels of fresh (unweathered) Prudhoe Bay crude oil (obtained from oil/SPM stirred-chamber experiments (Payne et al., 1987b)). Thus, the oiled SPM used in the experiments was representative of the type material that would be encountered after an oil spill event in SPM-rich waters. In general, the experiments focused on interactions of frazil and sediment in the water column. Two types of water samples were collected: the first was water siphoned from mid-water depth, and the second was interstitial water that drained from the floating frazil-slush samples.

8.3.4.3 Results and Discussion -- Interaction of Frazil with Suspended Sediment

In the experiments presented in Table 8-4, the water column samples and frazil ice samples were taken during the temperature rise from T_m to T_e and then at half-hour and 2-hr intervals after collection of the original samples. The data in Table 8-4 and Figure 8-16 illustrate that the SPM concentrations in frazil/slush ice were significantly higher than in the water column immediately after the supercooling event. As in the wave-tank experiments, however, the frazil ice SPM concentrations subsequently decreased until, after 2 hr, they were lower than in the corresponding water-column samples. As shown by the data in the table, previous contamination of a sediment with oil did not have any significant effect on its behavior with the frazil ice compared to uncontaminated sediment.

From these data it appears that the question as to whether frazil ice is sticky in saltwater remains controversial. Specifically, while laboratory

236

Table 8-4

Results of Gravimetric Analyses of SPM Loads of Slush Ice and Water Column Samples Collected During the Racetrack Flume Experiments

Date	Time (hr)	Elapsed Time (min)	SPM Type	SPM LOAD IN: Water (mg/L)	Frazil Ice (mg/L)	Comments
17-Feb-87	1000	0	Unoiled	1,370	2,240	Current speed = 70 cm/sec; sampled immediately
17-Feb-87	1015	15	Jakolof 2	1,530		after supercooling
17-Feb-87	1346	0	Unoiled Jakolof 2	711	3,260	Current speed = 70 cm/sec; sampled immediately after supercooling
20-Feb-86	1947	0	Unoiled	54	74	Current speed = 70 cm/sec; sampled within 2
20-Feb-86	2017	30	Jakolof 2	64	43	minutes of maximum supercooling
20-Feb-86	2220	153		48	27	
26-Feb-86	1925	0	Unoiled	89	714	Current speed = 70 cm/sec; sampled immediately
26-Feb-86	1955	30	Jakolof 2	91	75	after supercooling
26-Feb-86	2127	122		54	38	
23-Feb-86	1350	0	Oiled	110	495	Current speed = 70 cm/sec; sampled immediately
23-Feb-86	1420	30	Jakolof 2	103	390	after supercooling
23-Feb-86	1550	120		86	77	
23-Feb-86	1801	0	Oiled	69	200	Current speed = 70 cm/sec; sampled immediately
23-Feb-86	1831	30	Jakolof 2	88	76	after supercooling
23-Feb-86	2001	120		80	50	

experiments conducted by Hanley and Tsang (1984) seem to show the nonsticky nature of saltwater frazil ice, the cold room studies above clearly suggest the formation of sticky frazil ice during the period when the water temperature rises from T_m to T_e. Also, the makeup of anchor ice observed in the Beaufort Sea clearly indicates a frazil origin (Reimnitz et al., in press) and, therefore, this too contradicts the former postulate.

In evaluating these and other laboratory study results, it is important to question the validity of laboratory experiments in which ice growth in a limited amount of water results in a change of water salinity and in which the supercooled stage is limited to a few minutes rather than a period of hours or days, as in nature. Even in natural settings, frazil that has risen to the surface is no longer sticky (Kempema et al., in prep.) and readily drops its

237
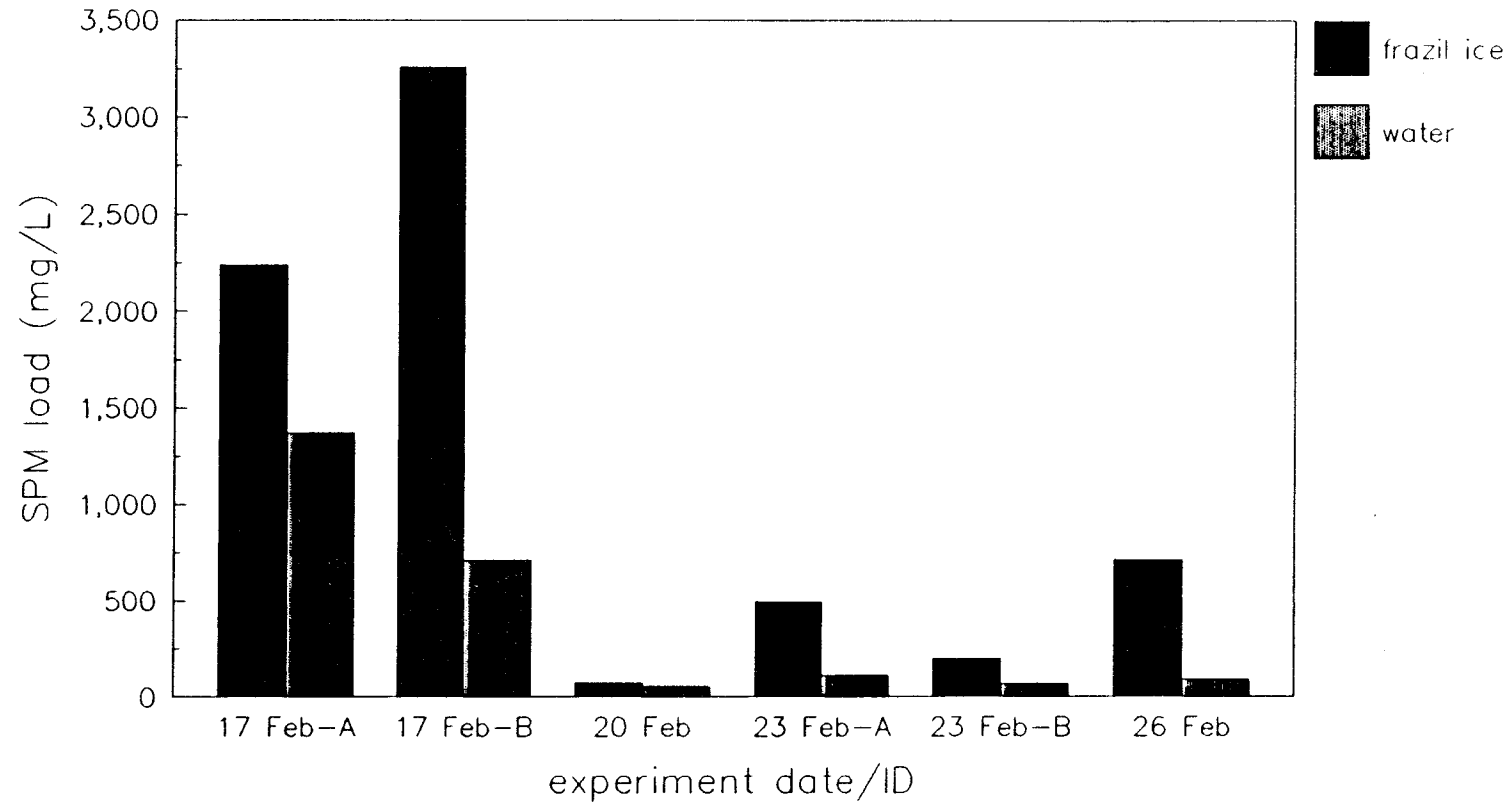
Figure 8-16.   SPM Loads in Frazil/Slush Ice Versus Water Column Samples Collected During the Racetrack Flume Experiments

sediment load when agitated. Therefore, the timing and method of sampling frazil in laboratory experiments may be critical because the frazil may be sticky for only a short period, while the water is near its maximum supercooling.

In the experiments described above, collection of water and frazil ice samples was tightly controlled to catch the critical phase when saltwater frazil may be sticky, which is the period when the temperature rises from T_m to T_e. Samples collected during this period were designated as time-zero samples, and subsequent samples at 0.5 and 2 hr thereafter show a decrease in the SPM load. This set of experiments strongly suggests that frazil crystals adhere to suspended particulates when there is significant supercooling, but that they lose adhesion when the temperature reaches T_e. In natural settings, significant supercooling will last for at least several hours, as opposed to a few minutes in a flume (Tsang, 1982). Therefore, saltwater frazil, in these settings, may be sticky for much longer than the few minutes observed in these experiments.

The data in Table 8-4 tend to support the idea that suspended sediment is scavenged by frazil because the sediment concentrations measured in frazil were higher than those in the water. However, some of the sediments seen in the frazil in the racetrack flume clearly were incorporated into flocs as they bounced and rolled along the bottom. The same process of flocs rolling along the bottom and picking up sediment has been described in rivers by Arden and Wigle (1972) and Osterkamp and Gosink (1983). Thus, there is still some question whether scavenging occurs by the sticky action of the frazil or whether it occurs by trapping of sediment particles at the interstices between ice crystals in flocs. Additional experiments, presented in Section 8.5, utilized inversion and vertical-column experimental systems to shed additional light on whether sediment inclusions in frazil occur within an individual ice crystal or just at the interstices between ice crystals. It is most likely that a combination of both mechanisms are important; however, if sediment is trapped at the interstices between frazil crystals, it is also possible that "stickiness" plays no part in sediment transport by ice.

Nevertheless, these studies (unlike the wave-tank experiments) illustrated that high loads of SPM materials could be entrained by growing frazil crystals when supercooling of the water could be controlled to simulate the behavior observed in nature. Presumably, the smaller water volume in the racetrack flume allowed better control of heat transfer and turbulence processes, compared to the ~2700 L contained in the wave tank where heat transfer was not sufficient to allow supercooling of the water for a longer sustained period of time. That is, as the seawater in the wave tank became supercooled (or approached supercooling) nucleation and initial formation of frazil ice was observed (possibly due to ice crystals in the air or insufficient turbulence in the tank itself), and extensive supercooling of the larger water volume in the wave tank could not be achieved.

8.3.4.4   Conclusions from Racetrack Flume Studies

The flume studies conducted at Kasitsna Bay demonstrated that saltwater frazil entrains high sediment loads during the period when the water temperature rises between T_m to T_e. This high sediment load is released back to the water column after T_e is reached. Thus, in the flume, saltwater frazil appears to be sticky for a few minutes when it is enveloped in supercooled water. In natural settings, supercooling can be maintained for at least several hours; thus, saltwater frazil may be sticky for at least that long.

Experiments conducted at Kasitsna Bay and at U.S. Geological Survey in Palo Alto (Kempema, 1986) showed that frazil forms readily in turbulent fresh- and saltwater. From those experiments frazil crystals were shown to have the same morphology in fresh- and saltwater, usually forming thin discs up to 5 mm in diameter. However, the morphology of frazil flocs and the way frazil interacts with sediment varies with salinity. Freshwater frazil flocs are somewhat larger and more cohesive than saltwater flocs.

Analysis of flume data suggests that the suspended sediment load in the water column decreases during periods of frazil formation. However, the scatter in the data makes this conclusion somewhat tentative, and more

measurements of suspended-sediment concentrations before and during frazil formation should be gathered in the future from natural settings.

The presence of petroleum contaminants does not appear to affect the incorporation of sediment into a saltwater frazil ice cover. Thus, oil-contaminated sediment may be incorporated into the ice cover during fall storms, and this may be a potential source of pollution dispersal.

The small amounts of sediment, water, and ice in flume studies, along with the short period of supercooling, require precise measurements. Ice growth in the flume can rapidly change water salinity, and these salinity changes are difficult to monitor and control. Thus, studies made in flumes, particularly when forming ice in saltwater, may be hard to extrapolate to larger, natural systems. Many remaining questions about frazil and anchor ice interactions with sediment will be difficult to resolve with flume studies, and future studies may have to concentrate on natural systems.

8.4   SELF-CLEANING OF SLUSH ICE

8.4.1   Introduction

With the racetrack flume experiments discussed in Section 8.3.4, it appears that sticky or active frazil ice can be generated initially during the supercooled period when frazil ice first forms. However, as demonstrated by the wave-tank experiments and the racetrack flume studies, the sediment load in the upper ice canopy did decrease with continued turbulence. This was demonstrated by the data in Tables 8-3 and 8-4 and was discussed in Sections 8.˜3 and 8.3.4, respectively.

This self-cleaning mechanism helps to explain the observed upper 1-10 cm of clean ice often seen in ice cores collected in the field. That is, if dirty slush ice is formed due to entrainment of suspended particulate material during initial ice formation, continued wave pumping with time can cause the upper surface to undergo significant self-cleaning. As the turbulence subsides and additional columnar ice formation beneath the upper slush ice

field occurs, a discontinuity of the sediment load would be noted with clean ice observed in the upper 1-10 cm of the frozen slush ice matrix, a dirtier cross-section of sediment-laden ice observed just above the columnar ice zone, and relatively clean columnar ice observed below the transition from slush (or congulation) ice to columnar ice.

8.4.2 Sprinkle Experiments to Look at the Rapid Loss of Suspended Particulate Material Through Slush Ice Undergoing Standing Wave Turbulence

Before examining the self-cleaning phenomena with coarse-grained sediment, a tube was inserted into the slush ice to measure the amount of freeboard or "dry" ice on top of the slush ice surface. Measurements indicated that there was approximately 0.5-1 cm of ice accumulation above the water surface. This suggested that sediments sprinkled on this material would be less apt to work their way into the interstitial water of the slush ice matrix and, thereby, be released to the bottom. To test this assumption, approximately 10 g of the coarse sand utilized for the sloping beach-face experiments were gently sprinkled onto the upper ice surface at an antinode in the standing wave patterns, and time-series photographs were taken over a 10-min interval. During this period, all of the sedimentary material rapidly penetrated through the slush ice field and returned to the bottom.

From these observations, it was concluded that any sediment actively scoured or entrained during the initial frazil ice formation event would have been quickly knocked free from the ice matrix or interstices as the ice accumulated in the active surface slush ice field being pumped by the passing wave train.

A modification of the sprinkle ice experiment was then repeated, except in this experiment coarse McDonald Spit sand was mixed into the slush ice layer within the wave tank to three different depths: on the surface, 5 cm deep, and 10 cm deep. Paddle turbulence was initiated, and settling was followed by time-lapse photography. As with the first sprinkle experiment, this test was again conducted at an antinode, and within 15 sec after starting

wave agitation in the slush, sand particles settled out of the bottom of the layer where the sand had been placed at the 10-cm depth. After 1 hr that depth was completely clean. The sand introduced at the 5-cm and 1-cm depths took longer to initiate downward advancement of the sediment grains; but even here, after 1 hr of wave agitation, all sediment was well on its way out of the slush layer. The experiment was then repeated with the sand placed at the upper surface at a node in the standing wave pattern with essentially no vertical wave motion. In this instance, the ice was much more densely packed than at the antinode, and after 2 hrs, essentially no sediment movement through the ice had occurred (Figures 8-17, 8-18, and 8-19). While these results were interesting and provided direct evidence of the importance of wave motion in the self-cleaning phenomena, some caution should be observed before placing too much emphasis on the antinode-versus-node observations. Specifically, the standing-wave pattern was an artifact of the wave-tank system, and it would not be expected to occur in nature, except possibly under very special circumstances such as the juxtaposition of longer ice floes and unique wind/wave patterns, etc.

8.4.3   Sausage-Tube Experiment -- Grain-Size Dependence

The wave-tank and racetrack flume chamber results discussed in Sections 8.3.3 and 8.3.4, coupled with the sprinkle experiments discussed above, made it apparent that a significant accumulation of sediment in an ice canopy could not be maintained if wave turbulence was continued for a significant period after the initial frazil ice formation event. Therefore, in an effort to determine if the self-cleaning mechanism due to passing wave trains through slush ice would preferentially remove or sort the SPM by grain size, a series of experiments were performed to evaluate the preferential retention of different size class sediments in a slush ice field subjected to turbulence introduced by 15-20 cm amplitude standing waves.

A sample of the Jakolof 2 sedimentary material used in the previous experiments was dispersed into an upper slush ice slurry contained in a 1-in diameter plastic sausage tube. The tube was first filled with slush ice at the same density as the surrounding slush ice in the open wave-tank system. The
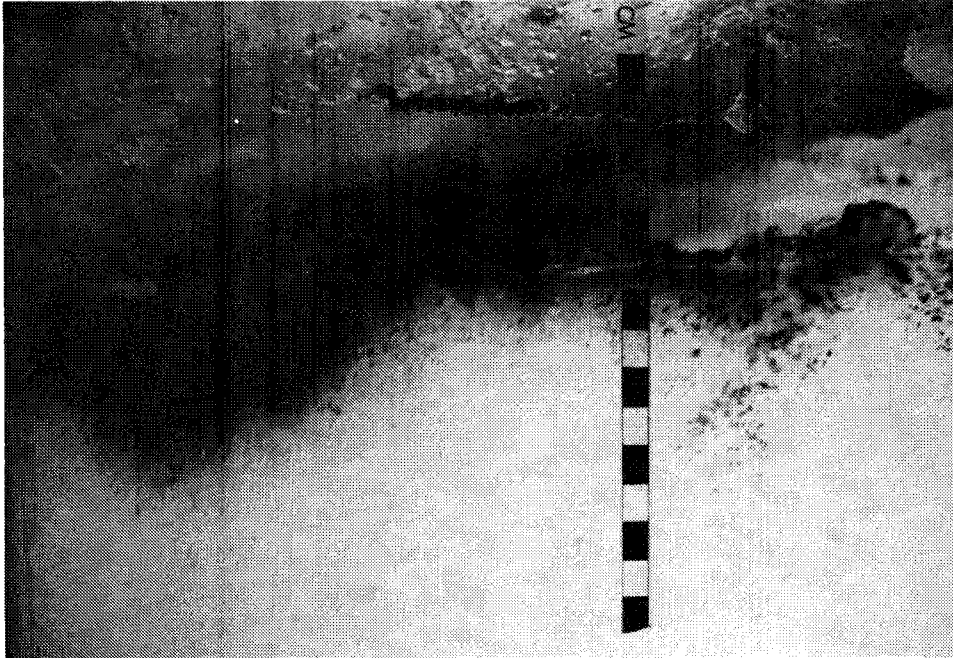
Figure 8-17. Time-Series Migration of Sedimentary Material Introduced at the Surface of Slush Ice at a Node in the Standing Wave Pattern of the Wave Tank Taken at Time Zero
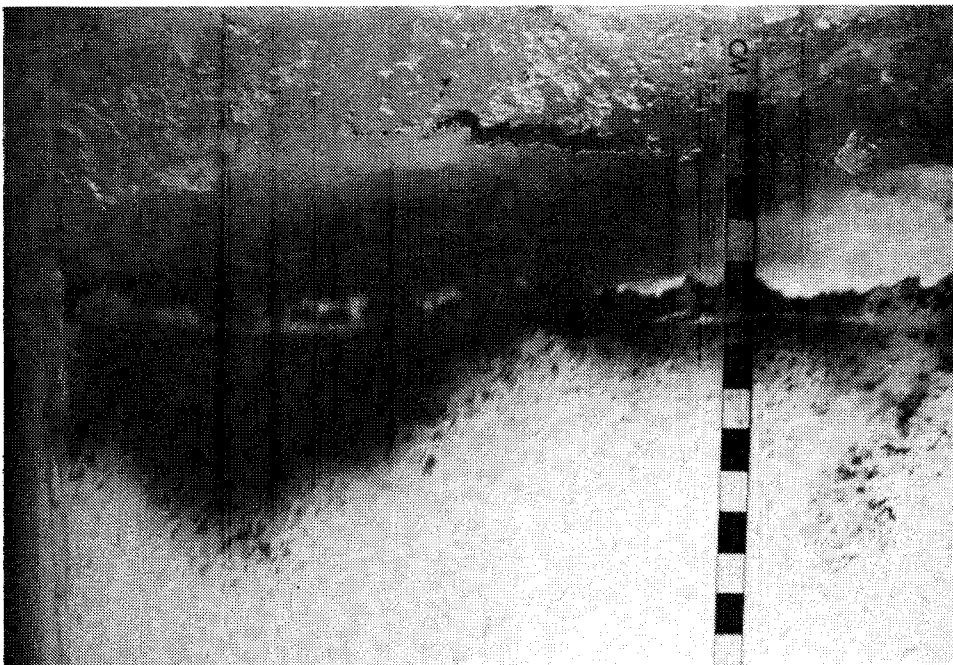
Figure 8-18. The sediment introduced in Figure 8-17 Above After an Elapsed Time of 6 Min at the Node

244

Figure 8-19.   The Sediment Introduced in Figure 8-17 Above After a Total Elapse Time of 2 Hr at the Node

sediment ice slurry was mixed in advance and carefully added to the top of the clean slush ice layer within the tube. The bag was then suspended at the position of an antinode in the wave tank with the wave generator off and sealed. Upon starting the wave generator, the sediment from the upper part of the slush layer immediately began to settle in the bag. After a few minutes the first grains were raining down into the water column within the sausage tube below. After 10 min of agitation in the wave field, the experiment was stopped, and two samples were collected, one from the bottom of the tube and one from the slush ice layer. The sediment grain-size data from these samples are presented in Table 8-5 and Figure 8-20. Clearly, there was preferential retention of the finer grain materials by the ice: the sample retained in the ice consisted of 11% mud (9% silt and 2% clay) and 88% sand; whereas, the material collected from the bottom of the sausage tube was 98.6% sand with only 1.4% mud (0.2% silt, 0.3 clay) passing through the slush ice field and accumulating in the water.

8.4.4 Racetrack Flume -- Self-Cleaning With Time

Examination of the data in Table 8-4 for 26 February 1986, shows that despite the elevated levels of SPM in the frazil ice immediately after supercooling and initial ice formation (714 mg/L), self-cleaning soon followed due to continued agitation or the termination of stickiness as the temperature changed from T_m to T_e (714 mg/L versus 75 mg/L half-an-hour later). Interestingly, the water-column concentrations remained constant over this time frame (89 mg/L versus 91 mg/L), suggesting that the decrease in SPM load in the slush ice was due to a change in its adhesive properties, rather than a simple change in turbulence (which would also affect the SPM load in the water column or interstitial water trapped with the slush ice). That is, the water-column concentrations remained constant throughout this time period, and thus, the drop in the slush ice levels (which were even below the water column concentration at that time) was not due to simple sedimentation from the declining overall turbulence. Thus, the data suggest a change in adhesion or stickiness over time in addition to the simple act of physically knocking the SPM out of the ice layer.

Table 8-5

Results of Gravimetric Analyses of SPM Loads in Surface Slush, Feed Water, and Drain Water Samples Collected During the Vertical Filtration Experiments

SEDIMENT SIZE DISTRIBUTION RETAINED IN ICE

Phi Size	mm	PARTICLE SIZE DISTRIBUTION Adjusted Weight	Weight Percent	Cumulative Percent	OVERALL SIZE CLASS DISTRIBUTION Size Class	Weight Percent
0.5	0.7071	0.0080	0.54	0.54	gravel	0.000
1.0	0.0500	0.0214	1.43	1.96	sand	88.846
1.5	0.3536	0.2016	13.48	15.45	silt	9.147
2.0	0.2500	0.4098	27.41	42.86	clay	2.007
2.5	0.1768	0.4031	26.97	69.83		
3.0	0.1250	0.1976	13.22	83.04		
3.5	0.0884	0.0748	5.00	88.04		
4.0	0.0625	0.0120	0.80	88.85		
4.5	0.0442	0.0667	4.47	93.31		
6.0	0.0156	0.0500	3.34	96.66		
11.0	0.0005	0.0500	3.34	100.00		

SEDIMENT SIZE DISTRIBUTION NOT RETAINED IN ICE

Phi Size	mm	PARTICLE SIZE DISTRIBUTION Adjusted Weight	Weight Percent	Cumulative Percent	OVERALL SIZE CLASS DISTRIBUTION Size Class	Weight Percent
0.5	0.7071	0.0187	0.19	0.19	gravel	0.000
1.0	0.5000	0.1680	1.73	1.92	sand	98.561
1.5	0.3536	2.0819	21.40	23.32	silt	1.163
2.0	0.2500	4.1358	42.52	65.84	clay	0.276
2.5	0.1768	2.2873	23.51	89.35		
3.0	0.1250	0.5788	5.95	95.30		
3.5	0.0884	0.2801	2.88	98.18		
4.0	0.0625	0.0373	0.38	98.56		
6.0	0.0156	0.0952	0.98	99.54		
11.0	0.0005	0.0448	0.46	100.0		
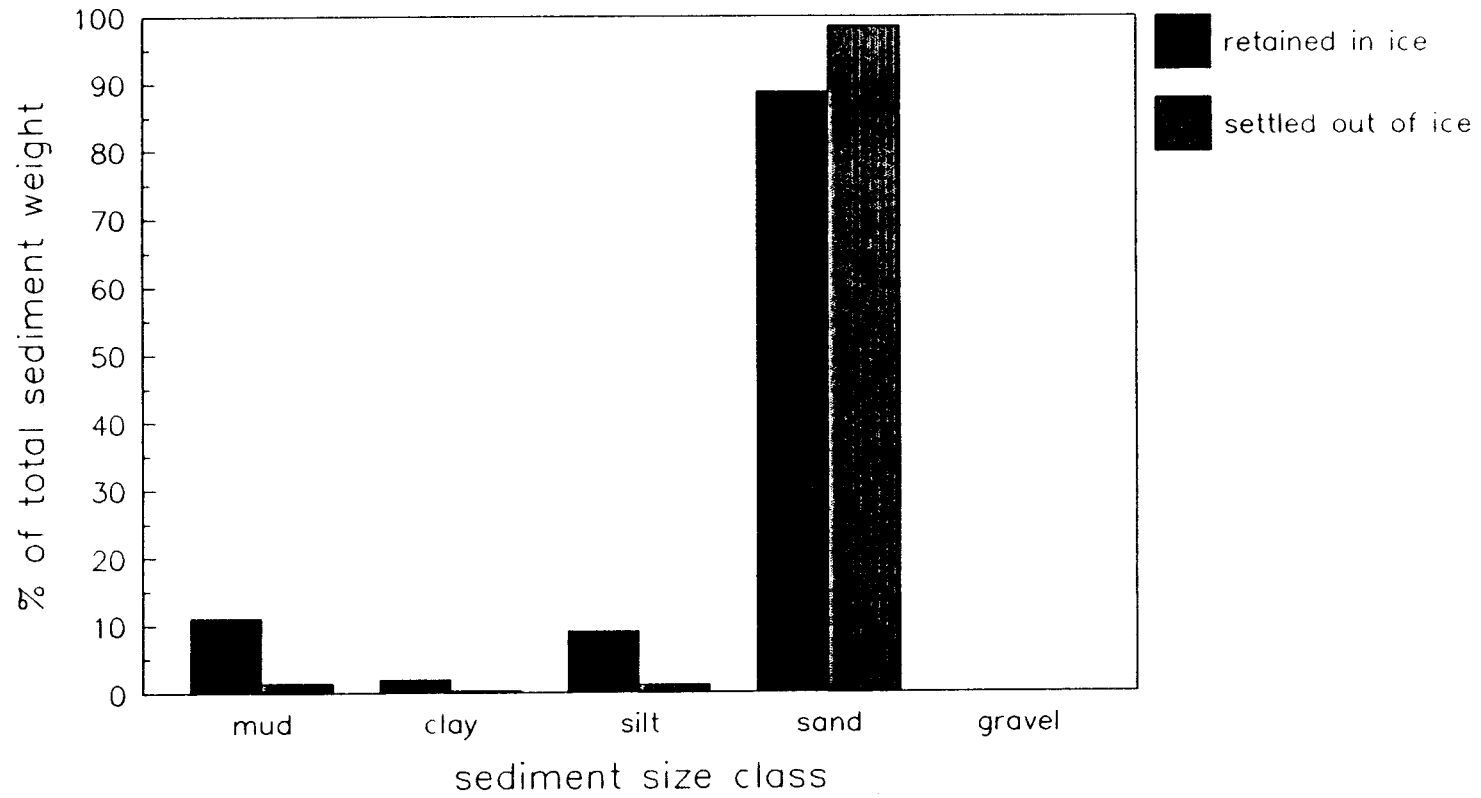
Figure 8-20. **Grain-Size Distributions of SPM Retained and Released by Slush Ice Contained in a Sausage Tube Placed in a Working Wave Train in the Wave Tank**

8.4.5   Additional Mechanisms for Self-Cleaning of Sediments in Sea Ice
         Canopies -- Movement of Fine-grained Sediment Particles in
         Seawater and Freshwater Slush Ice Slurries During Freeze-Front
         Advances

8.4.5.1 Introduction

In an effort to determine if there were other mechanisms of self-cleaning
of sediment-laden sea ice, experiments were performed to evaluate the effects
of advancing freeze-fronts on migrations of fine-grained sedimentary material
in seawater and freshwater slush ice slurries.

In previous sections of the report, various mechanisms have been dis-
cussed to explain the initial entrainment of sediments into slush ice canopies.
Following initial concentration of the frazil crystals into a slush ice layer
near the water surface, a downward freezing process in the ice can ensue to
form congelation ice, and this too can impart a significant change in the ice
structure and the retention of SPM and other impurities. Specifically, during
the downward freezing process, distinct changes will occur in the composition
of the ice relative to the initial ice slurry that tend to "purge" the ice of
constituents other than H_2O (Weeks and Ackley, 1982). For example, relatively
dense brine solutions are generated in the vicinity of the advancing freeze-
front due to salt rejection at ice water interfaces (Lake and Lewis, 1970).
Under the influence of both the advancing freeze-front (which progresses
downward from the air-ice interface) and gravity, these brine solutions flow
downward through the uncongealed slush ice matrix and into the underlying water
column (Lewis and Weeks, 1970). The rejection of brine during the freezing
process combined with the gravity-induced downward movement of the brine
through uncongealed slush ice have been hypothesized to produce a net movement
and accompanying concentration of sediment particles ahead of the advancing
freeze-front (Osterkamp and Gosink, 1984).

This mechanism can explain observed concentration profiles involving
low and high sediment loads in the surface and intermediate depth layers of sea
ice cores. The process can also lead to ultimate releases of fine-grained sed-
imentary material into underlying water columns. For example, high

249

concentrations of fine-suspended matter in quiescent water beneath a canopy of freezing slush ice have been noted during diving observations (Reimnitz and Dunton, 1979). If the freeze-front should advance beyond the sediment-laden intermediate layer in the slush ice, clear ice could form from below from relatively sediment-free water and produce a bottom layer of columnar ice with little or no sediment content. The net result of the preceding processes could produce the vertical concentration profiles of sediment noted in sea ice cores (see Section 8.1).

To investigate portions of the preceding mechanisms, several experiments were performed to evaluate aspects of movements of fine-grained sediment particles induced by advancing freeze-fronts in aqueous slush ice matrices. In one experiment, the horizontal migration of sediment particles induced by a laterally advancing freeze front was photographically documented. In a second experiment, release of fine-grained sediment from a seawater slush ice slurry undergoing freezing in a downward direction was monitored.

8.4.5.2 Methods and Materials

Lateral Freezing Experiment

A concentration of 1.79 gm dry wt/L of clay-sized particles was suspended in freshwater in a cylindrical container. The water in the container was initially near its freezing point. The container was then maintained in a refrigerated room at -8°C, with freezing of the aqueous suspension occurring inward from the container walls. The rate of advance of the freeze-front toward the center of the container was greater than the rate at which the particles settled out of suspension. At the conclusion of the experiment, horizontal thin sections were prepared from the solid ice "plug" removed from the container. The pattern of clay particles in the thin sections was documented photographically to evaluate the effect of the freeze-front advance on the particle distributions.

Sediment "Expulsion" Experiment

The sediment "expulsion" experiment was performed using a seawater slush ice slurry contained in a modified sediment trap placed in the walk-in cold room at Kasitsna Bay. The temperature in the room was maintained between -15°C and -20°C, and prechilled natural seawater and slush ice were obtained from the flowthrough wave tank under the influences of the cold ambient room temperature and the action of the wave-generating paddle. Natural sediment for the experiment was collected from the intertidal region of Jakolof Bay. Particle sizes larger than coarse sand were eliminated from the natural sediment by sieving through a 1-mm geological sieve before the experiment.

The modified sediment trap (shown schematically in Figure 8-21) served as the container for the prepared slush ice-sediment matrix in the experiment. The steep conical shape ensured that particles settling in the apparatus would pass efficiently to the bottom of the container for sample withdrawal. With the exception of the clear tubing at the bottom, the container was constructed of opaque fiberglass. To minimize mechanical movements that might induce unintentional releases of sediment from the slush ice, the container was secured in a protected corner of the cold room. To provide relevance to freezing processes in natural Arctic marine environments, the freeze-front in the container was allowed to advance only in a downward direction from the air-ice interface. An insulation blanket containing heat tape was wrapped around the container to ensure that freezing would not occur inward from the walls. Preliminary experimental runs were performed to adjust the thickness of the insulating heat tape/blanket wrap until neither freezing nor melting of slush ice occurred at the walls.

For the experiment, sediment was homogeneously mixed into 10 L of slush ice in seawater. Because the slush ice was produced in the wave tank in the cold room, the slurry was at or near its freezing point. Most, if not all, of the sediment particles in the initial sediment-ice slurry were in the interstitial water of the slurry matrix and, therefore, were capable of moving within the matrix. The concentration of sediment in the slurry was 1140 + 190 mg dry wt/L (mean + standard deviation; n - 3). Following transfer of the
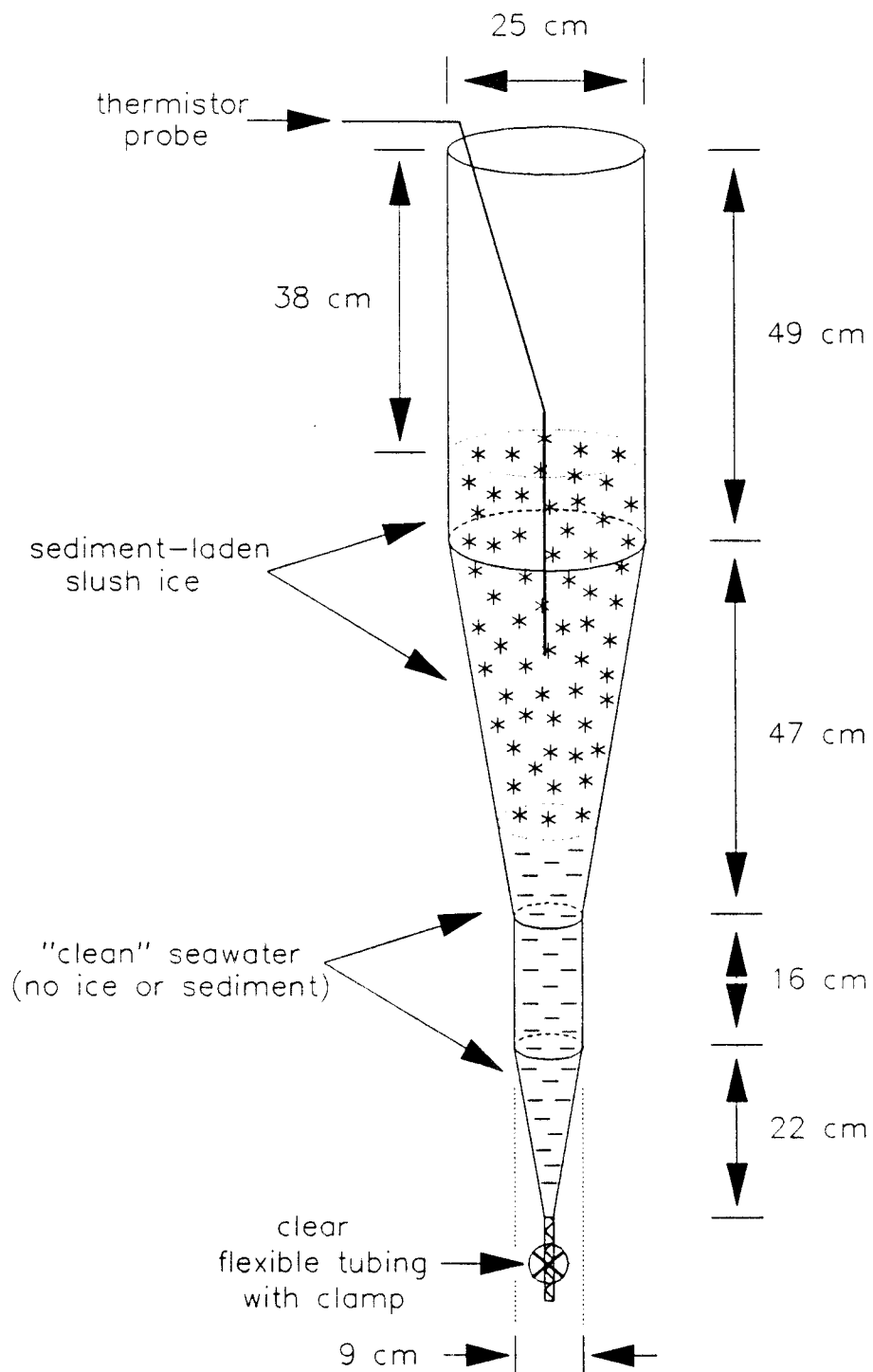
Figure 8-21. Schematic Representation of the Modified Sedimentation Trap Used for the Sediment "Expulsion" Experiment

sediment-ice slurry to the experimental container (Figure 8-21), cold ice-free seawater was introduced through the flexible tubing at the bottom of the container to "float" the slurry. Additions to the container of both the initial sediment-ice slurry and the subsequent seawater were done in a slow, gentle manner to minimize releases of sediment from the slurry. A thermistor probe was inserted to a depth of 25 cm in the slurry. After a 10-min interval, a small volume of water was drained from the flexible tubing at the bottom of the container to remove any sediment released during the complete "loading" process. The last of this initial "drained" water was collected for background (i.e., "time 0") sediment load and salinity determinations. At the conclusion of the "loading" process, the total depth of the slush ice layer in the container was estimated to be 45 cm (based on the initial 10 L volume of the sediment-slush ice slurry, the depth of the air-ice interface in the container, and the geometric dimensions of the container). The volume of ice-free water beneath the slurry was estimated to be 1.7 L.

During the experiment, water samples for "settled" sediment load and salinity measurements were removed through the flexible tubing at the bottom of the container at hourly intervals. The volume of these samples (always < 85 mL) was sufficient to collect all sediment that had "settled" to the bottom of the container between sampling events. In addition to the "time 0" measurements, collections of these water samples, as well as ice slurry temperature measurements with the thermistor probe, were made at periods of 1, 2, 3, 4, 5, and 7 hrs into the experiment. After the final sampling event, the air-ice interface in the container had only subsided approximately 1 cm due to withdrawal of < 500 mL of water for all sampling events between 1 and 7 hr. The design of the sampling strategy was intended to minimize effects of sample withdrawal on ice movements in the container.

Salinities in the water samples were measured with a Reichert temperature-compensated refractometer. Sediment quantities in water samples were determined gravimetrically in triplicate as described in Section 8.3.3. The quantity of "settled" sediment for a sample was determined from the mean of the gravimetric weight measurements (n = 3) and the volume of water sampled.

The "settled" sediment loads were calculated as means + 1 standard deviation unit.

8.4.5.3 Results

Lateral Freezing Experiment

For the lateral freezing experiment, the clay-sized particles were homogeneously distributed as a suspension in freshwater prior to the onset of freezing inward from the container walls. Photographic documentation of the horizontal distribution of the particles in the final frozen "plug" is shown in Figure 8-22. The sediment-particle distribution in the figure indicates that particles were "extruded" ahead of the laterally advancing freeze-front.

Sediment "Expulsion" Experiment

During the 7-hr duration of the sediment "expulsion" experiment, the seawater-ice slurry underwent a gradual freezing process. At "time 0", the ice matrix consisted of a dense-yet-loose crystal aggregate that could be easily penetrated by a blunt object. By 4 hr, the same blunt object could no longer be easily forced through the surface at the air-ice interface. During the evolving freezing process, temperatures at the 25-cm depth in the ice matrix declined from -1.79°C to -1.94°C, and salinities in the water beneath the ice increased from 33.5 ppt to slightly greater than 38 ppt (Figure 8-23). Quantities of "settled" sediment recovered from the flexible tubing outlet at the bottom of the container are shown in Figure 8-24. The total amount of sediment recovered during the experiment was 0.66 gm dry wt. This represented approximately 6% of the sediment in the initial ice slurry (i.e., [1.1 gm dry wt of sediment/L] x 10 L). Because mechanical disturbance of the container was avoided during the experiment and water in the sample collection tube at the conclusion of each sampling event was essentially "sediment-free," the values shown in Figure 8-24 should represent sediment "released" from the ice slurry between sampling events. In the absence of mechanical agitation, these sediment releases would be due to the progressive freezing process.

direction of
freeze front
advance

container wall

255
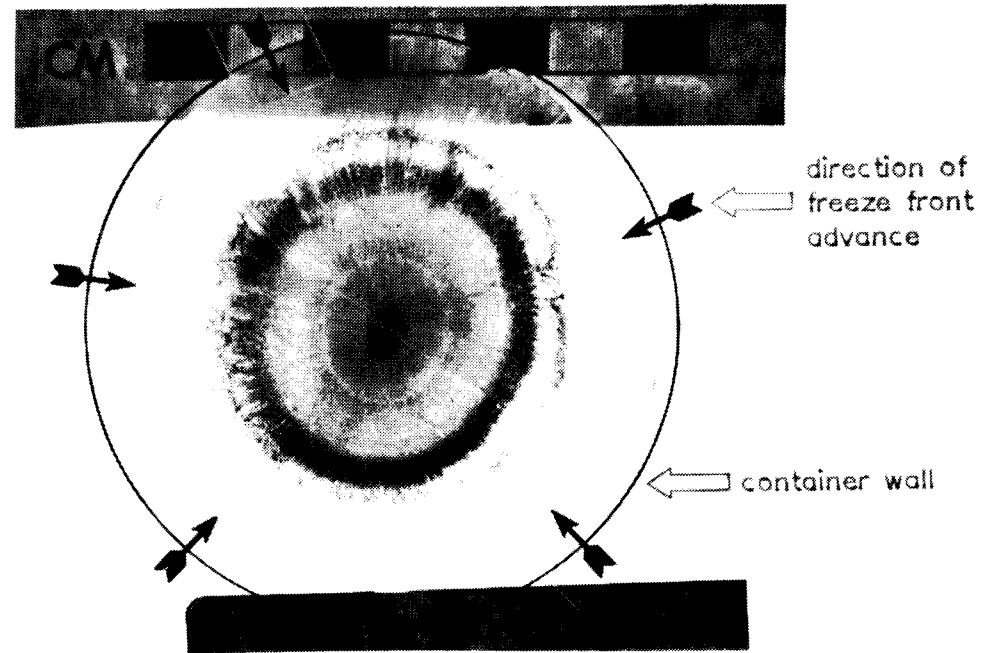
Figure 8-22.   Horizontal, Thin Section of the Final Solid Ice Plug Removed from the Cylindrical Vessel that Contained an Initial
Homogeneous Suspension of Clay-Sized Particles in Freshwater
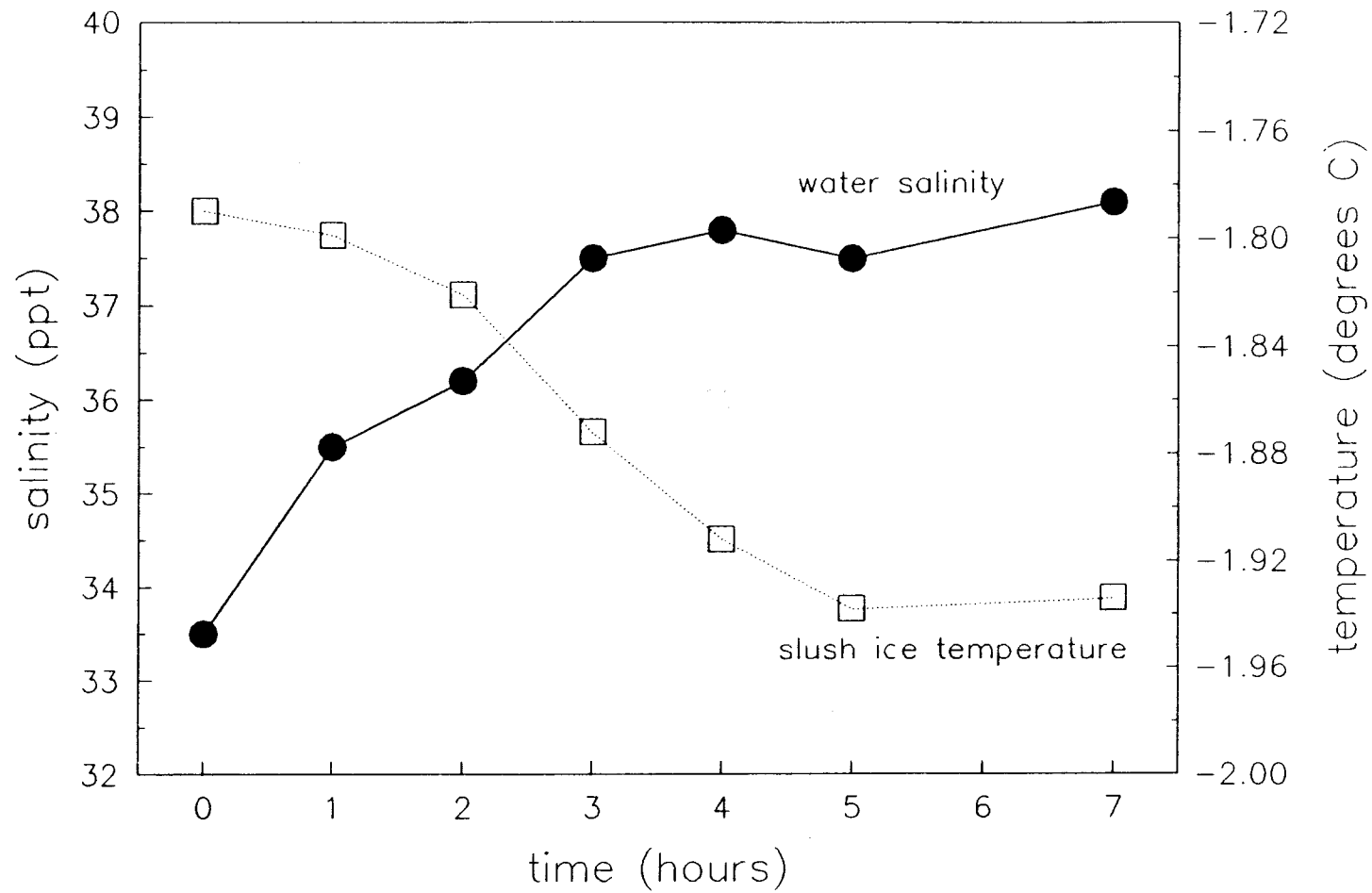
Figure 8-23. Time-Series Measurements of Temperature ($_o$C) in the Slush Ice Matrix (25-cm depth) and Salinity (parts per thousand, or ppt) in the Underlying Water Column in the Sediment "Expulsion" Experiment
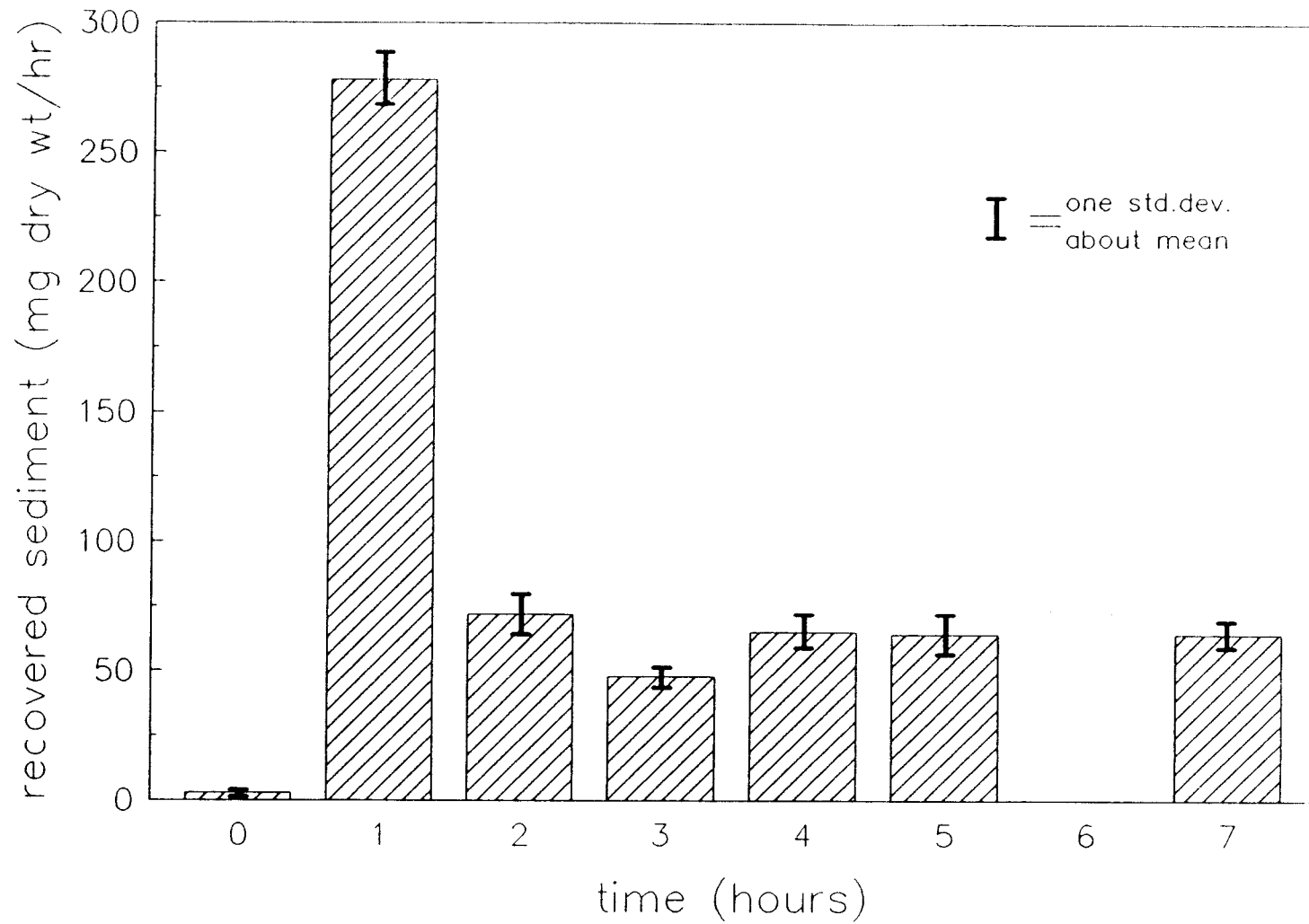
Figure 8-24. Time-Series Measurements of Sediment Loads (mg dry wt/hr) Collected from the Flexible Tubing at the Bottom of the Container in the Sediment "Expulsion" Experiment

The opaque fiberglass walls of the container prevented visual observation of events in the ice slurry during the experiment. Therefore, in an attempt to obtain information about sediment distributions in the congealed ice matrix at the conclusion of the experiment, the ice "plug" was gently removed from the container. Only the upper 27 cm of the "plug" were frozen solid, and a loose, noncohesive aggregate of ice crystals existed below the 27-cm depth. Although not quantified, substantial amounts of sediment remained in both the solid ice "plug" and the loose ice aggregate. A cross-section through the solid "plug" gave no visible evidence of vertical gradients in sediment concentrations, although the high residual amounts of sediment in the ice may have obscured concentration gradients generated by the freeze-front advance in the ice matrix.

8.4.5.4 Discussion

Photographic documentation of the final sediment distribution in the experiment involving the horizontal freeze-front advance in the freshwater ice slurry supports the contention that movement of sediment particles can occur during the freezing process and that this movement can be due to forces other than gravity alone. Both laboratory and theoretical studies have demonstrated that sediment particles up to several cm in diameter can be moved horizontally as well as vertically under the influence of advancing freeze-fronts in aqueous solutions (Corte, 1962; Uhlmann et al., 1964; Gilpin, 1980). In the latter studies, factors that affected particle "migrations" included the size and shape of particles as well as the rate of advance of a freeze-front. For example, smaller particles had a greater tendency to "migrate," and the fraction of particles in a given size class that moved a given distance increased with slower rates of freezing. If either the size of particles was too large or the rate of advance of a freeze-front was too rapid, particles became engulfed and frozen into an advancing ice matrix rather than "extruded" ahead of the freeze front. In the lateral freezing experiment (Figure 8-22), the size of the particles and the rate of the freeze-front advance were obviously conducive to the horizontal "migration" of particles. In addition to its relevance to the freezing processes in this study, the concept of particle "migration" ahead of an advancing freeze-front has also been successfully

258

applied to particle-sorting processes in natural sediment matrices such as permafrost zones during freeze-thaw cycles (e.g., Corte, 1963; Mackay, 1984; Anderson, 1988).

The purpose of the sediment "expulsion" experiment in the current study was to evaluate whether an advancing freeze-front in a congealing seawater slush ice slurry could induce "migration" and ultimate release of fine-grained sediment particles from the slurry. Because field studies have shown that mechanical agitation of sediment-laden slush ice can produce release of particulate material into an underlying water column (Dunton et al., 1982; Reimnitz and Kempema, 1987), special care was taken to minimize agitation of the sediment-laden slush ice in the experiment. Consequently, sediment released during the experiment (Figure 8-24) should have been the result of the particle "rejection" process, described above, during the evolving freezing process in the slush ice slurry. The results of this experiment also provide corroborative evidence to field observations of releases of fine-grained particulate material from a slush ice canopy into an underlying, relatively turbulence-free water column (e.g., diving observations noted in Reimnitz and Dunton, 1979). In terms of the relevance of the sediment "expulsion" experiment to real-world situations, the water beneath the slush ice layer experienced a substantial salinity increase in conjunction with the evolving freezing process. Field studies in shallow nearshore and lagoon areas of Arctic marine environments have documented salinity increases (due to brine rejection) that can approach 100 ppt during freezing (Walker, 1974; Hume and Schalk, 1976; Wiseman, 1979; Matthews, 1981; Matthews and Stringer, 1984). Consequently, results of the experiment in this section may be more appropriately extrapolated to shallow nearshore and coastal lagoon areas, as opposed to deep-water shelf or open oceanic environments where salinity changes would be less pronounced due to dilution.

While the sediment "expulsion" experiment by no means yields a detailed insight into the phenomenon of particle "rejection" ahead of an advancing freeze-front, the dynamic nature of retention or release of sedimentary material from a slush ice matrix can have broad implications for a variety of processes in regions affected by sea ice. Retention and subsequent release of

259

sedimentary material from an ice canopy (during either initial congelation ice formation or later melting of a solid ice canopy) can be important to studies relating to spatial transport of sediments by ice (Reimnitz and Kempema, 1987).

These experiments, in combination with the results presented in Sections 8.3 and the rest of Section 8.4, demonstrate that there are a number of mechanisms which are important for understanding both sediment incorporation and its ultimate fate and release from sea ice canopies. Consequently, an in-depth appreciation and understanding of the numerous factors contributing to retention and movement of fine-grained sedimentary material in congealing sea ice canopies is necessary before any speculations and modeling in a predictive sense can be initiated. In any event, the evolution of sediment-laden ice is clearly a stochastic process which makes predictive modeling difficult.

8.5 EXAMINATION OF OTHER MECHANISMS FOR THE FORMATION OF SEDIMENT-LADEN ICE CANOPIES -- SPM ENTRAINMENT BY RISING FRAZIL ICE CRYSTALS

8.5.1 Introduction

During all of the wave-tank studies, it was noted that SPM-laden sea-water splashed onto solid ice or other surfaces easily retained its SPM load as it was frozen in place. Thus, high sediment loads could at least be deposited onto the surface of existing ice floes that way. However, in all the wave-tank experiments, a high level of SPM could never be maintained in the surface ice canopy for a sustained period because of the self-cleaning mechanisms discussed in Section 8.4.

These observations lead to the hypothesis that in nature the varying levels of SPM in surface ice are dependent on the stochastic sequence of weather events during freezeup: SPM-laden slush ice will retain its sediment load only if the weather lies down quickly after a storm and the natural wave-dampening effect of the slush ice prevents further rainout of the sediment from the ice canopy as it freezes.

260

Expanding on the above hypothesis, it has been observed that the water-mixing depth in the Beaufort Sea can reach 18 to 20 m during a severe storm event. If the storm occurs during fall freezeup and the water is super-cooled to the point that frazil ice maintains itself in a "active" state for a sustained period, then significant adhesion of SPM might occur. However, even if the frazil ice is not maintained in a "sticky" state, the platelets could also be capable of passively scavenging (filtering) high loads of suspended particulate material from the water column as they work their way to the surface after the storm subsides. As this SPM-laden frazil ice reaches the surface, it can then either undergo self-cleaning, as observed in the wave-tank and racetrack flume experiments, or if the weather lies down quickly, grow thick enough fast enough so that residual wave turbulence subsides to the point at which additional self-cleaning of the ice by turbulent mechanisms is not a factor. In this manner, higher concentrations of suspended particulate material in a seasonal ice canopy would result, as observed in the field.

In an attempt to address this possible scenario, experiments were planned and undertaken to demonstrate first that a heavy SPM load could (at least) be established and maintained in the ice canopy under experimental conditions. Then, with that successful demonstration as a basis for further study, refinements were incorporated into the experimental methods to examine several mechanisms of SPM filtration and entrainment by rising frazil ice crystals. The following sections describe the results of those studies.

8.5.2   Wave-Tank Investigations of Surface Ice Canopy Loading by Physical Entrapment of SPM Into Rising Frazil and Slush Ice Crystals

Before proceeding with additional experiments to investigate the mechanisms outlined above, it was deemed necessary to demonstrate that high sediment loads could be generated in the ice canopy in the wave tank, even if artificial constraints had to be placed on the system to mimic a hypothesized ice-formation event in nature.

To undertake this experiment, a slush ice layer was allowed to form to a depth of 20 cm under constant wave turbulence in SPM-rich water generated

from "Jakolof Bay 2" sediment (see Table 8-2 for grain-size distributions). The wave paddle was then turned off, and subsamples of the surface slush ice and water column were collected for SPM-concentration determinations. As shown by the data in Table 8-6, the SPM load in the surface slush ice was 140 mg/L, and the water column beneath the slush ice had an SPM load of 276 mg/L. Immediately after these samples were collected, a 30-cm diameter cylinder was lowered through the surface slush ice and water column and allowed to rest on the bottom of the tank. To demonstrate that slush ice rising through this SPM-rich water column would entrain a higher SPM load and maintain that load with subsequent freezing in the absence of turbulence, the ice within the cylinder was vigorously mixed to the bottom and allowed to resurface. Additional aliquots of the surface ice, from inside the cylinder and from an un-mixed control area immediately adjacent to the cylinder, were then removed for SPM determinations, and the entire ice canopy within the wave tank was allowed to freeze without any additional turbulence.

After 14 hours, surface ice cores were removed from the ice canopy within the cylinder and the adjacent control area for examination and SPM analysis. The difference in SPM loads can easily be seen in the photographs of the cross sections of the cores (Figure 8-25), and it is even more apparent in the SPM gravimetric data presented in Table 8-6. As shown by the data in the

Table 8-6

Gravimetric Analyses of SPM Loads in the Surface Ice Canopy During Investigations of Physical Entrapment of SPM by Rising Frazil and Slush Ice Crystals

| Date | Time (hr) | SPM LOADS (mg/L) | | Slush Ice After Mixing With SPM-Rich Water |
		Water	Slush Ice Control	
16-Feb-86	2230	276	140	1078
17-Feb-86	1300	NA	109	581
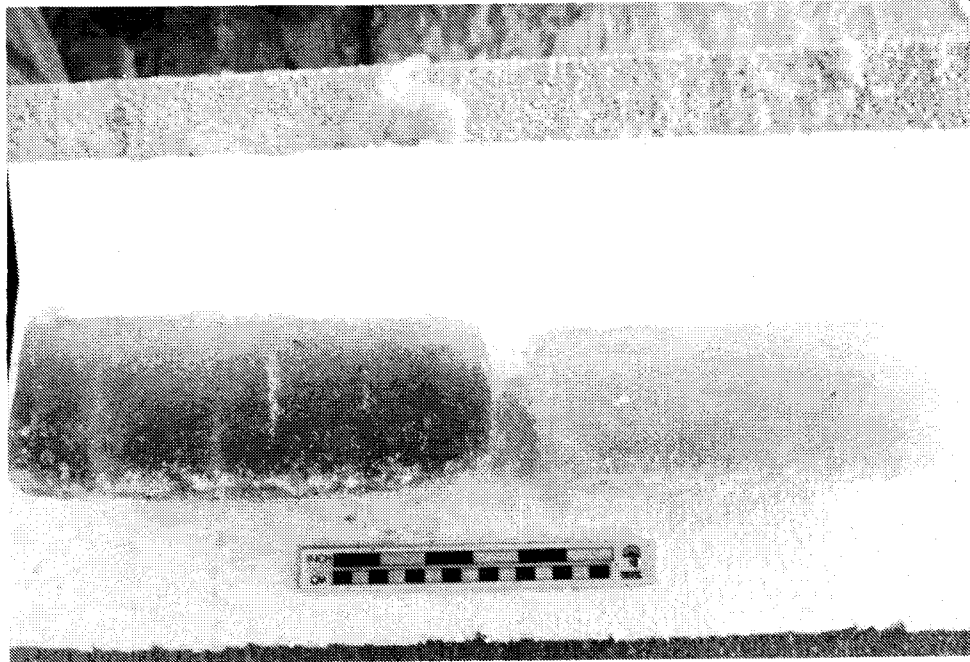
Figure 8-25. Side-By-Side Comparison of Surface Cores from the Vertical Cylinder/Wave-Tank Experiment

The core from the slush ice that was mixed inside the cylinder with the underlying SPM-laden seawater is on the left and the core from the adjacent control area is on the right.

table, the ambient SPM load in the control area from the surrounding ice layer was 140 mg/L at the initiation of the experiment, whereas the SPM load trapped within the ice mixed down into the water column inside the experimental cylinder was nearly 1080 mg/L. With subsequent freezing, the ice loading in both the slush ice control outside of the stirred cylinder and within the stirred cylinder decreased. However, an elevated level of 581 mg/L of suspended sedimentary material was maintained within the ice canopy that had been rapidly mixed into underlying SPM-rich water and then allowed to freeze in the absence of further turbulence.

The results of the cylinder experiment indicated that high levels of SPM could be generated in the wave-tank system; however, even in this instance there was some self-cleaning which may have been due to the advancing freeze-front mechanism described in Section 8.4.5.

These experiments support the earlier hypothesis that if an elevated load of SPM is generated in the water column during a storm, then it can be trapped and maintained by rising frazil and slush ice if the weather lies down very quickly after the frazil/slush ice sediment matrix surfaces. As additional ice growth ensues in the form of columnar ice (as would be the case if freezing continued under calm conditions, e.g., Payne et al., 1987a) a layer of relatively clean columnar ice would develop beneath the "dirty" surface layer. This scenario explains the observations from field studies which have shown a significant discontinuity in the SPM load at the slush ice/columnar ice interface (Osterkamp and Gosink, 1984; Wang, 1979; Weeks and Hamilton, 1962).

8.5.3   Kasitsna Bay Laboratory Tests of Current-Driven Filtration of SPM-Laden Water By Frazil/Slush Ice Pans

8.5.3.1 Introduction

In the field and in wave-tank studies, frazil ice has been observed to exist as formations of porous masses of crystals bonded together to varying degrees. Depending on the state of freezing, it is sometimes possible to force an arm through the matrix, and at other times it may require some force to

penetrate the material at all. Naidu (1980) proposed that seawater containing suspended sediment may flow through the porous formations of frazil ice before, during and after freezeup, and that this mechanism may be used to explain the increased sediment loads observed in ice canopies under certain conditions. Ostercamp and Gosink (1984) presented additional theoretical calculations relating to the filtration mechanism in combination with direct entrainment of SPM by frazil ice (or derived forms of frazil ice) during ice formation under conditions of high turbulence as the most likely mechanisms for sediment entrainment in the sea ice cover.

The hydraulic gradient or driving force for the water flow across or through a frazil pan was assumed by Osterkamp and Gosink to have both horizontal and vertical components. If a horizontal current velocity of about 0.10 m/sec is blocked by a frazil pan of approximately 1 m in the direction of the flow, then a horizontal flow rate of 1.6 μm/sec was calculated through the pan. Substantially higher vertical flow rates were estimated for waves splashing over floating frazil ice. For example, a 0.1-m overflow on 1.0-m thick frazil implied a vertical flow rate of 0.3×10^{-3} m/sec. Given these theoretical estimates, Osterkamp and Gosink calculated that the vertical filtration mechanism could explain observed sediment loads in frazil flocs or pans with diameters much less than 1 m if the deposition time scale was on the order of 8 hr (or approximately the period of a storm event capable of raising waves sufficient to overtop the frazil) and the ambient SPM load in the water column was 1 mg/L. In these theoretical calculations, the efficiency of the filtration process and the permeability of the frazil ice matrix were unknown; however, the concept described in their paper served as the framework for a number of filtration experiments which were undertaken in the walk-in coldroom and wave-tank system at Kasitsna Bay as part of this experimental program.

8.5.3.2 Methods for Horizontal and Vertical Filtration Experiments

As described in Section 8.2, the experimental wave-tank system and plumbing configuration were designed to allow simulation of water currents through a frazil ice matrix. This was to be accomplished by recirculating chilled water through the input and exhaust headers specifically constructed in

the wave-tank system (see Figures 8-4 through 8-8). Flow controllers and plumbing in an adjacent control room allowed measurement of water flow rates through the upper and lower recirculating lines.

During initial scoping determinations, significant quantities of frazil ice were entrained into the exhaust headers and destroyed by the in-line pumping system in the adjacent control room. Therefore, plastic screen material of 1-mm mesh was installed over the exhaust headers in the tank to prevent entrainment of ice crystals by the recirculating system. Additional flow controls were installed to allow adjustment of the flow rate through the upper and lower recirculating system to further mitigate against entrainment of ice. After these initial modifications to the recirculation system, three attempts were undertaken to generate a sufficient horizontal current flow through the slush ice field in the wave tank to allow investigation of horizontal filtration of SPM by frazil ice pans.

Unfortunately, all attempts at executing this experiment failed. Four major factors contributed to the lack of success:

- The recirculating pump added an unacceptable heat load to the water in the recirculating system. That is, heat input from the recirculating system destroyed the slush ice field, and the cooling capacity of the refrigeration system in the coldroom was not sufficient to override this heat-input process.

- Because of restrictions in flow imparted by the screens placed on the exhaust header ports, the horizontal current in the tank could not be maintained at rates greater than 0.3 cm/sec (estimated by measuring the time required for neutrally buoyant plastic marker disks to transect a measured distance in the tank) in the absence of slush ice.

- Under these low current speeds, sufficient SPM loads could not be maintained in the wave tank to conduct the experiments in the absence of wave turbulence.

- When wave turbulence was introduced to maintain a higher SPM load in the water column, this same wave turbulence caused self-cleaning of the frazil ice and slush ice matrix as described in Section 8.4.

As a result of these complications, the use of the recirculating system was eventually abandoned, and a series of vertical and horizontal tube experiments were undertaken in which a clean slush ice matrix from the racetrack flume was isolated in an experimental tube and varying amounts of SPM-laden seawater were allowed to percolate (filter) through it.

During February and August 1986, a total of 6 vertical column and 3 horizontal tube filtration experiments were successfully completed. In each of these experiments SPM either from the wave tank or from the USGS racetrack flume was used as feed material, and in all cases, the SPM was derived from Jakolof Bay sediments (see Table 8-2 for grain size distributions). Replicate SPM loads were measured in the feed water and drain water (water passing through the slush ice), the interstitial water within the ice matrix, and at various depths within the ice cores contained in the tube. In all of the vertical tube experiments, the slush ice was maintained on top of a vertical water column by placing the slush ice to varying depths (10 to 30 cm) on top of fresh -1.83°C seawater and then introducing -1.83°C SPM-laden waters to the top of the tube while draining water from the bottom of the tube at a constant rate. Depending on the experiment, SPM-laden feed water was either collected from the racetrack flume or the wave tank, placed in a reservoir, and then transferred to the vertical tube with a siphon as shown in Figure 8-26.

At the conclusion of a filtration experiment, the underlying water supporting the ice plug was drained, and the tube containing the intact ice plug was placed back in the coldroom for approximately 1 hr for additional solidification of the ice core to allow it to be extruded as a continuous ice sediment matrix. Subsamples of the extruded ice core were then taken at various depths as illustrated in Figure 8-27.

8.5.3.3 Results of Vertical and Horizontal Slush Ice Filtration Experiments

Table 8-7 presents gravimetric SPM data, filtering times, and volumes filtered for the vertical column experiments. As shown by the data in the table, significant concentration and entrapment of SPM was routinely observed as SPM-laden water was allowed to filter through the slush ice contained within

267
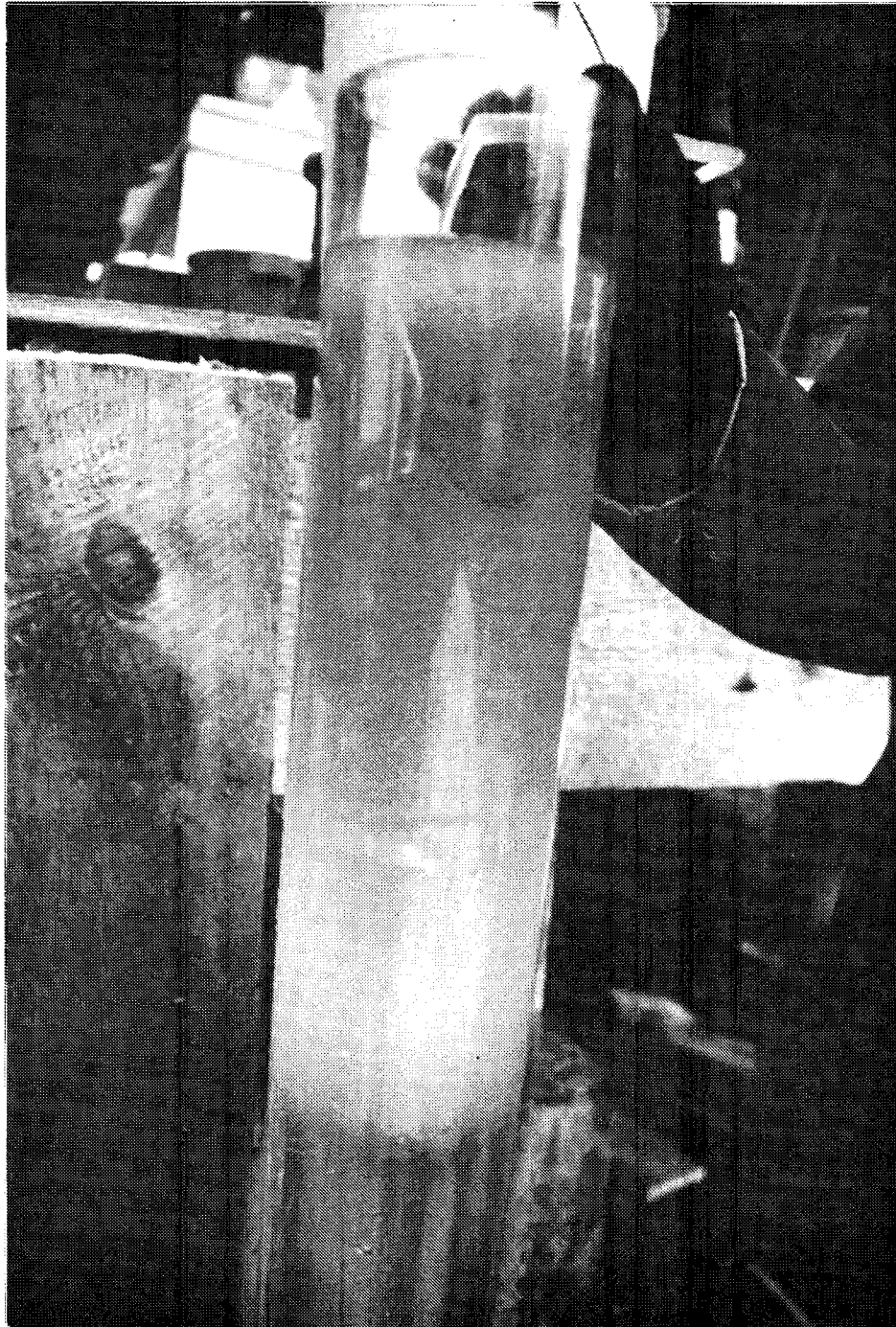
Figure 8-26. Entrapment of Suspended Particulate Material in the Slush Ice During a Vertical Filtration Experiment

Approximately 30 cm of congulation ice is supported by a clean water column, and SPM-laden "splash" water is introduced at the surface.

268
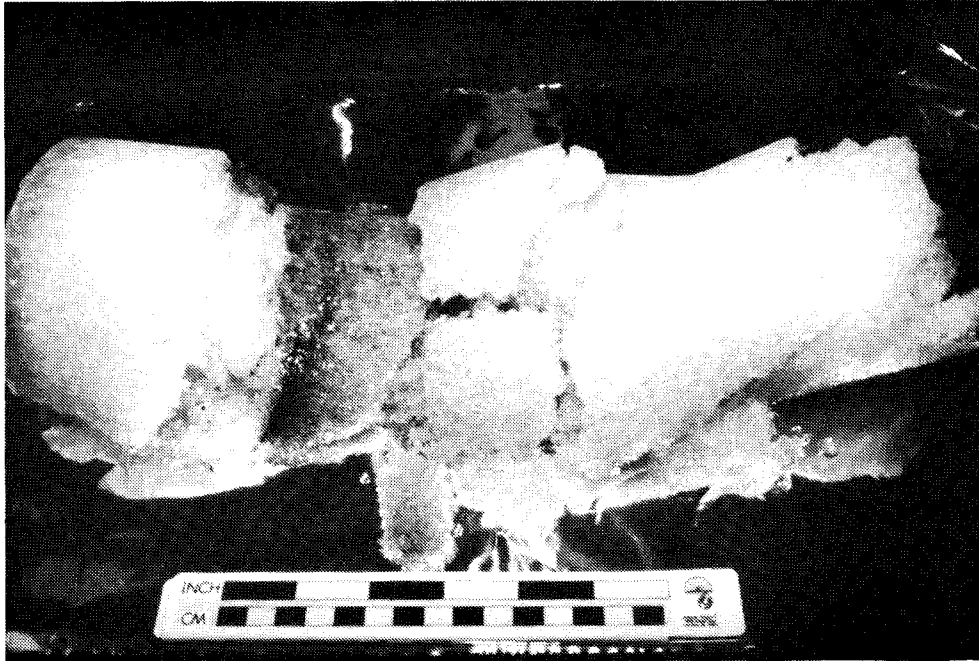
Figure 8-27. Extruded Sediment Core from Vertical Filtration Experiment Completed on 20 February 1986 Showing Dirty Ice at the 7- to 12-cm Depth with Relatively Clean Ice Present on Either Side

Table 8-7

Results of Gravimetric Analyses of SPM Loads in Feed Water, Drain Water, and Slush Ice Collected During Vertical Column Experiments

Date	SPM Type	Slush Ice Depth (ini/fin)[a] (cm)	Comments	SPM LOADS (mg/L)							
				Feed Water	Drain Water	(0-7)	(7-12)	(12-15)	(15-20)	(20-25)	(25-30)
18-Feb-86	Unoiled Jakolof sediment	10/20	Wave tank 2 SPM; 5 gal filtered in 15 min	157	151	190	NA	NA	NA	NA	NA
19-Feb-86	Unoiled Jakolof sediment	29/40	Wave tank 3 SPM; 4.5 gal filtered in 26 min	555	243	1,490	NA	NA	NA	NA	NA
27-Feb-86	Unoiled Jakolof sediment	19/28	SPM from flume; 2.5 gal filtered in 10 min	199	47	4,690	NA	NA	NA	348	NA
20-Feb-86	Oiled Jakolof sediment	29/34	SPM from flume; 5 gal filtered in 20 min	99	68	173	6,040	4,720	1,070	835	1,070
27-Feb-86	Oiled Jakolof sediment	25/30	SPM from flume; 3.5 gal filtered in 8 min	98	59	1160	NA	NA	149	NA	369
14-Aug-86	Unoiled Jakolof sediment	5	A 12-cm x 5-cm frazil pan was placed in a glass filter; 300 mL of feed water were allowed to filter through in approx. 2 min; final SPM load in ice was measured in triplicate (i.e., r = 3, CV = 20%)	21,064	10,141	8,750	NA	NA	NA	NA	NA

NA = not available
[a] (ini/fin) denotes initial and final slush ice depth in the column

the tube. In each case significantly elevated SPM loads were obtained in the slush ice compared to the feed water and drain water, and there appeared to be little variation in filtration efficiency when either unoiled or previously oiled SPM materials were used. As discussed in Section 8.3.4.2 for the racetrack flume experiments, the oiled SPM material was obtained from a stirred chamber oil/SPM interaction experiment conducted in a 28-L chamber (Payne et al., 1987b). Thus, the oiled SPM used in all of these studies was representative of the type of oiled SPM that would be encountered after an oil spill event in SPM-rich waters.

In most cases, the majority of the SPM material was trapped in the upper 0-10 cm of the slush ice matrix. However, in one experiment (20 February 1986) additional frazil/slush ice growth occurred in the vertical column, such that the upper 0-7 cm of ice was actually cleaner than the underlying ice from 7-12 cm which contained the highest SPM concentrations (see Figure 8-27). As the data in the table illustrate, a significant concentration gradient of SPM was noted from the upper surface to the bottom of the slush ice matrix in the vertical experiments. This gradient appeared to be present regardless of the initial concentration of the SPM load in the feed water and/or the previous oiling of the SPM load.

From the vertical column experiments described above, it was clear that SPM-laden water filtered through a vertical slush ice column produced elevated levels of SPM in the ice. However, the ice in those experiments had been manually scooped up from the water surface in the racetrack flume and placed on top of standing water in the tube. Therefore, another experiment (No. 32) was performed to examine the influence that natural slush ice accumulation, flocculation, and packing had on the filtration process. In this experiment, a frazil ice pan which had solidified in the wave tank under the influence of natural wave turbulence was removed and shaved down to fit inside a glass powder funnel. In this manner, the natural slush ice packing density and juxtaposition of the slush ice platelets were minimally altered. After the pan was placed in the funnel, loose ice shavings were packed around the side of the pan, and the pan was placed in the freezer for 20 min so that it adhered to the sides of the funnel. The sediment-laden water that was then introduced

271

into the funnel was thus filtered through the ice and not allowed to run down the space between the funnel and the side of the frazil ice pan.

The sediment slurry that was used in this experiment had an exceedingly high SPM load (21,000 mg/L), and it was introduced to the top of the frazil ice pan over a 2-min period. The entire volume of sediment/ seawater slurry poured onto the pan filtered through it, and it appeared that none of the water was retained in the ice lattice (i.e., 300 ml of slurry were added to the top of the ice and 300 ml were collected out of the bottom). Samples of the slush ice and filtrate were removed, melted, and analyzed gravimetrically for SPM content. The results from this experiment are also presented along with the other vertical column filtration data in Table 8-7. As the data illustrate, a substantial cleansing of the water column was noted with a reduction in SPM load from 21,000 mg/L in the feed water to 10,000 mg/L in the filtrate. The final slush ice SPM load was measured at 8,750 mg/L.

These data taken together with the other vertical column filtration experiments clearly illustrated the efficiency that slush ice has in removing SPM when introduced from above.

To examine the possibility of horizontal current-induced filtration, a series of horizontal filtration experiments were conducted during the summer 1986 program. In this case, the initial experiments utilized a 100-cm x 8-cm I.D. plastic tube filled with slush ice from the wave tank or racetrack flume. This tube was then suspended horizontally in the slush ice layer in the wave tank (Figure 8-28) and sediment-laden water was introduced at one end of the tube from either the racetrack flume or the water from beneath the ice canopy in the wave tank. The driving force for horizontal water migration through the tube was provided by initiating a siphon from the exit end of the tube which drained into a collection bucket located outside of the cold room. The total head differential in each of the horizontal tube experiments was measured and, as before, samples of the initial slush ice in the tube, the feed water (both at the initiation and termination of the experiments), and the drain water (at the initiation and termination of the experiments), as well as the slush ice

Figure 8-28. Installation of a Horizontal Tube in the Slush Ice Field to Evaluate the Horizontal Filtration Hypothesis of Sediment Removal

273

contained in the tube itself, were collected for gravimetric determinations of SPM loads.

The results of these horizontal filtration experiments are presented in Table 8-8. One of the surprising results from the horizontal experiments was a differentiation of clean and dirty ice within the horizontal tube itself. Figure 8-29 is a photograph of the horizontal tube after removal from the wave tank at the termination of Experiment No. 48. Quite clearly, the upper layer of the ice in the tube was relatively clean, while the lower third of the ice in the tube contained a significant amount of sedimentary material.

Because of this vertical segregation, there is some question as to the validity or applicability of the horizontal filtration results to real-world situations. Specifically, it is possible that slush ice SPM in the lower interstices of the slush ice in the tube would eventually be released to the water column and not retained under natural conditions. Nevertheless, the results of two experiments with the rigid tube (Nos. 46 and 48) showed some reduction in the SPM load from the initial and final feed water compared to the initial and final filtrate, and a significant SPM load was measured in the "dirty" lower slush ice contained in the tubes. In Experiment 46, the SPM load was fairly constant over the 1 hr of the experiment, whereas in Experiment 48, the SPM load in the feed water showed a decline over the course of the experiment. In the execution of Experiment 48, the filtration was allowed to run overnight. The purpose of the longer running experiment was to obtain filtration rates in a horizontal tube at lower flow rates over a longer period of time. At the initiation of the experiment, the feed water SPM load was 410 mg/L; after 14 hr the SPM load in the feed water had dropped to 268 mg/L. Even at that concentration, however, a significant reduction in the final filtrate water SPM load is noted by the final measured concentration of 115 mg/L. Based on the drop in the water depth in the wave tank used to feed the horizontal tube, a total of 430 L was calculated to have been filtered through the slush ice. As the water level in the wave tank dropped, the wave paddle did not interact with as much water, and as a result, the overall turbulence level in the tank also declined. This presumably was the cause of the lower level of SPM measured in the final feed water.

Table 8-8

**Results of Gravimetric Analyses of SPM Loads in Slush Ice, Feed Water, and Drain Water Samples
Collected During the Horizontal Filtration Experiments**

			SPM LOADS (mg/L)												
			Initial Feed Water: Mean + SD[a]		Initial Slush Ice: Mean + SD		Initial Filtrate Water: Mean + SD		Final Feed Water: Mean + SD		Final "Clean" Upper Slush Ice: Mean + SD		Final "Dirty" Lower Slush Ice: Mean + SD		Final Filtrate Water: Mean + SD	
Exp. No.	Date	Comments	Indiv	SD[a]	Indiv	SD	Indiv	SD	Indiv	SD	Indiv	SD	Indiv	SD	Indiv	SD
46	20-Aug-86	Rigid tube/horizontal filtration; Total water vol filtered = 29.5 L in 1 hr; Unoiled Jakolof sediment; Head pressure = 189 cm; Ice density = 60%	756 737	746	0	0	567 607	587	659 646	652	799 787 787	791 + 6	3,721 3,758 3,752	3,744 + 16	363 483	423
48	20-Aug-86	Rigid tube/horizontal filtration; Total water vol filtered = 430 L in 14 hr; Unoiled Jakolof sediment; Head pressure = 78 to 67 cm; Ice density = 61%	409 411	410	241 268	259	NA	NA	256 281	268	1,080 1,207	1,144	5,775 5,255	5,515	117 112	115
49	21-Aug-86	Flexible tube/horizontal filtration; Total water vol filtered = 34 L in 1 hr; Unoiled Jakolof sediment; Head pressure = 152 cm; Ice density = 61%	440 452 452	448 + 6	107 113 117	112 + 4	285 287 284	285 + 1	303 298 301	301 + 2	378 381 346	368 + 16	1,391 1,411 1,416	1,406 + 11	249 246 242	246 + 3

NA = not available
[a] standard deviations reported only for triplicate determinations

Figure 8-29.   Resultant Sediment Distribution from Horizontal Tube Filtration Experiment No. 48

Note the uneven distribution of the sedimentary material in the bottom portion of the tube due to the loosely packed nature of slush ice in the tube which allowed settling by gravity.

The ice density within the tube at the end of the experiment (based on the ultimate volume of water yielded on melting) was 61%. This density was very similar to that observed in Experiment 46. From these numbers it appears that significant melting of the slush ice in the horizontal tube during the execution of the 14-hr experiment did not occur.

To determine if the rigid tube utilized in the previous filtration experiments affected the overall results, the experiment was modified and a flexible tube was utilized instead. The flexible tube in this experiment consisted of an 10 cm long x 8 cm I.D. rigid plastic tube on the inflow and exit ends and a middle section that was a heavy plastic cylinder 9.9 cm I.D. and 55 cm long. In the execution of these experiments, the flexible plastic cylinder was filled with slush ice from the racetrack flume and then suspended in the wave tank using strings so that it was free to work back and forth in the waves in the tank.

During the execution of this experiment, it was noted that the slush ice density in the flexible tube was essentially the same as that in the rigid tube experiments, and as a result the tube was not free to work to as significant an extent as desired in the passing wave train in the tank. As a result, an upper and lower differentiation of clean and dirty slush ice was again observed with final SPM concentrations of 368 mg/L for the upper and 1406 mg/L for the significantly dirtier lower layers, respectively. As before there was sufficient evidence of cleaning in the water which passed through the slush ice field, with a final feed SPM load of 301 mg/L contrasted to a final filtrate SPM load of 246 mg/L.

In addition to the problems of artifically forcing water through the slush ice and the unnatural "upper" vs "lower" differentiation in the horizontal tube experiments, an additional shortcoming of the ice-filtration approach was that although total volumes of filtered SPM-laden water could easily be determined, the total volume of interstitial water and slush ice within each core could not be measured accurately. Thus, the SPM loads in different cross-sections of the ice cores could be determined, but the volume represented by

each cross-sectional area (interstitial volume versus slush ice volume) could not be determined accurately because the water was drained from the tube first. Additional complications on volume measurements in the filtration experiments were due to the increase in slush ice volume noted at the base of the vertical column experiments in every instance. The slush ice depth (centimeters) data in Table 8-7 denote the height of slush ice initially present in the vertical column experiment and the final height of slush ice after the experiment was completed. As illustrated by the data, the absolute amount of slush ice increased in each instance, presumably due to the formation of additional frazil after passage of the feed water, which was at or near freezing, through the vertical column slush-ice array.

Therefore, it was impossible from these experiments to obtain an overall mass balance or mass closure of total percent sediment entrained during each experiment. Thus, other than showing that SPM was readily removed from seawater percolating through a slush ice field, these experiments were subject to a number of complications, and they were not believed to be representative of what might be expected to occur under natural conditions. That is, in nature it is very unlikely that 5-10 gal volumes of SPM-laden water would be filtered through slush ice pans due to wave splashing events under any conceivable scenario. Also, it was reasoned that horizontal filtration was a highly unlikely mechanism because slush ice fields generally tend to move with the currents rather than be held in place and have SPM-laden water pass through them. Therefore, additional experimentation with vertical and horizontal filtration systems was discontinued, and the equipment was modified for the study of entrainment of SPM by frazil platelets rising through an SPM-rich water column as described below in Section 8.5.4.

8.5.4   Scavenging of Suspended Particulate Material by Rising Frazil Ice
         Platelets

8.5.4.1 Introduction

During the racetrack flume experiments, elevated SPM loads were observed in the freshly formed (and quite possibly "sticky") frazil ice during

278

the temperature transition from T_m to T_e (see Section 8.3.4). Also, the open cylinder experiment demonstrated that elevated levels of SPM could be trapped in a slush ice canopy after it was vigorously mixed into a sediment-laden water column and allowed to surface en masse and freeze in the absence turbulence (see Section 8.5.1). Therefore, another series of experiments was designed and undertaken to allow simulation of loosely packed frazil platelets rising through an extended water column containing various levels of SPM.

8.5.4.2 Methods

These experiments ultimately led to the vertical column/dry ice experiments considered in Section 8.5.5; however, as an initial series of scoping experiments, a 91-cm x 7.6-cm column was filled with water at the freezing point (-1.7°C) which contained a known and measured concentration of SPM. A limited amount of clean frazil ice from the racetrack flume was then introduced into the column to a depth of 10 cm, and the column was subjected to a series of end-for-end inversions. After each inversion, the column was held in a stationary vertical position in such a way that the frazil ice platelets, which rose due to their natural buoyancy, were exposed to SPM during their ascent. In this manner, it was hoped that the frazil would trap or remove SPM from the water column by either a physical filtration or a sticking process. Furthermore, by repeating the end-for-end inversion a number of times, a greater "distance traveled" by the rising platelets could be simulated.

Using this procedure, a series of experiments using both oiled and unoiled Jakolof SPM were completed. In each case, aliquots of feed water were removed for SPM determinations before any slush ice was added to the column, and then, after the frazil/slush ice was introduced, the tube was inverted a total of 23 times to simulate frazil rising through a 20-m water column. At the conclusion of each experiment, the system was allowed to stand in place in the cold room until all the frazil/slush ice congealed at the surface. The water was then drained from the tube, and both the slush ice and drain water were analyzed for SPM loads.

279

8.5.4.3 Results

Data from this set of experiments are presented in Table 8-9. In all five experiments, active filtration of SPM by the rising frazil/slush ice platelets could be observed, and in general, the SPM load in the resultant slush ice was higher than the load in water drained from the tube following the inversion experiment. Individual frazil ice crystals in the water column were composed of a regular discs from 1 mm to 1 cm in diameter. In some instances, many of these discs (10 to 75) were observed to adhere together in flocs up to 3-4 cm in diameter. These flocs ranged in shape from nearly spherical to platelike with regular appendages of frazil crystal groups. The shape of these flat flocs was very similar to that described by Tsang and O-Hanley (1984); however, those authors appeared to believe that these flocs were composed of an

Table 8-9

Results of Gravimetric Analyses of SPM Loads in Feed Water, Slush Ice, Interstitial Water, and Final Drain Water Samples Collected During the Inversion Tube/Inversion Experiments

| Exp. No. | Date | SPM Type | Slush Ice Depth (ini/fin)[a] (cm) | SPM LOADS (mg/L) | | | | Comments |
				Feed Water	Slush Ice	Interstitial Water	Drain Water	
17	19-Feb-86	Unoiled Jakolof sediment	25/12	495	300	NA	464	Wave tank 3 SPM; 23 inversions; pre-filter samples through 1-mm sieve before gravimetric weight measurements
22	21-Feb-86	Unoiled Jakolof sediment	29/18	188	161	34	69	Wave tank 3 SPM; 23 inversions/19 min; No prefiltration of samples
32	27-Feb-86	Unoiled Jakolof Sediment	22/16	NA	316	101	153	Wave tank 4 SPM; 23 inversions/20 min; No prefiltration of samples
20	20-Feb-86	Oiled Jakolof sediment	32/36	128	64(a) 98(b) 86(c)	37	88	Wave tank 3 SPM; 23 inversions; pre-filter samples through 1-mm seive; Ice depths: (a) 0–11 cm; (b) 11–22 cm; (c) 22–34 cm
30	27-Feb-86	Oiled Jakolof sediment	21/10	NA	136	NA	100	Wave tank 4 SPM; 23 inversions/19 min; No prefiltration of samples

NA = not available
[a] (ini/fin) denotes initial and final slush ice depth in the column

individual crystal. During each inversion, significant amounts of fine-grained organic debris and sedimentary material could be observed falling through the water column. As the ice worked its way up to the surface, SPM was observed to be reentrained and readily transported to the surface where the ice crystals were then congealed and compressed.

When the thicker ice flocs described above were observed to rise through the water column, significant quantities of sediment could be seen trapped in the interstices between individual platelets and on the upper face of those frazil ice crystal plugs. In this manner, the filtration hypothesis of Osterkamp and Gosink was partially confirmed, in that the water had to pass through these rather loose skeletal plugs of frazil mass during their ascent through the water column. The details of these processes were significantly different, however, from those originally proposed by Osterkamp and Gosink when describing their filtration hypothesis.

In addition to the physical lifting of the sediment load in the water column, convection currents were also set up within the clear tube as the frazil and slush ice crystals rose. Small eddies of sediment-laden water were observed swirling in the underside of the frazil and slush ice crystals during this rising period. When additional ice migrated to the surface, this SPM too was reentrained as ice crystals from below contacted it.

As noted by the data in the Table 8-9, the ice at the top of the column following these inversions was significantly dirtier than the "drain water" in the water column beneath it; however, after an additional period of standing, the sample precipitated very small but observable SPM particles from the bottom of the loose skeletal ice matrix at the top of the column. This was particularly true if the column was disturbed before the slush ice had congealed sufficiently and was, in fact, somewhat of a problem when several of the columns were drained. Similar SPM rainout has been observed in the field by divers who have reported a constant rain of SPM material from the loose skeletal layer beneath an ice canopy when it is disturbed by a diver's hand (Reimnitz and Dunton, 1979). As noted in Sections 8.3 and 8.4, much of this

SPM load in the upper ice canopy would also continue to be lost if the ice canopy were worked or pumped by passing wave action. However, if the freezeup conditions were such that additional agitation of the surface slush ice were discontinued, then much of this sediment material would be frozen in place in the interstices between the individual slush ice crystals.

These data suggested that the simple rise of loose frazil platelets through the water column was sufficient to scavenge SPM, overcome the negative buoyancy of the SPM particles, and result in an elevated SPM load in the upper ice canopy. As with the racetrack flume studies and the vertical and horizontal filtration experiments, previous oiling of the SPM material did not appear to significantly affect its interaction with the rising frazil ice crystals; however, the limited number of data points and difficulties encountered in conducting the experiments, preclude a statistical analysis of the data.

It was believed that the lack of any more enhanced removal of SPM load from the water column was due to the fact that the frazil platelets were not in an active or "sticky" stage of growth, because it was impossible to maintain the water in the inversion column in a supercooled state. Therefore, the procedure was modified to allow frazil ice crystals to be formed in situ at the base of the experimental column and then rise through the SPM-laden water by their own buoyancy as they grew in the supercooled fluid. These experiments are described in the following section.

8.5.5   Vertical Column Studies to Examine the Removal and Filtration of
         SPM by Actively Growing and "Sticky" Frazil Ice During Its in situ
         Formation and Rise to the Surface in Supercooled Seawater

8.5.5.1 Introduction

The maximum depth of penetration by frazil crystals has not been theoretically determined, but Dayton et al., 1969 observed frazil ice to a depth of 33 m under the Antarctic ice sheet and Reimnitz (personal communication) has suggested that frazil ice platelets can be formed in turbulent and supercooled waters to depths of 20-30 m during severe storms at the beginning of fall

freezeup.   As the turbulence subsides following a storm, the frazil platelets increase in size and rise through the water column to form slush ice at the surface. If the storm event occurs in coastal or shallow waters, the SPM loads in the supercooled water column can be in excess of several hundred mg/L. Then, as the frazil platelets rise, they serve as active (sticky) or passive filters, removing much of the SPM from the water column and concentrating it in the upper congelation ice.   Depending on subsequent freezing events, the congelation ice can either undergo self-cleaning due to wind/wave action (as described in Section 8.4) or freeze in place as the weather lies down to permanently encapsulate the SPM in the surface ice canopy (as described in Section 8.5.1).   As the turbulence subsides, additional growth of columnar ice beneath the congulation ice can occur, and under these conditions, a significant discontinuity in the SPM load would be expected (as has been observed in the field).

8.5.5.2 Experimental Methods and Initial Observations

The following sections describe an extensive series of experiments completed to examine the removal and filtration of SPM by actively growing (and possibly sticky) frazil ice crystals during their rise to the surface in supercooled seawater.   These experiments were performed in a 182-cm x 8-cm (inside diameter) plastic tube, which was filled with well-mixed SPM-laden seawater and secured vertically in the coldroom at Kasitsna Bay. A magnetic stir bar was placed in the tube, and the base of the tube was then placed in a methanol foot bath on top of a magnetic stir motor as shown in Figure 8-30. The temperature of the water in the tube was closely monitored, and stirring was introduced via the magnetic stirrer to allow supercooling of the seawater before the ice-formation event.   Then, just before the initiation of ice formation, additional vertical mixing of the water column was imparted by raising and lowering a lead-weighted plumb mixer repeatedly in the column (Figure 8-31).   Following this final mixing event, dry ice was added to the methanol foot bath to catalyze in situ frazil ice crystal formation in the bottom of the tube. These frazil platelets then gradually rose to the surface as they grew.

Figure 8-30. **Photograph of the 182 cm Tall Vertical Column for the In Situ Frazil Ice Formation/ Rising Experiments**

The bucket at the base of the column contains the dry ice/methanol needed to initiate frazil ice formation.

Figure 8-31. Utilization of a Lead-Weight Plumb Mixer to Ensure a Homogeneous Sediment Distribution at the Initiation of a Rising Frazil Platelet Experiment

285

The tube was graduated in 10 cm marks so that the rising velocity of frazil ice platelets (and rising and settling velocities of SPM) could be measured during the course of an experiment.

With the addition of the dry ice to the methanol bath, minute (0.5 to 3 mm) frazil platelets formed spontaneously at the base of the tube. These were subject to the magnetic stirring action up to a height of approximately 50 cm from the base. These smaller, 0.5- to 3-mm frazil platelets appeared to be neutrally buoyant in the water column because they did not readily rise until they had grown in size to at least 7 to 10 mm. Rapid growth of these frazil ice crystals then generated flat platelets with a crystal diameter of approximately 1-2 cm within 2 min. These agglomerated into larger flocs as they rose through the water column. When these frazil platelets and flocs were 50-60 cm from the base of the column, they were no longer subject to the circular water turbulence from the magnetic stirrer. At that point, they started to rise in a random floating manner until they intersected with (and were compressed in) the upper surface slush ice zone.

On several occasions, as 2- to 4-cm ice crystals grew, a herringbone pattern was observed on the crystal surface. When these crystals impacted sediment grains during their rise, the material appeared to stick to the herringbone pattern on the ice crystal surface. Specifically, when the ice crystals rotated 90° from a horizontal to vertical position, the sediment grains were not released from the ice crystal, and in certain instances they were transported to the surface even after the ice crystals had turned over, and the sediment grains had adhered to the bottom side of the rising ice platelets. This attachment was very fragile, because when such ice crystals impacted the upper slush ice surface (and were compressed due to additional frazil ice accumulation from below), the grains were partially released from the original platelet. In such instances, the sediment grains were quickly trapped in the interstices of rising flocs from below, and in that manner they rapidly accumulated in the frazil and slush ice layer at the surface.

In addition to the herringbone pattern which was occasionally observed, other 1- to 2-cm crystals interacted with similar sized platelets to form random and flat "snowflake" patterns with 3- to 4-cm cross-sectional areas. Occasionally irregular appendages of additional ice crystals protruded at steep angles from the original horizontal rising snowflake crystal pattern. These were extremely fragile also; however, it was possible to observe the entrapment of SPM grains at the interstices of these crystal matrices.

As larger flocs of frazil platelets rose, small trails of suspended particulate material were observed in their wakes. In several experiments, it was possible to track individual ice crystals or flocs over the entire 120-cm rise through the water column. By timing these assents, rise velocities of 2.1 to 3.0 cm/sec were calculated.

In general, each experiment continued until a total slush ice depth of 35 to 55 cm had accumulated at the surface. At that point, the experiment was terminated. The vertical column was removed from the dry ice/methanol foot bath and carefully taken from the cold room. Throughout this process, the column was kept in a vertical position, and every attempt was made to minimize disturbance to the ice crystal matrix. The upper ice surface was then scooped from the vertical column into a prechilled beaker (to minimize initial thawing) with a specially adapted stainless-steel ladle, taking care to minimize any SPM loss. In some of the experiments, the interstitial water which was removed with the surface slush ice was then carefully decanted from the prechilled beaker containing the harvested slush ice to allow separate volume estimates and SPM load determinations for both the surface slush ice field and associated interstitial water. The water column beneath the surface frazil ice layer was then well mixed to ensure complete homogeneity, and additional subsamples were removed for gravimetric SPM determinations. In several experiments, aliquots of the initial (prefreeze) water column, the final slush ice surface layer, and the postfreeze water column were also examined for salinity. When previously oiled SPM was used in the experiment, subsamples were also collected from the

287

prefreeze water column, the slush ice layer, and the postfreeze water column for petroleum hydrocarbon determinations using procedures described in Section 4.2.7.

A large number of initial scoping experiments were performed in which sediment or sand particles were introduced to the top of the column and allowed to fall through the water column as the frazil ice platelets rose. This approach proved unsatisfactory, however, because a homogeneous sediment load in the water column could not be obtained and because the procedure was very difficult to replicate. Therefore, as noted above, the sediment load was ultimately introduced before frazil formation and mixed before installation of the vertical column into the corner of the coldroom.

A total of 20 different experiments were performed in which low, medium, and high SPM loads were introduced to the column. "Jakolof 2" SPM was used in all of the experiments, and it was presieved < 53 μm size fractions. The previous oiling of the SPM was also examined as a variable to see if this affected SPM scavenging by the rising frazil crystals. Additional experiments also were undertaken with samples of small algae and plankton and, finally, freshwater.

8.5.5.3 Results of SPM Load Analyses from the Vertical Column/Dry Ice
        Experiments

Experimental data collected during the vertical column experiments are presented in Tables 8-10, 8-11, and 8-12. The data in Table 8-10 are for low (10-15 mg/L) concentrations of SPM, both with and without previous oiling. Table 8-11 presents a similar data set for medium (40 to 90 mg/L) SPM loads in the water column, and Table 8-12 presents data for high SPM loading (500 to 8000 mg/L) and the additional experiments conducted with plankton and freshwater.

Each experiment type was completed in replicate, and additional replicate subsamples within each experiment were analyzed in an effort to provide a statistically valid data base on frazil ice scavenging phenomena. Thus, for low and medium SPM load experiments, a series of at least three experiments were performed with both unoiled and oiled sediments, and for most

288

Table 8-10

Results of Gravimetric Analyses of Water Column, Surface Slush Ice, Interstitial Water, and Postfreeze Water Column Samples Collected During the Vertical Column Studies

Exp. No.	Date	Comments	Initial Water Column: Indiv	Mean + SD	Surface Slush Ice: Indiv	Mean + SD	Interstitial Water: Indiv	Mean + SD	Postfreeze Water Column: Indiv	Mean + SD
					SPM LOADS (mg/L)					
58	24-Aug-86	Replicate Expt. #1; Low load of < 53 μm unoiled Jakolof SPM; Salinity (ppt)—Initial 31.0; Slush ice 25.5; Postfreeze water 32.5; Frazil rise rate = 2.5 cm/sec; Final slush ice depth = 50 cm	20.8		18.4 17.7 18.7	18.3 + 0.4	NA	NA	10.6	
59	24-Aug-86	Replicate Expt. #2; Low load of < 53 μm unoiled Jakolof SPM; Salinity (ppt)—Initial 31.0; Slush ice 24.2; Postfreeze water 31.5; Frazil rise rate = 3.0 cm/sec; Final slush ice depth = 55 cm	20.6		18.8 19.3 20.3	19.5 + 0.6	NA	NA	11.5 12.1	11.8
63	02-Sep-86	Replicate Expt. #3; Low load of < 53 μm unoiled Jakolof SPM; Final slush ice depth = 65 cm	11.2 14.9 12.5	12.9 + 1.5	19.0 16.3 19.7	18.3 + 1.5	NA	NA	8.2 11.5 12.1	10.6 + 1.7
45B	18-Aug-86	Replicate Expt. #1; Low load of < 53 μm oiled Jakolof SPM; Final slush ice depth = 50 cm	10.3		9.5		NA	NA	11.6	
60A	31-Aug-86	Replicate Expt. #2; Low load of < 53 μm oiled Jakolof SPM; Final slush ice depth = 60 cm; Rate of formation of surface ice canopy = 6.7 cm/min	13.6 15.2	14.4	14.4 13.7 13.4	13.8 + 0.4	NA	NA	11.0 12.2	11.6
60B	31-Aug-86	Replicate Expt. #3; Low load of < 53 μm oiled Jakolof SPM; Frazil rise rate = 2.4 cm/sec; Final slush ice depth = 60 cm; Rate of formation of surface ice canopy = 6.0 cm/min	12.3 12.1	12.2	9.3 12.1	10.7	NA	NA	9.1 10.5	9.8
60C	31-Aug-86	Replicate Expt. #4; Low load of < 53 μm oiled Jakolof SPM; Final slush ice depth = 65 cm; Rate of formation of surface ice canopy = 4.1 cm/min	11.2		7.8 8.1 7.7	7.9 + 0.2	NA	NA	7.0 10.8	8.9

NA = not available

Table 8-11

Results of Gravimetric Analyses of SPM Loads in Initial Water Column Slush Ice, Interstitial Water, and Postfreeze Water During Vertical Column Studies Starting with Medium SPM Loads

			SPM LOADS (mg/L)							
			Initial Water Column:		Surface Slush Ice:		Interstitial Water:		Postfreeze Water Column:	
				Mean +		Mean +		Mean +		Mean +
Exp. No.	Date	Comments	Indiv	SD	Indiv	SD	Indiv	SD	Indiv	SD
62A	02-Sep-86	Replicate Expt. #1; Medium load of < 53 μm unoiled Jakolof SPM; Final slush ice depth = 65 cm; Rate of formation of surface ice canopy = 8.1 cm/min	59.9 67.3 66.6	64.6 + 3.3	84.4 89.7 89.0	87.7 + 2.4	NA	NA	37.4 41.6 44.3	41.1 + 2.8
62B	02-Sep-86	Replicate Expt. #2; Medium load of < 53 μm unoiled Jakolof SPM; Final slush ice depth = 65 cm; Rate of formation of surface ice canopy = 6.5 cm/min	53.6 55.7 58.8	56.1 + 2.1	74.3 79.1 77.4	76.9 + 2.0	NA	NA	36.3 40.5 42.0	39.6 + 2.4
62C	02-Sep-86	Replicate Expt. #3; Medium load of < 53 μm unoiled Jakolof SPM; Subsamples analyzed for hydrocarbons by FID-GC; Column-fast ice ring at base of column slowed ice growth; Final slush ice depth = 60 cm; Rate of formation of surface ice canopy = 3.8 cm/min	65.9		75.6 78.0 84.9	79.5 + 4.0	NA	NA	41.5	
62D	02-Sep-86	Replicate Expt. #4; Medium load of < 53 μm unoiled Jakolof SPM; Final slush ice depth = 60 cm; Rate of formation of surface ice canopy = 6.7 cm/min	54.8 60.7 61.5	59.0 + 3.0	38.0 49.4 44.3	43.9 + 4.7	NA	NA	41.9 44.9 43.1	43.3 + 1.2
61A	31-Aug-86	Replicate Expt. #1; Medium load of < 53 μm oiled Jakolof SPM; Ice growth was very rapid and crystals appeared larger (4–7 cm) than in Exp. Reps. #2 and #3; Final slush ice depth = 65 cm; Rate of surface ice canopy = 8.1 cm/min	45.5 21.2 27.1	31.3 + 10.4	45.0 60.3 59.4	54.9 + 7.0	NA	NA	15.5 30.9	23.2
61B	31-Aug-86	Replicate Expt. #2; Medium load of < 53 μm oiled Jakolof SPM; Ice observed to rise in 5–6 cm flocs across the entire tube diameter; Subsamples analyzed for hydrocarbons by FID-GC; Final slush ice depth = 60 cm; Rate of formation of surface ice canopy = 6.0 cm/min	69.7 77.4	73.6	45.2 65.5 52.5	54.4 + 8.4	NA	NA	40.2 45.2	42.7
61C	31-Aug-86	Replicate Expt. #3; Medium load of < 53 μm oiled Jakolof SPM; Final slush ice depth = 58 cm; Rate of formation of surface ice canopy = 5.0 cm/min	24.5 37.6 38.4	33.5 + 6.4	59.1 54.2 64.3	59.2 + 4.1	NA	NA	35.3 52.1 44.8	44.1 + 6.9

Table 8-11 (Continued)

		MASS BALANCE CONSIDERATIONS						
Exp. No.	Date	Total SPM Mass (mg)	Initial Water Vol (mL)	Final Ice Canopy Depth (cm)	Total Slush Ice Vol (mL)	SPM Mass in Ice (mg)	Post-Freeze Water Vol (mL)	SPM Mass in Post-Freeze Water (mg)
62A	02-Sep-86	591	9,144	21	1,055	92.5	8,089	332
62B	02-Sep-86	513	9,144	14	703	54.1	8,440	334
62C	02-Sep-86	602	9,144	12	603	47.9	8,541	354
62D	02-Sep-86	539	9,144	17	854	37.5	8,290	192
61A	31-Aug-86	286	9,144	17	854	46.9	8,290	192
61B	31-Aug-86	673	9,144	16	820	44.6	8,324	355
61C	31-Aug-86	306	9,144	18	904	53.5	8,240	363

NA = not available

Table 8-12

Results of Gravimetric Analyses of SPM Loads in Initial Water Column Slush Ice, Interstitial Water, and Postfreeze Water During Vertical Column Studies Starting with Heavy SPM Loads

Exp. No.	Date	Comments	SPM LOADS (mg/L)							
			Initial Water Column:	Mean + SD	Surface Slush Ice:	Mean + SD	Interstitial Water:	Mean + SD	Postfreeze Water Column:	Mean + SD
			Indiv	SD	Indiv	SD	Indiv	SD	Indiv	SD
50	22-Aug-86	Experiment #1; Very heavy load of < 53 μm unoiled Jakolof SPM; Initial salinity = 31.5 ppt; Water was totally opaque due to SPM load; Very loose slush ice packing to a final total depth of 30 cm	8,165 7,771	7,968	4,161 4,217 4,066	4,148 + 62	3,343 3,426 3,277	3,349 + 61	5,794 5,918 5,932	5,881 + 62
52	22-Aug-86	Experiment #2; Heavy load of < 53 μm unoiled Jakolof SPM; Initial salinity = 30.0 ppt; Initial sediment added until flashlight beam was visible through the column only as a bright spot; Loose slush ice packing to a final total depth of 30 cm	1,585 1,641 1,656	1627 + 30	2,165 2,055	2,110	2,050 1,121	1,586	1,316 1,247	1,282
55	24-Aug-86	Experiment #3; Intermediate load of < 53 μm unoiled Jakolof SPM; Initial salinity = 31.5 ppt; Slush ice formed to total depth of 40 cm	526 537 522	528 + 6	653 604 520	593 + 55	762 620 641	674 + 63	397 400 418	405 + 9
56	25-Aug-86	Natural plankton > 333 μm from Kasitsna Bay surface tow on 24-Aug-86; Primarily copepods (ranging up to 1.5 mm in length), amphipods, crab zoea larvae, small coelenterate medusae, and shed barnacle exoskeltons	36	36	131 147 158	145 + 11	18	18	13	13
54	24-Aug-86	Freshwater frazil expt.; Intermediate load of < 53 μm unoiled Jakolof SPM; Ice crystals and flocs were much larger (4-7 cm) than in seawater experiments and difficult to sample without breaking and SPM loss	822 851 861	845 + 17	370 361	366	401 435 454	430 + 22	476 507 503	495 + 14

Table 8-12 (Continued)

MASS BALANCE CONSIDERATIONS

Exp. No.	Date	Total SPM Mass (mg)	Initial Water Vol (mL)	Final Ice Canopy Depth (cm)	Final Water Depth - Ice (cm)	Total Slush Ice + Interstitial Water Vol (mL)	Total Slush Vol (mL)	Total Interstitial Water Vol (mL)	SPM Mass in Slush Ice (mg)	SPM Mass In Interstitial Water (mg)	Post-Freeze Water Vol (mL)	SPM Mass in Post-Freeze Water (mg)	Summed SPM Mass in Slush Ice + Interstitial Water + Postfreeze Water (mg)
50	22-Aug-86	72,859	9,144	30	4	1,507	201	1,306	834	4,375	8,943	52,592	57,800
52	22-Aug-86	14,877	9,144	30	5	1,507	265	1,242	559	1,971	8,879	11,383	13,912
55	24-Aug-86	4,828	9,144	40	8	2,010	402	1,608	238	1,084	8,742	3540	4,862
56	25-Aug-86	329	9,144	50	6	2,512	276	2,236	40	40	8,867	115	196
54	24-Aug-86	7,727	9,144	60	11	3,014	553	2,462	202	1,059	8,591	4,253	5,513

experiments, triplicate measurements of SPM loads in the starting seawater, the final frazil ice matrix, the interstitial water, and postfreeze water column samples were completed. When experimental conditions (limited sample size, availability of storage containers, or time) allowed only two replicates of a given matrix type to be sampled for SPM determinations, the individual values and the averages are presented. It was not always possible to obtain samples of interstitial water between the frazil platelets, and in these instances, the missing data are designated by NA.

Examination of the data in Table 8-10 shows that there was evidence of entrainment of SPM in the surface slush ice with an enriched SPM load compared to the final postfreeze (drain) water in all three experiments where unoiled SPM was used. In the four experiments where previous oiling of the sediment or SPM had taken place, the SPM load in the upper ice canopy was approximately the same as that in the initial water column or in the final postfreeze water column at the conclusion of the experiment. Thus, when oiled SPM was used at these lower SPM levels, it was not clear that any "active" scavenging of the SPM occurred. This suggests that previously oiled SPM may not be as subject to sticking or scavenging by the rising frazil ice platelets as unoiled SPM. In this case then, the oiled SPM, which was measured in the upper ice canopy, may have been simply filtered by passive frazil ice and trapped in the interstitial water within the surface slush ice matrix.

Table 8-11 presents the results from the frazil ice/SPM experiments completed with intermediate SPM loads. Four replicate experiments were run with both unoiled and oiled SPM, and as shown by the data in the table, the experiments completed with unoiled SPM (at an initial ambient concentration of 60 mg/L) all showed a cleansing of the SPM load from the water column. In addition, an enriched SPM load in the surface slush ice compared to the initial water column load occurred in three of the four experiments. The relative precision within each experiment was very good, and with the exception of the low slush ice load for Experiment 62D, there appeared to be excellent agreement among the tests.

Unfortunately, the results from the oiled SPM experiments were more ambiguous. High SPM loads were noted in the surface slush ice in all three experiments, but enrichment of oiled SPM in the surface slush ice compared to the initial water column was noted in only two of the three experiments. There also appeared to be a cleansing of the postfreeze water column of SPM (as shown by the reduced SPM load compared to the initial water column before initiation of the experiment); however, this was the case in only two out of the three experiments, and significantly greater heterogeneity was noted in the postfreeze water samples in one experiment (61B).

Nevertheless, in all seven experiments, rising frazil platelets significantly removed suspended particulate material from the water column, and this process was slightly more efficient with unoiled compared to oiled SPM. Specifically, the unoiled SPM materials yielded surface slush ice SPM loads that were higher (in absolute magnitude) than those observed with the oiled SPM, and similar cleansing of postfreeze water column loads was measured in all unoiled SPM experiments, while the results were more variable when oiled SPM was used.

An overall mass balance was attempted with each of the mid-level SPM experiments. These data, which were derived from measured volume and SPM loads in slush ice and pre- and postfreeze water column samples, are also presented in Table 8-11. A complete mass closure was not obtained in any of the experiments; however, approximately 70% of the SPM load could be accounted for in this experimental series. Unfortunately, when these medium-level SPM load experiments were performed, interstitial water in the surface slush ice matrix was not sampled separately, and gravimetric data on SPM loads in the interstitial water are therefore unavailable. Such measurements were, however, completed at the very heavy SPM loads and, as the data in Table 8-12 illustrate, much better overall mass closure was obtained.

When considering the data in Table 8-12, it should be noted that the initial SPM concentrations were exceedingly high. Nevertheless, at unoiled SPM concentrations of approximately 500, 1600, and 8000 m/L, the data clearly illustrate that elevated levels of SPM are trapped by the surface slush ice

(on the order of the initial seawater values) and that similar SPM values are present in the entrained interstitial water within the slush ice matrix. In all three cases, a significant cleanup of the water column was noted. When the SPM loads were measured in the interstitial water collected with the surface slush ice, a much more accurate overall mass balance (approaching 80-100%) was possible. As shown by the mass balance data in Table 8-12, actual mass of SPM in the surface slush ice, the interstitial water associated with that slush ice, and final postfreeze water mass could be tracked to a high degree of precision and accuracy when compared to the total SPM mass initially introduced into the water column.

In these experiments, three different loads of SPM were intentionally used to span a wide range in the initial water column in order to determine if the SPM affected the slush ice packing density at the heavy loads. A loose packing of the slush ice did appear at these higher SPM loads, and the overall ice formation depths were only 30 cm, compared to the 60 cm packings and denser ice crystal matrices noted at lower SPM loads (as shown in Table 8-11). It is possible that the heavy SPM loads encountered affected frazil ice vertical migration by imparting a change in the frazil platelet buoyancy.

Additional vertical column experiments at heavy SPM loads were not undertaken with oiled SPM. As noted earlier, the oiled SPM samples used in all these experiments were from stirred chamber oil/SPM interaction experiments, and these could not be completed at the 5- to 73-gm levels necessary to supply the amounts required for the vertical column experiments described in Table 8-12.

Table 8-12 also presents the results of one experiment which was performed using natural plankton samples from Kasitsna Bay. The plankton were obtained by a surface tow of a plankton net with a 330 μm mesh size on 24 August 1986. The plankton material consisted primarily of copepods (ranging up to 0.15 mm), amphipods, crab zoea larvae, small coelenterate medusae, and shed barnacle exoskeletons. Water samples in this vertical column experiment (No. 56) had a total surface slush ice depth of 50 cm. The surface slush ice

296

contained large amounts of organic matter, including living plankton of a larger size class than that in the postfreeze water. In this instance, over 35% of the total SPM mass comprised of plankton was trapped in the upper surface ice. Based on observation and gravimetric analyses, the capacity of the rising frazil ice to concentrate the plankton was highly efficient. In addition, the surface slush ice sample contained not only greater densities of plankton compared to the postfreeze water (on a volume basis), but it also contained higher densities of larger copepods, amphipods, barnacle ex-oskeletons, and larger plankton and organic debris, demonstrating a selective filtration of the larger organisms. The fauna in the interstitial water and postfreeze water column was comprised almost entirely of small copepods. There was only minimal evidence of other fauna and pieces of macro-algae. Similar behavior of surfacing ice has been reported in the Antarctic. Examination of the mass closure data for the plankton experiment showed that a total account-ing of approximately 60% of the material introduced into the column was possi-ble.

Finally, Table 8-12 presents the results from a vertical column exper-iment conducted with freshwater frazil ice. In this case, an intermediate load of unoiled Jakolof SPM was used at a starting concentration of approximately 845 mg/L. The surface slush ice at the end of the experiment contained an SPM load of 366 mg/L, and the interstitial water contained 430 mg/L. Thus, the SPM loads sticking to the ice and trapped in the interstitial water were similar to, but slightly less than, the initial water column concentration. Nevertheless, there was significant cleansing of the water column, as shown by the post-freeze water column SPM load of 495 mg/L. The overall mass balance SPM with the freshwater experiment was reasonably good at 71%.

In the freshwater experiment, the ice crystals and flocs were noted to be larger (4 to 7 cm) than those observed with seawater. Because of their larger size, they were more difficult to harvest without disturbing the ice crystals and causing loss of SPM during the sampling process. Thus, the surface slush ice SPM load, may have been somewhat higher than the value reported in Table 8-12. Nevertheless, the experiment did show that freshwater

frazil is capable of scavenging SPM from the water column, although the efficiency did not appear to be as great as that observed with seawater frazil.

The mass closure data for all the experiments in Table 8-12 indicate that both active scavenging of SPM onto rising (possibly "sticky") frazil ice and passive entrapment of SPM-laden interstitial water are important mechanisms for explaining high loads of final SPM in surface ice canopies. Therefore, with the encouraging results obtained when in situ frazil formation was catalyzed by addition of dry ice to the surrounding foot bath, the next logical step was to undertake studies using a thermally jacketed vertical column such that control and measurement of heat transfer could be completed during the execution of the experiments. Such heat transfer data are critical for ultimate modeling of frazil ice formation. These experiments are described in detail in the following Section (8.6). With this jacketed column, it was intended that a series of experiments similar to those described above be undertaken; however, rates of heat transfer were to be carefully controlled and measured.

8.6 INITIATION OF THERMALLY JACKETED VERTICAL COLUMN STUDIES IN SUPPORT OF MODELING OIL/ICE/SPM INTERACTIONS

8.6.1 Introduction

With the successful completion of the vertical column studies using a dry ice/methanol foot bath to initiate frazil ice formation, additional experiments were undertaken using a thermally jacketed column. The purpose of these latter studies was to control and obtain data on the heat transfer processes during the frazil ice formation and SPM scavenging event. Such data are essential for any attempt at eventually modeling the interactions of oil, ice, and suspended particulate material.

In the laboratory, it is important to be able to control the various independent variables that can affect the results of such interactions. For oil/SPM interactions these independent variables are:

1) Oil droplet formation rate and size distribution

2) SPM size distribution and total concentration

3) Total oil concentration

4) Sediment type

5) Oil type and degree of weathering

6) Level of turbulence.

With the exception of the oil droplet formation rate and size distribution, the stirred chamber experiments described in Sections 4 and 5 of this report successfully allowed examination of the other variables (2 through 6) on oil/SPM interactions.

When sea ice is added to the system, the following additional independent variables must be considered:

7) Ice formation rate

8) Degree of supercooling

9) Heat transfer rate to the environment

10. Ice crystal size.

As described in previous sections of this report, the degree of super-cooling and ice crystal size could be measured (but not necessarily controlled) during the execution of the experiments. This was not the case, however, with the control (let alone measurement) of the rate of heat transfer to the environment coupled with the ice formation rate.

8.6.2   Ice Formation Rate and Heat Transfer to the Environment

These two variables are roughly equivalent, depending upon the degree of supercooling and any temperature gradients in the system. In order to control and measure the heat transfer to the environment, it must be possible to expose the laboratory (or water column) experimental system to a fluid of

controlled temperature (lower than the experimental system) and <u>measure</u> the change in temperature of that fluid after contact with the experimental (water column) system.

The remainder of this section describes the design and construction of a laboratory apparatus to allow control and measurement of heat transfer rates and levels of turbulence during oil/ice/SPM interaction experiments. This apparatus was installed at the Kasitsna Bay Laboratory during February 1987, and initial scoping experiments were successfully completed as described in the following sections. Unfortunately, additional studies, beyond these initial tests, were never undertaken due to the change in program scope and the necessary focus on oil/SPM interactions alone, as considered in Sections 1-7 of this report.

8.6.3   Ice-Column Design

The criteria for design of the ice-column were as follows:

1) The system should be able to measure and control heat transfer rates including rates comparable to typical natural rates.

2) The system should be able to measure and control turbulence levels including levels comparable to natural systems.

3) The system should allow visual observation of the Oil/Ice/SPM interactions.

In order to meet these criteria the system shown in Figures 8-32 and 8-33 was designed. The column was designed to be compatible and complementary to the successful experiments described in Sections 8.5.5. This column configuration gives a large area for heat transfer per unit volume of water. Plexiglas was chosen as the primary material of construction in order to allow visual observations.

The inside experimental water column was constructed of 0.3-cm thick plexiglas tubing (9.5 cm I.D., 10.1 cm O.D.), which was 152 cm tall. This yielded a capacity of about 10 L. The outer column, or jacket, was 0.64-cm

300

5 1/2" O.D.

4" O.D.

Water column (10 liter)

Heat transfer jacket (volume ≈ 5.5 liter)

d

Bulkheads with O-ring seals

4'

5'

Swagelok fitting for ethylene glycol/water inlet flow

Bottom plate with hole for Thermocouple
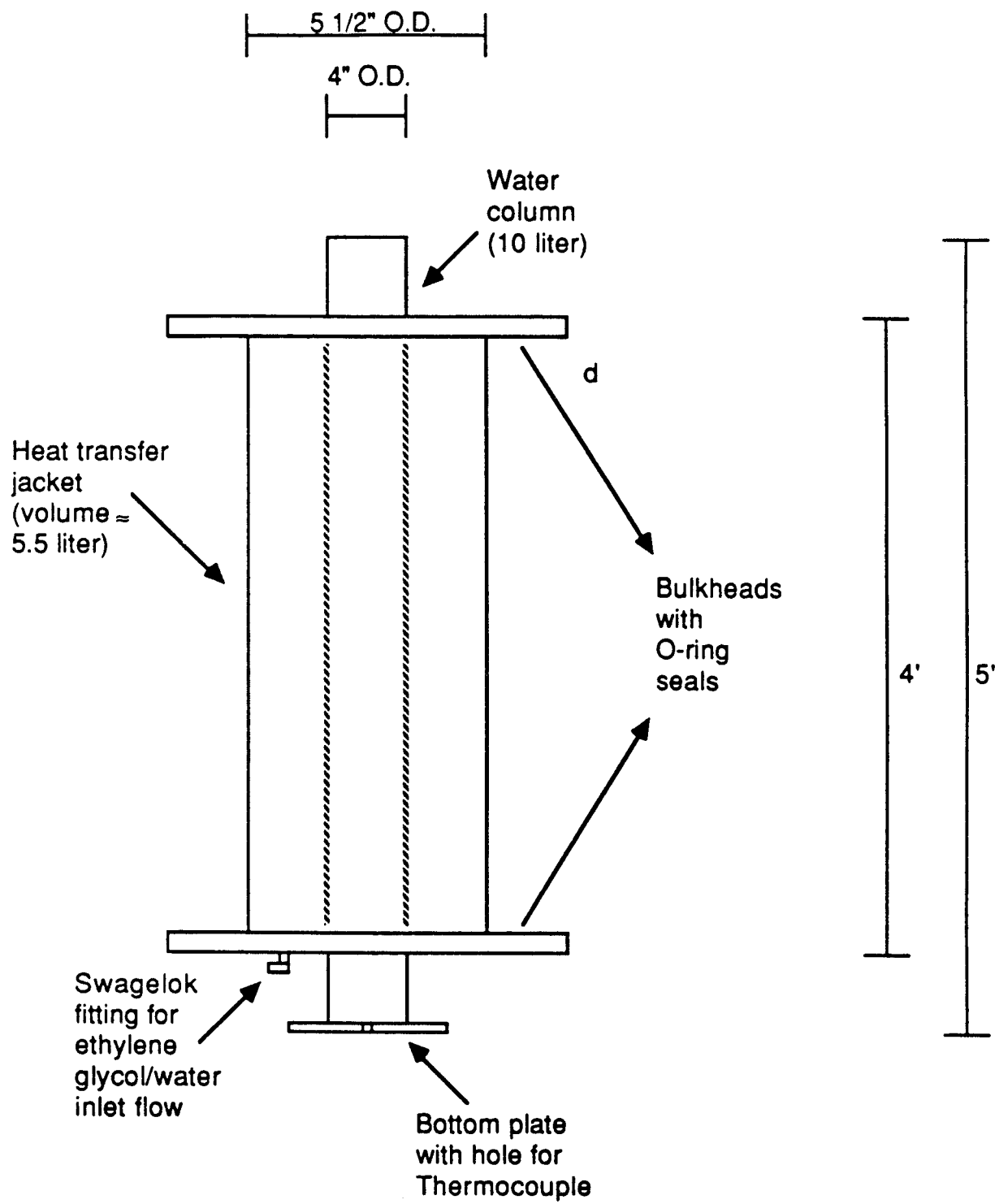
Figure 8-32.   Ice Column Design
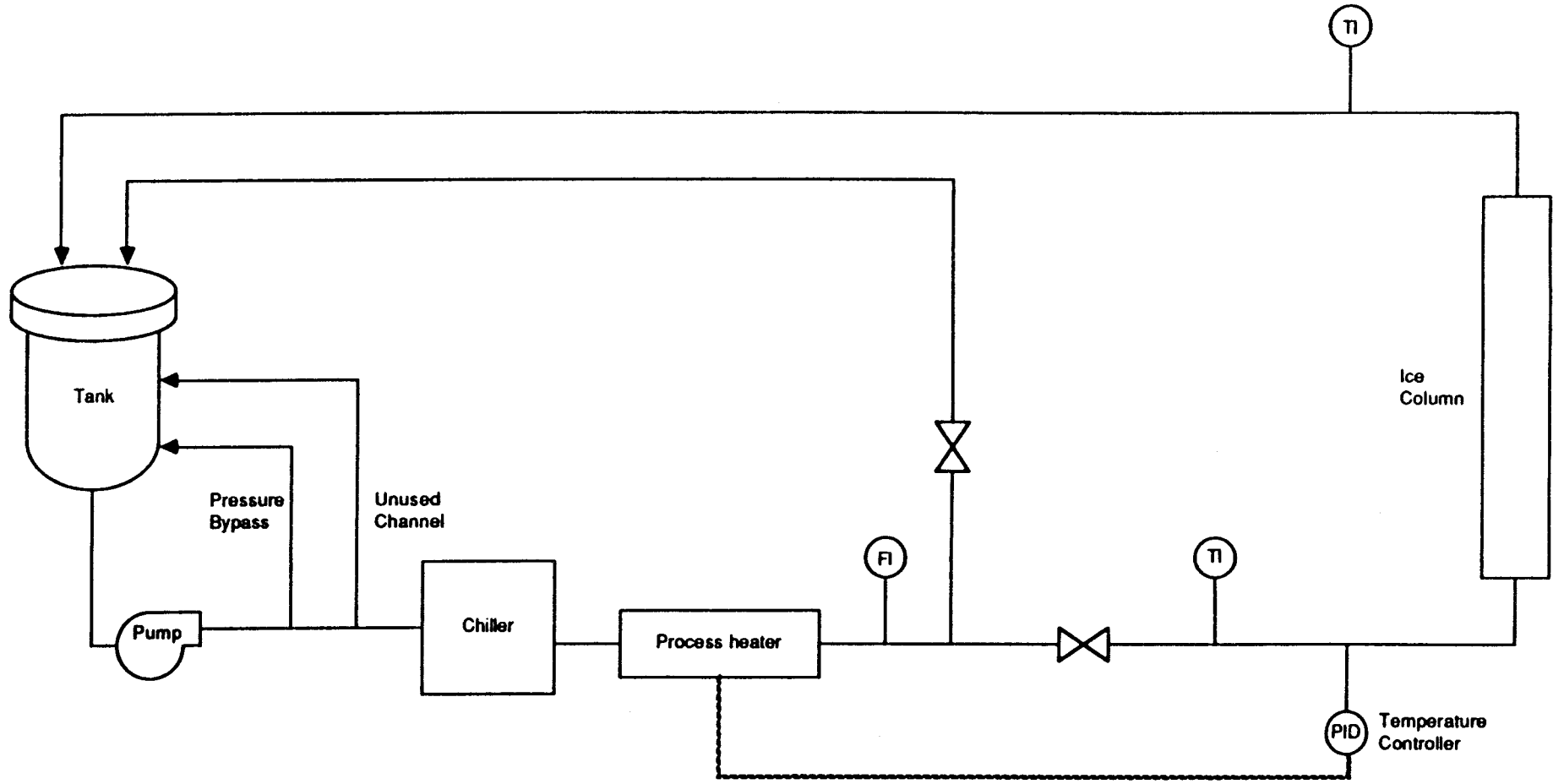
Figure 8-33.   Process and Instrumentation Diagram for Ice Column

thick plexiglas, 12.7 cm I.D., and 122 cm long. The volume of the annulus formed by the jacket and inside experimental water column was about 5.5 L.

The heat-transfer medium was a mixture of ethylene glycol and water. This medium is relatively easy to work with, readily available, inexpensive, and it has well-known properties. In order to contain the ethylene glycol/water mixture within the 5.5-L annulus surrounding the experimental column, removable bulkheads with neoprene O-rings were built. These seals worked well in preliminary tests conducted in February 1987. Flow of heat transfer fluid into the annulus was achieved through Swagelok fittings installed into the plexiglas bulkhead at the bottom of the column. Flow of fluid out of the annulus was allowed to "spill" over the top bulkhead and flow through a PVC "collection" tube back to the recirculating system.

The flow of heat-transfer fluid was achieved using portions of a salvaged Pelco refrigerated coolant recirculator. With minor modifications, this system was installed within the walk-in coldroom at Kasitsna Bay (to maximize potential cooling of the heat transfer fluid), and it was successful in providing the required heat removal and flow control for the experimental water column system installed in the adjacent control room (i.e., not within the walk-in coldroom itself).

As shown in Figure 8-33, the temperature and flowrate of the heat-transfer fluid and the temperature of the water column were measured. The temperature measurements were obtained using type J thermocouples and Omega Engineering temperature readouts. The flowrate was measured using a precision rotameter.

In "A Model of Grease Ice Growth in Small Leads," Bauer and Martin (1983) give values of heat fluxes at the ocean surface of about 1000 W/m^2. They assume an upper ocean-mixing layer about 0.5 m thick, so the heat transfer per unit volume is 2000 W/m^3. The volume of the water in the

experimental jacketed ice column was about 10 L or 0.01 m^3. Therefore, the required heat transfer for the experimental system was about (2000)(0.01) W or 20 W. The jacketed ice column was designed to achieve a maximum of 100 W of heat transfer with the ability to control lower rates.

The original design for control of temperature of the heat transfer fluid utilized a process controller with an on/off control of the chiller. This worked satisfactorily for the initial scoping experiments; however, this design was ultimately found to be unacceptable because of the long response time of the chiller. Therefore, the design was improved by utilizing a small process heater downstream of the chiller to control the temperature of the ethylene glycol/water mixture flowing into the annulus. This new design is shown in the P&ID diagram (Figure 8-33); however, it never was installed because of the aforementioned change in program direction.

Mechanical energy input into the system was achieved using a small, variable speed motor mounted above the water column. A 1/2-in diameter precision ground shaft, equipped with various propellers was lowered into the water column and attached to the motor. The system was designed to allow the eventual installation of the General Thermodynamics Model M-1 Torque meter used in the oil/SPM interaction kinetics experiments described in Section 4.2.1. Thus, it would ultimately have been possible to quantify turbulence within the jacketed column experimental system, as was described in Sections 4.2 and 5.2.2.4 of this report.

8.6.4   Preliminary Experiments

During February 1987, a series of experiments were performed to shake down the jacketed ice column and ensure that initial design criteria were met. Experiments using both freshwater and seawater were completed in which water was introduced into the experimental column and then frazil ice produced. All of the experiments were successful in producing frazil ice after the water column had reached supercooled conditions. All of the equipment performed to design, except for the control loop (as discussed above). The heat transfer achieved during these experiments allowed approximately 20-30% of the water column to be frozen during a 2- to 3-hr time period.

304

8.6.5   Summary

The results of the initial scoping and shakedown experiments with the jacketed ice column indicated that it would be a useful tool in the study of oil/ice/SPM interaction studies. Most of the independent variables important to such interactions could be controlled or at least measured in the system, and although some aspects of the system operation still needed to be refined, it was considered to be essentially ready for studies similar to those described in Section 8.5.5, in which other variables, such as SPM type, degree of oiling, turbulence, salinity, etc. could be introduced.

The system is in place at the NOAA Laboratory at Kasitsna Bay, and with minor additional effort, it could be utilized should frazil ice/SPM interactions and quantifications be required as part of additional studies. The system showed great promise, and coupled with the results from the "dry ice" vertical column experiments presented in Section 8.5.5, is (in our opinion) the obvious direction for continued attempts to study and model oil/ice/SPM interactions.

9.0   QA/QC

9.1   SPM CHARACTERIZATION

For the various physical and chemical properties measured in the sediment/SPM types used for experiments, the following QC measures were employed. Duplicate analyses were conducted on 50% of the samples submitted for TOC and 20% of the samples for hydrocarbon content. Insufficient sample volumes precluded replicate analyses for other parameters. Tables 5-3 and 5-4 in Section 5.1 present the results of the duplicate measurements for TOC and total resolved hydrocarbons, respectively. For TOC, relative percent differences (RPDs) for replicates ranged from 1 to 22%. Replicate measurements for the hydrocarbon content in Yukon Delta sediment were less than the analytical detection limit, while the replicates for Grewingk glacial till were 1.2 and 2.2 μg/g.

9.2   ISOTHERM DEVELOPMENT

The QA/QC measures employed during isotherm development consisted of analyses of duplicate _experimental_ samples for approximately 20% of all samples and the determination of linear correlation coefficients (LCC) for each isotherm. Tables 5-10 through 5-12 summarize values not only for maximum adsorption capacities but also for LCCs. LCC values approaching 1.0 are indicative of a high degree of fit of data to a straight line. As shown in Tables 5-10 through 5-12, of the 22 LCCs, 15 had values greater than 0.90, 6 had values of 0.80-0.90, and 1 (ethylbenzene with Grewingk glacial till) had a value of 0.78. The fact that all of these LCCs are near 1.0 not only allows for confidence in extrapolating to the maximum adsorption capacities at the tested initial concentrations in the experiments but also provides assurance that the isotherms were bracketed properly.

The determinations of partition coefficients were conducted in triplicate by examining three of the dosages within each isotherm set. The coefficient of variation (CV) arising from triplicate K_p determinations are

306

presented in parentheses in Table 5-13. The majority of the CV values were at or below 25%, which indicates acceptable precision at the low concentrations encountered.

The results of analyses of duplicate samples collected during isotherm experiments can be found in Tables 9-1, 9-2 and 9-3 for Cuts #4, #7, and #10, respectively. The relative percent difference (RPD) for Cut #4 duplicates show consistent and excellent precision for all compounds with RPD values ranging from 2.6% to 5.3%. RPDs for Cut #7 compounds (Table 9-2) are consistently around 25% for the duplicates of the Yukon Delta sediment, while the RPDs for Grewingk glacial till were near 10% for all compounds except 1,1'-biphenyl. The three sets of RPDs presented in Table 9-3 for Cut #10 ranged from 0.56% to 27.6%. The latter values for RPDs are acceptable, and the range of the values results primarily from inherent problems and errors associated with addressing Cut #10 as a whole.

9.3 OIL DROPLET NUMBER DENSITY COUNTS

As described in Sections 4.2.6, oil droplet number densities in a sample from a stirred reaction vessel experiment were determined by counting the number of oil droplets in five randomly chosen photographic fields. Mean values for the numbers from the five fields were then determined. As described in Section 5.2.2, these mean values were first transformed to their equivalent natural logarithmic values and a linear regression line fit to the transformed data for all time points between 1 and 15 minutes in a given experiment.

To evaluate fits of transformed number density data to anticipated linear trends over time, product-moment correlation coefficients "r" (Sokal and Rohlf, 1981) were calculated for the reaction rate constants "k" for every stirred reaction vessel experiment. The fraction of the variability in a given data set that can be accounted for by the linear fit to the data is equal to the square of the product-moment correlation coefficient (r^2). A value of 1.00 for r^2 would indicate a perfect fit of data to an expected trend. Values of r^2 for the stirred reaction vessel experiments are summarized in Table 9-4. Data in the table are separated by 1) salinity and/or 2) sediment or SPM type in a

307

Table 9-1

Results of QA/QC Duplicate Sample Analyses for Cut #4 Isotherms with Sieved Yukon Delta Sediment (YD)

Compound	AVERAGE CONCENTRATION (μg/l)/RPD[a] Samples YD-4-5a&b
Toluene	1,180/2.6%
Ethylbenzene	695/4.3%
m&p-xylene	2,840/3.9%
o-xylene	1,670/4.7%
Ethylmethylbenzene	120/5.3%
C_3-benzene	44/4.1%
C_3-benzene	48/4.6%

[a] relative percent difference

Table 9-2

Results of QA/QC Duplicate Sample Analyses for Cut #7 Isotherms with Sieved Grewingk Till (KB) and Yukon Delta Sediment (YD)

Compound	AVERAGE CONCENTRATION (μg/l)/RPD[a] Samples KB-7-1a&b	AVERAGE CONCENTRATION (μg/l)/RPD[a] Samples YD-7-1a&b
Tetramethylbenzene	25.6/10.2%	22.6/25.7%
C_4-benzene	75.5/13.3%	65.1/26.1%
Naphthalene	1,110/8.6%	1,010/23.8%
2-methylnaphthalene	842/9.7%	770/23.4%
1-methylnaphthalene	723/11.9%	637/23.6%
1,1'-biphenyl	31.2/48.1%	15.9/27.7%

[a] relative percent difference

Table 9-3

Results of QA/QC Duplicate SampleAnalyses for Cut #10 Isotherms with Sieved Grewingk Till (KB), Yukon Delta Sediment (YD), and Turnagain Arm (TA) SPM

Sample Designation	Total Cut #10 Average Concentration (µg/l) and RPD[a]
KB1-10-3a&b	12.3/27.6%
YD-10-3a&b	35.7/.056%
TA-10-3a&b	9.83/9.3%

[a] relative percent difference

particular experiment, with the mean values for r^2 for the resulting groups also being indicated. As shown, values for r^2 were generally > 0.90 in all experiments with a specific sediment or SPM phase and salinities of 14-31 ppt. Such values indicate high degrees of fit of the data to the expected logarithmic declines in oil droplet number densities over time that result from interactions of oil drops with available sediment or SPM particles. Low values of r^2 (i.e., usually < 0.60) in experiments were consistently observed either with no SPM phase present or at a salinity of 0 ppt. In both of the latter instances, the low values for r^2 were indicative of an absence of interactions between the oil drops and an SPM phase.

9.4 GRAVIMETRIC SPM WEIGHT DETERMINATIONS

The gravimetric method used to obtain SPM load measurements is described in Section 4.2.7. The majority of measurements for this parameter in both SPM settling velocity experiments (Section 5.3) and ice-related experiments (Section 8) were performed in triplicate (i.e., either triplicate samples were collected and analyzed at a specific sampling event or triplicate subsamples were removed for analysis from a given parent sample). In all instances where triplicate measurements were made, the data were reported as mean values. The corresponding values for the standard deviations and the coefficients of variation (CV) associated with specific mean values also were calculated. CVs for triplicate gravimetric measurements of SPM loads in

309

Table 9-4

Summary of Linear Regression Fits to Time-Series Oil Droplet Count Data for Generation of "k" Reaction Rate Constants in Experiments
(r^2 = square of product-moment correlation coefficient)

Date	Exp. No.	SPM Type	Oil Type	Sal (ppt)	"k" r^2: Indiv	"k" r^2: Mean
Jul-09-88	A	Grewingk till	Unweathered Prudhoe Bay crude	0	0.46	
Jul-09-88	B	Grewingk till	12-day weathered Prudhoe Bay crude	0	0.15	
Jul-18-88	B	Grewingk till	Unweathered No. 1 fuel	0	0.54	0.49
Feb-20-88	A	Yukon Delta sediment	Unweathered Prudhoe Bay crude	0	0.57	
Apr-18-88	A	Yukon Delta sediment	12-day weathered Prudhoe Bay crude	0	0.50	
Jul-20-88	B	Yukon Delta sediment	Unweathered No. 1 fuel	0	0.73	
Jul-10-88	A	Grewingk till	Unweathered Prudhoe Bay crude	14	0.95	
Jul-18-88	C	Grewingk till	Unweathered No. 1 fuel	15	0.97	
Feb-24-88	A	Yukon Delta sediment	Unweathered Prudhoe Bay crude	14	0.88	0.94
Apr-19-88	A	Yukon Delta sediment	12-day weathered Prudhoe Bay crude	14	0.94	
Jul-20-88	A	Yukon Delta sediment	Unweathered No. 1 fuel	14	0.97	
Jul-30-87	A	Grewingk till	Unweathered Prudhoe Bay crude	30	0.93	
Aug-29-87	A	Grewingk till	Unweathered Prudhoe Bay crude	30	0.90	
Sep-20-87	A	Grewingk till	Unweathered Prudhoe Bay crude	30	0.79	
Nov-14-87	A	Grewingk till	Unweathered Prudhoe Bay crude	30	0.97	
Nov-16-87	A	Grewingk till	Unweathered Prudhoe Bay crude	30	0.90	
Nov-17-87	A	Grewingk till	Unweathered Prudhoe Bay crude	30	0.98	0.94
Jul-15-88	A	Grewingk till	12-day weathered Prudhoe Bay crude	29	0.97	
Jul-15-88	B	Grewingk till	12-day weathered Prudhoe Bay crude	29	0.97	
Jul-15-88	C	Grewingk till	12-day weathered Prudhoe Bay crude	29	0.99	
Jul-17-88	A	Grewingk till	12-day weathered Prudhoe Bay crude	29	0.97	
Aug-03-87	A	Grewingk till	R/T Glacier Bay oil	30	0.94	
Jul-19-88	A	Grewingk till	Unweathered No. 1 fuel	30	0.94	
Feb-21-88	A	Yukon Delta sediment	Unweathered Prudhoe Bay crude	28	0.92	
Feb-23-88	A	Yukon Delta sediment	Unweathered Prudhoe Bay crude	29	0.82	
Apr-15-88	A	Yukon Delta sediment	12-day weathered Prudhoe Bay crude	29	0.95	0.92
Apr-16-88	A	Yukon Delta sediment	12-day weathered Prudhoe Bay crude	29	0.91	
Apr-17-88	A	Yukon Delta sediment	12-day weathered Prudhoe Bay crude	29	0.96	
Jul-19-88	C	Yukon Delta sediment	Unweathered No. 1 fuel	30	0.94	
Nov-12-87	-	Turnagain Arm SPM	Unweathered Prudhoe Bay crude	30	0.98	
Jul-17-88	B	Turnagain Arm SPM	Unweathered Prudhoe Bay crude	29	0.86	0.94
Jul-17-88	C	Turnagain Arm SPM	12-day weathered Prudhoe Bay crude	29	0.94	
Jul-18-88	A	Turnagain Arm SPM	Unweathered No. 1 fuel	30	0.97	
Jul-10-88	B	Beaufort sediment	Unweathered Prudhoe Bay crude	30	0.94	
Jul-12-88	A	Beaufort sediment	12-day weathered Prudhoe Bay crude	30	0.97	0.89
Jul-15-88	D	Beaufort sediment	Unweathered No. 1 fuel	30	0.96	
Jul-18-88	D	Beaufort sediment	Unweathered No. 1 fuel	30	0.68	
Jul-10-88	C	Beaufort peat	Unweathered Prudhoe Bay crude	30	0.96	0.91
Jul-12-88	B	Beaufort peat	12-day weathered Prudhoe Bay crude	30	0.87	
Jul-19-88	B	Jakolof sediment	Unweathered No. 1 fuel	30	0.93	
Jul-11-88	D	Kotzebue sediment	Unweathered Prudhoe Bay crude	30	0.97	0.93
Jul-14-88	A	Kotzebue sediment	12-day weathered Prudhoe Bay crude	30	0.88	
Jul-11-88	B	Peard Bay sediment	Unweathered Prudhoe Bay crude	30	0.96	0.96
Jul-13-88	B	Peard Bay sediment	12-day weathered Prudhoe Bay crude	30	0.95	

Table 9-4 (Continued)

Date	Exp. No.	SPM Type	Oil Type	Sal (ppt)	"k" r^2: Indiv	"k" r^2: Mean
Jul-11-88	C	Prudhoe Bay sediment	Unweathered Prudhoe Bay crude	30	0.89	0.93
Jul-13-88	C	Prudhoe Bay sediment	12-day weathered Prudhoe Bay crude	31	0.96	
Feb-19-88	C	None	Unweathered Prudhoe Bay crude	0	0.34	
Feb-19-88	B	None	Unweathered Prudhoe Bay crude	13	0.44	
Jul-29-87	B	None	Unweathered Prudhoe Bay crude	30	0.20	
Aug-31-87	A	None	Unweathered Prudhoe Bay crude	30	0.01	
Nov-12-87	A	None	Unweathered Prudhoe Bay crude	30	0.53	
Nov-13-87	A	None	Unweathered Prudhoe Bay crude	30	0.08	0.29
Feb-19-88	A	None	Unweathered Prudhoe Bay crude	30	0.05	
Apr-13-88	C	None	12-day weathered Prudhoe Bay crude	0	0.37	
Apr-13-88	A	None	12-day weathered Prudhoe Bay crude	29	0.26	
Apr-14-88	A	None	12-day weathered Prudhoe Bay crude	29	0.16	
Aug-02-87	A	None	R/T Glacier Bay oil	30	0.32	
Jul-14-88	B	None	Unweathered No. 1 fuel	29	0.67	

ice-related experiments (Section 8) and settling chamber experiments (Section 5.3) are summarized in Figures 9-1(a) and (b), respectively. As illustrated, the CVs for SPM load measurements were generally < 20% when SPM loads were greater than approximately 20 mg dry wt/L. At low SPM loads (i.e., < 20 mg/L), the CVs were frequently higher because gravimetric measurements approached the detection limits for the analytical balance. While measurements for gravimetric SPM loads in samples for this NOAA program were not always made in triplicate, the trends summarized in Figure 9-1 should be indicative of variabilities to be expected for all single-point measurements.

9.5 HYDROCARBON DETERMINATIONS BY FID-GC

The filtration and analysis procedures used to collect and measure quantities of oil that existed either as free oil droplets or in association with SPM are summarized in Section 4.2.7. The results of tests to document the

a) ice-related experiments
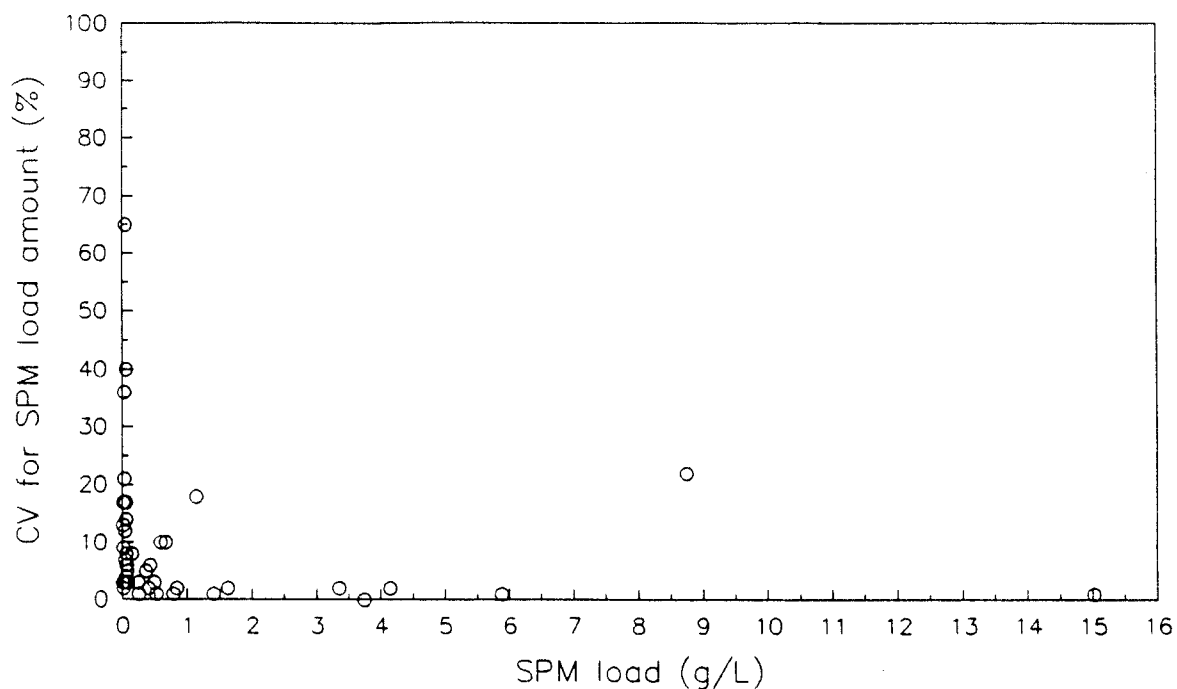
b) settling chamber experiments
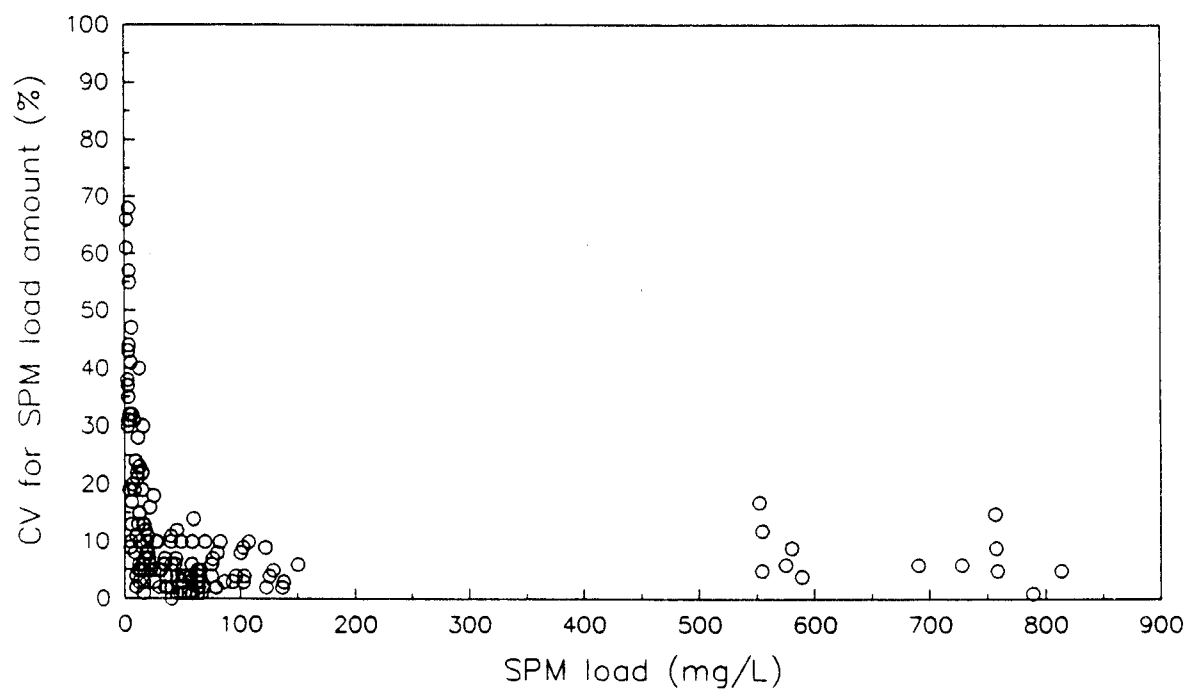
Figure 9-1.   **Coefficients of Variation (CVs) for Gravimetric SPM Load Measurements (n = 3) Versus Mean Values for the Corresponding SPM Loads**

(a) Ice-related experiments (Section 8). (b) Settling chamber experiments (Section 5.3).

312

efficiency of these procedures for recovering oil from samples has been presented in a previous report to MMS (Section 3.1.1 in Payne et al., 1987b).

For the current NOAA program, duplicate samples were frequently collected and analyzed for oil content in experiments involving oil additions. Values for resulting relative percent differences (RPD) in the oil values for duplicate measurements have been calculated and the data are illustrated in Figure 9-2. As shown, RPDs were generally < 30% for total oil loads varying from approximately 4 to 125 mg oil/L. Furthermore, this index of reproducibility for oil measurements appears to be largely independent of the type of oil detected (i.e., unweathered and 12-day weathered Prudhoe Bay crude oil, unweathered No. 1 fuel oil, and naturally weathered North Slope crude oil recovered from the R/T GLACIER BAY spill event in Cook Inlet). The data in Figure 9-2 can be used as estimators for variabilities in other single-point measurements for oil loads.
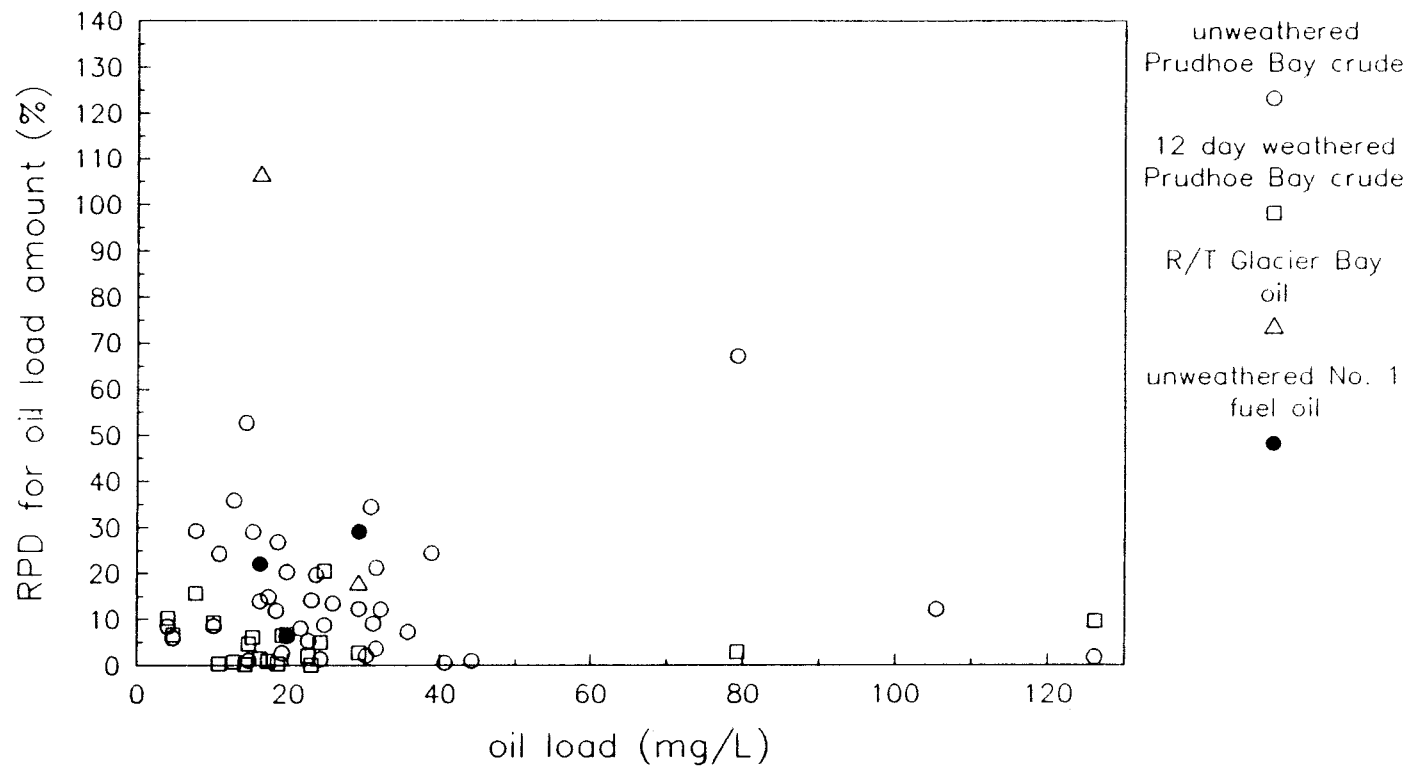
Figure 9-2. **Relative Percent Difference (RPDs) for Oil Concentration Measurements (n = 2) Versus Mean Concentrations for the Corresponding Concentrations**

Indicated oil types in the figure include unweathered and 12-day weathered Prudhoe Bay crude oil, unweathered No. 1 fuel oil, and naturally weathered North Slope crude oil recovered from the R/T Glacier Bay spill event in Cook Inlet, AK.

10.0 BIBLIOGRAPHY

Adams, C.E., and G.L. Weatherly. 1981. Some effects of suspended sediment stratification on an oceanic bottom boundary layer. J. Geophys. Res. 86:4161-72.

Allen, T. 1981. Particle Size Measurement. London: Chapman and Hall. 678 pp.

Anderson, S.P. 1988. The upfreezing process: Experiments with a single clast. Geol. Soc. Am. Bull. 100:609-21.

Aravamudan, K.S., K. Raj, and G. Marsh. 1981. Simplified models to predict the breakup of oil on rough seas. 1981 Oil Spill Conference.

Arden, R.S., and T.S. Wigle. 1972. Dynamics of ice formation in the upper Niagara River. In: International Symposium on the Role of Snow and Ice in Hydrology. Vol. 2, 1296-1313. Banff, Alberta, United Nations Education, Scientific and Cultural Organization/World Meteorological Association/-International Association of Hydrological Sciences.

Atlas, R.M., M.I. Venkatesan, I.R. Kaplan, R.A. Feely, R.P. Griffiths, and R.Y. Morita. 1983. Distribution of hydrocarbons and microbial populations related to sedimentation processes in lower Cook Inlet and Norton Sound, Alaska. Arctic 36:251-61.

Baker, E.T., 1983. Suspended particulate matter distribution, transport, and physical characteristics in the North Aleutian Shelf and St. George Basin lease areas. Final Report submitted to National Oceanic and Atmospheric Administration, NOAA Project No. R7120897. 134 pp.

Baldwin, R.R., and S.G. Daniel. 1953. The solubility of gases in lubricating oils and fuels. J. Petroleum Inst. 39(351):105-24.

Barnes, H.T. 1982. Ice Engineering. Montreal: Renouf Publishing Company.

Barnes, P.W. and D. Fox. 1979. Sediment-laden first-year sea ice, central Beaufort Coast, Alaska. Environmental Assessment of the Alaskan Continental Shelf, 231-243. Annual Reports of Principal Investigators. Boulder, CO: NOAA, Outer Continental Shelf Environmental Assessment Program.

Barnes, P.W., E. Reimnitz, and D. Fox. 1982. Ice rafting of fine-grained sediment, a sorting and transport mechanism, Beaufort Sea, Alaska. J. Sed. Petrology 52:493-502.

Bassin, N.J., and T. Ichiye. 1977. Flocculation behavior of suspended sediments and oil emulsions. J. Sed. Petrology 47:671-77.

Benedicks, Carl and Sederhom, Per, 1943, Regarding the formation of anchor (ground) ice: Arkiv for Matematik, Astronomi, och Fysik 29(22)1-7.

Benson, C.S., and Osterkamp, T.E. 1974. Underwater ice formation in rivers as a vehicle for sediment transport. In: Oceanography of the Bering Sea, 401-2. Fairbanks: Institute of Marine Science, University of Alaska.

Birkner, F.B., and J.J. Morgan. 1968. Polymer flocculation kinetics of dilute colloidal suspensions. Am. Waterworks Assoc. J. 60:175.

Black, C.A., D.D. Evans, J.L. White, L.E. Ensminga, and F.E. Clark, eds. 1965. Methods of Soil Analysis, Part 1. Physical and Mineralogical Properties, 548-67. Madison, WI: American Society of Agronomy, Inc.

Boehm, P.D. 1987. Transport and transformation processes regarding hydro-carbon and metal pollutants in offshore sedimentary environments. In: Long-term Environmental Effects of Offshore Oil and Gas Development, ed. D.F. Boesch and N.N. Rabalais. New York: Elsevier Applied Science Publishing Co., Inc.

-- in press. Transport and transformation processes regarding hydrocarbon and metal pollutants in OCS sedimentary environments. Background paper prepared for the Interagency Committee on Ocean Pollution Research Development and Monitoring; Predictive Assessment for Studies of Long-Term Impacts of OCS Activities. Chauvin, LA: Louisiania Universities Marine Consortium.

Boehm, P.D., and D.L. Fiest. 1980. Aspects of the transport of petroleum hydrocarbons to the offshore benthos during the IXTOC-I blowout in the Bay of Compeche. In: Proceedings of a Symposium, Preliminary Results From the September 1979 Researcher/Pierce IXTOC-1 cruise, 207-36. Bay Biscayne, FL: NOAA Office of Marine Pollution Assessment.

Boehm, P.D., D.L. Fiest, and A. Elskus. 1981. Comparative weathering patterns of hydrocarbons from the Amoco Cadiz oil spill observed at a variety of coastal environments. In: Proceedings of the Interatinal Symposium, Amoco Cadiz Fates and Effects of the Oil Spill, 159-73. Brest, France: Centre Oceanogigue de Bretagne.

Boehm, P.D., D.L. Fiest, D. Mackay, and S. Patterson. 1982. Physical-chemical weathering of petroleum hydrocarbons from the IXTOC I blowout: Chemical measurements and weathering model. In: Environmental Science and Technology, 16,498-505.

Bouwmeester, R.J.B., and R.B. Wallace. 1985. The break-up of an oil film due to wind-wave action. In: Proceedings of the Eighth Annual Arctic Marine Oilspill Program, 14-25. Michigan State University: Dept. of Civil Engineering.

-- 1986. Dispersion of oil on a water surface due to wind and wave action. Final Report submitted to the U.S. Department of Transportation, University Research Program, Washington, D.C. Michigan State University: Department of Civil and Environmental Engineering. 139 pp.

-- 1986. Oil entrainment by breaking waves. In: Proceedings of the Ninth Arctic Marine Oilspill Program Technical Seminar, 39-49. Michigan State University: Dept. of Civil Engineering.

Bretscher, M.S. 1985. The molecules of the cell membrane. Sci. Am. 253(4):100.

Bronson, M.T. 1988. Trace contaminants in surface sediment of the northern Bering Sea: A statistical review. Submitted to NOAA/Ocean Assessments Division. Anchorage, AK 99513.

Brooks, J.M., D.A. Wiesenburg, and R.A. Burke. 1980. Gaseous and volatile hydrocarbons in the Gulf of Mexico following the IXTOC-1 blow-out. Results from the 9/79 Researcher/Pierce IXTOC-1 cruise. In: Proceedings of a Symposium, Preliminary Results From the September 1979 Researcher/Pierce IXTOC-1 Cruise, 53-83. Bay Biscayne, FL: NOAA Office of Marine Pollution Assessment.

Businger, J.A., and S.P.S. Arya. 1974. Height of the mixed layer in the stably stratified planetary boundary layer. Adv. Geophys. 18A:73-92.

Buss, B.A., and K.S. Rodolfo. 1972. Suspended sediments in continental shelf waters off Cape Hatteras, North Carolina. In: Shelf Sediment Transport: Process and Pattern, ed. D.P. Swift, D.B. Duane, and O.H. Pilkey, 263-80. Stroudsburg, PA: Dowden, Hutchinson and Ross, Inc.

Cacchione, D.A., and D.E. Drake. 1979. Sediment transport in Norton Sound physical chemistry of the emulsifying agent. In: Proc. International Congress Surface Activity, 426-38.

Calgon Corporation Activated Carbon Division. The laboratory evaluation of granular carbons for liquid phase applications. #23-60a.

Campbell, N.J. and A.E. Collin. 1958. The discoloration of Foxe Basin ice. Jour. Fish. Res. Board Can. 15:1175-88.

Carslaw, H.S. and J.C. Jaeger. 1959. Conduction of Heat in Solids, 2d ed. Great Britain: Oxford at the Clarendon Press.

Carstens, M.R., R.M. Nielson, and H.D. Altinbilek. 1969. Bed forms generated in the laboratory under oscillatory flow: analytical and experimental study. Tech. Memo No. 28. U.S. Army Corps. Engr., Coastal Engr. Rsch. Ctr.

Carstens, T. 1966. Experiments with supercooling and ice formation in supercooled water. Geofysiske Publikasjoner XXVI(9)1-18.

Clayton, W. 1983. The Theory of Emulsions and Emulsification. Blaksitions, Sons and Co.

Coleman, H.J., E.M. Shelton, D.T. Nichols, and C.J. Thompson. 1978. Analyses of 800 crude oils from the United States oil fields. BETC/RI-78/14. Bartlesville, OK: Bartlesville energy Technology Center.

317

Corte, A.E. 1962. Vertical migration of particles in front of a moving freezing plane. J. Geophys. Res. 67:1085-90.

-- 1963. Particle sorting by repeated freezing and thawing. Science 142:499-501.

Davies, J.T. 1957. A quantitative kinetic theory of emulsion type i, physical chemistry of the emulsifying agent. In: Proc. International Congress Surface Activity, 426-38.

Dayton, P.K., G.A. Robilliard, and A.L. DeVries. 1969. Anchor ice formation in McMurdo Sound, Antarctica, and its biological effects. Science 163:273-74.

deLappe, B.W., R.W. Riseborough, J.C. Shopshire, W.R. Sisteck, E.F. Letterman, D.R. deLappa and J.R. Payne. 1979. The partitioning of petroleum related compounds between the mussel Mytilus californianus and seawater in the Southern California Bight. Draft Final Report II-15.0, Interdial Study of the Southern California Bight. Submitted to the Bureau of Land Management, Washington, D.C.

Delvigne, G.A.L., J.A. Roelivink, and C.E. Sweeney. 1986. Research on Vertical Turbulent Dispersion of Oil Droplets and Oil Particles: Literature Review. OCS Study MMS 86-0029, 138 pp.

Delvigne, G.A.L., J.A. van der Stel, and C.E. Sweeney. 1987. Measurement of vertical turbulent expulsion and diffusion of oiled droplets and oiled particles. Submitted to the Department of the Interior, Minerals Management Service, Anchorage, AK. Redmon, WA: Engineering Hydraulics, Inc. and Delft, the Netherlands: Delft Hydraulics Laboratory. 501 pp.

Drake, D.E. 1976. Suspended sediment transport and mud deposition on continental shelves. In: Marine Sediment Transport and Environmental Management, ed. D.J. Stanley and D.J. Swift, 127-158. New York: Wiley-Interscience.

-- 1977. Suspended matter in nearshore water of the Beaufort Sea. U.S. Geological Survey Open-File Report 77-477. C1-C13.

Drake, D.E., R.L. Kolpack, and P.J. Fischer. 1972. Sedimentary transport on the Santa Barbara-Oxnard Shelf, Santa Barbara Channel, California. In: Shelf Sediment Transport: Process and Pattern, ed. D.P. Swift, D.B. Duane and O.H. Pilkey, 307-32. Stroudsburg, PA: Dowden, Hutchinson and Ross, Inc.

Dunton, K.H., E. Reimnitz, and S. Schonberg. 1982. An arctic kelp community in the Alaskan Beaufort Sea. Arctic 35:465-84.

Eganhouse, R.P. and J.A. Calder. 1976. The solubility of medium molecular weight aromatic hydrocarbons and the effects of hydrocarbon co-solutes and salinity. Geochim. Cosmochim. Acta 40:555-61.

Encyclopedia Britannica, 1981. Ice in rivers and lakes. In: Encyclopedia Britannica, Vol. i, 165-70. Chicago: Encyclopedia Britannica, Inc.

Feely, R.A., J.D. Cline, and G.L. Massoth. 1978. Transport mechanisms and hydrocarbon adsorption properties of suspended matter in Lower Cook Inlet. In: Environmental Assessment of the Alaskan Continental Shelf, Vol. 8, 11-72. Annual Report to Outer Continental Shelf Environmental Assessment Program. Boulder, CO: Environmental Research Laboratories, National Oceanographic and Atmospheric Administration.

Feely, R.A., G.S. Massoth, A.J. Paulson, M.F. Lamb, and E.A. Martin. 1981. Distribution and elemental composition of suspended matter in Alaskan Coastal Waters. NOAA Technical Memorandum ERL PMEL-27. 119 pp.

Forrester W.D. 1971. Distribution of suspended oil particles following the grounding of the tanker Arrow. J. Mar. Res. 29:151-70.

Fornwalt, H.J., and R.A. Hutchins. 1966 (reprint). Purifying liquids with activated carbons. Chem. Engr. April 11.

Foulds, D.M., and Wigle, T.E. 1977. Frazil--the invisible strangler. J. Am. Water Works Assoc. April, 196-99.

Gad, J. 1978. Arch. Anat. Physiol. 181.

Gearing, J.N., P.J. Gearing, T. Wade, J.G. Quinn, H.B. McCarty, J. Farrington, and R.F. Lee. 1979. The rates of transport and fates of petroleum hydrocarbons in a controlled marine ecosystem and a note on analytical variability. In: Proceedings of the 1979 Oil Spills Conference, 555-65. Washington, D.C.: American Petroleum Institute.

Gearing, P.J., J.N. Gearing, R.J. Pruell, T.L. Wade, and J.G. Quinn. 1980. Partitioning of No. 2 fuel oil in controlled estuarine ecosystems. Sediments and suspended particulate matter. Environ. Sci. Tech. 4:1129-36.

Gearing, J.N. and P.J. Gearing. 1983 (submitted). Effects of suspended load and solubility on sedimentation of petroleum hydrocarbons in controlled estuarine ecosystems. Can. J. Fish. Aquatic Sci.

Gilpin, R.R. 1980. Theoretical studies of particle engulfment. J. Colloid and Interface Sci. 74:44-63.

Gleen, D.R., et al. 1982. Fate of chemically dispersed oil in the sea. A report on two field experiments. Report EPS4-EC-82-5. Canada: Environmental Impact Control Directorate.

Grant, W.D., L. Boyer, and L.P. Sanford. 1982. The effects of bioturbation on the initiation of motion of intertidal sands. J. Mar. Res. 40:659-77.

Grant, W.D., and S.M. Glenn. 1983a. A continental shelf bottom boundary layer model. Vol. 1: Theoretical model development. Technical Report to the American Gas Association. 167 pp.

-- 1983b. A continental shelf bottom boundary layer model. Vol. 2: Model/data comparison. Technical report to the American Gas Association. 63 pp.

-- 1983c. A continental shelf bottom boundary layer model. Vol. 3: Users Manual. Technical report to the American Gas Association. 189 pp.

Grant, W.D., and O.S. Madsen. 1979. Combined wave and current interaction with a rough bottom. J. Geophys. Res. 84(C4):1797-1808.

-- 1982. Moveable bed roughness in unsteady oscillatory flow. J. Geophys. Res. 87(C1):469-81.

-- 1986. The continental shelf bottom boundary layer. Am. Rev. Fluid Mech. 18:265-306.

Grant, H.L., H.L. Moilliet, and W.M. Vogel. 1968. Some observations of the occurrence of turbulence in and above the thermocline. J. Fluid Mech. 34(3):443-48.

Griffiths, R.P., and R.Y. Morita. 1980. Study of microbial activity and crude oil-microbial interactions in the waters and sediments of Cook Inlet and the Beaufort Sea. Final Report to the NOAA OCSEAP office. Juneau, AK.

Groves, M.J. 1978. Spontaneous emulsification. Chem. Industry 12:417.

Gundlach, E.R., K.J. Finkerlstein, and J.L. Sadd. 1981. Impact and persistence of IXTOC-1 oil on the South Texas Coast. In: Proceedings of the 1981 Oil Spills Conference, 477-85. Washington, D.C.: American Petroleum Institute.

Gunther, H., W. Rosenthall, T.J. Weare, B.A. Worthington, K. Hasselmann, and J.A. Ewing. 1979. A hybrid parametrical wave prediction model. J. Geophys. Res. 84(C9):5727-38.

Gurwitsch. 1913. Wissenschaftliche Grundlagen der Erdolbearbeitung. Translation by Moore. London: Chapman and Hall, Ltd.

Hanley, T. O'D. and Tsang, G. 1984. Formation and properties of frazil in saline water. Cold Regions Science and Technology, Vol. 8, 209-21.

Hann, R.W., Jr. 1977. Fate of oil from the supertanker Metula. In: Proceedings of the 1977 Oil Spills Conference, 465-68. Washington, D.C.: American Petroleum Institute.

Hartung, R. and G.W. Klingler. 1968. Sedimentation of floating oils. Papers of the Michigan Academy of Science, Arts, and Letters 53:23-27.

Hayes, M.O., E.R. Gundlach, and L. D'Ozouville. 1979. Role of dynamic coastal processes in the impact and dispersal of the Amoco Cadiz oil spill. (March, 1978) Brittany, France. In: Proceedings of the 1979 Oil Spills Conference, 193-98. Washington, D.C.: American Petroleum Institute.

Head, K.H.   1980. Manual of Soil Laboratory Testing. Vol. 1: Soil Classifi-cation and Compaction Testing. London: Pentech Press. 339 pp.

Huang, C.P. 1976. Solid-solution interface: Its role in regulating the chem-ical composition of natural waters. In: Transport Processes in Lakes and Oceans. Np.

Huang, C.P. and H.A. Elliott. 1977. The stability of emulsified crude oils as affected by suspended particles.   In: Fate and Effects of Petroleum Hydrocarbons in Marine Ecosystems and Organisms, ed. D.A. Wolfe, 413-20. Oxford: Pergamon Press.

Hume, J.D. and M. Schalk.   1976.   The effects of ice on the beach and nearshore, Point Barrow, Arctic Alaska. Rev. Geogr. Montr. 30:105-114.

Hunt, J. R. 1981. Particle dynamics in Seawater: Implication for predicting the fate of discharged particles. Environ. Sci. Technol. 16:303-9.

-- Self-similar particle-size distributions during coagulation. Theory and experimental verification. J. Fluid Mech. 122:169.

Hyland, J.L., and E.D. Schneider.   1976. Petroleum hydrocarbons and their effects on marine organisms, populations, communities, and ecosystems. In: Proceedings of the Symposium on Sources, Effects and Sinks of Hydrocarbons in the Aquatic Environment, 464-506.   Washington, D.C.: The American Institute of Biological Sciences. American University.

Inman, D.L., and C.E. Nordstrom.   1977.   On the tectonic and morphologic classification of coasts. J. Geol. 79:1-21.

Johansson, S., U. Larsson, and P.D. Boehm. 1980. The *Tsesis* oil spill impact on the pelagic ecosystem. Mar. Pollution Bull. 11:284-93.

Johnson, F.G.   1977.   Sublethal biological effects of petroleum hydrocarbon exposures: Bacteria, algae, and invertebrates. In: Effects of Petroleum on Arctic and Subarctic Marine Environments and Organisms. Vol. 2. Biological Effects, ed. D.C. Malins, 271-318. New York: Academic Press.

Jordan. R.E. and J.R. Payne. 1980. Fate and Weathering of Petroleum Spills in the Marine Environment.   A Literature Review and Synopsis. Ann Arbor Science Publishers, Inc. Ann Arbor, Michigan. 174 p.

Kaminski and McBain. 1949. Proc. Royal. Soc. A 198:447.

Kaplan, I.R., M.I. Venkatesan, S. Brenner, E. Ruth, J. Bonilla, and D. Meredith. 1979. Characterization of organic matter in sediments from Gulf of Alaska, Bering and Beaufort Seas.   Annual reports of principal investigators. OCSEAP research unit 480. 5:597-659.

Kaplan, I.R., M.I. Venkatesan, E. Ruth, D. Meredith. 1980. Characterization of organic matter in sediments from Cook Inlet and Norton Sound. Annual reports. OCSEAP research unit 480. 3:296-352.

321

Karickhoff, S.W. 1981. Semi-empirical estimation of sorption of hydrophobic pollutants on natural sediments and soils. Chemosphere 10:833-46.

Karickhoff, S.W., D.S. Brown, and T.A. Scott. 1978. Sorption of hydrophobic pollutants on natural sediments. Water Res. 13:241-48.

Karrick, N.L. 1977. Alterations in petroleum resulting from physicochemical and microbiological factors. In: Effects of Petroleum on Arctic and Subarctic Marine Environments and Organisms. Vol 1. Nature and Fate of Petroleum, ed. D.C. Malins, 225-99. New York: Academic Press.

Kempema, E.W., E. Reimnitz, and R.E. Hunter. 1986. Flume studies and field observations of the interaction of frazil ice and anchor ice with sediment. U.S. Geological Survey Open-File Report 86-515. 48 pp.

Kempema, E.W., E. Reimnitz, and P.W. Barnes (in prep). Sea ice sediment entrainment and rafting in the arctic. Submitted to J. Sed. Petrology.

Kirstein, B.E. and C.L. Clary. 1989. User's Manual for the Computer Codes: OILSPMXS, SPONLY, OILSMP3. Submitted to the National Oceanic and Atmospheric Administration, Outer Continental Shelf Environmental Assessment Program. Anchorage, AK.

Kivisild, H.R. 1970. River and lake ice terminology. In: Proceedings of International Association for Hydraulic Research Symposium on Ice and Its Action on Hydraulic Structures, Paper 1.0. Iceland. 14 pp.

Kolpack, R.L. 1971. Biological and oceanographic survey of the Santa Barbara Channel oil spill, 1969-1970. Vol. 2. Physical, Chemical, and Geological Studies. Los Angeles, CA: Allen Hancock Foundation, University of Southern California.

Laevastu, and Fukahara. 1985. In: Oil on the Bottom of the Sea: A Simulation Study of Oil Sedimentation and Its Effects on the Bristol Bay Ecosystem, Research Unit 463, January 1985.

Lake, R.A., and E.L. Lewis. 1970. Salt rejection by sea ice during growth. J. Geophys. Res. 75:583-97.

Lee, R.F., W.S. Gardner, J.W. Anderson, J.W. Blaylock, and J. Barwell-Clarke. 1978. Environ. Sci. Tech. 12:832-38.

Leibovich, S. 1975. A Natural Limit to the Containment and Removal of Oil Spills at Sea. Ocean Engineering. Vol. 3. Np.

Leibovich, S. and J.L. Lundey. 1981. A Theoretical Appraisal of the Joint Effects of Turbulence and of Langmuir Circulations on the Dispersion of Oil Spilled in the Sea. Washington, D.C.: U.S. Dept. of Transportation.

Lewis, E.L. 1980. The practical salinity scale, 1978, and its antecedents. IEEE J. Ocean Engr. OE5(1)3-16.

Lewis, E.L. and W.F. Weeks. 1970. Sea ice: some polar contrasts. In: Proceedings of the Symposium on Antarctic Ice and Water Masses, ed. G. Deacon, 23-34. Tokyo, Japan: Scientific Committee on Arctic Research, Cambridge, England.

Lick, W. 1987. The transport of sediments in aquatic systems. In: Fate and Effects of Sediment-bound Chemicals in Aquatic Systems, ed. K.L. Dickson, A.W. Maki, and W.A. Brungs, 61-74. New York: Pergamon Press.

Lin, J.T., M. Gad-el-Hak, and H.T. Liu. 1978. A Study to Conduct Experiments Concerning Turbulent Dispersion of Oil Slicks. U.S. Coast Guard Rpt. CG-D-54-78. Washington, D.C.: U.S. Dept. of Transportation.

Liu, S.K. 1983. Letter (RAND) to T. Laevastu.

-- 1985. Range of Turbulent Energy Dissipation Rates in Arctic Seas. Personal Communication.

Liu, S.K. and J. J. Leendertse. 1982. Modeling of tides and circulation in the Bering/Chukchi Sea, Part 1. Preliminary analysis of simulation results. Draft report for National Oceanic and Atmospheric Administration, Juneau, Alaska.

Longuet-Higgins, M.S. 1969. On wave breaking and the equilibrium spectrum of wind-generated waves. Proc. Roy. Soc. London A310:151-59.

Lyman, W.J., W.F. Ruehl, and D.H. Rosenblatt. 1982. Handbook of Chemical Property Estimation Methods. New York: McGraw-Hill Inc.

McAuliffe, C.D. 1966. Solubility in water of paraffin, cycloparaffin, olefin, acetylene, cycloolefin, and aromatic hydrocarbons. J. Phys. Chem. 70:1267-75.

McAuliffe, C.D. 1977a. Dispersal and alteration of oil discharged on a water surface. In: Fate and Effects of Petroleum Hydrocarbons in Marine Ecosystems and Organisms, ed. D.A. Wolfe, 19-83. New York: Pergamon Press.

-- 1977b. Evaporation and solution of C_2 to C_{10} hydrocarbons from crude oils on the sea surface. In: Fate and Effects of Petroleum Hydrocarbons in Marine Ecosystems and Organisms, ed. D.A. Wolfe, 363-71. New York: Pergamon Press.

McAuliffe, C.D., et al. 1975. Chevron Main Pass Block 41 Oil Spill: Chemical and Biological Investigations. Proceedings of the Joint Conference on Prevention and Control of Oil Spills. San Francisco.

Mackay, D., A. Bobra, and D.W. Chan. 1982. Vapor pressure correlations for low-volatility environmental chemicals. Environ. Sci. Technol. 16:645-49.

Mackay, D., and K. Hossain. 1983. An exploratory study of naturally and chemically dispersed oil. Department of Chemical Engineering and Applied Chemistry, University of Toronto (internal paper).

Mackay, J.R. 1984. The frost heave of stones in the active layer above permafrost with downward and upward freezing. Arctic and Alpine Res. 16:439-46.

McManus, D.A., V. Kolla, D.M. Hoplins, and C.H. Nelson. 1977. Distribution of bottom sediments on the continental shelf, North Bering Sea. U.S. Geological Survey Professional Paper 759-C.

Madsen, O.S., and W.D. Grant. 1976. Quantitative description of sediment transport by waves. Proc. Coastal Engr. Conf., 15th. 2. 1093-1112. J. Phys. Oceanogr., 7:248-55.

Malinky, G., and D.G. Shaw. 1979. Modeling the association of petroleum hydrocarbons and sub-arctic sediments. In: Proceedings of the 1979 Oil Spills Conference, 621-24. Washington, D.C.: American Petroleum Institute.

Manley, R.S.J., and S.G. Mason. 1952. Particle motions in sheared suspensions. II. Collisions of uniform spheres. J. of Colloid Science, 7:354.

Martin, S. 1981. Frazil ice in rivers and oceans. Ann. Rev. Fluid Mech. 13:379-97.

Martin, S., and P. Kauffman. 1981. A field and laboratory study of wave damping by grease ice. J. Glaciology 27(96):283-313.

Matthews, J.B. 1981. Observations of under-ice circulation in a shallow lagoon in the Alaskan Beaufort Sea. Ocean Management 6:223-34.

Matthews, J.B. and W.J. Stringer. 1984. Spring breakup and flushing of an Arctic lagoon estuary. J. Geophys. Res. 89(C2):2073-79.

Means, J.C., S.G. Wood, J.J. Hassett, and W.C. Banwart. 1980. Sorption of polynuclear aromatic hydrocarbons by sediments and soils. Environ. Sci. Technol. 14:1524.

Mercier, R.S. 1985. The reactive transport of suspended particles: Mechanisms and modeling. Joint Program in Oceanography and Ocean Engineering. Doctoral dissertation. Massachusetts Institute of Technology and Woods Hole Oceanographic Institution WHOI-85-23.

Meyer-Peter, E., and R. Muller. 1948. Formulas for bed-load transport. Proc. Intl. Assn. Hydraulic Struc. Tsch. 2:39-64.

Meyers, P.A., and J.G. Quinn. 1973. Association of hydrocarbons and mineral particles in saline solutions. Nature 244:23-24.

-- 1973. Factors affecting the association of fatty acids with mineral particles in sea water. Geochemica et Cosmochimica Acta, 37:1745-59.

Michel, Bernard. 1972. Properties and processes of river and lake ice. In: The Role of Ice and Snow in Hydrology. International Association for Scientific Hydrology Publication 1(107):454-81.

Milgram, J.H., et al. 1978. Effects of Oil Slick Properties on the Dispersion of Floating Oil into the Sea. Washington, D.C.: U.S. Dept. of Transportation.

Miller, I., and J.E. Freund. 1965. Probability and Statistics for Engineering. New York: Prentice-Hall.

Muench, R.D., and K. Ahlnas. 1976. Ice movement and distribution in the Bering Sea from March to June 1974. J. Geophys. Res. 81:4467-76.

Muench, R.D., R.B. Tripp, and J.D. Cline. 1981. Circulation and hydrography of Norton Sound. In: The Eastern Bering Sea Shelf: Oceanography and Resources, Vol 1, ed. D.W. Hood and J.A. Calder, 77-97. Washington, D.C.: U.S. Dept. of Commerce.

Munk, W.H. 1947. A critical wind speed for air-sea boundary processes. J. Mar. Resources 6:1-3.

Nelson, C.H. and J.S. Creager. 1977. Displacement of Yukon-derived sediment from Bering Sea to Chukchi Sea during Holocene time. Geol. 5:141-46.

NRC (National Research Council). 1985. Oil in the Sea, Inputs, Fates, and Effects. Washington, D.C.: National Academy Press.

O'Melia, C. 1980. Aquasols: The behavior of small particles in aquatic systems. Environ. Sci. Technol. 14:1052.

Osterkamp, T.E. 1978. Frazil ice formation: A review. J. Hydraulics Div., Am. Soc. Civ. Engr. 104(HY9)1239-55.

Osterkamp, T.E., and J.P. Gosink. 1983. Frazil ice formation and ice cover development in interior Alaska streams. Cold Regions Sci. and Technol. 8:43-56.

-- 1984. Observations and analyses of sediment-laden sea ice. In: The Alaskan Beaufort Sea: Ecosystems and Environments, ed. P.W. Barnes, D.M. Schell, and E. Reimnitz, 73-93. Orlando, FL: Academic Press.

Overbeek, J.T.G. 1952. Stability of hydrophobic colloids and emulsions. In: Colloid Science, Vol. 1, ed. H.R. Kruyt. New York: Elsevier Publishing Co.

Owen, M.W. 1977. Problems in modeling the transport, erosion, and deposition of cohesive sediments. In: The Sea, Vol. 6., ed. E.D. Goldberg, I.N. McCave, J.J. O'Brien, and T.H. Steele, 515-37. New York: Interscience.

Owen, P.R. 1964. Saltation of uniform grains in air. J. Fluid Mech. 20:225-42.

Parker, P.L., and S. Macko. 1978. An intensive study of the heavy hydrocarbons in the suspended particulate matter in seawater. In: The South Texas Outer Continental BLM Study, Chap. 11. Washington, D.C.: Bureau of Land Management.

Patten, B.G. 1977. Sublethal biological effects of petroleum hydrocarbon exposures: fish. In: Effects of Petroleum on Arctic and Subarctic Marine Environments and Organisms. Vol. 2. Biological Effects, ed. D.C. Malins, 319-35. New York: Academic Press.

Pavlou, S.P., and R.N. Dexter. 1979. Distribution of polychlorinated biphenyls (PCB) in estuarine ecosystems. Testing the concept of equilibrium partitioning in the marine environment. Environ. Sci. Technol. 13:65.

Payne, J.R., B.E. Kirstein, R.F. Shokes, N.L. Guinasso, L. Carver, K.R. Fite, R.E. Jordan, P.J. Mankiewicz, G.S. Smith, W.J. Paplawsky, T.G. Fanara, and J. Lambach. 1980. Multivariant analysis of petroleum weathering under marine conditions. Interim Quarterly Report Submitted to National Oceanic and Atmospheric Administration, Juneau, AK.

Payne, J.R., G.S. Smith, P.J. Mankiewicz, R.F. Shokes, N.W. Flynn, V. Moreno, and J. Altamirano. 1980. Horizontal and vertical transport of dissolved and particulate-bound higher-molecular-weight hydrocarbons from the IXTOC-1 blow-out. In: Proceedings of a Symposium, Preliminary Results From the September 1979 Researcher/Pierce IXTOC-1 cruise, 119-67. Bay Biscayne, FL: NOAA Office of Marine Pollution Assessment.

Payne, J.R., B.E. Kirstein, R.F. Shokes, N.L. Guinasso, L. Carver, K.R. Fite, R.E. Jordan, P.J. Mankiewicz, G.S. Smith, W.J. Paplawsky, T.G. Fanara, and J. Lambach. 1981. Multivariant analysis of petroleum weathering in the marine environment-subarctic. Annual Report submittal to National Oceanic and Atmospheric Administration, Juneau, AK.

Payne, J.R., B.D. Kirstein, G.D. McNabb Jr., J.L. Lambach, R.I. Redding, R.E. Jordan, W. Hom, C. deOliveira, G.S. Smith, D.M. Baxter, and R. Gaegel. 1984a. Multivariate analysis of petroleum weathering in the marine environment--subarctic. In: Environmental Assessment of the Alaskan Continental Shelf. Vol. 21 and 22. Juneau, AK: U.S. Department of Commerce, National Oceanic and Atmospheric Administration.

Payne, J.R., G.D. McNabb Jr., B.D. Kirstein, R.I. Redding, J.L. Lambach, C.R. Phillips, L.E. Hachmeister, and S. Martin. 1984b. Development of a Predictive Model for the Weathering of Oil in the Presence of Sea Ice. Final Report submitted to the National Oceanic and Atmospheric Administration, Outer Continental Shelf Environmental Assessment Program. Anchorage, AK.

Payne, J.R., and D. McNabb Jr. 1984. Weathering of petroleum in the marine environment. Mar. Tech. Soc. J. 18(3):24-42.

Payne, J.R., and C.R. Phillips. 1985a. Petroleum Spills in the Marine Environment. The Chemistry and Formation of Water-in--Oil Emulsions and Tar Balls. Chelsea, MI: Lewis Publishers, Inc. 148 pp.

-- 1985b. Photochemistry of Petroleum in Water. Environ. Sci. Tech. 19(7):569-79.

Payne, J.R., C.R.. Phillips, and W. Hom. 1987. Transport and transformations: Water column processes. Background paper for Interagency Committee on Ocean Pollution Research Development and Monitoring; Predictive Assessment for Studies of Long-Term Impacts of OCS Activities. Chauvin, LA: Louisiana Universities Marine Consortium.

Payne, J.R., J.R. Clayton, Jr., G.D. McNabb, Jr., C.R. Phillips, L.E. Hachmeister, B.E. Kirstein, R.T. Redding, C.C. Clary, G.S. Smith. and G.H. Farmer. 1987a. Development of a Predictive Model for the Weathering of Oil in the Presence of Sea Ice. U.S. Dep. Commer., NOAA, OCSEAP Final Rep. 59(1988):147-465.

Payne, J.R., B.E. Kirstein, J.R. Clayton, Jr., C. Clary, R. Redding, G.D. McNabb, Jr., and G. Farmer. 1987b. Integration of Suspended Particulate Matter and Oil Transportation Study. Final Report. Submitted to Minerals Management Service, Environmental Studies, Anchorage, AK. San Diego, CA: Science Applications International Corporation.

Piotrovich, P.P. 1956. Formation of depth-ice. Priroda 9:94-95.

Poirier, O.A., and G.A. Thiel. 1941. Deposition of free oil by sediments settling in sea water. Bull. Am. Assoc. Petrol. Geol. 25:(12)2170-80.

Pope, S.B. 1979. The relationship between the probability approach and particle models for reaction in homogeneous turbulence. Combustion and Flame 35:41-45.

Pope, S.B. 1981. A Monte Carlo method for the PDF equations of turbulent reactive flow. Combustion Science and Technology, 25:159-74.

Pope, S.B. 1982. An improved turbulent mixing model. Combustion Science and Technology, 28:131-45.

Quinn, J.G. In press. Sedimentation of petroleum in the marine environment. Background paper prepared for the National Academy of Science, Petroleum in the Marine Environment. Washington, D.C.: National Academy of Sciences.

Raj, P.K. 1977. Theoretical Study to Determine the Sea State Limit for the Survival of Oil Slicks on the Ocean. U.S. Coast Guard Rpt. CG-61505A.

Raschevsky. 1928. Z. Phys. 46:585.

Reed, M., T.W. Kana, and E.R. Dundlach. Nd. Development testing and verification of an oil spill surf zone mass transport model, June 1988. Final Report. Submitted to the Department of the Interior, Minerals Management Service, Anchorage, AK. Narragansett, RI: Applied Science Associates, Inc.; Columbia, SC: Coastal Science and Engineering, Inc.; and Narragansett, RI: E-Tech, Inc. 178 pp. + 2 appendices.

Reimnitz, E., and K. Dunton. 1979. Diving observations of the soft ice layer under the fast ice at DS-11 in the Steffanson Sound Boulder Patch. In: Environmental Assessment of the Alaskan Continental Shelf, Principal Investigators' Reports, March 1979. National Oceanic and Atmospheric Administration. 9:210-30.

Reimnitz, E., and E.W. Kempema. 1987. Field observations of slush ice generated during freeze-up in Arctic coastal waters. Mar. Geol. 77:219-31.

Reimnitz, E., E.W. Kempema, and P.W. Barnes. 1986. Anchor ice and bottom freezing in high-latitude marine sedimentary environments: observations from the Alaskan Beaufort Sea. U.S. Geological Survey Open-File Report 86-298. 17 pp.

-- 1987. 'Anchor ice, seabed freezing, and sediment dynamics in shallow Arctic seas. J. Geophys. Res. 92:14,671-78.

-- In press. Effects of anchor ice and seabed freezing on sediment dynamics in shallow Arctic seas. J. Geophys. Res. 19 pp.

Reineck, H.E., and I.B. Singh. 1980. Depositional Sedimentary Environments. Berlin: Springer-Verlag. 549 pp.

Rohm and Haas Company. 1979. Amberlite Ion Exchange Resins Laboratory Guide. Philadelphia: Rohm and Hass Company.

Rudolfo, K.S. 1970. Annual suspended sediment supplied to the California continental borderland by the southern California watershed. J. Sed. Petrol. 40:666-71.

Sabljic', A. 1987. On the prediction of soil sorption coefficients of organic pollutants from molecular structure: Application of molecular topology model. Environ. Sci. Tech. 21:358-66.

Sadd, J.L., E.R. Gundlach, W. Ernst, and G.I. Scott. 1980. Distribution, size, and oil content of tar mets and the extent of buried oil along the South Texas Shoreline. In: Research Planning Institute Report to the National Oceanic and Atmospheric Administration, 14-20. Boulder, CO: Office of Marine Pollution Assessment.

Saffman, P.G., and J.S. Turner. 1956. On the collision of drops in turbulent clouds. J. Fluid Mech. 1:16.

Schaefer, V.J. 1950. The formation of frazil and anchor ice in cold water. Trans. Am. Geophys. Union 31:885-93.

Schubel, J.R. 1974. Effects of tropical storm Agnes on the suspended solids of northern Chesapeake Bay. In: Suspended Solids in Water, ed. R.J. Gibbs, 113-32. New York: Plenum Press.

Seuss, E. 1968. Calcium carbonate interactions with organic compounds. Ph.D. thesis. Bethlehem, PA: Leheigh University.

Sharma, G.D., F.F. Wright, J.J. Burns, and P.C. Burbank. 1974. Sea surface circulation, sediment transport, and marine mammal distribution, Alaska Continental Shelf. ERTS Final Report, Natl. Tech. Serv. Report E74-10711.

Shaw, D.G. 1977. Hydrocarbons in the water column. In: Fates and Effects of Petroleum Hydrocarbons in Marine Ecosystems and Organisms, ed. D.A. Wolfe. N.p.

Shoemaker, D.P., and C.W. Garland. 1962. Experiments in Physical Chemistry. New York: McGraw-Hill.

Shonting, D. H., P. Temple, and J. Roklan. 1970. The Wind Wave Turbulence Observation Program (WAVTOP). U.S. Coast Guard Report. CG-D-68-79.

Siebert, P.C. 1979. Simple sedimentation methods, including the Andreason pipette and the Cahn sedimentation balance. In: Particle Size Analysis, ed. J.D. Stockham and E.G. Fochtman, 45-55. Ann Arbor, MI: Ann Arbor Science Publishers, Inc.

Smith, J.D., and S.R. McLean. 1977a. Spatially averaged flow over a wavy surface. J. Geophys. Res. 32:1735-46.

-- 1977b. Boundary layer adjustments to bottom topography and suspended sediment. In: Bottom Turbulence, ed. J.C.J. Nihoul, 123-52. The Netherlands: Elsevier Scientific Publishing Co.

Smoluchowski, M. 1916. Z. Physik Chemie. XCII:129.

Sobey, R.J. 1986. Wind-wave prediction. Ann. Rev. Fluid Mech. 18:169-72.

Sokal, R.R., and F.J. Rohlf. 1981. Biometry. San Francisco: W.H. Freeman and Co.

Stackelburg, W., Klockner and Mohrhauer. 1949. Kolloidzschr 115:53.

Steen, W.C., D.F. Paris, and G.L. Baughman. 1978. Partitioning of selected polychlorinated biphenyls to natural sediments. Water Res. 12:655.

Stewart, R.W., and H.L. Grant. 1962. The determination of the rate of dissipation of turbulent energy near the sea surface in the presence of waves. J. Geophys. Res. 67(8):3177.

Straughn, D. 1977. Biological survey of intertidal areas in the straits of Magellan in January, 1975, five months after the Metula oil spill. In: Fate and Effects of Petroleum Hydrocarbons in Marine Organisms and Ecosystems, ed. D.A. Wolfe, 247-60. Elnsford, NY: Pergamon Press.

Sutton, C., and J.A. Calder. 1974. Solubility of higher-molecular-weight n-paraffins in distilled water and seawater. Environ. Sci. Tech. 8:654-47.

-- 1975. Solubility of alkylbenzenes in distilled water and seawater at 25.0°C. J. Chem. Engr. Data 20:320-22.

Tsang, G. 1982. Frazil and anchor ice: a monograph. Ottawa, Canada: National Research Council Subcommittee on Hydraulics of Ice Covered Rivers.

Tsang, G., and T. O'D. Hanley. 1985. Frazil formation in water of different salinities and supercoolings. J. Glaciology 31:74-85.

Uhlmann, D.R., B. Chalmers and K.A. Jackson. 1964. Interaction between particles and a solid-liquid interface. J. Appl. Phys. 35:2986-93.

Venkatesan, N.I., M. Sandstrom, S. Brenner, E. Ruth, J. Bonilla, I.R. Kaplan, and W.E. Reed. 1981. Organic geochemistry of surficial sediments from the eastern Bering Sea. In: The Eastern Bering Sea Shelf: Oceanography and Resources, ed. D.W. Hood and J.A. Calder, 389-409. Washington, D.C.: U.S. Department of Commerce.

Wade, T.L. and J.G. Quinn. 1980. Incorporation, distribution and fate of saturated petroleum hydrocarbons in sediments from a controlled marine ecosystem. Marine Environmental Research, 3: 15-33.

Walker, H.J. 1974. The Colville River and the Beaufort Sea: Some interactions. In: The Coast and Shelf of the Beaufort Sea, ed. J.C. Reed and J.E. Sater, 513-539. Arlington, VA: Arctic Institute of North America.

Wallace, R.B., T.M. Rushlow, and R.J.B. Bouwmeester. 1986. In situ measurement of oil droplets using an image processing system. In: Proceedings of the Ninth Arctic Marine Oil Spill Program Technical Seminar, 421-31. Department of Civil and Environmental Engineering, Michigan State University.

Weeks, W.F., and S.F. Ackley. 1982. The growth, structure, and properties of sea ice. CRREL Monograph 82-1. Hanover, NH: Cold Regions Research and Engineering Laboratory. 130 pp.

White, S.J. 1970. Plane bed thresholds of find grained sediments. Nature 228:152-53.

Wiberg, P., and J.D. Smith. 1983. A comparison of field data and theoretical models for wave-current interactions at the bed on the continental shelf. Continental Shelf Res. 2:147-62.

Wigle, T.E. 1970. Investigations into frazil, bottom ice, and surface ice formation in the Niagara River. In: Proceedings of the Symposium on Ice and Its Action on Hydraulic Structures. Reykjavik, Iceland: International Association for Hydraulic Research. Paper No. 2.8. 16 pp.

Wilson D.J. and D. Mackay. 1986. Behavior of oil in freezing situations. Department of Chemical Engineering and Applied Chemistry, University of Toronto. 65 pp.

Winters, J.K. 1978. Fate of petroleum derived aromatic compounds in seawater held in outdoor tanks. In: South Texas Outer Continental Shelf BLM Study, Ch. 12. Washington D.C.: Bureau of Land Management.

Wiseman, W.J., Jr. 1979. Hypersaline bottom water: Peard Bay, Alaska. Estuaries 2:189-93.

Wolfe, D.A. 1987. Interactions of spilled oil with suspended materials and sediments in aquatic systems. In: Fate and Effects of Sediment-Bound Chemicals in Aquatic Systems, ed. K.L. Dickson, A.W. Maki, and W.A. Brungs, New York: Pergamon Press.

Wotherspoon, P., G. Swiss, R. Kowalchuk, and J. Armstrong. 1985. Oil and ice computer model. Final Report to the Environmental Studies Revolving Funds, Ottawa, Canada. Report #012. Calgary, Canada: Vendome Petroleum Ltd.

Zurcher, F., and M. Thuer. 1978. Rapid weathering processes of fuel oil in natural waters: Analyses and interpretations. Environ. Sci. Tech. 12:838-43.

APPENDIX A

SPM MINERALOGICAL DATA

THE X-RAY DIFFRACTION ANALYSES OF 3 ALASKAN SILT SAMPLES

INTRODUCTION

Three samples of Alaskan silt were received in the laboratory for X-ray diffraction analysis. It was requested that the mineral phases present in the silt samples be determined by this method. The following report represents the results of the studies and is respectfully submitted.

SAMPLES

Samples were received with the following designations:

1. Yukon Delta Sediment, <53 microns
2. Grewingk Glacial Till, <53 microns
3. Turnagain Arm SPM

SAMPLE PREPARATION AND STUDY METHODS

As these samples were received as fine powders, no preparation was necessary other than drying the samples and packing them into standard holders which were run in a Philips Electronics X-ray diffractometer equipped with a crystal monochrometer. The operating conditions are marked on the enclosed X-ray diffraction charts.

X-ray diffraction is a crystal structure analysis method using the atomic arrays within the crystals as a three dimensional diffraction grating to diffract a monochromatic beam of X-rays. The angles at which the beam is diffracted are used to calculate the interplanar atomic spacings (d-spacings) giving information about how the atoms are arranged within the crystalline compounds. These patterns are compared to over 50,000 data entries in the powder diffraction file.

In order to identify some of the minor phases, additional studies were made using gravimetric techniques to separate the fine fractions, especially to determine if possible clay phases were present. This was done by settling out the larger than 10 micron fraction, then concentrating the less than 10 micron fraction that remained in suspension, this fraction was allowed to dry on a piece of microscope slide into an oriented layer. After running these preparations through the diffractometer, they were additionally studied after heating to 500 degrees C.

DISCUSSION

The enclosed X-ray diffraction charts are marked with the interplanar atomic spacing measurements (d-spacings) in angstrom units and with the corresponding Miller Index (hkl) of the crystallographic plane causing each reflection. Phase identification was made by comparison with standard data in the JCPDS/ASTM diffraction files.

The samples are fairly similar with alpha-quartz and feldspar as the major constituents and minor amounts of both mica and a chlorite mineral. A few minor unidentified peaks are also found which indicate the presence of an unknown phase. Severe interference from other peaks prevent complete identification. A summary of the X-ray diffraction data is presented on the next page.

TURNAGAIN

This sample contains minor phases of both CHLORITE and an ILLITE clay derivative of mica. The analysis of these silts was not straight forward. It was at first thought a kaolinitic clay was present by the peak at 12.2 angstroms, but heat treatment at 500 degrees C failed to decompose the clay into the amorphous meta-kaolin (compare XRD charts #79857 and #79859). This fact and the presence of the 14 angstrom peak which did not shift to a smaller value upon heating (indicative of montmorillonite clay) confirmed CHLORITE as the preferred identification. The remainder of the peaks appear to match the amphibole mineral, HORNBLENDE, in addition to the quartz and feldspar.

GREWINGK GLACIAL TILL

A strong minor amount of a chlorite mineral is found in this sample in addition to the major quartz and feldspar concentrations. A minor amount of illite is also present along with a trace of the horneblende amphibole.

YUKON DELTA SEDIMENT

This sample is different as compared to the two samples. This Yukon silt has only a trace of the chlorite mineral. Even an oriented sample did not show enough of a chlorite pattern for a definitive identification. This sediment also appears to have two different feldspar group minerals. The major form is the plagioclase form found in the other two samples. LABRADORITE shows the closest match to this pattern. A lesser amount of a potassium feldspar such as MICROCLINE or SANDINE appears to be present. In Sandine a portion of the potassium is relaced by sodium. Interference by the other patterns makes it impossible to differentiate between these two forms.

SUMMARY OF THE X-RAY DIFFRACTION DATA

SAMPLE	ALPHA-QUARTZ	FELDSPAR	CHLORITE	MICA	OTHER
Turnagain	Major	Intermediate +	Minor	Minor	Hornblende - Minor
Yukon	Major	Intermediate +	Trace ?	Trace	Sanadine/Microcline Intermediate
Grewingk	Major	Intermediate +	Minor +	Trace	Hornblende - Trace

d=1.68Å α-QUARTZ (202)
d=1.78Å
d=1.81Å α-QUARTZ (003)
d=1.83Å α-QUARTZ (112)
d=1.87Å
d=1.97Å α-QUARTZ (201)
d=2.13Å α-QUARTZ (200)
d=2.23Å α-QUARTZ (111)
d=2.30Å α-QUARTZ (102)
d=2.34Å
d=2.40Å CHLORITE
d=2.49Å α-QUARTZ (110)
d=2.75Å FELDSPAR (241)
d=2.48Å
d=2.98Å
d=3.35Å CHLORITE (005)
d=3.17Å FELDSPAR (041)
d=3.03Å FELDSPAR (131)
d=3.24Å FELDSPAR (220)
d=3.53Å CHLORITE (004)
d=3.70Å FELDSPAR
d=3.81Å FELDSPAR
d=3.91Å FELDSPAR (111)
d=4.09Å FELDSPAR (201)
d=4.28Å α-QUARTZ (101)
d=4.53Å
d=4.98Å CHLORITE (003)
d=5.09Å MICA (ω)
d=6.55Å FELDSPAR (110)
d=7.23Å CHLORITE (002)
d=8.67Å HORNBLENDE (020)
d=10.39Å MICA (001)   ILLITE
d=14.7Å CHLORITE (001)

20°2θ
40°2θ
60°2θ
30°2θ
20°2θ
10°2θ

d=1.50Å

60°2θ d=1.54Å α - QUARTZ (211)

d=1.67Å α - QUARTZ (203)

d=1.70Å

50°2θ d=1.82Å α - QUARTZ (112)

d=1.85Å

d=1.88Å CHLORITE (151), (205)

d=1.98Å α - QUARTZ (201)

d=2.01Å CHLORITE (137), (204)

d=2.13Å α - QUARTZ (200)

d=2.16Å HORNBLEND (351)

40°2θ d=2.28Å α - QUARTZ (111)

d=2.28Å α - QUARTZ (102)

d=2.40Å CHLORITE (153), (204)

d=2.46Å α - QUARTZ (110)

d=2.56Å FELDSPAR (241), CHLORITE (132), (042)

d=2.60Å CHLORITE (151), (204)

d=2.62Å

d=2.71Å HORNBLEND (151)

d=2.82Å CHLORITE (015)

30°2θ d=2.95Å FELDSPAR (041)

d=3.00Å FELDSPAR (131)

d=3.18Å FELDSPAR (002)

d=3.34Å α - QUARTZ (101)

d=3.41Å FELDSPAR (112)

d=3.53Å CHLORITE (004)

d=3.66Å FELDSPAR (131)

d=3.77Å FELDSPAR (111)

d=3.86Å FELDSPAR (111)

d=4.02Å FELDSPAR (201)

d=4.25Å α - QUARTZ (100)

10°2θ d=4.48Å MICA (110)

d=4.72Å FELDSPAR (021), CHLORITE (003)

d=5.01Å MICA (004)

d=6.37Å FELDSPAR (020)

d=7.08Å CHLORITE (001)

d=10.28Å MICA (002)

TECHNOLOGY OF MATERIALS

341

d = 1.37Å α - QUARTZ (301)

d = 1.39Å α - QUARTZ (212)

d = 1.42Å α - QUARTZ (302)

d = 1.45Å α - QUARTZ (113)

d = 1.52Å

60°2θ   d = 1.54Å α - QUARTZ (211)

d = 1.57Å

d = 1.67Å α - QUARTZ (202)

d = 1.71Å
d = 1.74Å

50°2θ   d = 1.82Å α - QUARTZ (112)

d = 1.85Å
d = 1.88Å

d = 1.98Å α - QUARTZ (201)
d = 2.0Å

d = 2.13Å α - QUARTZ (203)

d = 2.12Å SANIDINE (060)

40°2θ   d = 2.23Å α - QUARTZ (111)

d = 2.22Å α - QUARTZ (102)

d = 2.34Å

d = 2.45Å α - QUARTZ (110)

d = 2.51Å FELDSPAR (224)

d = 2.56Å

d = 2.70Å DIOPSIDE AUGITE ROOM

d = 3.00Å SANIDINE (022)
d = 2.92Å FELDSPAR (041)
d = 2.90Å SANIDINE (13)

30°2θ

d = 3.18Å FELDSPAR (002)

d = 3.26Å SANIDINE (202),(220)

d = 3.5Å
α - QUARTZ (15)

d = 3.46Å FELDSPAR (112)

d = 3.67Å FELDSPAR (131)

d = 3.78Å FELDSPAR (111)   SANIDINE (13)

d = 4.02Å FELDSPAR (201)

d = 4.23Å α - QUARTZ (100)

20°2θ   d = 4.44Å MICA (001)

TECHNOLOGY OF MATERIALS

342

343

This Report No. 884201-D1-7/8 is hereby respectfully submitted to SAIC and has been authorized by P.O. #5278019.

TECHNOLOGY OF MATERIALS

By _____
William E. Gardner
Laboratory Director

WEG/jb

April 19, 1988.

THE X-RAY DIFFRACTION ANALYSIS OF FIVE SEDIMENTS

INTRODUCTION

Five sediment samples were received in the laboratory for X-ray diffraction analysis. It was requested that the mineral phases present in the silt samples be determined by this method. The following report represents the results of the studies and is respectfully submitted.

SAMPLES

Samples were received with the following designations:

1. 882130-05A Beauford Sea
2. 882130-06A Jakolöf
3. 882130-07A Peard Bay
4. 882130-08A Prudhoe Bay
5. S82130-09A Kotzebue

SAMPLE PREPARATION AND STUDY METHODS

Initial studies were made of the as-received sediments. As they were received as the less-than 53 micron fraction, no preparation was necessary for this study other than drying the samples and packing them into standard holders which were run in a Philips Electronics X-ray diffractometer equipped with a crystal monochrometer. The operating conditions are marked on the enclosed X-ray diffraction charts.

In order to identify some of the minor phases, additional studies were made. Acetone slurries of the sediments were were allowed to dry on pieces of microscope slides into oriented layers. After running the X-ray diffraction scans of the as-received preparations,

they were additionally studied after heating to 550 degrees C, then run again in the diffractometer.

In order to differentiate between the montmorillonite clays and the chlorites, additional studies were made by exposing the heat-treated, oriented preparations to ethylene glycol vapor for 24 hours to determine if the (001) layer expansion occurred, indicative of the montmorillonite group.

DISCUSSION

The enclosed X-ray diffraction charts are marked with the interplanar atomic spacing measurements (d-spacings) in angstrom units and with the corresponding Miller Index (hkl) of the crystallographic plane causing each reflection. Phase identification was made by comparison with standard data in the JCPDS/ASTM diffraction files.

The samples are fairly similar with alpha-quartz as the major constituent with lesser amounts of other minerals such as feldspar, kaolinite, mica and a chlorite mineral. The heat-treatment studies allowed differentiation of the kaolinite in the presence of chlorite. Kaolinite becomes the amorphous meta-kaolin between 500 and 600 degrees C. This effect is clearly observed in XRD charts 80313 vs. 80329.

At a temperature of 550 degrees C, the peak occuring at 14A should collapse due to inter-layer water loss if this peak is caused by

montmorillonite. The dehydrated montmorollinite then should produce a peak at 9A which can be re-expanded to 17A by absorbing ethlene glycol. This peak shift did not occure, identifying the 14 A peak as entirely due to chlorite.

No hornblende or related amphibole minerals were found in any of these sediments. A summary of the X-ray diffraction data is presented on the next page. However a few comments will be made pertaining to specific sediments.

Beauford Bay

This sample contains minor to intermediate amounts of both an ILLITE clay derivative of mica and a CHLORITE mineral. The identification of the illite clay was made possible by the oriented study, as relatively strong peaks other than those caused by (00ℓ) reflections were found. This would not occur in the oriented studies with the more ordered mica minerals. Heat-treating the sediment caused a noticeable attenuation of the 7.1A peak due to meta-kaolinite formation, indicating that both KAOLINITE clay and CHLORITE contribute to this 7A reflection.

Peard Bay

This sediment is similar to the the other samples with a minor to intermediate concentration of chlorite along with the high quartz content. Illite concentration in this sample is only a trace to minor concentration. A minor amount of OLIVINE, $(Mg,Fe)_2SiO_4$, may

also be present in this sediment, however certainty cannot be assigned on the presence of only the peak at d=2.78A.

Prudhoe Bay

An intermediate amount of CALCITE ($CaCO_3$) and a minor amount of the related carbonate mineral, DOLOMITE, $CaMg(CO_3)_2$ are are both found only in this sediment. Chlorite and illite are both found as minor constituents along with the greater amount of kaolinite which is found in this sediment.

Kotzebue

The highest chlorite content was found in this sediment. Slight attenuation of the 7.12A peak after heat-treatment indicates a minor concentration of kaolinite is also contained in this sample. A minor amount of olivine may also be present in this sediment along with the more significant quartz and feldspar content.

The Jakalof sediment is similar to the other samples, however it contains only a trace of illite.

SUMMARY OF THE X-RAY DIFFRACTION MINERALOGY

SAMPLE	–QUARTZ	FELDSPAR	CHLORITE	ILLITE	KAOLITE	OTHER
Beauford Sea - 05A	Major	Minor+	Minor+	Minor+	Intermed.	–
Jakalof -06A	Major	Intermed.	Minor	Trace	Minor	–
Peard Bay -07A	Major	Minor	Minor+	Minor-	Minor	Olivine?
Prudhoe Bay-08A	Major	Minor+	Minor	Minor+	Minor+	Calcite(Intermed.) Dolomite(Minor+)
Kotzebue -09A	Major	Intermed.	Intermed.	Minor+	Minor	Olivine?

350

351

d=1.82Å α-Quartz (112)

d=2.12Å α-Quartz (211)

d=2.24Å α-Quartz (111)
d=2.28Å α-Quartz (202)

d=2.39Å Chlorite (132)

d=2.46Å α-Quartz (110)

d=2.57Å Chlorite

d=2.79Å Quartz?

d=2.99Å Feldspar (131)

d=3.21Å Feldspar (040)

d=3.35Å
α-Quartz (101)

d=3.11Å
d=3.49Å Chlorite/Kaolinite
d=3.67Å Feldspar
d=3.77Å Feldspar
d=3.94Å Feldspar
d=4.11Å Feldspar

d=4.26 α-Quartz (100)

d=4.47Å Illite (020)(110)

d=4.71Å Chlorite

d=5.0 Illite (001)

d=7.1 Chlorite/Kaolinite (002)/(001)

d=10 Illite (001)

d=14 Chlorite (001)

352

d=4.252 α-Quartz (201)

d=1.604 Calcite (1.17)

d=4.252 α-Quartz (001)

d=3.348 α-Quartz (112)

d=3.034 Calcite (116)
d=3.034 Calcite (100)

d=1.932 α-Quartz (200)
d=1.977

d=2.285 Calcite (211)
d=2.457 α-Quartz (205)

d=2.81 Dolomite
d=2.282 α-Quartz (111)
d=2.282 α-Quartz

d=2.458 α-Quartz (102)
d=2.285 Calcite (116)
d=3.035 Calcite (130)(Ar)

TECHNOLOGY OF MATERIALS
X-RAY DIFFRACTION JPL
X-RAY SPECTROGRAPHIC

Sample: Precalor Bay

d=3.035 Dolomite

d=3.035 Calcite (204)

d=3.343 Feldspar (040)

d=3.343 α-Quartz 0.

d=4.5 Kaolinite (002)

d=3.034 Calcite (1.11)
d=4.04 Feldspar (201)

d=4.252 α-Quartz (100)
d=4.57

d=4.457 Kaolinite (001)

d=3.59 ZZ (112)(201)

d=7.149 Kaolinite (001)

d=4 ZZ Mica (001)

354

d = 1.376Å α-Quartz(203), (301)
d = 1.382Å α-Quartz(201)

d = 1.418Å α-Quartz(300)

d = 1.453Å α-Quartz(113)

d = 1.541Å α-Quartz(211)

d = 1.661Å α-Quartz(103)
d = 1.674Å α-Quartz(202)

d = 1.804Å α-Quartz(003)
d = 1.817Å α-Quartz(112)

d = 1.910Å

d = 1.980Å α-Quartz(102)

d = 2.13Å α-Quartz(110)

d = 2.241Å α-Quartz(111)
d = 2.281Å α-Quartz(102)

d = 2.281Å Calcite(104)
d = 2.46Å α-Quartz(101)
d = 2.570Å

d = 2.57Å Chlorite/Kaolinite

d = 2.77Å Olivine?
d = 2.99Å Illite(110), Chlorite(005)

d = 3.09Å Feldspar(137)

d = 3.20Å Feldspar(204)

α-Quartz(101)

d = 3.57Å Kaolinite/Chlorite

d = 4.04Å Feldspar

d = 4.27Å α-Quartz(100)

d = 4.5Å Chlorite/Kaolinite
d = 4.70Å Chlorite(001), (002)
d = 5.03Å Illite(002)

d=1.542Å α-Quartz

d=1.672Å α-Quartz (203)

d=1.817Å α-Quartz (112)

d=1.962Å α-Quartz

d=2.12Å α-Quartz (200)

d=2.24Å α-Quartz (200)
d=2.23Å α-Quartz (111)
d=2.28Å α-Quartz (102)

d=2.39Å Chlorite (113)

d=2.45Å α-Quartz (112)

d=2.56Å Chlorite/Kaolinite

d=2.97Å Calcite (005), Illite (114)

d=3.03Å

d=3.17Å Feldspar (040)

d=3.34Å α-Quartz (101)

d=3.55Å Chlorite/Kaolinite

d=4.26Å α-Quartz (100)

d=4.48Å Illite (110),(020)

d=4.74Å Chlorite

d=9.99Å Illite (001)

d=7.14Å Chlorite/Kaolinite (002)(001)

d=9.9Å Illite (001)

356

This Report No. 888011-D1-12 is hereby respectfully submitted to SAIC and has been authorized by P.O. #5336451.

TECHNOLOGY OF MATERIALS

By _William E. Gardner_
William E. Gardner
Laboratory Director

WEG/amg

November 8, 1988

APPENDIX B

FIELD VALIDATION STUDIES OF OIL WEATHERING
RELATED TO THE EXXON VALDEZ OIL SPILL

Field Validation Studies of Oil Weathering
Related to the EXXON VALDEZ Oil Spill

1.0 INTRODUCTION

Since the Trans-Alaska pipeline commenced operation in 1977, activities related to both drilling operations and commercial transport have provided the potential for large-scale releases or spills of oil into coastal environments of Alaska. Until recently, the lack of sizeable accidents or mishaps involving spills has been noteworthy. However, on 24 March 1989 the EXXON VALDEZ oil tanker became grounded on Bligh Reef near the port of Valdez. Following rupture of cargo tanks in the vessel, more than 10 million gallons of Prudhoe Bay crude oil were released into the marine waters of Prince William Sound. Within the first week following the incident, oil had impacted an area of approximately 900 square miles in the Sound to the southwest of the site of the grounding. With time, substantial portions of the oil also moved out of the Sound and impacted coastal waters further southwest along the Kenai Peninsula, Kodiak Island, and even areas as far as the Aleutian Islands.

In anticipation of the possibility of major oil spills in arctic and subarctic marine waters of Alaska, SAIC has been responsible for conducting numerous programs for NOAA OCSEAP and MMS to evaluate and develop numerical models describing the behavior of oil released into coastal marine environments. Major emphasis and interest in these programs has been directed toward scenarios for potential releases of oil into Alaskan waters. Titles of Final Reports produced by SAIC during the conduct of these programs have included: 1) Multivariate Analysis of Petroleum Weathering in the Marine Environment---Sub Arctic (Payne et al., 1984a), 2) Development of a Predictive Model for the Weathering of Oil in the Presence of Sea Ice (Payne et al., 1984b), 3) Development of a Predictive Model for the Weathering of Oil in the Presence of Sea Ice (Payne et al., 1987a), 4) Integration of Suspended Particulate Matter and Oil Transportation Study (Payne et al., 1987b), and 5) Oil/Ice/Sediment Interactions During Freezeup and Breakup (Payne et al., the current report). In particular, major analytical and modeling efforts in these programs have included the following:

- detailed investigations of temporal changes in the chemical and physical properties of oil released into marine waters (e.g., composition and rheological properties of the oil),

- the effect that these changes have on the behavior and fate of the oil,

- interactions of oil and suspended particulate material (SPM) in a water column as functions of 1) the type and degree of prior weathering of the oil, 2) the type of particulate material, 3) the salinity of the water, and 4) the level of turbulence, and

- effects of oil/SPM interactions on sedimentation rates of SPM and oil as functions of 1) the extent of oil/SPM interactions, 2) the type of particulate material, and 3) the salinity of the water.

Laboratory components in the programs have normally involved experimental efforts on size scales ranging from routine laboratory vessels (e.g., ≤ 10 L) to 2800-L flow-through seawater wavetanks. Results from these relatively "small-scale" experimental setups have provided necessary numerical data and insight into the behavior of spilled oil. Information from the experiments has then been used to support and verify aspects of the numerical models developed for predicting the behavior of spilled oil.

In the context of the programs performed by SAIC, it has not been possible to test aspects of the models on scales larger than that of the 2800-L wavetanks. However, a spill-of-opportunity of large-scale proportions did become available for investigating and/or corroborating aspects of the laboratory and wavetank experiments with the grounding of the EXXON VALDEZ and the release of more than 10 million gallons of Prudhoe Bay crude oil into the waters of Prince William Sound. With the support of NOAA OCSEAP in Anchorage, SAIC did mobilize and initiate a field-sampling effort for studies in the Prince William Sound area within three weeks of the spill incident. Results of the field study are included in this appendix.

2.0 METHODS AND MATERIALS

To provide a necessary support platform for both collection and initial processing of samples, the NOAA Launch 1273 was transported by NOAA OCSEAP from Prudhoe Bay to Valdez (AK) in early April 1989. Samples for oil analyses were subsequently collected in the field by three SAIC scientists (J. Payne, J.

Clayton, and D. McNabb) and the NOAA skipper of Launch 1273 (Lt. Cmdr. Pat Harman) from 12-15 April 1989. Locations selected for collections of samples were based primarily on precruise overflight surveys and real-time information from NOAA HAZMAT support personnel in Valdez regarding locations of oil in the Prince William Sound area.

Three types of field samples were collected for analyses of oil during the cruise: 1) bulk oil samples, 2) water column samples, and 3) surficial flocculant layer of sediment samples in shallow, nearshore areas. Bulk oil samples were collected from both surface slicks on the water as well as exposed intertidal beach areas. Samples of oil on the water's surface (i.e., mousse and/or sheen) were obtained by "skimming" the oil from the surface into precleaned glass containers. Oil samples from exposed beach areas were collected into precleaned glass containers with stainless steel or teflon-coated utensils. All bulk oil samples were stored in screw-cap glass containers with aluminum-foil cap liners. For hydrocarbon content and composition determinations, a known weight of an oil sample was dissolved in methylene chloride and analyzed by FID-GC (see below).

Water column samples were collected with a 10-L G/O sampling bottle (General Oceanics) attached to a metal hydrowire cable. The sampling bottle was initially passed through the air-water interface in a closed configuration, opened at depth for sample collection, and closed before retrieval through the water's surface. Determinations of salinity in water samples were made with a Reichert temperature-compensated refractometer. The filtration technique described in Section 4.2.7 of this report was used onboard the NOAA Launch 1273 to separate whole-water samples into two fractions: 1) a "dissolved" fraction and (2) a "suspended particulate material (SPM)/dispersed oil droplet" fraction. Briefly, the procedure involved initial vacuum filtration of a known volume of a water sample through a previously tared (at Kasitsna Bay) polyester membrane filter (0.4 μm pore size). The aqueous filtrate, designated as the dissolved fraction of the sample, was subsequently back-extracted with methylene chloride to recover dissolved hydrocarbons. Following filtration of the dissolved fraction, the filter was immediately subjected to additional vacuum filtration with 1) distilled water (to remove residual sea salts), 2) methanol, and 3) methylene chloride. The methanol and methylene chloride

filtrates were combined to form the SPM/dispersed oil fraction of the sample, which was subsequently analyzed for SPM/dispersed hydrocarbons by FID-GC (on return to Kasitsna Bay following the cruise). The solvent-rinsed polyester filter was subsequently maintained in a desiccator until a final gravimetric weight measurement could be made at Kasitsna Bay to determine the total particulate load in the initial whole-water sample.

Samples of surficial flocculant layers of sediment from shallow, nearshore areas were collected by lowering precleaned teflon tubing to near the sediment-water interface. Vacuum suction was applied to the tubing to retrieve fine-grained particulate material from the sediment surface into a precleaned 5-gal glass carboy. The pump used to generate suction for the sampling apparatus was located downstream of the carboy. Following collection, a subsample of the surface sediment sample was processed with the polyester filtration technique described above to obtain an SPM/dispersed hydrocarbon fraction as well as the total particulate load extracted for the sample.

The following rheological properties were determined for bulk oil samples collected during the cruise: 1) kinematic viscosity, 2) oil/water and oil/air interfacial surface tension, 3) density, and 4) water content. Viscosity measurements were performed at 38°C (100°F) with a Fisher Scientific Viscometer, No. A97. Interfacial surface tension measurements were determined with a Surface Tensiomat, Model 21 (Fisher Scientific Co.). Density was determined by measuring the weight of a known volume of an oil sample (measurements being made at oil temperatures of 7°-18°C). Determinations of water content in oil samples of unweathered Prudhoe Bay crude and EXXON VALDEZ cargo crude were made by Karl Fisher titration. Azeotropic distillations (ASTM Method D-95) were used for water content measurements in all field samples of oil collected during the cruise because of the high water content in the samples.

Hydrocarbon content and composition in sample extracts (i.e., dissolved and SPM/dispersed fractions of water and surface sediment samples as well as bulk oil samples) were determined by flame-ionization-detector gas chromatography (FID-GC). All GC analyses were performed on a Hewlett-Packard 5840A gas chromatograph located at the University of Alaska/NOAA field

laboratory at Kasitsna Bay, AK. Quantities of paraffinic hydrocarbon compounds in sample extracts were determined by comparison to a standard solution containing n-alkanes with even- and odd-numbers of carbon atoms from n-C_{12} through n-C_{32} plus the isoprenoid compounds pristane and phytane. Polynuclear aromatic hydrocarbons (PAHs) were determined by comparison to a standard solution containing 2-ring through 5-ring aromatic compounds from naphthalene to benzo[ghi]perylene.

3.0 RESULTS

3.1 SAMPLING LOCATIONS AND CRUISE OBSERVATIONS

Sampling efforts were centered in the western portion of Prince William Sound for purposes of directing studies toward areas that were most heavily impacted by oil released from the EXXON VALDEZ. Selections of specific sampling sites were based in large part on reliable information about locations of oil that were supplied by NOAA HAZMAT team overflights and observations prior to and during the cruise. In addition, areas were selected where potential SPM loads in the water column might be slightly elevated (e.g., near glacial sources and shallow bays fed by freshwater streams) compared to the extremely clean and deeper open waters in Prince William Sound. The actual sampling locations (shown in Figure B-1) were concentrated in 5 areas: 1) Herring Bay on the west side of Knight Island, 2) Northwest Bay on Eleanor Island, 3) the open-water passage between Naked and Eleanor Islands, 4) near the face of the Nellie Juan Glacier in Port Nellie Juan, and 5) near the face of the Columbia Glacier in Columbia Bay. A summary of the sampling locations, times and types of samples collected in Prince William Sound is presented in Table B-1. As indicated, three types of samples were collected: 1) bulk oil samples (designated by the letter "M") from either the water's surface or exposed beach faces; 2) water column samples that were separated into dissolved ("A") and suspended particulate/dispersed oil ("DP") fractions; and 3) surficial flocculant layer of sediment samples ("N") in shallow, nearshore areas. In addition to the samples collected in Prince William Sound, a surface oil sample was obtained by the fishing vessel MAD VIKING on 19 April 1989 from water approximately one mile off Point Adam on the west end of the Kenai Peninsula.
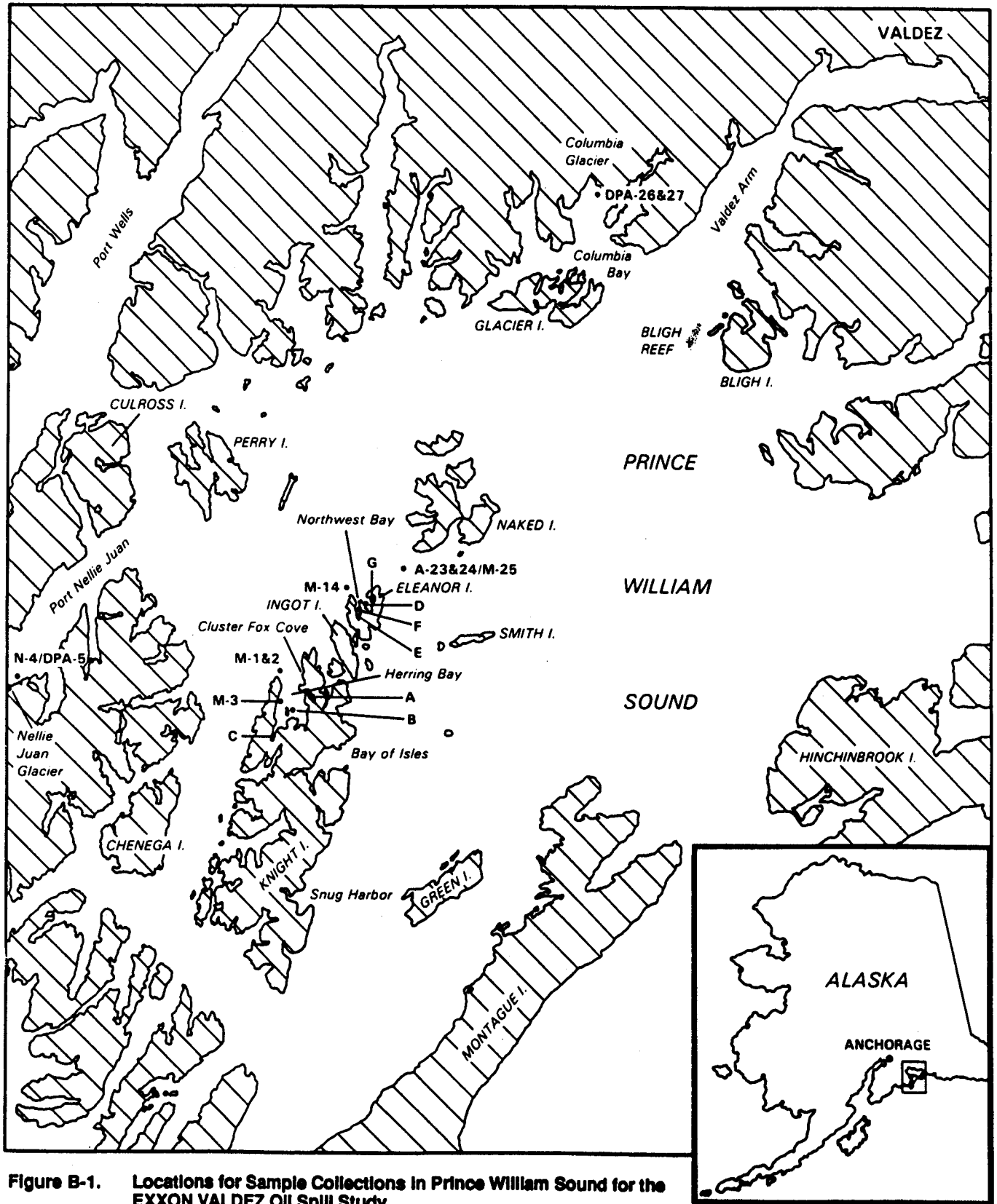
Figure B-1. **Locations for Sample Collections in Prince William Sound for the EXXON VALDEZ Oil Spill Study**

Table B-1

Locations and Types of Samples Collected During the EXXON VALDEZ Oil Spill Study

oil	water	sed	sampling depth (m)	location	date	time	general comments
	DPA-5		1	face of Nellie Juan Glacier	13-Apr-89	9:00	
		N-4	5	face of Nellie Juan Glacier	13-Apr-89	9:30	surface flocculent layer/sediment sample
M-1			0	Herring Bay, Knight Is.	13-Apr-89	13:25	mousse sample from surface of water
M-2			0	Herring Bay, Knight Is.	13-Apr-89	13:30	mousse sample from surface of water
M-3			0	Herring Bay, Knight Is.	13-Apr-89	14:00	sheen sample from surface of water
	DPA-6		1	Cluster Fox Cove, Herring Bay	13-Apr-89	17:30	near FW runoff; oiled adjacent beach
		N-7	3	Cluster Fox Cove, Herring Bay	13-Apr-89	18:00	surface flocculent layer/sediment sample
M-8			-	Cluster Fox Cove, Herring Bay	13-Apr-89	19:00	bulk oil from beach
M-9			0	Sta. A, Herring Bay, Knight Is.	13-Apr-89	20:40	sheen sample from water's surface
M-10			0	Sta. B, Herring Bay, Knight Is.	13-Apr-89	21:15	waxy oil sample from water's surface
M-11			0	Sta. C, Herring Bay, Knight Is.	14-Apr-89	8:30	bulk oil from inside containment boom
	DPA-12		10	Sta. C, Herring Bay, Knight Is.	14-Apr-89	9:00	adjacent to boomed oil for M-11
	DPA-13		1	Sta. C, Herring Bay, Knight Is.	14-Apr-89	9:00	adjacent to boomed oil for M-11
M-14			0	1/4 mi. W. of NW Bay, Eleanor Is.	14-Apr-89	11:00	mousse sample from water's surface
M-15			0	Sta. D, NW Bay, Eleanor Is.	14-Apr-89	13:00	mousse sample from water's surface
	DPA-16		1	Sta. E, NW Bay, Eleanor Is.	14-Apr-89	14:00	
		N-17	2	Sta. E, NW Bay, Eleanor Is.	14-Apr-89	15:00	surface flocculent layer/sediment sample
	DPA-18		1	Sta. F, NW Bay, Eleanor Is.	14-Apr-89	15:28	
M-19			0	Sta. F, NW Bay, Eleanor Is.	14-Apr-89	15:30	sheen sample from surface of water
		N-20	2	Sta. F, NW Bay, Eleanor Is.	14-Apr-89	15:45	surface flocculent layer/sediment sample
	DPA-21		1	Sta. G, NW Bay, Eleanor Is.	14-Apr-89	17:10	
		N-22	3	Sta. G, NW Bay, Eleanor Is.	14-Apr-89	17:30	surface flocculent layer/sediment sample
	A-23		1	between Naked & Eleanor Is.	14-Apr-89	18:20	beneath oil slick; calm water conditions
	A-24		30	between Naked & Eleanor Is.	14-Apr-89	18:30	beneath oil slick; calm water conditions
M-25			0	between Naked & Eleanor Is.	14-Apr-89	18:40	mousse sample from water's surface
	DPA-26		1	face of Columbia Glacier	15-Apr-89	13:00	
	DPA-27		5	face of Columbia Glacier	15-Apr-89	13:15	water column suction sample

NOTES:

1) DPA in sample code denotes separate "particulate/dispersed" (DP) and "dissolved" (A) fractions obtained from whole water sample

The samples collected from Herring Bay in Prince William Sound were obtained from a number of locations in the eastern, western, and southern portions of the bay. Surface oil (i.e., sheen or mousse) was present on the water and/or beached oil was present in exposed intertidal areas at all locations selected for sampling. Water column samples DPA-12 and DPA-13 were actually collected immediately adjacent to oil being held within a containment boom at Station C (i.e., the head of a cove at the south end of Herring Bay). Clarities of the water columns at all locations were quite high, reflecting low SPM loads that were subsequently measured in the water samples from the bay (see Section 3.3 below). Light microscopy was used to examine the surficial flocculant layer of sediment samples collected from Cluster Fox Cove on the east side of Herring Bay (i.e., N-7). While in close proximity to heavily oiled intertidal beach areas and oil sheens on the water's surface, microscopic observations of this sample gave no indication of a presence of dispersed oil droplets. In fact, the sample was composed almost exclusively of organic matter with large quantities of viable biota including centric and pennate diatoms, harpacticoid copepods, nematodes, and a variety of small, motile flagellates.

Samples from Northwest Bay on Eleanor Island were also associated with areas impacted by spilled oil. Heavily oiled beaches were common in the sampling areas. If not present at the time of specific sampling events, surface oil slicks (i.e., sheen or mousse) on the water's surface had been present at all sampling locations within several hours of actual sample collections. Clarities of the water columns at all sampling locations in Northwest Bay were again extremely high, reflecting low SPM loads in the water (see Section 3.3 below).

The sampling stations in the passage between Naked and Eleanor Islands were in open water where the depth of the water column was 260-280 m. Samples were collected in several wide (i.e., 100-200 m across) bands of oil sheen and mousse that provided 100% coverage of the water's surface at the sampling location. Dead calm conditions (i.e., little or no wind and wave action) prevailed at the site during the period of sampling.

In contrast to the preceding sampling areas, sampling locations near both the Nellie Juan Glacier and the Columbia Glacier were in areas with no visible presence of prior exposure to oil released from the EXXON VALDEZ. While water clarity near the Nellie Juan Glacier was high, the water column near the Columbia Glacier did have a "milky" appearance from a shipboard vantage point. These observations regarding water clarity were reflected in measured SPM loads at both sites (see Section 3.3 below).

3.2 BULK OIL SAMPLES--PHYSICAL PROPERTIES

Physical properties were determined in bulk oil samples from Herring Bay (Knight Island), Northwest Bay (Eleanor Island), and Pt. Adam (on the west end of the Kenai Peninsula) as well as unweathered Prudhoe Bay crude and a sample of the cargo crude carried by the EXXON VALDEZ. Results of measurements are summarized in Table B-2. It should be emphasized that oil sampled during the cruise had been undergoing natural weathering in the field for almost three weeks at the time of collections. As shown in Table B-2, field samples of oil did exhibit substantial differences when compared to unweathered crude. For example, viscosities in oil samples from the field had increased from < 30 to $\geq$ 450 centipoise (with one mousse sample having a viscosity of 2,700 centipose), oil/water interfacial surface tensions had decreased from 23.3 to $\leq$ 9 dynes/cm, densities had increased from 0.81 to 0.92-0.95 g/mL, and water contents had increased from approximately 0.1% to 30-70%. Previous studies documenting temporal changes in these physical properties of Prudhoe Bay crude oil during weathering in outdoor, flow-through seawater wavetanks have been performed by SAIC for NOAA (Payne et al., 1984a; Payne and McNabb, 1984). Results from the latter studies are illustrated in Figure B-2. Comparison of results from these previous studies with measurements in the Prince William Sound samples (i.e., Table B-2) show remarkably good agreement. Consequently, the previous studies on weathering of crude oil in the flow-through wavetanks proved to be extremely accurate for predicting physical properties of the oil released from the EXXON VALDEZ over time.

370

Table B-2

Physical Properties of Oil Samples Collected During the EXXON VALDEZ Oil Spill Study

sample ID	oil type	station ID	viscosity at 38 C (centipoise)	surface tension (dynes/cm)		density (g/mL)	water content (% by weight)
				oil/water	oil/air		
	unweathered PB crude		<30	23.3	31.9	0.81	0.0148
	EXXON VALDEZ cargo crude		NA	NA	NA	NA	0.119
M-1	floating oil	mouth of Herring Bay, Knight Is.	NA	6.8	36.5	NA	57.8
M-2	floating oil	mouth of Herring Bay, Knight Is.	NA	5.5	39.9	NA	45.0
M-8	beached oil	Cluster Fox Cove, Herring Bay	750	4.5	34.9	0.92	30.9
M-11	floating oil	Sta. C, Herring Bay, Knight Is.	2700	5.5	35.0	0.92	45.4
M-14	floating oil	1/4 mi. W. of NW Bay, Eleanor Is.	900	4.3	36.4	0.93	52.9
M-15	floating oil	Sta. D, NW Bay, Eleanor Is.	450	4.1	37.9	0.94	53.6
	floating oil	Pt. Adam, Kenai Peninsula	850	9.0	39.7	0.95	69.4

NOTES:
1) NA indicates not analyzed

371

WATER INCORPORATION BY OIL VS. WEATHERING TIME

DENSITY VS. WEATHERING TIME OF PB CRUDE OIL

WATER/OIL AND OIL/AIR INTERFACIAL TENSIONS VS. WEATHERING TIME

VISCOSITY VS. WEATHERING TIME
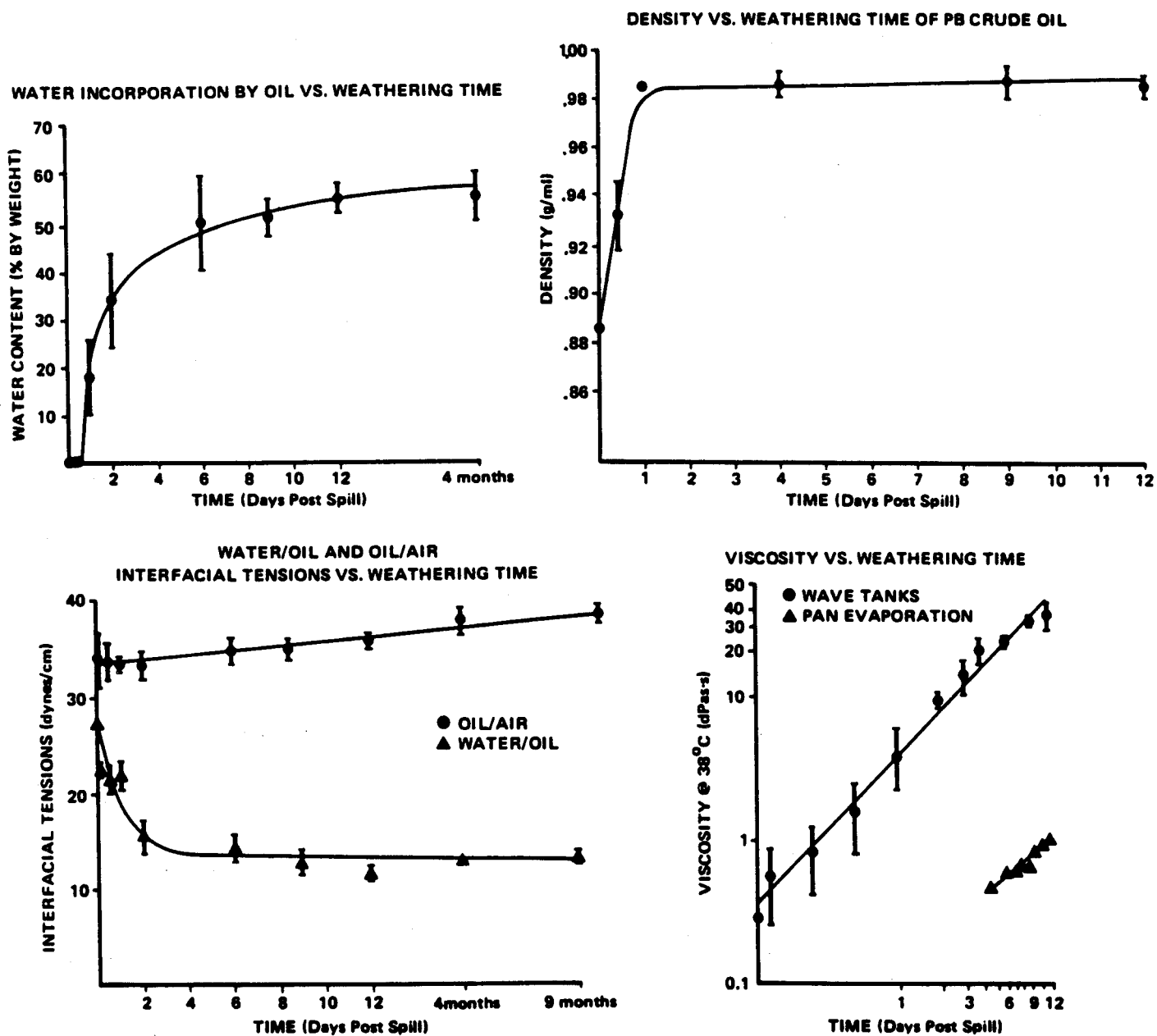
Figure B-2. **Changes in Various Physical Properties of Prudhoe Bay Crude Oil as a Function of Weathering Time.**

Weathering of the crude is marked by increases in density, water content, and viscosity and a decrease in oil/water interfacial surface tension. The figure is taken from Payne and McNabb (1984).

372

3.3 WATER COLUMN AND SURFICIAL FLOCCULANT LAYER OF SEDIMENT
SAMPLES---PARTICULATE CONCENTRATIONS AND SALINITY MEASUREMENTS

Concentrations of particle loads and salinities were determined in water column and surface sediment samples collected from Herring Bay (Knight Island), Northwest Bay (Eleanor Island), near the face of the Nellie Juan Glacier, and near the face of the Columbia Glacier. Results of the measurements are presented in Table B-3. SPM concentrations were extremely low in all water column samples, with loads generally being < 1 mg dry weight/L. Even the "milky" water near the face of the Columbia Glacier had SPM concentrations of only 4.3-4.6 mg/L. The higher particle concentrations measured in the surficial flocculant layer of sediment samples reflect recoveries of fine-grained sediment particles from sediment-water interfaces. Salinities in water samples were generally between 27 and 29 ppt, except for sample DP-6 (salinity - 22 ppt) that was collected in the vicinity of three small freshwater streams discharging into Cluster Fox Cove on the east side of Herring Bay.

3.4 HYDROCARBON CONTENT AND CHARACTERIZATION IN SAMPLES

FID-GC analyses were performed for hydrocarbon content and characterization in bulk oil samples, dissolved and SPM/dispersed fractions of water column samples, and SPM/dispersed fractions of surface sediment samples.

To evaluate changes in chemical composition due to natural weathering processes following release of the oil from the EXXON VALDEZ, the relative compositions of paraffinic hydrocarbons in oil samples collected during the cruise were compared with that of unweathered Prudhoe Bay crude. For this purpose, mass ratios of individual n-alkanes between $n-C_{12}$ and $n-C_{32}$ (plus pristane and phytane) were calculated relative to $n-C_{18}$. Plots of the ratios are presented in Figure B-3 for oil samples from Herring Bay (M-3) and Northwest Bay (M-15) as well as unweathered Prudhoe Bay crude. Good agreement is shown in all three samples for paraffins with molecular weights > $n-C_{17}$. However, dramatic declines in the ratios for paraffins < $n-C_{16}$ are observed in the samples collected from the field, while no such decline is observed in the unweathered crude. Almost identical changes in the composition of crude oil

Table B-3

Particulate Load and Salinity in Water Samples
from EXXON VALDEZ Oil Spill Study

sample ID	station ID	sampling depth (m)	particulate load (mg dry wt/L)	water salinity (ppt)
WATER COLUMN SAMPLES:				
DP-5	face of Nellie Juan Glacier	1	1.18	NA
DP-6	Cluster Fox Cove, Herring Bay	1	0.86	22
DP-12	Sta. C, Herring Bay, Knight Is.	10	0.65	28
DP-13	Sta. C, Herring Bay, Knight Is.	1	0.36	28
DP-16	Sta. E, NW Bay, Eleanor Is.	1	2.22	29
DP-18	Sta. F, NW Bay, Eleanor Is.	1	0.43	NA
DP-21	Sta. G, NW Bay, Eleanor Is.	1	0.00	NA
DP-26	face of Columbia Glacier	1	4.57	27
DP-27	face of Columbia Glacier	5	4.32	NA
SURFACE FLOCCULENT LAYER/SEDIMENT SAMPLES:				
N-4	face of Nellie Juan Glacier	5	89.2	NA
N-7	Cluster Fox Cove, Herring Bay	3	95.4	27
N-17	Sta. E, NW Bay, Eleanor Is.	2	110.3	NA
N-20	Sta. F, NW Bay, Eleanor Is.	2	70.6	NA
N-22	Sta. G, NW Bay, Eleanor Is.	3	63.2	NA

NOTES:
1) NA indicates not analyzed
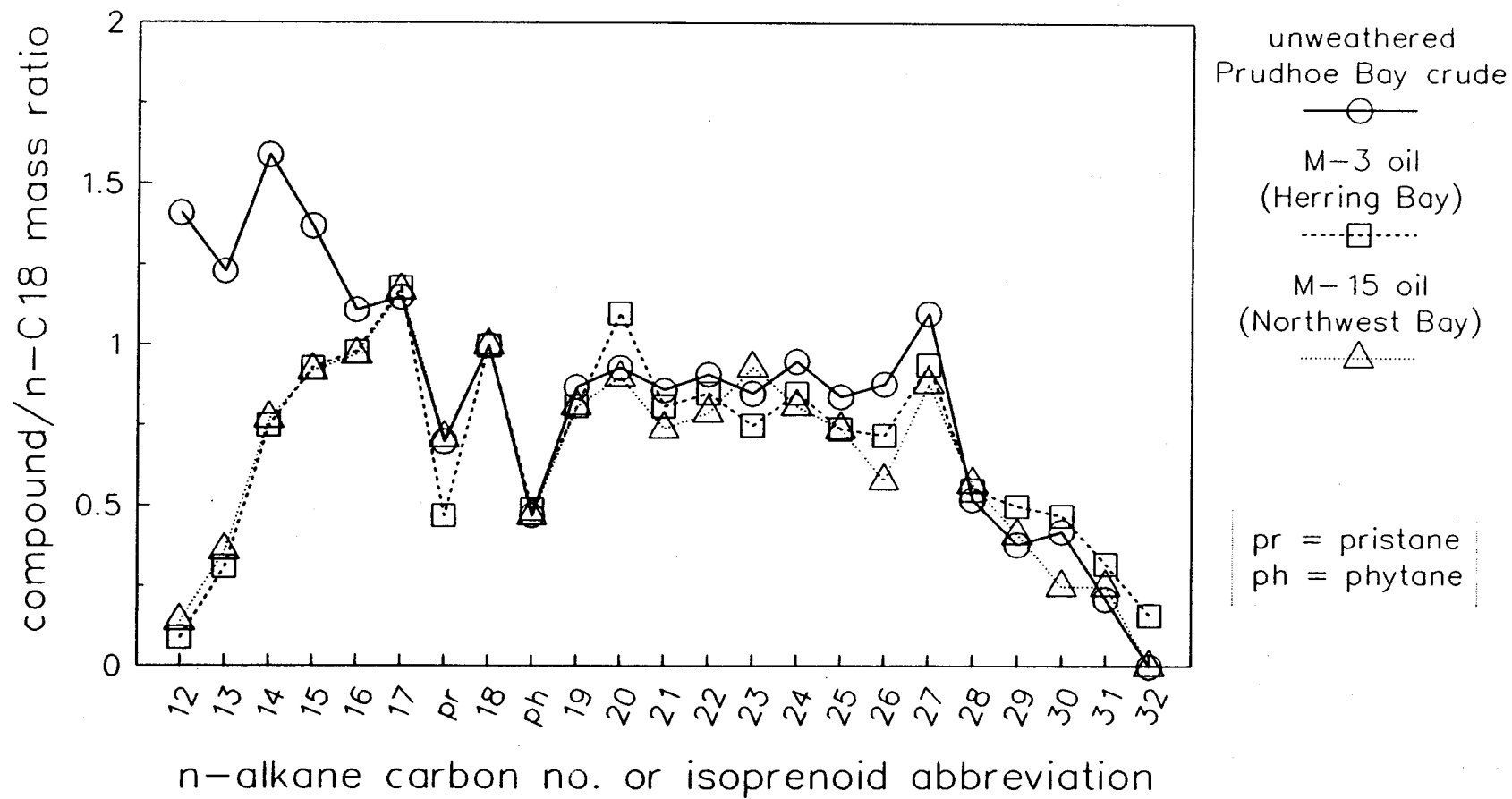
Figure B-3. **Mass Ratios of N-Alkanes (n-C$_{12}$ through n-C$_{32}$) and Pristane and Phytane to n-C$_{18}$ for Unweathered Prudhoe Bay Crude Oil and Prince William Sound Oil Samples from Herring Bay (M-3) and Northwest Bay (M-15)**

during comparable periods of natural weathering (i.e., 2-3 weeks) have been documented in previous flow-through seawater wavetank studies (Payne et al., 1984a; Payne and McNabb, 1984). Therefore, as with measurements for the physical properties, previous SAIC studies on the weathering of crude oil again proved to be extremely accurate for predicting the weathered composition of oil released from the EXXON VALDEZ over time.

Analyses by FID-GC were also performed on the dissolved fractions of water column samples collected during the cruise. While no aliphatic hydrocarbons were detected in the dissolved fractions of any samples, several polynuclear aromatic hydrocarbons were detected at a number of sampling locations. Results of the PAH measurements are summarized in Table B-4. PAH compounds detected included naphthalene, one and two methyl-substituted naphthalenes, biphenyl, and fluorene. While levels of these compounds were relatively low in all samples, detection of one or more of the compounds in samples from Herring Bay, Northwest Bay, and the passage between Naked and Eleanor Islands presumably reflect dissolution from surface oil slicks present at these locations. It should be emphasized that both the types and concentrations of the dissolved aromatics measured in the water column samples from Prince William Sound are remarkably similar to results obtained in the flow-through seawater wavetanks discussed in Payne et al. (1984a) and Payne and McNabb (1984). Consequently, previous studies performed by SAIC for NOAA also proved very accurate for predicting aspects of the chemical composition of the water column beneath oil released from the EXXON VALDEZ after 2-3 weeks of natural weathering in the field.

The presence of part-per-trillion-level aromatics in dissolved fractions of water column samples from near the face of the Columbia Glacier was unanticipated and remains unclear. No visible evidence of a presence of oil was apparent at this location during sampling. Sample contamination appears to be the most likely explanation; however, water column samples obtained with entirely different sampling techniques and devices (i.e., the G/O sampling bottle and the teflon tube/suction sampling device; samples A-26 and A-27, respectively) both show a similar presence of aromatics. An additional complicating factor which makes sample contamination difficult to understand is that the dissolved hydrocarbons were higher in the Columbia Bay water samples

Table B-4

PAH Compounds in "Dissolved" Fractions of Whole Water Samples from EXXON VALDEZ Oil Spill Study

sample ID	station ID	sampling depth (m)	PAH concentration (ug/L)					
			naph	2-MeNa	1-MeNa	biphenyl	2,6-DiMeNa	fluorene
A-5	face of Nellie Juan Glacier	1	0.000	0.000	0.000	0.000	0.000	0.000
A-6	Cluster Fox Cove, Herring Bay	1	0.095	0.166	0.158	0.065	0.000	0.000
A-12	Sta. C, Herring Bay, Knight Is.	10	0.169	0.184	0.188	0.000	0.000	0.000
A-13	Sta. C, Herring Bay, Knight Is.	1	0.068	0.098	0.108	0.000	0.000	0.000
A-16	Sta. E, NW Bay, Eleanor Is.	1	0.234	0.575	0.547	0.155	0.154	0.066
A-18	Sta. F, NW Bay, Eleanor Is.	1	0.192	0.207	0.211	0.000	0.000	0.000
A-21	Sta. G, NW Bay, Eleanor Is.	1	0.313	0.334	0.349	0.000	0.000	0.000
A-23	between Naked and Eleanor Is.	1	0.092	0.156	0.157	0.000	0.000	0.000
A-24	between Naked and Eleanor Is.	30	0.047	0.067	0.086	0.000	0.000	0.000
A-26	face of Columbia Glacier	1	0.135	0.165	0.155	0.096	0.000	0.000
A-27	face of Columbia Glacier	5	0.107	0.112	0.102	0.000	0.000	0.000

(A-26, A-27) compared to the open-water samples between Naked and Eleanor Islands (A-23, A-24), even though the latter samples were taken before the Columbia Bay Station. Shipboard contamination of the samples appears unlikely as an explanation because a subsequent method blank processed with the shipboard solvents used for these samples showed no evidence of aromatics.

As for the SPM/dispersed fractions of water column and surficial flocculant layer of sediment samples collected in Prince William Sound, paraffinic hydrocarbons were detected at all locations. Concentrations of n-alkanes $\geq$ n-C_{12} (and pristane and phytane) are summarized in Table B-5. At the final volumes of sample extracts used for the FID-GC analyses, no aromatic hydrocarbons and no paraffins > n-C_{21} were detected in any samples. It should be noted from the values in Table B-5, however, that the concentrations of the detected paraffins were quite low (i.e., < 0.4 μg/L). These low concentrations presumably reflect the lack of direct transport of dispersed oil droplets as oil/SPM agglomerates to the sediments as a result of the extremely low levels of SPM recovered in all of the water samples.

4.0 DISCUSSION

The physical properties summarized for oil samples in Table B-2 have very important implications for the behavior of the oil released from the EXXON VALDEZ. For example, densities of all oil samples collected from the field were $\leq$ 0.95 g/mL. Even following removal of all light-end compounds from Prudhoe Bay crude oil by distillation during refining operations, the density of the nondistillable residuum for the oil is still only 0.99 g/mL (Coleman et al., 1978). In contrast, the density of seawater is approximately 1.024 g/mL. Therefore, oil released from the EXXON VALDEZ would not be expected to sink by itself even following extensive weathering.

While not being directly subject to sinking, the fresh crude released from the EXXON VALDEZ could be dispersed/driven into the water column by turbulence from wave and/or wind action. However, dispersed oil droplets greater than a given size (e.g., > 50 μm in diameter) would quickly return to the water's surface in the absence of continued turbulence. Extremely low levels of natural turbulence due to wind and wave action were encountered at essentially

378

Table B-5

Paraffinic Hydrocarbons in "SPM/Dispersed" Fractions of Water Samples from EXXON VALDEZ Oil Spill Study

sample ID	station ID	samp depth (m)	n-alkane/isoprenoid concentration (ug/L)											
			nC-12	nC-13	nC-14	nC-15	nC-16	nC-17	pristane	nC-18	phytane	nC-19	nC-20	nC-21
WATER COLUMN SAMPLES:														
DP-5	face of Nellie Juan Glacier	1	0.000	0.000	0.000	0.048	0.077	0.119	0.063	0.075	0.036	0.059	0.000	0.000
DP-6	Cluster Fox Cove, Herring Bay	1	0.098	0.210	0.261	0.463	0.532	0.418	0.227	0.224	0.100	0.140	0.107	0.134
DP-12	Sta. C, Herring Bay, Knight Is.	10	0.182	0.276	0.239	0.361	0.430	0.362	0.196	0.180	0.074	0.090	0.000	0.000
DP-13	Sta. C, Herring Bay, Knight Is.	1	0.097	0.174	0.181	0.296	0.342	0.289	0.147	0.118	0.054	0.090	0.000	0.000
DP-16	Sta. E, NW Bay, Eleanor Is.	1	0.101	0.174	0.177	0.290	0.328	0.298	0.155	0.146	0.051	0.087	0.000	0.000
DP-18	Sta. F, NW Bay, Eleanor Is.	1	0.272	0.383	0.288	0.361	0.421	0.367	0.196	0.164	0.064	0.090	0.000	0.000
DP-21	Sta. G, NW Bay, Eleanor Is.	1	0.145	0.256	0.216	0.308	0.341	0.297	0.166	0.139	0.056	0.000	0.000	0.000
DP-26	face of Columbia Glacier	1	0.102	0.157	0.141	0.216	0.250	0.228	0.125	0.105	0.044	0.000	0.000	0.000
DP-27	face of Columbia Glacier	5	0.118	0.186	0.147	0.218	0.261	0.223	0.129	0.105	0.046	0.000	0.000	0.000
SURFACE FLOCCULENT LAYER/SEDIMENT SAMPLES:														
N-7	Cluster Fox Cove, Herring Bay	3	0.26	0.78	0.64	1.39	1.53	1.71	1.10	1.20	0.46	1.16	1.01	1.54
N-17	Sta. E, NW Bay, Eleanor Is.	2	1.03	1.90	1.47	2.15	2.68	2.90	1.83	1.96	1.03	1.59	1.44	1.44
N-20	Sta. F, NW Bay, Eleanor Is.	2	1.40	2.28	1.70	2.11	2.23	2.07	1.01	0.91	0.43	0.00	0.00	0.00
N-22	Sta. G, NW Bay, Eleanor Is.	3	0.58	1.01	0.82	1.08	1.20	1.32	1.98	0.96	1.02	0.87	0.00	1.09

all sampling locations during the Prince William Sound study on the NOAA Launch 1273. Consequently, low levels of dispersed oil would be expected. In fact, only very low levels of hydrocarbons were detected in the SPM/dispersed fractions of the water column samples, even in the immediate proximity of surface oil slicks (e.g., samples DP-12 and DP-13 that were collected adjacent to oil held by a containment boom in Herring Bay). As a further point relating to the potential for dispersion of oil into water columns, the viscosity of the oil from the EXXON VALDEZ did increase during natural weathering processes in the Prince William Sound area (e.g., Table B-2). With increasing viscosity, sizes of oil droplets dispersed into a water column by a given amount of turbulence would be expected to become larger, further enhancing the tendency for the droplets of dispersed oil to return rapidly to the water's surface. This would also favor low levels of dispersed oil in water columns.

Based on preceding considerations of densities and viscosities of oil derived from the EXXON VALDEZ, incorporation of oil into the water column would most likely require either 1) direct interactions with SPM loads in the water or 2) resuspension of oiled sediment/particle substrates from oiled beaches (e.g., by storm events). In either of the latter circumstances, oil would be subject to transport and eventual deposition in offshore benthic environments due to sinking of oiled/SPM agglomerates. Estimates of the potential for transport of oil to benthic environments due to sinking of oiled/SPM particles have been made by Boehm (1987). For example, massive transport and deposition of oil could occur at SPM concentrations > 100 mg/L. At SPM loads of 10-100 mg/L, considerable oil/SPM interactions could still occur (accompanied by transport and deposition) in the presence of sufficient turbulent mixing. In contrast, no appreciable interaction and transport of oil to the seabed would be expected at SPM concentrations < 10 mg dry weight/L. As noted in Table B-3, SPM concentrations in the Prince William Sound areas sampled for this study were always < 5 mg dry weight/L. Extremely calm water conditions (i.e., low levels of turbulence) were also present at the sampling locations. In light of these latter facts, the extremely low levels of oil measured in both the water column and the surficial flocculant layer of sediment samples at locations in Prince William Sound seem reasonable.

In summary, measurements of physical properties and chemical composition of bulk oil samples as well as concentrations of specific aromatics in dissolved fractions of water column samples from Prince William Sound show remarkably good agreement with values obtained from previous oil weathering studies performed by SAIC for NOAA (Payne et al., 1984a; Payne and McNabb, 1984). Such agreement demonstrates the validity of the preceding studies as accurate "tools" for predicting properties and the behavior of crude oil released into arctic and subarctic marine waters. As for oil/SPM interactions, the extremely low levels of SPM encountered in the water columns in the Prince William Sound study precluded direct validation of results from previous laboratory investigations of oil droplet/SPM interactions and sinking behavior of oil/SPM agglomerates.

5.0 REFERENCES

Boehm, P.D. 1987. Transport and transformation processes regarding hydrocarbon and metal pollutants in offshore sedimentary environments. In: Long Term Environmental Effects of Offshore Oil and Gas Development, ed. Boesch, D.F. and N.N. Rabelais. Elsevier Applied Science Publishers, Ltd. pp. 708.

Coleman, H.J., E.M. Shelton, D.T. Nichols, and C.J. Thompson. 1978. Analyses of 800 crude oils from the United States oil fields. BETC/RI-78/14, Bartlesville Energy Technology Center. Bartlesville, Oklahoma.

Payne, J.R. and G.D. McNabb, Jr. 1984. Weathering of petroleum in the marine environment. Mar. Tech. Soc. Jour. 18(3):24-42.

Payne, J.R., B.E. Kirstein, G.D. McNabb, Jr., J.L. Lambach, R.T. Redding, R.E. Jordan, W. Hom, C. de Oliveira, G.S. Smith, D.M. Baxter, and R. Geagel. 1984a. Multivariate Analysis of Petroleum Weathering in the Marine Environment---Sub Arctic. In: Environmental assessment of the Alaskan continental shelf---Final Reports of principal investigators. Vol. 21 and 22. U.S. Department of commerce, National Oceanic and Atmospheric Administration. Juneau, AK.

Payne, J.R., G.D. McNabb, Jr., B.E. Kirstein, R.I. Redding, J.L. Lambach, C.R. Phillips, L.E. Hachmeister, and S. Martin. 1984b. Development of a Predictive Model for the Weathering of Oil in the Presence of Sea Ice. Final Report submitted to the National and Oceanic Administration, Outer Continental Shelf Environmental Assessment Program. Anchorage, AK.

Payne, J.R., J.R. Clayton, Jr., G.D. McNabb, C.R. Phillips, L.E. Hachmeister, B.E. Kirstein, R.T. Redding, C.L. Clary, G.S. Smith, and G.H. Farmer. 1987a. Development of a Predictive Model for the Weathering of Oil in the Presence of Sea Ice. Final Report. Submitted to NOAA/Ocean Assessments Division, Anchorage, AK. San Diego, CA: Science Applications International Corporation.

Payne, J.R., B.E. Kirstein, J.R. Clayton, Jr., C.L. Clary, R.I. Redding, G.D. McNabb, Jr., and G.H. Farmer. 1987b. Integration of Suspended Particulate Matter and Oil Transportation Study. Final Report. Submitted to Minerals Management Service, Environmental Studies, Anchorage, AK. San Diego, CA: Science Applications International Corporation.

USER'S MANUAL FOR THE COMPUTER CODES:
OILSPMXS
SPMONLY
OILSPM3

by

Bruce E. Kirstein and Cheryl L. Clary

Science Applications International Corporation
10210 Campus Point Drive
San Diego, California 92121

Final Report
Outer Continental Shelf Environmental Assessment Program
Research Unit 680

June 30, 1989

385
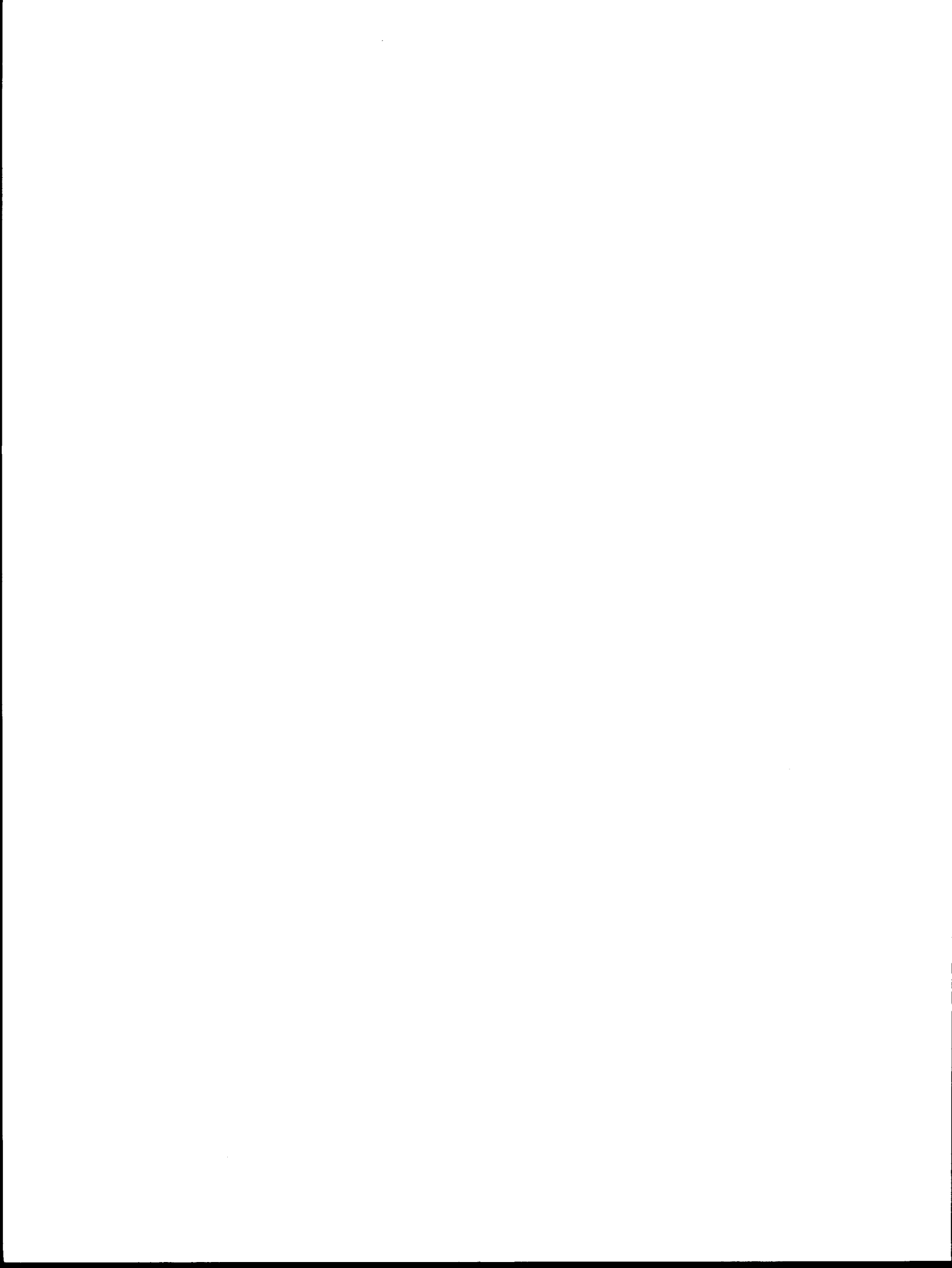
1.0   CODE DESCRIPTIONS

This document is a compilation of the code-user's instructions for the three computer codes OILSPMXS, SPMONLY, and OILSPM3 described in Chapter 6 of Payne et al. (1989). The intent of this user's manual is to describe how to input data and operate the codes. All internal and external references referred to in this manual are the same as those in Payne et al. (1989). Details of the mathematical bases for these three computer codes can also be found in Chapter 3 of Payne et al. (1989).

OILSPMXS is the coding of an analytical solution for one-dimensional transport of oil and SPM where the SPM concentration exceeds the oil concentration to such an extent that the SPM concentration does not change substantially due to the oil-SPM interactions. Typically, if the number density of SPM particles exceeds the number density of oil droplets by a factor of 10, this code can be used.

SPMONLY is the coding of an analytical solution for one-dimensional transport of sediment in the absence of oil. It was used primarily to check the numerical code that follows and to provide a mathematically-consistent SPM concentration profile at steady state to start the numerical integration. Any SPM profile that is "reasonable" can be used. Other SPM profiles not at steady state can also be used, but no coding has been provided to do so.

OILSPM3 is a numerical integration code that solves the one-dimensional transport equations for oil droplets and SPM that are interacting. There are virtually no restrictions on the use of this code.

The choice of a source term for oil is an important consideration. The oil source term used in the codes is a decaying exponential because virtually any time-varying source of oil from the open-ocean oil weathering code has followed this trend. Furthermore, exponentials are do-able in a mathematical sense. A series of exponential oil-source terms can also be used with the requirement that the code be run for each exponential and the results

added together. However, a single exponential source term is all that has been used to date.

The codes are one-dimensional. Therefore, the user must recognize that they do not describe any three-dimensional environmental situations. However, this is the only limitation mathematically. Because the describing partial differential equations are linear (i.e., additive and homogeneous), the usual superposition theorem can be used to obtain other results (e.g., the adding of exponential oil-source terms being one).

The sample problems presented herein illustrate the "best" estimate of available input parameters. Additional estimates for input parameters can be extracted from the experimental data in Chapter 5 of Payne et al. (1989), and Chapter 7 (conclusions and major findings) should be consulted by anyone interested in using the model. As users become more experienced with the models and gain real-world experience, better estimates for input parameters should follow. One of the major purposes of a model is to predict reality, or attempt to do so, by adjusting parameters until reality is predicted.

1.1 CODE-USE DESCRIPTION: OILSPMXS

The mathematical model that describes the interaction of oil droplets with excess SPM is coded in BASIC and named OILSPMXS.BAS. The mathematics are described in Section 3.1 of Payne et al. (1989). This code should be run from a compiled and linked executable file. The executable file should be a "stand-alone" and not require a run-time library.

Upon running OILSPMXS by typing the .EXE file name, the screen will display a prompt asking the user if the parameters are to be "edited" or "entered," as illustrated in Table 1. The user can then enter "edit" as illustrated. Previously stored values of the parameters will be displayed as shown in Table 2. It is recommended that the user "edit" parameters rather than "enter" because the stored parameters are in the range of interest for environmental applications. Any of the displayed parameters can be changed (i.e., edited by typing "yes" to the prompt), as illustrated in Table 2. Upon

Table 1.   Initial Screen Prompt From OILSPMXS.BAS.

OIL DROPLETS INTERACTING WITH EXCESS SPM.
CODE NAME IS OILSPMXS.BAS, VERSION OF 8-3-88 @ 0718

WANT TO EDIT OR ENTER INPUT PARAMETERS ? edit

Table 2.   Screen Display of Parameter Editing From OILSPMXS.BAS.

OIL DROPLETS INTERACTING WITH EXCESS SPM.
CODE NAME IS OILSPMXS.BAS, VERSION OF 8-3-88 @ 0718

1. RISE VELOCITY, CM/SEC = .001
2. TURBULENT DIFFUSIVITY, CM*CM/SEC = 100
3. DEPTH, METERS = 10
4. NUMBER OF ROOTS = 25
5. ROOT ERROR LIMIT = 1.000D-06
6. EXPONENTIAL FLUX TERM, 1/SEC = 4.600D-05
7. INITIAL OIL FLUX, GRAM/(CM*CM*SEC) = 1.800D-05
8. DISAPPEARANCE RATE CONSTANT, 1/SEC = 9.400D-04
9. NUMBER OF DEPTH VALUES = 27
10. PRINT THE ROOTS? YES

WANT TO CHANGE ANY? yes

ENTER THE LINE NUMBER TO BE CHANGED? 3

ENTER THE DEPTH, METERS ? 20

entering "yes" the parameter line number that is to be changed is entered (e.g., in Table 2 the depth is changed to 20 m). After each edit the entire parameter list is displayed. The code will continue execution only after "no" is entered at the parameter-change prompt as illustrated in Table 3.

The code executes in the compiled and linked mode in a few seconds. The initial output is a summary of the input parameters and the roots of the transcendental function (also referred to as eigenvalues) for the problem. Each page of the output begins with a header identifying the code name and version. This information is coded into the source through character strings and any user that changes the code is urged also to make these changes (in the first few lines of the source). By doing this, a record is maintained that can be of great value in documenting results. An example of the first page of output is illustrated in Table 4.

The calculated oil droplet concentration profile for a user-entered time of 1 hr is illustrated in the output in Table 5. The dimensionless time printed just under the time of 1 hr is printed to provide the user with a number that can be used to gauge how close the results are to a steady state value. Typically, dimensionless times greater than 1.0 are indicative of a result that is very close to steady state, and entering a greater time will not markedly change the results. However, this dimensionless time is printed only as a gauge, and in some cases the steady state may be a zero-concentration profile. Note in the calculated results in Table 5 that the oil-droplet concentration varies from 5.04 x 10^{-5} gm/cm^3 (50.4 ppm) at the surface to 1.05 x 10^{-5} gm/cm^3 (10.5 ppm) at a depth of 5 m, and to 0 gm/cm^3 at the bottom. The zero concentration at the bottom is the result of the (imposed) boundary condition described in the derivation.

A summary of the total material balance for oil droplets is printed after the concentration profile. This summary provides information with respect to the quantity of oil droplets dispersed into the water at the surface, in this example (i.e., Table 5) 0.0597 grams at 1 hour; the mass of unattached oil droplets in the water, 0.0151 grams; oil attached to SPM, 0.0415 grams; and oil attached to the bottom, 0.0032 grams. The latter three masses

Table 3. Screen Display of Parameters to be Used in Calculation, with a Final User Response of "no", From OILSPMXS.BAS.

```
OIL DROPLETS INTERACTING WITH EXCESS SPM.
CODE NAME IS OILSPMXS.BAS, VERSION OF 8-3-88 @ 0718

1.  RISE VELOCITY, CM/SEC =   .001
2.  TURBULENT DIFFUSIVITY, CM*CM/SEC =   100
3.  DEPTH, METERS =   10
4.  NUMBER OF ROOTS =   25
5.  ROOT ERROR LIMIT =   1.000D-06
6.  EXPONENTIAL FLUX TERM, 1/SEC =   4.600D-05
7.  INITIAL OIL FLUX, GRAM/(CM*CM*SEC) =   1.800D-05
8.  DISAPPEARANCE RATE CONSTANT, 1/SEC =   9.400D-04
9.  NUMBER OF DEPTH VALUES =   27
10. PRINT THE ROOTS? YES

WANT TO CHANGE ANY? no
```

Table 4. Printed Output of Problem Parameters From OILSPMXS.BAS.

```
CODE NAME IS OILSPMXS.BAS, VERSION OF 8-3-88 @ 0718
RUN TIME = 07:15:01, RUN DATE = 08-03-1988

THIS CODE SOLVES THE TRANSIENT ADVECTION-DISPERSION EQUATION FOR
OIL DROPLETS WITH FIRST-ORDER REACTION LOSS.

PROBLEM IDENTIFICATION: PRE-LOADED PARAMETER TEST CASE

OIL DROPLET RISE VELOCITY =  .001  CM/SEC, DEPTH =  10   METERS

TURBULENT DIFFUSIVITY =  100   CM*CM/SEC

ERROR LIMIT FOR THE ROOTS =  1.000D-06

VX*L/(2*K) = -5.000D-03 UNITLESS

THE 25 ROOTS OF F(BETA) = BETA*COTANGENT(BETA) + VX*L/(2*K)

        ROOT            F(BETA)        ERROR CODE
      1.568D+00       -4.111D-07           1
      4.711D+00        3.831D-07           1
      7.853D+00       -7.362D-08           1
      1.100D+01       -2.266D-08           1
      1.414D+01        4.998D-07           1
      1.728D+01        3.937D-07           1
      2.042D+01       -4.653D-07           1
      2.356D+01       -8.318D-08           1
      2.670D+01        2.939D-07           1
      2.984D+01        3.739D-07           1
      3.299D+01        1.577D-07           1
      3.613D+01       -5.745D-07           1
      3.927D+01        3.101D-07           1
      4.241D+01       -7.179D-07           1
      4.555D+01        6.801D-07           1
      4.869D+01       -9.371D-07           1
      5.184D+01        5.586D-08           1
      5.498D+01        6.808D-07           1
      5.812D+01        7.541D-07           1
      6.126D+01        5.503D-08           1
      6.440D+01        2.015D-07           1
      6.754D+01       -9.391D-07           1
      7.069D+01       -5.765D-08           1
      7.383D+01        9.708D-07           1
      7.697D+01       -6.114D-07           1

EXPONENTIAL FLUX TERM =  4.600D-05 1/SEC

INITIAL OIL FLUX =  1.800D-05 GRAMS/(CM*CM*SEC)

FIRST ORDER DISAPPEARANCE RATE CONSTANT, 1/SEC =  9.400D-04 1/SEC

ZETA-BAR IS REAL ( <> VX/(2*K) ) AND EQUAL TO  2.990D-03 1/CM (IZBAR = 1)
```

Table 5. Calculated Oil-Droplet Concentration Profile at 1 Hour From OILSPMXS.BAS.

```
CODE NAME IS OILSPMXS.BAS, VERSION OF 8-3-88 @ 0718
RUN TIME = 07:15:01, RUN DATE = 08-03-1988

CALCULATED RESULTS ********************************

CONCENTRATION PROFILE (GM/CC) FOR TIME =  1.000D+00 HOURS
DIMENSIONLESS TIME, K*T/L**2 =   3.600D-01

          DEPTH          OIL CONC
          (CM)           (GM/CC)
        0.000D+00        5.040D-05        (SURFACE)
        3.846D+01        4.484D-05
        7.692D+01        3.988D-05
        1.154D+02        3.546D-05
        1.538D+02        3.152D-05
        1.923D+02        2.800D-05
        2.308D+02        2.487D-05
        2.692D+02        2.207D-05
        3.077D+02        1.957D-05
        3.462D+02        1.733D-05
        3.846D+02        1.534D-05
        4.231D+02        1.355D-05
        4.615D+02        1.195D-05
        5.000D+02        1.052D-05
        5.385D+02        9.225D-06
        5.769D+02        8.062D-06
        6.154D+02        7.011D-06
        6.538D+02        6.057D-06
        6.923D+02        5.187D-06
        7.308D+02        4.390D-06
        7.692D+02        3.654D-06
        8.077D+02        2.969D-06
        8.462D+02        2.327D-06
        8.846D+02        1.717D-06
        9.231D+02        1.131D-06
        9.615D+02        5.614D-07
        1.000D+03        0.000D+00        (BOTTOM)

TOTAL GRAMS OF OIL DISPERSED INTO THE WATER COLUMN =  5.972D-02

GRAMS OF FREE OIL DROPS IN THE WATER COLUMN =  1.507D-02
GRAMS OF OIL DROPS ATTACHED TO SPM =  4.147D-02
GRAMS OF FREE OIL DROPS ATTACHED TO THE BOTTOM =  3.179D-03

TOTAL GRAMS OF OIL ACCOUNTED FOR IN THE CALCULATION =  5.972D-02
```

must sum to the mass of oil dispersed in order to "close" the material balance. Thus, the last line of output accounts for 0.0597 g of oil. The material balance must close for each calculation; lack of successful closure indicates an error in the calculation.

The oil-droplet concentration profile at 10 hr is presented in Table 6 and is to be compared with the profile at 1 hr in Table 5. Note that the 10-hr concentrations are considerably decreased relative to the 1-hr concentrations. This is due to the loss of oil through reaction and loss of oil to the bottom. Note that the dispersion is modeled as a decaying exponential, (line #6 in Table 2) and as a result the oil-droplet flux from the surface goes to zero at large values of time.

The sample problem illustrated in Tables 1 through 6 is based on an $(\epsilon/\nu)^{1/2}$ value of 10 sec^{-1}. However, a review of the literature (Table 7) for energy dissipation rates in the ocean shows that a value of 0.01 $erg/cm^3/sec$ can be expected (and down to 0.0003 $erg/cm^3/sec$ also). On a per-unit mass-of-fluid basis this value becomes 0.01 cm^2/sec^3, and dividing by a kinematic viscosity of 0.01 cm^2/sec yields $(\epsilon/\nu)^{1/2} = 1\ sec^{-1}$. The rate constant for oil-droplet loss with an excess SPM load of 100 mg/L then will be 0.000094 sec^{-1} (decreased by a factor of 10 from the previous case). Calculated results for this rate constant at 1 and 10 hr are presented in Tables 8 through 10. Note that the free oil-droplet concentration profile with the decreased α_c in Table 8 is greater than that in Table 5. The reason for this difference is that in the case with a smaller oil-loss rate constant, more oil remains in the water column. This is also illustrated by the mass of oil attached to SPM at 1 hour; for $\alpha_c = 0.00094$ the oil mass attached is 0.0415 grams (Table 5) while for $\alpha_c = 0.000094$ the oil mass attached is 0.00834 grams (Table 9). The corresponding calculation at 10-hr is presented in Table 6-10 and is to be compared with Table 6.

1.2   CODE-USE DESCRIPTION: SPMONLY

The mathematical model which describes the transport of SPM with a first-order reaction loss is coded in BASIC and named SPMONLY.BAS. The

Table 6. Calculated Oil-Droplet Concentration Profile at 10 Hours From OILSPMXS.BAS.

```
CODE NAME IS OILSPMXS.BAS, VERSION OF 8-3-88 @ 0718
RUN TIME = 07:15:01, RUN DATE = 08-03-1988

CALCULATED RESULTS ********************************

CONCENTRATION PROFILE (GM/CC) FOR TIME =  1.000D+01 HOURS
DIMENSIONLESS TIME, K*T/L**2 =  3.600D+00

          DEPTH          OIL CONC
          (CM)           (GM/CC)
        0.000D+00       1.145D-05       (SURFACE)
        3.846D+01       1.020D-05
        7.692D+01       9.083D-06
        1.154D+02       8.087D-06
        1.538D+02       7.197D-06
        1.923D+02       6.404D-06
        2.308D+02       5.695D-06
        2.692D+02       5.062D-06
        3.077D+02       4.496D-06
        3.462D+02       3.990D-06
        3.846D+02       3.537D-06
        4.231D+02       3.131D-06
        4.615D+02       2.767D-06
        5.000D+02       2.439D-06
        5.385D+02       2.144D-06
        5.769D+02       1.877D-06
        6.154D+02       1.636D-06
        6.538D+02       1.416D-06
        6.923D+02       1.215D-06
        7.308D+02       1.030D-06
        7.692D+02       8.583D-07
        8.077D+02       6.984D-07
        8.462D+02       5.478D-07
        8.846D+02       4.046D-07
        9.231D+02       2.667D-07
        9.615D+02       1.325D-07
        1.000D+03       0.000D+00       (BOTTOM)

TOTAL GRAMS OF OIL DISPERSED INTO THE WATER COLUMN =  3.166D-01

GRAMS OF FREE OIL DROPS IN THE WATER COLUMN =  3.459D-03
GRAMS OF OIL DROPS ATTACHED TO SPM =  2.843D-01
GRAMS OF FREE OIL DROPS ATTACHED TO THE BOTTOM =  2.881D-02

TOTAL GRAMS OF OIL ACCOUNTED FOR IN THE CALCULATION =  3.166D-01
```

Table 7. Observed Energy Dissipation Rates

Depth (m)	ε(ergs/cm^3/sec)	References
1	6.4 E-2	Liu (1985)
1-2	3.0 E-2	Stewart & Grant (1962)
15	3.0 E-2	Stewart & Grant (1962)
15	2.5 E-2	Grant et al. (1968)
15	1.0 E-2	Liu (1985)
27	5.2 E-3	Grant et al. (1968)
36	1.5 E-1	Belyaev (1975)*
40	2.65 E-3	Liu (1985)
43	3.0 E-3	Grant et al. (1968)
58	4.8 E-3	Grant et al. (1968)
73	1.9 E-3	Grant et al. (1968)
89	3.4 E-4	Grant et al. (1968)
90	3.1 E-4	Grant et al. (1968)
100	6.25 E-4	Liu (1985)
140	3.7 E-2	Belyaev (1975)*

*In Raj (1977).

Unit Conversions

$$1 \text{ erg/cm}^3/\text{sec} = 1 \text{ cm}^2/\text{sec}^3 \text{ water}$$
$$= 10^{-4} \text{ watts/kg water}$$
$$= 10^{-7} \text{ watts/cm}^3$$

Reference:

Kirstein et al., "Observed Energy Dissipation Rates", Interim Report, Integration of Suspended Particulate Matter and Oil Transportation Study, submitted to MMS, November 1, 1985.

Table 8.   Printed Output of Problem Parameters From OILSPMXS.BAS (with $a_c=0.000094$ sec^{-1}).

```
CODE NAME IS OILSPMXS.BAS, VERSION OF 8-3-88 @ 0718
RUN TIME = 10:42:31, RUN DATE = 08-03-1988

THIS CODE SOLVES THE TRANSIENT ADVECTION-DISPERSION EQUATION FOR
OIL DROPLETS WITH FIRST-ORDER REACTION LOSS.

PROBLEM IDENTIFICATION: PRE-LOADED PARAMETER TEST CASE

OIL DROPLET RISE VELOCITY = .001 CM/SEC, DEPTH = 10 METERS

TURBULENT DIFFUSIVITY = 100 CM*CM/SEC

ERROR LIMIT FOR THE ROOTS = 1.000D-06

VX*L/(2*K) = -5.000D-03 UNITLESS

THE 25 ROOTS OF F(BETA) = BETA*COTANGENT(BETA) + VX*L/(2*K)

        ROOT          F(BETA)         ERROR CODE
      1.568D+00      -4.111D-07            1
      4.711D+00       3.831D-07            1
      7.853D+00      -7.362D-08            1
      1.100D+01      -2.266D-08            1
      1.414D+01       4.998D-07            1
      1.728D+01       3.937D-07            1
      2.042D+01      -4.653D-07            1
      2.356D+01      -8.318D-08            1
      2.670D+01       2.939D-07            1
      2.984D+01       3.739D-07            1
      3.299D+01       1.577D-07            1
      3.613D+01      -5.745D-07            1
      3.927D+01       3.101D-07            1
      4.241D+01      -7.179D-07            1
      4.555D+01       6.801D-07            1
      4.869D+01      -9.371D-07            1
      5.184D+01       5.586D-08            1
      5.498D+01       6.808D-07            1
      5.812D+01       7.541D-07            1
      6.126D+01       5.503D-08            1
      6.440D+01       2.015D-07            1
      6.754D+01      -9.391D-07            1
      7.069D+01      -5.765D-08            1
      7.383D+01       9.708D-07            1
      7.697D+01      -6.114D-07            1

EXPONENTIAL FLUX TERM = 4.600D-05 1/SEC

INITIAL OIL FLUX = 1.800D-05 GRAMS/(CM*CM*SEC)

FIRST ORDER DISAPPEARANCE RATE CONSTANT, 1/SEC = 9.400D-05 1/SEC

ZETA-BAR IS REAL ( <> VX/(2*K) ) AND EQUAL TO 6.928D-04 1/CM (IZBAR = 1)
```

Table 9.   Calculated Oil-Droplet Concentration Profile at 1 Hour From OILSPMXS.BAS (with $a_c = 0.000094$ sec^{-1}).

```
CODE NAME IS OILSPMXS.BAS, VERSION OF 8-3-88 @ 0718
RUN TIME = 10:42:31, RUN DATE = 08-03-1988

CALCULATED RESULTS  *********************************

CONCENTRATION PROFILE (GM/CC) FOR TIME =  1.000D+00 HOURS
DIMENSIONLESS TIME, K*T/L**2 =  3.600D-01

          DEPTH          OIL CONC
          (CM)           (GM/CC)
       0.000D+00       9.647D-05        (SURFACE)
       3.846D+01       9.068D-05
       7.692D+01       8.512D-05
       1.154D+02       7.977D-05
       1.538D+02       7.463D-05
       1.923D+02       6.970D-05
       2.308D+02       6.498D-05
       2.692D+02       6.044D-05
       3.077D+02       5.610D-05
       3.462D+02       5.193D-05
       3.846D+02       4.794D-05
       4.231D+02       4.411D-05
       4.615D+02       4.044D-05
       5.000D+02       3.691D-05
       5.385D+02       3.353D-05
       5.769D+02       3.027D-05
       6.154D+02       2.713D-05
       6.538D+02       2.410D-05
       6.923D+02       2.117D-05
       7.308D+02       1.832D-05
       7.692D+02       1.556D-05
       8.077D+02       1.286D-05
       8.462D+02       1.022D-05
       8.846D+02       7.625D-06
       9.231D+02       5.063D-06
       9.615D+02       2.526D-06
       1.000D+03       0.000D+00        (BOTTOM)

TOTAL GRAMS OF OIL DISPERSED INTO THE WATER COLUMN =  5.972D-02

GRAMS OF FREE OIL DROPS IN THE WATER COLUMN =  4.073D-02
GRAMS OF OIL DROPS ATTACHED TO SPM =  8.342D-03
GRAMS OF FREE OIL DROPS ATTACHED TO THE BOTTOM =  1.064D-02

TOTAL GRAMS OF OIL ACCOUNTED FOR IN THE CALCULATION =  5.972D-02
```

Table 10. Calculated Oil-Droplet Concentration Profile at 10 Hours From OILSPMXS.BAS (with $a_c = 0.000094$ sec^{-1}).

```
CODE NAME IS OILSPMXS.BAS, VERSION OF 8-3-88 @ 0718
RUN TIME = 10:42:31, RUN DATE = 08-03-1988

CALCULATED RESULTS ********************************

CONCENTRATION PROFILE (GM/CC) FOR TIME =  1.000D+01 HOURS
DIMENSIONLESS TIME, K*T/L**2 =  3.600D+00
```

DEPTH (CM)	OIL CONC (GM/CC)	
0.000D+00	2.988D-05	(SURFACE)
3.846D+01	2.855D-05	
7.692D+01	2.725D-05	
1.154D+02	2.597D-05	
1.538D+02	2.471D-05	
1.923D+02	2.346D-05	
2.308D+02	2.224D-05	
2.692D+02	2.102D-05	
3.077D+02	1.983D-05	
3.462D+02	1.865D-05	
3.846D+02	1.748D-05	
4.231D+02	1.632D-05	
4.615D+02	1.518D-05	
5.000D+02	1.405D-05	
5.385D+02	1.293D-05	
5.769D+02	1.182D-05	
6.154D+02	1.071D-05	
6.538D+02	9.619D-06	
6.923D+02	8.531D-06	
7.308D+02	7.450D-06	
7.692D+02	6.375D-06	
8.077D+02	5.305D-06	
8.462D+02	4.238D-06	
8.846D+02	3.175D-06	
9.231D+02	2.115D-06	
9.615D+02	1.057D-06	
1.000D+03	0.000D+00	(BOTTOM)

```
TOTAL GRAMS OF OIL DISPERSED INTO THE WATER COLUMN =  3.166D-01

GRAMS OF FREE OIL DROPS IN THE WATER COLUMN =  1.434D-02
GRAMS OF OIL DROPS ATTACHED TO SPM =  1.028D-01
GRAMS OF FREE OIL DROPS ATTACHED TO THE BOTTOM =  1.995D-01

TOTAL GRAMS OF OIL ACCOUNTED FOR IN THE CALCULATION =  3.166D-01
```

mathematics is described in Section 3.1.2 of Payne et al. (1989). This code should be run from a compiled and linked executable file. The executable file should be a "stand-alone" and not require a run-time library.

Upon running SPMONLY by typing in the .EXE file name, the screen will display a prompt asking the user if the parameters are to be "edited" or "entered". It is recommended that the user enter "edit" because the parameters stored in the code are in the range of interest of environmental applications. Any of the displayed parameters can be changed (i.e., edited) by typing "yes" in response to the prompt. Upon entering "yes" the parameter line number that is to be changed is entered. After each edit the entire parameter list is displayed. The code will continue to execute only after "no" is entered at the parameter-change prompt as illustrated in Table 11.

Upon entering "no" the prompt will ask the user if cotangent values from Abramowitz and Stegun are to be used. The Abramowitz and Stegun cotangent values are double-precision cotangent values as described in the Handbook of Mathematical Functions (M. Abramowitz and I.A. Stegun, page 76). The reason this cotangent calculation was used is the recognition that some BASIC software does not have double-precision trigonometric functions, and in the early stages of coding an error limit of less than 1.DO-05 could not be attained in solving for the roots of the transcendental function (eigenfunction). Most of the time it will make no difference if the Abramowitz and Stegun cotangent values are used or if the single-precision machine function is used. For the example illustrated in Table 11, "no" is entered. The prompt will then ask for a time to calculate the SPM concentration profile.

The results of a calculation are illustrated in Tables 12 through 14. Table 12 provides documentation of the code name and version, an echo of the input parameters, and the roots of the transcendental function (eigenfunction). The code name and version are printed as a header on each page of output to provide a means of documenting results. These two identification items are coded into the source through character strings, and any user that changes the code is urged to make these changes (in the first few lines of the source).

400

Table 11.   Screen Display of Parameter List for SPMONLY.BAS.

```
SUSPENDED-PARTICULATE-MATTER (SPM) CALCULATION
CODE NAME IS SPMONLY.BAS, VERSION OF 8-4-88 @ 0746

1.   TERMINAL VELOCITY, CM/SEC =   .001
2.   TURBULENT DIFFUSIVITY, CM*CM/SEC =   100
3.   DEPTH, METERS =   10
4.   NUMBER OF ROOTS =   25
5.   ROOT ERROR LIMIT =   1.000D-06
6.   SPM-LOSS RATE CONSTANT, 1/SEC =   9.400D-07
7.   FLUX RATE, GM/SEC*CM*CM =   4.600D-05
8.   DEPOSITION RATE, CM/SEC =   4.600D-02
9.   NUMBER OF DEPTH VALUES =   49
10.  PRINT THE ROOTS? YES

WANT TO CHANGE ANY? N

DO YOU WANT ABRAMOWITZ & STEGUN COTANGENT VALUES? NO

ENTER THE TIME IN HOURS ? 1.

TIME ENTERED IS   1.000D+00

IS THIS CORRECT ? yes
```

Table 12. Printed Output From SPMONLY Documenting Problem Parameters.

```
CODE NAME IS SPMONLY.BAS, VERSION OF 8-4-88 @ 0746
RUN TIME = 08:12:02, RUN DATE = 08-04-1988

THIS CODE SOLVES THE 1-D TRANSIENT ADVECTION-DISPERSION EQUATION FOR SPM
(ANALYTICAL SOLUTION) WITH FIRST-ORDER REACTION LOSS.

TERMINAL VELOCITY = 1.000D-03 CM/SEC, DEPTH = 10.0 METERS

TURBULENT DIFFUSIVITY = 100.0 CM*CM/SEC

FLUX RATE FROM THE BOTTOM = 4.600D-05 GM/SEC*CM*CM

DEPOSITION RATE = 4.600D-02 CM/SEC

ERROR LIMIT FOR THE ROOTS = 1.000D-06

A = VX/(2*K) = 5.000D-06 1/CM

ROOTS CALCULATED USING MACHINE FUNCTIONS.

THE 25 ROOTS OF F(BETA)=BETA*COTANGENT(BETA)-K*((A*L)^2-A*KS*L+BETA^2)/(KS*L)

        ROOT          F(BETA)        ERROR CODE
     6.319D-01       1.685D-07           1
     3.281D+00       9.872D-07           1
     6.355D+00      -6.364D-07           1
     9.473D+00      -1.659D-07           1
     1.260D+01      -8.777D-07           1
     1.574D+01      -3.807D-07           1
     1.887D+01       4.496D-07           1
     2.201D+01       6.450D-07           1
     2.515D+01      -7.795D-07           1
     2.829D+01      -4.485D-08           1
     3.143D+01      -6.668D-07           1
     3.457D+01       9.841D-07           1
     3.771D+01       1.799D-07           1
     4.085D+01       5.034D-07           1
     4.399D+01       6.818D-07           1
     4.713D+01      -7.496D-07           1
     5.027D+01      -3.562D-07           1
     5.342D+01      -9.183D-07           1
     5.656D+01      -4.542D-07           1
     5.970D+01      -8.393D-07           1
     6.284D+01      -6.561D-07           1
     6.598D+01       7.975D-07           1
     6.912D+01      -9.499D-08           1
     7.226D+01       5.386D-07           1
     7.540D+01       3.503D-07           1

INITIAL SPM FLUX = 4.600D-05 GRAMS/(CM*CM*SEC)

FIRST-ORDER SPM DISAPPEARANCE RATE CONSTANT, 1/SEC = 9.400D-07 1/SEC
```

Table 13.   Printed Output From SPMONLY, SPM Profile at 1 Hour.

```
CODE NAME IS SPMONLY.BAS, VERSION OF 8-4-88 @ 0746
RUN TIME = 08:12:02, RUN DATE = 08-04-1988

CONCENTRATION PROFILES AT TIME =  1.000D+00 HOURS **********************

          DEPTH           SPM CONC.
           CM             GM/CM**3
        0.000D+00         7.772D-05 (SURFACE)
        2.083D+01         7.781D-05
        4.167D+01         7.805D-05
        6.250D+01         7.845D-05
        8.333D+01         7.899D-05
        1.042D+02         7.968D-05
        1.250D+02         8.053D-05
        1.458D+02         8.152D-05
        1.667D+02         8.267D-05
        1.875D+02         8.397D-05
        2.083D+02         8.542D-05
        2.292D+02         8.702D-05
        2.500D+02         8.877D-05
        2.708D+02         9.067D-05
        2.917D+02         9.273D-05
        3.125D+02         9.493D-05
        3.333D+02         9.729D-05
        3.542D+02         9.980D-05
        3.750D+02         1.025D-04
        3.958D+02         1.053D-04
        4.167D+02         1.083D-04
        4.375D+02         1.114D-04
        4.583D+02         1.146D-04
        4.792D+02         1.181D-04
        5.000D+02         1.217D-04
        5.208D+02         1.254D-04
        5.417D+02         1.293D-04
        5.625D+02         1.333D-04
        5.833D+02         1.375D-04
        6.042D+02         1.418D-04
        6.250D+02         1.463D-04
        6.458D+02         1.510D-04
        6.667D+02         1.558D-04
        6.875D+02         1.607D-04
        7.083D+02         1.658D-04
        7.292D+02         1.711D-04
        7.500D+02         1.765D-04
        7.708D+02         1.820D-04
        7.917D+02         1.877D-04
        8.125D+02         1.936D-04
        8.333D+02         1.996D-04
        8.542D+02         2.057D-04
        8.750D+02         2.120D-04
        8.958D+02         2.184D-04
        9.167D+02         2.250D-04
        9.375D+02         2.317D-04
        9.583D+02         2.386D-04
        9.792D+02         2.456D-04
        1.000D+03         2.527D-04 (BOTTOM)

GRAMS OF SPM (UNATTACHED) IN THE WATER COLUMN = 1.362D-01
GRAMS OF SPM ATTACHED TO OIL = 2.395D-04

GRAMS OF SPM IN WATER + ATTACHED = 1.365D-01

GRAMS OF SPM FROM THE BOTTOM (FROM VX*C-K*DC/DX) = 1.365D-01
GRAMS OF SPM FROM THE BOTTOM (FROM -F0+KS*C) = 1.365D-01
```

Table 14.   Printed Output From SPMONLY, SPM Profile at 6 Hours.

```
CODE NAME IS SPMONLY.BAS, VERSION OF 8-4-88 @ 0746
RUN TIME = 08:12:02, RUN DATE = 08-04-1988

CONCENTRATION PROFILES AT TIME =  6.000D+00 HOURS ************************

        DEPTH                 SPM CONC.
         CM                   GM/CM**3
      0.000D+00            5.395D-04 (SURFACE)
      2.083D+01            5.397D-04
      4.167D+01            5.399D-04
      6.250D+01            5.402D-04
      8.333D+01            5.406D-04
      1.042D+02            5.411D-04
      1.250D+02            5.416D-04
      1.458D+02            5.422D-04
      1.667D+02            5.429D-04
      1.875D+02            5.437D-04
      2.083D+02            5.445D-04
      2.292D+02            5.455D-04
      2.500D+02            5.465D-04
      2.708D+02            5.476D-04
      2.917D+02            5.487D-04
      3.125D+02            5.500D-04
      3.333D+02            5.513D-04
      3.542D+02            5.527D-04
      3.750D+02            5.541D-04
      3.958D+02            5.557D-04
      4.167D+02            5.573D-04
      4.375D+02            5.590D-04
      4.583D+02            5.608D-04
      4.792D+02            5.626D-04
      5.000D+02            5.645D-04
      5.208D+02            5.665D-04
      5.417D+02            5.686D-04
      5.625D+02            5.708D-04
      5.833D+02            5.730D-04
      6.042D+02            5.753D-04
      6.250D+02            5.776D-04
      6.458D+02            5.801D-04
      6.667D+02            5.826D-04
      6.875D+02            5.852D-04
      7.083D+02            5.879D-04
      7.292D+02            5.906D-04
      7.500D+02            5.934D-04
      7.708D+02            5.963D-04
      7.917D+02            5.992D-04
      8.125D+02            6.022D-04
      8.333D+02            6.053D-04
      8.542D+02            6.085D-04
      8.750D+02            6.117D-04
      8.958D+02            6.150D-04
      9.167D+02            6.183D-04
      9.375D+02            6.217D-04
      9.583D+02            6.252D-04
      9.792D+02            6.288D-04
      1.000D+03            6.324D-04 (BOTTOM)

GRAMS OF SPM (UNATTACHED) IN THE WATER COLUMN =  5.717D-01
GRAMS OF SPM ATTACHED TO OIL =  6.677D-03

GRAMS OF SPM IN WATER + ATTACHED =  5.784D-01

GRAMS OF SPM FROM THE BOTTOM (FROM VX*C-K*DC/DX) =  5.784D-01
GRAMS OF SPM FROM THE BOTTOM (FROM -F0+KS*C) =  5.784D-01
```

Tables 13 and 14 illustrate the calculated SPM profiles at 1 and 6 hr, respectively. At 1 hr the SPM concentration varies from 7.7×10^{-5} gm/cm^3 (77 ppm) at the surface to 2.5×10^{-4} gm/cm^3 (250 ppm) at the bottom, while at 6 hr the SPM at the surface is 5.4×10^{-4} gm/cm^3 (540 ppm) and at the bottom 6.3×10^{-4} gm/cm^3 (630 ppm). Note that the SPM profile is "flattening out" at 6 hr (i.e., the SPM concentration in the water column is approaching steady state and is expected to be "flat").

A total material balance for the SPM is printed below each concentration profile. SPM can reside in the water column or be removed from the water column through reaction with oil. These two masses <u>must</u> sum to the SPM mass put into the water column at the bottom. This is illustrated in Table 13 where 0.1362 g are in the water column and 0.000239 g are attached to oil (by reaction). These two masses sum to 0.1365 g, which is equal to the SPM mass fluxed into the water at the bottom by $-F_o + k_s C$ or the mass fluxed <u>away from</u> the bottom by $\nu_x C - k(dC/dx)$. Similar results are illustrated in Table 14.

1.3   CODE-USE DESCRIPTION: OILSPM3

The mathematical model that describes the interaction of oil droplets and SPM where SPM is not required to be in excess is coded in BASIC and named OILSPM3.BAS. The "3" in the code name pertains to the fact that this model calculates <u>three</u> changing concentration profiles: oil droplets, SPM, and oil-SPM agglomerate. The mathematics are described in Section 3.1.3 of Payne et al. (1989). This code <u>must</u> be run from a compiled and linked executable file. The executable file should be a "stand-alone" and not require a run-time library.

Upon running OILSPM3 by typing the .EXE file name, the screen will display a prompt asking the user if the parameters are to be "edited" or "entered". It is recommended that the user enter "edit" because the parameters stored in the code are in the range of interest of environmental applications. Any of the displayed parameters can be changed (i.e., edited) by typing "yes" in response to the prompt. Upon entering "yes", the parameter line number that is to be changed is entered. After each edit the entire parameter list is displayed. The code will continue to execute only after "no" is entered at the parameter-change prompt as illustrated in Tables 15a and 15b. These two tables

405

Table 15a. First (of two) Screen Display of Parameters to be Used in Calculation, with a Final User Response of "no", From OILSPM3.

```
INTERACTING OIL DROPLETS AND SPM CALCULATION
CODE NAME IS OILSPM3.BAS, VERSION OF 8-9-88 @ 0643

1.   TURBULENT DIFFUSIVITY, CM*CM/SEC =  1.00D+02
2.   OIL RISING VELOCITY, CM/SEC =  1.00D-02
3.   OIL-SPM RATE CONSTANT FOR OIL LOSS, CC/(GM*SEC) =  9.40D-02
4.   OCEAN DEPTH, METERS =  1.00D+01
5.   NUMBER OF GRID POINTS =  49
6.   INITIAL OIL-DISPERSON FLUX SZERO, GRAMS/(CM*CM*SEC) =  1.80D-05
7.   OIL-DISPERSON GAMMA, 1/SEC =  4.60D-05
8.   MAXIMUM TIME, HOURS =  10.00
9.   PRINT INTERVAL, HOURS = 0.500
10.  USE STEADY-STATE OIL PROFILE TO START: NO
11.  COUPLE THE CONCENTRATIONS: YES
12.  COUPLING ITERATIONS =  3

WANT TO CHANGE ANY? no
```

Table 15b. Second Screen Display of Parameters to be Used in Calculation, with a Final User Response of "no", From OILSPM3.

```
INTERACTING OIL DROPLETS AND SPM CALCULATION
CODE NAME IS OILSPM3.BAS, VERSION OF 8-9-88 @ 0643

1.   SPM SETTLING VELOCITY, CM/SEC =  1.00D-03
2.   OIL-SPM AGGLOMERATE SETTLING VELOCITY, CM/SEC =  1.00D-03
3.   OIL-SPM RATE CONSTANT FOR SPM LOSS, CC/(GM*SEC) =  9.40D-02
4.   SPM SOURCE FLUX TERM, GM/(CM^2*SEC) =  4.60D-05
5.   SPM DEPOSITION RATE CONSTANT, CM/SEC =  4.60D-02
6.   USE STEADY-STATE SPM PROFILE TO START: YES

WANT TO CHANGE ANY? no

TIME FOR UNITY DIMENSIONLESS TIME, HOURS =  2.814D-01

THE TIME STEP WILL BE THE ABOVE TIME DIVIDED BY   20.000

IS THIS ACCEPTABLE? yes
```

illustrate the parameter input list for OILSPM3. Table 15a illustrates mainly oil-related options and integration parameters such as the number of grid points. Because OILSPM3 is a numerical integration code, it is not possible just to enter a "time" and then calculate the concentration profiles. The code must integrate up to a specified time from an initial condition. The initial condition recommended for oil in the water column is zero (i.e., oil is spilled at time - 0. This condition is implemented by line 10 in Table 15a, where a "no" is entered to the prompt: USE STEADY-STATE OIL PROFILE TO START.

The reason this option exists is for material-balance testing calculations only. The user should always make sure that line 10 has a response of "no." Material-balance testing is used to make sure the code calculation accounts for all the masses in the water. This is difficult in numerical integrations because mass transfer changes rapidly in the initial stages of the calculation (i.e., the profiles are quite steep in the early stages of calculation. However, if a "smooth" profile, such as a steady-state profile, is used initially, the early integration errors do not exist; and for purposes of finding programming errors the calculated results are much easier to interpret.

Table 15b illustrates mainly SPM and oil-SPM agglomerate related parameters and the selection of the maximum allowable time step to be used in the Crank-Nicolson integration. Note that line 6 in this table specifies that a steady-state SPM profile is used to start the calculation. In other words, oil is spilled in water that has sediment. The dimensionless time referred to in this table is used as a gauge to select a maximum time step. Experience has resulted in selecting a time step on the order of 1/20 of this dimensionless time. It is recommended that at least 20 be entered. However, if a larger number is entered, compute time will increase accordingly.

The code execute time is on the order of many minutes on a 80286-based personal computer. If an 8088-based machine is used, expect one-half hour or longer. The initial output is illustrated in Table 16 where the code version is documented and the input parameters for the calculation are also documented.

408

Table 16.   Initial Output of Problem Parameters for OILSPM3.

```
FINITE-DIFFERENCE SOLUTION FOR INTERACTING OIL DROPLETS AND SPM.

CODE NAME IS OILSPM3.BAS, VERSION IS 8-9-88 @ 0643
RUN TIME WAS 06:42:48, AND RUN DATE WAS 08-09-1988

PROBLEM PARAMETERS ARE AS FOLLOWS:

VERTICAL TURBULENT DIFFUSIVITY, CM*CM/SEC =  100.00
WATER DEPTH, METERS =  10.0

OIL RISING VELOCITY, CM/SEC =  1.00D-02
OIL-SPM RATE CONSTANT FOR OIL LOSS, CC/(GM*SEC) =  9.400D-02
OIL DISPERSION RATE, GM/(CM*CM*SEC) = (0.18D-04)*EXP((-0.46D-04)*SECONDS)

SPM SETTLING VELOCITY, CM/SEC =  1.00D-03
OIL-SPM RATE CONSTANT FOR SPM LOSS, CC/(GM*SEC) =  9.40D-02
SPM BOTTOM SOURCE FLUX, GM/(CM^2*SEC) =  4.60D-05
SPM DEPOSITION RATE CONSTANT, CM/SEC =  4.60D-02

OIL-SPM AGGLOMERATE SETTLING VELOCITY, CM/SEC =  1.00D-03

TIME STEP, HOURS =  5.62D-03, INTEGRATION TIME, HOURS =  10.00
SPECIFIED PRINT INTERVAL, HOURS =  0.500

THE INITIAL OIL WATER-COLUMN LOADING, GRAMS =  0.000D+00
THE INITIAL SPM WATER-COLUMN LOADING, GRAMS =  9.950D-01
```

Table 17a presents the calculated oil-droplet, SPM and oil-SPM agglomerate concentration profiles at 0.5 hour, and Table 17b presents the total material balance for these species. The SPM concentration profile is close to 0.001 gm/cm^3 because of the values selected for the SPM source flux [at 4.6 x 10^{-5} $gm/(cm^2$ sec)] and the SPM deposition rate constant (4.6 x 10^{-2} cm/sec). The oil-droplet concentration profile ranges from 7.8 x 10^{-5} gm/cm^3 (78 ppm) at the surface to 0 at the bottom. The zero concentration at the bottom is an imposed boundary condition and essentially results in an upper bound flux of oil to the bottom. Likewise, the oil-SPM agglomerate concentration is 0 at the bottom.

Table 17b illustrates the total material balance calculation for the three transporting species. Note that the oil fluxed into the water at the surface is 0.03109 g, while the calculation accounted for 0.03091 g as oil that was in the water, lost at bottom (transported to the bottom), and lost through reaction. This difference should be zero; it is not because of numerical integration errors and can be made smaller by decreasing the grid spacing, the time step, or both. The SPM material balance closes by accounting for 0.9950 g, and the oil-SPM agglomerate almost closes by accounting for 0.004827 g in the water and lost to the bottom compared to 0.004825 g produced by reaction. Closing these material balances to four significant digits is considered reasonable given the assumptions and limitation of the data and calculation.

The oil-droplet, SPM and oil-SPM agglomerate concentration profiles and total material balance at 10 hr are presented in Tables 18a and 18b. Note that the time at the end of the calculation was 7:34 and the start time 6:42 for an integration to 10 hr with a time-step size of 0.00562 hr on a grid size of 20.83 cm (over 10 m, 51 grid points including 1 grid point outside each boundary for central differences). The SPM-concentration profile is still close to 0.001 gm/cm^3 and the oil-droplet concentration varies from 3.159 x 10^{-5} (32 ppm) at the surface to 0 at the bottom. This concentration is decreasing from the 0.5-hr value because the oil-dispersion source term is a

410

Table 17a. Calculated Oil-Droplet SPM and Oil-SPM Agglomerate Profiles at 0.5 Hour From OILSPM3.

```
FINITE-DIFFERENCE SOLUTION FOR INTERACTING OIL DROPLETS AND SPM.

CODE NAME IS OILSPM3.BAS, VERSION IS 8-9-88 @ 0643
RUN TIME WAS 06:42:48, AND RUN DATE WAS 08-09-1988


CONCENTRATION PROFILES AT TIME = 0.500 HOURS  ****************************
```

DEPTH (CM)	OIL CONC (GM/CC)	SPM CONC (GM/CC)	OIL-SPM CONC (GM/CC)	
0.000D+00	7.832D-05	9.856D-04	8.807D-06	(SURFACE)
2.083D+01	7.476D-05	9.858D-04	8.792D-06	
4.167D+01	7.131D-05	9.860D-04	8.747D-06	
6.250D+01	6.798D-05	9.863D-04	8.675D-06	
8.333D+01	6.476D-05	9.865D-04	8.578D-06	
1.042D+02	6.164D-05	9.868D-04	8.459D-06	
1.250D+02	5.864D-05	9.871D-04	8.320D-06	
1.458D+02	5.574D-05	9.874D-04	8.163D-06	
1.667D+02	5.294D-05	9.877D-04	7.990D-06	
1.875D+02	5.025D-05	9.880D-04	7.803D-06	
2.083D+02	4.765D-05	9.883D-04	7.605D-06	
2.292D+02	4.516D-05	9.886D-04	7.396D-06	
2.500D+02	4.276D-05	9.889D-04	7.179D-06	
2.708D+02	4.045D-05	9.892D-04	6.954D-06	
2.917D+02	3.824D-05	9.895D-04	6.724D-06	
3.125D+02	3.612D-05	9.899D-04	6.490D-06	
3.333D+02	3.408D-05	9.902D-04	6.252D-06	
3.542D+02	3.213D-05	9.905D-04	6.013D-06	
3.750D+02	3.027D-05	9.908D-04	5.772D-06	
3.958D+02	2.848D-05	9.911D-04	5.531D-06	
4.167D+02	2.677D-05	9.915D-04	5.291D-06	
4.375D+02	2.514D-05	9.918D-04	5.052D-06	
4.583D+02	2.358D-05	9.921D-04	4.816D-06	
4.792D+02	2.210D-05	9.924D-04	4.581D-06	
5.000D+02	2.068D-05	9.928D-04	4.350D-06	
5.208D+02	1.932D-05	9.931D-04	4.123D-06	
5.417D+02	1.803D-05	9.934D-04	3.899D-06	
5.625D+02	1.680D-05	9.937D-04	3.680D-06	
5.833D+02	1.562D-05	9.940D-04	3.465D-06	
6.042D+02	1.450D-05	9.943D-04	3.254D-06	
6.250D+02	1.343D-05	9.946D-04	3.048D-06	
6.458D+02	1.241D-05	9.949D-04	2.847D-06	
6.667D+02	1.144D-05	9.952D-04	2.651D-06	
6.875D+02	1.051D-05	9.955D-04	2.459D-06	
7.083D+02	9.622D-06	9.957D-04	2.271D-06	
7.292D+02	8.773D-06	9.960D-04	2.088D-06	
7.500D+02	7.959D-06	9.963D-04	1.910D-06	
7.708D+02	7.178D-06	9.966D-04	1.735D-06	
7.917D+02	6.428D-06	9.968D-04	1.564D-06	
8.125D+02	5.705D-06	9.971D-04	1.397D-06	
8.333D+02	5.007D-06	9.974D-04	1.233D-06	
8.542D+02	4.331D-06	9.976D-04	1.073D-06	
8.750D+02	3.674D-06	9.979D-04	9.143D-07	
8.958D+02	3.035D-06	9.981D-04	7.584D-07	
9.167D+02	2.410D-06	9.983D-04	6.044D-07	
9.375D+02	1.797D-06	9.986D-04	4.519D-07	
9.583D+02	1.192D-06	9.988D-04	3.006D-07	
9.792D+02	5.942D-07	9.990D-04	1.501D-07	
1.000D+03	0.000D+00	9.992D-04	0.000D+00	(BOTTOM)

Table 17b. Total Material Balance for Oil-Droplets, SPM and Oil-SPM Agglomerate at 0.5 Hour From OILSPM3.

```
MATERIAL BALANCE INFORMATION (FOR 1 CM*CM COLUMN OF WATER):

OIL IN THE WATER COLUMN, GRAMS = 2.688D-02
OIL LOST TO THE BOTTOM, GRAMS = 1.612D-03
OIL LOST THROUGH REACTION WITH SPM, GRAMS = 2.413D-03

OIL IN WATER + LOST AT BOTTOM + LOST THROUGH REACTION, GRAMS = 3.091D-02
OIL FLUXED INTO WATER + INITIAL LOADING, GRAMS = 3.109D-02


SPM (UNATTACHED) IN THE WATER COLUMN, GRAMS = 9.926D-01
SPM LOST THROUGH REACTION WITH OIL, GRAMS = 2.413D-03

SPM IN WATER + LOST THROUGH REACTION, GRAMS = 9.950D-01
SPM FLUXED INTO WATER AT BOTTOM + INITIAL LOADING, GRAMS = 9.950D-01


OIL-SPM AGGLOMERATE IN THE WATER COLUMN, GRAMS = 4.496D-03
OIL-SPM AGGLOMERATE FLUXED TO THE BOTTOM, GRAMS = 3.309D-04

OIL-SPM IN WATER + LOST TO BOTTOM, GRAMS = 4.827D-03
OIL-SPM AGGLOMERATE PRODUCED BY REACTION, GRAMS = 4.825D-03


VECTOR CONVERGENCE, OIL = 3.06D-14, SPM = 6.01D-15 ON  3 ITERATIONS.
```

Table 18a. Calculated Oil-Droplet, SPM and Oil-SPM Agglomerate Profiles at 10 Hours From OILSPM3.

```
FINITE-DIFFERENCE SOLUTION FOR INTERACTING OIL DROPLETS AND SPM.

CODE NAME IS OILSPM3.BAS, VERSION IS 8-9-88 @ 0643
RUN TIME WAS 06:42:48, AND RUN DATE WAS 08-09-1988


CONCENTRATION PROFILES AT TIME = 10.000 HOURS   ****************************
```

DEPTH (CM)	OIL CONC (GM/CC)	SPM CONC (GM/CC)	OIL-SPM CONC (GM/CC)	
0.000D+00	3.159D-05	9.366D-04	2.168D-05	(SURFACE)
2.083D+01	3.081D-05	9.368D-04	2.167D-05	
4.167D+01	3.004D-05	9.371D-04	2.163D-05	
6.250D+01	2.927D-05	9.373D-04	2.157D-05	
8.333D+01	2.852D-05	9.375D-04	2.148D-05	
1.042D+02	2.777D-05	9.378D-04	2.136D-05	
1.250D+02	2.702D-05	9.381D-04	2.121D-05	
1.458D+02	2.629D-05	9.384D-04	2.105D-05	
1.667D+02	2.556D-05	9.387D-04	2.086D-05	
1.875D+02	2.483D-05	9.390D-04	2.064D-05	
2.083D+02	2.411D-05	9.393D-04	2.040D-05	
2.292D+02	2.340D-05	9.396D-04	2.014D-05	
2.500D+02	2.269D-05	9.400D-04	1.986D-05	
2.708D+02	2.199D-05	9.403D-04	1.955D-05	
2.917D+02	2.130D-05	9.407D-04	1.923D-05	
3.125D+02	2.061D-05	9.411D-04	1.888D-05	
3.333D+02	1.992D-05	9.415D-04	1.851D-05	
3.542D+02	1.924D-05	9.419D-04	1.813D-05	
3.750D+02	1.857D-05	9.423D-04	1.773D-05	
3.958D+02	1.790D-05	9.427D-04	1.731D-05	
4.167D+02	1.723D-05	9.432D-04	1.687D-05	
4.375D+02	1.657D-05	9.436D-04	1.641D-05	
4.583D+02	1.591D-05	9.441D-04	1.594D-05	
4.792D+02	1.526D-05	9.445D-04	1.546D-05	
5.000D+02	1.461D-05	9.450D-04	1.496D-05	
5.208D+02	1.397D-05	9.455D-04	1.444D-05	
5.417D+02	1.333D-05	9.460D-04	1.391D-05	
5.625D+02	1.269D-05	9.465D-04	1.337D-05	
5.833D+02	1.206D-05	9.470D-04	1.282D-05	
6.042D+02	1.143D-05	9.475D-04	1.225D-05	
6.250D+02	1.081D-05	9.480D-04	1.167D-05	
6.458D+02	1.019D-05	9.485D-04	1.108D-05	
6.667D+02	9.566D-06	9.490D-04	1.048D-05	
6.875D+02	8.950D-06	9.496D-04	9.876D-06	
7.083D+02	8.337D-06	9.501D-04	9.259D-06	
7.292D+02	7.727D-06	9.507D-04	8.633D-06	
7.500D+02	7.120D-06	9.512D-04	7.999D-06	
7.708D+02	6.515D-06	9.518D-04	7.358D-06	
7.917D+02	5.913D-06	9.523D-04	6.711D-06	
8.125D+02	5.313D-06	9.529D-04	6.057D-06	
8.333D+02	4.715D-06	9.535D-04	5.398D-06	
8.542D+02	4.119D-06	9.541D-04	4.734D-06	
8.750D+02	3.526D-06	9.546D-04	4.066D-06	
8.958D+02	2.934D-06	9.552D-04	3.394D-06	
9.167D+02	2.344D-06	9.558D-04	2.719D-06	
9.375D+02	1.756D-06	9.564D-04	2.042D-06	
9.583D+02	1.169D-06	9.570D-04	1.362D-06	
9.792D+02	5.839D-07	9.576D-04	6.814D-07	
1.000D+03	0.000D+00	9.582D-04	0.000D+00	(BOTTOM)

Table 18b. Total Material Balance for Oil-Droplets, SPM and Oil-SPM Agglomerate at 10 Hours From OILSPM3.

```
MATERIAL BALANCE INFORMATION (FOR 1 CM*CM COLUMN OF WATER):

OIL IN THE WATER COLUMN, GRAMS =  1.501D-02
OIL LOST TO THE BOTTOM, GRAMS =  2.001D-01
OIL LOST THROUGH REACTION WITH SPM, GRAMS =  1.013D-01

OIL IN WATER + LOST AT BOTTOM + LOST THROUGH REACTION, GRAMS =  3.164D-01
OIL FLUXED INTO WATER + INITIAL LOADING, GRAMS =  3.166D-01


SPM (UNATTACHED) IN THE WATER COLUMN, GRAMS =  9.458D-01
SPM LOST THROUGH REACTION WITH OIL, GRAMS =  1.013D-01

SPM IN WATER + LOST THROUGH REACTION, GRAMS =  1.047D+00
SPM FLUXED INTO WATER AT BOTTOM + INITIAL LOADING, GRAMS =  1.047D+00


OIL-SPM AGGLOMERATE IN THE WATER COLUMN, GRAMS =  1.358D-02
OIL-SPM AGGLOMERATE FLUXED TO THE BOTTOM, GRAMS =  1.890D-01

OIL-SPM IN WATER + LOST TO BOTTOM, GRAMS =  2.026D-01
OIL-SPM AGGLOMERATE PRODUCED BY REACTION, GRAMS =  2.025D-01


VECTOR CONVERGENCE, OIL = 9.98D-16, SPM = 6.55D-16 ON  3 ITERATIONS.

END OF RUN WAS 07:34:47
```

decaying exponential. The oil-SPM agglomerate concentration varies from 2.168 x 10^{-5} gm/cm^3 to 0; also, note this oil-SPM agglomerate concentration(s) is higher than the 0.5-hr value because the oil-SPM agglomerate has been produced over the 9.5 hr interval.

The total material balance at 10 hours presented in Table 18b illustrates that numerical integration errors improve (i.e., decrease) as the calculation "steps out" in time. Note that the oil put into the water from the surface is 0.3166 g while the calculation accounts for 0.3164 g. The material balances for the other two species close to four digits.

The vector convergence numbers that appear at the end of each of the material balance calculations are the average final errors in trial vectors used in the calculation. In other words, to solve for an oil-droplet concentration profile, the SPM concentration (vector) must be "guessed." Likewise, to solve for the SPM-concentration profile the oil-droplet concentration (vector) must be guessed. The average error in the concentrations is printed to indicate how well (or not) the calculation proceeded. For the case illustrated here the average error between "guessed" and "calculated" concentrations is 9.9 x 10-16 g/cm^3 for oil and 6.55 x 10^{-16} for SPM, which is considered sufficiently small.

1.4   CODE LIMITATIONS AND PERSPECTIVE

An important aspect of the three calculations described here is that they are one dimensional. For the sample problems discussed, a water-column depth of 10 m is used with an area (top or bottom) of 1 cm^2. Note that if 0.5 cm of oil is spilled and this oil transports into the water, the oil droplet concentration could be 0.4gm/1000cm^3 or 400 ppm if there are no oil-loss mechanisms. For the case where oil is removed at the bottom the resulting concentrations will be lower. Clearly this oil concentration is much higher than ever observed in the ocean. The main reason for not predicting a lower oil concentration is that the one-dimensional calculation does not

consider horizontal dispersion or spreading of the oil. Thus, the one-dimensional calculations are conservatively too high. Then the question arises: What good are the calculations?

Besides providing upper bound estimates of concentrations, these calculations also provide an estimate of the time required for things to happen in the water column. Also, the sensitivity of the input parameters can be investigated to learn what is or is not important with respect to a specific objective. For example, the oil deposition mechanisms are the boundary conditions at the bottom for the oil and the oil-SPM agglomerate, and the relative importance of these two processes can be investigated with respect to the parameters that will affect them (i.e., oil rise velocity, oil-SPM reaction rate, and oil-SPM settling velocity).

These calculations (codes) are not usable by interfacing them with other codes (i.e., with an ocean circulation code). The only part of the calculation that is usable is the oil-SPM reaction rate that is of the form: $\alpha_c CS$. This reaction rate is written on a per-unit volume basis, and an ocean-circulation model in three dimensions must then integrate this expression for the loss of oil, loss of SPM, and production of oil-SPM agglomerate. Thus, the relatively simple reaction rate expression is quite difficult to use in an environmental situation, if for no other reason than the environmental situations of interest are three dimensional.

416

APPENDIX A

CODE LISTING FOR OILSPMXS.BAS

```
100 DEFDBL A-H,K-Z
110 REM THIS CODE SOLVES THE ADVECTION-DISPERSION EQUATION FOR OIL
120 REM DROPS WITH EXCESS SPM AND FIRST-ORDER REACTION LOSS.
130 DIM BETA(50),C(50),XDEPTH(50),PT(50),COSR(50),SINR(50)
140 DIM EXPTERM(50),CONTERM(50),MASTERM(50),REATERM(50),FLXTERM(50)
150 DIM ICHECK(50)
160 PIE=3.1415926536#
170 PIE2=PIE/2#
180 TOFS=CHRS(12)
190 CODES="OILSPMXS.BAS"
200 VERS="8-3-88 @ 0718"
210 RTIMES=TIMES
220 RDATES=DATES
230 REM ITIME=1
240 REM EBIG IS THE MAXIMUM ARGUMENT AN EXPONENTIAL IS ALLOWED TO BE
250 EBIG=30#
260 VXIN=.001#:K=100#:L=10#:RERROR=.000001#:GAMMA=.000046#
270 ALPHA=.00094#:NZERO=.000018#:NROOT=25:IEX=27:AN1S="YES"
280 HEADS="PRE-LOADED PARAMETER TEST CASE"
290 CLS
300 GOSUB 4020
310 PRINT:INPUT"WANT TO EDIT OR ENTER INPUT PARAMETERS ";AN2S
320 TEST2S=LEFTS(AN2S,2)
330 IF TEST2S="ED" GOTO 560
340 IF TEST2S="ed" GOTO 560
350 PRINT:INPUT"ENTER AN IDENTIFICATION LINE: ";HEADS
360 PRINT:INPUT"ENTER THE OIL-DROP RISE VELOCITY, CM/SEC (TRY -0.001) ";VX
370 REM SEE THE LETTER TO MAURI PELTO FROM BRUCE KIRSTEIN, 28 JULY 1987
380 REM FOR THE VERTICAL TURBULENT DIFFUSIVITY
390 PRINT:INPUT"ENTER THE TURBULENT DIFFUSIVITY, CM*CM/SEC (TRY 100) ";K
400 PRINT:INPUT"ENTER THE DEPTH, METERS (TRY 10.0) ";L
410 PRINT:INPUT"ENTER THE NUMBER OF ROOTS TO BE DETERMINED (TRY 25) ";NROOT
420 PRINT:PRINT"ENTER THE ERROR LIMIT FOR THE ROOTS (TRY 1.0D-06) ";
430 INPUT RERROR
440 REM SEE THE LETTER TO DAVE LIU FROM BRUCE KIRSTEIN, 1-JULY-83 FOR
450 REM CALCULATION OF THE DISPERSION RATE CONSTANTS
460 PRINT:INPUT"ENTER THE EXPONENTIAL FLUX TERM, 1/SEC (TRY 4.6D-05) ";GAMMA
470 PRINT:PRINT"ENTER THE INITIAL OIL FLUX, GRAM/(CM*CM*SEC) (TRY 1.8D-05) ";
480 INPUT NZERO
490 PRINT:PRINT"ENTER THE DISAPPEARANCE RATE CONSTANT, 1/SEC (TRY 0.00094) ";
500 INPUT ALPHA
510 PRINT:INPUT"ENTER THE NUMBER OF DEPTH VALUES TO EVALUATE (TRY 27) ";IEX
520 IF IEX<50 GOTO 550
530 PRINT:PRINT"NUMBER OF DEPTH VALUES MUST BE LESS THAN 50, RE-ENTER."
540 GOTO 510
550 PRINT:INPUT"WANT TO PRINT THE ROOTS (SAY NO) ";AN1S
560 CLS
570 GOSUB 4020
580 PRINT:PRINT"1.  RISE VELOCITY, CM/SEC = ";VXIN
590 PRINT"2.  TURBULENT DIFFUSIVITY, CM*CM/SEC = ";K
600 PRINT"3.  DEPTH, METERS = ";L
610 PRINT"4.  NUMBER OF ROOTS = ";NROOT
620 PRINT"5.  ROOT ERROR LIMIT = ";
630 PRINT USING"##.###^^^^";RERROR
640 PRINT"6.  EXPONENTIAL FLUX TERM, 1/SEC = ";
650 PRINT USING"##.###^^^^";GAMMA
660 PRINT"7.  INITIAL OIL FLUX, GRAM/(CM*CM*SEC) = ";
670 PRINT USING"##.###^^^^";NZERO
680 PRINT"8.  DISAPPEARANCE RATE CONSTANT, 1/SEC = ";
690 PRINT USING"##.###^^^^";ALPHA
700 PRINT"9.  NUMBER OF DEPTH VALUES = ";IEX
710 PRINT"10. PRINT THE ROOTS? ";AN1S
720 PRINT:INPUT"WANT TO CHANGE ANY";ANS
730 TESTS=LEFTS(ANS,1)
```

```
740 IF TESTS="N" GOTO 980
750 IF TESTS="n" GOTO 980
760 PRINT:INPUT"ENTER THE LINE NUMBER TO BE CHANGED";IL
770 ON IL GOTO 780,800,820,840,860,880,900,920,940,960
780 PRINT:INPUT"ENTER THE RISE VELOCITY, CM/SEC ";VXIN
790 GOTO 560
800 PRINT:INPUT"ENTER THE TURBULENT DIFFUSIVITY, CM*CM/SEC ";K
810 GOTO 560
820 PRINT:INPUT"ENTER THE DEPTH, METERS ";L
830 GOTO 560
840 PRINT:INPUT"ENTER THE NUMBER OF ROOTS TO BE DETERMINED ";NROOT
850 GOTO 560
860 PRINT:INPUT"ENTER THE ERROR LIMIT FOR THE ROOTS ";RERROR
870 GOTO 580
880 PRINT:INPUT"ENTER THE EXPONENTIAL FLUX TERM, 1/SEC ";GAMMA
890 GOTO 560
900 PRINT:INPUT"ENTER THE INITIAL OIL FLUX, GRAM/(CM*CM*SEC) ";NZERO
910 GOTO 560
920 PRINT:INPUT"ENTER THE DISPPEARANCE RATE CONSTANT, 1/SEC ";ALPHA
930 GOTO 560
940 PRINT:INPUT"ENTER THE NUMBER OF DEPTH VALUES TO EVALUATE ";IEX
950 GOTO 560
960 PRINT:INPUT"WANT TO PRINT THE ROOTS? ";AN1$
970 GOTO 560
980 REM BEGIN THE CALCULATION
990 TEST1$=LEFT$(AN1$,1)
1000 LCM=100#*L
1010 LCM2=LCM*LCM
1020 VX=-VXIN
1030 A=VX/(2#*K)
1040 A2=A*A
1050 AL=A*LCM
1060 AL2=AL*AL
1070 EAL=EXP(AL)
1080 EMAL=1#/EAL
1090 VX2=VX/2#
1100 VXLK=VX*LCM+2#*K
1110 K2=2#*K
1120 IEARLY=1
1130 IPAGE=0
1140 GOSUB 4070
1150 LPRINT:LPRINT"THIS CODE SOLVES THE TRANSIENT ADVECTION-DISPERSION";
1160 LPRINT" EQUATION FOR"
1170 LPRINT"OIL DROPLETS WITH FIRST-ORDER REACTION LOSS."
1180 LPRINT:LPRINT"PROBLEM IDENTIFICATION: ";HEAD$
1190 LPRINT:LPRINT"OIL DROPLET RISE VELOCITY = ";VXIN;
1200 LPRINT" CM/SEC, DEPTH = ";L;
1210 LPRINT" METERS"
1220 LPRINT:LPRINT"TURBULENT DIFFUSIVITY = ";K;
1230 LPRINT" CM*CM/SEC"
1240 LPRINT:LPRINT"ERROR LIMIT FOR THE ROOTS = ";
1250 LPRINT USING"##.###^^^^";RERROR
1260 LPRINT:LPRINT"VX*L/(2*K) = ";
1270 LPRINT USING"##.###^^^^";AL;
1280 LPRINT" UNITLESS"
1290 IF TEST1$="N" GOTO 1350
1300 IF TEST1$="n" GOTO 1350
1310 LPRINT:LPRINT"THE ";
1320 LPRINT USING"##";NROOT;
1330 LPRINT" ROOTS OF F(BETA) = BETA*COTANGENT(BETA) + VX*L/(2*K)"
1340 LPRINT:LPRINT"          ROOT          F(BETA)        ERROR CODE"
1350 FOR I = 1 TO NROOT
1360 ICHECK(I)=1
1370 XR=PIE*CDBL(I)
1380 XL=XR-PIE
1390 FOR IHALF = 1 TO 50
```

```
1400 X=(XL+XR)/2#
1410 FX=X*COS(X)/SIN(X)+AL
1420 TEST=ABS(FX)
1430 IF TEST<RERROR GOTO 1510
1440 IF FX>0# GOTO 1470
1450 XR=X
1460 GOTO 1480
1470 XL=X
1480 NEXT IHALF
1490 ICHECK(I)=2
1500 REM STORE CONVENIENT FORMS OF THE ROOTS
1510 X2=X*X
1520 BETA(I)=X
1530 EXPTERM(I)=ALPHA+K*(A2+X2/LCM2)
1540 COSR(I)=COS(X)
1550 SINR(I)=SIN(X)
1560 REM SEE PAGE 15 FOR THE SERIES CONCENTRATION TERM
1570 CONTERM(I)=X/((GAMMA-EXPTERM(I))*(VXLK*COSR(I)-K2*X*SINR(I)))
1580 REM SEE PAGE 42 FOR THE SERIES MASS-IN-WATER TERM
1590 MASTERM(I)=X*CONTERM(I)*(1#-EMAL*(AL*SINR(I)/X+COSR(I)))/(X2+AL2)
1600 REM SEE PAGE 43 FOR THE SERIES MASS-LOST-BY-REACTION TERM
1610 REATERM(I)=MASTERM(I)/EXPTERM(I)
1620 REM SEE PAGE 33 FOR THE SERIES MASS-LOST-AT-THE-BOTTOM TERM
1630 FLXTERM(I)=X*CONTERM(I)/EXPTERM(I)
1640 IF TEST1$="N" GOTO 1710
1650 LPRINT TAB(5);
1660 LPRINT USING"##.###^^^^";BETA(I);
1670 LPRINT TAB(19);
1680 LPRINT USING"##.###^^^^";FX;
1690 LPRINT TAB(36);
1700 LPRINT USING"##";ICHECK(I)
1710 NEXT I
1720 LPRINT:LPRINT"EXPONENTIAL FLUX TERM = ";
1730 LPRINT USING"##.###^^^^";GAMMA;
1740 LPRINT" 1/SEC"
1750 LPRINT:LPRINT"INITIAL OIL FLUX = ";
1760 LPRINT USING"##.###^^^^";NZERO;
1770 LPRINT" GRAMS/(CM*CM*SEC)"
1780 LPRINT:LPRINT"FIRST ORDER DISAPPEARANCE RATE CONSTANT, 1/SEC = ";
1790 LPRINT USING"##.###^^^^";ALPHA;
1800 LPRINT" 1/SEC"
1810 NZL=4#*NZERO*K/LCM
1820 REM SEE PAGE 25 OF THE DERIVATION NOTES FOR ZETA-BAR.
1830 ALPHAK=ALPHA/K
1840 GAMMAK=GAMMA/K
1850 REM ZGAMMA2 IS ZETA-BAR SQUARED ON PAGE 25.
1860 ZGAMMA2=A2+ALPHAK-GAMMAK
1870 REM THIS ZERO-SWITCH WAS INSTALLED 8-3-88, TO REMOVE, JUST REMOVE
1880 REM THE REM'S DOWN TO ZGAMMA2=0#
1890 IF ABS(ZGAMMA2)<1D-20 THEN ZGAMMA2=0#
1900 REM PRINT:PRINT"ZGAMMA2 = ";
1910 REM PRINT USING"##.######^^^^";ZGAMMA2
1920 REM PRINT:INPUT"WANT TO ZERO IT (YES IF LESS THAN 1.0D-20) ";AN$
1930 REM TEST$=LEFT$(AN$,1)
1940 REM IF TEST$="N" GOTO 1940
1950 REM IF TEST$="n" GOTO 1940
1960 REM ZGAMMA2=0#
1970 REM SET THE ZETA-BAR SWITCH FOR REAL (=1), REAL 'A' WHICH MEANS
1980 REM THAT GAMMA=ALPHA (=2), IMAGINARY (=3), OR A HARD ZERO (=4)
1990 REM SEE PAGES 25-27 FOR THE SPECIAL CASES OF ZETA-BAR.
2000 IF ZGAMMA2<>0# GOTO 2030
2010 IZBAR=4
2020 GOTO 2170
2030 IF ALPHA<>GAMMA GOTO 2070
2040 IZBAR=2
2050 ZGAMMA=A
```

```
2060 GOTO 2140
2070 IF ZGAMMA2>0# GOTO 2100
2080 IZBAR=3
2090 GOTO 2120
2100 IZBAR=1
2110 GOTO 2130
2120 ZGAMMA2=-ZGAMMA2
2130 ZGAMMA=SQR(ZGAMMA2)
2140 ARG=ZGAMMA*LCM
2150 COSZ=COS(ARG)
2160 SINZ=SIN(ARG)
2170 ON IZBAR GOTO 2180,2200,2220,2240
2180 LPRINT:LPRINT"ZETA-BAR IS REAL ( <> VX/(2*K) )";
2190 GOTO 2260
2200 LPRINT:LPRINT"ZETA-BAR IS REAL ( = VX/(2*K) )";
2210 GOTO 2260
2220 LPRINT:LPRINT"ZETA-BAR IS IMAGINARY";
2230 GOTO 2260
2240 LPRINT:LPRINT"ZETA-BAR IS EQUAL TO ZERO";
2250 GOTO 2290
2260 LPRINT" AND EQUAL TO ";
2270 LPRINT USING"##.###^^^^";ZGAMMA;
2280 LPRINT" 1/CM";
2290 LPRINT" (IZBAR =";
2300 LPRINT USING"##";IZBAR;
2310 LPRINT")"
2320 ON IZBAR GOTO 2330,2330,2390,2410
2330 EXP1=EXP(ARG)
2340 EXP2=1#/EXP(ARG)
2350 SINH=(EXP1-EXP2)/2#
2360 COSH=(EXP1+EXP2)/2#
2370 LTERM=NZERO/(VX2*SINH+K*ZGAMMA*COSH)
2380 GOTO 2420
2390 LTERM=NZERO/(VX2*SINZ+K*ZGAMMA*COSZ)
2400 GOTO 2420
2410 LTERM=2#*NZERO/VXLK
2420 GOSUB 4070
2430 LPRINT:LPRINT"CALCULATED RESULTS ***********************************"
2440 PRINT:INPUT"ENTER THE TIME, HOURS ";TH
2450 PRINT:PRINT"TIME ENTERED IS ";
2460 PRINT USING"##.###^^^^";TH
2470 PRINT:INPUT"IS THIS CORRECT ";AN$
2480 TEST$=LEFT$(AN$,1)
2490 IF TEST$="N" GOTO 2440
2500 IF TEST$="n" GOTO 2440
2510 T=3600#*TH
2520 DTIME=K*T/LCM2
2530 EGAMT=EXP(-GAMMA*T)
2540 IF IEX=0 GOTO 3030
2550 REM LOAD THE X VALUES
2560 XSTEP=LCM/CDBL(IEX-1)
2570 FOR I = 1 TO IEX
2580 XDEPTH(I)=(I-1)*XSTEP
2590 NEXT I
2600 FOR I = 1 TO IEX
2610 X=XDEPTH(I)
2620 EAX=EXP(A*X)
2630 ARG=ZGAMMA*(LCM-X)
2640 ON IZBAR GOTO 2650,2650,2680,2700
2650 EXP1=EXP(ARG)
2660 CLEAD=EAX*LTERM*EGAMT*(EXP1-1#/EXP1)/2#
2670 GOTO 2710
2680 CLEAD=EAX*LTERM*EGAMT*SIN(ARG)
2690 GOTO 2710
2700 CLEAD=EAX*LTERM*EGAMT*(LCM-X)
2710 SUM1=0#
```

```
2720 FOR IROOT = 1 TO NROOT
2730 ARG=EXPTERM(IROOT)*T
2740 IF ARG>EBIG GOTO 2780
2750 TEMP1=CONTERM(IROOT)*EXP(-ARG)*SIN(BETA(IROOT)*(1#-X/LCM))
2760 SUM1=SUM1+TEMP1
2770 NEXT IROOT
2780 C(I)=CLEAD-NZL*EAX*SUM1
2790 REM NOW INCREMENT TO NEXT X
2800 NEXT I
2810 REM CHECK FOR NEGATIVE CONCENTRATIONS WHICH CAN OCCUR FOR TIMES
2820 REM TOO SMALL, I.E., THE CONCENTRATION PROFILE HAS NOT HAD TIME
2830 REM TO TOUCH THE BOTTOM
2840 REM IEARLY IS THE SWITCH THAT DENOTES WHEN THE TIME IS TOO SMALL
2850 IEARLY=1
2860 FOR I = 1 TO IEX
2870 IF C(I)<0# GOTO 2910
2880 PT(I)=C(I)
2890 NEXT I
2900 GOTO 2970
2910 IEARLY=2
2920 IEX1=I
2930 FOR I = IEX1 TO IEX
2940 C(I)=0#
2950 PT(I)=C(I)
2960 NEXT I
2970 LPRINT:LPRINT"CONCENTRATION PROFILE (GM/CC) FOR TIME = ";
2980 LPRINT USING"##.###^^^^";TH;
2990 LPRINT" HOURS"
3000 LPRINT"DIMENSIONLESS TIME, K*T/L**2 = ";
3010 LPRINT USING"##.###^^^^";DTIME
3020 GOSUB 3790
3030 REM CALCULATE THE MASS OF OIL IN THE WATER AT TIME T, THE LOSS OF OIL
3040 REM THROUGH REACTION, AND THE LOSS OF OIL AT THE BOTTOM
3050 ON IZBAR GOTO 3060,3080,3100,3120
3060 CWLEAD=LTERM*(ZGAMMA*EAL-A*SINH-ZGAMMA*COSH)/(A2-ZGAMMA2)
3070 GOTO 3170
3080 CWLEAD=LTERM*(LCM*EAL-SINH/A)/2#
3090 GOTO 3170
3100 CWLEAD=LTERM*(ZGAMMA*EAL-A*SINZ-ZGAMMA*COSZ)/(A2+ZGAMMA2)
3110 GOTO 3170
3120 REM CHECK FOR A=0 OR GAMMA=0.
3130 IF A<>0# GOTO 3160
3140 CWLEAD=NZERO*LCM2/VXLK
3150 GOTO 3170
3160 CWLEAD=-2#*NZERO*(LCM/A+(1#-EAL)/A2)/VXLK
3170 IF GAMMA>0# GOTO 3200
3180 CRLEAD=CWLEAD*T
3190 GOTO 3220
3200 CRLEAD=CWLEAD*(1#-EGAMT)/GAMMA
3210 CWLEAD=CWLEAD*EGAMT
3220 ON IZBAR GOTO 3230,3230,3230,3280
3230 IF GAMMA>0# GOTO 3260
3240 CFLEAD=LTERM*K*ZGAMMA*EAL*T
3250 GOTO 3320
3260 CFLEAD=LTERM*K*ZGAMMA*EAL*(1#-EGAMT)/GAMMA
3270 GOTO 3320
3280 IF GAMMA>0# GOTO 3310
3290 CFLEAD=K2*NZERO*EAL*T/VXLK
3300 GOTO 3320
3310 CFLEAD=K2*NZERO*EAL*(1#-EGAMT)/(GAMMA*VXLK)
3320 SUM1=0#
3330 SUM2=0#
3340 SUM3=0#
3350 FOR I = 1 TO NROOT
3360 ARG=EXPTERM(I)*T
3370 EXP1=0#
```

```
3380 IF ARG<EBIG THEN EXP1=EXP(-ARG)
3390 SUM1=SUM1+EXP1*MASTERM(I)
3400 SUM2=SUM2+(1#-EXP1)*REATERM(I)
3410 SUM3=SUM3+(1#-EXP1)*FLXTERM(I)
3420 NEXT I
3430 CWMASS=CWLEAD-4#*NZERO*K*EAL*SUM1
3440 CRMASS=(CRLEAD-4#*NZERO*K*EAL*SUM2)*ALPHA
3450 CFMASS=CFLEAD-4#*NZERO*K*K*EAL*SUM3/LCM2
3460 IF IEX>0 GOTO 3510
3470 LPRINT:LPRINT"TIME = ";
3480 LPRINT USING"##.###^^^^";TH;
3490 LPRINT" HOURS, DIMENSIONLESS TIME, K*T/L**2 = ";
3500 LPRINT USING"##.###^^^^";DTIME
3510 IF GAMMA>0# GOTO 3540
3520 FLUXED=NZERO*T
3530 GOTO 3550
3540 FLUXED=NZERO*(1#-EGAMT)/GAMMA
3550 LPRINT:LPRINT"TOTAL GRAMS OF OIL DISPERSED INTO THE WATER COLUMN = ";
3560 LPRINT USING"##.###^^^^";FLUXED
3570 LPRINT:LPRINT"GRAMS OF FREE OIL DROPS IN THE WATER COLUMN = ";
3580 LPRINT USING"##.###^^^^";CWMASS
3590 LPRINT"GRAMS OF OIL DROPS ATTACHED TO SPM = ";
3600 LPRINT USING"##.###^^^^";CRMASS
3610 ON IEARLY GOTO 3660,3620
3620 LPRINT"THE CONCENTRATION PROFILE HAS NOT 'TOUCHED' THE ";
3630 LPRINT"BOTTOM YET"
3640 CFMASS=0#
3650 GOTO 3690
3660 LPRINT"GRAMS OF FREE OIL DROPS ATTACHED TO THE BOTTOM = ";
3670 IF CFMASS<0# THEN CFMASS=0#
3680 LPRINT USING"##.###^^^^";CFMASS
3690 TOTOIL=CFMASS+CRMASS+CWMASS
3700 LPRINT:LPRINT"TOTAL GRAMS OF OIL ACCOUNTED FOR IN THE CALCULATION = ";
3710 LPRINT USING"##.###^^^^";TOTOIL
3720 CLS
3730 PRINT:INPUT"WANT TO DO IT AGAIN ";ANS$
3740 TEST$=LEFT$(ANS$,1)
3750 IF TEST$="Y" GOTO 2420
3760 IF TEST$="y" GOTO 2420
3770 LPRINT TOF$
3780 END
3790 REM PRINT SUBROUTINE
3800 LPRINT:LPRINT"        DEPTH";
3810 LPRINT TAB(21);
3820 LPRINT"OIL CONC"
3830 LPRINT"        (CM)";
3840 LPRINT TAB(22);
3850 LPRINT"(GM/CC)"
3860 FOR I = 1 TO IEX
3870 LPRINT TAB(5);
3880 LPRINT USING"##.###^^^^";XDEPTH(I);
3890 LPRINT TAB(20);
3900 LPRINT USING"##.###^^^^";PT(I);
3910 IF I>1 GOTO 3950
3920 LPRINT TAB(36);
3930 LPRINT"(SURFACE)"
3940 GOTO 4000
3950 IF I<IEX GOTO 3990
3960 LPRINT TAB(36);
3970 LPRINT"(BOTTOM)"
3980 GOTO 4000
3990 LPRINT" "
4000 NEXT I
4010 RETURN
4020 REM SUBROUTINE TO PRINT SCREEN HEADER.
4030 PRINT"OIL DROPLETS INTERACTING WITH EXCESS SPM.
```

```
4040 PRINT"CODE NAME IS ";CODE$;
4050 PRINT", VERSION OF ";VER$
4060 RETURN
4070 REM SUBROUTINE TO PRINT PAGE HEADER.
4080 LPRINT TOF$
4090 LPRINT"CODE NAME IS ";CODE$;
4100 LPRINT", VERSION OF ";VER$
4110 LPRINT"RUN TIME = ";RTIME$;
4120 LPRINT", RUN DATE = ";RDATE$;
4130 IPAGE=IPAGE+1
4140 LPRINT TAB(65);
4150 LPRINT"PAGE ";
4160 LPRINT USING"##";IPAGE
4170 RETURN
```

APPENDIX B
CODE LISTING FOR SPMONLY.BAS

```
100 DEFDBL A-H,K-Z
110 REM THIS CODE SOLVES THE ADVECTION-DISPERSION EQUATION FOR OIL
120 REM DROPS WITH EXCESS SPM AND FIRST-ORDER REACTION LOSS.
130 DIM BETA(50),C(50),XDEPTH(50),PT(50),COSR(50),SINR(50)
140 DIM EXPTERM(50),CONTERM(50),MASTERM(50),REATERM(50),FLXTERM(50)
150 DIM ICHECK(50)
160 PIE=3.1415926536#
170 PIE2=PIE/2#
180 TOFS=CHR$(12)
190 CODE$="OILSPMXS.BAS"
200 VER$="8-3-88 @ 0718"
210 RTIME$=TIME$
220 RDATE$=DATE$
230 REM ITIME=1
240 REM EBIG IS THE MAXIMUM ARGUMENT AN EXPONENTIAL IS ALLOWED TO BE
250 EBIG=30#
260 VXIN=.001#:K=100#:L=10#:RERROR=.000001#:GAMMA=.000046#
270 ALPHA=.00094#:NZERO=.000018#:NROOT=25:IEX=27:AN1$="YES"
280 HEAD$="PRE-LOADED PARAMETER TEST CASE"
290 CLS
300 GOSUB 4020
310 PRINT:INPUT"WANT TO EDIT OR ENTER INPUT PARAMETERS ";AN2$
320 TEST2$=LEFT$(AN2$,2)
330 IF TEST2$="ED" GOTO 560
340 IF TEST2$="ed" GOTO 560
350 PRINT:INPUT"ENTER AN IDENTIFICATION LINE: ";HEAD$
360 PRINT:INPUT"ENTER THE OIL-DROP RISE VELOCITY, CM/SEC (TRY -0.001) ";VX
370 REM SEE THE LETTER TO MAURI PELTO FROM BRUCE KIRSTEIN, 28 JULY 1987
380 REM FOR THE VERTICAL TURBULENT DIFFUSIVITY
390 PRINT:INPUT"ENTER THE TURBULENT DIFFUSIVITY, CM*CM/SEC (TRY 100) ";K
400 PRINT:INPUT"ENTER THE DEPTH, METERS (TRY 10.0) ";L
410 PRINT:INPUT"ENTER THE NUMBER OF ROOTS TO BE DETERMINED (TRY 25) ";NROOT
420 PRINT:PRINT"ENTER THE ERROR LIMIT FOR THE ROOTS (TRY 1.0D-06) ";
430 INPUT RERROR
440 REM SEE THE LETTER TO DAVE LIU FROM BRUCE KIRSTEIN, 1-JULY-83 FOR
450 REM CALCULATION OF THE DISPERSION RATE CONSTANTS
460 PRINT:INPUT"ENTER THE EXPONENTIAL FLUX TERM, 1/SEC (TRY 4.6D-05) ";GAMMA
470 PRINT:PRINT"ENTER THE INITIAL OIL FLUX, GRAM/(CM*CM*SEC) (TRY 1.8D-05) ";
480 INPUT NZERO
490 PRINT:PRINT"ENTER THE DISAPPEARANCE RATE CONSTANT, 1/SEC (TRY 0.00094) ";
500 INPUT ALPHA
510 PRINT:INPUT"ENTER THE NUMBER OF DEPTH VALUES TO EVALUATE (TRY 27) ";IEX
520 IF IEX<50 GOTO 550
530 PRINT:PRINT"NUMBER OF DEPTH VALUES MUST BE LESS THAN 50, RE-ENTER."
540 GOTO 510
550 PRINT:INPUT"WANT TO PRINT THE ROOTS (SAY NO) ";AN1$
560 CLS
570 GOSUB 4020
580 PRINT:PRINT"1.  RISE VELOCITY, CM/SEC = ";VXIN
590 PRINT"2.  TURBULENT DIFFUSIVITY, CM*CM/SEC = ";K
600 PRINT"3.  DEPTH, METERS = ";L
610 PRINT"4.  NUMBER OF ROOTS = ";NROOT
620 PRINT"5.  ROOT ERROR LIMIT = ";
630 PRINT USING"##.###^^^^";RERROR
640 PRINT"6.  EXPONENTIAL FLUX TERM, 1/SEC = ";
650 PRINT USING"##.###^^^^";GAMMA
660 PRINT"7.  INITIAL OIL FLUX, GRAM/(CM*CM*SEC) = ";
670 PRINT USING"##.###^^^^";NZERO
680 PRINT"8.  DISAPPEARANCE RATE CONSTANT, 1/SEC = ";
690 PRINT USING"##.###^^^^";ALPHA
700 PRINT"9.  NUMBER OF DEPTH VALUES = ";IEX
710 PRINT"10. PRINT THE ROOTS? ";AN1$
720 PRINT:INPUT"WANT TO CHANGE ANY";ANS$
730 TEST$=LEFT$(AN$,1)
```

```
740 IF TEST$="n" GOTO 970
750 PRINT:INPUT"ENTER THE LINE NUMBER TO BE CHANGED";IL
760 ON IL GOTO 770,790,810,830,850,870,890,910,930,950
770 PRINT:INPUT"ENTER THE TERMINAL VELOCITY, CM/SEC ";VX
780 GOTO 550
790 PRINT:INPUT"ENTER THE TURBULENT DIFFUSIVITY, CM*CM/SEC ";K
800 GOTO 550
810 PRINT:INPUT"ENTER THE DEPTH, METERS ";L
820 GOTO 550
830 PRINT:INPUT"ENTER THE NUMBER OF ROOTS TO BE DETERMINED ";NROOT
840 GOTO 550
850 PRINT:INPUT"ENTER THE ERROR LIMIT FOR THE ROOTS ";RERROR
860 GOTO 570
870 PRINT:INPUT"ENTER THE SPM-LOSS RATE CONSTANT, 1/SEC ";ALPHA
880 GOTO 550
890 PRINT:INPUT"ENTER THE FLUX RATE, GM/SEC*CM*CM ";F0
900 GOTO 550
910 PRINT:INPUT"ENTER THE DEPOSTION RATE, CM/SEC ";KS
920 GOTO 550
930 PRINT:INPUT"ENTER THE NUMBER OF DEPTH VALUES TO EVALUATE ";IEX
940 GOTO 550
950 PRINT:INPUT"WANT TO PRINT THE ROOTS? ";AN1$
960 GOTO 550
970 REM BEGIN THE CALCULATION
980 TEST1$=LEFT$(AN1$,1)
990 PRINT:INPUT"DO YOU WANT ABRAMOWITZ & STEGUN COTANGENT VALUES";AN$
1000 TEST$=LEFT$(AN$,1)
1010 IF TEST$="N" THEN AANDS=1
1020 IF TEST$="n" THEN AANDS=1
1030 LCM=100#*L
1040 LCM2=LCM*LCM
1050 A=VX/(2#*K)
1060 A2=A*A
1070 AL=A*LCM
1080 AL2=AL*AL
1090 EAL=EXP(AL)
1100 EMAL=1#/EAL
1110 VX2=VX/2#
1120 VXLK=VX*LCM+2#*K
1130 K2=2#*K
1140 K2L=K2/LCM
1150 TERM2=A*KS*LCM
1160 TERM3=LCM*KS-2#*K
1170 TERM4=A*KS*LCM2/K
1180 TERM5=KS*LCM/K
1190 TERM6=LCM*KS+K2
1200 IEARLY=1
1210 IPAGE=0
1220 GOSUB 4030
1230 LPRINT:LPRINT"THIS CODE SOLVES THE 1-D TRANSIENT ADVECTION-";
1240 LPRINT"DISPERSION EQUATION FOR SPM"
1250 LPRINT"(ANALYTICAL SOLUTION) WITH FIRST-ORDER REACTION LOSS."
1260 LPRINT:LPRINT"TERMINAL VELOCITY = ";
1270 LPRINT USING"##.###^^^^";VX;
1280 LPRINT" CM/SEC, DEPTH = ";
1290 LPRINT USING"###.#";L;
1300 LPRINT" METERS"
1310 LPRINT:LPRINT"TURBULENT DIFFUSIVITY = ";
1320 LPRINT USING"####.#";K;
1330 LPRINT" CM*CM/SEC"
1340 LPRINT:LPRINT"FLUX RATE FROM THE BOTTOM = ";
1350 LPRINT USING"##.###^^^^";F0;
1360 LPRINT" GM/SEC*CM*CM"
1370 LPRINT:LPRINT"DEPOSITION RATE = ";
1380 LPRINT USING"##.###^^^^";KS;
1390 LPRINT" CM/SEC"
```

```
1400 LPRINT:LPRINT"ERROR LIMIT FOR THE ROOTS = ";
1410 LPRINT USING"##.###^^^^";RERROR
1420 LPRINT:LPRINT"A = VX/(2*K) = ";
1430 LPRINT USING"##.###^^^^";A;
1440 LPRINT" 1/CM"
1450 IF TEST1$="N" GOTO 1580
1460 IF TEST1$="n" GOTO 1580
1470 LPRINT:LPRINT"ROOTS CALCULATED USING";
1480 IF AANDS=2 THEN LPRINT" ABRAMOWITZ AND STEGUN."
1490 IF AANDS=1 THEN LPRINT" MACHINE FUNCTIONS."
1500 LPRINT:LPRINT"THE ";
1510 LPRINT USING"##";NROOT;
1520 LPRINT" ROOTS OF F(BETA)=BETA*COTANGENT(BETA)-";
1530 LPRINT"K*((A*L)^2-A*KS*L+BETA^2)/(KS*L)
1540 LPRINT:LPRINT"          ROOT          F(BETA)        ERROR CODE"
1550 GOTO 1610
1560 LPRINT:LPRINT"THE NUMBER OF ROOTS USED IS ";
1570 LPRINT USING"####";NROOT
1580 REM START ON THE FIRST ZERO-PIE INTERVAL
1590 TESTI=(AL2-TERM4)/TERM5
1600 REM IF TESTI>1 THERE IS NO ROOT.
1610 FOR I = 1 TO NROOT
1620 IF I>1 GOTO 1650
1630 NOROOT=1#
1640 IF TESTI<=1# THEN NOROOT=0#
1650 ICHECK(I)=1
1660 XR=PIE*CDBL(I+NOROOT)
1670 XL=XR-PIE
1680 FOR IHALF = 1 TO 50
1690 X=(XL+XR)/2#
1700 IF AANDS=2 GOTO 1730
1710 FX=COS(X)/SIN(X)-((AL2/X)-(TERM4/X)+X)/TERM5
1720 GOTO 1750
1730 GOSUB 3530
1740 FX=FCOTX-((AL2/X)-(TERM4/X)+X)/TERM5
1750 TEST=ABS(FX)
1760 ICHECK(I)=IHALF
1770 IF TEST<RERROR GOTO 1850
1780 IF FX>0# GOTO 1810
1790 XR=X
1800 GOTO 1820
1810 XL=X
1820 NEXT IHALF
1830 ICHECK(I)=99
1840 REM STORE CONVENIENT FORMS OF THE ROOTS.
1850 X2=X*X
1860 BETA(I)=X
1870 PEXPT(I)=K*(A2+X2/LCM2)
1880 EXPTERM(I)=ALPHA+PEXPT(I)
1890 SUMTEMP(I)=LCM*(KS-LCM*PEXPT(I)+TERM2)
1900 COSR(I)=COS(X)
1910 SINR(I)=SIN(X)
1920 REM SEE PAGE 29 FOR THE SERIES CONCENTRATION TERM
1930 CONTERM(I)=X/(EXPTERM(I)*(TERM6*X*SINR(I)-SUMTEMP(I)*COSR(I)))
1940 REM SEE PAGE 9 CC FOR THE SERIES MASS-IN-WATER TERM
1950 MASTERM(I)=CONTERM(I)*(VX*AL+K2L*X2)*SINR(I)/((LCM/K)*PEXPT(I))
1960 REM SEE PAGE 12(CC) FOR THE SERIES MASS-LOST-BY-REACTION TERM
1970 REATERM(I)=MASTERM(I)/EXPTERM(I)
1980 REM SEE PAGE 19(CC) FOR THE SERIES MASS-LOST-AT-THE-BOTTOM TERM
1990 FLXTERM(I)=((K2L/2#)*K2L*X2+VX*VX2)*SINR(I)*CONTERM(I)/EXPTERM(I)
2000 BFLUX(I)=(VX*SINR(I)+K2L*X*COSR(I))*CONTERM(I)/EXPTERM(I)
2010 IF TEST1$="N" GOTO 2100
2020 IF TEST1$="n" GOTO 2100
2030 LPRINT TAB(5);
2040 LPRINT USING"##.###^^^^";BETA(I);
2050 LPRINT TAB(19);
```

```
2060 LPRINT USING"##.###^^^^";FX;
2070 LPRINT TAB(38);
2080 IF ICHECK(I)<51 THEN ICHECK(I)=1
2090 LPRINT USING"##";ICHECK(I)
2100 NEXT I
2110 LPRINT:LPRINT"INITIAL SPM FLUX = ";
2120 LPRINT USING"##.###^^^^";F0;
2130 LPRINT" GRAMS/(CM*CM*SEC)"
2140 LPRINT:LPRINT"FIRST-ORDER SPM DISAPPEARANCE RATE CONSTANT, 1/SEC = ";
2150 LPRINT USING"##.###^^^^";ALPHA;
2160 LPRINT" 1/SEC"
2170 ALPHAK=ALPHA/K
2180 ZETA2=A2+ALPHAK
2190 ZZETA=SQR(ZETA2)
2200 ARG=ZZETA*LCM
2210 EXP1=EXP(ARG)
2220 EXP2=1#/EXP(ARG)
2230 SINH=(EXP1-EXP2)/2#
2240 COSH=(EXP1+EXP2)/2#
2250 ZHYP=2#*K*ALPHA+VX*KS
2260 LTERM=1#/(K2*KS*ZZETA*COSH+ZHYP*SINH)
2270 BLEAD=(VX*SINH+K2*ZZETA*COSH)*LTERM
2280 REM START THE CALCULATION.
2290 PRINT:INPUT"ENTER THE TIME IN HOURS ";TYME
2300 PRINT:PRINT"TIME ENTERED IS ";
2310 PRINT USING"##.###^^^^";TYME
2320 PRINT:INPUT"IS THIS CORRECT ";AN$
2330 TEST$=LEFT$(AN$,1)
2340 IF TEST$="N" GOTO 2290
2350 IF TEST$="n" GOTO 2290
2360 T=3600#*TYME
2370 REM LOAD THE X VALUES
2380 XSTEP=LCM/CDBL(IEX-1)
2390 FOR I = 1 TO IEX
2400 XDEPTH(I)=(I-1)*XSTEP
2410 NEXT I
2420 FOR I = 1 TO IEX
2430 X=XDEPTH(I)
2440 EAX=EXP(-A*(LCM-X))
2450 ARG=ZZETA*X
2460 EXP1=EXP(ARG)
2470 EXP1R=1#/EXP(ARG)
2480 CLEAD2=K2*ZZETA*(EXP1+EXP1R)/2#
2490 CLEAD1=LTERM*((VX*(EXP1-EXP1R)/2#)+CLEAD2)
2500 SUM1=0#
2510 FOR IROOT = 1 TO NROOT
2520 ARG=EXPTERM(IROOT)*T
2530 IF ARG>EBIG GOTO 2600
2540 TRIGARG=BETA(IROOT)*X/LCM
2550 SINTERM=VX*SIN(TRIGARG)
2560 COSTERM=K2L*BETA(IROOT)*COS(TRIGARG)
2570 TEMP1=CONTERM(IROOT)*EXP(-ARG)*(SINTERM+COSTERM)
2580 SUM1=SUM1+TEMP1
2590 NEXT IROOT
2600 C(I)=F0*EAX*(CLEAD1-SUM1)
2610 REM NOW INCREMENT TO NEXT X
2620 NEXT I
2630 REM CHECK FOR NEGATIVE CONCENTRATIONS WHICH CAN OCCUR FOR TIMES
2640 REM TOO SMALL, I.E., THE CONCENTRATION PROFILE HAS NOT HAD TIME
2650 REM TO TOUCH THE BOTTOM.
2660 REM IEARLY IS THE SWITCH THAT DENOTES WHEN THE TIME IS TOO SMALL.
2670 IEARLY=1
2680 FOR I = 1 TO IEX
2690 J=IEX-I+1
2700 IF C(J)<0# GOTO 2720
2710 NEXT I
```

```
2720 IEARLY=2
2730 IEX1=I
2740 FOR I = IEX1 TO IEX
2750 J=IEX-I+1
2760 C(J)=0#
2770 NEXT I
2780 REM NOW PRINT THE CONCENTRATION PROFILES
2790 GOSUB 4030
2800 LPRINT:LPRINT"CONCENTRATION PROFILES AT TIME = ";
2810 LPRINT USING"##.###^^^^";TYME;
2820 LPRINT" HOURS ***********************"
2830 LPRINT:LPRINT TAB(9);
2840 LPRINT"DEPTH";
2850 LPRINT TAB(27);
2860 LPRINT"SPM CONC."
2870 LPRINT TAB(10);
2880 LPRINT"CM";
2890 LPRINT TAB(27);
2900 LPRINT"GM/CM**3"
2910 FOR I=1 TO IEX
2920 LPRINT"        ";
2930 LPRINT USING"##.###^^^^";XDEPTH(I);
2940 LPRINT"           ";
2950 LPRINT USING"##.###^^^^";C(I);
2960 IF I>1 GOTO 3000
2970 LPRINT TAB(36);
2980 LPRINT"(SURFACE)"
2990 GOTO 3050
3000 IF I<IEX GOTO 3040
3010 LPRINT TAB(36);
3020 LPRINT"(BOTTOM)"
3030 GOTO 3050
3040 LPRINT" "
3050 NEXT I
3060 REM CALCULATE THE MASS OF OIL IN THE WATER AT TIME T, THE LOSS OF OIL
3070 REM THROUGH REACTION, AND THE LOSS OF OIL AT THE BOTTOM.
3080 CWLEAD=LTERM*K2*SINH
3090 CRLEAD=ALPHA*CWLEAD
3100 CFLEAD=CRLEAD
3110 SUM1=0#
3120 SUM2=0#
3130 SUM3=0#
3140 SUM4=0#
3150 FOR I = 1 TO NROOT
3160 ARG=EXPTERM(I)*T
3170 EXP1=0#
3180 IF ARG<EBIG THEN EXP1=EXP(-ARG)
3190 SUM1=SUM1+EXP1*MASTERM(I)
3200 EXPM1=1#-EXP1
3210 SUM2=SUM2+EXPM1*REATERM(I)
3220 SUM3=SUM3+EXPM1*FLXTERM(I)
3230 SUM4=SUM4+EXPM1*BFLUX(I)
3240 NEXT I
3250 CWMASS=F0*(CWLEAD-SUM1)
3260 CRMASS=F0*(CRLEAD*T-ALPHA*SUM2)
3270 CFMASS=F0*(CFLEAD*T+SUM3)
3280 IF IEX>0 GOTO 3330
3290 LPRINT:LPRINT"TIME = ";
3300 LPRINT USING"##.###^^^^";TYME
3310 LPRINT" HOURS, DIMENSIONLESS TIME, K*T/L**2 = ";
3320 LPRINT USING"##.###^^^^";DTIME
3330 LPRINT:LPRINT"GRAMS OF SPM (UNATTACHED) IN THE WATER COLUMN = ";
3340 LPRINT USING"##.###^^^^";CWMASS
3350 LPRINT"GRAMS OF SPM ATTACHED TO OIL = ";
3360 LPRINT USING"##.###^^^^";CRMASS
3370 TOTSPM=CRMASS+CWMASS
```

```
3380 LPRINT:LPRINT"GRAMS OF SPM IN WATER + ATTACHED = ";
3390 LPRINT USING"##.###^^^^";TOTSPM
3400 LPRINT:LPRINT"GRAMS OF SPM FROM THE BOTTOM (FROM VX*C-K*DC/DX) = ";
3410 LPRINT USING"##.###^^^^";CFMASS
3420 SEDIMENT=F0*T-KS*F0*(BLEAD*T-SUM4)
3430 LPRINT"GRAMS OF SPM FROM THE BOTTOM (FROM -F0+KS*C) = ";
3440 LPRINT USING"##.###^^^^";SEDIMENT
3450 CLS
3460 PRINT:INPUT"WANT TO DO IT AGAIN ";ANS
3470 TEST$=LEFT$(ANS,1)
3480 IF TEST$="Y" GOTO 2280
3490 IF TEST$="y" GOTO 2280
3500 LPRINT TOF$
3510 LPRINT TOF$
3520 END
3530 REM SUBROUTINE TO CALCULATE COTANGENT FROM M. ABRAMOWITZ
3540 REM AND I.R. STEGUN, HANDBOOK OF MATHEMATICAL FUNCTIONS,
3550 REM SEE PAGE 76, EQUATION 4.3.103.
3560 FLIP=0
3570 REM THIS CALCULATES THE SERIES APPROX FOR XCOT(X).
3580 AC2=-.333333341#:AC4=-.0222220287#:AC6=-.0021177168#
3590 AC8=-.00020785041#:AC10=-.00002626191#
3600 REM UNWIND THE ARGUMENT TO LESS THAN PIE/4.
3610 REM ADJUST X TO A 2PI FRAME.
3620 YI=(X/TWOPIE -CDBL(INT(X/TWOPIE)))*TWOPIE
3630 IF (YI>0)AND(YI<PIE2) THEN IQUAD=1
3640 IF (YI>PIE2)AND(YI<PIE) THEN IQUAD=2
3650 IF (YI>PIE)AND(YI<PIE*1.5#) THEN IQUAD=3
3660 IF (YI>PIE*1.5#)AND(YI<TWOPIE) THEN IQUAD=4
3670 IF (YI=PIE2) OR (YI=PIE*1.5#) THEN IQUAD=5
3680 IF (YI=PIE)OR(YI=TWOPIE)OR(YI=0) THEN IQUAD=6
3690 ON IQUAD GOTO 3700,3720,3740,3760,3940,3960
3700 Y=YI
3710 GOTO 3770
3720 Y=PIE-YI
3730 GOTO 3770
3740 Y=YI-PIE
3750 GOTO 3770
3760 Y=TWOPIE-YI
3770 TEST=PIE4-Y
3780 IF TEST>0# GOTO 3820
3790 XI=Y
3800 Y=PIE2-XI
3810 FLIP=1
3820 YSQ=Y*Y
3830 SREMAIN=YSQ*(AC8+(AC10)*YSQ)
3840 SCOTX=1#+YSQ*(AC2+YSQ*(AC4+YSQ*(AC6+SREMAIN)))
3850 TCOTX=SCOTX/Y
3860 IF IQUAD=2 THEN TCOTX=-TCOTX
3870 IF IQUAD=4 THEN TCOTX=-TCOTX
3880 REM SO NOW WE REALLY HAVE COTX FOR THE ZERO TO PIE/4 WEDGE.
3890 IF FLIP=1 GOTO 3920
3900 FCOTX=TCOTX
3910 GOTO 3970
3920 FCOTX=1#/TCOTX
3930 GOTO 3970
3940 FCOTX=0#
3950 GOTO 3970
3960 FCOTX=1D+21
3970 RETURN
3980 REM SUBROUTINE TO PRINT SCREEN HEADER.
3990 PRINT"SUSPENDED-PARTICULATE-MATTER (SPM) CALCULATION
4000 PRINT"CODE NAME IS ";CODENS;
4010 PRINT", VERSION OF ";VER$
4020 RETURN
4030 REM SUBROUTINE TO PRINT PAGE HEADER.
```

431

```
4040 LPRINT TOF$
4050 LPRINT"CODE NAME IS ";CODEN$;
4060 LPRINT", VERSION OF ";VER$
4070 LPRINT"RUN TIME = ";RTIME$;
4080 LPRINT", RUN DATE = ";RDATE$;
4090 IPAGE=IPAGE+1
4100 LPRINT TAB(65);
4110 LPRINT"PAGE ";
4120 LPRINT USING"##";IPAGE
4130 RETURN
```

APPENDIX C
CODE LISTING FOR OILSPM3BAS

```
100  REM
110  DEFDBL A-H,O-Z
120  REM THIS CODE IS THE SIMULTANEOUS OIL-SPM SOLVER AND CAN BE USED
130  REM TO SOLVE FOR OIL ALONE OR SPM ALONE WITH AN ARBITRARY INITIAL
140  REM CONDITION.   CRANK-NICOLSON INTEGRATION IS USED.
150  DIM A(3,101),C(101),U(101),Y(101),X(101),PNT(101)
160  DIM B(3,101),S(101),V(101),Z(101),CG(101),SG(101)
170  DIM D(3,101),W(101),Q(101),G(101),R(101)
180  CODEN$="OILSPM3.BAS"
190  VER$="8-9-88 @ 0643"
200  TOF$=CHR$(12)
210  RTIME$=TIME$:RDATE$=DATE$
220  CLS
230  GOSUB 9250
240  REM SET THE PAGE COUNTER TO ZERO.
250  IPAGE=0
260  REM SPECIFY SOME OIL PARAMETERS:
270  VDIFFA=100#:VOIL=.01#:ALPHO=.094#:DEPTH=10#:NPOINTSA=49
280  SZER=.000018#:GAMM=.000046#:TYMEMAX=.5#:PINT=.5#:TDIVIDE=20#
290  REM SPECIFY SOME SPM PARAMETERS:
300  VSPM=.001#:ALPHS=.094#:FZER=.000046#:SKZER=.046#:PIE2=9.869589#
310  VASPM=.001#:SECONDS=3600#:IEULER=1:ICRATE=3
320  ANSP$="YES":ANOP$="NO":ANCP$="YES"
330  PRINT:PRINT"WANT TO 'ENTER' NEW PARAMETERS OR 'EDIT' RECOMMENDED";
340  INPUT" VALUES";ANS$
350  TESTA$=LEFT$(ANS$,2)
360  IF TESTA$="EN" GOTO 390
370  IF TESTA$="en" GOTO 390
380  GOTO 610
390  CLS
400  GOSUB 9250
410  PRINT:PRINT"ENTER THE VERTICAL-TURBULENT DIFFUSIVITY, CM*CM/SEC";
420  INPUT", (TRY 100)";VDIFFA
430  PRINT:PRINT"ENTER THE OIL RISING VELOCITY, CM/SEC, (TRY 0.001)";
440  INPUT VOIL
450  PRINT:PRINT"ENTER THE OIL-SPM RATE CONSTANT FOR OIL LOSS, CC/(GM*SEC)";
460  INPUT", (TRY .094)";ALPHO
470  PRINT:INPUT"ENTER THE OCEAN DEPTH, METERS, (TRY 10)";DEPTH
480  PRINT:PRINT"ENTER THE NUMBER OF GRID POINTS (MAXIMUM 99,";
490  PRINT" MUST BE ODD, TRY 49)";
500  REM THIS IS THE NUMBER OF POINTS WITHIN THE WATER COLUMN AND DOES
510  REM NOT INCLUDE THE EXTERIOR TWO POINTS.
520  INPUT NPOINTSA
530  PRINT:PRINT"THE OIL-DISPERSION FLUX IS: SZERO*EXP(-GAMMA*TIME)"
540  PRINT:INPUT"ENTER SZERO, GRAMS/(CM*CM*SEC), (TRY 1.8D-05)";SZER
550  PRINT:INPUT"ENTER GAMMA, 1/SEC, (TRY 4.6D-05)";GAMM
560  PRINT:INPUT"ENTER THE MAXIMUM TIME, HOURS";TYMEMAX
570  PRINT:INPUT"ENTER THE PRINT INTERVAL, HOURS";PINT
580  PRINT:INPUT"USE STEADY-STATE OIL PROFILE TO START (SAY NO): ";ANOP$
590  PRINT:INPUT"COUPLE THE CONCENTRATIONS: ";ANCP$
600  PRINT:INPUT"COUPLING ITERATIONS (TRY 5) ";ICRATE
610  CLS
620  GOSUB 9250
630  PRINT:PRINT"1.   TURBULENT DIFFUSIVITY, CM*CM/SEC = ";
640  PT=VDIFFA
650  GOSUB 7210
660  PRINT"2.   OIL RISING VELOCITY, CM/SEC = ";
670  PT=VOIL
680  GOSUB 7210
690  PRINT"3.   OIL-SPM RATE CONSTANT FOR OIL LOSS, CC/(GM*SEC) = ";
700  PT=ALPHO
710  GOSUB 7210
720  PRINT"4.   OCEAN DEPTH, METERS = ";
730  PT=DEPTH
740  GOSUB 7210
```

```
750 PRINT"5.   NUMBER OF GRID POINTS = ";
760 IPT=NPOINTSA
770 GOSUB 7240
780 PRINT"6.   INITIAL OIL-DISPERSON FLUX SZERO, GRAMS/(CM*CM*SEC) = ";
790 PT=SZER
800 GOSUB 7210
810 PRINT"7.   OIL-DISPERSON GAMMA, 1/SEC = ";
820 PT=GAMM
830 GOSUB 7210
840 PRINT"8.   MAXIMUM TIME, HOURS = ";
850 PRINT USING"###.##";TYMEMAX
860 PRINT"9.   PRINT INTERVAL, HOURS = ";
870 PRINT USING"#.###";PINT
880 PRINT"10. USE STEADY-STATE OIL PROFILE TO START: ";ANOP$
890 PRINT"11. COUPLE THE CONCENTRATIONS: ";ANCP$
900 PRINT"12. COUPLING ITERATIONS = ";
910 PRINT USING"##";ICRATE
920 PRINT:INPUT"WANT TO CHANGE ANY";ANS$
930 TESTB$=LEFT$(ANS$,1)
940 IF TESTB$="N" GOTO 1230
950 IF TESTB$="n" GOTO 1230
960 PRINT:INPUT"ENTER THE LINE NUMBER TO BE CHANGED";LN
970 ON LN GOTO 980,1000,1020,1040,1060,1090,1110,1130,1150,1170,1190,1210
980 PRINT:INPUT"ENTER THE TURBULENT DIFFUSIVITY, CM*CM/SEC";VDIFFA
990 GOTO 610
1000 PRINT:INPUT"ENTER THE OIL RISING VELOCITY, CM/SEC";VOIL
1010 GOTO 610
1020 PRINT:INPUT"ENTER THE OIL-SPM RATE CONSTANT, CC/(GM*SEC)";ALPHO
1030 GOTO 610
1040 PRINT:INPUT"ENTER THE OCEAN DEPTH, METERS";DEPTH
1050 GOTO 610
1060 PRINT:PRINT"ENTER THE NUMBER OF GRID POINTS (MAXIMUM 99,";
1070 INPUT" MAKE IT ODD, TRY 49)";NPOINTSA
1080 GOTO 610
1090 PRINT:INPUT"ENTER SZERO, GRAMS/(CM*CM*SEC) ";SZER
1100 GOTO 610
1110 PRINT:INPUT"ENTER GAMMA, 1/SEC";GAMM
1120 GOTO 610
1130 PRINT:INPUT"ENTER THE MAXIMUM TIME, HOURS";TYMEMAX
1140 GOTO 610
1150 PRINT:INPUT"ENTER THE PRINT INTERVAL, HOURS";PINT
1160 GOTO 610
1170 PRINT:INPUT"USE STEADY-STATE OIL PROFILE TO START: ";ANOP$
1180 GOTO 610
1190 PRINT:INPUT"COUPLE THE CONCENTRATIONS: ";ANCP$
1200 GOTO 610
1210 PRINT:INPUT"COUPLING ITERATIONS (TRY 5) ";ICRATE
1220 GOTO 610
1230 REM CHECK THE NUMBER OF GRID POINTS.
1240 IF NPOINTSA<100 GOTO 1300
1250 CLS
1260 PRINT:PRINT"THE NUMBER OF GRID POINTS EXCEEDS ARRAY CAPACITY";
1270 PRINT" OF 99."
1280 PRINT:INPUT"ENTER THE NUMBER OF GRID POINTS (MAKE IT ODD)";NPOINTSA
1290 GOTO 610
1300 REM ENTER OR EDIT THE SPM PARAMETERS
1310 CLS
1320 IF TESTA$="EN" GOTO 1350
1330 IF TESTA$="en" GOTO 1350
1340 GOTO 1460
1350 GOSUB 9250
1360 PRINT:INPUT"ENTER THE SPM SETTLING VELOCITY, CM/SEC (TRY 0.001)";VSPM
1370 PRINT:PRINT"ENTER THE OIL-SPM AGGLOMERATE SETTLING VELOCITY,";
1380 INPUT" CM/SEC (TRY 0.0001)";VASPM
1390 PRINT:PRINT"ENTER THE OIL-SPM RATE CONSTANT FOR SPM LOSS,";
1400 INPUT" CC/(GM*SEC), TRY 0.094";ALPHS
```

435

```
1410 PRINT:PRINT"ENTER THE SPM BOTTOM SOURCE FLUX TERM, GM/CM^2*SEC";
1420 INPUT" (TRY 4.6D-05)";FZER
1430 PRINT:PRINT"ENTER THE SPM BOTTOM DEPOSITION RATE CONSTANT, CM/SEC,";
1440 INPUT" (TRY 0.046)";SKZER
1450 PRINT:INPUT"WANT TO START OFF WITH STEADY-STATE SPM";ANSP$
1460 CLS
1470 GOSUB 9250
1480 PRINT:PRINT"1.  SPM SETTLING VELOCITY, CM/SEC = ";
1490 PT=VSPM
1500 GOSUB 7210
1510 PRINT"2.  OIL-SPM AGGLOMERATE SETTLING VELOCITY, CM/SEC = ";
1520 PT=VASPM
1530 GOSUB 7210
1540 PRINT"3.  OIL-SPM RATE CONSTANT FOR SPM LOSS, CC/(GM*SEC) = ";
1550 PT=ALPHS
1560 GOSUB 7210
1570 PRINT"4.  SPM SOURCE FLUX TERM, GM/(CM^2*SEC) = ";
1580 PT=FZER
1590 GOSUB 7210
1600 PRINT"5.  SPM DEPOSITION RATE CONSTANT, CM/SEC = ";
1610 PT=SKZER
1620 GOSUB 7210
1630 PRINT"6.  USE STEADY-STATE SPM PROFILE TO START: ";ANSP$
1640 PRINT:INPUT"WANT TO CHANGE ANY";ANS$
1650 TESTB$=LEFT$(ANS$,1)
1660 IF TESTB$="N" GOTO 1830
1670 IF TESTB$="n" GOTO 1830
1680 PRINT:INPUT"ENTER THE LINE NUMBER TO BE CHANGED";LN
1690 ON LN GOTO 1700,1720,1750,1770,1790,1810
1700 PRINT:INPUT"ENTER THE SPM SETTLING VELOCITY, CM/SEC";VSPM
1710 GOTO 1460
1720 PRINT:PRINT"ENTER THE OIL-SPM AGGLOMERATE SETTLING VELOCITY,";
1730 INPUT" CM/SEC ";VASPM
1740 GOTO 1460
1750 PRINT:INPUT"ENTER THE OIL-SPM RATE CONSTANT FOR SPM LOSS";ALPHS
1760 GOTO 1460
1770 PRINT:INPUT"ENTER THE SPM BOTTOM SOURCE FLUX TERM";FZER
1780 GOTO 1460
1790 PRINT:INPUT"ENTER THE SPM BOTTOM DEPOSITION RATE CONSTANT";SKZER
1800 GOTO 1460
1810 PRINT:INPUT"USE STEADY-STATE SPM PROFILE TO START: ";ANSP$
1820 GOTO 1460
1830 REM INITIALIZE THE SPM CONCENTRATION PROFILE.
1840 TESTSPM$=LEFT$(ANSP$,1)
1850 ISPM=1
1860 IF TESTSPM$="Y" THEN ISPM=2
1870 IF TESTSPM$="y" THEN ISPM=2
1880 TESTOIL$=LEFT$(ANOP$,1)
1890 IOIL=1
1900 IF TESTOIL$="Y" THEN IOIL=2
1910 IF TESTOIL$="y" THEN IOIL=2
1920 REM IS COUPLING ON?
1930 ICPLE=1
1940 TESTCPL$=LEFT$(ANCP$,1)
1950 IF TESTCPL$="N" THEN ICPLE=2
1960 IF TESTCPL$="n" THEN ICPLE=2
1970 REM THE ACTUAL NUMBER OF POINTS IS NPOINTSA+2 BECAUSE THERE IS
1980 REM A POINT AT -DX ON THE LEFT BOUNDARY AND A POINT AT +DX ON
1990 REM THE RIGHT BOUNDARY.  THE REASON FOR DOING THIS IS THAT
2000 REM CENTRAL DIFFERENCE APPROXIMATIONS ARE USED FOR THE DERIVATIVES
2010 REM AT THE BOUNDARIES.
2020 NPOINTS=NPOINTSA+2
2030 APOINTS=CDBL(NPOINTS)
2040 NPOINTS1=NPOINTS-1
2050 NPOINTS2=NPOINTS-2
2060 NPOINTS3=NPOINTS-3
```

```
2070 REM THE BOTTOM BOUNDARY CONDITION IS C=0 FOR OIL ALWAYS,
2080 J(NPOINTS1)=0#
2090 REM AS IS W=0 FOR THE OIL-SPM AGGLOMERATE.
2100 D(NPOINTS1)=0#
2110 REM START THE CALCULATION.
2120 REM THE WORKING UNITS ARE GRAM-CENTIMETER-HOUR.
2130 DEPTH1=DEPTH*100#
2140 DEPTH2=DEPTH1*DEPTH1
2150 REM EXAMINE K*T*PIE^2/L^2 TO DETERMINE THE TIME REQUIRED
2160 REM FOR UNIT DIMENSIONLESS TIME, SEE SECTION 3.8, PAGE 113
2170 REM OF CARSLAW AND JAEGER FOR A SIMILAR PROBLEM.
2180 VDIFF=VDIFFA*SECONDS
2190 TUNITY=DEPTH2/VDIFF/PIE2
2200 PRINT:PRINT"TIME FOR UNITY DIMENSIONLESS TIME, HOURS = ";
2210 PRINT USING"##.###^^^^";TUNITY
2220 PRINT:PRINT"THE TIME STEP WILL BE THE ABOVE TIME DIVIDED BY ";
2230 PRINT USING"####.###";TDIVIDE
2240 PRINT:INPUT"IS THIS ACCEPTABLE";ANS$
2250 TESTB$=LEFT$(ANS$,1)
2260 IF TESTB$="Y" GOTO 2310
2270 IF TESTB$="y" GOTO 2310
2280 PRINT:INPUT"ENTER THE VALUE YOU WANT";TDIVIDE
2290 GOTO 2220
2300 REM SET THE TIME STEP.
2310 DT=TUNITY/TDIVIDE
2320 REM NOW COMPUTE THE REQUIRED TIME STEP WHICH IS LESS THAN
2330 REM THE CURRENT VALUE OF DT TO 'STEP' ON A PRINT INTERVAL.
2340 TYME=0#
2350 TYME9=.9999#*TYMEMAX
2360 PINT9=.9999#*PINT
2370 NSTEPS=FIX(PINT/DT)+1
2380 ASTEPS=CDBL(NSTEPS)
2390 DT=PINT/ASTEPS
2400 RDT=1#/DT
2410 REM SET THE FINAL PRINT SWITCH.
2420 IPFINAL=1
2430 REM SET UP THE PARAMETERS IN THE CORRECT UNITS OF GRAM-CM-HOUR.
2440 REM USE CM/HOUR FOR THE RISING OR SETTLING VELOCITY.
2450 REM THE OIL RISING VELOCITY IS NEGATIVE BECAUSE THE UP-DIRECTION
2460 REM IS NEGATIVE, POSITIVE IS DOWN.
2470 VROIL=-VOIL*SECONDS
2480 VRSPM=VSPM*SECONDS
2490 VRAGG=VASPM*SECONDS
2500 REM USE 1/HOUR FOR THE RATE CONSTANT WITH UNIT SPM CONCENTRATION
2510 REM OR GM/(CM^3*HOURS) WHEN A REAL SPM CONCENTRATION IS USED.
2520 ALPHAO=ALPHO*SECONDS
2530 ALPHAS=ALPHS*SECONDS
2540 REM THE RATE CONSTANT FOR THE APPEARANCE OF THE OIL-SPM AGGLOMERATE
2550 REM IS THE SUM OF THE TWO INDIVIDUAL RATE CONSTANTS.
2560 ALPHAB=ALPHAO+ALPHAS
2570 SZERO=SZER*SECONDS
2580 FZERO=FZER*SECONDS
2590 SKZERO=SKZER*SECONDS
2600 GAMMA=GAMM*SECONDS
2610 REM NUMBER OF UNKNOWN OIL CONCENTRATIONS SOLVED FOR MUST BE SET
2620 REM TO L FOR THE SPARSE-MATRIX SOLVING ROUTINE.  THIS ROUTINE
2630 REM SOLVES FOR THE N-2 UNKNOWNS AND THE OTHER UNKNOWN IS SOLVED
2640 REM FOR 'OFF-LINE.'  THE REASON FOR THIS IS AS FOLLOWS:
2650 REM THE NUMBER OF GRID POINTS IS NPOINTS, HENCE THE NUMBER OF
2660 REM OF UNKNOWN OIL CONCENTRATIONS IS NPOINTS.  BUT, THE OIL
2670 REM CONCENTRATION AT THE OCEAN BOTTOM IS 0., I.E., C(NPOINTS1)=0.
2680 REM BECAUSE OF THIS PARTICULAR ZERO OIL CONCENTRATION, THE 'OIL'
2690 REM SYSTEM OF EQUATIONS IS SOLVED THROUGH NPOINTS-2 ONLY, AND THE
2700 REM LAST UNKNOWN OIL CONCENTRATION IS SOLVED FOR AT THE 'END.'
2710 REM SOLVING SUBROUTINE.
2720 L=NPOINTS2
```

437

```
2730 LM1=L-1
2740 LM2=L-2
2750 APOINTS1=CDBL(NPOINTS3)
2760 DX=DEPTH1/APOINTS1
2770 DX2=DX*DX
2780 DX4=4#*DX
2790 REM CALCULATE THE EULER INTEGRATION PARAMETERS
2800 REM FOR THE INTEGRATION OF THE FLUX OF OIL TO THE BOTTOM,
2810 REM THE OIL REACTION LOSS, THE NET SPM FLUX AND THE SPM
2820 REM REACTION LOSS.
2830 EDTDX=VDIFF*DT/DX
2840 REM AND FOR THE REACTION LOSS.
2850 EDT=DT
2860 REM SET UP THE SIMPSONS INTEGRATION PARAMETERS.  DO NOT INCLUDE
2870 REM C(1) AND C(N) IN THE INTEGRATION BECAUSE THEY ARE OUTSIDE THE
2880 REM BOUNDARIES.
2890 ISMP42=(NPOINTSA-3)/2
2900 HSMP3=DX/3#
2910 ALPHAO2=ALPHAO/2#
2920 ALPHAS2=ALPHAS/2#
2930 ALPHAB2=ALPHAB/2#
2940 DOILDX=VDIFF/DX
2950 DOILDX2=VDIFF/DX2
2960 DOILDX22=DOILDX2/2#
2970 V4XO=VROIL/DX4
2980 V4XS=VRSPM/DX4
2990 V4XB=VRAGG/DX4
3000 REM THE C(I) ARRAY STORES THE OIL CONCENTRATION PROFILE AT THE
3010 REM CURRENT TIME, THE U(I) ARRAY STORES THE CALCULATED OIL
3020 REM CONCENTRATION PROFILE AT THE NEXT TIME (STEP).
3030 REM THE A(3,N) ARRAY STORES THE COEFFICIENTS FOR THE CRANK-
3040 REM NICOLSON ALGORITHM FOR THE OIL.
3050 REM ALSO, THE S(I) ARRAY STORES THE SPM CONCENTRATION PROFILE AT THE
3060 REM CURRENT TIME, THE V(I) ARRAY STORES THE CALCULATED SPM
3070 REM CONCENTRATION PROFILE AT THE NEXT TIME (STEP).
3080 REM THE B(3,N) ARRAY STORES THE COEFFICIENTS FOR THE CRANK-
3090 REM NICOLSON ALGORITHM FOR THE SPM.
3100 REM THE MAIN DIAGONAL ELEMENT IS 'DIAGC1' FOR THE C(I,J+1).
3110 REM THE MAIN DIAGONAL ELEMENT IS 'DIAGC2' FOR THE C(I,J).
3120 DIAGC1=DOILDX2+RDT
3130 DIAGC2=DOILDX2-RDT
3140 REM THE MAIN DIAGONAL ELEMENT IS 'DIAGS1' FOR THE S(I,J+1).
3150 REM THE MAIN DIAGONAL ELEMENT IS 'DIAGS2' FOR THE S(I,J).
3160 DIAGS1=DIAGC1
3170 DIAGS2=DIAGC2
3180 REM THE MAIN DIAGONAL ELEMENT IS 'DIAGB1' FOR THE W(I,J+1).
3190 REM THE MAIN DIAGONAL ELEMENT IS 'DIAGB2' FOR THE W(I,J)
3200 DIAGB1=DIAGC1
3210 DIAGB2=DIAGC2
3220 REM THE UPPER DIAGONAL IS 'UDIAG'
3230 UDIAGC=DOILDX22-V4XO
3240 UDIAGS=DOILDX22-V4XS
3250 UDIAGB=DOILDX22-V4XB
3260 REM THE LOWER DIAGONAL IS 'BDIAG'
3270 BDIAGC=DOILDX22+V4XO
3280 BDIAGS=DOILDX22+V4XS
3290 BDIAGB=DOILDX22+V4XB
3300 GOSUB 9300
3310 LPRINT:LPRINT"PROBLEM PARAMETERS ARE AS FOLLOWS:"
3320 LPRINT:LPRINT"VERTICAL TURBULENT DIFFUSIVITY, CM*CM/SEC = ";
3330 LPRINT USING"####.##";VDIFFA
3340 LPRINT"WATER DEPTH, METERS = ";
3350 LPRINT USING"###.#";DEPTH
3360 LPRINT:LPRINT"OIL RISING VELOCITY, CM/SEC = ";
3370 LPRINT USING"##.##^^^^";VOIL
3380 LPRINT"OIL-SPM RATE CONSTANT FOR OIL LOSS, CC/(GM*SEC) = ";
```

438

```
3__0  LPRINT USING"##.###^^   ";ALPHO
3400  LPRINT"OIL DISPERSION RATE, GM/(CM*CM*SEC) = (";
3410  LPRINT USING"#.##^^   ";SZER;
3420  LPRINT")*EXP((-";
3430  LPRINT USING"#.##^^^^^";GAMM;
3440  LPRINT")*SECONDS)"
3450  LPRINT:LPRINT"SPM SETTLING VELOCITY, CM/SEC = ";
3460  LPRINT USING"##.##^^^^^";VSPM
3470  LPRINT"OIL-SPM RATE CONSTANT FOR SPM LOSS, CC/(GM*SEC) = ";
3480  LPRINT USING"##.##^^^^^";ALPHS
3490  LPRINT"SPM BOTTOM SOURCE FLUX, GM/(CM^2*SEC) = ";
3500  LPRINT USING"##.##^^^^^";FZER
3510  LPRINT"SPM DEPOSITION RATE CONSTANT, CM/SEC = ";
3520  LPRINT USING"##.##^^^^^";SKZER
3530  LPRINT:LPRINT"OIL-SPM AGGLOMERATE SETTLING VELOCITY, CM/SEC = ";
3540  LPRINT USING"##.##^^^^^";VASPM
3550  LPRINT:LPRINT"TIME STEP, HOURS = ";
3560  LPRINT USING"##.##^^^^^";DT;
3570  LPRINT", INTEGRATION TIME, HOURS = ";
3580  LPRINT USING"###.##";TYMEMAX
3590  LPRINT"SPECIFIED PRINT INTERVAL, HOURS = ";
3600  LPRINT USING"##.###";PINT
3610  REM SAVE THE DEPTHS.
3620  FOR I = 1 TO NPOINTS2
3630  X(I)=(I-1)*DX
3640  NEXT I
3650  REM ZERO THE ARRAYS.
3660  FOR I = 1 TO NPOINTS
3670  S(I)=0#
3680  C(I)=0#
3690  W(I)=0#
3700  SG(I)=0#
3710  CG(I)=0#
3720  NEXT I
3730  REM IF THE REACTION RATE CONSTANTS ARE GREATER THAN ZERO,
3740  REM TURN ON THE CROSS TERMS.
3750  IF ALPHAO=0# GOTO 3790
3760  FOR I = 1 TO NPOINTS
3770  SG(I)=1#
3780  NEXT I
3790  IF ALPHAS=0# GOTO 3830
3800  FOR I = 1 TO NPOINTS
3810  CG(I)=1#
3820  NEXT I
3830  OILZERO=0#
3840  ON IOIL GOTO 3930,3850
3850  REM CALCULATE A STEADY STATE (GAMMA=0) OIL CONCENTRATION PROFILE.
3860  GOSUB 8830
3870  FOR I = 1 TO NPOINTSA
3880  PNT(I)=C(I+1)
3890  NEXT I
3900  REM INTEGRATE THE INITIAL NONZERO OIL PROFILE.
3910  GOSUB 8330
3920  OILZERO=SUM1
3930  LPRINT:LPRINT"THE INITIAL OIL WATER-COLUMN LOADING, GRAMS = ";
3940  LPRINT USING"##.###^^^^^";OILZERO
3950  SPMZERO=0#
3960  ON ISPM GOTO 4060,3970
3970  REM CALCULATE A STEADY-STATE SPM CONCENTRATION PROFILE.
3980  GOSUB 8460
3990  REM AND LOAD THE SPM STEADY-STATE PROFILE.
4000  FOR I = 1 TO NPOINTSA
4010  PNT(I)=S(I+1)
4020  NEXT I
4030  REM INTEGRATE THE INITIAL NONZERO SPM PROFILE.
4040  GOSUB 8330
```

```
4050 SPMZERO=SUM1
4060 LPRINT"THE INITIAL SPM WATER-COLUMN LOADING, GRAMS = ";
4070 LPRINT USING"##.###    ";SPMZERO
4080 REM FILL IN SOME ELEMENTS WHICH DO NOT CHANGE.
4090 AEXTRA=-DOILDX/2#
4100 DEXTRA=AEXTRA
4110 A(2,1)=-AEXTRA
4120 A(1,1)=VROIL
4130 B(1,1)=VRSPM
4140 BEXTRA2=DOILDX/2#
4150 BEXTRA1=-BEXTRA2
4160 B(2,1)=BEXTRA2
4170 B(1,1)=VRSPM
4180 Z(1)=0#
4190 REM THE NEXT THREE STATEMENTS REFER TO THE OIL-SPM AGGLOMERATE.
4200 D(2,1)=-DEXTRA
4210 D(1,1)=VRAGG
4220 G(1)=0#
4230 REM INTEGRATE THE INITIAL OIL CONCENTRATION PROFILE.
4240 FOR I = 1 TO NPOINTSA
4250 PNT(I)=C(I+1)
4260 NEXT I
4270 GOSUB 8330
4280 OILP=SUM1
4290 REM INTEGRATE THE INITIAL SPM CONCENTRATION PROFILE.
4300 FOR I = 1 TO NPOINTSA
4310 PNT(I)=S(I+1)
4320 NEXT I
4330 GOSUB 8330
4340 SPMP=SUM1
4350 REM THE INITIAL OIL-SPM AGGLOMERATE CONCENTRATION PROFILE IS
4360 REM ALWAYS ZERO,
4370 AGLP=0#
4380 REM AS IS THE INTEGRAL OF THE FLUX TO THE BOTTOM.
4390 AGFLUX=0#
4400 REM THE INTEGRATION OF THE PROFILES IS DONE AT EACH TIME
4410 REM INCLUDING T=0.  THIS IS THE START OF THE EULER INTEGRATION.
4420 OILFLUX=(C(NPOINTS2)-C(NPOINTS))/4#
4430 OILLOSS=OILP/2#
4440 SPMCONC=S(NPOINTS1)/2#
4450 SPMLOSS=SPMP/2#
4460 REM IS COUPLING ON?
4470 ON ICPLE GOTO 4480,4600
4480 REM INTEGRATE THE INITIAL OIL*SPM CONCENTRATION PROFILE.
4490 FOR I = 1 TO NPOINTSA
4500 PNT(I)=C(I+1)*S(I+1)
4510 NEXT I
4520 GOSUB 8330
4530 REM AND INTEGRATE WITH RESPECT TO TIME.
4540 CROSS=SUM1/2#
4550 ICNT=0
4560 FOR I = 1 TO NPOINTS
4570 CG(I)=C(I)
4580 SG(I)=S(I)
4590 NEXT I
4600 REM DO AN INITIAL PRINT.
4610 GOSUB 6230
4620 REM START THE CALCULATION.
4630 REM FILL IN THE OIL AND SPM TRIDIAGONAL ELEMENTS INTO THE
4640 REM A(3,NPOINTS) AND B(3,NPOINTS) ARRAYS.
4650 REM FILL THE UPPER OIL DIAGONAL STARTING WITH A(1,2) AND RUNNING
4660 REM THROUGH NPOINTS3.
4670 FOR I = 2 TO NPOINTS3
4680 A(1,I)=UDIAGC
4690 NEXT I
4700 REM FILL THE MAIN OIL DIAGONAL STARTING WITH A(2,2) AND RUNNING
```

```
....  REM THROUGH NPOINTS2.
....  FOR I = 2 TO NPOINTS2
4730  REM NOW GUESS THE SEDIMENT VECTOR AND COMPUTE ALPHA-PRIME
4740  REM FOR EACH POSITION IN THE WATER COLUMN.
4750  REM LEAVE AT UNITY FOR NOW, 2-13-38.
4760  A(2,I)=-DIAGC1-ALPHAO2*SG(I)
4770  NEXT I
4780  REM FILL THE LOWER OIL DIAGONAL STARTING WITH A(3,1) AND RUNNING
4790  REM THROUGH NPOINTS3.
4800  FOR I = 1 TO NPOINTS3
4810  A(3,I)=BDIAGC
4820  NEXT I
4830  REM FILL Y(1) WITH THE OIL BOUNDARY CONDITION AT THE TYME+DT STEP.
4840  Y(1)=SZERO*EXP(-GAMMA*(TYME+DT))
4850  REM FILL Y(I) VECTOR STARTING WITH Y(2) AND RUNNING THROUGH NPOINTS1.
4860  FOR I = 2 TO NPOINTS1
4870  IM=I-1
4880  IP=I+1
4890  Y(I)=-BDIAGC*C(IM)+(DIAGC2+ALPHAO2*SG(I))*C(I)-UDIAGC*C(IP)
4900  NEXT I
4910  REM FILL THE UPPER SPM DIAGONAL STARTING WITH B(1,2) AND RUNNING
4920  REM THROUGH NPOINTS1.  FILL THE MAIN SPM DIAGONAL STARTING
4930  REM WITH B(2,2) AND RUNNING THROUGH NPOINTS1 WITH THE GUESS
4940  REM OF THE OIL CONCENTRATION.
4950  FOR I = 2 TO NPOINTS1
4960  B(1,I)=UDIAGS
4970  B(2,I)=-DIAGS1-ALPHAS2*CG(I)
4980  NEXT I
4990  REM FILL IN THE LAST B(2,NPOINTS) ELEMENT.
5000  B(2,NPOINTS)=BEXTRA1
5010  REM FILL THE LOWER SPM DIAGONAL STARTING WITH B(3,1) AND RUNNING
5020  REM THROUGH NPOINTS2.
5030  FOR I = 1 TO NPOINTS2
5040  B(3,I)=BDIAGS
5050  NEXT I
5060  B(3,NPOINTS1)=VRSPM-SKZERO
5070  REM FILL Z(I) VECTOR STARTING WITH Z(2) AND RUNNING THROUGHT
5080  REM NPOINTS1, NOTE THAT Z(1) IS ALWAYS 0.
5090  FOR I = 2 TO NPOINTS1
5100  IM=I-1
5110  IP=I+1
5120  Z(I)=-BDIAGS*S(IM)+(DIAGS2+ALPHAS2*CG(I))*S(I)-UDIAGS*S(IP)
5130  NEXT I
5140  REM AND FILL IN Z(NPOINTS).
5150  Z(NPOINTS)=-FZERO
5160  REM NOW SOLVE THE SYSTEM OF EQUATIONS.
5170  GOSUB 7640
5180  GOSUB 7850
5190  REM IS COUPLING ON?
5200  ON ICPLE GOTO 5210,5400
5210  ICNT=ICNT+1
5220  IF ICNT>ICRATE GOTO 5380
5230  ERROIL=0#
5240  ERRSPM=0#
5250  FOR I = 1 TO NPOINTS
5260  ERROIL=ERROIL+ABS(CG(I)-U(I))
5270  ERRSPM=ERRSPM+ABS(SG(I)-V(I))
5280  CG(I)=U(I)
5290  SG(I)=V(I)
5300  NEXT I
5310  ERROIL=ERROIL/APOINTS
5320  ERRSPM=ERRSPM/APOINTS
5330  PRINT:PRINT"OIL ERROR = ";
5340  PRINT USING"##.##^^^^";ERROIL;
5350  PRINT", SPM ERROR = ";
5360  PRINT USING"##.##^^^^";ERRSPM
```

```
5370 GOTO 4610
5380 REM RESET THE ITERATION COUNTER.
5390 ICNT=0
5400 REM INCREMENT TIME, IPNTED=1 MEANS A PRINT AT THIS TIME
5410 REM HAS NOT OCCURRED.
5420 TYME=TYME+DT
5430 PRINT:PRINT"TIME = ";
5440 PRINT USING"##.###^^^^";TYME
5450 IPNTED=1
5460 REM RELOAD THE CONCENTRATION VECTORS AND SAVE THE AVERAGE OIL-SPM
5470 REM CONCENTRATION PRODUCT.
5480 FOR I = 1 TO NPOINTS
5490 R(I)=C(I)*S(I)+U(I)*V(I)
5500 C(I)=U(I)
5510 S(I)=V(I)
5520 NEXT I
5530 REM NOW SOLVE FOR THE OIL-SPM AGGLOMERATE CONCENTRATION PROFILE.
5540 REM FILL IN THE OIL-SPM AGGLOMERATE TRIDIAGONAL ELEMENTS INTO THE
5550 REM D(3,NPOINTS) ARRAY.
5560 REM FILL THE UPPER OIL-SPM DIAGONAL STARTING WITH D(1,2) AND RUNNING
5570 REM THROUGH NPOINTS3.
5580 FOR I = 2 TO NPOINTS3
5590 D(1,I)=UDIAGB
5600 NEXT I
5610 REM FILL THE MAIN OIL-SPM DIAGONAL STARTING WITH D(2,2) AND RUNNING
5620 REM THROUGH NPOINTS2.
5630 FOR I = 2 TO NPOINTS2
5640 D(2,I)=-DIAGB1
5650 NEXT I
5660 REM FILL THE LOWER OIL-SPM DIAGONAL STARTING WITH D(3,1) AND RUNNING
5670 REM THROUGH NPOINTS3.
5680 FOR I = 1 TO NPOINTS3
5690 D(3,I)=BDIAGB
5700 NEXT I
5710 REM FILL G(1) WITH THE OIL-SPM BOUNDARY CONDITION AT THE TYME+DT STEP.
5720 G(1)=0#
5730 REM FILL G(I) VECTOR STARTING WITH G(2) AND RUNNING THROUGH NPOINTS1.
5740 FOR I = 2 TO NPOINTS1
5750 IM=I-1
5760 IP=I+1
5770 G(I)=-BDIAGB*W(IM)+DIAGB2*W(I)-UDIAGB*W(IP)-ALPHAB2*R(I)
5780 NEXT I
5790 REM NOW SOLVE FOR THE OIL-SPM AGGLOMERATE CONCENTRATION PROFILE.
5800 GOSUB 8080
5810 REM AND STORE THE NEW VECTOR IN W(I).
5820 FOR I = 1 TO NPOINTS
5830 W(I)=Q(I)
5840 NEXT I
5850 REM INTEGRATE THE OIL CONCENTRATION PROFILE.
5860 FOR I = 1 TO NPOINTSA
5870 PNT(I)=C(I+1)
5880 NEXT I
5890 GOSUB 8330
5900 OILP=SUM1
5910 REM INTEGRATE THE SPM CONCENTRATION PROFILE.
5920 FOR I = 1 TO NPOINTSA
5930 PNT(I)=S(I+1)
5940 NEXT I
5950 GOSUB 8330
5960 SPMP=SUM1
5970 REM INTEGRATE THE OIL-SPM AGGLOMERATE CONCENTRATION PROFILE.
5980 FOR I = 1 TO NPOINTSA
5990 PNT(I)=W(I+1)
6000 NEXT I
6010 GOSUB 8330
6020 AGLP=SUM1
```

```
6030 ON ICPLE GOTO 6040,6120
6040 REM INTEGRATE THE OIL*SPM CONCENTRATION PROFILE.
6050 FOR I = 1 TO NPOINTSA
6060 PNT(I)=C(I+1)*S(I+1)
6070 NEXT I
6080 GOSUB 8330
6090 REM AND INTEGRATE WITH RESPECT TO TIME.
6100 CROSSL=SUM1
6110 CROSS=CROSS+CROSSL
6120 REM INTEGRATE THE FLUX OF OIL TO THE BOTTOM AND REACTION LOSS,
6130 REM SPM DEPOSITION AND REACTION LOSS.
6140 OILFLUX=OILFLUX+(C(NPOINTS2)-C(NPOINTS))/2#
6150 OILLOSS=OILLOSS+OILP
6160 SPMCONC=SPMCONC+S(NPOINTS1)
6170 SPMLOSS=SPMLOSS+SPMP
6180 REM INTEGRATE THE OIL-SPM AGGLOMERATE FLUX TO THE BOTTOM.
6190 AGFLUX=AGFLUX+(W(NPOINTS2)-W(NPOINTS))/2#
6200 REM IS IT TIME TO PRINT?
6210 IF TYME<=PINT9 GOTO 6380
6220 PINT9=.9999#*(PINT+TYME)
6230 REM DO A PRINT.
6240 GOSUB 9300
6250 LPRINT:LPRINT
6260 LPRINT:LPRINT"CONCENTRATION PROFILES AT TIME = ";
6270 LPRINT USING"##.###";TYME;
6280 LPRINT" HOURS   ***************************"
6290 GOSUB 7270
6300 LPRINT:LPRINT"MATERIAL BALANCE INFORMATION ";
6310 LPRINT"(FOR 1 CM*CM COLUMN OF WATER):"
6320 REM CALCULATE THE TOTAL MASS OF OIL IN THE WATER COLUMN,
6330 REM WHICH WAS DONE ABOVE.
6340 LPRINT:LPRINT"OIL IN THE WATER COLUMN, GRAMS =";
6350 LPRINT USING"##.###^^^^";OILP
6360 REM CALCULATE THE MASS OF OIL FLUXED TO THE BOTTOM.
6370 BMASSO=(OILFLUX-(C(NPOINTS2)-C(NPOINTS))/4#)*EDTDX
6380 LPRINT"OIL LOST TO THE BOTTOM, GRAMS = ";
6390 LPRINT USING"##.###^^^^";BMASSO
6400 ON ICPLE GOTO 6410,6440
6410 CROSS2=(CROSS-CROSSL/2#)*EDT
6420 AMASSO=ALPHAO*CROSS2
6430 GOTO 6450
6440 AMASSO=ALPHAO*(OILLOSS-OILP/2#)*EDT
6450 LPRINT"OIL LOST THROUGH REACTION WITH SPM, GRAMS = ";
6460 LPRINT USING"##.###^^^^";AMASSO
6470 TOTALO=AMASSO+BMASSO+OILP
6480 LPRINT:LPRINT"OIL IN WATER + LOST AT BOTTOM + LOST THROUGH REACTION,";
6490 LPRINT" GRAMS = ";
6500 LPRINT USING"##.###^^^^";TOTALO
6510 REM CALCULATE THE OIL FLUXED INTO THE WATER AT THE SURFACE.
6520 IF GAMMA=0# GOTO 6550
6530 SURFACE=SZERO*(1#-EXP(-GAMMA*TYME))/GAMMA
6540 GOTO 6560
6550 SURFACE=SZERO*TYME
6560 SURFACE=SURFACE+OILZERO
6570 LPRINT"OIL FLUXED INTO WATER + INITIAL LOADING,";
6580 LPRINT" GRAMS = ";
6590 LPRINT USING"##.###^^^^";SURFACE
6600 LPRINT:LPRINT:LPRINT"SPM (UNATTACHED) IN THE WATER COLUMN, GRAMS = ";
6610 LPRINT USING"##.###^^^^";SPMP
6620 ON ICPLE GOTO 6630,6650
6630 SPMREAC=ALPHAS*CROSS2
6640 GOTO 6660
6650 SPMREAC=ALPHAS*(SPMLOSS-SPMP/2#)*EDT
6660 LPRINT"SPM LOST THROUGH REACTION WITH OIL, GRAMS = ";
6670 LPRINT USING"##.###^^^^";SPMREAC
6680 TOTALS=SPMREAC+SPMP
```

```
6700 LPRINT:LPRINT"SPM IN WATER + LOST THROUGH REACTION";
6710 LPRINT", GRAMS = ";
6710 LPRINT USING"##.###      ";TOTALS
6720 SPMFLUX=FZERO+TYME-SPZERO+(SPMCONC-S(NPOINTS1)/2#)*EDT
6730 LPRINT"SPM FLUXED INTO WATER AT BOTTOM + INITIAL LOADING";
6740 LPRINT", GRAMS = ";
6750 SPMFLUX=SPMFLUX+SPMZERO
6760 LPRINT USING"##.###      ";SPMFLUX
6770 REM PRINT THE OIL-SPM AGGLOMERATE INFORMATION.
6780 LPRINT:LPRINT:LPRINT"OIL-SPM AGGLOMERATE IN THE WATER COLUMN, GRAMS = ";
6790 LPRINT USING"##.###      ";AGLP
6800 BMASSA=(AGFLUX-(W(NPOINTS2)-W(NPOINTS))/4#)*EDTDX
6810 LPRINT"OIL-SPM AGGLOMERATE FLUXED TO THE BOTTOM, GRAMS = ";
6820 LPRINT USING"##.###      ";BMASSA
6830 TOTALA=AGLP+BMASSA
6840 LPRINT:LPRINT"OIL-SPM IN WATER + LOST TO BOTTOM, GRAMS = ";
6850 LPRINT USING"##.###      ";TOTALA
6860 AGRATE=ALPHAB*CROSS2
6870 LPRINT"OIL-SPM AGGLOMERATE PRODUCED BY REACTION, GRAMS = ";
6880 LPRINT USING"##.###      ";AGRATE
6890 ON ICPLE GOTO 6900,6970
6900 LPRINT:LPRINT:LPRINT"VECTOR CONVERGENCE, OIL =";
6910 LPRINT USING"##.##      ";ERROIL;
6920 LPRINT", SPM =";
6930 LPRINT USING"##.##      ";ERRSPM;
6940 LPRINT" ON ";
6950 LPRINT USING"##";ICRATE;
6960 LPRINT" ITERATIONS."
6970 IPNTED=2
6980 REM HAS THE SPECIFIED INTEGRATION TIME BEEN ATTAINED?
6990 IF TYME>=TYME9 GOTO 7030
7000 REM THE INTEGRATION TIME HAS NOT BEEN ATTAINED,
7010 REM TAKE ANOTHER STEP.
7020 GOTO 4620
7030 REM CHECK TO SEE IF A FINAL PRINT IS REQUIRED.
7040 IF IPNTED=2 GOTO 7120
7050 REM DO A FINAL PRINT.
7060 ON IPFINAL GOTO 7070,7120
7070 IPFINAL=2
7080 LPRINT:LPRINT
7090 LPRINT:LPRINT"FINAL PRINT FROM LAST TIME STEP";
7100 LPRINT" (NOT NECESSARILY ON A PRINT INTERVAL):"
7110 GOTO 6260
7120 LPRINT:LPRINT"END OF RUN WAS ";TIME$
7130 CLS
7140 LPRINT:INPUT"WANT TO DO ANOTHER CALCULATION";AGAIN$
7150 TESTC$=LEFT$(AGAIN$,1)
7160 IF TESTC$="Y" GOTO 610
7170 IF TESTC$="y" GOTO 610
7180 LPRINT TOF$
7190 LPRINT TOF$
7200 END
7210 REM PRINT 3-PLACE SCIENTIFIC NOTATION.
7220 PRINT USING"##.##      ";PT
7230 RETURN
7240 REM PRINT 3-PLACE FIXED NOTATION.
7250 PRINT USING"###";IPT
7260 RETURN
7270 REM THIS IS THE RESULT PRINTING ROUTINE.
7280 REM PRINT THE HEADER.
7290 LPRINT:LPRINT"         DEPTH";
7300 LPRINT TAB(21);
7310 LPRINT"OIL CONC";
7320 LPRINT TAB(36);
7330 LPRINT"SPM CONC";
7340 LPRINT TAB(50);
```

```
        LPRINT"OIL-SPM CONC"
            LPRINT"         CM)";
7370 LPRINT TAB(22);
7380 LPRINT"(GM/CC)";
7390 LPRINT TAB(37);
7400 LPRINT"(GM/CC)";
7410 LPRINT TAB(52);
7420 LPRINT"(GM/CC)"
7430 FOR I = 1 TO NPOINTSA
7440 J=I+1
7450 LPRINT TAB(5);
7460 LPRINT USING"##.###^^^^  ";X(I);
7470 LPRINT TAB(20);
7480 LPRINT USING"##.###^^ ^";C(J);
7490 LPRINT TAB(35);
7500 LPRINT USING"##.###^^^^";S(J);
7510 LPRINT TAB(50);
7520 LPRINT USING"##.###^^^^";W(J);
7530 IF I>1 GOTO 7570
7540 LPRINT TAB(63);
7550 LPRINT"(SURFACE)"
7560 GOTO 7620
7570 IF I<NPOINTSA GOTO 7610
7580 LPRINT TAB(63);
7590 LPRINT"(BOTTOM)"
7600 GOTO 7620
7610 LPRINT
7620 NEXT I
7630 RETURN
7640 REM THIS IS THE SPARSE MATRIX SOLVING ROUTINE FOR THE OIL
7650 REM CONCENTRATION VECTOR.
7660 REM SEE THE DERIVATION NOTES OF 7-14-86.
7670 A(1,2)=A(1,2)-AEXTRA*A(3,1)/A(2,1)
7680 FOR I = 2 TO L
7690 IM1=I-1
7700 ATEMP=A(3,IM1)/A(2,IM1)
7710 A(2,I)=A(2,I)-A(1,IM1)*ATEMP
7720 Y(I)=Y(I)-Y(IM1)*ATEMP
7730 NEXT I
7740 REM NOW PICK UP U(N).
7750 Y(NPOINTS1)=Y(NPOINTS1)-Y(NPOINTS2)*BDIAGC/A(2,NPOINTS2)
7760 U(NPOINTS)=Y(NPOINTS1)/UDIAGC
7770 REM NOW BACK SUBSTITUTE AND STORE THE SOLUTION IN THE U VECTOR.
7780 U(L)=Y(L)/A(2,L)
7790 FOR I = 1 TO LM2
7800 IN=L-I
7810 U(IN)=(Y(IN)-A(1,IN)*U(IN+1))/A(2,IN)
7820 NEXT I
7830 U(1)=(Y(1)-A(1,1)*U(2)-AEXTRA*U(3))/A(2,1)
7840 RETURN
7850 REM THIS IS THE SPARSE MATRIX SOLVING ROUTINE FOR THE SPM
7860 REM CONCENTRATION VECTOR.
7870 B(1,2)=B(1,2)-BEXTRA1*B(3,1)/B(2,1)
7880 FOR I = 2 TO NPOINTS1
7890 IM1=I-1
7900 BTEMP=B(3,IM1)/B(2,IM1)
7910 B(2,I)=B(2,I)-B(1,IM1)*BTEMP
7920 Z(I)=Z(I)-Z(IM1)*BTEMP
7930 NEXT I
7940 B(3,NPOINTS1)=B(3,NPOINTS1)-BEXTRA2*B(1,NPOINTS2)/B(2,NPOINTS2)
7950 Z(NPOINTS)=Z(NPOINTS)-BEXTRA2*Z(NPOINTS2)/B(2,NPOINTS2)
7960 B(2,NPOINTS)=B(2,NPOINTS)-B(3,NPOINTS1)*B(1,NPOINTS1)/B(2,NPOINTS1)
7970 Z(NPOINTS)=Z(NPOINTS)-B(3,NPOINTS1)*Z(NPOINTS1)/B(2,NPOINTS1)
7980 V(NPOINTS)=Z(NPOINTS)/B(2,NPOINTS)
7990 FOR I = 1 TO NPOINTS2
8000 IN=NPOINTS-I
```

```
8010 V(IN)=(Z(IN)-B(1,IN)*V(IN+1))/B(2,IN)
8020 NEXT I
8030 REM NOW PICK UP THE EXTRA TERM AT THE TOP OF THE MATRIX, NOTE
8040 REM THAT Z(1)=0.
8050 V(1)=(B(1,1)*V(2)+BEXTRA1*V(3))/B(2,1)
8060 V(1)=-V(1)
8070 RETURN
8080 REM THIS IS THE SPARSE MATRIX SOLVING ROUTINE FOR THE OIL-SPM
8090 REM AGGLOMERATE CONCENTRATION VECTOR.
8100 REM THE COLUMN VECTOR CONTAINING THE 'LAST-TIME-STEP' INFORMATION
8110 REM IS G(I), I.E., THIS IS 'Y'
8120 REM SEE THE DERIVATION NOTES OF 7-14-86.
8130 D(1,2)=D(1,2)-DEXTRA*D(3,1)/D(2,1)
8140 FOR I = 2 TO L
8150 IM1=I-1
8160 DTEMP=D(3,IM1)/D(2,IM1)
8170 D(2,I)=D(2,I)-D(1,IM1)*DTEMP
8180 G(I)=G(I)-G(IM1)*DTEMP
8190 NEXT I
8200 REM THE NEW OIL-SPM AGGLOMERATE CONCENTRATION PROFILE IS
8210 REM STORED IN Q(I).
8220 REM NOW PICK UP Q(N).
8230 G(NPOINTS1)=G(NPOINTS1)-G(NPOINTS2)*BDIAGB/D(2,NPOINTS2)
8240 Q(NPOINTS)=G(NPOINTS1)/UDIAGB
8250 REM NOW BACK SUBSTITUTE AND STORE THE SOLUTION IN THE Q VECTOR.
8260 Q(L)=G(L)/D(2,L)
8270 FOR I = 1 TO LM2
8280 IN=L-I
8290 Q(IN)=(G(IN)-D(1,IN)*Q(IN+1))/D(2,IN)
8300 NEXT I
8310 Q(1)=(G(1)-D(1,1)*Q(2)-DEXTRA*Q(3))/D(2,1)
8320 RETURN
8330 REM INTEGRATION OF THE PNT(I) VECTOR BY SIMPSONS RULE.
8340 REM THE PARAMETERS ISMP42 AND HSMP3 MUST BE CALCULATED IN
8350 REM THE MAIN ROUTINE BEFORE THE FIRST CALL.
8360 REM ISMP42 IS THE NUMBER OF (4,2) PAIRS IN THE INTEGRATION SUM
8370 REM AND IS EQUAL TO (NPOINTSA-4)/2, AND HSMP3 IS THE INTERVAL
8380 REM DELTA-X DIVIDED BY 3.
8390 SUM1=PNT(1)
8400 FOR I = 1 TO ISMP42
8410 K=2*I
8420 SUM1=SUM1+4#*PNT(K)+2#*PNT(K+1)
8430 NEXT I
8440 SUM1=(SUM1+4#*PNT(K+2)+PNT(K+3))*HSMP3
8450 RETURN
8460 REM SUBROUTINE TO CALCULATE THE STEADY STATE SPM PROFILE.
8470 REM CALCULATE SOME TERMS USED THROUGHOUT.  THERE IS NO REACTION-
8480 REM RATE CONSTANT FOR SPM LOSS IN THE STEADY-STATE SPM PROFILE
8490 REM BECAUSE THERE MUST BE AN OIL CONCENTRATION, AND THERE IS NOT.
8500 REM IF THERE IS A NEED TO PUT A REACTION-LOSS TERM IN,
8510 REM ADD ALPHAS*OILCONC/VDIFF TO SQRARG, AND ADD
8520 REM 2*VDIFF*ALPHAS*OILCONC TO BRACKET (SEE BELOW).  BUT, OILCONC
8530 REM MUST BE DEFINED AND IT MUST BE UNIFORM IN THE WATER COLUMN.
8540 VX2K=VRSPM/(2#*VDIFF)
8550 SQRARG=VX2K*VX2K
8560 REM IF THE SQUARE-ROOT ARGUMENT IS ZERO, THE STEADY-STATE SPM
8570 REM PROFILE IS FZERO/SKZERO.
8580 IF SQRARG<>0# GOTO 8640
8590 CSPM=FZERO/SKZERO
8600 FOR I = 1 TO NPOINTS
8610 S(I)=CSPM
8620 NEXT I
8630 GOTO 8820
8640 ZETAZ=SQR(SQRARG)
8650 TWOKZ=2#*VDIFF*ZETAZ
8660 TWOKKZ=TWOKZ*SKZERO
```

```
8670 BRACKET=VRSPM*SKZERO
8680 REM CALCULATE THE DENOMINATOR ONLY ONCE.
8690 EXPTERM=EXP(ZETAZ*DEPTH1)
8700 SINHL=(EXPTERM-1#/EXPTERM)/2#
8710 COSHL=(EXPTERM+1#/EXPTERM)/2#
8720 DENOM=(TWOKZ*COSHL+BRACKET*SINHL)/FZERO
8730 FOR I = 1 TO NPOINTS
8740 X=CDBL(I-2)*DX
8750 HARG=ZETAZ*X
8760 EXPTERM=EXP(HARG)
8770 SINHX=(EXPTERM-1#/EXPTERM)/2#
8780 COSHX=(EXPTERM+1#/EXPTERM)/2#
8790 EXPLEAD=EXP(VX2K*(X-DEPTH1))
8800 S(I)=EXPLEAD*(VRSPM*SINHX+TWOKZ*COSHX)/DENOM
8810 NEXT I
8820 RETURN
8830 REM SUBROUTINE TO CALCULATE A STEADY-STATE OIL PROFILE
8840 REM WITH EXPONENTIAL DISERSION (GAMMA) SET TO ZERO,
8850 REM OTHERWISE THERE IS NO STEADY STATE PROFILE, SEE
8860 REM PAGE 25 OF 12-9-87.
8870 REM IT IS RECOMMENDED THAT A STEADY-STATE OIL PROFILE NOT BE USED.
8880 REM USING SUCH A STEADY-STATE OIL PROFILE IS SOMEWHAT ODD, I.E.,
8890 REM THE WATER USUALLY HAS SPM IN IT TO START WITH AND OIL IS
8900 REM THEN SPILLED.  IT IS DIFFICULT TO CONCEIVE OF A SITUATION WHERE
8910 REM OIL IS AT STEADY STATE IN THE WATER, BUT THIS SUBROUTINE IS HERE
8920 REM ANYWAY, MAINLY AS A TESTING ROUTINE TO GET THINGS GOING IN
8930 REM MATHEMATICAL SENSE.
8940 REM CHECK TO SEE IF VROIL=0.
8950 IF VROIL<>0# GOTO 9030
8960 IF ALPHAO>0# GOTO 9030
8970 SSOIL=SZERO/VDIFF
8980 FOR I = 1 TO NPOINTS
8990 X=CDBL(I-2)*DX
9000 C(I)=SSOIL*(DEPTH1-X)
9010 NEXT I
9020 GOTO 8820
9030 AOIL=VROIL/(2#*VDIFF)
9040 REM USE THE CORRECT REACTION CONSTANT FOR OIL LOSS, NOTE THAT THERE
9050 REM MUST BE AN SPM CONCENTRATION ASSOCIATED WITH THE OIL-LOSS CONSTANT.
9060 REM SEE PAGES 25A OF 12-9-87 AND 25B OF 8-8-88 OF THE DERIVATION
9070 REM NOTES FOR COMMENTS ON THIS AND ALSO A SPECIAL CASE WHEN
9080 REM THE REACTION CONSTANT IS LARGE.
9090 ALPHAU=ALPHAO*FZER/SKZER
9100 ZETAO2=AOIL*AOIL+ALPHAU/VDIFF
9110 ZETAO=SQR(ZETAO2)
9120 EXP1=EXP(ZETAO*DEPTH1)
9130 EXP2=1#/EXP1
9140 SINHO=(EXP1-EXP2)/2#
9150 COSHO=(EXP1+EXP2)/2#
9160 SSOIL=SZERO/(VDIFF*ZETAO*COSHO+SINHO*VROIL/2#)
9170 FOR I = 1 TO NPOINTS
9180 X=CDBL(I-2)*DX
9190 EXPLEAD=EXP(AOIL*X)
9200 EXP1=EXP(ZETAO*(DEPTH1-X))
9210 SINH=(EXP1-1#/EXP1)/2#
9220 C(I)=SSOIL*EXPLEAD*SINH
9230 NEXT I
9240 RETURN
9250 REM SUBROUTINE TO PRINT HEADER ON THE SCREEN.
9260 PRINT"INTERACTING OIL DROPLETS AND SPM CALCULATION"
9270 PRINT"CODE NAME IS ";CODEN$;
9280 PRINT", VERSION OF ";VER$
9290 RETURN
9300 REM SUBROUTINE TO PRINT PAGE HEADER.
9310 LPRINT TOF$
9320 LPRINT"FINITE-DIFFERENCE SOLUTION FOR INTERACTING OIL DROPLETS";
```

```
9330 LPRINT" AND 5PM."
9340 LPRINT:LPRINT"CODE NAME IS ";CCDEN$;
9350 LPRINT", VERSION IS ";VER$
9360 LPRINT"RUN TIME WAS ";RTIME$;
9370 LPRINT", AND RUN DATE WAS ";RDATE$;
9380 IPAGE=IPAGE+1
9390 LPRINT TAB(65);
9400 LPRINT"PAGE ";
9410 LPRINT USING"###";IPAGE
9420 RETURN
```

U.S. DEPARTMENT OF COMMERCE
NATIONAL OCEANIC AND ATMOSPHERIC ADMINISTRATION
NATIONAL OCEAN SERVICE

Alaska Office
Federal Bldg., U.S. Courthouse, Room A13
222 W. Eighth Ave., #56
Anchorage, Alaska 99513-7543

OFFICIAL BUSINESS
PENALTY FOR PRIVATE USE $300

FOURTH-CLASS MAIL
POSTAGE AND FEES PAID
U.S. Department of Commerce
Permit Number G-19

SPECIAL FOURTH CLASS

CLASS OF POSTAL SERVICE